Metabolic characterisation and modulation of the immune response to biomaterials for bone tissue engineering

Lianne Shanley

B.A. (Hons) Molecular Medicine

A thesis submitted to

Trinity College Dublin

for the degree of

Doctor of Philosophy

Supervisor: Prof. Aisling Dunne

Co-supervisor: Prof. Daniel Kelly

2025

Declaration of Authorship

I declare that this thesis has not been submitted as an exercise for a degree at this or any other university and it is entirely my own work, except where otherwise stated. I agree to deposit this thesis in the University's open access institutional repository or allow the library to do so on my behalf, subject to Irish Copyright Legislation and Trinity College Library conditions of use and acknowledgement.

Lianne Shanley

Acknowledgements

Firstly, to my supervisor, Professor Aisling Dunne, and co-supervisor, Professor Daniel Kelly. Aisling, thank you for placing your trust in me since day one. You have not only been there to advise and guide me throughout this project, but also to give words of encouragement and support when needed. Thank you for all that you've done, navigating the twists and turns of the last few years with professionalism and compassion. I feel very lucky to have had you as my mentor. Danny, thank you for always being open to running through data, offering your guidance and advice, and sitting through countless immunometabolism presentations over the years. It has been a pleasure to work as part of your lab, and I'm truly grateful to have been given the opportunity to do so.

Thank you to my thesis committee, Professors Ed Lavelle and Ursula Fearon, for supporting me as I progressed through the years, and for offering some fantastic suggestions and pointers along the way.

To Olwyn, on whose work this project was built. Thank you for getting me up and running in the lab whilst you were also wrapping up, and for your patience with me since then, whether it be answering (numerous) queries about data analysis, proofing of papers and transfer theses, and teaching me to 'think immunology like a bioengineer'!

To Hannah and Sinead, the Dunne lab gals. Suffice to say, this PhD would not have been the same without you both. Thank you for teaching me how the lab was run, and for all the times you offered your advice and support. I cannot count how often you were there to troubleshoot experiments, listen to presentation after presentation, and bear witness to all the ups and downs of the last 4+ years, often with a sympathetic ear or a coffee (/Coke Zero) to hand. Hannah, for all your ketoacid advice and HO-1 help, and everything in between. Sinead, for always being willing to act as a soundboard, advise on all things immunoengineering, and head out for a little treat when things just weren't going our way (and oftentimes when they were, too).

Well, Gearóid! You've been such a great addition to the Dunne lab, and I've thoroughly enjoyed all our natters, silliness, consultations, and pep talks. You're a great scientist and pal, and you're going to do wonderful things wherever you go.

To the McLoughlin and Stevenson labs, with special mention to Emilio, Clíodhna, Seán, Alanna, Mei, and Aziz as the PhD reading room contingent. Emilio, you have been such an immense help during this PhD, so often going above and beyond to give incredible advice (both lab and skincare-related), help out with experiments, being there to have a chat (often far later than we intended to stay!), and imparting the immortal words of reassurance: "Every people flumble". Clíodhna, thank you for being the best Ents Officer not only to the McLoughlin lab, but the whole lot of us, and for always being there for a chat or a late-night sushi run. Alanna, thank you for always being up for a good natter, and Seán, you really were an excellent muse. Mei, it's been such a pleasure working with you these last few years, and Aziz, the dragon, best of luck with the rest of your PhD. To Tracey, Simon, Brenda, Jonah, Juber, past members Claudia, Eva, Jenny, Andy, Richard, Eoin, Michelle, Lowela, and of course to Vivienne, for holding the entire place together.

To the Kelly lab and members of TCBE past and present, all a wonderful bunch of scientists, and always willing to lend a hand and offer some much-needed bioengineering advice. A particular thank you to Gabi, Fran, Kyle, and Nadia, without whom 'Operation: Rats' could never have happened. A special thank you to past members, Dave, for getting the hydrogels up and running, and Fiona, for giving up so much of your time to advise and help out in the chaos of the surgeries. To Simon, whose help has avoided so many near-disasters over the years.

To Stéphane, mon fellow AMBER pamplemousse, you have been an incredible friend and colleague over the years. Thank you for all your help, your support, and your endless kindness. I'm very proud to have watched you grow as a scientist and I'm so happy to have shared this experience with you. To Meena, for all the chats and the commiserations (of which there were many) over the years. It's been wonderful working alongside you and I'm excited to see where you go next! To Nuno, former member of the Monaghan lab, for giving so much time and support to the metabolism experiments.

To all the teaching lab team, who never fail to pick us up with their kind words and endless help. You made the labs a joy to work in, and there's not a tighter ship to be found running in Trinity. To Liam McCarthy and Liam Cross, for being the go-tos for everything and anything. To Gavin McManus, for your limitless patience with my confocal queries. To Barry and Aoife, for all the help with everything flow: I don't know how I'd have gotten through without having you both to run to with a proposed panel or in a flow-related panic. Thank you to Laavanya, for your tireless work with CMU and constantly going above and beyond to ensure everything is kept running, and to Daniel, Ciarán, and Rustam, for all your help with the surgeries.

To all my friends that have been there for the last four years (and well beyond that). You have all been such pillars of support and never fail to pick me up or cheer me on, depending on what the day requires. There are too many of you to name without these acknowledgements getting (even more) ridiculous, but I'd like to extend a particular thank you to Ailbhe, Bronwyn, and Anne-Marie, the best SAD Supports I could ask for, and a special mention to James, who was always there for a good debrief over a cup of tea (whether he wanted to be or not).

Lastly, but by no means least, to my family. To my nanny and grandad, who I'm sure will cite the origins of this PhD as being at their kitchen table (could sitting for hours learning how to draw cartoon mice have had an influence here?). Shauna and Emma, my little-ish sisters, you're a gas pair (sometimes). Thank you to my Mum and Dad, my biggest supporters since day one, for always being there to offer advice, cheer me on, pick me up when I'm down, and help me regain a sense of perspective when it was needed most. I love you all very much.

Thank you for everything.

Abstract

The limited capacity of many tissues and organs to adequately repair and regenerate lies at the heart of numerous healthcare challenges. Difficulties faced in promotion of tissue healing and regrowth have begun to be tackled by the incorporation of biomaterial approaches into clinical practice, with the ultimate goal being functional tissue regeneration. While traditional biomaterial design centred around 'immune-inert' biomaterials that would elicit minimal immune response from a host system, it is now evident that the immune system functions as a critical determinant of implant integration, failure, and success. Given this, there is a pressing need to thoroughly characterise how the immune system not only recognises, but also responds to biomaterials. Materials intended for bone-tissue applications are one such class of biomaterials that stand to benefit from the incorporation of immunology research into bone-based biomaterial design. As our understanding of 'osteoimmunology' expands, so too does our appreciation of the immune processes that can contribute to regeneration of functional bone tissue. As such, efforts are underway to further understand the processes that contribute to destruction at the implant site, and leverage those that facilitate repair and regeneration.

The studies presented in this thesis first examine the effect of micron and nano-sized hydroxyapatite (HA) particles on the metabolic profile of human macrophages, given that metabolic reprogramming is now known to impact on macrophage function. Results from this chapter demonstrate that HA particle size can differentially impact on macrophage metabolism, with micron-sized particles preferentially driving a metabolic shift favouring glycolysis, accompanied by pro-inflammatory macrophage polarisation. Furthermore, it is shown that blockade of particle phagocytosis reduces surrogate markers of glycolysis at the gene expression level and attenuates micronHA-driven pro-inflammatory polarisation, furthering not only our insight into the use of HA in orthopaedic biomaterials, but also our understanding of the destructive processes that can occur at the site of biomaterial implantation that can contribute to orthopaedic implant wear and eventual failure.

This thesis then investigates the effect of novel immunomodulatory ketoacids (indole pyruvate [IP] and hydroxyphenyl pyruvate [HPP]), derived from the parasite *Trypansoma*

brucei (T. brucei), on the inflammatory and regenerative profile of human macrophages. Results reveal differential effects on human macrophages compared to other immune cells and demonstrate for the first time that these ketoacids have potential pro-regenerative effects. This work is furthered by interrogation of the effect of IP on the osteoblastic differentiation of human mesenchymal stem cells (MSC), demonstrating that IP can potentially promote early osteogenesis and mineralisation of MSC.

The final chapter explores the effects of a novel hyaluronic acid hydrogel on primary human macrophages. It is demonstrated that this material is biocompatible, and modulation of hydrogel stiffness in the range achieved (1 – 10 kPa) has no significant effect on macrophage polarisation. It is then attempted to incorporate the ketoacid, IP, into the hydrogel and deliver it into a rat bone defect site. Follow-on assessment of *ex vivo* tissue demonstrates that IP-loaded hydrogel leads to an upregulation in osteogenic gene expression at seven days post-implantation.

Overall, the work in this thesis furthers our understanding of the human macrophage response to HA biomaterial particulates and posits immunometabolism a worthy strategy to further characterise the immune response to biomaterials, as well as reveal potential novel therapeutic targets for tissue repair and regeneration. This thesis also demonstrates the pro-regenerative potential of a novel immunomodulatory ketoacid for bone tissue engineering applications, and presents a novel hyaluronic acid hydrogel as a potential delivery platform for immunomodulators in a bone regenerative context. Ultimately, by furthering our understanding of biomaterial-immune system interactions, and how we can capitalise on such for therapeutic benefit, we stand to create a new class of 'immune-informed' biomaterials that hold the potential to tackle existing healthcare challenges around biomaterial implantation strategies.

Publications, Conference Proceedings, and Awards

First author publications:

Shanley L.C., Mahon O.R., O'Rourke S.A., Neto N.G.B., Monaghan M.G., Kelly D.J., Dunne A. Macrophage metabolic profile is altered by hydroxyapatite particle size. *Acta Biomaterialia* 2023.

Shanley L.C., Fitzgerald H.K., O'Rourke S.A., Dunne A. Endogenous drivers of altered immune cell metabolism. *Experimental Biology and Medicine* 2022.

Shanley L.C., Mahon O.R., Kelly D.J., Dunne A. Harnessing the innate and adaptive immune system for tissue repair and regeneration: Considering more than macrophages. *Acta Biomaterialia* 2021.

Co-author publications:

Petrousek S.R., Kronemberger G.S., O'Rourke S.A., **Shanley L.C.,** Dunne A., Kelly D/J, Hoey D.A. Human macrophage polarisation and regulation of angiogenesis and osteogenesis is dependent on culture extracellular matrix and dimensionality. *Biochemical and Biophysical Research Communications* 2024.

O'Rourke S.A., **Shanley L.C**., Dunne A. The Nrf2-HO-1 System and Inflammageing. *Frontiers in Immunology* 2024.

Freeman F.E., Dosta P., **Shanley L.C.**, Ramirex Tamez N., Riojas Javelly C.J., Mahon O.R., Kelly D.J., Artzi N. Localised Nanoparticle-Mediated Delivery of miR-29b Normalises the Dysregulation of Bone Homeostasis Caused by Osteosarcoma whilst Simultaneously Inhibiting Tumor Growth. *Advanced Materials* 2023.

O'Rourke S.A., Neto N.G.B., Devilly E., **Shanley L.C.,** Fitzgerald H.K., Monaghan M.G., Dunne A. Cholesterol crystals drive metabolic reprogramming and M1 macrophage polarisation in primary human macrophages. *Atherosclerosis* 2022.

Conference proceedings:

British Society for Immunology, December 2023, Belfast, N.I., UK. **Shanley L.C.,** Mahon O.R., O'Rourke S.A., Neto N.G.B., Monaghan M.G., Kelly D.J., Dunne A. Macrophage metabolic profile is altered by hydroxyapatite particle size. Poster presentation.

Bioengineering in Ireland, 28th Annual Conference, January 2023, Meath, Ireland. **Shanley L.C.,** Mahon O.R., O'Rourke S.A., Neto N.G.B., Monaghan M.G., Kelly D.J., Dunne A. Particle size alters macrophage metabolism: implications for bone tissue engineering. Oral presentation.

British Society for Immunology, December 2022, Liverpool, UK. **Shanley L.C.,** Mahon O.R., O'Rourke S.A., Neto N.G.B., Monaghan M.G., Kelly D.J., Dunne A. Particle size alters macrophage metabolism: implications for bone tissue engineering. Poster presentation.

Irish Society for Immunology, September 2022, Maynooth, Kildare, Ireland. **Shanley L.C.,** Mahon O.R., O'Rourke S.A., Neto N.G.B., Monaghan M.G., Kelly D.J., Dunne A. Macrophage metabolic profile is altered by hydroxyapatite particle size. Poster presentation.

Gordon Research Conference in Immunoengineering, July 2022, Ventura Beach, California, USA. **Shanley L.C.,** Mahon O.R., O'Rourke S.A., Neto N.G.B., Monaghan M.G., Kelly D.J., Dunne A. Macrophage metabolic profile is altered by hydroxyapatite particle size. Poster presentation.

Bioengineering in Ireland, 27th Annual Conference, May 2022, Galway, Ireland. **Shanley L.C.,** Mahon O.R., O'Rourke S.A., Neto N.G.B., Monaghan M.G., Kelly D.J., Dunne A. Particle size alters macrophage metabolism: implications for bone tissue engineering. Oral presentation.

British Society for Immunology, December 2021, Edinburgh. **Shanley L.C.,** Mahon O.R., O'Rourke S.A., Neto N.G.B., Monaghan M.G., Kelly D.J., Dunne A. Particle size alters macrophage metabolism: implications for bone tissue engineering. Poster presentation.

European Macrophage and Dendritic Cell Society, June 2021, Virtual conference. **Shanley L.C.,** Mahon O.R., O'Rourke S.A., Neto N.G.B., Monaghan M.G., Kelly D.J., Dunne A. Particle size alters macrophage metabolism: implications for bone tissue engineering. E-poster presentation.

Awards:

First Place - IUA National 'Thesis in 3' (3MT), Royal Irish Academy, November 2023

Audience Choice - IUA National 'Thesis in 3' (3MT), Royal Irish Academy, November 2023

First Place - Trinity College Dublin 'Thesis in 3' (3MT), Trinity College Dublin, March 2023

Audience Choice - Trinity College Dublin 'Thesis in 3' (3MT), Trinity College Dublin, March 2023

RAMI Bronze Medal - Royal Academy of Medicine in Ireland - 28th Annual Conference of the RAMI Section of Bioengineering, The Johnstown Estate, Enfield, Co.Meath, January 2023

First Place - BinI 'Biomaterials' Track - 27th Annual Conference of the RAMI Section of Bioengineering, The Galmont, Co.Galway, May 2022

Abbreviations

2-DG	2-Deoxyglucose
3-PO	3-(3-Pyridinyl)-1-(4-pyridinyl)-2-propen-1-one
AhR	Aryl hydrocarbon receptor
ALP	Alkaline phosphatase
AMP	Adenosine monophosphate
AMPK	AMP-activated protein kinase
ANG1	Angiopoietin 1
ANOVA	Analysis of variance
ANXA1	Annexin A1
AP	Activator protein
AR	Alizarin red
ARE	Antioxidant response element
Arg1	Arginase1
Arnt	AhR nuclear translocators
AT-RvD1	Aspirin-triggered resolving D1
ATP	Adenosine triphosphate
BACH1	BTB and CNC homology 1
BaP	Benzo[*a*]pyrene
BHB	Beta-hydroxybutyrate
BMDC	Bone marrow derived dendritic cells
BMDM	Bone marrow derived macrophages
BMP	Bone morphogenic protein
BMSC	Murine bone marrow stromal cells
BSA	Bovine serum albumin
CaP	Calcium phosphate
CCL	Chemokine ligand
CD	Cluster of differentiation
CIA	Collagen-induced arthritis
CM	Conditioned media

CO	Carbon monoxide
CoPP	Cobalt protoporphyrin
COVID	Coronavirus disease
CPC	Cetylpyridinium chloride
cRPMI	Complete RPMI
CST	Cell Signalling Technologies
CXCL	Chemokine (C-X-C motif) ligand
DAMP	Damage associated molecular pattern
DC	Dendritic cells
DK	Diclofenac potassium
DMEM	Dulbecco's Modified Eagle Medium
DMF	Dimethyl fumarate
DMSO	Dimethyl sulfoxide
DNA	Deoxyribonucleic acid
DQ-ova	DQ-ovalbumin
EAE	Experimental autoimmune encephalomyelitis
ECAR	Extracellular acidification rate
ECAR	Extracellular acidification rate
ECL	Electrochemiluminescence
ECM	Extracellular matrix
EDTA	Ethylenediaminetetraacetic acid
EGCG	Epigallocatechine-3-gallate
ELISA	Enzyme-lined immunosorbent assay
ERK	Extracellular signal-regulated kinase
ETC	Electron transport chain
FADH	Flavin adenine dinucleotide
FAO	Fatty acid oxygen pathway
FAS	Fatty acid synthesis pathway
FBR	Foreign body response
FBS	Foetal bovine serum
FCCP	Carbonyl cyanide-p-tripluoromethoxyphenylhydrazone
FCS	Forward scatter

FGF	Fibroblast growth factor
FICZ	6-formylindolo[3,2-b]carbazole
FLIM	Fluorescence lifetime imagine microscopy
FLIM	Fluorescence Lifetime Imaging Microscopy
FMO	Fluorescence minus one
FMO	Fluorescence minus one
G6P	Glucose-6-phosphate
GAG	Glycolsaminoglycan
GAPDH	Glyceraldehyde-3-phosphate dehydrogenase
GO-PEI	Polyethylenimine-functionalised graphene oxide
GPa	Gigapascals
GSR	Glutathione reductase
GVD	Graft-versus-host disease
HA	Hydroxyapatite
HEK	Human embryonic kidney
HEK	Human embryonic kidney
hgDMEM	High-glucose DMEM
HIF	Hypoxia inducible factor
HIF1α	Hypoxia inducible factor 1 alpha
HK2	Hexokinase II
HO	Heme oxygenase
HPLC	High-performance liquid chromoatography
HPP	4-hydroxyphenyl pyruvate
HRP	Horseradish peroxidase
HUVEC	Human umbilical vein endothelial cells
HyA	Hyaluronic acid
HyA-TA	Tyramine-conjugated hyaluronic acid
IBD	Irritable bowel disease
iDC	Immature dendritic cell
IFNγ	Interferon gamma
IL	Interleukin
ILC	Innate lymphoid cell

iNOS	Inducible nitric oxide synthase
IP	Indole-3-pyruvate
IP-CM	IP-conditioned media
JNK	Janus kinase
KEAP	Kelch-like ECH-associated protein 1
kPa	Kilopascal
LPS	Lipopolysaccharide
M-CSF	Macrophage colony stimulation factor
MACS	Magnetic-activated cell sorting
MAPK	Map kinase
MFI	Mean fluorescence intensity
MFN	Mitofusin
MI	Myocardial infarction
micronHA	Micron-sized hydroxyapatite
MMP	Matrix metalloproteinase
mRNA	Messenger RNA
MS	Multiple sclerosis
MSC	Mesenchymal stem/stromal cell
MSN	Mesoporous silica nanoparticles
MSU	Monosodium urate
mTOR	Mammalian target of rapamycin
NADH	Nicotinamide adeneine dinucleotide
NADH	Nicotinamide adenine dinucleotide and hydrogen
nanoHA	Nano-sized hydroxyapatite
NF-kb	Nuclear factor kappa-light-chain-enhancer of activated B cells
NK	Natural Killer
NLR	Nod-like receptor
NLRP3	NLR family pyrin domaining containing 3
NMR	Nuclear magnetic resonance
NO	Nitric oxide
NP	Nanoparticles

NQO-1	NAD(P)H Quinone Oxidoreductase 1
Nrf2	Nuclear factor erythroid 2-related factor
OA	Osteoarthritis
OCN	Osteocalcin
OCR	Oxygen consumption rate
OCR	Oxygen consumption rate
OPN	Osteopontin
PAMP	Pathogen associated molecular pattern
PBMC	Peripheral blood mononuclear cells
PBMC	Peripheral blood mononuclear cell
PBS	Phosphate-buffered saline
PCL	Polycaprolactone
PCR	Polymerase chain reaction
PDGF	Platelet derived growth factor
PE	Polyethylene
PEEK	Polyetheretherketone
PEG	Polyethylene glycol
PEGDA	Poly (ethylene glycol) diacrylate
PFA	Paraformaldehyde
PFKFB3	Phosphofructokinase
PI	Propidium iodide
PKM2	Pyruvate kinase isoform 2
PKM2	Pyruvate kinase M2
PLA	Poly lactic acid
PLGA	Poly (lactic co-glycolic acid)
PLLA	Poly (L-lactide)
PMMA	Polymethyl methylacrylate
PP	Phenyl pyruvate
PPP	Pentose phosphate pathway
PRR	Pathogen recognition receptor
PVDF	Polyvinylidene difluoride
RA	Rheumatoid arthritis

rBMSC	Rat bone marrow stomal cells
RGD	Arginylglycylaspartic acid
RHAMM	Receptor for hyaluronan-mediated motility
RIPA	Radioimmunoprecipitation assay buffer
RNA	Ribonucleic acid
ROI	Region of interest
ROS	Reactive oxygen species
RPMI	Roswell Park Memorial Institute
RSV	Respiratory syncytial virus
RT	Room temperature
RT-qPCR	Quantitative reverse transcription polymerase chain reaction
RUNX2	Runt-related transcription factor
SD	Standard deviation
SDS-PAGE	Sodium dodecyl sulphate polyacrylamide gel electrophoresis
SEAP	Secreted embryonic alkaline phosphatase
SEC-CM	Macrophage secretome-conditioned media
SEM	Standard error of the mean
SEM	Standard error of the mean
siRNA	Small interfering RNA
SnPP	Tin protoporphoryin
SPM	Specialised pro-resolving mediator
SSC	Side scatter
STAT	Signal transducer and activator of transcription
T2D	Type 2 diabetes
TbcASAT	Cytoplasmic aspartate aminotransferase
TBST	Tris-buffered saline with TWEEN™
TCA	Tricarboxylic acid
TCDD	2,3,7,8-tetrachlorodibenzo-p-dioxin
TCP	Tissue culture plastic
TGF-β	Tissue growth factor beta
Th	T helper
TIMP	Tissue inhibitor of metalloproteinase

TLR	Toll-like Receptor
TNF	Tumour necrosis factor
Treg	Regulatory T cell
UHMWPE	Ultra-high molecular weight polyethylene
VEGF	Vascular endothelial growth factor
VML	Volumetric muscle loss
WNT	Wingless/Integrated
XRE	Xenobiotic-response elements
YAP	Yes-associated protein
ZnPP	Zinc protoporphyrin

Table of Contents

Declaration of Authorship ..... *ii*

Acknowledgements ..... *iii*

Abstract ..... *vi*

Publications, Conference Proceedings, and Awards ..... *viii*

Abbreviations ..... *xi*

Table of Contents ..... *xviii*

Table of Figures ..... *xxii*

Table of Tables ..... *xxvi*

Chapter One: Introduction *1*

1.1 The immune system in tissue repair **2**
1.1.1 Innate immunity in tissue repair 3
1.1.2 Macrophages in tissue repair 5
1.1.3 Adaptive immunity in tissue repair 7

1.2 Novel immunomodulatory strategies for tissue repair and regeneration **9**
1.2.1 The heme-oxygenase system and HO-1 10
1.2.2 HO-1 in inflammation and tissue repair 11
1.2.3 HO-1 inducers as therapeutics 12
1.2.4 Immunomodulatory ketoacids 13

1.3 Immunomodulatory biomaterials for tissue repair and regeneration **14**
1.3.1 Particle size and shape for immunomodulation 15
1.3.2 Biomaterial stiffness for immunomodulation 16
1.3.3 Immunomodulation through targeting pro-inflammatory factors 17
1.3.4 Immunomodulation through targeting anti-inflammatory factors 19

1.4 Immunometabolism: implications for tissue engineering **22**
1.4.1 Macrophage metabolism: implications for tissue engineering 24

1.5 Biomaterials in bone tissue engineering **25**

1.6 Research question **28**

1.7 Specific aims **29**

Chapter Two: Materials and Methods *30*

2.1 Materials **31**
2.1.1 Cell culture 30
2.1.2 Inhibitors and reagents 31
2.1.3 Western blotting 31
2.1.4 Primary antibodies 32
2.1.5 Secondary antibodies 32
2.1.6 Flow cytometry 32
2.1.7 Seahorse XF analyser materials 34
2.1.8 Confocal microscopy 34
2.1.9 Polymerase Chain Reaction (PCR) materials 34
2.1.10 Fluorescence Lifetime Imaging Microscopy (FLIM) 36
2.1.11 Enzyme-linked Immunosorbent Assay (ELISA) 36
2.1.12 Hyaluronic acid hydrogels 36

2.1.13 Alizarin red staining 36

2.2 Methods 37

2.2.1 Cell culture 37
2.2.1.1 Isolation of PBMCs from human venous blood 37
2.2.1.2 Isolation of $CD14^+$ monocytes 37
2.2.1.3 Culture of monocyte-derived macrophages 38
2.2.1.4 Macrophage lifting 38
2.2.1.5 Culture of adult human bone marrow-derived mesenchymal stem cells (MSC) 39
2.2.1.6 Neutral red viability assay 39
2.2.1.7 Macrophage conditioned media experiment 40
2.2.2 Flow cytometry 40
2.2.2.1 Cell surface marker staining 40
2.2.2.2 Annexin V & PI staining 40
2.2.2.3 Acquisition, compensation, and analysis 40
2.2.3 SDS-PAGE, gel staining, and western blot 41
2.2.3.1 Sample preparation 41
2.2.3.2 SDS-PAGE 41
2.2.3.3 Transfer of proteins onto PVDF membrane 42
2.2.3.4 Immunodetection of proteins 42
2.2.4 Polymerase Chain Reaction (PCR) 43
2.2.4.1 Cell treatments 43
2.2.4.2 RNA extraction 43
2.2.4.3 cDNA synthesis 44
2.2.4.4 Real-time polymerase chain reaction (PCR) 45
2.2.5 Measurement of cytokine production by ELISA 47
2.2.6 Seahorse XF Analyser 48
2.2.6.1 Macrophage seahorse experiments 48
2.2.6.2 Seahorse analysis 48
2.2.7 Confocal imaging of mitochondria 51
2.2.8 Fluorescence Lifetime Imaging Microscopy (FLIM) 51
2.2.9 Preparation of micron and nano hydroxyapatite particle suspensions 52
2.2.9.1 Synthesis of nano hydroxyapatite particles 52
2.2.9.2 Preparation of micron hydroxyapatite particle suspension 52
2.2.9.3 Assessment of endotoxin contamination 52
2.2.10 Hyaluronic acid hydrogel fabrication 53
2.2.11 Alizarin red staining 53
2.2.12 Rat femoral defect model 54
2.2.12.1 Surgical procedure 54
2.2.12.2 Characterisation of immune cell subsets and gene expression analysis 54
2.2.13 Statistical analysis 55

Chapter Three: Macrophage metabolic profile is altered by hydroxyapatite particle size 59

3.1 Introduction 60

3.2 Hypothesis 61

3.3 Specific Aims 61

3.4 Results 63

3.4.1 Micron and nano-sized hydroxyapatite particles are not contaminated with endotoxin 63
3.4.2 Micron and nano-sized hydroxyapatite particles do not impact on cell viability 63
3.4.3 MicronHA particles, but not nanoHA, upregulate surrogate markers of glycolysis in primary human macrophages 64
3.4.4 MicronHA particles upregulate oxidative phosphorylation-associated mRNA expression of *ATP5b* at 24 hours post-stimulation, and do not affect *MFN1* and *MFN2* 65
3.4.5 MicronHA and nanoHA particles differentially impact on mitochondrial fusion and fission 65

3.4.6 MicronHA particles alter primary human macrophage metabolism at 6 and 24 hours 66
3.4.7 MicronHA particles, but not nanoHA, alter primary human macrophage bioenergetics to favour glycolysis over oxidative phosphorylation 67
3.4.8 Inhibition of micronHA particle uptake decreases expression of surrogate markers of glycolysis at the mRNA level in primary human macrophages 68
3.4.9 Inhibition of micronHA particle uptake decreases expression of pro-inflammatory cytokines in primary human macrophages 68
3.4.10 Glycolytic inhibitors 2-DG and 3-PO decrease pro-inflammatory macrophage marker expression at the mRNA level and attenuate pro-inflammatory cytokine secretion in primary human macrophages 69

3.5 Discussion 91

Chapter Four: Immunomodulatory and regenerative potential for Trypanosoma brucei-derived ketoacids in primary human macrophages and mesenchymal stem cells..... 96

4.1 Introduction 97

4.2 Hypothesis 99

4.3 Specific Aims 99

4.4 Results 100
4.4.1 IP and HPP are non-toxic to primary human macrophages 100
4.4.2 HPP upregulates HO-1 to a greater extent than IP in primary human macrophages 100
4.4.3 IP and HPP activate the aryl hydrocarbon receptor (AhR) and Nrf2 in primary human macrophages 101
4.4.4 IP and HPP attenuate LPS-induced inflammatory gene expression, but not cytokine production, in primary human macrophages 102
4.4.5 IP and HPP modulate macrophage metabolic responses in primary human macrophages 103
4.4.6 IP and HPP drive vascularisation- and regeneration-associated gene expression in primary human macrophages 104
4.4.7 IP-conditioned macrophage media does not significantly impact on pro-osteogenic and pro-regenerative gene expression in human mesenchymal stem cells 104
4.4.8 IP does not significantly impact on the viability of human mesenchymal stem cells 105
4.4.9 IP upregulates HO-1 in human mesenchymal stem cells 106
4.4.10 IP upregulates AhR- and Nrf2-related gene expression and activates Nrf2 in human mesenchymal stem cells 106
4.4.11 IP upregulates vascular-associated and growth factor gene expression in human mesenchymal stem cells 107
4.4.12 IP potentially promotes osteoblastic differentiation of human mesenchymal stem cells 107
4.4.13 IP-mediated upregulation of *RUNX2* and *VEGF* is dependent on AhR activation 108

4.5 Discussion 134

Chapter Five: A hyaluronic acid hydrogel delivery system for immunomodulators in the context of bone regeneration 144

5.1 Introduction 145

5.2 Hypothesis 147

5.3 Specific Aims 148

5.4 Results 149
5.4.1 Hyaluronic acid hydrogels do not impact on the viability or differentiation ability of primary human macrophages and monocytes 149
5.4.2 Macrophages can polarise in response to stimuli when seeded on hyaluronic acid hydrogel surfaces of different stiffnesses, and stiffness does not impact on macrophage polarisation... 149
5.4.3 The impact of hyaluronic acid hydrogel stiffness on the immune cell environment in a rat femoral defect model 151

5.4.4 The impact of hyaluronic acid hydrogel stiffness on gene expression in a rat femoral defect model 153
5.4.5 IP-loaded hyaluronic acid hydrogels behave similarly to stiff (10 kPa) hyaluronic acid hydrogels 154
5.4.6 IP-loaded hydrogels are capable of temporally upregulating aryl hydrocarbon receptor-associated gene CYP1A1 155
5.4.7 The early effect of IP-loaded hyaluronic acid hydrogels on gene expression 155
5.4.8 IP-loaded hydrogels do not impact on immune cell environment in a rat femoral defect model 156
5.4.9 IP-loaded hydrogels upregulate pro-osteogenic *BMP2* and *RUNX2* gene expression, and pro-regenerative *TGFβ1* gene expression, in a rat femoral defect model 157

5.5 Discussion 182

Chapter Six: General Discussion 194

6.1 General discussion 195

6.2 Limitations and future work 203

6.3 Conclusion 205

References 206

Table of Figures

Figure 1.1 – The immune microenvironment in tissue healing **9**

Figure 1.2 – Regulation of HO-1 expression **12**

Figure 1.3 – Biomaterial-based targeting of pro and anti-inflammatory factors for immunomodulation **22**

Figure 1.4 – Schematic summary of major metabolic pathways used by pro-inflammatory and anti-inflammatory immune cells **25**

Figure 2.1 – Isolation of PBMCs from buffy coat packs **56**

Figure 2.2 – Analysis of macrophage purity by flow cytometry **57**

Figure 2.3 – Hyaluronic acid hydrogel fabrication **58**

Figure 3.1 – MicronHA and nanoHA particles are not contaminated by endotoxin **70**

Figure 3.2 – MicronHA and nanoHA particles do not significantly impact on primary human macrophage viability **71**

Figure 3.3 – MicronHA particles upregulate surrogate markers of glycolysis at the mRNA level **72**

Figure 3.4 – MicronHA particles upregulate expression of the glycolytic markers GLUT1 and HK2 ..... **73**

Figure 3.5 – IL-4 pre-polarised macrophages upregulate glycolytic genes upon exposure to micronHA particles to a lesser extent than unpolarised macrophages **74**

Figure 3.6 – Primary human macrophages increase *ATP5b* expression at 24 hours post micronHA stimulation **75**

Figure 3.7 – MicronHA particles promote mitochondrial fission **76**

Figure 3.8 – MicronHA particles alter macrophage metabolism at 6 hours **77**

Figure 3.9 – MicronHA particles alter macrophage metabolism at 24 hours **78**

Figure 3.10 – MicronHA stimulation temporally increases basal and maximum rates of glycolysis in primary human macrophages **79**

Figure 3.11 – NanoHA stimulation does not impact on the basal and maximum rates of glycolysis in primary human macrophages **80**

Figure 3.12 – MicronHA stimulation does not significantly impact on the basal and maximum rates of respiration in primary human macrophages **81**

Figure 3.13 – NanoHA stimulation does not impact on the basal and maximum rates of respiration in primary human macrophages **82**

Figure 3.14 – MicronHA particles, but not nanoHA, drive a temporal metabolic shift to favour glycolysis in primary human macrophages **83**

Figure 3.15 – Inhibition of phagocytosis attenuates micronHA-induced upregulation of surrogate markers of glycolysis in primary human macrophages **84**

Figure 3.16 – Inhibition of phagocytosis attenuates micronHA-induced pro-inflammatory cytokine secretion in primary human macrophages. **85**

Figure 3.17 – Inhibition of glycolysis using 2-DG attenuates micronHA-driven M1-marker mRNA expression in primary human macrophages..... **86**

Figure 3.18 – Inhibition of glycolysis using 2-DG attenuates micronHA-driven pro-inflammatory cytokine secretion in primary human macrophages **87**

Figure 3.19 – Inhibition of glycolysis using 3PO attenuates micronHA-driven M1-marker mRNA expression in primary human macrophages..... **88**

Figure 3.20 – Inhibition of glycolysis using 3PO attenuates micronHA-driven pro-inflammatory cytokine secretion in primary human macrophages **89**

Figure 3.21 – Summary schematic of findings..... **95**

Figure 4.1 – IP and HPP are non-toxic to primary human macrophages **110**

Figure 4.2 – HPP upregulates HO-1 in a dose-dependent manner to a greater extent than IP in primary human macrophages **111**

Figure 4.3 – IP and HPP upregulate mRNA expression of *CYP1A1* over time in primary human macrophages..... **112**

Figure 4.4 – IP and HPP upregulate mRNA expression of *GSR* and *NQO1* over time in primary human macrophages..... **113**

Figure 4.5 – IP and HPP activate Nrf2 at 3 hours in primary human macrophages..... **114**

Figure 4.6 – IP and HPP attenuate LPS-induced mRNA expression of *CXCL9* and *CXCL10* in primary human macrophages..... **115**

Figure 4.7 – IP and HPP have no significant effect on the production of pro-inflammatory cytokines TNF and IL-6, but increase production of IL-8, in LPS-stimulated primary human macrophages **116**

Figure 4.8 – IP and HPP have no significant effect on the production of anti-inflammatory cytokine IL-10 in primary human macrophages **117**

Figure 4.9 – IP attenuates glycolysis in LPS-stimulated macrophages..... **118**

Figure 4.10 – HPP attenuates glycolysis in LPS-stimulated macrophages..... **119**

Figure 4.11 – IP and HPP attenuate the glycolytic shift that occurs in LPS-stimulated macrophages **120**

Figure 4.12 – IP and HPP upregulate vascularisation-associated genes in primary human macrophages **121**

Figure 4.13 – IP and HPP upregulate mRNA expression of growth factor *TGFβ1* in primary human macrophages **122**

Figure 4.14 – The effect of IP-conditioned macrophage media on osteogenic gene expression and growth factor gene expression in human mesenchymal stem cells..... **123**

Figure 4.15 – IP is non-toxic to human mesenchymal stem cells..... **124**

Figure 4.16 – IP induces HO-1 in a dose-dependent manner in human mesenchymal stem cells..... **125**

Figure 4.17 – IP induces HO-1 in a temporal manner in human mesenchymal stem cells **126**

Figure 4.18 – IP induces AhR and Nrf2-associated genes *CYP1A1* and *NQO1*, and Nrf2-associated gene *GSR* in human mesenchymal stem cells **127**

Figure 4.19 – IP activates Nrf2 in human mesenchymal stem cells at 24 hours **128**

Figure 4.20 – IP upregulates vascularisation-associated and growth factor genes in human mesenchymal stem cells **129**

Figure 4.21 – IP upregulates osteogenic genes in human mesenchymal stem cells **130**

Figure 4.22 – IP exposure enhances mineralisation of human mesenchymal stem cells at 14 days **131**

Figure 4.23 – AhR antagonist CH223191 reduces IP-induced upregulation of *CYP1A1* gene expression in human mesenchymal stem cells **133**

Figure 4.24 – AhR antagonist CH223191 attenuates IP-induced mRNA expression of *VEGF-A* and *RUNX2* in human mesenchymal stem cells **139**

Figure 4.25 – Summary schematic of findings **143**

Figure 5.1 – Hyaluronic acid hydrogels do not impact on primary human macrophage viability **158**

Figure 5.2 – Hyaluronic acid hydrogels do not impact on the ability of monocytes to differentiate into macrophages **159**

Figure 5.3 – Alteration of crosslinker concentration produces 2% hyaluronic acid hydrogels ranging in stiffness between 1 kPa and 10 kPa **160**

Figure 5.4 – Macrophages can polarise in response to stimuli when seeded atop hyaluronic acid hydrogel surfaces of 1 kPa and 10 kPa **161**

Figure 5.5 – Hyaluronic acid hydrogel surfaces and stiffness do not significantly impact on macrophage polarisation marker expression **162**

Figure 5.6 – Hyaluronic acid hydrogel stiffness does not significantly impact on macrophage polarisation marker expression in response to stimuli **163**

Figure 5.7 – Hyaluronic acid hydrogel surfaces, but not hydrogel stiffness, impact on macrophage secretion of TNF, but not IL-6 or IL-8 ..... **164**

Figure 5.8 – Hyaluronic acid hydrogel stiffness does not impact on immune microenvironment in a rat femoral defect model **165**

Figure 5.9 – 1 kPa hyaluronic acid hydrogels decrease inflammatory and promote regenerative monocytes compared to empty defect **166**

Figure 5.10 – 1 kPa and 10 kPa hyaluronic acid hydrogels do not significantly impact on macrophage phenotype in a rat femoral defect model **167**

Figure 5.11 – 10 kPa hyaluronic acid hydrogels promote an increase in $CD4^-/CD8^+$ T cells compared to 1 kPa hydrogels in a rat femoral defect model **168**

Figure 5.12 – 1 kPa hyaluronic acid hydrogels decrease *IL1Ra* and increase *TGFβ3* mRNA expression in a rat femoral defect model **169**

Figure 5.13 – mRNA expression of macrophage activation markers *CD80*, *CD86*, and *CD163* are not affected by hyaluronic acid hydrogel stiffness in a rat femoral defect model **170**

Figure 5.14 – mRNA expression of osteogenic genes *BMP2* and *RUNX2* following implantation of 1 kPa and 10 kPa hydrogels into a rat femoral defect model **171**

Figure 5.15 – IP-gel behaves similarly to 10 kPa HyA-gel in the presence of hyaluronidase **172**

Figure 5.16 – *CYP1A1* mRNA expression is upregulated at days 1,2,3, and between days 4-6, in human mesenchymal stem cells treated with IP-gel conditioned media..... **173**

Figure 5.17 – *BMP2* mRNA expression, but not *RUNX2*, *OCN*, or *VEGF-A*, is upregulated in human mesenchymal stem cells treated with IP, HyA-gel conditioned media, and IP-gel conditioned media at day 1 ..... **174**

Figure 5.18 – IP-loaded hyaluronic acid hydrogel does not impact on immune microenvironment in a rat femoral defect model **175**

Figure 5.19 – Monocyte subsets are not significantly impacted on following implantation of hyaluronic acid hydrogels with and without IP into a rat femoral defect model **176**

Figure 5.20 – Macrophage subsets are not significantly impacted on following implantation of hyaluronic acid hydrogels with and without IP into a rat femoral defect model **177**

Figure 5.21 – T cell subsets are not significantly impacted on following implantation of hyaluronic acid hydrogels with and without IP into a rat femoral defect model **178**

Figure 5.22 – mRNA expression of inflammatory and regenerative-associated genes following implantation of hyaluronic acid hydrogels with and without IP into a rat femoral defect model **179**

Figure 5.23 – mRNA expression of macrophage activation markers *CD80* and *CD86*, but not *CD163*, are upregulated following implantation of hyaluronic acid hydrogels with and without IP into a rat femoral defect model **180**

Figure 5.24 – mRNA expression of osteogenic genes *BMP2* and *RUNX2* are upregulated following implantation of IP-loaded hyaluronic acid hydrogels into a rat femoral defect model **181**

Figure 5.25 – Summary schematic of findings **193**

Table of Tables

Table 2.1 – Western blot buffers **32**
Table 2.2 – Antibodies for *in vitro* macrophage studies **33**
Table 2.3 – Antibodies for *in vivo* immune cell profiling **33**
Table 2.4 – Human primer sequences **35**
Table 2.5 – Rat primer sequences **36**
Table 2.6 – Composition of SDS-polyacrylamide gels **42**
Table 2.7 – Immunoblotting antibody dilutions **43**
Table 2.8 – Components and volumes required for 2X RT Master Mix **45**
Table 2.9 – cDNA Reverse Transcription Reaction **45**
Table 2.10 – Components and volumes required for qPCR reaction **46**
Table 2.11 – Thermal cycling parameters for TaqMan real-time PCR **46**
Table 2.12 – Components and volumes required for the iTaq Universal SYBR Green reaction **46**
Table 2.13 – Thermal cycling parameters for iTaq Universal SYBR Green real-time PCR **47**
Table 2.14 – Seahorse protocol **49**
Table 2.15 – Seahorse calculations **50**

Chapter One

Introduction

Sections of this chapter have been peer-reviewed and published in *Acta Biomaterialia* (DOI: 10.1016/j.actbio.2021.02.023, 2021)

1.1 The immune system in tissue repair

The limited capacity of many tissues and organs to repair and regenerate is at the heart of numerous healthcare challenges. When controlled, the tissue healing response allows for resolution of inflammation and restoration of tissue architecture and homeostasis. A dysfunctional response, on the other hand, often leads to fibrosis and scarring at the injury site which can impair healing and result in organ failure [1]. A number of globally prevalent conditions such as heart disease, severe musculoskeletal defects, and organ failure comprise those most urgently demanding improved therapeutic strategies that enhance the tissue repair process. A thorough understanding of the cellular processes underlying tissue healing and repair is therefore crucial in the development of appropriate and effective therapies that engineer regenerative mechanisms to combat debilitating disease processes.

As the number of tissue repair models used in research has grown and evolved over the last few decades, our understanding of tissue repair and the ability to integrate this knowledge with the pathogenesis of relevant diseases has also expanded. A prevailing concept derived from study findings across a number of species indicates that the tissue regenerative capacity inherent to organisms lesser in complexity, such as fish and amphibians, diminishes as the immune competency of more complex organisms, namely mammals, increases [2, 3]. It is now well accepted that the immune system plays a pivotal role in tissue healing, with immune cells directly affecting the host response at the injury site and influencing the activity of related tissue-specific cell populations and both recruited and tissue-resident stem cells. Indeed, the immune system has been shown to both positively and negatively regulate the tissue repair process, resulting in either effective tissue regeneration or fibrosis and scarring, respectively [2, 4].

In mammals, the normal tissue healing process progresses in four overlapping phases: haemostasis, inflammation, repair (also termed proliferation or granulation), and remodelling (also termed maturation) [5] (Fig. 1.1). To ensure optimal healing, these phases must progress in a tightly controlled manner, with aberration resulting in impairment that can lead to fibrosis and heightened potential for organ failure. The

progression of these phases is heavily reliant on the contribution of immune cells, particularly during the inflammatory phase, which dictates the efficacy of subsequent tissue repair and remodelling [6, 7].

Inflammation begins with neutrophil influx, followed by monocyte infiltration and subsequent differentiation into macrophages, in a process that is dependent on location and stimuli received [8]. Signals from these innate cells recruit lymphocytes to the site of injury, which then engage in crosstalk and influence further innate immune responses. This phase resolves naturally in the case of acute wounds and is marked primarily by the transition of inflammatory macrophages at the injury site to a pro-reparative population. The subsequent repair phase is characterised by the onset of angiogenesis along with collagen synthesis and the deposition of extracellular matrix (ECM), with the final phase of regeneration involving the maturation of the newly formed vessels and remodelling of tissue. Immune cells exert critical influence over the processes of remodelling and regeneration in their clearance of cellular debris, along with their effects on the proliferation and differentiation of tissue specific stem/progenitor cell populations. This is exemplified in the case of bone regeneration, in which the crosstalk between immune cells and osteoprogenitor cells is integral to the initiation and propagation of osteogenesis and associated activities.

An ever-growing wealth of evidence supports our understanding that aberrant cellular activity in the inflammatory phase often results in impaired tissue healing and defective host responses, with over-fibrosis and scarring a major outcome of such. Given the complex role immune cells of both the innate and adaptive immune system play in the tissue repair process, a thorough understanding of their individual contributions to healing and their interaction with other cells that are involved in tissue repair and regeneration, particularly tissue specific stem/progenitor cells, is required.

1.1.1 Innate immunity in tissue repair

The cells of the innate immune system function as the first line of defence against pathogenic assault, or as first responders in the event of tissue injury. The role of the innate immune system as orchestrator of inflammation and tissue repair is well

documented, with a plethora of innate immune cells exerting different functions to coordinate responses that can either direct repair or further propagate destructive processes. Neutrophils are derived from common myeloid progenitors in the immune reservoirs of the body (the bone marrow and spleen) and function by secreting antimicrobial agents and proteases that control infection at the injury site [9]. They predominate during the beginning of the acute inflammatory response and large numbers are recruited from the peripheral blood by chemoattractants released by cells in response to damage associated molecular patterns (DAMPs) following injury [9, 10], with neutrophils implicated as playing a role in angiogenesis [11] and facilitation of normal tissue healing [12]. Natural killer (NK) cells function as the sentinels of the innate immune system. Depending on their received stimuli, NK cells are instructed to either tolerate or attack an invading pathogen [13], and parallels are drawn between NK cells and cytotoxic $CD8^+$ T cells of the adaptive immune system regarding their functionality [14]. They are well-defined in terms of their regulation of the adaptive immune system, with a growing body of evidence detailing their efficacy in mediating host immunity to viral pathogens [15]. In the case of tissue healing, NK cells have been shown to function as regulators of the inflammatory phase, with evidence to date indicating a net negative effect of NK cells on the tissue repair process [16-18]. Innate lymphoid cells (ILCs), a recently classified family of innate immune cells, have emerged as cellular populations that share properties with cells of the adaptive immune system but do not display antigen-specific receptors. In this way, they are often described as the “innate counterparts of T cells” [19]. ILCs can be found in both lymphoid organs and non-lymphoid tissues. They are primarily tissue-resident and found in abundance in mucosal tissues, interacting with immune cells to promote immunity and mediate inflammation and tissue repair [20]. Of particular relevance to tissue healing, ILCs are enriched in barrier tissues such as the skin, intestine, and the lung, and have been documented as playing a role in the maintenance of tissue integrity by promotion of tissue remodelling, whilst also playing a role in mediation of inflammatory diseases [21]. Dendritic cells (DCs) are considered as “bridging” cells between the innate and adaptive arms of the immune system. DCs play a similar phagocytic role to macrophages in their recognition of invading pathogens and are heavily involved in the instruction of T and B cell responses post-trauma, primarily in their antigen-presenting capabilities. They can also activate the pro-reparative T cell subset, regulatory

T cells (Tregs), an adaptive immune cell subset vital for tissue regeneration [22]. DCs express pattern recognition receptors (PRRs) which recognize pathogenic and foreign materials and propagate signalling. Depending on the PRR stimulated, DCs exhibit an immunogenic or tolerogenic phenotype [23]. DC enrichment has also been shown to play a positive role in tissue repair in a murine model of burn wound healing [24]. Although it is evident that the innate immune response to tissue repair involves the concerted action of a number of innate immune cell types, there is particular focus given to macrophages given their critical and complex role in influencing tissue reparative processes.

1.1.2 Macrophages in tissue repair

Whilst tissue healing and tissue repair requires the presence and concerted actions of a plethora of cell types, the involvement of macrophages across all stages of tissue repair and their extensive interaction with stem and progenitor cells has indicated that targeting macrophage-mediated responses holds wide-ranging therapeutic potential [25]. Their crucial role in the repair process across multiple tissue types has been demonstrated by depleting macrophage populations in several models of tissue injury. Seminal works in salamander and murine models exemplified the detrimental effect of macrophage depletion on limb regeneration and muscle repair [6, 26]. Bolstering evidence for the critical contribution of the macrophage component, a recent comparative study in which single-cell RNA-seq was used to compare immune cell populations between salamander and murine models of tissue regeneration showed an earlier recruitment of macrophages exhibiting heightened expression of matrix metalloproteinases (MMPs) in the salamander as compared to the more immuno-competent murine model [27].

Macrophages originate from myeloid precursor cells in the bone marrow compartment and persist in the host system either within the circulation where they differentiate from monocytes through extravasation through the endothelium, or residing in tissues in which they rapidly proliferate in response to injury [28]. There is evidence to support that these subsets can play opposing but important roles in healing in a tissue-dependent manner, with studies involving inhibition or depletion of monocytes and macrophages showing a

more pro-inflammatory role for macrophages derived from monocytes, in comparison to a more regenerative role for those macrophages that are tissue resident [29-31].

An early paradigm introduced in 2000 that has greatly evolved in recent years is that depicting macrophage plasticity and polarisation states. These states exist across a spectrum of diverse, plastic phenotypes, with one end of the spectrum correlating to an "M1-like" or pro-inflammatory phenotype and the other referring to an anti-inflammatory "M2-like" phenotype, which in turn determines their functionality [32]. Broadly speaking, M1-like macrophages are induced by pro-inflammatory stimuli (*in vitro*, the classic "M1-like" activators are lipopolysaccharide [LPS] and interferon-γ [IFNγ]) and they act to orchestrate the initial acute inflammatory response to tissue assault. M1-like macrophages engage in phagocytosis of foreign particles and clearance of debris at the wound site, a process which propagates a pro-inflammatory secretome. The release of pro-inflammatory cytokines and growth factors acts to counter the hypoxic conditions at the site of tissue damage or injury, with molecules including platelet-derived growth factor (PDGF) and vascular endothelial growth factor (VEGF) promoting formation of new vessels and cellular proliferation.

M2-like macrophages are induced *in vitro* and in certain *in vivo* settings by anti-inflammatory cytokines such as interleukin (IL)-4 and IL-13, along with glucocorticoids, prostaglandins, and modulators of metabolism, and these macrophages play a key role in tissue healing and remodelling [33]. They secrete factors including transforming growth factor (TGF)-β1 and anti-inflammatory cytokine IL-10 that instruct cells at the injury site such as fibroblasts to move towards a reparative phenotype and deposit ECM [34, 35]. The latter phases of repair and remodelling require predominance of the M2-like macrophage population, facilitating dampening of inflammation and destructive processes and upregulation of healing-associated activities. Under normal healing conditions, the initial predominant population of M1-like macrophages shifts towards M2-like as the reparative phase begins [36]. This shift from M1-like to M2-like can be attributed to the effect of a number of stimulatory molecules, and was recently shown in a murine model of musculoskeletal injury to be particularly dependent on the protein

annexin A1 (ANXA1), a major driver of resolution of inflammation signalling through the AMP-activated protein kinase (AMPK)-governed pathway [37].

Indeed, a large number of studies have shown that higher M2/M1 ratios correlate with heightened tissue repair and a reduction in fibrosis and scarring in the wake of tissue injury, largely caused by a local reduction in inflammatory mediators [38-41]. A caveat to macrophage modulation lies in the critical temporal roles of various macrophage phenotypes and functions, with their delicate balance and inextricable interplay with cells of the adaptive immune system rendering them both an attractive therapeutic target and a potential hinderance to immunomodulation. Supporting this, a recent study uncovering the contribution of macrophages to deleterious collagen deposition during scar formation in both a zebrafish and a murine model of cardiac tissue repair implicates macrophages as an apparent 'double-edged sword' in tissue restorative processes [42], further pointing to the importance of macrophages in research into tissue repair and regeneration, and indicating that they should continue to be considered as either central or peripheral components in the majority of immunomodulation strategies, depending on the intended target cell population or populations and tissue types.

1.1.3 Adaptive immunity in tissue repair

In addition to the critical role of the innate immune system in tissue healing and repair, the adaptive immune system has also been documented to play a role in driving and coordinating pro-reparative responses in the wake of injury. The adaptive arm of the immune system is primarily responsible for the development of immunological memory, and is found only in vertebrates. The function of the adaptive immune system is mediated primarily *via* B and T cells. The major role of B cells is in their presentation of antigen to T cells and resultant influence over the adaptive immune response. While studies regarding the role of B cells in tissue repair and wound healing are limited in number compared to T cells, it has been shown that $CD19^-$ null mice (a murine model of B cell deficiency) in which cutaneous wound healing was examined, a lack of B cells resulted in inhibited healing accompanied by an increase in pro-inflammatory cellular infiltration and cytokine expression [43], and indeed further works evidenced the ability of mature B cells to

accelerate wound healing in a mouse model of skin wound healing [44]. There is ample evidence supporting the crucial role of T cells in tissue repair and regeneration through modulation of inflammation during the healing process. T cells develop in the thymus and are broadly grouped into $CD4^+$ and $CD8^+$ subsets. These naïve T cells, in response to antigen stimulation, can then differentiate into either $CD8^+$ cytotoxic effector and memory T cells or $CD4^+$ T helper (Th) cells which can exert positive or negative effects on tissue healing. Seminal work in the field has indicated that cytotoxic $CD8^+$ T cell presence at the injury site is associated with poor tissue regenerative outcomes, with a high number of $CD8^+$ cytotoxic T cells at the bone fracture site having a negative impact on bone regeneration in both mice and humans [45, 46]. In contrast, a prevalence of $CD4^+$ Th cells has been shown to contribute to effective tissue regeneration [47]. Furthermore, regulatory T cells (Tregs) have been evidenced to exert an influential role in tissue regeneration by engaging in crosstalk with neutrophils, directing macrophage polarization, and regulating helper T cells, and have been shown in a number of tissue repair models to be regulators of the healing response [48, 49]. Tregs notably polarize macrophages towards an M2-like phenotype and are seen to persist as a T cell subpopulation at the injury site even as overall T cell numbers decrease [50, 51]. There is therefore evidence to support a vital role for the adaptive immune system in tissue repair and regeneration, and further highlights the importance of thorough characterisation of the immune response in the context of therapies that seek to promote tissue repair and regeneration.

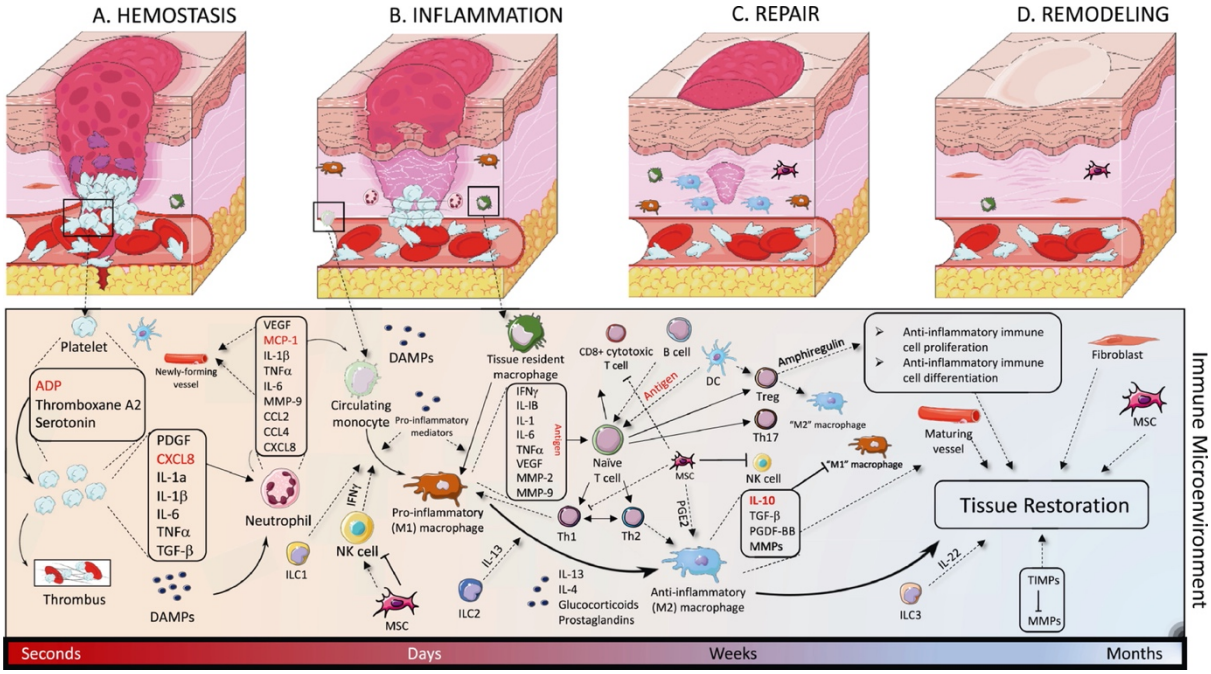

Figure 1.1 The immune microenvironment in tissue healing: Depiction of the immune microenvironment during the stages of tissue healing detailing the main cellular components and their contribution to progression.

1.2 Novel immunomodulatory strategies for tissue repair and regeneration

With growing appreciation for the role of the immune system in dictating and driving reparative and regenerative responses, there is expanding interest into exploration of novel immunomodulators that promote a favourable immune response in the context of tissue repair and, ultimately, regeneration. One such class of immunomodulators garnering interest is that of heme-oxygenase (HO) inducers, such as cobalt protoporphyrin (CoPP), hemin, and plant-derived phytochemicals such as quercetin, carnosol, and curcumin, which have proven efficacious with respect to exerting anti-inflammatory effects on individual immune cell subsets [52-54], and also in *in vivo* models of inflammatory disease [55, 56]. Additionally, recent works implicate heme oxygenase-1 (HO-1) induction in promotion of tissue repair [57-59] and in osteogenic differentiation of mesenchymal stem cells (MSC) [60-62].

1.2.1 The heme-oxygenase system and HO-1

Heme oxygenases are enzymes that catalyse the first rate-limiting step in the breakdown of heme, an iron-containing porphyrin that functions as a component of biological proteins such as haemoglobin and myoglobin, cytochromes, and enzymes (e.g: haem peroxidase). The heme oxygenase pathway catalyses heme breakdown to yield carbon monoxide (CO), iron, and biliverdin, which is further reduced to bilirubin, and this pathway is strongly implicated in the progression and resolution of tissue injury. Injury or damage to tissue results in release of free heme, which is cytotoxic, and degradation of heme by HO exerts a range of protective functions in its anti-inflammatory, antioxidant, and antiapoptotic activity [63].

Of the two functional isoforms that exist in mammalian cells, HO-1 and HO-2 (encoded by *HMOX1* and *HMOX2* respectively), HO-1 exists as a stress-inducible isozyme, whereas HO-2 is constitutively expressed in certain tissues. HO-1 is upregulated in response to a number of pro-oxidant and inflammatory stimuli, and given its key role in mitigating oxidative damage that plays a role in driving tissue destructive processes, HO-1 is emerging as a therapeutic target in tissue repair. Control of HO-1 is largely under the redox-sensitive transcription factor nuclear factor erythroid 2 (NF-E2)-related factor 2 (Nrf2) [64]. Nrf2 is bound to protein Kelch-like ECH-associated protein 1 (KEAP1) in the cytoplasm under homeostatic conditions, in which it is readily ubiquitinated and degraded, thereby suppressing its activity [65, 66]. Nrf2 activation occurs in the presence of Nrf2 activators such as reactive oxygen species (ROS) which result in modification of the cysteine residues of KEAP1, allowing for the release and stabilisation of Nrf2. Nrf2 can then translocate into the nucleus where it binds to the antioxidant response element (ARE) and promotes expression of antioxidant genes [67], such as *HMOX1* [68]. HO-1 expression is counter-regulated by BTB and CNC homology 1 (BACH1), a transcriptional repressor and heme sensor, which is capable of binding the *HMOX1* promoter and repressing its transcriptional activity [69]. When intracellular levels of heme are high, free heme can bind to BACH1 and cause it to dissociate from the ARE. Dissociated BACH1 is then exported from the nucleus, ubiquitinated, and degraded, which allows for *HMOX1* transcription to proceed [70, 71]. It is worth noting that, while Nrf2 and BACH1 are the primary regulators of HO-1, other

transcription factors such as HIF1α have been shown to regulate HO-1 expression [72]. Within the HMOX1 promoter, binding sites for the pro-inflammatory transcription factors NFκB and activator protein (AP)-1 have also been identified [73], bolstering the evidence for inflammation-induced upregulation of HO-1 as a protective mechanism in immune cells, and can account for studies in which HO-1 induction occurs through Nrf2-independent mechanisms [66]. Other HO-1 inducers have been documented to act *via* intermediate signalling pathways such as mitogen activated kinases (MAPKs), ERK, JNK, and p38, and STAT3-mediated HO-1 induction by anti-inflammatory IL-10, as well as AMPK-mediated upregulation in response to metabolic intermediates and HO-1 inducers [54, 74-76].

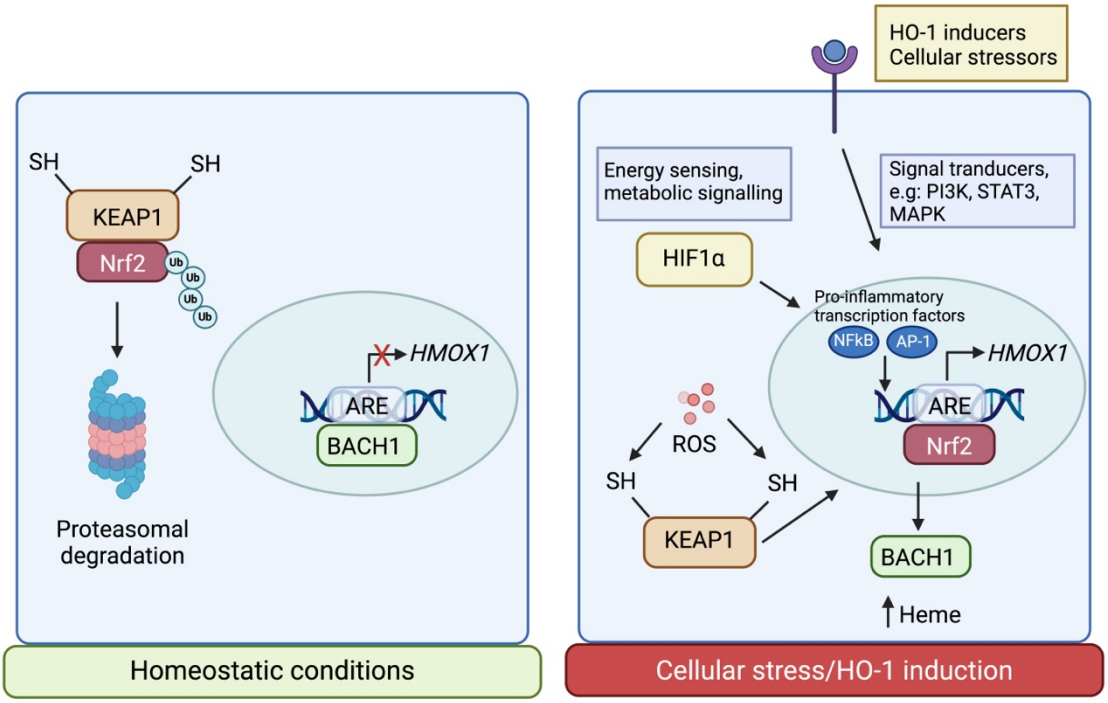

Figure 1.2: Regulation of HO-1 expression, adapted from Campbell, Fitzgerald *et al*., 2021.

1.2.2 HO-1 in inflammation and tissue repair

The anti-inflammatory properties of HO-1 have been widely studied [52, 63, 77-79], with HO-1 deficiency in humans and animal models linked to chronic inflammation [80-82]. HO-1 induction by common inducers hemin and CoPP was shown to inhibit the formation of

the NLRP3 inflammasome and reduce mature IL-1β secretion in primary human macrophages, THP-1 cells, and murine macrophages, as well as reducing IL-1β secretion *in vivo* by MSU crystals [53]. Exemplifying the role of HO-1 in modulating inflammation, HMOX1$^{-/-}$ mice display significantly higher production of pro-inflammatory cytokines such as IL-6, IL-12, and TNF compared to wild-type mice [81], and decreased IFNβ production when challenged with LPS [83], and HO-1 induction has shown benefit in dampening inflammation linked to inflammatory diseases such as atherosclerosis and autoimmune conditions [84, 85].

Linked with this, the importance of HO-1 in tissue protection has been demonstrated in patients with HO-1 genetic deficiencies that exhibit damage to the liver, kidneys, and vasculature as a result of heme and iron accumulation [86], and in murine models in which HO-1 deficiency leads to high levels of circulating heme and inflammation [87]. HO-1 deficient mice were shown to exhibit delayed wound closure and angiogenesis, concomitant with an increase in oxidative stress and inflammation [57], and HO-1 has also been implicated in the regulation of diabetic wound healing. Diabetic mice showed delayed induction of HO-1 in response to hemin compared to wild type, and local delivery of HO-1 transgene resulted in increased neovascularisation and improved wound closure [57]. Hemin has also been demonstrated to promote wound healing in diabetic rats, with promotion of angiogenesis and a reduction in pro-inflammatory cytokines such as TNF [58, 59]. Taken together, there is evidence to support a link between the anti-inflammatory effects of HO-1 and its ability to promote tissue repair, positing HO-1 as an attractive target in tissue reparative therapeutic strategies.

1.2.3 HO-1 inducers as therapeutics

HO-1 induction poses a promising strategy in the development of therapeutics to mitigate inflammation-driven and tissue-destructive processes. Indeed, HO-1 inducers have conferred benefit in inflammatory and autoimmune diseases and disease models such as RA [55, 88], and multiple sclerosis (MS) [89], as well as organ rejection and graft failure [90-92]. Notably, in recent years HO-1 has been implicated as a possible therapeutic strategy in the treatment of COVID-19 [93], given that hemin-induced HO-1 was shown to

mitigate cytokine storm and tissue injury in murine models of sepsis and renal damage [94], as well as recent works demonstrating that CoPP-induced HO-1 can inhibit influenza A and RSV viral replication [95]. However, certain limitations surrounding use of some existing HO-1 inducers in a therapeutic context lie in their poor oral bioavailability, as well as studies using these compounds at supra-physiological concentrations [96, 97], with other common inducers exhibiting cytotoxicity at high doses [98], and so investigation is ongoing into identification of alternative, novel HO-1 inducers that could potentially mitigate current challenges to clinical translation.

1.2.4 Immunomodulatory ketoacids

The parasite *Trypanosoma brucei* (*T.brucei*) is the causative agent of sleeping sickness, which can be fatal. One element by which this parasite survives within its host is by using immune-evasion strategies, allowing it to evade host clearance [99, 100]. It has been long documented that *T.brucei* infection results in a high level of circulating amino acid-derived ketoacids in the host system [101-104]; the aromatic amino acids tryptophan, tyrosine, and phenylalanine are converted to yield indole pyruvate (IP), hydroxyphenylpyruvate (HPP), and phenyl pyruvate (PP) respectively, through the expression of a parasitic cytoplasmic aspartate aminotransferase (TbcASAT) [105]. Work has evidenced the immunomodulatory capabilities of these ketoacids, with IP, HPP, and PP capable of suppressing the immune response by activation of Nrf2 and modulation of immune cell metabolism [78, 105, 106]. IP in particular has proven efficacious in the context of inflammatory disease, with administration shown to alleviate inflammation in murine models of colitis by reducing pro-inflammatory cytokine expression [107]. IP additionally has been shown to attenuate LPS-driven prostaglandin production in bone marrow-derived macrophages (BMDM) and primary human macrophages [106]. Work by the Dunne group has exemplified the ability of these ketoacids to attenuate production of pro-IL-1β in murine glia and BMDM, and reduce pro-inflammatory cytokines IL-6 and TNF in glia, but not BMDM, and this was additionally shown to be mediated via the HO-1/Nrf2 pathway [78]. Further work demonstrated the ability of IP and HPP to induce HO-1 and attenuate LPS-induced pro-inflammatory responses in human dendritic cells, as well as reducing the LPS-driven switch to glycolysis [108]. As such, these aromatic ketoacids are

now being considered as novel HO-1 inducers with potential therapeutic benefit, with their ability to activate the heme oxygenase pathway linked to their anti-inflammatory, immunomodulatory abilities. The effects of IP in particular have been shown to be exerted *via* activation of the aryl hydrocarbon receptor (AhR) [105, 106, 109]. The AhR is a cytosolic transcription factor that is activated in response to AhR agonists such as environmental toxins, or tryptophan and tryptophan derivatives, primarily comprised of indole-based compounds [110]. Under homeostatic conditions, the AhR exists in cytoplasmic complexes with various proteins, with binding of the AhR to an AhR ligand resulting in the translocation of the AhR complex into the nucleus and binding to the AhR nuclear translocators (Arnt). Once there, AhR-Arnt heterodimers can bind xenobiotic-responsive elements (XREs) and upregulate responsive genes [111]. The AhR has been implicated in inflammatory responses of immune cells, and thus its activation has been linked with the anti-inflammatory abilities of the ketoacid IP. Given their documented anti-inflammatory abilities across a range of immune cells and in inflammatory disease models, as well as newly emerging evidence to support HO-1 induction and Nrf2 activation, *T.brucei*-derived ketoacids pose a worthy avenue of investigation as potential novel immunomodulators for tissue repair.

1.3 Immunomodulatory biomaterials for tissue repair and regeneration

With an array of immune cell subtypes implicated as crucial players in tissue repair and regeneration, it is unsurprising that a vast range of immunomodulatory strategies are employed in the design of regenerative therapeutics. Although these strategies have advanced the field of regenerative medicine to a considerable degree, there still exist multiple limitations when attempting to target various components of such a complex and interdependent system during tissue regeneration. There remain many unmet clinical challenges, such as in the case of large-scale tissue defects that hold limited regenerative capacity, and biomaterial intervention is a commonplace strategy in instances where native tissue has become damaged or destroyed. Traditionally, the optimal biomaterial was thought to be “immune-inert”, but now opinion is changing to reflect our understanding that the human immune system mounts a response against all biomaterials

to various degrees, and interest is growing into characterisation and manipulation of this response for therapeutic benefit. The field of immunomodulatory bioengineering, or immunoengineering, has now emerged. Immunoengineering is a relatively new area which applies engineering approaches in the context of the immune system, either by biomaterial alone, or in combination with stem cells, growth factors, or drugs, and this approach holds the potential to address clinical challenges to biomaterial-based therapies [112]. As our understanding of biomaterial-mediated immune-modulation grows, so too does our potential to further characterise and manipulate immune-mediated destructive processes that are known to occur at the site of implantation, such as in the case of orthopaedic implant materials that are prone to wear and loosening. Studies are ongoing into modulation of various biomaterial parameters for the goal of immunomodulation, with parameters such as particle size and shape [113, 114], stiffness [115, 116], surface topography [117-119], surface chemistry [120-123], and porosity [124, 125] comprising elements of biomaterial design that can impact on immune cell functionality. Particular focus has been given to particle size and shape and biomaterial stiffness in terms of how these parameters impact on macrophage function, especially given the plastic nature of macrophages and their potent effects on subsequent immune processes in tissue repair and regeneration.

1.3.1 Particle size and shape for immunomodulation

Particle size and shape are two physical biomaterial characteristics that have been shown to be immunomodulatory in their influence of the foreign body response (FBR) [113]. This is largely due to the extent to which they influence macrophage phagocytosis and, consequently, polarisation and healing outcomes. In a 2014 study, smaller poly (lactic co-glycolic acid) (PLGA) microspheres (5, 30μm) supported increased phagocytosis and macrophage infiltration in a rat subcutaneous model, an effect which was not observed with microspheres of greater size (>30μm) [113]. A recent study investigating the relationship between hydroxyapatite (HA) particle size (0.1μm, 5μm, 20μm, and 100μm) and shape (needle-shaped/spherical; smooth/rough surface) and the innate immune response saw smaller, needle-shaped HA particles enhancing cytokine secretion and the inflammatory response, whilst larger, spherical HA particles did not induce a strong

immune reaction [114]. In terms of macrophage response and osteogenesis, it was shown that nano-sized HA particles preferentially polarised human macrophages towards an M2-like phenotype *via* IL-10 when compared to the effect of commercially available micro-sized HA particles [126]. A study investigating the effect of particle shape in murine alveolar macrophages demonstrated that gold nanorods are preferentially taken up *via* micropinocytosis compared to nanospheres, with more rapid uptake of shorter rods when compared to their longer counterparts. The longer rods that persisted were shown to induce greater levels of inflammatory cytokines IL-1a and TNF [127]. Supporting the ability of particle shape to modulate macrophage polarisation, it was shown that while both spherical and rod-shaped particles induced inflammation, rods induced an inflammasome-mediated inflammatory response *via* induction of IL-1β in murine bone marrow-derived dendritic cells (BMDC) while spheres resulted in a more non-specific inflammation [128]. Particle shape and size are therefore an important consideration in the context of biomaterial design, both in terms of surface coatings in their initial recognition by the immune system, and when considering the effect of biomaterial degradation on host response.

1.3.2 Biomaterial stiffness for immunomodulation

Macrophages are capable of sensing the physical properties of biomaterials and respond to such by rearrangement of their cytoskeleton, in turn affecting motility, cell function, and polarisation state [129]. Biomaterial stiffness is one such property known to be sensed by macrophages, and this parameter can be modulated during biomaterial fabrication [116]. An initial demonstration of this capability was achieved using polyacrylamide beads of identical surface properties and different stiffnesses. When BMDM were cultured on these beads, it was found that the microbeads of greater stiffness had a higher likelihood of being phagocytosed by macrophages than their softer counterparts [115]. This was further supported by culturing of macrophages on polyethylene glycol arginylglycylaspartic acid (PEG-RGD) hydrogels of varying stiffnesses, ranging from 130-840 kPa, in which an increase in stiffness positively correlated with an increased inflammatory response upon LPS-stimulation [130]. Recently it was shown that culturing of the monocytic THP-1 cell line on a stiff plastic plate resulted in an M1-like phenotype in

comparison to cells seeded on a softer, agarose substrate, the latter of which led to an M2-like phenotype [131]. However, recent studies have also reported findings that human macrophages cultured on stiff 3D-crosslinked collagen (0.1 kPa) exhibited an M2-like, pro-reparative phenotype when compared to those seeded on a 0.03 kPa pure collagen control [132], and BMDMs cultured on low stiffness polyacrylamide hydrogels were more pro-inflammatory than those cultured on higher stiffness hydrogels [133], illustrating that stiffness alone may not be taken as an ultimate determinant of macrophage polarisation state and needs to be considered in the context of an interplay of factors.

1.3.3 Immunomodulation through targeting pro-inflammatory factors

Given the critical role of inflammation in tissue repair, the direct targeting of inflammatory factors using biomaterials has emerged as a potential pro-reparative strategy. In this regard, many investigations into modulation of the immune response have focused on targeting pro and anti-inflammatory mediators, and there exists in-depth review of biomaterial-mediated induction of the inflammatory response *via* formation of the inflammasome [134]. Therapeutic strategies targeting inflammation are of particular relevance to biomaterial-mediated tissue regeneration in that they also pose an avenue for modulation or tempering of the FBR and potential fibrosis and scarring that can result from inflammation in the wake of biomaterial implantation.

The pro-inflammatory cytokine TNF has been implicated as a major contributor to detrimental outcomes post-injury. This has been demonstrated particularly in the context of macrophage- mediated responses, and reduction or inhibition of TNF as an associated effect of common painkillers such as aspirin and ibuprofen has shown promise in the context of tissue repair and regeneration [3, 135]. Serving as an example of the beneficial effect of TNF inhibition, bone tissue regeneration was shown to be positively influenced by the biomaterial mediated delivery of anti-TNF antibodies in a diabetic rat model [136]. Cardiac tissue, too, has been shown to benefit from inhibiting TNF, with the use of gold nanoparticles to knockdown TNF in RAW 264.7 macrophages *in vitro* and subsequently in an *in vivo* rodent model of myocardial infarction (MI), resulting in improved cardiac function [137]. Hyaluronic acid (HyA), shown to exert anti-inflammatory effects in its high

molecular weight form [138], has also proven effective in delivering anti-TNF to modulate inflammation in a burn wound model, resulting in a decrease in nonviable tissue and lessened pro-inflammatory cytokine secretion at the wound site when compared to HyA alone and saline controls [139]. The efficacy of TNF targeting, therefore, provides not only an effective strategy to modulate inflammation, but also supports the targeting of major pro-inflammatory cytokines to achieve a more pro-regenerative immune cell landscape.

Targeting of the pro-inflammatory cytokine interleukin-1 (IL-1) and its receptor (IL-1R1) is particularly notable in the context of biomaterial-mediated immunomodulation, with inhibition of IL-1R1 signalling shown to enhance the tissue regenerative activity of MSC [140]. A recent investigation building on this demonstrated the negative impact of IL-1R1 activation on the osteo-regenerative capabilities of MSC [141]. In this study, the inhibition of IL-1 pro-inflammatory signalling through the co-delivery of IL-1 receptor agonist (IL-1Ra) and pro-osteogenic growth factors BMP-2 and PDGF-BB via a fibrin-based biomaterial scaffold resulted in enhanced bone regeneration *in vivo* when compared to growth factors alone in a murine critical-sized calvarial defect.

Given the potency of targeting pro-inflammatory signalling in driving a pro-regenerative outcome, therapeutic strategies that seek to target the nuclear factor kappa b (NFκB) signalling pathway, a central pathway in pro-inflammatory mediation across a range of diseases and regenerative processes [3, 142], have also proven useful in aiding tissue repair and regeneration. For example, it has been shown that curcumin-loaded nanoparticles effectively inhibited the activation of NF-κB and downregulated inflammatory markers alongside decreased infiltration of inflammatory monocytes in an *in vivo* model of experimental autoimmune encephalomyelitis (EAE), holding promise for the future combatting of degenerative or destructive diseases such as MS and graft-versus-host disease (GVD) [143]. In the context of bone regeneration, pro-inflammatory cytokine-stimulated NFκB signalling has previously been shown to inhibit osteogenic differentiation of MSC [144], rendering inhibition of NFκB signalling an attractive strategy in bone regeneration. Small interfering RNA (siRNA)-based NFκB targeting has also risen as an effective means of blocking NFκB signalling, with use of hybrid micelles to co-deliver siRNA targeting p65 (RelA, a member of the NFκB signalling family) and dexamethasone, a

glucocorticoid that inhibits transcription of NFκB and is commonly employed in treatment of rheumatoid arthritis, effectively reducing inflammation and inducing polarisation of macrophages from a pro to anti-inflammatory state in a murine model of collagen-induced arthritis (CIA) [145].

Toll-like receptors (TLRs), a set of pattern-recognition receptors expressed on many immune cell subsets, have been shown to play a role in tissue regeneration which can be attributed in part to their activation of the pro-inflammatory NFκB signalling pathway, as well as the induction of TNF among other pro-inflammatory cytokines. They therefore pose a potential up-stream target of pro-inflammatory signalling and have thus been employed in biomaterial-mediated immunomodulation, with TLR4 targeting proving particularly effective in tissue regeneration. TLR4 activation in murine renal and cardiac ischemia-reperfusion models has been shown to contribute to pro-inflammatory responses that mediate organ failure, with $TLR4^{-/-}$ mice shown to exhibit decreased inflammation, smaller infarct sizes, and protection against tubular damage and immune cell infiltration [146, 147]. However, it is clear that inhibiting certain influencers of inflammatory signalling must be considered in the context of the complex cellular interplay at the defect site, a caveat supported by a recent *in vitro* study using LPS-primed MSCs in which TLR4 had been silenced that displayed diminished wound healing ability, in contrast with their LPS-primed only MSC controls which promoted neutrophil activation, NET formation, and increased healing [148]. TLR4 signalling, too, has been demonstrated to be a regulator of wound healing *in vivo*, with $TLR4^{-/-}$ mice exhibiting slower wound healing, which was postulated to be as a result of TLR4-induced TGF-β and activation of CCL5, an immune cell chemokine [149].

1.3.4 Immunomodulation through targeting anti-inflammatory factors

In contrast to the targeting of pro-inflammatory pathways, which generally aims to inhibit or dampen the activity of pro-inflammatory mediators, anti-inflammatory strategies usually seek to skew host responses towards a desired state typically *via* the delivery of cytokines that have direct anti-inflammatory function. The appropriate temporal dampening or modulation of inflammation is often desirable in the context of tissue

regeneration, with biomaterial-mediated delivery of anti-inflammatory factors representing a promising route towards immunomodulation for tissue repair.

Delivery of IL-4, an M2-like macrophage polarising cytokine, *via* intraperitoneal injection of mesoporous silica nanoparticles (MSNs) in a murine model has been shown to induce M2-like macrophage polarisation and lower ROS production, demonstrating the potential of exogenous IL-4 delivery for improving tissue repair [150]. Similarly, functionalisation of TiO_2 nanotubes with IL-4 and attachment of RGD peptide resulted in M2-like macrophage polarisation and enhanced production of the pro-reparative cytokine IL-10, and also appears to improve MSC osteogenic differentiation *in vitro* [151]. IL-4-conjugated gold nanoparticles implanted into murine skeletal muscle were shown to lead to a twofold increase in the M2a-like macrophage population (one of the four distinct M2-like macrophage subsets and that which is most strongly associated with anti-inflammatory and wound healing actions [152]) and a twofold decrease in M1-like macrophages [153]. Another recent study has found that alginate hydrogels loaded with anti-inflammatory molecules, either CSF-1 alone or in conjunction with IL-4, or IL-4, IL-6, and IL-13, have resulted in faster tissue repair *in vivo* using a rat model of ischemia-reperfusion. Subsequent injection of biomaterials loaded with M-CSF and IL-4 were then shown to result in reduced fibrosis and increased cardiac function in a rat MI model, supporting use of biomaterial-mediated cytokine delivery for the healing of damaged cardiac tissue [154].

It is worth noting that, given the complex and spatiotemporal role of macrophage phenotype in tissue repair, appreciation for the need of an M1-like phenotype early on in the repair process has come to light. Demonstrating this, a bone scaffold that sequentially delivered M1-like and M2-like polarizing cytokines *via* physically adsorbed IFNγ and biotinylated IL-4 respectively has been investigated in a murine subcutaneous implantation model. Overall, this sequential cytokine delivery method resulted in improved vascularisation *in vivo* in comparison to either an IFNγ or IL-4 scaffold alone, exemplifying the necessity of controlled transition of M1- like to M2-like macrophages required for vascularization and angiogenesis [155], and highlighting the tissue-specific requirements for a spectrum of inflammation states at different stages of repair as a consideration in therapeutic delivery of immunomodulatory cytokines.

In addition to loading of IL-4 as an M2-polarising cytokine, delivery of IL-10 has also been investigated as a means of inducing M2-like macrophage polarisation and promoting tissue repair. Indeed, loading of alginate nanoparticles with IL-10 has displayed potent polarisation towards a reparative phenotype in a rat model of arthritis [156], while more recently it has been demonstrated that direct supplementation of recombinant IL-10 in culture media resulted in induction of robust *BMP2*, *ALP*, and *OPN* gene expression in human MSC, demonstrating a role for IL-10 not only in macrophage polarisation but also in promoting osteogenesis [126]. Of particular note, a recent study by Sok *et al.* employed PEG-hydrogels to locally deliver IL-10 and the specialised pro-resolving mediator (SPM) aspirin-triggered resolving D1 (AT-RvD1) resulting in increased infiltration of pro-regenerative macrophages, dendritic cells, and T cells in a murine model of tissue injury, highlighting the efficacy of local bioactive molecule delivery in inducing the desired response of multiple immune cell subtypes [157].

The TGFβ isoforms 1-3 have been shown to play a key role in multiple stages of tissue healing and regeneration [158], with the TGFβ1 isoform particularly implicated in skeletal muscle re- pair [159] and scar formation [35]. TGFβ1, although known to hold pro-inflammatory capabilities, has also been shown to function as a major anti-inflammatory modulator in tissue regeneration and therefore indicated as a therapeutic target. TGFβ1 and IL-10 are frequently used to influence dendritic cell activity *in vitro*, and it was demonstrated that immobilisation of TGFβ1 and IL-10 on PEG hydrogel surfaces inhibited immature dendritic cell (iDC) maturation, advocating for the efficacy of designing an immunosuppressive biomaterial for therapeutic benefit [160].

Given the potency of targeting inflammatory signalling in the context of the immune response and the wealth of evidence strongly suggesting that such responses can be modulated *via* biomaterial intervention, it is reasonable to suggest that biomaterial-mediated targeting of inflammatory activities represents a particularly promising means of generating pro-regenerative environments *in vivo*.

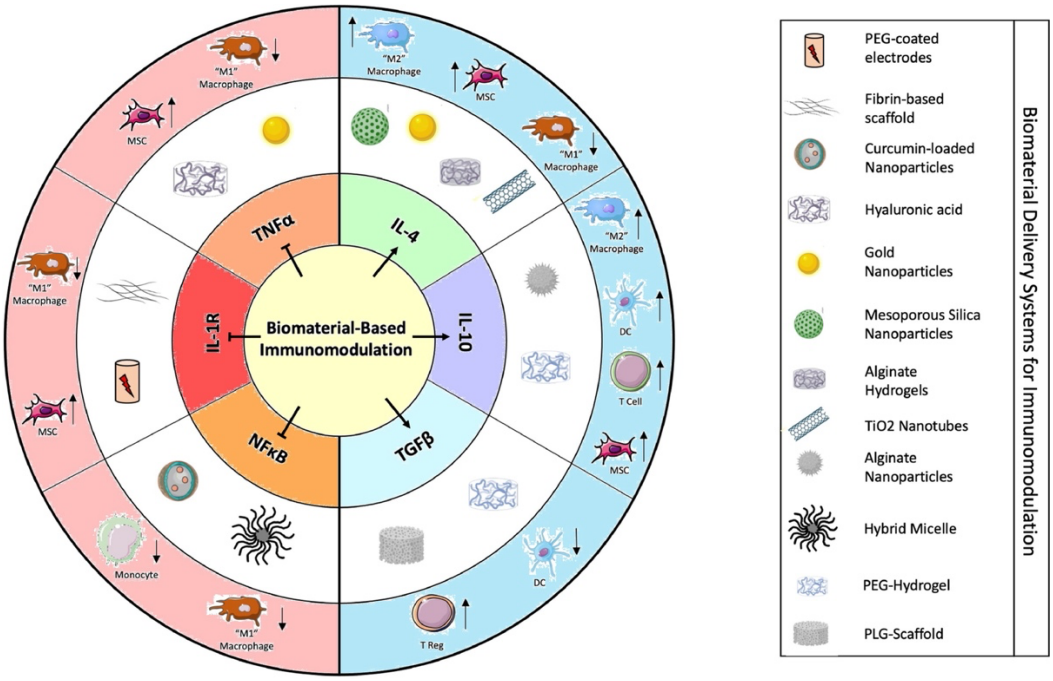

Figure 1.3 Biomaterial-based targeting of pro and anti-Inflammatory factors for immunomodulation: A summary schematic of biomaterials discussed as examples of biomaterial-based immunomodulation by targeting pro and anti-inflammatory factors, with a legend to identify key biomaterial types. From the centre outwards this depicts the factor targeted whether by inhibition or delivery, the biomaterial used to implement this, and the cell type influenced.

1.4 Immunometabolism: implications for tissue engineering

Despite significant advances made in recent years in taking biomaterials from bioactive to immuno-informed, there remains a substantial gap in our understanding of the immune response to various biomaterials and their physiochemical properties, as well as a need for novel immunomodulatory therapeutic options in the field of tissue engineering. The field of immunometabolism is rapidly expanding, with extensive research in recent years leading to an appreciation for the role of immune cell metabolism in dictating cellular phenotype and function. As such, immunometabolism provides a novel means of further characterising the immune cell response to biomaterials, and potentially indicates new means of therapeutic targeting for functional tissue regeneration.

Generally, immune cells exert specific effector functions that can be coupled to changes in metabolic processes, and it has been demonstrated that immune-stimulatory molecules such as IL-4 or LPS have the ability to induce cells to favour different metabolic pathways [161]. The glycolytic pathway is most strongly associated with pro-inflammatory immune cell responses. Glycolysis involves the uptake of extracellular glucose (a simple sugar that results from the breakdown of complex carbohydrates) which is then converted to pyruvate for conversion into lactate or entry into the tricarboxylic acid (TCA) cycle. Glycolysis also feeds into the pentose phosphate pathway (PPP) which can generate biosynthetic intermediates such as nucleotides and amino acids. Glycolysis is a relatively inefficient pathway for adenosine triphosphate (ATP) production, yielding a net of 2 ATP molecules per glucose unit, but functions to provide intermediates and meet the demands of growing and proliferating cells. The TCA cycle and oxidative phosphorylation, by contrast, is a highly efficient generator of ATP, generating 36 molecules of ATP per unit of glucose. Immune cells generally employ oxidative phosphorylation as their preferred metabolic pathway when quiescent or non-proliferative, and when exerting anti-inflammatory functions. The TCA cycle generates NADH and $FADH_2$ which then facilitate oxidative phosphorylation by acting as electron donors in the mitochondrial electron transport chain (ETC).

Dysregulated immune cell metabolism is increasingly being recognised as playing a contributory role in a number of inflammatory diseases such as RA, osteoarthritis (OA), and type 2 diabetes (T2D) [161-163]. For example, it has been demonstrated that metabolites associated with glycolysis are increased in the synovia of RA patients, as well as an upregulation of surrogate markers of glycolysis at the gene expression level, whilst mitochondrial dysfunction plays a role in the pathogenesis of osteoarthritis [162, 164, 165]. It was shown that substitution of galactose for glucose in the culture medium of osteoarthritic chondrocytes reversed markers of mitochondrial dysfunction and reduced their pro-catabolic metabolism that contributes to disease progression [166], highlighting the pivotal role of immunometabolism in inflammatory disease progression.

As such, strategies for interrogating and targeting immunometabolism for therapeutic benefit are emerging as worthy players. Cancer treatment in particular has benefitted from the inhibition of glycolysis due to the reliance of tumour cells on 'Warburg metabolism', or aerobic glycolysis for survival and proliferation [167]. 2-deoxyglucose (2-DG), a glucose analogue, has shown success at the experimental and clinical level [168, 169]. Anti-inflammatory strategies that include dimethyl fumarate (DMF), metformin, and methotrexate have emerged as effective metabolism-targeting therapeutics to combat inflammatory conditions such as EAE, T2D, and RA respectively [170]. A recent study demonstrated that incorporation of itaconate, a metabolite known to exert anti-inflammatory functions, into a biomaterial backbone, resulted in immunomodulation through reduction of the inflammatory response, lending support to the relevance of studying immunometabolism in the context of the host response to biomaterials [171]. Furthermore, a molybdenum-containing bioactive glass ceramic displaced enhanced periodontal tissue regeneration in canines, mediated *via* modulation of the macrophage metabolic response from glycolysis towards mitochondrial oxidative phosphorylation [172]. Assessment of the metabolic response of immune cells to biomaterials therefore not only provides additional means of characterising the host immune response, but may also reveal novel therapeutic targets to enhance functional tissue regeneration.

1.4.1 Macrophage metabolism: implications for tissue engineering

Macrophages are one such immune cell that is appreciated to utilise different metabolic pathways to exert different functions [161, 173]. Under homeostatic conditions, macrophages rely on oxidative phosphorylation to generate ATP, but upon activation they exhibit a metabolic shift to favour glycolysis as their primary means of energy production. M1-like macrophages, commonly stimulated *in vitro* by LPS and IFNγ, utilise a range of metabolic pathways in addition to glycolysis [174]. They exhibit an induction of the pentose phosphate pathway (PPP) resulting in generation of ROS and nitric oxide (NO) production [161, 175], and also rely on fatty acid synthesis (FAS) as a result of citrate accumulation, which in turn promotes production of inflammatory mediators such as TNF [176, 177]. M2-like macrophages, on the other hand, are induced by a range of stimuli such as IL-4 and IL-13 *in vitro*, and exhibit a metabolic reliance on oxidative

phosphorylation [178, 179] which is crucial for M2-like activation. M2-like macrophages have also been shown to employ fatty acid oxidation (FAO) to fuel mitochondrial oxidative phosphorylation [180]. Given the crucial role of macrophages in recognition of, and response to, biomaterial implantation, it is evident that thorough characterisation of biomaterial-macrophage interactions are imperative to improving biomaterial-based therapies. The profiling of the metabolic response of macrophages to biomaterials therefore serves to not only further characterise macrophage-biomaterial interaction, but offers a potential new avenue for therapeutic exploitation.

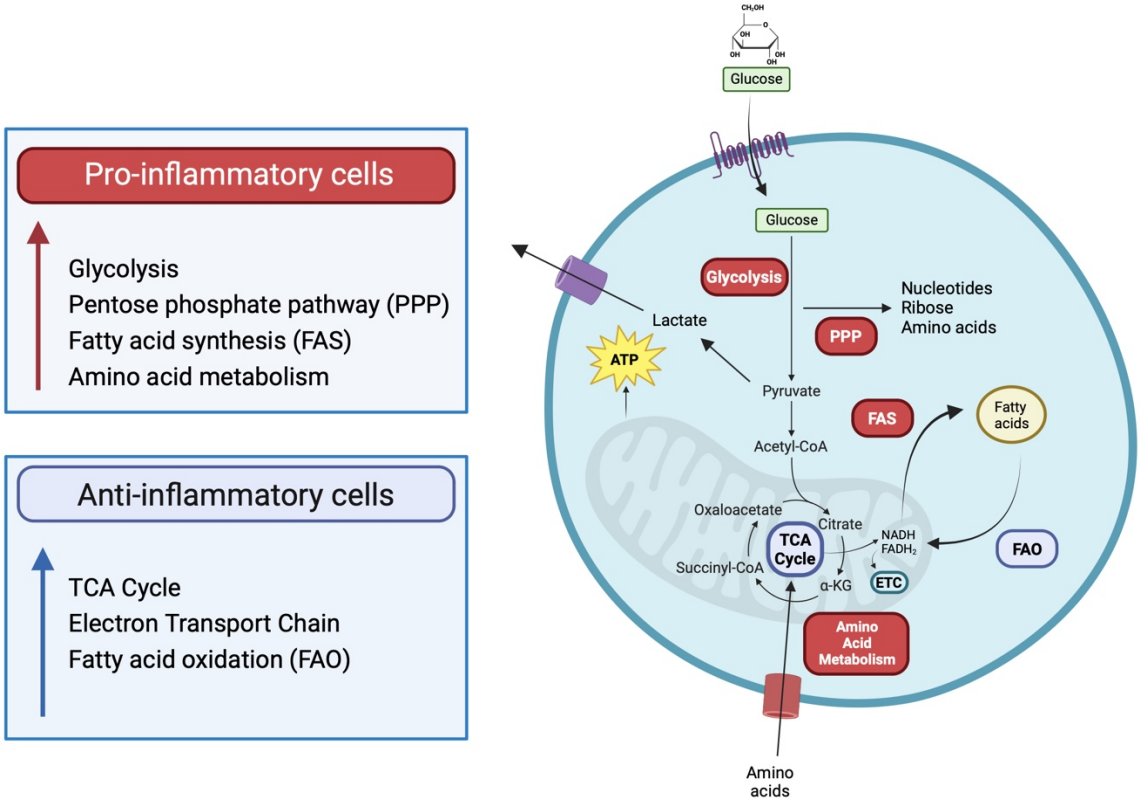

Figure 1.4 Schematic summary of major metabolic pathways used by pro-inflammatory and anti-inflammatory immune cells. Adapted from O'Neill, *et al.* 2016 and Shanley, *et al.* 2022.

1.5 Biomaterials in Bone Tissue Engineering

Bone is one of the main human tissues for which therapeutic intervention can be dramatically improved by biomaterial implantation. The optimal biomaterial in bone tissue engineering supports healing and tissue repair at the implant site, eventually degrading *in situ* as the host bone regenerates and regains function. Grafting of vascularised autografts

and allografts functions as a current first-line treatment for bone defects, but present numerous challenges that include shortage of donors, donor site morbidity, scarring, and immunogenicity [181]. Ideally, the use of biomaterials would allow for an off-the-shelf, patient-tailorable approach that would capitalise on the host repair process and engineer a pro-regenerative response, eventually leading to full restoration of natural host bone. The recent line of investigation into the field of "osteo-immunology", and the evidence indicating host immune response as a dictator of biomaterial implant success has highlighted the development of immunomodulatory biomaterials as a promising therapeutic strategy for bone tissue engineering [182].

The three basic elements of bone tissue engineering are scaffolds, cells, and growth factors [183] with initial emphasis placed primarily on the design of biologically inert materials. This, as well as the need for mechanical strength, longevity of the implant, and relative ease of manufacture led to the commonplace usage of metal-based materials in the development of implants and prostheses in orthopaedics. Given the issues that arise at the bone-metal interface (for example, ion release leading to inflammation and adverse host tissue responses) these implants are commonly treated with other materials to render them biocompatible. In the case of bone tissue repair, materials initially used for biocompatibility included synthetic polymers (e.g: polymethyl methacrylate [PMMA], polyetheretherketone [PEEK]), and ceramics (e.g: aluminium- and zirconium-based) [135].

Taken together, this formed the basis for the first generation of biomaterials in bone tissue repair: mechanically stable, biocompatible and, critically, biologically inert. It was the emergence of the advantageous bioactive component that led to the onset of the second generation of biomaterials including, but not limited to, synthetic polymers (for example poly (L-lactic acid) [PLLA] and polycaprolactone [PCL]) and natural polymers (primarily collagen-based), calcium phosphates, calcium carbonates, calcium sulphates, and bioactive glasses. Now, with the ever-expanding wealth of knowledge in the fields of bone tissue engineering and osteoimmunology, a third generation of biomaterials are in development; those which combine the advantages of the first and second and build upon that to create materials capable of inducing specific biological responses, the most critical

of which concern the cells of the immune system and their influence on the process of bone healing.

Calcium phosphates are regarded as biomaterials of choice as their composition closely mirrors that of native bone, with human bone comprised of approximately 70% calcium phosphate (CaP) mineral. Hydroxyapatite (HA) is one such naturally occurring CaP material that exhibits osteoconductivity *in vivo* and has been utilised primarily as an implant coating to improve implant biocompatibility and fixation [184]. Early work demonstrating the biocompatibility and efficacy of HA in bone tissue engineering applications showed new bone deposition around HA ceramic implants when implanted subcutaneously in a canine model [185] and work since has sought to refine means of HA incorporation into biomaterial implants for superior integration and tissue regeneration. One means by which this has been done is by the use of nanophase HA, or nanoHA, with nanoHA shown to increase osteoblast lineage commitment [186], as well as promote bone volume concomitant with a pro-regenerative immune microenvironment in a rat femoral defect model [126]. Currently, research into the immunomodulatory potential of bone-based biomaterials involves mechanisms such as the tuning of inherent biomaterial properties like particle size, and imbuing the material with immunomodulatory biomolecules that can be released in a controlled manner to affect both immune response and consequent regenerative processes [187]. As such, research is ongoing into investigating appropriate biomaterials for delivery of novel immunomodulators.

Hydrogels are one such biomaterial showing promise in the field of bone tissue engineering, both alone and as a delivery platform for immunomodulatory therapeutics. Hydrogels are 3D polymeric structures with a high water content, and can be derived from natural or synthetic sources. Natural hydrogels, such as those derived from collagen, fibrinogen, and hyaluronic acid, offer an advantage over synthetic in that they display superior biocompatibility, whilst synthetic hydrogels offer greater mechanical strength and tunability [188]. Hydrogels have emerged as a platform for immunomodulation in the promotion of tissue regeneration [189], and consequently have begun to be used as effective delivery platforms for immunomodulators in the context of bone tissue regeneration, recently reviewed [190, 191].

1.6 Research Question

The limited capacity for many tissues to repair and regrow post-damage or destruction lies at the heart of numerous healthcare challenges. There has been vast expansion of research into the vital contribution of the immune system in driving and dictating reparative and regenerative responses. Numerous immune cell subsets are critically involved in driving and modulating tissue healing processes post-injury, and additionally mediate tissue regeneration through their interactions with progenitor cells. One strategy seeking to surmount the current challenges to adequate tissue regeneration is by the incorporation of biomaterials. It is therefore advantageous to thoroughly characterise the interaction of the immune system with various biomaterials intended for clinical use in order to gain a robust understanding of current clinical challenges and outcomes, as well as to inform the design of the future generation of biomaterials for superior integration and tissue regeneration. This includes investigation into the impact of biomaterials on immune cell metabolism, given our growing appreciation of the extent to which immunometabolism dictates immune cell phenotype and function. Interrogation of immunometabolism in the context of the host response to biomaterials not only allows for more robust characterisation of biomaterial-immune system interaction, but also offers the potential to identify novel therapeutic targets, such as investigation into the use of metabolic inhibitors to inhibit unfavourable or promote beneficial immune responses, or targeting certain metabolites that can enhance biomaterial success. Overall, immunometabolism offers an exciting avenue to aid in addressing currently unmet clinical needs that surround biomaterial intervention.

Bone tissue is one such tissue that stands to benefit from incorporation of immunological and immunometabolic insights into tissue engineering and biomaterial-mediated strategies, with a need for new means of characterisation and manipulation of the immune response to allow for the design of 'immune-informed' bone-based biomaterials. Interrogation of existing and novel immunomodulators also offers potential for identification of novel immunomodulatory therapeutics capable of not only manipulating the immune response, but also promoting the regeneration of functional tissue *in situ*.

This work aims to interrogate the immune response to biomaterials that are currently used clinically for bone-based applications, including investigation into whether biomaterial particulates are capable of impacting on the metabolic profile of human macrophages, as well as investigate the potential of novel immunomodulators to interact with cells of the immune system and progenitor cells for the ultimate goal of enhancing bone repair and regeneration in an *in vivo* system.

1.7 Specific Aims

- To determine if biomaterial particulates are capable of impacting on the metabolic profile of primary human macrophages.
- To investigate the impact of novel immunomodulatory ketoacids on primary human macrophage phenotype and osteogenic potential of human mesenchymal stem cells.
- To interrogate the effect of hyaluronic acid hydrogels and hydrogel stiffness on primary human macrophage phenotype *in vitro* and immune profile *in vivo*.
- To investigate hyaluronic acid hydrogels as a potential delivery system for novel immunomodulators for the goal of bone regeneration *in vivo*.

Chapter Two

Materials and Methods

2.1 Materials

2.1.1 Cell culture

Lymphoprep was purchased from StemCell as manufactured by Axis-Shield poC. MagniSort Human CD14 Positive Selection Kit was purchased from eBioscience. Dulbecco's Modified Eagle Medium (DMEM) and Roswell Park Memorial Institute (RPMI)-1640 Medium were purchased from Gibco. The following were purchased from Sigma-Aldrich: Dulbecco's Phosphate-Buffered Saline (PBS), L-Glutamine, Penicillin-Streptomycin solution, Foetal Bovine Serum (FBS), Ethylenediaminetetraacetic Acid (EDTA), Trypsin-EDTA solution, Trypan Blue solution, Dimethyl Sulfoxide (DMSO), L-ascorbic acid-2-phosphate, dexamethasone, and β-Glycerol phosphate, Neutral red cytotoxicity assay kit (TOX4). Human recombinant Monocyte Colony-Stimulating Factor (M-CSF), IL-4, and IFNγ were purchased from Miltenyi Biotec. MagniSort Human CD14 Positive Selection kit was purchased from Thermo Fisher Scientific.

2.1.2 Inhibitors and reagents

Ultrapure lipopolysaccharide (LPS) from E. Coli O111:B4 was purchased from Enzo Life Sciences. 2-deoxyglucose (2-DG) and 3PO were purchased from Sigma Aldrich. Cytochalasin B was purchased from Cayman Chemicals. Hydroxyapatite particles (HA) were purchased from Sigma Aldrich. Indole-3-pyruvate and 4- hydroxyphenyl pyruvate were purchased from Merck and dissolved in RPMI or DMEM to a final concentration of 2 mM prior to use. Aryl hydrocarbon receptor (AhR) antagonist, CH223191, was purchased from Merck.

2.1.3 Western blotting

All chemicals used were purchased from Sigma-Aldrich unless otherwise stated. Acrylamide was purchased from Fisher Scientific. SeeBlue Plus2 Pre-Stained Protein Standard was purchased from Invitrogen. Immobilon polyvinylidene difluoride (PVDF) membrane and Enhanced Chemiluminescent (ECL) Horseradish-Peroxidase (HRP) Substrate were purchased from Merck Millipore.

Table 2.1 Western blot buffers.

Buffer	**Reagents**
1 M Tris-HCl (pH 6.8)	121.4 g Tris, 1 L diH_20
1.5 M Tris-HCl (pH 8.8)	181.71 g Tris, 1 L diH_20 10% SDS: 10 g SDS, 100 mL diH_20 10% Ammonium Persulfate (APS): 100 mg APS, 10 mL diH_20
10X Running Buffer (pH 8.3)	30.3 g Tris, 144 g Glycine, 1 L diH_20 (diluted to 1X with diH_20)
10X Transfer Buffer (pH ~8)	30 g Tris, 144 g Glycine, 1 L diH_20 (diluted to 1X with diH_20)
10X Tris-buffered Saline with Tween-20 (TBST) (pH 7.6)	24.2 g Tris, 88 g NaCL, 10 mL Tween-20, 990 mL diH_20 (diluted to 1X with diH_20)

2.1.4 Primary antibodies

GLUT1 and Hexokinase 2 (HK2) were purchased from Abcam. Nrf2 was purchased from Cell-Signalling Technologies (CST). HO-1 was purchased from Enzo Life Sciences. Anti-β-actin-peroxidase was purchased from Sigma-Aldrich.

2.1.5 Secondary antibodies

Anti-rabbit IgG (whole molecule)-peroxidase and anti-mouse IgG (whole molecule)-peroxidase were purchased from Sigma-Aldrich.

2.1.6 Flow cytometry

OneComp Beads were purchased from Biosciences. Fixable Viability Dye eFluor506 and Annexin V & PI Staining Kit were purchased from eBioscience. BD Cytofix/Cytoperm Fixation/Permeabilisation Kit was purchased from Becton Dickinson (BD) Biosciences. Fcγ Receptor block was purchased from eBioscience. Anti-CD32 (Rat Fcγ block) was purchased from BD Biosciences. The following fluorochrome-conjugated antibodies were purchased from eBioscience (Table 2.1):

Table 2.2 Antibodies for *in vitro* macrophage studies.

Specificity	**Fluorochrome**	**Clone**	**Supplier**
CD14	FITC	HCD14	Biosciences
CD11b	APC-Cy7	ICRF44	Biosciences
CD163	BV421	eBioGHI/61	Biosciences
CD206	APC	19.2	Biosciences
CD86	PerCP-Cy7	IT2.2	Biosciences
CD80	PerCP-Cy5	2D10	Biosciences
CD40	eFluor450	5C3	Biosciences

Table 2.3 Antibodies for *in vivo* immune cell profiling.

Specificity	**Fluorochrome**	**Clone**	**Supplier**
CD8a	BV421	OX-8	Becton Dickinson
CD4	BV605	OX-35	Becton Dickinson
CD161a	BV480	10/78	Becton Dickinson
CD11b/c	PE-Cy7	OX-42	Becton Dickinson
CD45R	BV711	HIS24	Becton Dickinson
CD45 (Leukocyte Common Antigen)	APC-Cy7	OX-1	Becton Dickinson
CD3	APC	1F4	Becton Dickinson
CD86 (B7-2)	BV786	24F	Becton Dickinson
CD163	BV650	HIS36	Becton Dickinson
His48	FITC	HIS48	Invitrogen/Fisher
CD68	PE	ED1	Invitrogen/Fisher
CD43	PerCP/Cy5.5	W3/13	BioLegend

2.1.7 Seahorse XF analyser materials

Seahorse XF/XFe 96 well cell culture microplates, extracellular flux assay kits, XF calibrant and XF assay media was purchased from Agilent Technologies. Oligomycin A was purchased from Cayman Chemicals. Carbonyl cyanide-p-trifluoromethoxyphenylhydrazone (FCCP) was purchased from Santa Cruz Biotechnology. Rotenone, antimycin A, and 2-deoxy-D-glucose (2-DG) were purchased from Sigma-Aldrich.

2.1.8 Confocal microscopy

Cell culture microplates were purchased from iBidi. Mitotracker Red™ was purchased from Invitrogen. Hoechst 33342 was purchased from ThermoFisher. Confocal microscope used was the Leica SP8 Scanning Confocal.

2.1.9 Polymerase Chain Reaction (PCR) materials

High pure RNA Isolation Kit was purchased from Roche. Applied Biosystems High-Capacity cDNA transcription kit, TaqMan fast universal PCR Master Mix and TaqMan probes for eukaryotic 18S rRNA, human *CXCL9*, *CXCL10*, *CXCL19*, *CXCL11*, *MRC1*, and *CCL13* were purchased from Biosciences. iTaq Universal SYBR Green Supermix was purchased from Bio-Rad Laboratories. Forward and reverse oligonucleotide primers for all primers used were purchased from Sigma-Aldrich. The primer sequences are as follows:

Table 2.4 Human primer sequences.

Gene	**Forward**	**Reverse**
GAPDH	ACAGTTGCCATGTAGACC	TTTTTGGTTGAGCACAGG
HIF1α	GAAACTTCTGGATGCTGGTGATTT	GCAATTCATCTGTGCTTTCATGTCA
HIF2α	AAGCTCCTCTCCTCAGTTTGCT	GTACAAGTTGTCCATCTGCTGG
HK2	TTCTTGTCTCAGATTGAGAGTGAC	TTGCAGGATGGCTCGGACTTG
GLUT1	GAACTCTTCAGCCAGGGTCC	ACCACACAGTTGCTCCACAT
PFKFβ3	CCATGAAAGTCCGGAAGCAATG	GCTTTTGACATCTCTCAAGGCAG
PKM2	ATGTTGATATGGTGTTTGCG	ATTTCATCAAACCTCCGAAC
VEGF	GCAGAATCATCACGAAGTGGTG	TCTCGATTGGATGGCAGTAGCT
PDGF-BB	GGGCAGGGTTATTTAATATGG	AATCAGGCATCGAGACAG
TGF-β	AACCCACAACGAAATCTATG	CTTTTAACTTGAGCCTCAGC
β-actin	GGACTTCGAGCAAGAGATGG	AGCACTGTGTTGGCGTACAG
BMP2	TCCACCATGAAGAATCTTTG	TAATTCGGTGATGGAAACTG
RUNX2	AAGCTTGATGACTCTAAACC	TCTGTAATCTGACTCTGTCC
OCN	TTCTTTCCTCTTCCCCTTG	CCTCTTCTGGAGTTTATTTGG
ANG1	TACTCAGTGGCTGCAAAAACTTGA	ATCTCCGACTTCATGTTTTCCACA
FGF	AAGAGCGACCCTCACATCAAG	ACACTCCTTTGATAGACACAACTC
NQO1	TGAAGAAGAAAGGATGGGAG	TTTACCTGTGATGTCCTTTC
GSR	GACCTATTCAACGAGCTTTAC	CAACCACCTTTTCTTCCTTG
CYP1A1	CATTAACATCGTCTTGGACC	TCTTGGATCTTTCTCTGTACC

Table 2.5 Rat primer sequences.

Gene	Forward	Reverse
FoxP3	GAAGATGGCATTGACAAAAG	CATGTTGTGGAAGAACTCTG
IFNγ	GAAAGCCTAGAAAGTCTGAAG	AGTATTTTCGTGTTACCGTC
TNF	CTCACACTCAGATCATCTTC	GAGAACCTGGGAGTAGATAAG
Timp1	TTGATAGCTTCCAGTAAAGC	GAATCCTTTGAGCATCTTAGTC
VEGF-A	GATAGAGTATATCTTCAAGCCG	CTCATCTCTCCTATGTGCTG
CD86	CACAAGCTTTGATAGGGATAAC	TTCTTGTTTCATTCTGAGCC
CD163	ATAGTCTGCTCACGATACATAG	GACATAAGACATGAGCATCTTC
IL1Ra	CATTGATGGAAAGAAGCCTG	TCAAAATCTGAGTCCTTGTC
CD80	GCTTCAGAAGAAGAAATGAGG	AATTCAAGGAAGGCAAATGG
TGFB1	GGAAATCAATGGGATCAGTC	CTGAAGCAGTAGTTGGTATC
TGFB3	CTGTCCATGTCATACCTTTC	TGTCCACTCCTTTGAATTTG
Runx2	AGAGTCAGATTACAGATCCC	TGTCATCATCTGAAATACGC
BMP2	CTATATGCTCGACCTGTACC	CTCATTTCTGAAAGTTCCTCG
HPRT	ACTGGTAAAACAATGCAGAC	CCTGAAGTGCTCATTATAGTC

2.1.10 Fluorescence Lifetime Imaging Microscopy (FLIM)

35 µm tissue culture dishes dishes were purchased from Sarstedt, Germany. Phenol-free RPMI media was purchased from Biosciences.

2.1.11 Enzyme-linked immunosorbent assay (ELISA)

Human IL-6, IL-8, TNF, and IL-10 uncoated ELISA kits were purchased from Invitrogen.

2.1.12 Hyaluronic acid hydrogels

Non-sterile HyA-TA (lyophilised), sterile horseradish peroxidase (HRP) were kindly provided by the Duffy Lab (NUIG) as supplied by Contipro (Czech Republic). H_20_2 solution was purchased from Sigma-Aldrich.

2.1.13 Alizarin red staining

Alizarin Red and cetylpyridinium chloride were purchased from Sigma.

2.2 Methods

2.2.1 Cell culture

Cells were cultured at 37 °C with an atmosphere of 95% humidity and 5% CO_2. Cell culture media was supplemented with 10% FBS, 2 mM L-Glutamine, 100 U/ml penicillin and 100 µg/ml streptomycin unless stated otherwise. Cell numbers and viability were determined by performing cell counts in trypan blue. Cells were diluted in trypan blue and 10 µl was loaded onto a Hycor KOVA Glasstic cell counter slide and viewed under a light microscope. Cell viability was assessed by dye exclusion. The number of viable cells was determined using the following formula:

$$\text{Number of cells/ml} = \#\text{ cells counted} \times \text{dilution factor} \times 10^4$$

2.2.1.1 Isolation of PBMCs from human venous blood

This study was approved by the research ethics committee of the School of Biochemistry and Immunology, Trinity College Dublin and is in accordance with the Declaration of Helsinki. PBMCs were isolated from leukocyte-enriched buffy coat packs (the plasma depleted fraction of anti-coagulated blood) obtained from anonymous healthy donors with consent from the Irish Blood Transfusion Service, St James' Hospital, Dublin. Blood was diluted in sterile PBS and centrifuged at 2500 rpm for 10 minutes at room temperature, with the brake off. The buffy coat layer containing leukocytes was removed and diluted in sterile PBS. 25 ml of diluted buffy coat was layered over 17.5 ml LymphoPrep, and PBMCs were isolated by density-gradient centrifugation at 2000 rpm for 20 minutes at room temperature, with the brake off (Figure 2.1). The PBMC layer was removed from the interface of the gradient and washed twice in sterile PBS by centrifugation at 1800 rpm for 10 minutes at room temperature. Isolated PBMCs were re-suspended in RPMI.

2.2.1.2 Isolation of $CD14^+$ monocytes

$CD14^+$ monocytes were isolated from PBMCs by magnetic-activated cell sorting (MACS), using the Magnisort CD14 positive selection kits (eBioscience). PBMCs were washed in

MACS buffer (PBS supplemented with 2% FBS and 2 mM EDTA) and pelleted by centrifugation at 300 g for 5 minutes. PBMCs were re-suspended in MACS buffer at 1 x 10^8 cells/ml in a 12 x 75 mm 5 ml tube and incubated with anti-CD14 biotin (10 µl per 100 µl cells) for 10 minutes at room temperature. Cells were then washed in 4 ml MACS buffer and pelleted by centrifugation at 300 g for 5 minutes. Supernatant was discarded, cells were re-suspended in their original volume of MACS buffer and incubated with MagniSort positive selection beads (15 µl per 100 µl cells) for 10 minutes at room temperature. The volume was then adjusted to 2.5 ml and the tube placed inside the magnetic field of a Magnisort magnet for 5 minutes. The negative fraction was then poured off by inverting the tube while held inside the Magnisort magnet, and the remaining cells were re-suspended in 2.5 ml MACS buffer. This step was repeated three times and then the positive fraction containing the $CD14^+$ monocytes was re-suspended in RPMI and counted.

2.2.1.3 Culture of monocyte-derived macrophages

Primary human macrophages were cultured from $CD14^+$ monocytes isolated from healthy human PBMCs. Purified $CD14^+$ monocytes were cultured at 1 x 10^6 cells/ml in RPMI supplemented with human recombinant M-CSF (50 ng/ml). On the third day of culture half the media was carefully removed from the wells and replaced with fresh media containing M-CSF. On the sixth day of culture the purity of macrophages was determined by expression of CD14 and CD11b by flow cytometry: $CD14^+$ $CD11b^+$ cells were defined as fully differentiated macrophages (Figure 2.2).

2.2.1.4 Macrophage lifting

For hydrogel experiments, monocytes were plated at 1 x 10^6 cells/ml in complete RPMI (cRPMI) supplemented with M-CSF (50 ng/ml) in a 25 cm^2 low attachment flask (Corning) at a final volume of 10 ml/flask. At 6 days of culture, $CD14^+$/$CD11b^+$ macrophages were washed with PBS prior to incubation with pre-warmed Versene™ (Gibco) at 37 °C for 5 minutes. Cells were then collected in suspension and centrifuged at 300g for 5 minutes. The pellet was resuspended in cRPMI and cells were counted and plated.

2.2.1.5 Culture of adult human bone marrow-derived mesenchymal stem cells (MSC)

Bone marrow aspirates, obtained from anonymous donors (Lonza), were washed in PBS and centrifuged at 900g for 10 mins. Supernatant was gently aspirated, and cells were plated at 4000-5000 MSCs/cm^2 in complete media (DMEM, 10% FBS, 1% P/S, 5 ng/ml bFGF2). Cells were cultured for up to two weeks (until colonies form and cells proliferate), with media being replenished every 3-4 days. Cells were washed with PBS in between feedings to dislodge red blood cells. Adherent cells were expanded up to P2 and were characterized by their plastic adherence and fibroblastic nature. Colony Forming Unit assays were used to quantify proliferation, and Trilineage Potential assays were used to determine pluripotency. For *in vitro* assays, MSC were seeded at 1 x 10^5 cells/ml in standard culture media, high glucose Dulbecco's modified Eagle's medium (4.5 mg/mL D-glucose and 200 mM L-glutamine; hgDMEM) supplemented with 10% fetal bovine serum (FBS) and penicillin (100 U/mL)–streptomycin (100 g/mL) and expanded in a humidified atmosphere at 37 °C, 5% CO_2, and 20% pO_2.

2.2.1.6 Neutral red viability assay

Cells were incubated with 10% neutral red solution (N-2889, TOX4 kit, Sigma) for 1 hour. After incubation, media was removed and cells were washed with Neutral Red assay fixative (N-4270) once and fixative was removed. Cells were then solubilised with Neutral Red assay solubilisation solution (N-4395) at the equivalent volume to that of the original media in each well. The cell plate was shaken at room temperature for 10 minutes to ensure homogeneity of the solution and absorbance was read at 540 nm and 690 nm. Cell viability was determined relative to untreated cells using the below formula:

$$(B1\text{-}B2/A1\text{-}A2) \times 100$$

B1: absorbance of treated cells at 540 nm; B2: absorbance of treated cells at 690 nm; A1: absorbance of untreated control cells at 540 nm; A2: absorbance of untreated control cells at 690 nm.

2.2.1.7 Macrophage conditioned media experiment

Primary human macrophages were cultured with 1 mM IP for 24 hours. Conditioned media (CM) was harvested and centrifuged at 300 x g for 10 minutes to remove any cellular debris. Macrophages were cultured in IP-free RPMI for a further 24 hours prior to harvesting and centrifugation of CM. Human MSC were cultured in CM for 48 hours prior to assessment of gene expression by RT-qPCR.

2.2.2 Flow cytometry

2.2.2.1 Cell surface marker staining

Cells were first stained with a Fixable Viability dye (FixVia eFluor 506 for macrophages, Live/Dead Aqua for rat tissue digests) for 15 minutes at room temperature. Cells were Fc blocked for 15 minutes prior to staining for surface markers. Cells were stained with fluorochrome conjugated antibodies specific to markers of interest prior to fixation with 4% paraformaldehyde (PFA), and then washed and acquired on a FACSCantoTM II (BD Biosciences) or Aurora cytometer (Cytek). Compensation beads singly stained with every fluor channel utilised were acquired to adjust for spectral overlap. An unstained sample was also run as a control.

2.2.2.2 Annexin V & PI staining

For assessment of MSC viability under IP treatment, MSC were stained with fluorochrome-conjugated anti-Annexin V and PI. Cells were washed in 1x Annexin V binding buffer and pelleted by centrifugation at 300 g for 5 minutes. Supernatant was discarded and the cells were incubated in 100 µl 1x binding buffer containing 5 µl fluorochrome-conjugated anti-Annexin V and 10 µl PI for 15 minutes at room temperature. 400 µl of 1x binding buffer was added to the cells prior to immediate acquisition using the BD FACSCanto II flow cytometer.

2.2.2.3 Acquisition, compensation, and analysis

Where flow cytometry experiments contained more than one fluorochrome, single-stained controls were prepared for each fluorochrome using BD CompBeads in order to

calculate spectral compensation. Samples were acquired on a BD FACSCanto II flow cytometer or Aurora cytometer (Cytek). All flow cytometry data analysis was performed using FlowJo v10 (Treestar Inc) software.

2.2.3 SDS-PAGE, gel staining, and western blot

2.2.3.1 Sample preparation

For GLUT1 and HK2 blots cells were lysed by the addition of RIPA buffer (100 µl per 1 x 10^6 cells) containing 1% phosphatase inhibitor cocktail 3. Samples were centrifuged at 16,000 g for 5 minutes and lysates were transferred to fresh microcentrifuge tubes. Samples were stored at -20 °C. For HO-1 and Nrf2 blots cells were lysed according to the CST protocol, as follows: cells were lysed in 1X Laemmli buffer (10 µl of 5X Laemmli buffer containing 20% β-mercaptoethanol, in 40 µl de-ionised water) containing 1% phosphatase inhibitor cocktail 3. Cells were transferred to micro-centrifuge tubes and sonicated for 10 min to shear DNA and reduce viscosity. Samples were boiled at 100 °C for 5 minutes prior to being cooled on ice. Samples were then centrifuged at 16,000 g for 5 minutes prior to collection of the supernatant and transfer into fresh micro-centrifuge tubes. Samples were then stored at -20 °C.

2.2.3.2 SDS-PAGE

Samples lysed in RIPA were prepared by the addition of 5x Laemmli buffer (containing 20% β-mercaptoethanol) in a ratio of 1:5 prior to boiling at 100 °C for 5 minutes. Depending on the size of the target protein, either 10% or 12% polyacrylamide gels were used (see Table 2.3 for composition of gels). Samples and a pre-stained protein standard were loaded and resolved through the gel at 120 volts (V) for 90 minutes.

Table 2.6 Composition of SDS-Polyacrylamide Gels.

	2x 10% RESOLVING GEL (ml)	**2x 12% RESOLVING GEL (ml)**	**2x STACKING GEL (ml)**
30% Acrylamide	5	6	0.67
H_20	5.9	4.9	2.7
1.5M TRIS	3.8	3.8	--
1M TRIS	--	--	0.5
10% SDS	0.15	0.15	0.04
10% APS	0.15	0.15	0.04
Temed	0.006	0.006	0.006

2.2.3.3 Transfer of proteins onto PVDF membrane

A wet transfer sandwich was prepared in the following order: sponge, filter paper, gel, PVDF membrane, filter paper, sponge. PVDF membrane was first activated by submersion in methanol. All other components of the transfer sandwich were first submerged in transfer buffer. The transfer sandwich was placed into the transfer system with the gel on the cathode side and the membrane on the anode side. After ensuring that there were no air bubbles in the system, the proteins were transferred at 200 milliamperes (mA) for 75-90 minutes.

2.2.3.4 Immunodetection of proteins

Following the transfer, the membrane was incubated in blocking buffer under agitation for 1 hour at room temperature. For detection of specific proteins the blocking buffer and diluent was 5% (w/v) milk in 1 X TBST. The membrane was incubated in primary antibody (see Table 2.4 for dilutions) with agitation overnight at 4 °C. The membrane was washed 5 times for 5 minutes each with 1X TBST prior to incubation in secondary antibody (Table 2.7) for 2 hours at room temperature. The membrane was washed a further 5 times for 5 minutes each and then developed with freshly prepared ECL using Chemi-Luminescent gel documentation system (Alpha-Innotech). Densitometric analysis was used to quantify the protein bands using Biorad software.

Table 2.7 Immunoblotting antibody dilutions.

Primary Antibody	**Dilution**	**Secondary Antibody**	**Dilution**
Anti-Hexokinase 2	1:1000	Anti-mouse	1:2000
Anti-GLUT1	1:1000	Anti-rabbit	1:2000
Anti-HO-1	1:1000	Anti-rabbit	1:2000
Anti-Nrf2	1:1000	Anti-rabbit	1:2000
Anti-β-actin-peroxidase	1:50000	--	--

2.2.4 Polymerase Chain Reaction (PCR)

2.2.4.1 Cell treatments

Human macrophages were plated at a concentration of 1 x 10^6 cells/ml in a 12-well plate and stimulated with particles or ketoacids for the appropriate time points. Human MSC were cultured at a concentration of 1 x 10^5 cells/ml in a 12 or 6 well plate and stimulated with IP or CM for the appropriate timepoints. Following treatments, RNA was extracted using the high pure RNA Isolation Kit as described below.

2.2.4.2 RNA extraction

Supernatants were removed and cells were washed once with PBS before the addition of 400 µl of lysis/-binding buffer and 200 µl of PBS per well. The lysates were transferred to a High Pure Filter Tube that was inserted into a collection tube. Samples were centrifuged at 8,000 g for 15 seconds. The flowthrough liquid was discarded and 90 µl of DNase incubation buffer with 10 µl DNase I was added to each Filter Tube and incubated for 15 minutes at room temperature. 500 µl of Wash Buffer I was then added to the Filter Tubes which were centrifuged at 8,000 g for 15 seconds. The flow-through liquid was discarded and 500 µl of Wash Buffer II was added to the Filter Tubes which were centrifuged again at 8,000 g for 15 seconds. The flow-through liquid was discarded and a further 200 µl of Wash Buffer II was added to Filter Tubes and centrifuged at 13,000 g for 2 minutes. The

collection tubes were discarded, and the Filter Tubes were placed into sterile, RNase-free 1.5 ml microcentrifuge tubes. 50 µl of Elution Buffer was added to the filter tubes and centrifuged at 8,000 x g for 1 minute. The concentration of eluted RNA in each sample was determined using a NanoDrop 2000c UV-Vis Spectrophotometer and then equalised by the addition of Elution Buffer where necessary.

2.2.4.3 cDNA synthesis

cDNA synthesis was then carried out using the High-Capacity cDNA reverse transcription kit (Applied Biosystems). A 2X Reverse Transcription (RT) master mix was prepared with the components in Table 2.8.

Table 2.8 Components and volumes required for 2X RT Master Mix

Component	**Volume added (per sample)**
10X RT Buffer	2 µl
25X dNTP Mix (100mM)	0.8 µl
10X RT Random Primers	2 µl
Multiscribe Reverse Transcriptase	1 µl
Total added (per well)	5.8 µl

14.2 µl of RNA and 5.8 µl of the 2X RT master mix were added to RNase-free PCR tubes and the reverse transcription (see Table 2.9) was performed using the Mini Amp Thermal Cycler.

Table 2.9 cDNA Reverse Transcription Reaction

	Step 1	**Step 2**	**Step 3**	**Step 4**
Temperature (°C)	23	37	85	4
Time (minutes)	10	120	5	Indefinitely

2.2.4.4 Real-time polymerase chain reaction (PCR)

Two protocols were used for analysis of gene expression by real-time PCR.

1. TaqMan protocol:

Real-time PCR was carried out on transcripts using the TaqMan fast universal PCR Master Mix (Applied Biosystems) and predesigned TaqMan gene expression primers. Samples were made up as detailed in Table 2.10, into a 96-well PCR microplate. The PCR reaction is detailed in Table 2.11.

Table 2.10 Components and volumes required for qPCR reaction.

Component	**Volume added (per sample)**
18S RNA Probe	0.5 µl
Target Probe	0.5 µl
TaqMan Universal PCR Master Mix	4.5 µl
cDNA sample	4.5 µl
Total volume (per reaction)	10 µl

Table 2.11 Thermal cycling parameters for TaqMan real-time PCR:

	Step 1	**Step 2**	**Step 3**	**Step 4**	**Step 5**	**Step 6**
Temperature (°C)	95	95	60	Plate Read	72	Go to Step 2
Time (seconds)	10 (mins)	15	30	-	30	X 40

2. iTaq Universal SYBR Green protocol:

Real-time PCR was carried out on human mesenchymal stem cell cDNA transcripts using the iTaq Universal SYBR Green Supermix and oligonucleotide primers. Reactions were made up as detailed in Table 2.12 in a 96-well PCR microplate. The PCR reaction is detailed in Table 2.13.

Table 2.12 Components and volumes required for iTaq Universal SYBR Green reaction.

Component	**Volume added (per sample)**
Forward Primer	0.8 µl
Reverse Primer	0.8 µl
RNase free water	7.4 µl
iTaq Universal SYBR Green	9.5 µl
cDNA Sample	1.5 µl
Total volume	20 µl

Table 2.13 Thermal cycling parameters for iTaq Universal SYBR Green real-time PCR.

	Step 1	**Step 2**	**Step 3**	**Step 4**	**Step 5**	**Step 6**
Temperature (°C)	95	95	60	Plate Read	72	Go to Step 2
Time (seconds)	10 (mins)	15	30	-	30	X 40

The real-time PCR reactions (detailed in Table 2.11 and Table 2.13) were performed using the BioRad CFX Touch Real-Time PCR detection system. For each sample, mRNA concentration was normalised using the crossing threshold of the housekeeping genes, 18s ribosomal RNA or β-actin. Gene expression, relative to untreated samples, was determined using the $2^{-\Delta\Delta Ct}$ method.

2.2.5 Measurement of cytokine production by ELISA

The concentrations of human TNF, IL-6, IL-8, and IL-10 production were quantified by ELISA, according to the manufacturer's protocol. 75 µl of capture antibody diluted in coating buffer was applied to high-binding 96-well plates (Greiner Bio-one). Plates were incubated overnight at 4 °C, capture antibody was removed, and non-specific binding sites were blocked with appropriate blocking solution (1% (w/v) BSA) for 1 hour at room temperature. After blocking, plates were washed in PBS-tween solution, dried, and supernatant samples were loaded into wells in triplicates either neat or diluted appropriately with assay diluent. A standard curve of serially diluted recombinant cytokine standard was also loaded onto the plates in triplicate. Blank wells, containing assay diluent only, were included on each plate to allow the subtraction of background from each sample. Samples were incubated overnight at 4 °C. After washing, biotinylated detection antibody was added to each well and incubated for 2 hours at room temperature. Plates were washed and horseradish-peroxidase (HRP) conjugated to streptavidin was applied to wells for 30 minutes in the dark. Wells were thoroughly washed and the substrate, TMB, was added. The enzyme-mediated colour reaction was protected from light while developing and stopped with the addition of 1M H_2SO_4. The optical density of the colour was determined by measuring the absorbance at 450 nm using a microtiter plate reader.

A standard curve was generated using serially diluted protein standards and used to determine the concentration of cytokine in the supernatant.

2.2.6 Seahorse XF/XFe 96 Analyser

2.2.6.1 Macrophage seahorse experiments

The Seahorse XF/XFe 96 analyser simultaneously measures in real time the oxygen consumption rate (OCR), a measure of the rate of oxidative phosphorylation, and extracellular acidification rate (ECAR), a measure of the rate of glycolysis, in the medium directly surrounding a monolayer of cells. Macrophages were cultured at 1 x 10^6 cells/ml for 6 days prior to re-seeding at 2 × 10^5 cells/well in a Seahorse 96-well microplate and allowed to rest for 5 hours prior to HA or nanoHA stimulation for 3, 6, and 24 hours, or IP or HPP treatment for 6 hours followed by LPS stimulation for 3 hours. The Seahorse cartridge plate was hydrated with XF calibrant fluid and incubated in a non-CO_2 incubator at 37 °C for a minimum of 8 hours prior to use. 30 minutes prior to placement into the XF/XFe analyser, cell culture medium was replaced with complete XF assay medium (Seahorse Biosciences; supplemented with 10 mM glucose, 1 mM sodium pyruvate, 2 mM L-glutamine, and pH adjusted to 7.4) and incubated in a non-CO_2 incubator at 37°C. Blank wells (XF assay medium only) were prepared without cells for subtracting the background oxygen consumption rate (OCR) and extracellular acidification rate (ECAR) during analysis. Oligomycin (1 µM), carbonyl cyanide-p-trifluoromethoxyphenylhydrazone (FCCP) (1 µM), rotenone (500 nM), and antimycin A (500 nM) and 2-deoxy-D-glucose (2-DG) (25 mM) were prepared in XF assay medium and loaded into the appropriate injection ports on the cartridge plate and incubated for 10 minutes in a non-CO_2 incubator at 37 °C. OCR and ECAR were measured over time with sequential injections of oligomycin, FCCP, rotenone and antimycin A and 2-DG.

Table 2.14 Seahorse Protocol.

Step	**Action**
1	Equilibrate
2	Mix (3 mins)
3	Wait (2 mins)
4	Measure (3 mins)
5	Repeat steps 2-4 x2
6	Inject Port A
7	Repeat steps 2-4 x3
8	Inject port B
9	Repeat steps 2-4 x3
10	Inject port C
11	Repeat steps 2-4 x3
12	Inject port D
13	Repeat Steps 2-4 x3
14	End protocol

2.2.6.2 Seahorse analysis

Analysis of results was performed using Wave software (Agilent Technologies). The rates of basal glycolysis, max glycolysis, glycolytic reserve, basal respiration, max respiration, ATP production and respiratory reserve were calculated as detailed in Table 2.15.

Table 2.15 Seahorse Calculations.

Rate	Calculation
Non-glycolytic ECAR	Average ECAR values after 2-DG treatment.
Basal glycolysis	Average ECAR values prior to oligomycin treatment – non-glycolytic ECAR
Max glycolysis	Average ECAR values after oligomycin & before FCCP treatment
Glycolytic reserve	Max glycolysis – basal glycolysis
Non-mitochondrial OCR	Average OCR values after rotenone/antimycin A & before 2-DG treatment
Basal respiration	Average OCR values prior to oligomycin treatment – non-mitochondrial OCR
Max respiration	Average OCR values after FCCP & before rotenone/antimycin A treatment
Non-ATP respiration	Average of OCR values after oligomycin & before FCCP treatment
ATP Production	Basal respiration – non-ATP respiration
Respiratory reserve	Max respiration – basal respiration
Mitochondrial production rate	OCRATP (pmol O2/min) *2 (pmol O/pmol O2) *P/O (pmol ATP/pmol O)
Glyco ATP Production Rate	Equivalent to glycoPER (pmol H+/min)
ATP Production Rate	GlycoATP Production Rate + mitoATP Production Rate

2.2.7 Confocal imaging of mitochondria

Following treatment with either micronHA or nanoHA, cells were incubated with MitoTracker™ Red CMX Ros (50 nM) to stain mitochondria, and Hoechst (5 μg/ml) for visualisation of the nucleus. Cells were washed 3 times in cold PBS and cRPMI was replenished. Cells were imaged using a Leica SP8 scanning confocal microscope, and image analysis was performed using CellProfiler™ (script written by Dr. Nuno G.B. Neto).

2.2.8 Fluorescence Lifetime Imaging Microscopy (FLIM)

Two-photon excited NAD(P)H- Fluorescence Lifetime Imaging Microscopy (FLIM) was used to measure the levels of free and protein-bound NADH within cells and was performed on a custom multiphoton system. A titanium:sapphire laser (Chameleon, Coherent®) was used for multiphoton excitation. A water-immersion 25x objective (Olympus, 1.05NA) was utilised on an upright (Olympus BX61WI) laser scanning microscope. Two-photon excitation of nicotinamide adenine dinucleotide phosphate (NAD(P)H) fluorescence was performed with 760 nm excitation wavelength. A 455/90 nm bandpass filter was used to isolate NAD(P)H fluorescence signal. 512x512 pixel images were acquired with a pixel dwell time of 3.81 μs and 30-second collection time. A PicoHarp 300 TCSPC system operating in the time-tagged mode coupled with a PMA hybrid detector (PicoQuanT GmbH) was used for fluorescence decay measurements yielding 256 time bins per pixel. At least three images for each model were acquired. Afterwards, regions of interest (ROI) were selected, and the NAD(P)H fluorescence decay was analysed. For the NAD(P)H fluorescence decay analysis, an overall decay curve was generated by the contribution of all pixels in the ROI area. Afterwards, it was fitted with a double exponential decay curve (Equation (1):

$$I(t) = \alpha_1 e^{-t/\tau 1} + \alpha_2 e^{-t/\tau 2} + c$$

I(t) represents the fluorescence intensity at time (t) after laser excitation. α1 and α2 represent the fraction of the overall signal comprised of a short and long lifetime component, respectively. τ1 and τ2 are the long and short lifetime components, respectively. C corresponds to background light. χ2 is calculated to evaluate the goodness

of multi-exponential fit to the raw fluorescence decay data—the lowest χ2 values were considered in this study. For NAD(P)H, a two-component fit was used to differentiate between the free (τ1) and protein-bound (τ2) NAD(P)H. The average lifetime (τavg) of NAD(P)H for each pixel is calculated by a weighted average of both the free and bound lifetime contributions (Equation 2):

$$\tau_{avg} = (\alpha 1 \times \tau 1) + (\alpha 2 \times \tau 2) / (\alpha 1 + \alpha 2)$$

2.2.9 Preparation of micron and nano hydroxyapatite particle suspensions

2.2.9.1 Synthesis of nano hydroxyapatite particles

Bone mimetic nano-sized Hydroxyapatite (nanoHA) particles were prepared following a previously described protocol [192]. Briefly, a solution of 20 mM calcium chloride was added to a solution of 12 mM sodium phosphate, containing 0.017% DARVAN 821A (RT Vanderbilt) as the dispersant, and nanoHA particles were precipitated. This solution was centrifuged, reconstituted in endotoxin-free water, and filtered through a 0.2 µm filter to remove aggregated particles.

2.2.9.2 Preparation of micron hydroxyapatite particle suspension

Commercial micronHA particles ($Ca_5(OH)(PO_4)3$ were purchased from Sigma-Aldrich (Cat# 04238), weighed out, and resuspended at a concentration of 10 mg/ml in endotoxin-free water, sonicated for 10 min, and stored at 4 °C. Particles were thoroughly vortexed immediately prior to use.

2.2.9.3 Assessment of endotoxin contamination

In-house synthesized nanoHA and micronHA particles (Sigma Aldrich [Cat# 04238]) were first tested for lipopolysaccharide (LPS) contamination using the HEK-Blue™ hTLR4 assay system (Invivogen). HEK-blue cells (5 x 10^5 cells/ml) expressing TLR4 were stimulated with LPS (10–100 ng/ml; positive control), micron or nano HA particles (250 µg/ml) for 24 hours. The expression of SEAP which is under the control of NF-kB and AP-1 was tested by

incubating cell supernatants with HEK-blue detection medium for 30 minutes at 37 °C and absorbance was read at 650 nm.

2.2.10 Hyaluronic acid hydrogel fabrication

The following protocol describes steps for the preparation of tyramine-conjugated hyaluronic acid (HyA-TA) hydrogel with a concentration of 2% w/v. This concentration is modifiable as required. Nonsterile HyA-TA was added to PBS and rolled at 4 °C overnight. Once homogenous, the solution was then double filtered before being split equally into 2 falcon tubes. HRP (15 µl/ml for soft gels, 60 µl/ml for stiff gels) was added to tube 1 and stirred for ~1 min. 0.1 % H_20_2 (15 µl/ml for soft gels, 60 µl/ml for stiff gels) was added to tube 2 and stirred for ~1 min. 3 ml of tube 1 and 3 ml of tube 2 were drawn into two syringes, respectively. These syringes were attached using a gel mixer (pictured) before being extruded simultaneously into a mould at a volume of 200 µl/gel and allowed to gelate (Figure 2.3).

2.2.11 Alizarin Red staining

To evaluate calcium deposition, MSC in monolayer culture were stained with alizarin red (AR) after treatment and 14 days subsequent culture in osteogenic induction media or control media. Cell culture supernatants were removed, and cells were rinsed with PBS prior to being fixed in 100% ethanol for 10 minutes at room temperature. This was removed and cells were rinsed again with PBS prior to the addition of 1% AR. AR was removed after 20 minutes, cells were washed with deionised water, and fixed again with 100 % ethanol. Stained samples were air-dried and images were captured using phase transmission microscope (Olympus, UK). Semi-quantitative analysis of AR staining was done through extraction of the dye using 10% cetylpyridinium chloride and measurement of absorbance at 540 nm.

2.2.12 Rat femoral defect model

2.2.12.1 Surgical procedure

Critically sized (5 mm) femoral defects were created in immune-competent adult Wistar Han rats (>12 weeks old) following an established procedure [193]. Hydrogels were made in a custom silicon mold and were press-fit into the defect site, and repair tissue was harvested for analysis at 1 week post-implantation. One defect was created per animal and n=9 hydrogels were implanted per condition. Briefly, anaesthesia was induced and maintained by isoflurane-oxygen throughout the surgery. The rats were also injected with buprenorphine and meloxicam to provide pain relief during and after surgery. The shaft of the left femur was exposed by dissection and the periosteum was scraped back to allow access to the bone. A weight-bearing polyetheretherketone (PEEK) internal fixation plate was secured to the exposed femur with four screws into pre-drilled holes. A 5 mm mid-diaphyseal defect was then created using a dental drill fitted with 2 small circular parallel saw blades welded to a narrow straight rod separated with a 5 mm spacer. The defect site was thoroughly irrigated with saline to remove bone debris before it was treated with a hydrogel. The wounds were closed with sutures and the rats were allowed to recover. On dates of scheduled explant retrieval, rats were sacrificed by CO_2 asphyxiation. The femur, with the PEEK plate fixator intact, was carefully separated from the adjacent hip and knee joints for analysis.

2.2.12.2 Characterization of immune cell subsets and gene expression analysis

Tissue surrounding the hydrogel, and the hydrogel itself, were harvested at 1 week post-surgery and cells were recovered by digestion in a Collagenase digestion cocktail (Collagenase D (2 mg/ml), DNAse I (0.1 mg/ml) and Hyaluronidase (0.5 mg/ml) for 30 minutes at 37°C and 255 rpm. Cells were blocked by incubating in anti-CD32 (Rat Fcγ) blocker (BD Pharmingen; 1 µg/ml) for 10 min. To discriminate live from dead cells, cells were stained with LIVE/DEAD Aqua for an additional 30 min. Staining was performed with fluorescent antibodies specified in Table 2.3. Cells were acquired using the Aurora cytometer (Cytek). Analysis was completed using FlowJo version 9.2 (Tree Star). In order to assess gene expression, digested single-cell suspensions were lysed in lysis buffer

(ROCHE) and RNA was isolated according to the manufacturer's protocol (ROCHE). cDNA was made using the High-Capacity cDNA reverse transcription kit (Applied Biosystems) and genes were assessed as detailed in Table 2.5.

2.2.13 Statistical Analysis

All experiments were performed in at least three healthy donors (defined by N), or in at least 3 replicates for MSC work (defined by n). Data was assessed using one-way ANOVA for the analysis of more than two groups, with Dunnett's post-test (against controls) or Tukey's multiple comparisons test, where applicable. Kruskal-Wallis test was used for analysis of nonparametric data as determined by normality test. Student's t-test was used for analysis of two groups only. All statistical analysis was performed on GraphPad Prism™ 9.00 (GraphPad Software) where p value < 0.05 were deemed significant and denoted by an asterisk. *$p \leq 0.05$, **$p \leq 0.01$, ***$p \leq 0.001$, ****$p \leq 0.0001$.

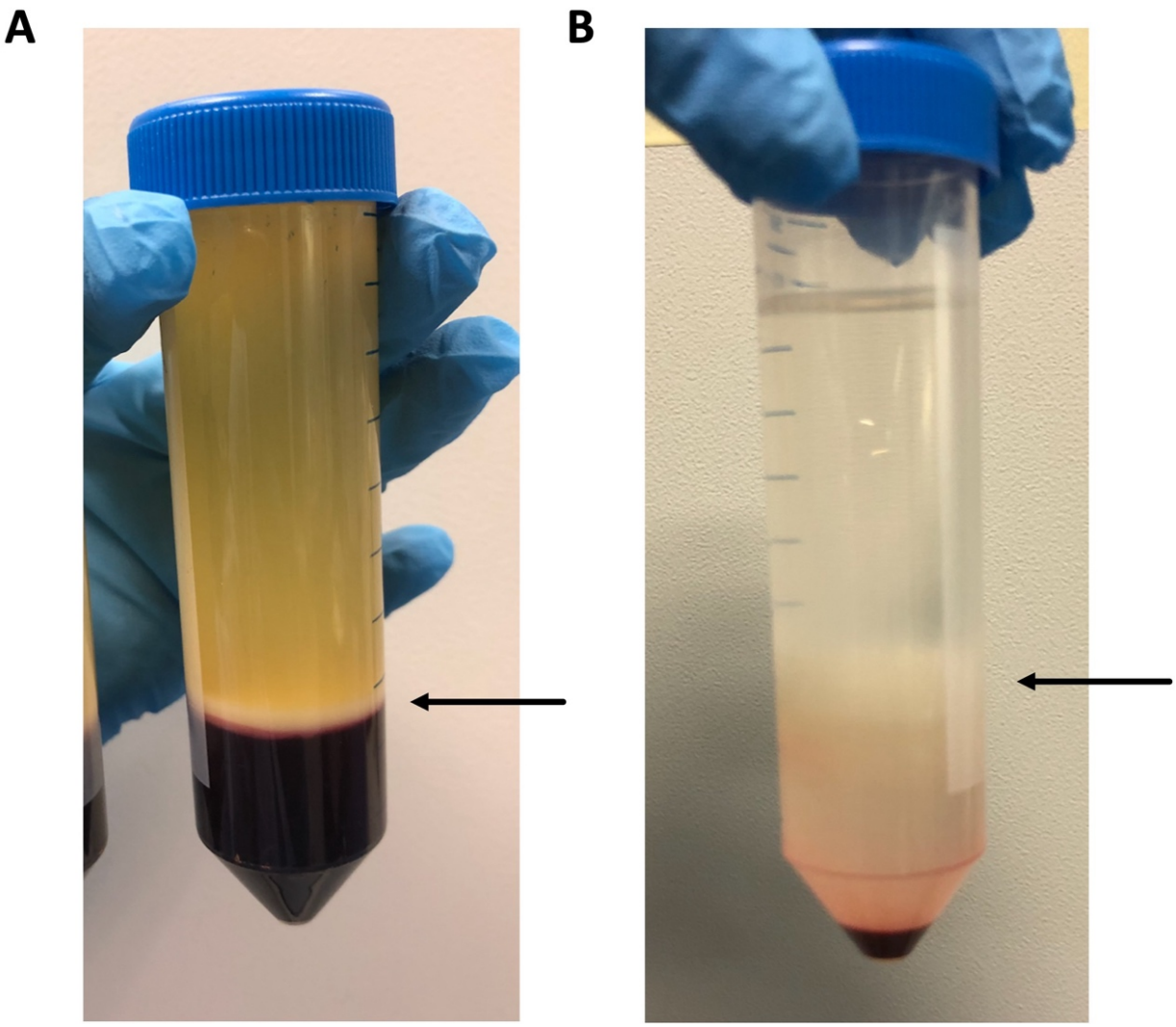

Figure 2.1: Isolation of PBMCs from buffy coat packs.

Blood was diluted 1 in 2 with sterile PBS and centrifuged at 2500 rpm for 10 mins with the brake off. After separation, the leukocyte-rich buffy coat layer (A) was removed and diluted in sterile PBS before being layered over Lymphoprep and centrifuged at 2000 rpm for 20 mins at room temperature with the brake off. The mononucleocyte-rich layer (B) at the interface between PBS and the lymphoprep layer was removed for further processing, and the waste discarded.

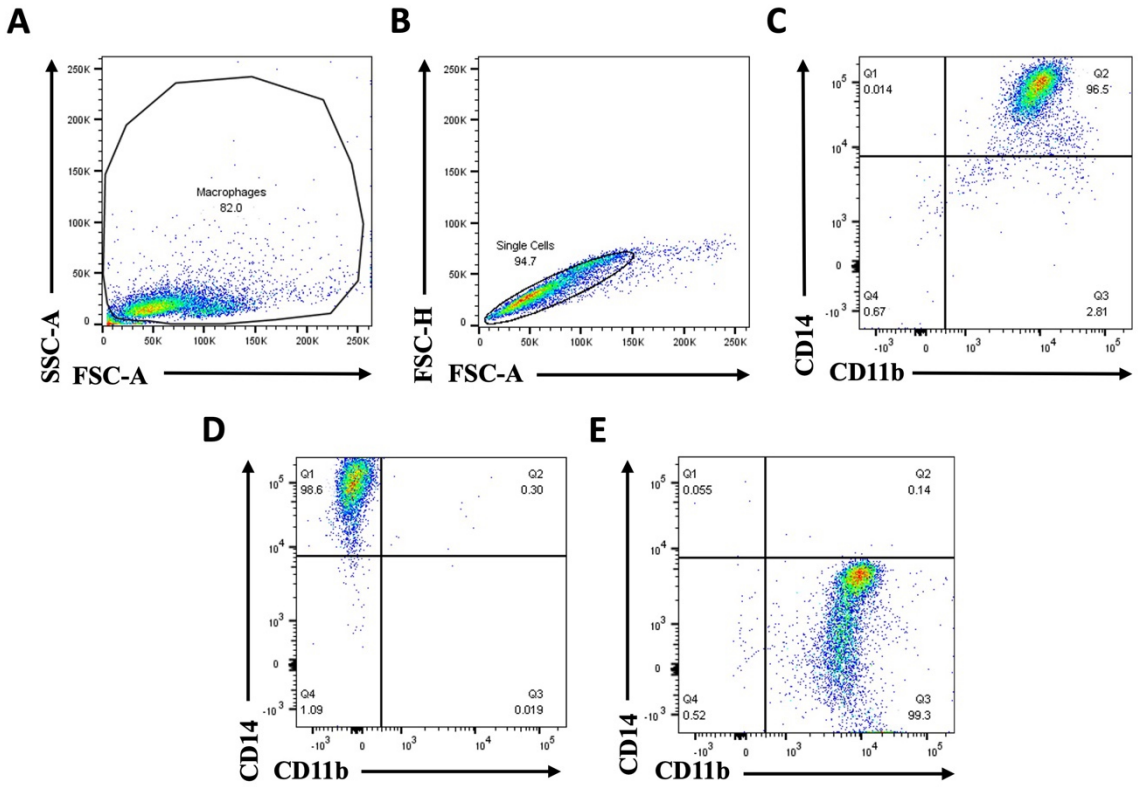

Figure 2.2: Analysis of macrophage purity by flow cytometry.

Human monocyte-derived macrophages were identified as $CD14^{+}/CD11b^{+}$ by flow cytometry. (A) Dead cells and cellular debris were excluded on the basis of size (FSC) and granularity (SSC). (B) Single cells were then gated on based on FSC-H and FSC-A. (D-E) FMO defined CD14 vs CD11b gate was then applied to macrophage sample to determine (C) purity of the macrophage population.

A

DUFFY LAB

Procedure	Double Filtration
To be carried out	Under aseptic conditions (within cell culture fume hood)
Materials Required	Liquid to filter in 50 ml falcon
	2x sterile 50 ml falcons
	2x sterile 10 ml syringes
	2x sterile 18G needles
	2 x sterile syringe filters

Figure 1: Double filtration procedure

B

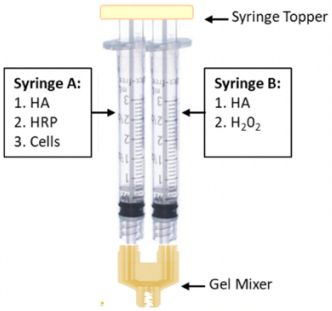

Figure 2: Gel forming apparatus

C

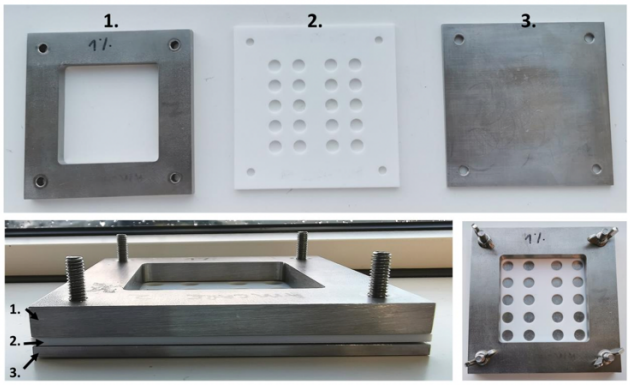

Figure 3: Gel moulds set-up. Each well holds 200 µL of gel. Can be sterilised using an autoclave.

Figure 2.3: Hyaluronic acid hydrogel fabrication.

HyA-TA is dissolved in PBS, double filtered under a laminar flow hood, and split into two equal parts. 15-60 µl /mL HRP is added to one part and stirred. 15-60 µl /ml H_20_2 is added to the second part and stirred (A). 3 mL HA+HRP is drawn into a 3 mL syringe (syringe A) using an 18G needle. 3 mL HA+ H_20_2 is drawn into a second syringe (syringe B) using an 18G needle. Syringe A and and syringe B are attached to a gel mixer (B) and extruded simultaneously into a gel mould (C) in volumes of 200 µl. *Images taken from DuffyLab protocol.*

Chapter Three

Macrophage metabolic profile is altered by hydroxyapatite particle size

This chapter has been peer-reviewed and published in *Acta Biomaterialia* (DOI: 10.1016/j.actbio.2023.01.058, 2023)

3.1 Introduction

Immunometabolism is a rapidly expanding field that focuses on the intimate link between the metabolic phenotype of immune cells and their functionality. Innate immune cells such as macrophages generally rely on oxidative phosphorylation as their basal means of energy production but exhibit a shift to favour glycolysis on exposure to cellular stressors and under conditions in which oxygen is limiting. This in turn allows for the rapid generation of metabolic and biosynthetic intermediates that contribute to the production of inflammatory mediators and reactive oxygen species (ROS) [161]. Such metabolic reprogramming is generally associated with polarisation towards a pro-inflammatory phenotype and, unsurprisingly, dysregulated immunometabolism has now been recognised as a feature of many immune mediated diseases and cancers [163, 194-196]. While it is well accepted that pathogen-associated molecules such as lipopolysaccharide (LPS) can promote a shift to favour glycolysis in both murine and human macrophages, focus is now moving to identify other drivers of altered macrophage metabolism in disease-specific contexts. For example, it has recently been shown that exposure to damage or disease-associated molecular patterns (DAMPs) such as gout-associated monosodium urate (MSU) crystals, osteoarthritis-associated calcium-containing crystals, or cholesterol crystals that are deposited in atherosclerotic plaques, drive a glycolytic metabolic profile, concomitant with the polarisation of primary human macrophages to an M1-like phenotype [197-199].

While MSU and cholesterol crystals represent endogenous disease-associated particulates, particulate materials derived from exogenous sources such as bone-mimetic hydroxyapatite (HA), commonly employed in the development of scaffolds for bone tissue engineering and as a coating for orthopaedic implant materials given its known osteoconductive properties, are now emerging as modulators of immune response with potential implications for immunometabolism [200-204]. Indeed, HA has been well studied in the context of macrophage responses, and it has been found that accumulation and recognition of HA particulates can have potent effects on subsequent immune cell-driven inflammatory responses. For example, it has been shown that the shape and size

of HA particles can differentially modulate immune cell effector function, with needle-shaped [114, 205] and micron-sized [199] particles preferentially driving an inflammatory monocyte and macrophage phenotype, characterised by production of pro-inflammatory cytokines such as TNF, IL-6, and IL-1β. These cytokines are well documented contributors to the FBR at the orthopaedic implant site and have also been shown to contribute to osteoclast differentiation and activation, leading to bone resorption, periprosthetic osteolysis and eventual aseptic implant loosening [206]. As a result, orthopaedic biomaterial design is relying on insights gained from immunological studies to mitigate these destructive processes and facilitate superior implant integration and tissue regeneration.

Nano-sized hydroxyapatite (nanoHA) has become an attractive alternative to traditionally used micronHA given its ability to promote an anti-inflammatory macrophage phenotype and exert pro-osteogenic effects on mesenchymal stem cells (MSC) [126]. NanoHA has been shown to promote differentiation of osteoblasts [207], with recent work further exploring the interaction of nanoHA with the adaptive immune cell component to regulate osteoblastic differentiation [208]. Despite advances made in recent years, there remains a pressing need for more thorough mechanistic studies into how particulate biomaterials, both in terms of their composition and tuneable parameters, drive immune cell responses preclusive to repair and those that facilitate tissue regeneration. In this chapter, HA particles in the micron and nanometre range (referred to hereon in as micronHA and nanoHA respectively) are used to investigate whether hydroxyapatite particle size impacts on the metabolism of primary human macrophages.

3.2 Hypothesis

Hydroxyapatite particle size alters the metabolism of primary human macrophages.

3.3 Specific Aims

- To investigate the effect of micronHA and nanoHA particles on metabolic profile of primary human macrophages.

- To examine a potential link between metabolic profile and micronHA-driven pro-inflammatory responses in primary human macrophages.
- To establish whether metabolic intervention could offer a potential therapeutic avenue in the context of bone-based biomaterials.

3.4 Results

3.4.1 Micron and nano-sized hydroxyapatite particles are not contaminated with endotoxin.

Endotoxin contamination poses a major challenge in assessment of the cellular response to biomaterials [209, 210]. To ensure micronHA and nanoHA particles were not contaminated with endotoxin prior to experimentation on primary human macrophages, HA particles were tested for the presence of LPS using the HEK-Blue™ TLR4 assay system. HEK-Blue™ TLR4 cells were stimulated with either LPS (0.1-100 ng/ml; positive control), micron HA (250 µg/ml), or nanoHA (250 µg/ml) for 24 hours. Supernatants were then incubated with HEK-blue detection medium for 30 minutes at 37 °C for detection of SEAP expression and read at 650 nm. Results show that micronHA and nanoHA particle preparations were not contaminated with endotoxin such that the threshold for HEK-Blue™ cell TLR4 activation was reached, and therefore particles were deemed suitable for experimental use with primary human macrophages (Figure 3.1).

3.4.2 Micron and nano-sized hydroxyapatite particles do not impact on cell viability.

Once micron and nanoHA particles were found to be endotoxin-free, it was next of interest to assess whether treatment with either particle preparation impacted on primary human macrophage viability. To this end, a neutral red cytotoxicity assay was used (TOX4, Sigma). Neutral red is a dye that is transported across the cell membrane of live cells and accumulates in the lysosome. Neutral red dye can then be extracted by cell lysis and quantified spectroscopically. Primary human macrophages were treated with micron or nanoHA (250 µg/ml) for 24 hours before being incubated with neutral red reagent for one hour at 37 °C. Cells were then washed thoroughly to ensure the removal of neutral red from the surrounding media. Neutral red dye was extracted from the remaining monolayer and read at 690 and 540 nm for quantification. Micron and nanoHA were found to not significantly impact on the viability of primary human macrophages (Figure 3.2).

3.4.3 MicronHA particles, but not nanoHA, upregulate surrogate markers of glycolysis in primary human macrophages.

It has previously been demonstrated that micronHA treatment results in the polarisation of primary human macrophages towards a pro-inflammatory phenotype, while nanoHA treatment preferentially results in anti-inflammatory macrophage polarisation [126, 199]. As pro-inflammatory immune cell function is strongly associated with a metabolic shift to favour glycolysis [161], the expression of genes encoding for key glycolytic markers upon micron and nanoHA treatment was investigated. Primary human macrophages were treated with micron or nanoHA particles over 3, 6, and 24 hours, or the positive control, LPS (100 ng/ml), for 24 hours, before established markers of glycolysis were assessed using RT-qPCR. It was observed that *GLUT1*, which encodes for the glucose transporter, and *HK2*, the rate-limiting enzyme in glycolysis, were significantly upregulated at 6- and 24-hours post-stimulation with micronHA particles (Figure 3.3 A-B). The mRNA encoding glyceraldehyde-3-phosphate dehydrogenase (*GAPDH*) and pyruvate kinase M2 (*PKM2*), key enzymes involved in regulation of glycolysis, were also found to be significantly upregulated at 24 hours post micronHA stimulation (Figure 3.3, C, E). An increase in phosphofructokinase (*PFKFB3*) was observed at 6 and 24 hours in micronHA particle-treated macrophages, albeit this was not significant (Figure 3.3 D). This was also the case for the transcription factor, *HIF1α*, which is known to be upregulated in macrophages undergoing a metabolic shift towards glycolysis, where it translocates to the nucleus to upregulate expression of pro-inflammatory cytokines [211, 212] (P=0.08 at 24 hours) (Figure 3.3 F). In contrast, nanoHA did not appear to impact on expression of any of the glycolytic genes assessed (Figure 3.3, A-F). This suggests that exposure of macrophages to micronHA particles, but not nanoHA, enhances transcription of key genes involved in glycolysis. Interestingly, micronHA particles were also capable of moderately increasing glycolytic genes *GLUT1, HK2, GAPDH,* and *HIF1α* in macrophages pre-polarised with IL-4, although not to as great an extent as that achieved upon micronHA stimulation of untreated macrophages alone (Figure 3.5). This suggests that micronHA particles are capable of driving expression of glycolysis-associated genes even in the presence of M2 polarising stimuli, which are known to induce a greater reliance on oxidative phosphorylation.

Having observed an upregulation of key glycolytic markers upon stimulation with micronHA, it was next of interest to validate this at the protein level. GLUT1 and HK2 were chosen, being the glucose transporter and first rate-limiting enzyme in glycolysis respectively, and therefore provide reliable indication that the upregulation observed at the mRNA level is being translated to the protein level. Macrophages were treated with micronHA and nanoHA over 3, 6, and 24 hours, before assessment by immunoblotting. Both GLUT1 and HK2 were found to be upregulated over time, with peak induction occurring at 24 hours post micronHA stimulation (Figure 3.4 A-B). Densitometric analysis revealed a significant increase in GLUT1 and HK2 at 24 hours post micronHA stimulation (Figure 3.4 B). In contrast, nanoHA stimulated macrophages did not drive expression of GLUT1 or HK2, with levels found to be comparable to that of untreated control cells (Figure 3.4 A-B).

3.4.4 MicronHA particles upregulate mRNA expression of oxidative phosphorylation-associated *ATP5b* at 24 hours post-stimulation, and do not affect *MFN1* and *MFN2*.

Given the upregulation in surrogate markers of glycolysis as a result of micronHA treatment, it was also of interest to investigate whether genes associated with oxidative phosphorylation were also affected by these HA particles in order to determine whether micronHA was promoting a metabolic shift towards glycolysis, or a more metabolically active macrophage profile overall. To this end, mRNA expression of *ATP5b* (complex V of the electron transport chain) as well as mitofusin-associated *MFN1* and *MFN2* were assessed after 3, 6, and 24 hours of stimulation with micronHA particles (250 µg/ml). *ATP5b* was significantly, albeit moderately (fold change 1.28-2) upregulated at 24 hours post micronHA stimulation (Figure 3.6 A), whilst *MFN1* and *MFN2* expression was not significantly altered as a result of treatment with micronHA (Figure 3.6 B-C).

3.4.5 MicronHA and nanoHA particles differentially impact on mitochondrial fusion and fission.

Alterations in mitochondrial dynamics are closely linked with the metabolic state of immune cells. Mitochondrial ROS (mtROS) production occurs as a result of, and promotes,

pro-inflammatory macrophage polarisation [213-215], and macrophages undergoing a shift to favour glycolysis exhibit a reduction in mitochondrial biogenesis and hence mitochondrial mass [216, 217]. It is also documented that mitochondrial fission, in which mitochondrial networks are broken apart into punctate structures, occurs in macrophages following LPS treatment and is associated with an upregulation in glycolysis [218, 219]. Given the observed upregulation of surrogate glycolytic markers upon micronHA treatment, it was of interest to investigate whether mitochondrial dynamics are altered as a result of stimulation with micron and nanoHA particles. Macrophages were stained with MitoTracker Red™ following stimulation with micron or nanoHA for 24 hours. The mitochondrial networks of micronHA treated macrophages showed significantly more punctate structures and had a lower aspect ratio and eccentricity (measures of deviation from circularity), indicating significantly more mitochondrial fission in micronHA stimulated macrophages compared to untreated and nanoHA-treated counterparts (Figure 3.7 A-C). By contrast, and while not significant, there was a trend towards an increase in mitochondrial aspect ratio and eccentricity upon nanoHA particle stimulation, with mitochondrial structures appearing as fused networks within the macrophages, indicating that nanoHA potentially promotes mitochondrial fusion (Figure 3.7 A-C). While further investigation is required, this data suggests that micronHA particle stimulation promotes mitochondrial fission and hence a reduced reliance on oxidative phosphorylation, whilst nanoHA stimulation appears to slightly promote mitochondrial fusion and suggests a sustained reliance on oxidative phosphorylation.

3.4.6 MicronHA particles alter primary human macrophage metabolism at 6 and 24 hours.

Having observed an upregulation of surrogate markers of glycolysis as a result of micronHA treatment, as well as changes in mitochondrial dynamics in response to micron and nano-sized HA particles, an emerging non-invasive imaging technique termed fluorescence lifetime imaging microscopy (FLIM) was employed to assess overall metabolic profile of macrophages post-particle stimulation. FLIM provides a quantitative live readout of particle-stimulated macrophage metabolism based on the excited state lifetime of endogenously fluorescent NADH. Free NADH has a short emission lifetime and is associated with glycolysis, whereas protein bound NADH has a longer emission lifetime

and is associated with oxidative phosphorylation, thus providing a means to identify both metabolic states. The calculated ratio of bound:free NADH is then used to indicate the metabolic state of the cell, with a lower τ_{avg} corresponding to a glycolytic metabolic profile and vice versa. Primary human macrophages were treated with micron or nanoHA for 6 and 24 hours to assess sustained metabolic profile and imaged using FLIM. A lower τ_{avg} as a result of micronHA stimulation compared to untreated control, and a higher τ_{avg} in nanoHA versus micronHA, was observed at 6 hours (Figure 3.8 A-C). At 24 hours, micronHA stimulated macrophages were found to have a significantly lower τ_{avg} than untreated and nanoHA stimulated macrophages, suggesting a heightened reliance on glycolysis as their primary metabolic pathway (Figure 3.9 B). NanoHA treated macrophages, by contrast, exhibited a significantly higher τ_{avg} than micronHA treated macrophages, suggesting a sustained reliance on oxidative phosphorylation (Figure 3.9 B).

3.4.7 MicronHA particles, but not nanoHA, alter primary human macrophage bioenergetics to favour glycolysis over oxidative phosphorylation.

In order to validate and complement the findings of FLIM analysis, it was next of interest to investigate the effect of HA particle size on the bioenergetic profile of macrophages. To this end, macrophage bioenergetics were assessed using the Seahorse XF analyser. Macrophages were seeded into a Seahorse microplate and stimulated with micron and nanoHA particles for 3, 6, or 24 hours. They were then placed in a Seahorse XF96 analyser in which the extracellular acidification rate (ECAR) and oxygen consumption rate (OCR) before and after injections of metabolic inhibitors oligomycin, FCCP, rotenone and antimycin A, and 2-deoxyglucose (2-DG) were measured. The basal and maximum rates of glycolysis were increased at all timepoints with micronHA stimulation, with significance achieved at 3 and 6 hours post particle treatment (Figure 3.10 B-C). NanoHA stimulation, by contrast, did not upregulate basal or max glycolysis in macrophages (Figure 3.11 B-C). Most notably, the ECAR:OCR ratio of micronHA treated macrophages was increased at all timepoints, with a significant increase occurring at 6 hours post micronHA stimulation (Figure 3.14 A). NanoHA treatment resulted in no observable increase in ECAR:OCR when compared to untreated control cells (Figure 3.14 B). Max respiration was modestly

increased upon micronHA stimulation (Figure 3.12). NanoHA did not appear to alter macrophage respiration (Figure 3.13).

3.4.8 Inhibition of micronHA particle uptake decreases expression of surrogate markers of glycolysis at the mRNA level in primary human macrophages.

In order to further investigate the mechanism by which metabolic alteration is induced in primary human macrophages in response to micronHA stimulation, and thus link metabolic phenotype with pro-inflammatory polarisation, it was investigated whether particle uptake is required for the observed effects on macrophage metabolism and effector function. To test this, macrophages were treated with the inhibitor of actin polymerization, cytochalasin B (5μm), for 45 minutes prior to stimulation with micronHA particles, and then assessed for expression of surrogate markers of glycolysis *GLUT1*, *HK2*, *PKM2*, *PFKFB3*, *GAPDH*, and *HIF1α*. It was found that inhibition of phagocytosis significantly attenuated the upregulation of all surrogate markers assessed at 24 hours post-stimulation (Figure 3.15 A-F), with additional attenuation of *PFKFB3* at 6 hours post micronHA-stimulation (Figure 3.15 D).

3.4.9 Inhibition of micronHA particle uptake decreases expression of pro-inflammatory cytokines in primary human macrophages.

In order to investigate whether the cytochalasin B-mediated attenuation of micronHA-driven mRNA expression of glycolytic genes was linked with the known micronHA-induced pro-inflammatory phenotype [126], and thus confirm that micronHA particle uptake was linked to pro-inflammatory polarisation, the expression of pro-inflammatory cytokines IL-6, TNF, and IL-8 was assessed by ELISA. It was seen that pre-treatment of primary human macrophages with cytochalasin B resulted in a decreased secretion of micronHA-induced IL-6 (Figure 3.16 A) and a trend towards reduced expression of TNF (Figure 3.16 B) as well as moderate reduction of IL-8 (Figure 3.16 C), together with the previous results suggesting that micronHA-induced metabolic rewiring to favour glycolysis and pro-inflammatory macrophage polarisation is dependent on particle uptake.

3.4.10 Glycolytic inhibitors 2-DG and 3PO decrease pro-inflammatory macrophage marker expression at the mRNA level and attenuate pro-inflammatory cytokine secretion in primary human macrophages.

Given the established link between macrophage metabolism and polarisation state, it was of interest to investigate whether metabolic alteration as a result of particle stimulation could be linked with the known effect of HA particle size on macrophage phenotype [126]. RT-qPCR was used to investigate mRNA expression of M1-like macrophage markers *CXCL9, CXCL10*, *CXCL11,* and *CCL19* in macrophages treated with micron and nanoHA in the presence or absence of glycolytic inhibitors 2-DG (25 mM) or 3PO (10 μM). Results demonstrate that 2-DG potently inhibited micronHA-induced expression of *CXCL9* and *CCL19* at 6 and 24 hours post-stimulation (Figure 3.17 A, D). *CXCL10* and *CXCL11* were more highly expressed at 6 hours and both genes were inhibited by 2-DG at this time-point (Figure 3.17 B, C). 3PO, an inhibitor of PFKFB3, significantly reduced mRNA expression of *CXCL10* at 6 hours post micronHA stimulation (Figure 3.19 B), while there was a trend towards decreased expression of *CXCL9* and *CXCL11* (Figure 3.19 A, C). Although not significant, a decrease in *CCL19* expression at 6 and 24 hours post micronHA stimulation was also observed (Figure 3.19 D). To validate these findings at the protein level, secretion of the pro-inflammatory cytokines IL-6, TNF, and IL-8 were assessed by ELISA. Pre-treatment of macrophages with 2-DG and 3PO was found to significantly decrease micronHA-induced production of IL-6 and TNF, complementing the observed attenuation of pro-inflammatory markers at the mRNA level (Figure 3.18 A-B, Figure 3.20 A-B). Production of pro-inflammatory chemokine IL-8 was assessed given its contributory role in recruitment of inflammatory cells and propagation of tissue destructive processes, with a significant decrease in micronHA-driven induction observed upon 2-DG pretreatment (Figure 3.18 C), and a trend towards a reduction in micronHA-driven IL-8 secretion upon 3PO treatment (Figure 3.20 C).

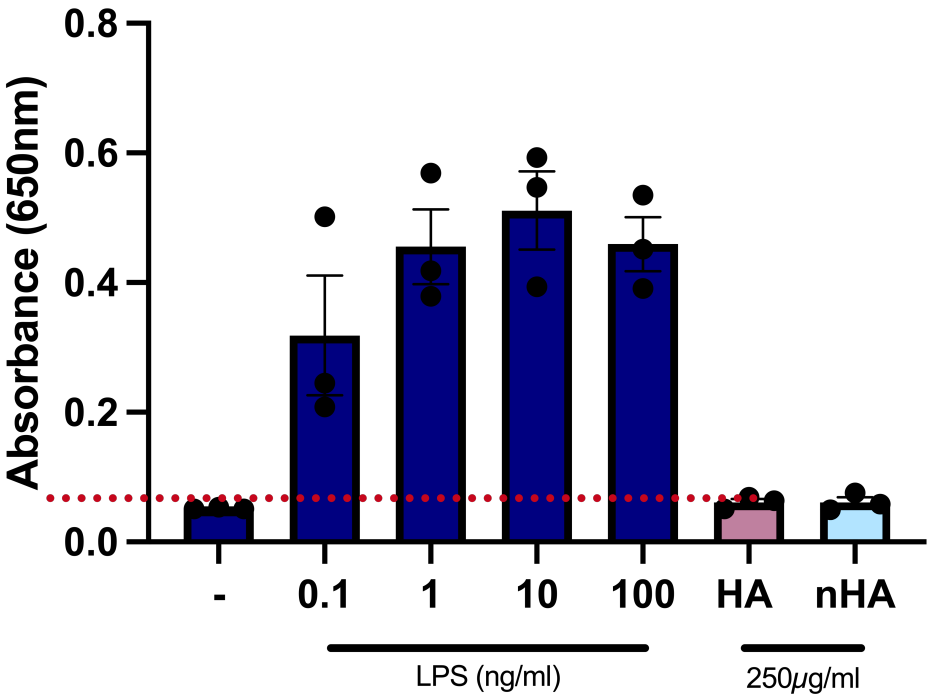

Figure 3.1 MicronHA and nanoHA particles are not contaminated by endotoxin.

HEK-blue^{TM} cells (5 x 10^5 cells/ml) were left either untreated, stimulated with LPS (0.1-100 ng/ml) (as a positive control) or stimulated with micronHA or nanoHA (250 µg/ml) for 24 hours. The expression of SEAP, under the control of NF-kB and AP-1, as a result of incubation with LPS or particulate preparations was measured by absorbance at 650 nm. Data are represented as mean ± SEM (n=3).

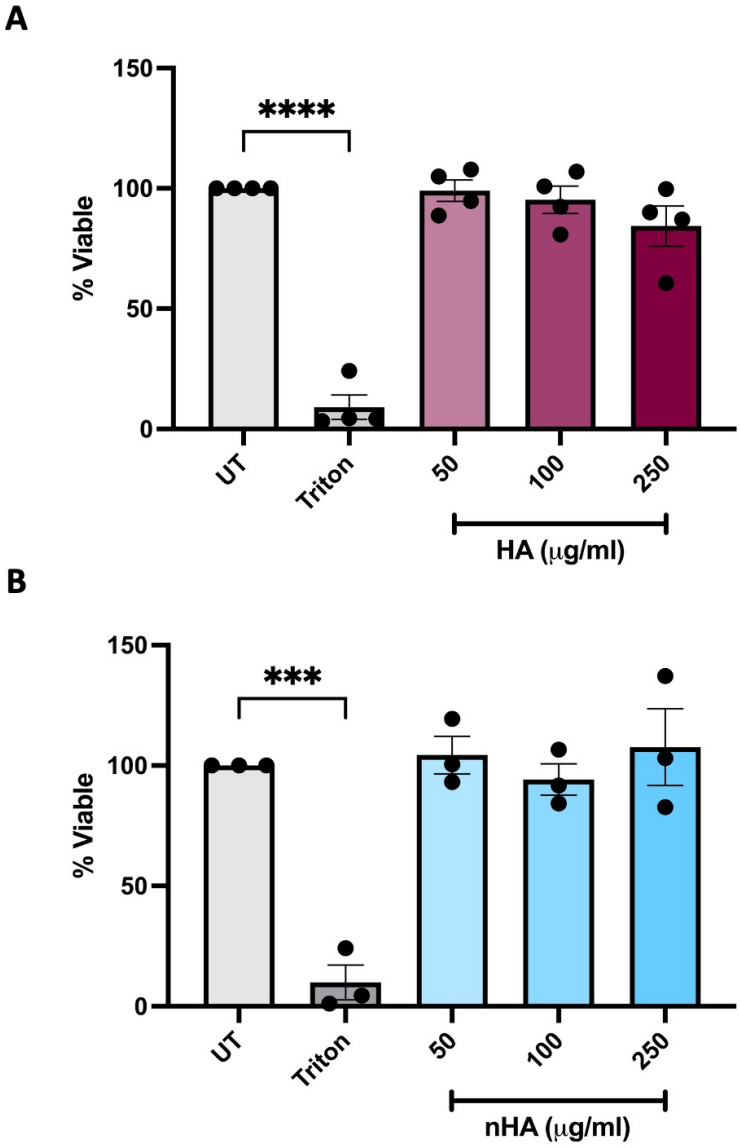

Figure 3.2 MicronHA and nanoHA particles do not significantly impact on primary human macrophage viability.

Primary human macrophages were seeded at a density of 1 x 10^6 cells/ml and stimulated with micronHA **(A)** or nanoHA **(B)** (50, 100, or 250 μg/ml) 24 hours. A neutral red based cytotoxicity assay (TOX4; Sigma) was used to assess cell viability. Pooled data (N=3-4 human donors) depicts percentage viability normalised to donor-matched untreated macrophages and data is depicted as mean ± SEM. Triton X-100 was used as a positive control. Data were analysed using one-way ANOVA with Dunnett's post-test. (***P≤0.001, ****P≤0.0001).

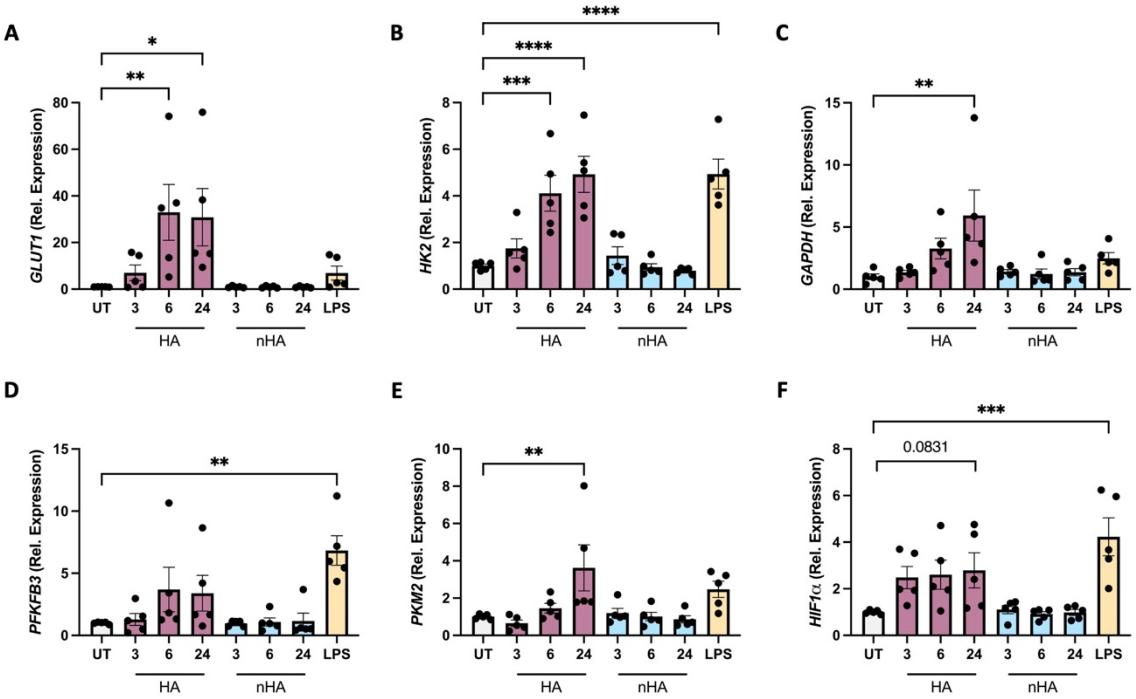

Figure 3.3 MicronHA particles upregulate surrogate markers of glycolysis at the mRNA level.

Primary human macrophages ($1x10^6$ cells) were stimulated with micron or nanoHA particles (250 µg/ml) for 3, 6, or 24 hours. mRNA expression of glycolytic markers **(A)** *GLUT1*, **(B)** *HK2*, **(C)** *GAPDH*, **(D)** *PFKFB3*, **(E)** *PKM2*, and **(F)** *HIF1α* were assessed by RT-qPCR. Pooled data (N=5) is represented as mean ± SEM. Bar graphs depict fold change in gene expression compared to untreated control and normalized to *β-actin* housekeeping gene. Data were analysed using one-way ANOVA with Tukey's post-test (*P≤0.05, **P≤0.01, ***P≤0.001, ****P≤0.0001).

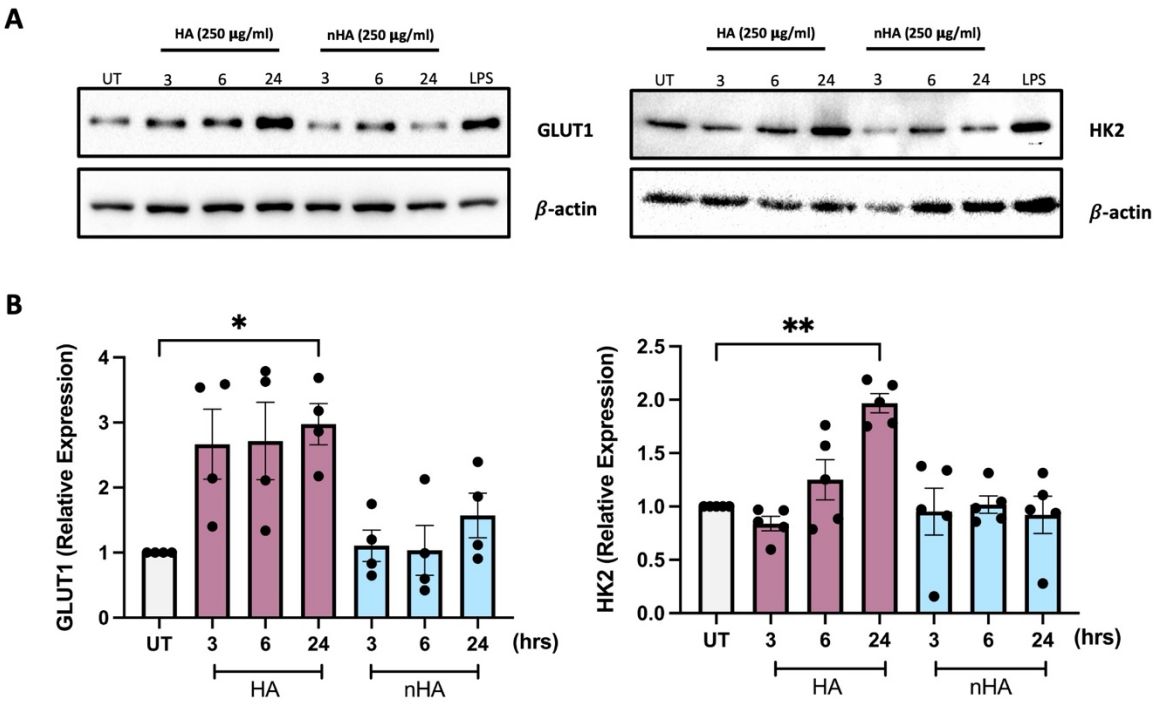

Figure 3.4 MicronHA particles upregulate expression of the glycolytic markers GLUT1 and HK2.

Primary human macrophages (1x10^6 cells) were stimulated micronHA or nanoHA (250 µg/ml) for 3, 6, or 24 hours. Protein production of glycolytic markers HK2 and GLUT1 was analysed by western blot. **(A)** Representative western blots for GLUT1 and HK2 in whole cell lysates in response to micronHA or nanoHA particles after 3, 6, and 24 hour stimulation. **(B)** Pooled data (HK2, N=5; GLUT1, N=4) depicting densitometric analysis of immunoblots using BioRad Software. Bar graphs illustrate mean ± SEM increase in protein expression relative to untreated control and normalised to *β-actin* housekeeping protein. Data were analysed using one-way ANOVA with Tukey's post-test (*P≤0.05, **P≤0.01).

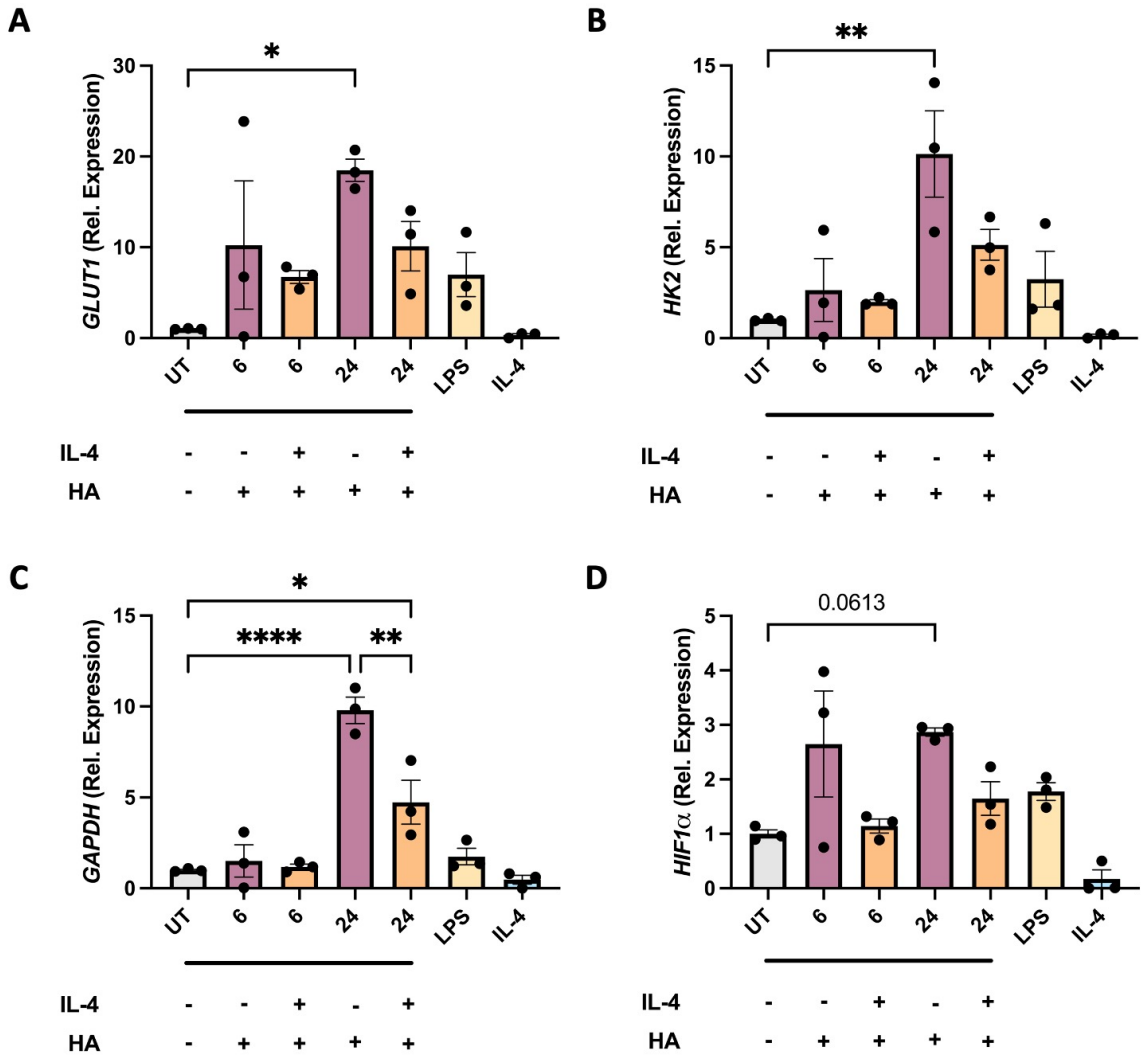

Figure 3.5 IL-4 pre-polarised macrophages upregulate glycolytic genes upon exposure to micronHA particles to a lesser extent than unpolarised macrophages.

Primary human macrophages (1 x 10^6 cells) were treated with micronHA (250 µg/ml) for 6 and 24 hours with and without 24-hour pre-treatment with IL-4. mRNA expression of **(A)** *GLUT1* **(B)** *HK2* **(C)** *GAPDH*, and **(D)** *HIF1α* were analysed by RT-qPCR. Pooled data (N=3) is represented as mean ± SEM. Data were analysed using one-way ANOVA with Tukey's post-test (*P≤0.05, **P≤0.01, ****P≤0.0001).

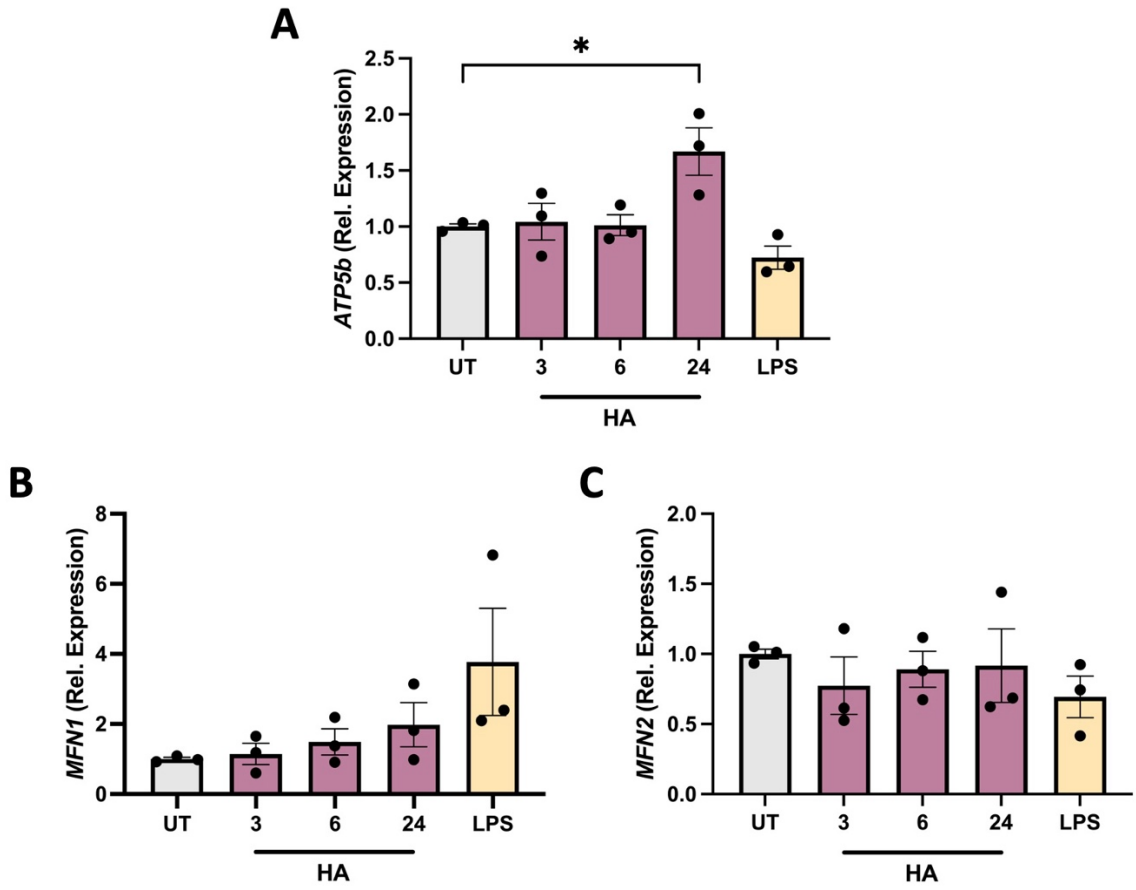

Figure 3.6 Primary human macrophages increase *ATP5b* expression at 24 hours post micronHA stimulation.

Primary human macrophages (1 x 10^6 cells) were treated with micronHA (250 µg/ml) for 3, 6, and 24 hours. mRNA expression of **(A)** *ATP5b* **(B)** *MFN1* **(C)** *MFN2* were analysed by real-time PCR. Pooled data (N=3) is represented as mean ± SEM. Data were analysed using one-way ANOVA with Tukey's post-test (*P≤0.05).

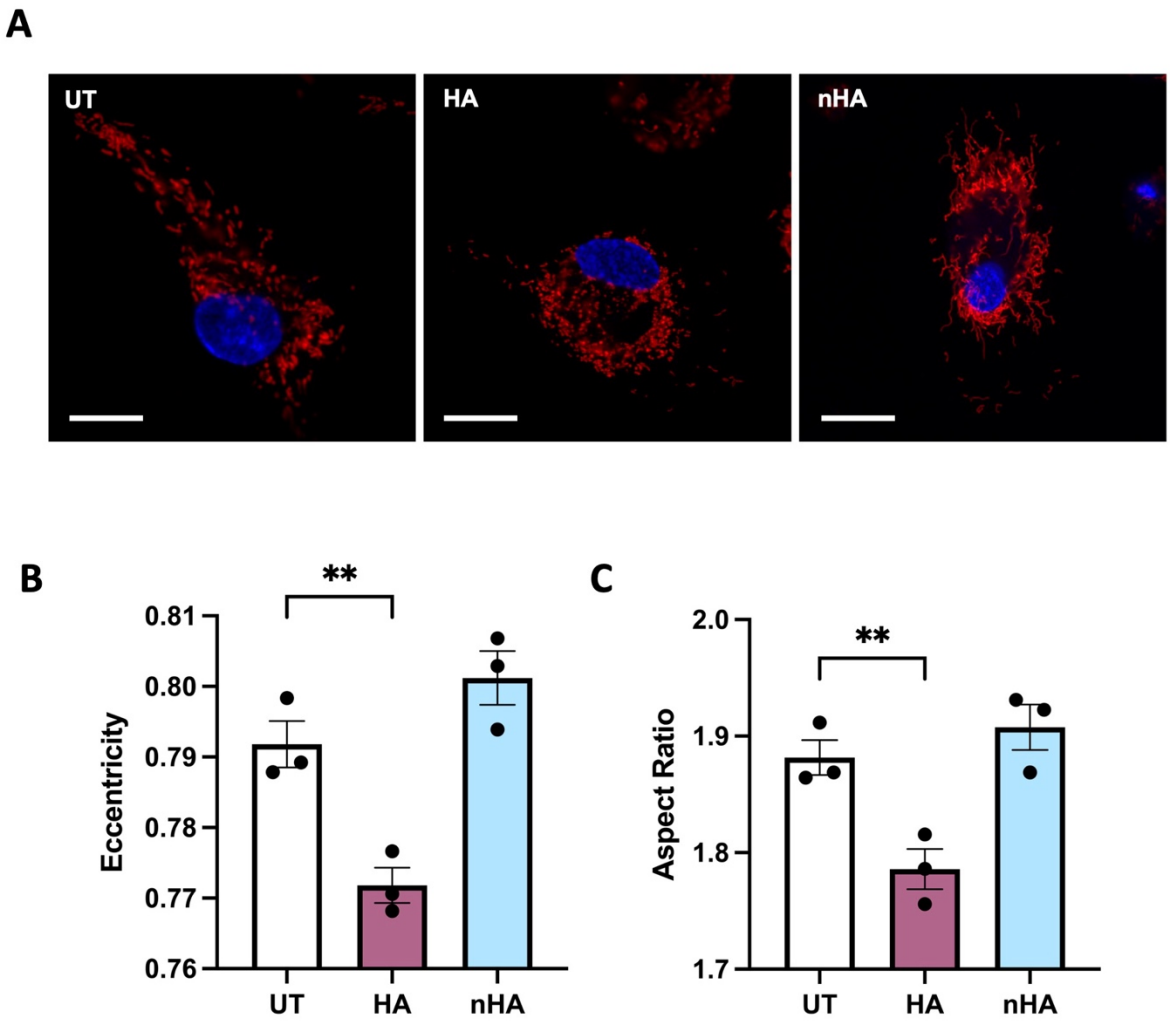

Figure 3.7 MicronHA particles promote mitochondrial fission.

Primary human macrophages (1x10^6 cells/condition) were treated with micron or nanoHA (250 µg/ml) for 24 hours. Cells were stained with MitoTracker Red^{TM} (Invitrogen) at a concentration of 50 nm and Hoechst 33342 (5 µg/ml) for nuclear visualisation 30 mins prior to imaging. Cells were washed with PBS and imaged using a fluorescent microscope (Leica SP8 Scanning confocal). **(A)** Representative images (with zoom) of stained mitochondrial network of untreated, micronHA, and nanoHA stimulated macrophages, scale bar = 5 µM. Pooled data (N=3) of shape parameters of **(B)** mitochondrial eccentricity and **(C)** aspect ratio were determined using CellProfiler. Data are represented as mean ± SEM and were analysed using one-way ANOVA with Tukey's post-test (**P<0.01).

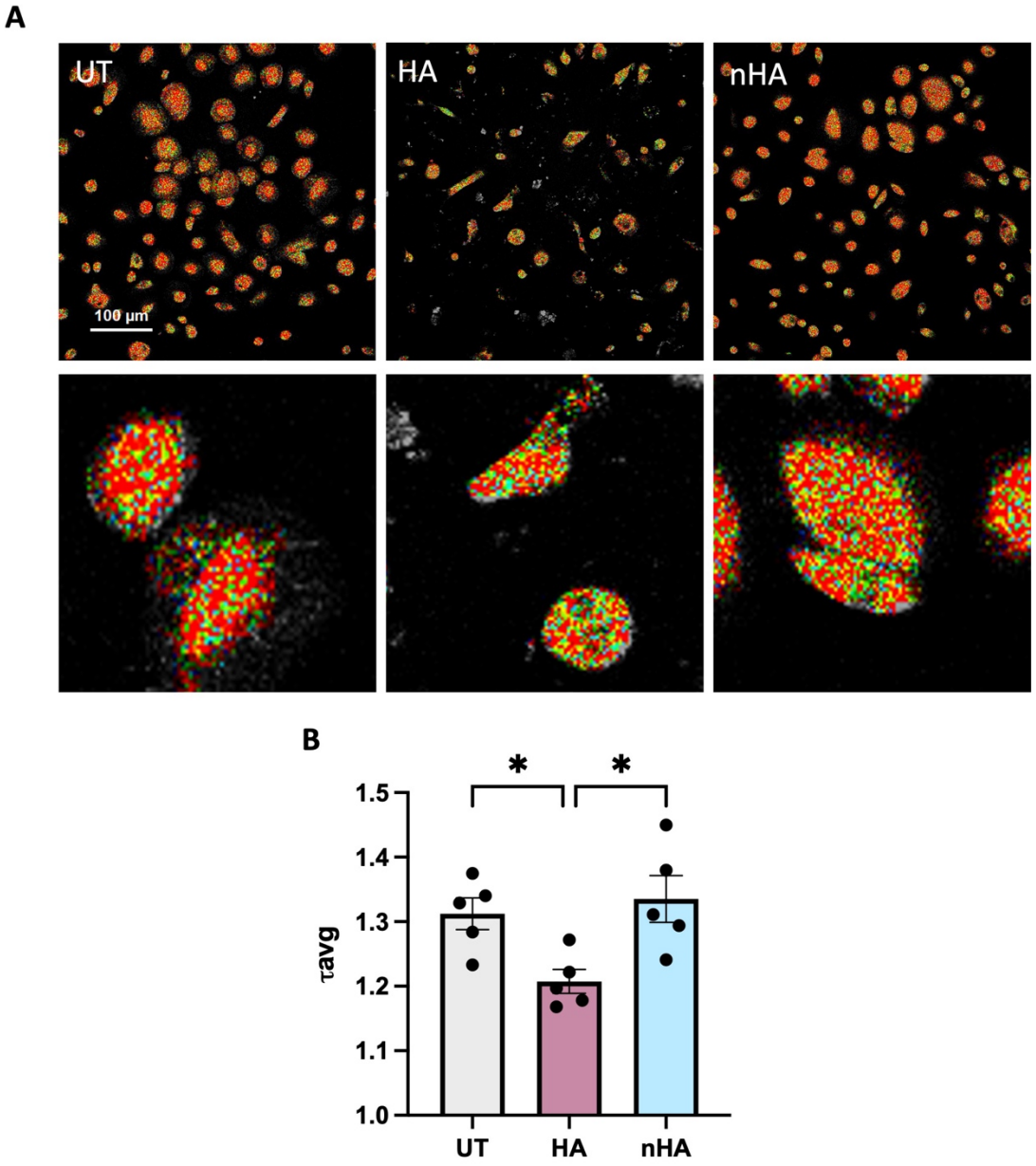

Figure 3.8 MicronHA particles alter macrophage metabolism at 6 hours.

Primary human macrophages (1x10^6 cells) were stimulated with micronHA or nanoHA particles (250 µg/ml) for 6 hours. Cells were then imaged using Fluorescence lifetime imaging microscopy (FLIM) for the detection of the endogenously fluorescent metabolic cofactor NAD(P)H. **(A)** Representative images of untreated, micron, or nanoHA treated macrophages. **(B)** Bar graph representing the ration of bound:free NADH (τavg). Pooled data (N=3) is represented as mean ± SEM. Data were analysed using one-way ANOVA with Tukey's post-test (*P≤0.05). *FLIM analysis performed by Nuno G.B. Neto.*

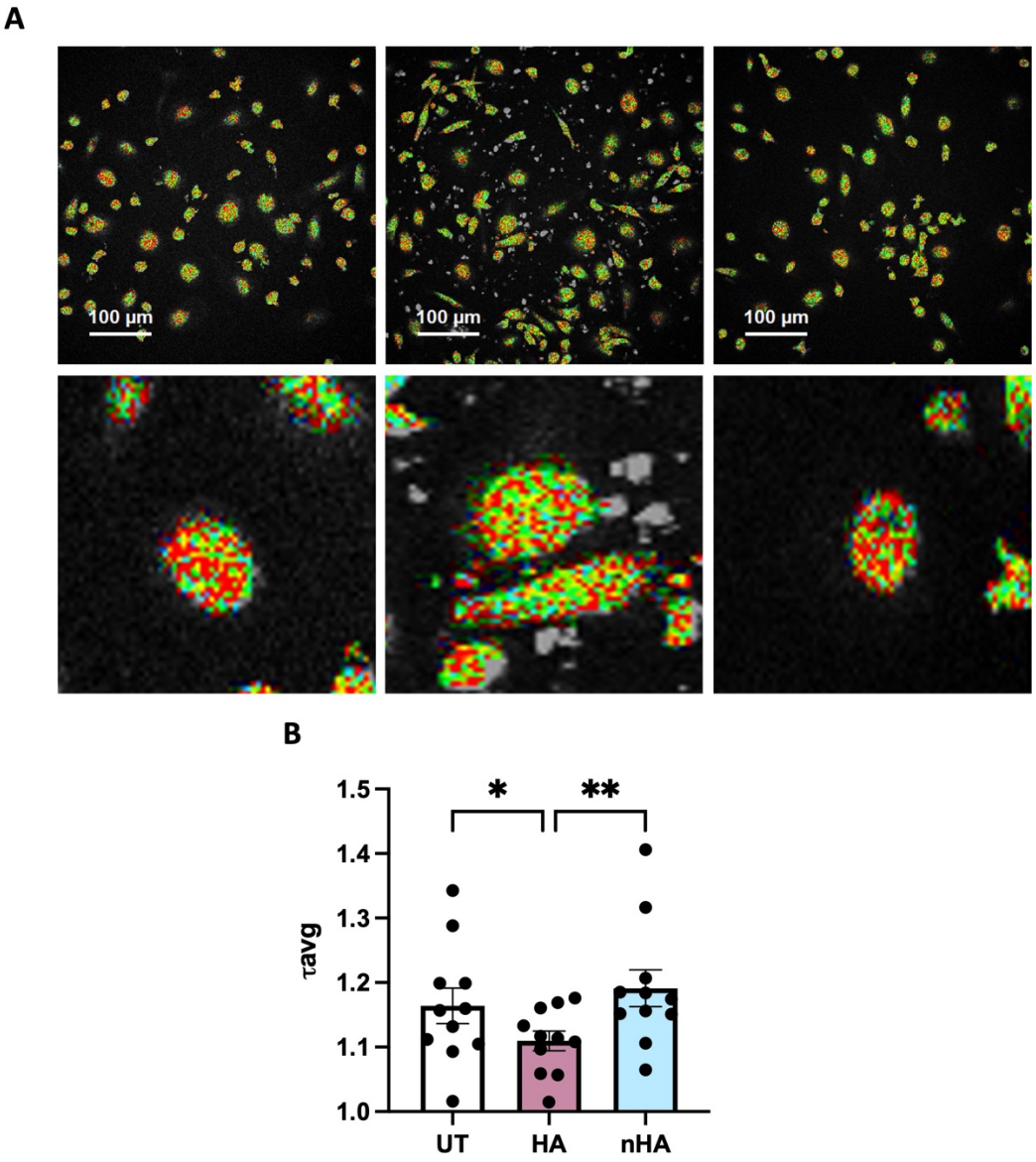

Figure 3.9 MicronHA particles alter macrophage metabolism at 24 hours.

Primary human macrophages (1x10^6 cells) were stimulated with micronHA or nanoHA particles (250 µg/ml) for 24 hours. Cells were then imaged using Fluorescence lifetime imaging microscopy (FLIM) for the detection of the endogenously fluorescent metabolic cofactor NAD(P)H. **(A)** Representative images of untreated, micron, or nanoHA treated macrophages. **(B)** Bar graph representing the ration of bound:free NADH (τavg). Pooled data (N=11) is represented as mean ± SEM. Data were analysed using one-way ANOVA with Tukey's post-test (*P≤0.05, **P≤0.01). *FLIM analysis performed by Nuno G.B. Neto.*

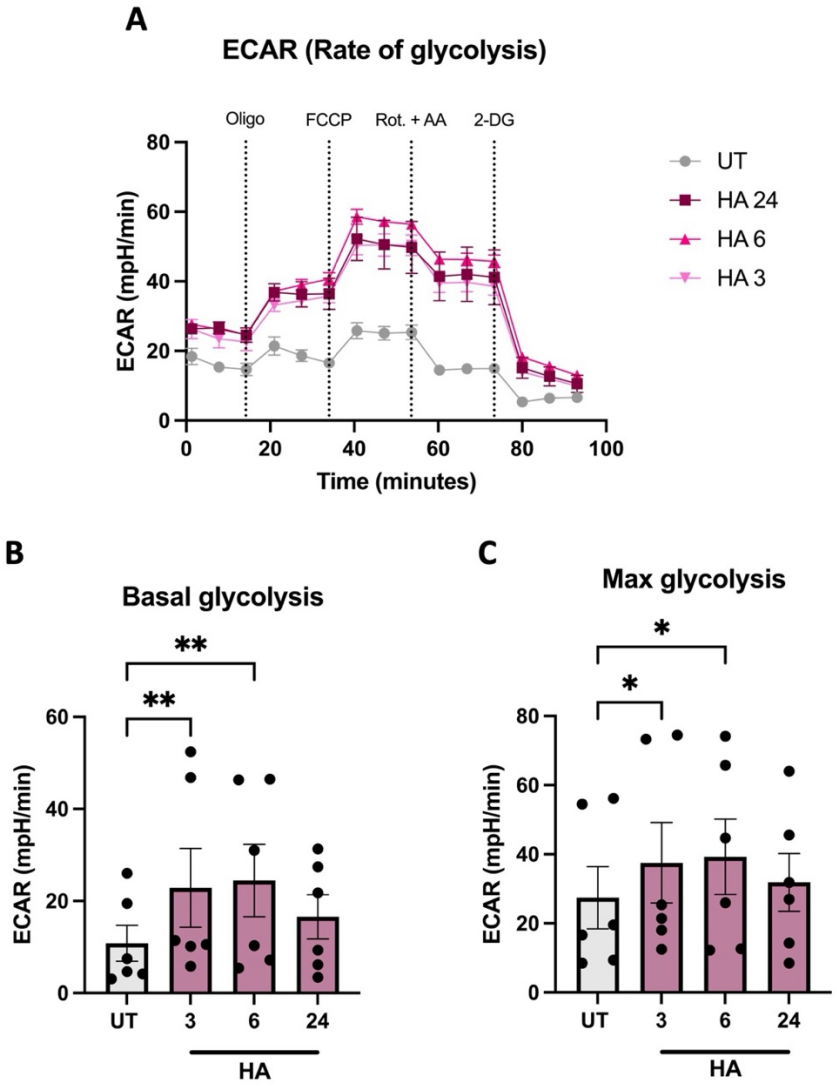

Figure 3.10 MicronHA stimulation temporally increases basal and maximum rates of glycolysis in primary human macrophages.

Primary human macrophages ($2x10^5$ cells) were stimulated with micronHA (250 µg/ml) for 3, 6, or 24 hours prior to placement in a Seahorse XF96 analyser. The extracellular acidification rate (ECAR) was measured before and after injections of oligomycin (1 µm), FCCP (1 µm), antimycin A (500 nm)/Rotenone (500 nm), and 2-DG (25 mM). **(A)** Representative ECAR measurements depicting rate of glycolysis over time for micronHA stimulation at each timepoint. **(B-C)** Pooled data (N=6) depicting the calculated mean basal and maximum rate of glycolysis at each timepoint. Data are represented as mean ± SEM and were analysed using Kruskal-Wallis with Dunn's post-test. (*P≤0.05, **P≤0.01)

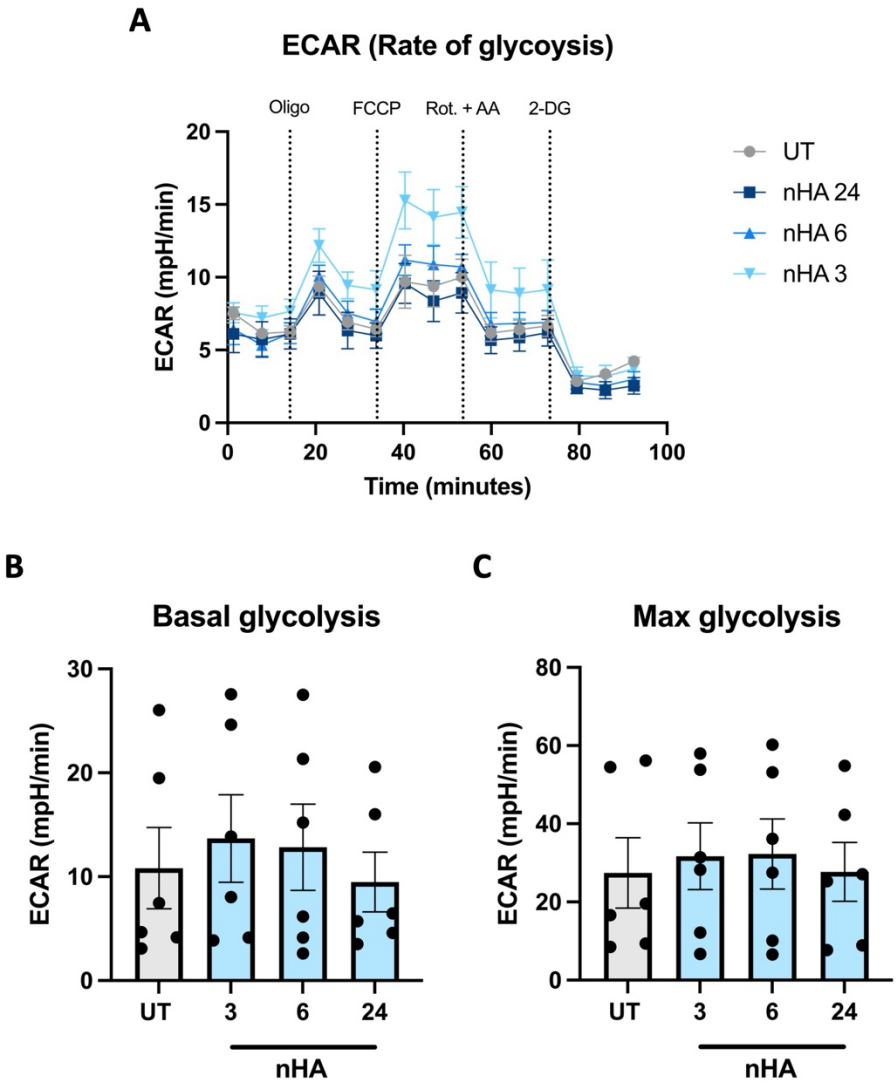

Figure 3.11 NanoHA stimulation does not impact on the basal and maximum rates of glycolysis in primary human macrophages.

Primary human macrophages ($2x10^5$ cells) were stimulated with nanoHA (250 µg/ml) for 3, 6, or 24 hours prior to placement in a Seahorse XF96 analyser. The extracellular acidification rate (ECAR) was measured before and after injections of oligomycin (1 µm), FCCP (1 µm), antimycin A (500 nm)/Rotenone (500 nm), and 2-DG (25 mM). **(A)** Representative ECAR measurements depicting glycolysis over time for nanoHA stimulation at each timepoint. **(B-C)** Pooled data (N=6) depicting the calculated mean basal and maximum rate of glycolysis at each timepoint. Data are represented as mean ± SEM and were analysed using Kruskal-Wallis with Dunn's post-test.

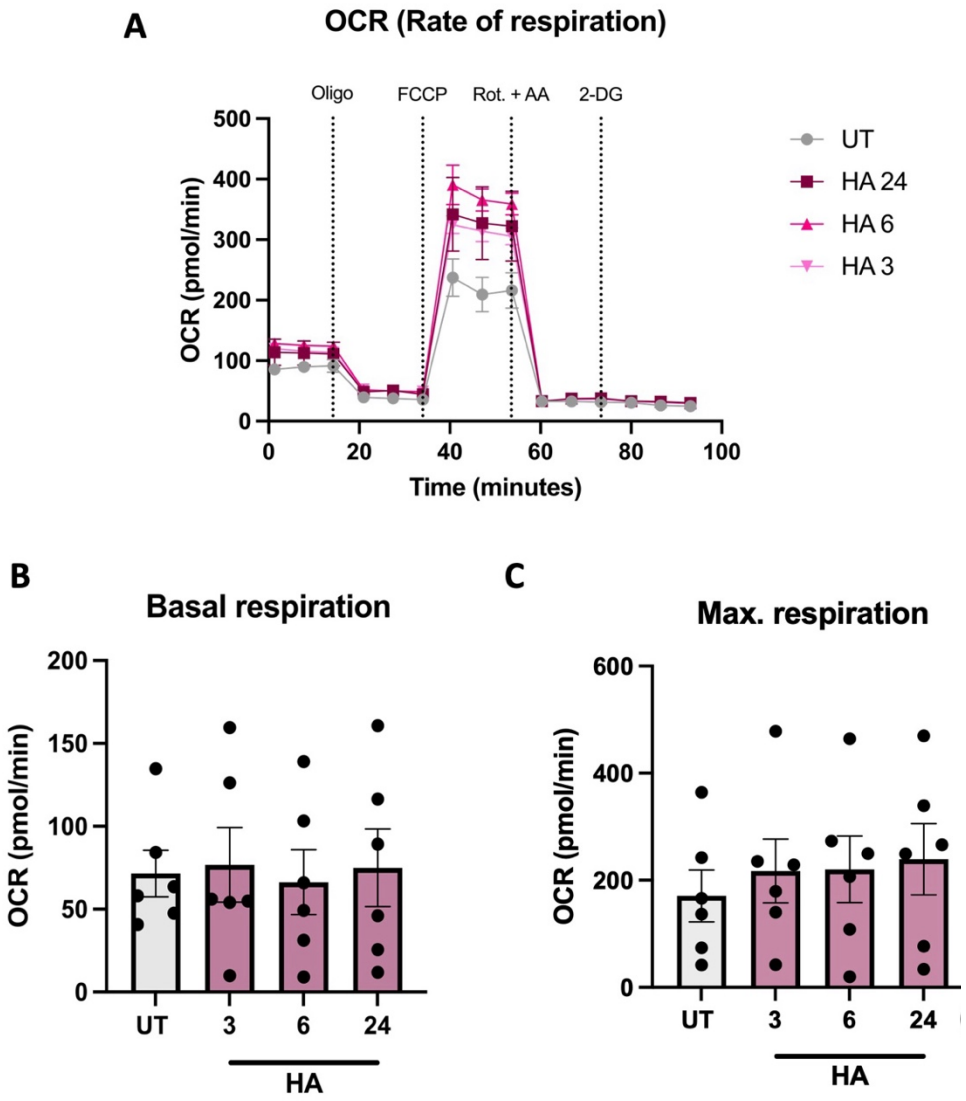

Figure 3.12 MicronHA stimulation does not significantly impact on the basal and maximum rates of respiration in primary human macrophages.

Primary human macrophages (2x10^5 cells) were stimulated with micronHA (250 µg/ml) for 3, 6, or 24 hours prior to placement in a Seahorse XF96 analyser. The oxygen consumption rate (OCR) was measured before and after injections of oligomycin (1 µm), FCCP (1 µm), antimycin A (500 nm)/Rotenone (500 nm), and 2-DG (25 mM). **(A)** Representative OCR measurements depicting respiration over time for particle stimulation at each timepoint. **(B-C)** Pooled data (N=6) depicting the calculated mean basal and maximum respiratory rates for each timepoint. Data are represented as mean ± SEM and were analysed using Kruskal-Wallis with Dunn's post-test.

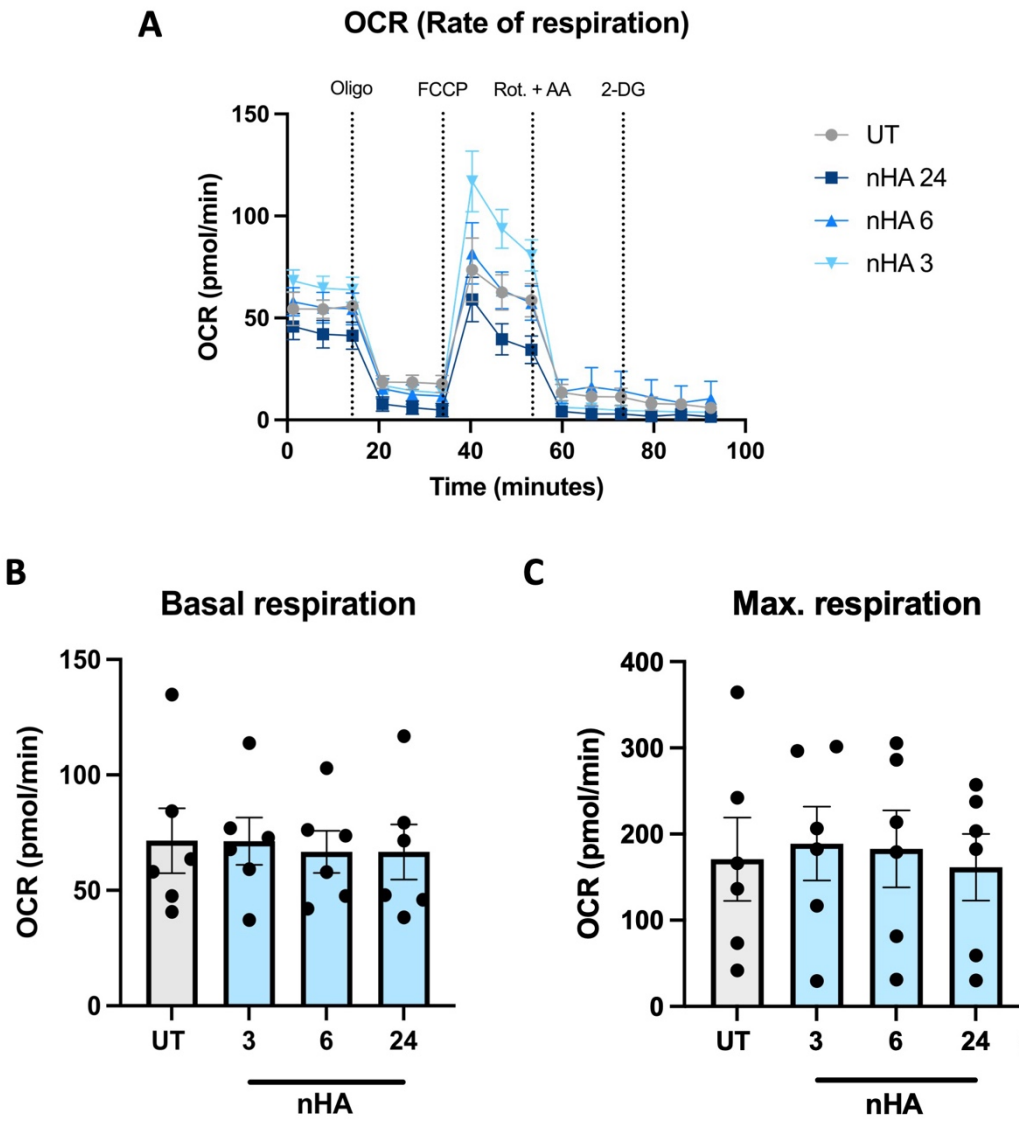

Figure 3.13 NanoHA stimulation does not impact on the basal and maximum rates of respiration in primary human macrophages.

Primary human macrophages (2x10^5 cells) were stimulated with nanoHA (250 µg/ml) for 3, 6, or 24 hours prior to placement in a Seahorse XF96 analyser. The oxygen consumption rate (OCR) was measured before and after injections of oligomycin (1 µm), FCCP (1 µm), antimycin A (500 nm)/Rotenone (500 nm), and 2-DG (25 mM). **(A)** Representative OCR measurements depicting respiration over time for particle stimulation at each timepoint. **(B-C)** Pooled data (N=6) depicting the calculated mean basal maximum respiratory rates for each timepoint. Data are represented as mean ± SEM and were analysed using Kruskal-Wallis with Dunn's post-test.

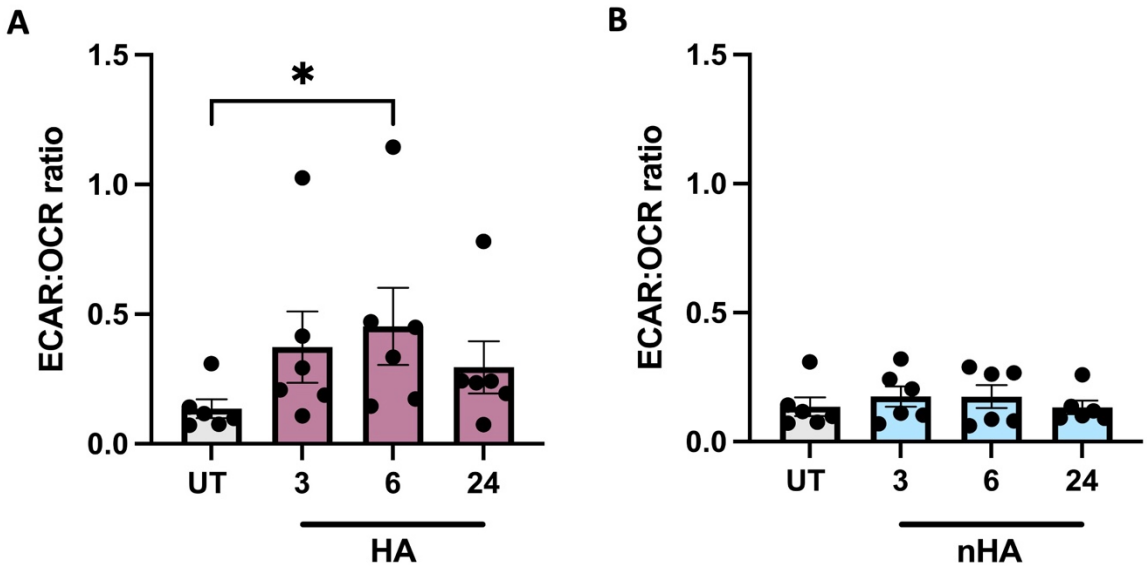

Figure 3.14 MicronHA particles, but not nanoHA, drive a temporal metabolic shift to favour glycolysis in primary human macrophages.

Primary human macrophages ($2x10^5$ cells) were stimulated with micronHA or nanoHA (250 µg/ml) for 3, 6, or 24 hours prior to placement in a Seahorse XF96 analyser. Basal rates of glycolysis and oxidative phosphorylation were measured by ECAR and OCR respectively. Pooled data (N=6) of the calculated mean ratio of ECAR:OCR for each particle stimulation timepoint. Data are represented as mean ± SEM and were analysed using Kruskal-Wallis with Dunn's post-test. (*P≤0.05)

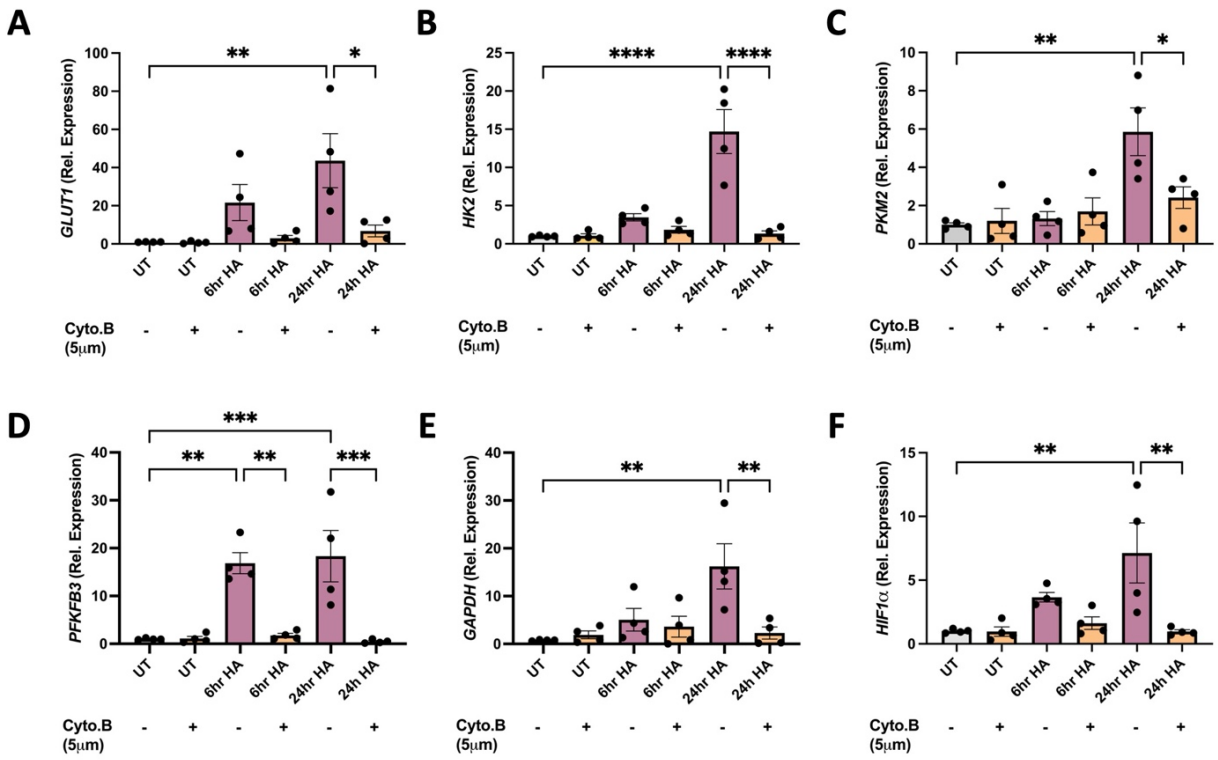

Figure 3.15 Inhibition of phagocytosis attenuates micronHA-induced upregulation of surrogate markers of glycolysis in primary human macrophages.

Primary human macrophages (1 x 10^6 cells) were stimulated with micronHA particles (250 µg/ml) for 6 or 24 hours in the presence or absence of phagocytic inhibitor cytochalasin B (5 µM). mRNA expression of glycolytic markers **(A)** *GLUT1*, **(B)** *HK2*, **(C)** *PKM2* **(D)** *PFKFB3*, **(E)** *GAPDH*, **(F)** *HIF1α*, was assessed by RT-qPCR and normalised to *β-actin* housekeeping gene (N=4). Data are represented as mean ± SEM and were analysed using one-way ANOVA with Tukey's post-test (*P≤0.05, **P≤0.01, ***P≤0.001).

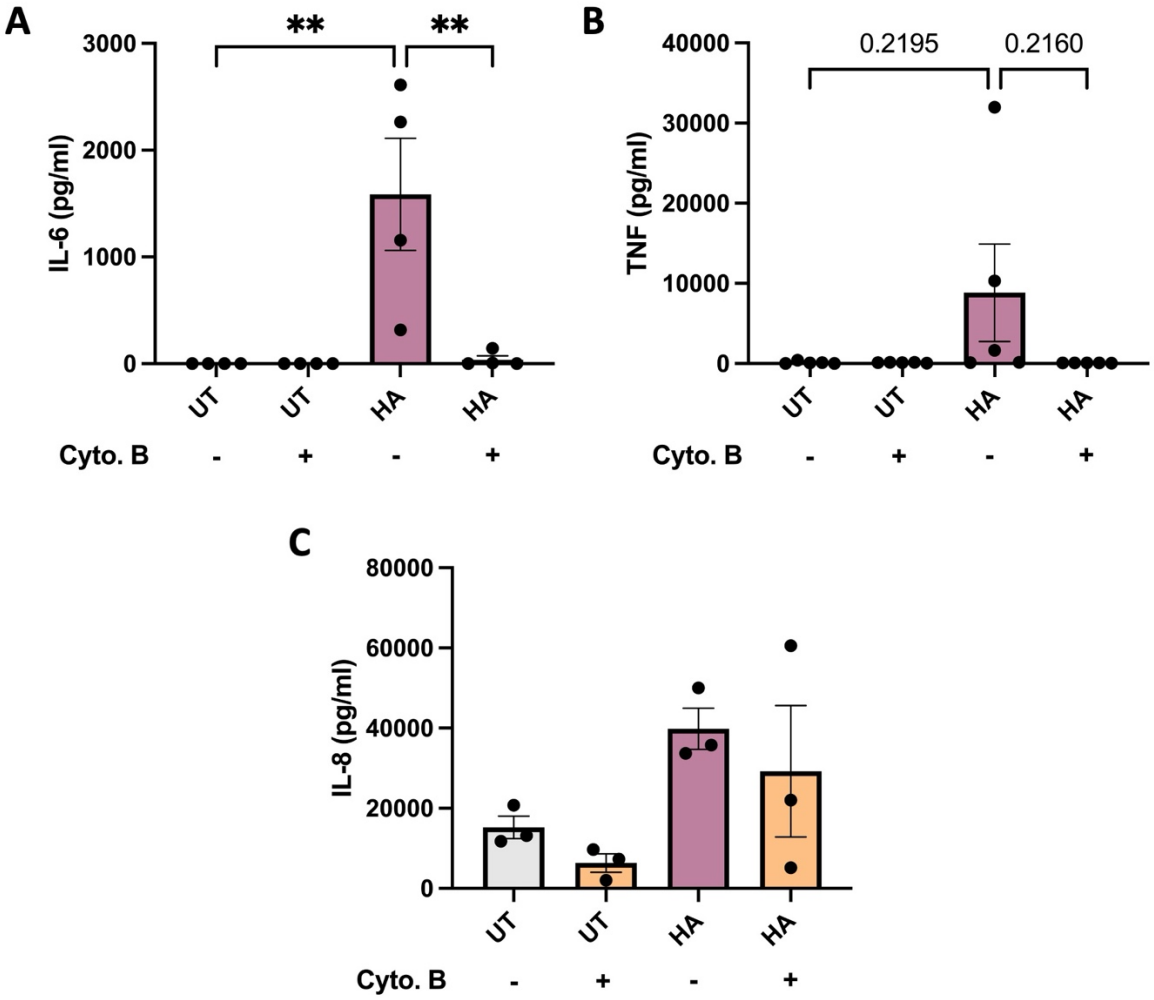

Figure 3.16 Inhibition of phagocytosis attenuates micronHA-induced pro-inflammatory cytokine secretion in primary human macrophages.

Primary human macrophages (1 x 10^6 cells) were stimulated with micronHA particles (250 µg/ml) for 24 hours in the presence or absence of phagocytic inhibitor cytochalasin B (5 µM). Supernatants were assessed for IL-6, TNF, and IL-8 production in the presence and absence of inhibitor, micronHA, or both inhibitor and micronHA **(A-C)** (N=3-4). Data are represented as mean ± SEM and were analysed using one-way ANOVA with Tukey's post-test (*P≤0.05, **P≤0.01, ***P≤0.001).

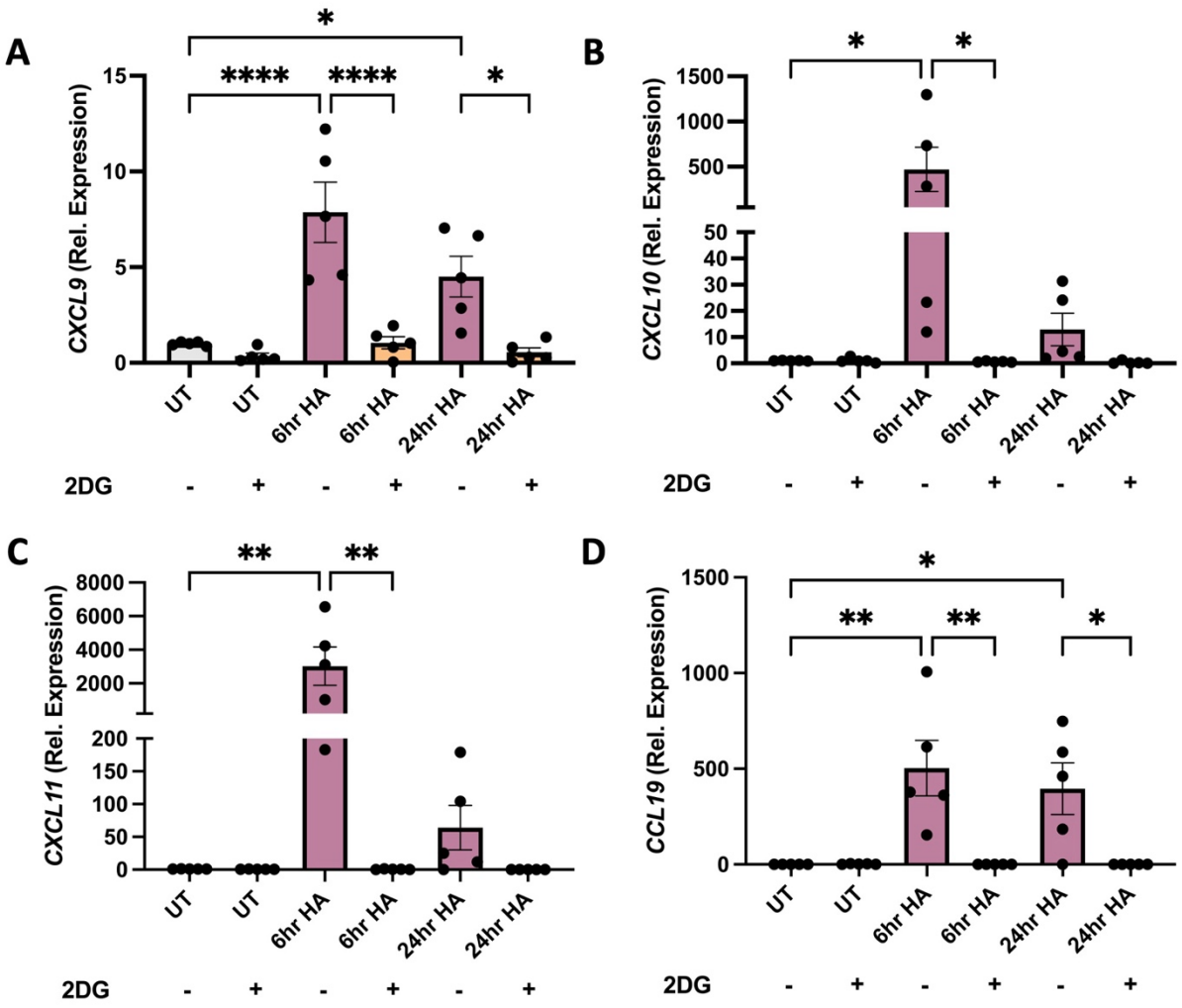

Figure 3.17 Inhibition of glycolysis using 2-DG attenuates micronHA-driven M1-marker mRNA expression in primary human macrophages.

Primary human macrophages (1 x 10^6 cells/ml) were stimulated with micronHA particles (250 µg/ml) for 6 or 24 hours in the presence or absence of glycolytic inhibitor 2-DG (25 mM). mRNA expression of M1-like markers **(A)** *CXCL9*, **(B)** *CXCL10*, **(C)** *CXCL11*, **(D)** *CCL19* were analysed by RT-qPCR. Pooled data (N=5) is represented as mean ± SEM. Data were analysed using one-way ANOVA with Tukey's post-test (*P≤0.05, **P≤0.01, ***P≤0.001, ****P≤0.0001).

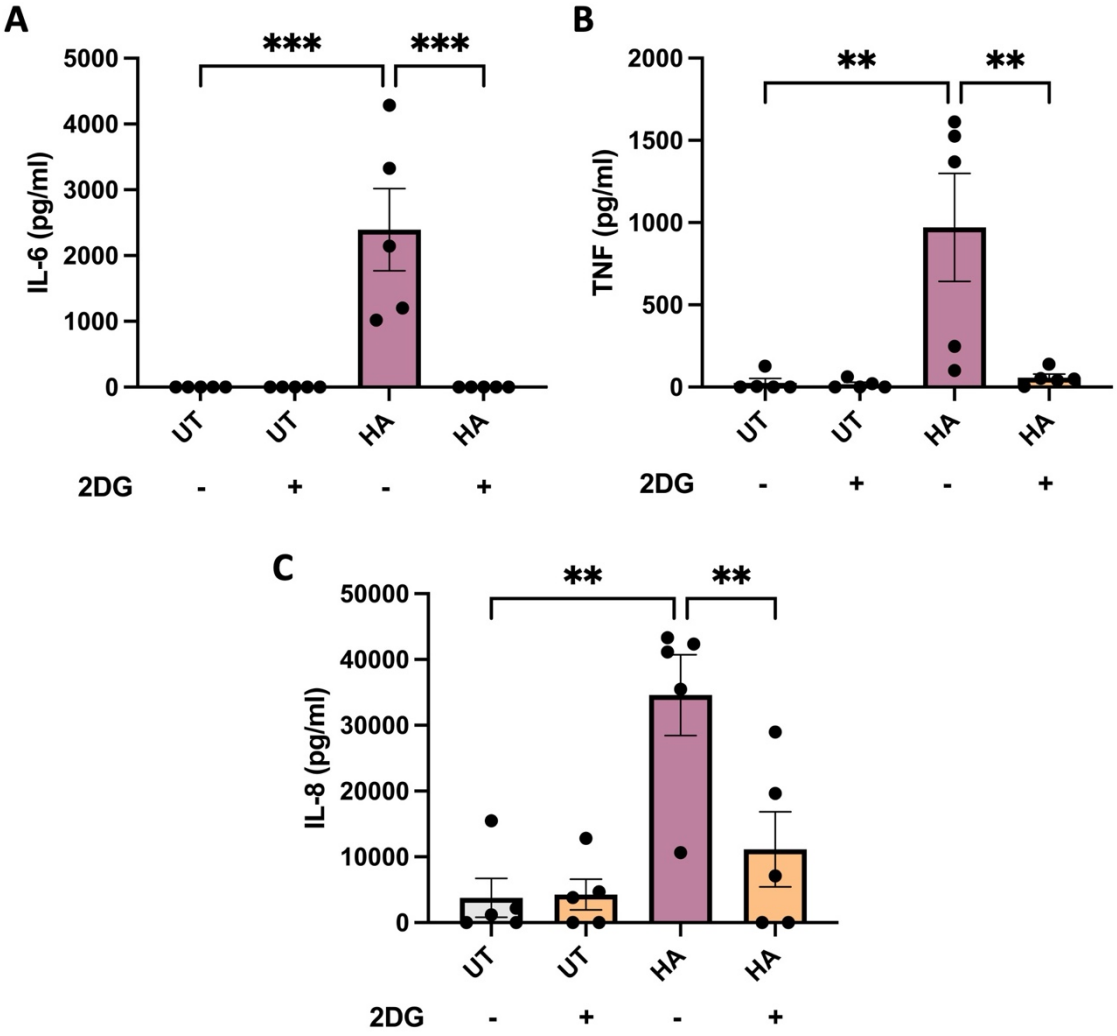

Figure 3.18 Inhibition of glycolysis using 2-DG attenuates micronHA-driven pro-inflammatory cytokine secretion in primary human macrophages.

Primary human macrophages (1 x 10^6 cells) were stimulated with micronHA particles (250 µg/ml) for 24 hours in the presence or absence of glycolytic inhibitor 2-DG (25 mM). **(A-C)** Supernatants were assessed for IL-6, TNF, and IL-8 production in the presence and absence of inhibitor, micronHA, or both inhibitor and micronHA (N=5). Data are represented as mean ± SEM and were analysed using one-way ANOVA with Tukey's post-test (*P≤0.05, **P≤0.01, ***P≤0.001).

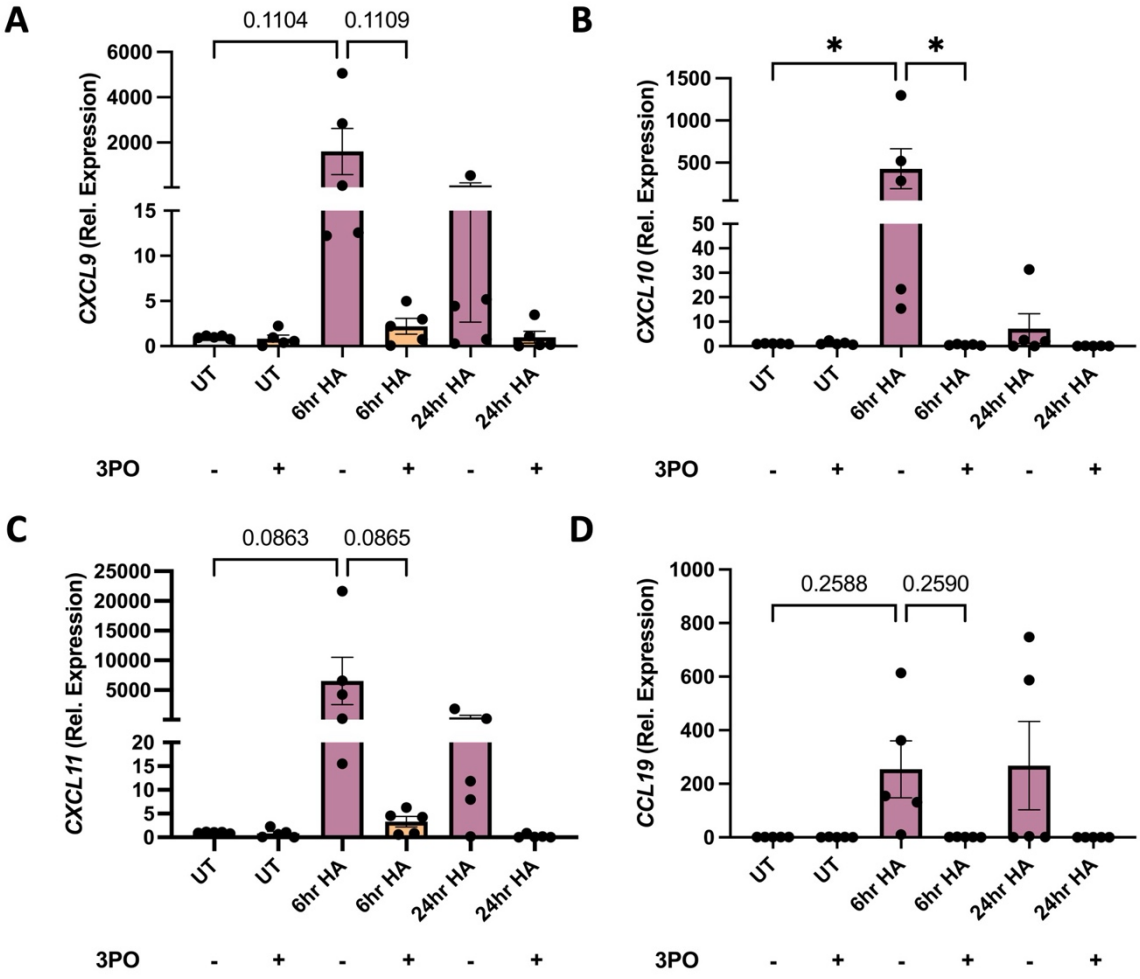

Figure 3.19 Inhibition of glycolysis using 3PO attenuates micronHA-driven M1-marker mRNA expression in primary human macrophages.

Primary human macrophages (1 x 10^6 cells) were stimulated with micronHA particles (250 µg/ml) for 6 or 24 hours in the presence or absence of glycolytic inhibitor 3PO (10 µm). mRNA expression of M1-like markers **(A)** *CXCL9*, **(B)** *CXCL10*, **(C)** *CXCL11*, **(D)** *CCL19* were analysed by real-time PCR. Pooled data (N=5) is represented as mean ± SEM. Data were analysed using one-way ANOVA with Tukey's post-test (*P≤0.05).

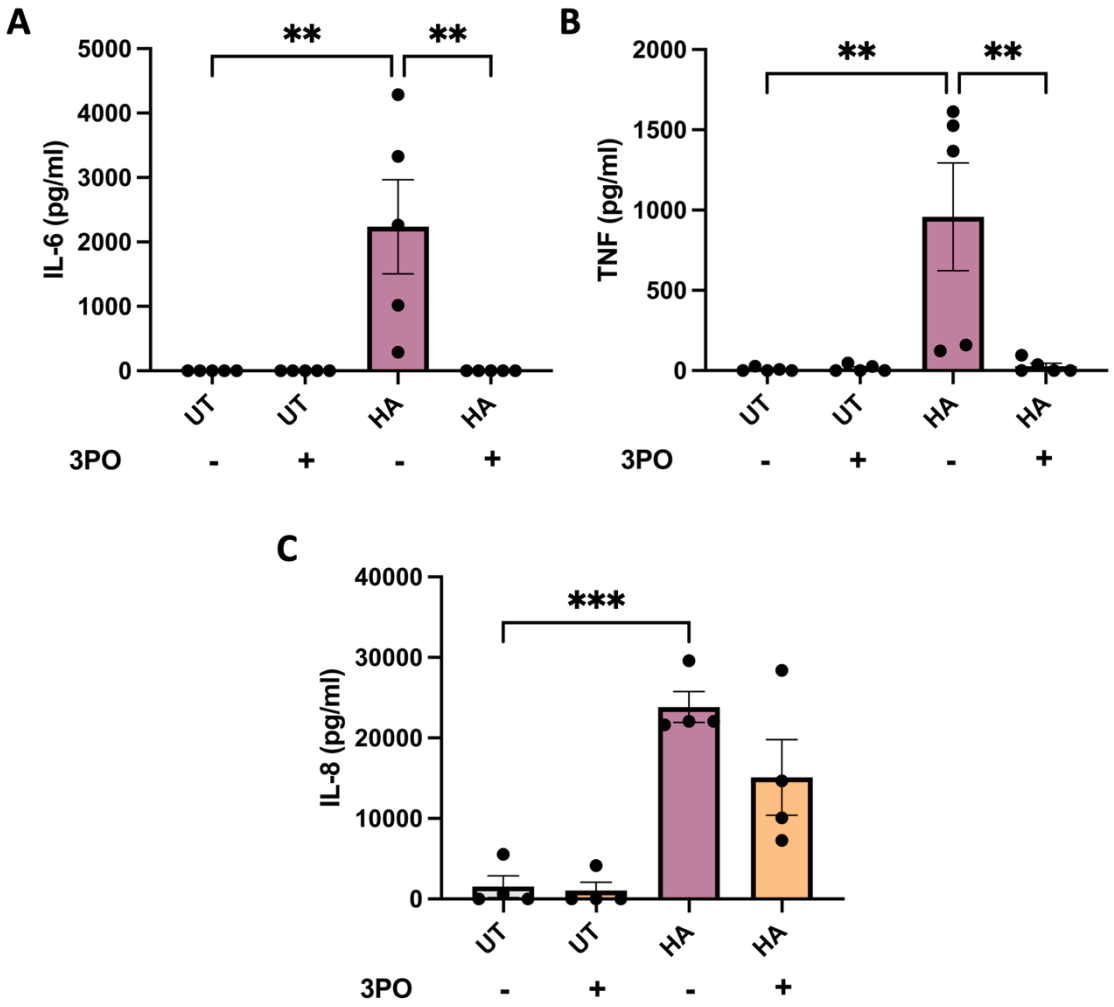

Figure 3.20 Inhibition of glycolysis using 3PO attenuates micronHA-driven pro-inflammatory cytokine secretion in primary human macrophages.

Primary human macrophages (1 x 10^6 cells) were stimulated with micronHA particles (250 µg/ml) for 24 hours in the presence or absence of glycolytic inhibitor 3PO (10 µM). Supernatants were assessed for **(A)** IL-6, **(B)** TNF, and **(C)** IL-8 production in the presence and absence of inhibitor, micronHA, or both inhibitor and micronHA (N=4-5). Data are represented as mean ± SEM and were analysed using one-way ANOVA with Tukey's post-test (*P≤0.05, **P≤0.01, ***P≤0.001).

3.5 Discussion

Wear debris generated at the host-biomaterial interface of orthopaedic implants is known to mediate detrimental effects through interactions with innate immune cells. For example, insoluble particulates such as hydroxyapatite crystals have been implicated as directly contributing to destructive arthropathy [220], and are well documented to resist digestion by macrophages [221]. This results in a host of clinical challenges, including periprosthetic osteolysis at the implant site, and the eventual need for revision/replacement surgeries. As a result, measures are currently underway to mitigate these destructive processes, and investigations into nanoscale materials such as nanoHA have yielded promising results, with nano-scale particles reported to preferentially polarise macrophages to an anti-inflammatory, pro-regenerative phenotype [126]. It is also becoming increasingly evident that immune cell phenotype is intricately linked to metabolic status, and that dysregulated metabolic reprogramming contributes to inflammatory processes in a number of diseases including OA, RA, and diabetes [162, 163, 222]. In this chapter it is demonstrated that micron, but not nano-sized HA particles, drive a metabolic shift to favour glycolysis, as evidenced by increased expression of surrogate markers of glycolysis, changes in cellular bioenergetics, and altered mitochondrial dynamics. Uptake of the particles is required for these metabolic changes to occur, while inhibition of micronHA-driven metabolic reprogramming attenuates pro-inflammatory macrophage responses. This chapter thus provides a novel mechanistic link between particle size, glycolytic profile, and pro-inflammatory macrophage polarisation.

It is now well established that pro-inflammatory macrophage polarisation correlates with metabolic rewiring to favour glycolysis over oxidative phosphorylation. Termed 'the Warburg effect', this phenomenon occurs even when oxygen is plentiful and facilitates the production of biosynthetic intermediates needed for a rapid inflammatory response [161, 170]. Key indicators of this shift include upregulation of enzymes and proteins required to drive glycolytic pathways. It was observed that treatment of primary human macrophages with micronHA resulted in upregulation of *GLUT1*, *HK2, GAPDH, HIF1α*, and *PFKFB3* in addition to *PKM2*, which is a key regulator of glycolytic pathways. It is worth noting that,

while *GAPDH* is often used as a housekeeping gene for data normalisation, it functions as a key enzyme in the glycolytic pathway and, as demonstrated with the use of micronHA particles, is altered by modulators of cellular metabolism. This therefore argues for the use of alternative housekeeping genes for studies in which glycolysis, and indeed metabolism in general, is under investigation.

While the extracellular acidification rate of the cells was increased upon micronHA stimulation compared to nanoHA treatment (demonstrating a significantly higher rate of glycolysis), a moderate increase in max respiration was also observed, indicating that micronHA treated macrophages are potentially more metabolically active overall. This observed effect is similar to that seen in more recent studies examining the effect of ultrahigh molecular weight polyethylene wear particles (UHMWPE) on murine macrophage metabolism, in which it was demonstrated that sterile UHMWPE particles led to simultaneous elevation of ECAR and OCR, with both increased glycolysis and oxidative phosphorylation implicated as contributors to UHMWPE-driven inflammation that can exacerbate periprosthetic osteolysis [223-225]. Given the observed effects, it will therefore be of interest to examine a wider range of metabolic pathways such as fatty acid oxidation and the pentose phosphate pathway to further robustly characterise the metabolic phenotype induced by HA particle size.

In terms of mitochondrial morphology and function, it has been shown that macrophage mitochondrial networks undergo fission in response to pro-glycolytic stimuli such as LPS [219], and here it is seen that this phenomenon occurs upon stimulation with micronHA, but not nanoHA. This is accompanied by decreased mitochondrial mass and increased ROS production [226]. In a biomaterial context, it has been demonstrated that positively charged polyethylenimine-functionalised graphene oxide (GO-PEI) mediates its cytotoxic effects in microglia *via* induction of mitochondrial fission, further supporting a role for dysregulated mitochondrial dynamics in biomaterial-mediated immune dysfunction [227]. It should be noted that, although not significant, a modest increase was observed in mitochondrial fusion in nanoHA treated macrophages, supporting the FLIM analysis, and indicating that nanoHA treatment may be playing a role in the sustained cellular respiration linked with a nanoHA-driven M2-like polarisation state. More detailed studies

of particle size and surface topography are required to determine if these properties can be altered to promote favourable changes in mitochondrial bioenergetics. Of note, the micron HA particles used in this study have a mean size of 1.3 μm, and there is evidence to demonstrate that particle size of >1 μm can be conducive to pro-inflammatory macrophage polarisation [221, 228-230]. Other studies have demonstrated that needle versus spherical shaped particles induce higher levels of pro-inflammatory cytokine secretion, hence it is plausible that particulate shape is also a driving factor in alteration of mitochondrial dynamics. Mitochondrial dysfunction is also known to prevent repolarisation of M1-like macrophages to an M2-like state [178]; therefore, these combined effects on mitochondrial morphology and function may preclude the pro-inflammatory to pro-reparative transition necessary for normal healing processes to occur.

There is a growing body of research implicating particulate-mediated metabolic reprogramming as key driver of inflammation [197, 199]. The list to date consists of endogenous disease-associated particulates such as gout-associated MSU crystals, osteoarthritis-associated calcium containing crystals and atherosclerosis-associated cholesterol crystals [197, 198, 231]. Micron- and nano-sized hydroxyapatite particles can now be added to this growing list of metabolic modulators. Other biomaterials such as PMMA particles likely have a similar effect, given their propensity to drive pro-inflammatory macrophage polarisation [221]. As mentioned above, further study will determine how particle size/shape can differentially affect metabolic pathways, and whether this can be artificially manipulated. Further research in this area may also lead to the identification of novel therapeutic targets. For example, inhibitors of PKM2 are currently being explored in the context of atherosclerosis [232] and SLE [233], while the metabolism altering drug, metformin, which is traditionally used to treat type II diabetes, is now showing potential as a treatment for autoimmune and inflammatory diseases, including RA and colitis, and has been shown *in vitro* to preclude ultra-high molecular weight polyethylene (UHMWPE)-driven elevated oxidative phosphorylation directly linked to increased mitochondrial ROS production and resultant pro-inflammatory cytokine secretion in BMDMs, and *in vivo* to attenuate UHMWPE-induced osteolysis in a mouse calvarial defect model [223, 225, 234, 235]. Of note, it was recently demonstrated that a 3D-printed glass ceramic scaffold coated with the trace element, molybdenum, promotes

M2 macrophage polarisation and a shift from glycolysis to oxidative phosphorylation in LPS-stimulated murine macrophages, as well as promoting periodontal tissue regeneration in canines [172]. Furthermore, metabolomics studies have identified anti-inflammatory metabolites such as itaconate and ß-hydroxybutyrate (BHB) that could potentially be incorporated into biomaterial scaffolds to engineer an anti-inflammatory, pro-regenerative immune response [171, 236].

Of note, ^{1}H NMR metabolomics has emerged as a valuable technique for interrogating cellular metabolism on a deep level, allowing for a thorough characterisation of the intracellular metabolome of immune cells. Graphene-based nanoparticles were shown to induce different metabolic profiles in murine RAW 264.7 macrophages depending on their size and functionalisation, with flavin mononucleotide-stabilised pristine graphene (PF-FMN) particles from 200 – 400 nm, and 100 – 200 nm, capable of increasing nitric oxide production and altering metabolites such as phosphocreatine and creatine in a manner similar to that seen upon LPS treatment [237]. It has also been shown that murine RAW 264.7 macrophages alter their metabolism and inflammatory response upon exposure to silk, silica, and PLGA nanoparticles ranging from 100 – 125 nm [238]. This study posits ^{1}H NMR metabolomics as a useful means of identifying not only immunometabolic reprogramming induced by particulate materials, but allows for identification of metabolites and other metabolic pathways at play. These works also highlight the ability of other nanoparticles, in addition to the potential of micronHA and nanoHA used within, to modulate cellular metabolism and macrophage phenotype in a manner similar to that seen in this chapter, with silica, silk, and PLGA particles inducing production of TNF at concentrations of 500 μg/ml and induction of M1-like macrophage markers. This also reiterates that not only size, but also particle composition plays a role in dictating macrophage metabolic and functional response, given that nanoHA particles with mean sizes falling between 50 -– 150 nm used in this chapter induce an anti-inflammatory macrophage by contrast.

Finally, it was observed that treatment of human macrophages with glycolytic inhibitors prevented micron HA-driven pro-inflammatory macrophage polarisation and inflammatory cytokine production, suggesting that targeting this aspect of particulate-

induced inflammation warrants further *in vivo* investigation. This undoubtedly requires careful consideration given the potential for 'off-target' effects and the differential use of metabolic pathways by different cell types. Furthermore, it is important to note that we use a limited number of macrophage surface markers to perform phenotypic analysis in this study. It is now widely accepted that the traditional "M1/M2" paradigm of macrophage classification is overly simplistic and it is far more likely that macrophages exhibit a much more complex response in displaying 'hybrid' phenotypic and functional characteristics of both pro and anti-inflammatory macrophages in response to external stimuli [239, 240]. The findings in this chapter nonetheless provide further insight into cellular changes that occur at the periprosthetic implant site and implicate metabolic targeting and modulation as a potentially effective strategy for tempering adverse inflammatory processes associated with biomaterial implantation.

In conclusion, it is demonstrated here for the first time that primary human macrophages alter their metabolic profile in response to hydroxyapatite exposure. Furthermore, it is shown that particle size is a determining factor in driving these changes. This not only broadens the range of immune cell parameters that we can assess and modulate when designing immune-informed biomaterials, but also highlights immunometabolism as a novel therapeutic avenue worthy of exploring in order to mitigate adverse post-implantation reactions.

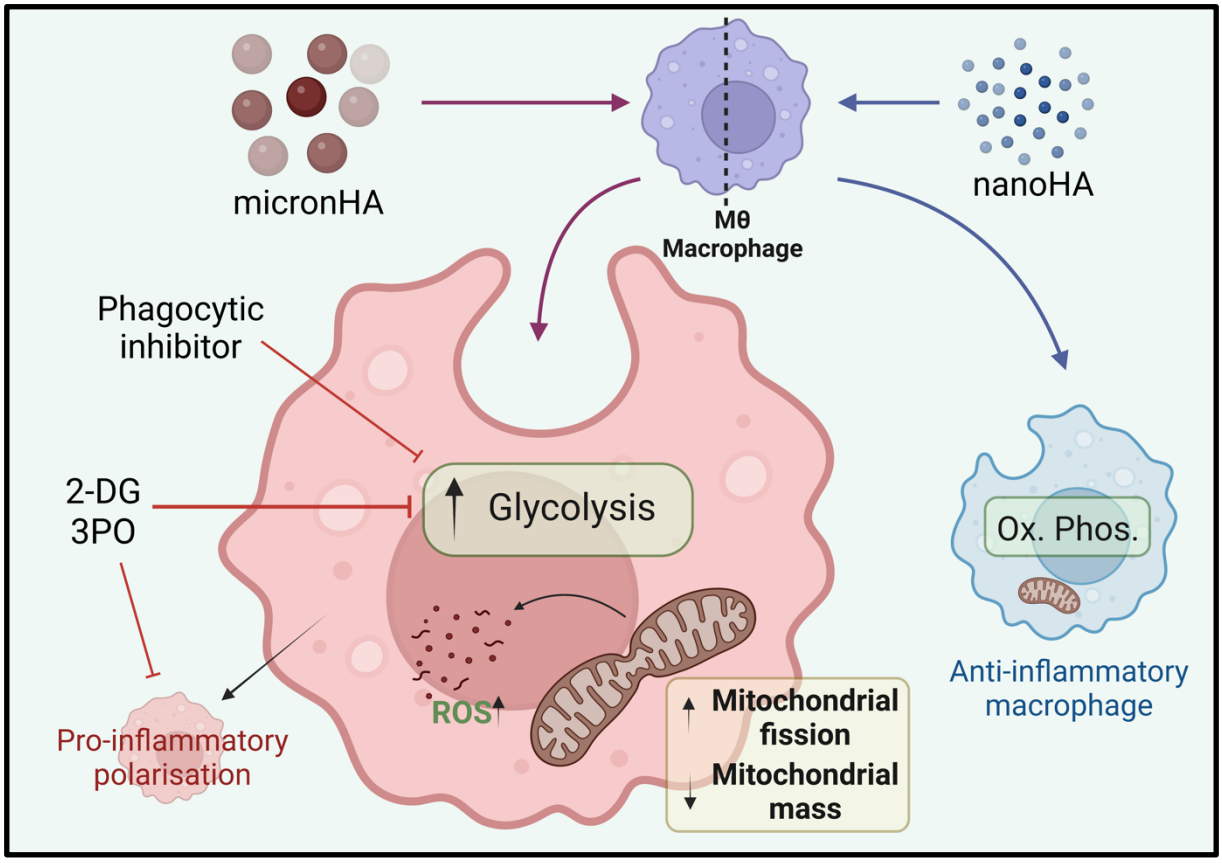

Figure 3.21 Summary schematic of findings.

Micron and nano-sized hydroxyapatite particles can alter the metabolism of primary human macrophages. MicronHA exposure, which is documented to lead to pro-inflammatory macrophage polarisation, results in a bioenergetic shift to favour glycolysis, concomitant with an upregulation in M1-like pro-inflammatory markers. Inhibition of phagocytosis results in an attenuation of glycolytic mRNA expression and reduces pro-inflammatory macrophage polarisation. Additionally, inhibition of glycolysis using 2-DG or 3-PO results in an attenuation of pro-inflammatory polarisation. Macrophages exposed to nanoHA, by contrast, do not exhibit a switch to glycolysis and instead preferentially rely on oxidative phosphorylation as their predominant means of energy production.

Chapter Four

Immunomodulatory and regenerative potential for *Trypanosoma brucei*-derived ketoacids in primary human macrophages and mesenchymal stem cells

4.1 Introduction

With growing appreciation of the interplay between the immune system and tissue regeneration, there now exists a pressing need for therapeutic strategies that marry anti-inflammatory and pro-regenerative potential in the context of tissue healing and regeneration. While an initial inflammatory response aids regeneration by facilitating the infiltration of immune cells and initiation of necessary processes such as angiogenesis and stem cell differentiation [241], it is well appreciated that the immune response must resolve this inflammation and switch from pro- to anti-inflammatory for normal healing and regenerative processes to continue [242, 243]. Failure to do so results in chronic inflammation that propagates deleterious processes, precluding repair and often resulting in tissue destruction. As such, there is growing need to explore the potential of novel therapeutics to exert dual anti-inflammatory, pro-regenerative effects across a range of tissue types. Given demonstration in the previous chapter that modulators of cellular metabolism and metabolites may pose a worthy therapeutic strategy in mitigation of inflammation-driven tissue destructive processes, this chapter interrogates the ability of amino acid-derived metabolites to manipulate primary human macrophage and MSC functionality with respect to inflammation and regeneration.

The aromatic ketoacids, indole pyruvate (IP) and hydroxyphenyl pyruvate (HPP), are products of amino acid metabolism that have been implicated as potential immunomodulators across a range of immune cell types [78, 105, 106]. The parasite *Trypanosoma brucei* (*T. brucei*) which is the causative agent of African Sleeping Sickness, is known to convert the amino acids tryptophan, tyrosine, and phenylalanine into IP, HPP, and phenyl pyruvate (PP) as a putative means of immune-evasion and prolonging survival in its infected host [78, 105, 244]. As a result, the immunomodulatory properties of these ketoacids have begun to be explored for potential therapeutic benefit, particularly in the context of inflammatory disease [78, 108]. IP in particular has potent anti-inflammatory effects in animal models of colitis and rheumatoid arthritis (RA) [107, 109], while in humans, IP has been identified as both a biomarker of and protective factor against RA. In support of this, decreased levels of IP are found in the plasma of RA patients compared to

healthy controls, and protective effects have been attributed to activation of the aryl hydrocarbon receptor (AhR) [109]. Further work has demonstrated that HPP and IP can reduce expression of the pro-inflammatory cytokines, IFNγ and IL-17, in human peripheral blood mononuclear cells (PBMC) isolated from patients with inflammatory bowel disease (IBD) and, moreover, both IP and HPP have been shown to modulate cellular metabolism by attenuating LPS-induced glycolysis in human DC with IP having a similar effect in murine macrophages [105, 108].

IP and HPP have recently been identified as novel inducers of the stress response protein, heme oxygenase 1 (HO-1), in murine glia and macrophages, as well as human DC. This occurs via activation of Nrf2, and the expression of HO-1 is linked to anti-oxidant and anti-inflammatory immune cell function [63]. Indeed, clinically relevant inducers of HO-1 are highly sought after given that upregulation of this enzyme has been shown to ameliorate disease in a number of animal models [107, 245-247]. In the context of tissue regeneration, and with respect to bone tissue, induction of HO-1 has shown promise in promoting osteoblastic differentiation of murine bone marrow stromal cells (BMSC), in which VEGF-driven HO-1 expression, as well as direct HO-1 induction by known HO-1 inducer cobalt protoporyphyrin (CoPP), was shown to induce osteoblastogenesis [60], while in human MSC, treatment with CoPP resulted in a decrease in adipogenic differentiation and an increase in osteoblastic differentiation [61, 62]. Additionally, it has been observed that MSC upregulate HO-1 on exposure to known osteogenic promotors such as osteogenic growth peptide (OGP) [61]. Furthermore, studies have indicated that pro-osteogenic effects can be mediated through activation of the transcription factor, Nrf2. In support of this, Nrf2 activation via deletion/knockdown of Keap1 (a negative regulator of Nrf2) in mice was shown to enhance the transcription of osteogenic genes in primary osteoblasts and resulted in increased bone formation [248], whilst Nrf2 knockout in primary osteoblasts and osteocytes was shown to decrease osteogenic gene expression [249]. Taken together, HO-1 induction and Nrf2 activation represent promising strategies not only for immune modulation, but also as potential promoters of osteogenesis and bone tissue regeneration.

Although the anti-inflammatory properties of IP and HPP have been documented in human DC and PBMC, as well as murine glia and BMDM, less is known regarding the effects of these ketoacids in primary human macrophages. This chapter aims to investigate the effects of these ketoacids in this cell type with particular focus on HO-1 expression and Nrf2 activation, immune modulation, and tissue regeneration-associated gene expression. Experiments will also be conducted to determine if the ketoacids have any impact on MSC differentiation, with particular focus on osteoblastic differentiation. IP will be the main focus of this chapter given its relative potency compared to HPP in driving cellular responses linked to inflammation, and given that IP is comparatively better studied in the literature with respect to inflammatory disease.

4.2 Hypothesis

The *T.brucei*-derived ketoacids, IP and HPP, can impact on the phenotype and activity of primary human macrophages, and can potentially promote osteoblastic differentiation of human mesenchymal stem cells.

4.3 Specific Aims

- To investigate if IP and HPP can impact on HO-1 expression and Nrf2 activation in primary human macrophages.
- To investigate the ability of ketoacids to modulate LPS-induced inflammatory mediator production in primary human macrophages.
- To investigate the effect of IP and HPP on primary human macrophage regeneration-associated gene expression.
- To examine whether IP and HPP can impact on LPS-driven metabolic alteration in primary human macrophages.
- To interrogate the effect of IP on regeneration-associated gene expression in human mesenchymal stem cells.
- To examine the ability of IP to impact on osteoblastic differentiation of human mesenchymal stem cells.

4.4 Results

4.4.1 IP and HPP are non-toxic to primary human macrophages.

At the time of this study, there were no published reports assessing the effects of both these ketoacids in primary human macrophages; hence, cell viability was assessed by flow cytometry prior to carrying out detailed experiments. Cells were treated with 500 or 1000 µM IP and HPP for 24 hours - these doses have been used in previously published studies using murine macrophages, glia, and human DC. Furthermore, they equate to the doses found circulating in the plasma of individuals infected with *T. brucei* [78, 105]. Cell viability was assessed using Fixable Viability dye eFluor 506 and plotted against corresponding untreated control. Neither concentration of IP or HPP was found to impact on cell viability and thus they were deemed suitable for further use (Figure 4.1 A-B).

4.4.2 HPP upregulates HO-1 to a greater extent than IP in primary human macrophages.

As IP and HPP have been studied as HO-1 inducers across a range of immune cell types, including murine glia and macrophages, as well as human DC, and given the putative anti-inflammatory activities associated with HO-1 induction, it was next of interest to investigate whether these ketoacids could upregulate HO-1 in primary human macrophages. To test this, macrophages were treated with increasing doses (250 – 1000 µM) of IP or HPP for 24 hours and HO-1 protein expression was assessed by western blot. Marginal induction of HO-1 was observed upon treatment with IP (0.75 – 1.6 fold change with 1000 µM) (Figure 4.2 A-B) while both 500 and 1000 µM HPP were found to significantly upregulate HO-1 expression (Figure 4.2 A, C). This demonstrates that HPP can induce HO-1 to a greater extent than IP in this cell type.

4.4.3 IP and HPP activate the aryl hydrocarbon receptor (AhR) and Nrf2 in primary human macrophages.

It has recently been reported that IP activates the AhR in BMDM [105, 106]. Cytochrome P450 1A1 (*CYP1A1*), which is under the control of the AhR, is commonly used as a readout for determining AhR activation. In order to determine if the ketoacids can activate the AhR in primary human macrophages in our hands, cells were treated with IP and HPP (1000 µM) for 3, 6, and 24 hours and *CYP1A1* mRNA expression was assessed over time using RT-qPCR. IP was found to significantly upregulate *CYP1A1* expression in macrophages at all timepoints tested (Figure 4.3 A-C), whilst HPP significantly upregulated *CYP1A1* expression at 3 and 6 hours (Figure 4.3 D-F).

It has also been demonstrated that ketoacids IP and HPP can induce HO-1 expression *via* activation of transcription factor Nrf2, and that this is potentially linked with signalling through the AhR [108]. The mRNA expression of *NQO1*, a gene which is regulated by both AhR and Nrf2 activity and therefore can function as a readout for both, and *GSR,* which is regulated by Nrf2, were assessed by RT-qPCR under both IP and HPP treatment conditions at 3, 6, and 24 hours. IP significantly upregulated *NQO1* mRNA at 6 hours, and both *GSR* and *NQO1* mRNA expression at 24 hours (Figure 4.4 B-C, E-F). HPP, by contrast, significantly upregulated *GSR* and *NQO1* mRNA expression at all timepoints tested (Figure 4.4, G-L). Western blotting was also used to assess the expression/accumulation of Nrf2, as a readout for Nrf2 activation. Macrophages were treated with IP and HPP (1000 µM) for 3, 6, and 24 hours and expression of Nrf2 was assessed. Nrf2 protein expression was found to be increased in the lysate of IP and HPP treated macrophages at 3 hours, with IP trending towards significance and HPP reaching significance at this early timepoint (Figure 4.5 A-B, G-H). Although an increase in Nrf2 protein was observed at 6 and 24 hours with both IP and HPP, this was not significant (Figure 4.5 C-F, I-L). Together, this suggests that IP and HPP may activate Nrf2 at an early timepoint in primary human macrophages, and taken with the observed increase in mRNA expression of *CYP1A1* as a readout for AhR activation, that this activation may occur *via*, or concomitantly with, signalling through the AhR.

4.4.4 IP and HPP attenuate LPS-induced inflammation-associated chemokine gene expression, but not inflammatory cytokine production, in primary human macrophages.

As mentioned above, IP and HPP have been shown to attenuate pro-inflammatory responses in a range of immune cells [78, 105, 106, 108]. In order to determine if these effects are observed in primary human macrophages, cells were pre-treated with IP and HPP (1000 µM) for 6 hours prior to stimulation with LPS (100 ng/ml) for 24 hrs. A 6 hour pre-treatment was chosen as Nrf2 expression was seen to be increased by 3 hours with IP and HPP, and as these ketoacids have been documented to act via Nrf2-mediated HO-1 induction, 6 hours would allow time for Nrf2 to exert its transcriptional activity. mRNA expression of the M1-associated macrophage markers, chemokines *CXCL9* and *CXCL10*, was then assessed using RT-qPCR. Both IP and HPP were found to significantly reduce LPS-induced *CXCL10* expression (Figure 4.6 B, D), whilst IP significantly reduced *CXCL9* mRNA expression (Figure 4.6 A, C) . These results suggest that both IP and HPP are capable of tempering LPS-associated inflammatory gene expression in primary human macrophages, and that IP may prove more potent at doing so than HPP.

To further this investigation at the functional level, the levels of LPS-induced pro-inflammatory cytokines TNF, IL-6, and chemokine IL-8 were assessed by ELISA in the presence or absence of IP or HPP. Macrophages were treated with IP or HPP (1000 µM) for 6 hours prior to stimulation with LPS (100 ng/ml) for a further 24 hours, and supernatants collected for measurement of cytokine. Despite promising results at the mRNA level, it was found that IP pre-treatment led only to a moderate reduction in LPS-stimulated TNF and IL-6 (Figure 4.7 A-B), whilst HPP pre-treatment prior to LPS stimulation resulted in a moderate increase in both cytokines (Figure 4.7 D-E). IL-8, by contrast, was significantly upregulated as a result of both IP and HPP pre-treatment prior to stimulation with LPS compared to LPS stimulation alone (Figure 4.7 C,F). These results suggest that IP, but not HPP, may exert a moderately ameliorative effect on production of pro-inflammatory cytokines TNF and IL-6, but not IL-8, whist HPP pre-treatment upregulates the LPS-driven production of all three pro-inflammatory mediators in primary human macrophages. Production of the anti-inflammatory cytokine, IL-10, was also assessed. In this case, HPP pre-treatment led to no observable difference in IL-10 production as

compared to LPS stimulation alone (Figure 4.8 B), whilst IP pre-treatment appeared to promote a mild increase in IL-10 production in combination with LPS stimulation (Figure 4.8 A). Taken together, these findings indicate that IP and HPP do not exert anti-inflammatory effects in primary human macrophages to as great an extent as has been documented in other immune cell types such as primary human DC and murine glia.

4.4.5 IP and HPP modulate metabolic responses in primary human macrophages.

Modulation of immune cell metabolism is now considered a promising therapeutic strategy to mitigate glycolysis-associated inflammation [170], and the ketoacids IP and HPP have been shown to attenuate glycolysis in human DC and BMDM [105, 108]. It was therefore of interest to examine whether the ketoacids can impact on primary human macrophage metabolism. LPS has been shown to promote an increased reliance on glycolysis in human immune cells and this is linked to a pro-inflammatory phenotype [161, 250, 251].

Macrophages were pre-treated with IP or HPP (1000 µM) for 6 hours prior to stimulation with LPS (100 ng/ml) for three hours. Seahorse analysis was then performed to assess the bioenergetic profile of the cells in the presence or absence of the ketoacids. The ECAR and OCAR were measured in order to give an indication of glycolysis and oxidative phosphorylation, respectively. Treatment with IP or HPP alone had no effect on basal and maximum rates of glycolysis; however LPS induced a trend towards increased glycolysis and this was reduced, albeit not significantly, in IP treated cells, with similar results observed with HPP (Figure 4.9 A-C, Figure 4.10 A-C), and reflected in the calculated ECAR:OCR ratios of IP and HPP pre-treated LPS-stimulated macrophages (Figure 4.11 A-B). While further work is needed, there is some evidence to suggest that IP and HPP are capable of modulating pro-glycolytic metabolic shifts induced by known inflammatory stimuli in primary human macrophages.

4.4.6 IP and HPP drive vascularisation- and regeneration-associated gene expression in primary human macrophages.

As indicated above, there is a pressing need for identification of novel therapeutics that hold not only anti-inflammatory potential, but also an ability to exert pro-regenerative effects in order to effectively promote tissue repair and regrowth. As is it known that macrophages not only co-ordinate tissue repair and regeneration through inflammatory activity, but also through the secretion of growth factors that recruit and promote differentiation of progenitor cells such as MSC, it was also of interest to examine the pro-regenerative potential of IP and HPP treated primary human macrophages. To this end, the expression of the vascularisation-associated genes, *VEGF-A*, *PDGF-BB*, and *ANG1,* were examined by RT-qPCR following treatment with IP and HPP for 24 hours. mRNA expression of the transforming growth factor *TGFβ1* was also assessed given its role in regulating tissue repair and regrowth. It was observed that IP treatment resulted in a significant upregulation of *VEGF-A* and *PDGF-BB*, which promote early vascularisation and maturation of vessels respectively, and a trend towards upregulation of *ANG1* (P=0.0798), which acts to stabilise vessels and regulates VEGF-mediated vessel permeability (Figure 4.12 A-C). HPP was found to significantly upregulate *VEGF-A*, and there was a trend towards increased *PDGF-BB* expression following HPP treatment (P=0.0915). *ANG1*, on the other hand, was not significantly upregulated (Figure 4.12 D-F). IP upregulated all three vascularisation-associated genes to a greater extent than HPP. Similarly, IP was found to significantly upregulate mRNA expression of *TGFβ1* which plays a regulatory role in osteogenic and chondrogenic differentiation of progenitor cells (Figure 4.13 A). Finally, a trend towards increased *TGFβ1* expression was observed as a result of HPP treatment (P=0.0781) (Figure 4.13 B).

4.4.7 IP-conditioned macrophage media does not significantly impact on pro-osteogenic and pro-regenerative gene expression in human mesenchymal stem cells.

Given the observed increases in genes associated with vascularisation and regeneration upon IP/HPP treatment in macrophages, it was next of interest to determine whether the ketoacid-conditioned macrophage secretome can impact on the osteogenic and

regenerative potential of human MSC. Given that more potent effects on the anti-inflammatory and pro-regenerative profile of macrophages were exerted by IP as opposed to HPP, and given that IP has been more extensively studied in the literature in the context of therapeutic potential, IP was chosen as the ketoacid with which to test this hypothesis. Primary human macrophages were left untreated (conditioned media [CM]), or pre-treated with IP (1000 µM) for 24 hours, after which the IP-conditioned media (IP-CM) was removed and replaced with fresh cRPMI, which was then collected after a further 24 hours. This second collection was to ensure that any potential observed effects on MSC were not the result of residual ketoacid in the media, but rather a response to the IP-conditioned macrophage secretome (SEC-CM). MSC were then treated with a media control (1:1 ratio DMEM and RPMI), or conditioned media at a 1:1 ratio with DMEM for 48 hours prior to assessment of pro-osteogenic and growth factor gene expression by RT-qPCR. It was observed that there was a slight increase in the expression of *BMP2* upon IP-CM and SEC-CM treatment (Figure 4.14 A), while IP-CM significantly increased mRNA expression of the osteogenic transcription factor, *RUNX2.* Furthermore, there was a small increase in expression of *RUNX2* upon SEC-CM treatment but this was not significant (Figure 4.14 B). While there was a trend towards increased expression of *FGF* with CM, IP-CM and SEC-CM (Figure 4.14 D), overall the effects observed were moderate. Finally, expression of osteogenesis-associated osteocalcin (*OCN*) and growth factors *TGFβ1/3* did not appear to be affected by any of the treatment conditions (Figure 4.14 C, E-F).

4.4.8 IP does not impact on the viability of human mesenchymal stem cells.

Given a small increase in the expression of *BMP2* and *FGF* as a result of IP-CM and SEC-CM treatment, and in the induction of *RUNX2* mRNA expression by IP-CM, as well as recent works implicating the potential of HO-1 inducers to impact on MSC differentiation, it was next of interest to test the ability of IP to directly impact on MSC gene expression and function. It was first necessary to ascertain that IP was non-toxic to MSC; therefore, cell viability was first assessed using Annexin V/PI staining following treatment of the cells with increasing doses of IP (250, 500, and 1000 µM). Annexin V^-/PI^- represented the viable cell population. Untreated controls were set at 100% and IP-treated MSC were compared to the average of untreated cells. No significant differences were found in cell viability as a

result of stimulation with any dose of IP used and IP was deemed suitable for further experimentation on MSC (Figure 4.15 A-B).

4.4.9 IP upregulates HO-1 in human mesenchymal stem cells.

As mentioned above, HO-1 expression and HO-1 inducers are now showing potential in the promotion of osteoblastic differentiation of MSC [61, 62, 252]. Even though a moderate effect on HO-1 expression was observed in primary human macrophages as a result of IP pre-treatment, HO-1 inducers including IP have been shown to potently increase expression of this enzyme in other cell types. Therefore, it was of interest to determine whether IP is capable of inducing HO-1 expression in MSC. To test this, MSC were treated with increasing doses (250, 500, 1000 μM) of IP for 24 hours prior to assessment of HO-1 protein expression by western blot. It was found that the highest dose (1000 μM) of IP significantly upregulated HO-1 expression in these cells (Figure 4.16 A-B). It was next of interest to assess the ability of IP to induce HO-1 in MSC over time, in order to examine whether IP-driven HO-1 induction in MSC is a temporal process, and whether induction of HO-1 is sustained over time. To test this, MSC were treated with IP (1000 μM) for 6, 24, or 48 hours before assessment of HO-1 induction by western blot. While IP did not induce HO-1 protein expression at 6 hours (Figure 4.17 A-B), there was again a significant upregulation at 24 hours (Figure 4.17 C-D), and this was sustained at 48 hours (Figure 4.17 E-F). These results confirm that IP is capable of directly inducing HO-1 expression in human MSC.

4.4.10 IP upregulates AhR- and Nrf2-related gene expression and activates Nrf2 in human mesenchymal stem cells.

Given previous results demonstrating that IP can induce upregulation of the AhR target gene, *CYP1A1*, as well as the AhR/Nrf2 related genes, *NQO1* and *GSR,* in primary human macrophages (Figure 4.3 A-F; Figure 4.4 A-L), it was of interest to examine whether IP had a similar effect in MSC. To test this, MSC were treated with IP (1000 μM) for 24 hours and the mRNA expression of AhR/Nrf2 regulated-genes was examined by RT-qPCR. It was found that *CYP1A1*, *NQO1*, and *GSR* were all significantly upregulated in MSC after 24

hours, providing indication that IP may activate the AhR and Nrf2 in these cells (Figure 4.18 A-C). To further confirm this at the protein level, and to ascertain whether putative IP-mediated Nrf2 activation is temporal in this cell type, Nrf2 expression over time was assessed using western blot. MSC were treated with IP (1000 µM) over 6, 24, and 48 hours prior to assessment of Nrf2 expression. It was found that Nrf2 expression was not significantly increased at 6 hours (Figure 4.19 A-B), but a significant increase was seen at 24 hours post-IP treatment (Figure 4.19 C-D). By 48 hours the increased expression of Nrf2 was no longer significant (Figure 4.16 E-F), together indicating that Nrf2 activation by IP occurs in a temporal manner in MSC.

4.4.11 IP upregulates vascular-associated and growth factor gene expression in human mesenchymal stem cells.

As IP treatment was found to induce mRNA expression of vascular-associated genes as well as growth factor expression in primary human macrophages, it was next of interest to test whether IP could induce similar pro-vascularisation and regeneration-associated genes in MSC. To test this, MSC were treated with IP (1000 µM) for 48 hours prior to assessment of vascularisation-associated *VEGF-A* and *PDGF-BB*, as well as *TGFβ1*, *TGFβ3*, and fibroblast growth factor (*FGF*) by RT-qPCR. It was found that IP significantly upregulated mRNA expression of *VEGF-A* at 48 hours, but had no discernible effect on *PDGF-BB* (Figure 4.20 A-B). mRNA expression of *TGFβ1* and *FGF* were also significantly increased at 48 hours, while a trend towards significance was observed for *TGFβ3* (P=0.0509) (Figure 4.20 C-E). This implies that IP may have potential pro-regenerative effects on MSC, with possible enhancement of vascularisation and production of soluble mediators that contribute to tissue repair and regrowth that warrants further investigation.

4.4.12 IP potentially promotes osteoblastic differentiation of human mesenchymal stem cells.

In order to further probe the potential for IP in the context of osteogenic differentiation of MSC, the ability of IP to directly impact on MSC mRNA expression of *BMP2*, *RUNX2*, and

OCN was assessed by RT-qPCR. MSC were treated with IP (1000 µM) for 48 hours and assessed for osteogenic mRNA expression. It was found that *BMP2*, *RUNX2*, and *OCN* were significantly upregulated at 48 hours (Figure 4.21 A-C). This complements what was seen at the gene expression level in the IP-treated macrophage conditioned media experiment regarding *RUNX2* expression and potential *BMP2* expression as a result of IP-CM exposure, and implicates IP as a potential promotor of osteoblastic differentiation in MSC. To investigate this further, an alizarin red assay was performed to assess MSC mineralisation as a result of IP exposure. MSC were treated with IP (1000 µM) for 48 hours before being cultured in expansion media (DMEM without osteogenic supplements) as a negative control, or osteogenic induction media (DMEM supplemented with osteogenic supplements 10 mM β-glycerol phosphate, 100 nM dexamethasone, and 0.05 mM ascorbic acid) for a further 14 days. Assessment of mineralisation on day 14 showed an enhanced appearance of calcification granules in the IP-conditioned group as compared to positive control (osteogenic induction media alone) (Figure 4.22 A), and further quantification by dye extraction showed a significant enhancement in mineralisation in the IP-conditioned group compared to positive control (osteogenic induction media alone) (Figure 4.22 B). This further implies that IP may promote osteoblastic differentiation of MSC in an *in vitro* model of osteogenesis.

4.4.13 IP-mediated upregulation of *RUNX2* and *VEGF* is dependent on aryl hydrocarbon receptor activation.

In order to test whether activation of the AhR (as indicated by the IP-induced upregulation of *CYP1A1*) is necessary for IP to mediate its potential pro-osteogenic and pro-regenerative effects in MSC, a selective AhR receptor antagonist, CH223191, was used. MSC were pre-treated with CH223191 (10 µM) for 1 hour prior to stimulation with IP (1000 µM) for 48 hours and gene expression was assessed by RT-qPCR. *CYP1A1* mRNA expression was assessed as a readout for AhR activation, and it was found that pre-treatment of cells with CH223191 significantly reduced IP-mediated induction of this gene (Figure 4.23). The effect of CH223191 pre-treatment on IP-induced osteogenic genes *BMP2*, *RUNX2*, and *OCN*, as well as vascular-associated *VEGF-A* and growth factors *TGFβ1* and *FGF* was next assessed. AhR inhibition with CH223191 significantly reduced IP-induced mRNA

expression of *VEGF-A* and *RUNX2* (Figure 4.24 B-C), while there was a trend towards reduced IP-induced *TGFβ1* mRNA expression (P=0.0725) (Figure 4.24 F). IP-induced *BMP2*, *FGF*, and *OCN* expression were not significantly impacted by CH223191 (Figure 4.24 A, D-E), with this preliminary evidence suggesting that IP may mediate some, but not all, observed effects in MSC via signalling through the AhR.

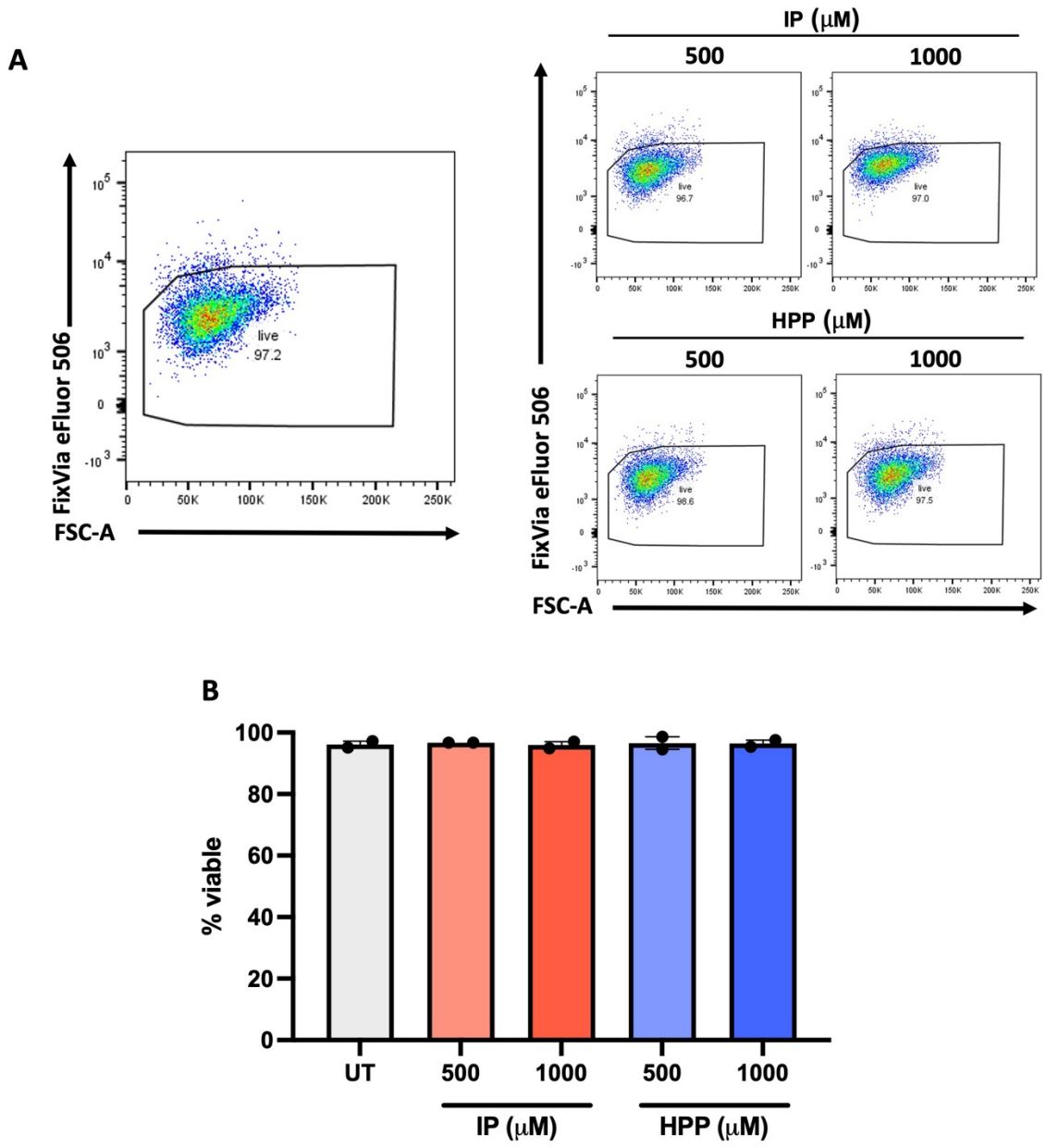

Figure 4.1 IP and HPP are non-toxic to primary human macrophages.

Primary human macrophages (1 x 10^6 cells) were left untreated (UT) or incubated with IP or HPP (500 and 1000 μM) for 24 hours. Cells were stained with FixVia eFluor 506 viability dye and analysed by flow cytometry. **(A)** Dot plots depicting Annexin V and PI expression from one representative experiment. **(B)** Pooled data showing the mean ± SEM of viable cells as compared to respective untreated control (N=2).

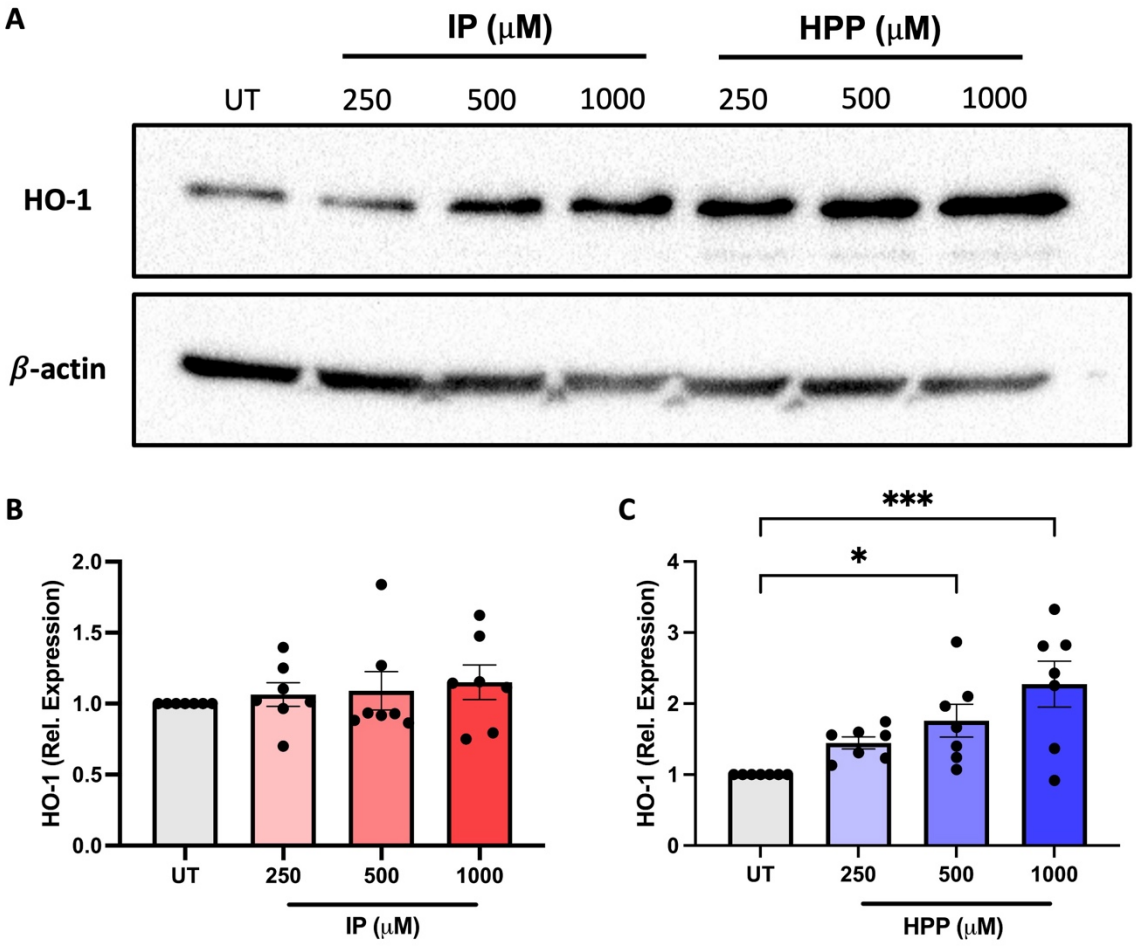

Figure 4.2 HPP upregulates HO-1 in a dose-dependent manner to a greater extent than IP in primary human macrophages.

Primary human macrophages (1 x 10^6 cells) were left untreated (UT) or incubated with **(A-B)** IP or **(A, C)** HPP (250 - 1000 μM) for 24 hours. HO-1 expression was detected by western blot. **(A)** Representative blot of HO-1 and corresponding β-actin protein. **(B, C)** Pooled data (N=7) depicting densitometric analysis of immunoblots using BioRad Software. Bar graphs illustrate mean ± SEM increase in protein expression relative to untreated control and normalised to β-actin housekeeping protein. Data were analysed using one-way ANOVA with Dunnett's post-test (*P≤0.05, ***P≤0.001).

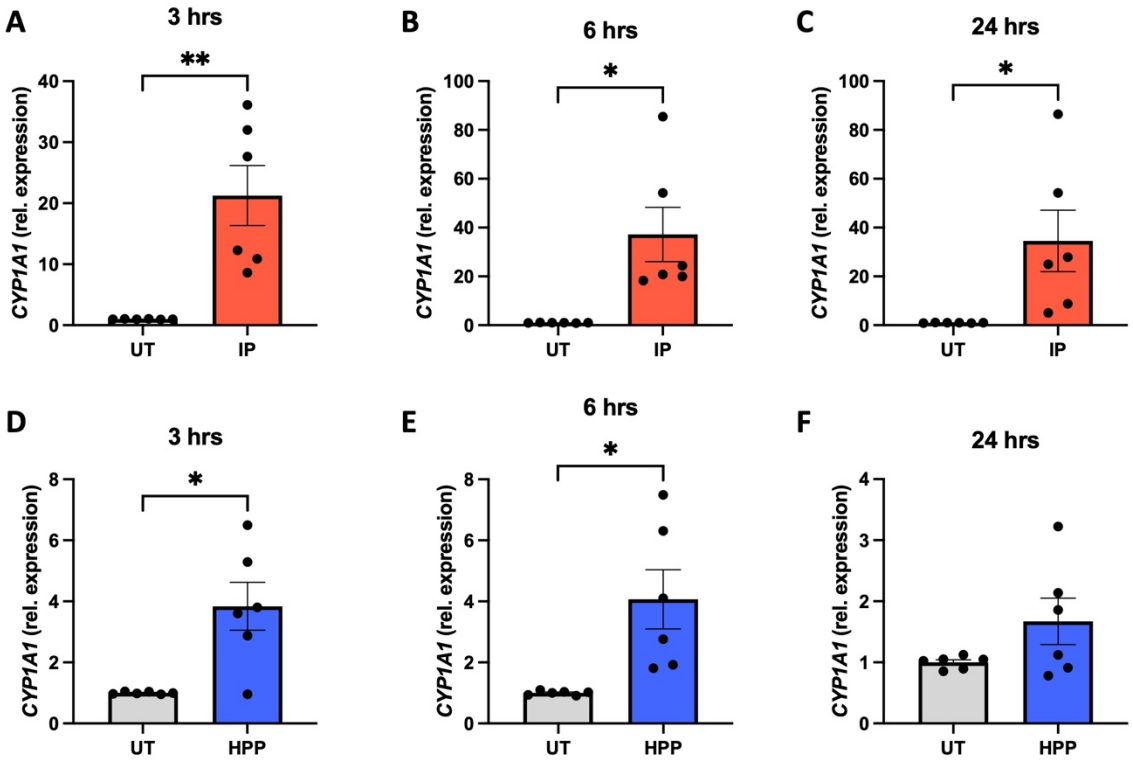

Figure 4.3 IP and HPP upregulate mRNA expression of *CYP1A1* over time in primary human macrophages.

Primary human macrophages (1 x 10^6 cells) were left untreated (UT) or incubated with **(A-C)** IP or **(D-F)** HPP (both 1000 µM) for 3, 6, or 24 hours. mRNA expression of *CYP1A1* was analysed by RT-qPCR. Pooled data (N=6) are represented as mean ± SEM. Data were analysed using Student's t-test (*P≤0.05, **P≤0.01).

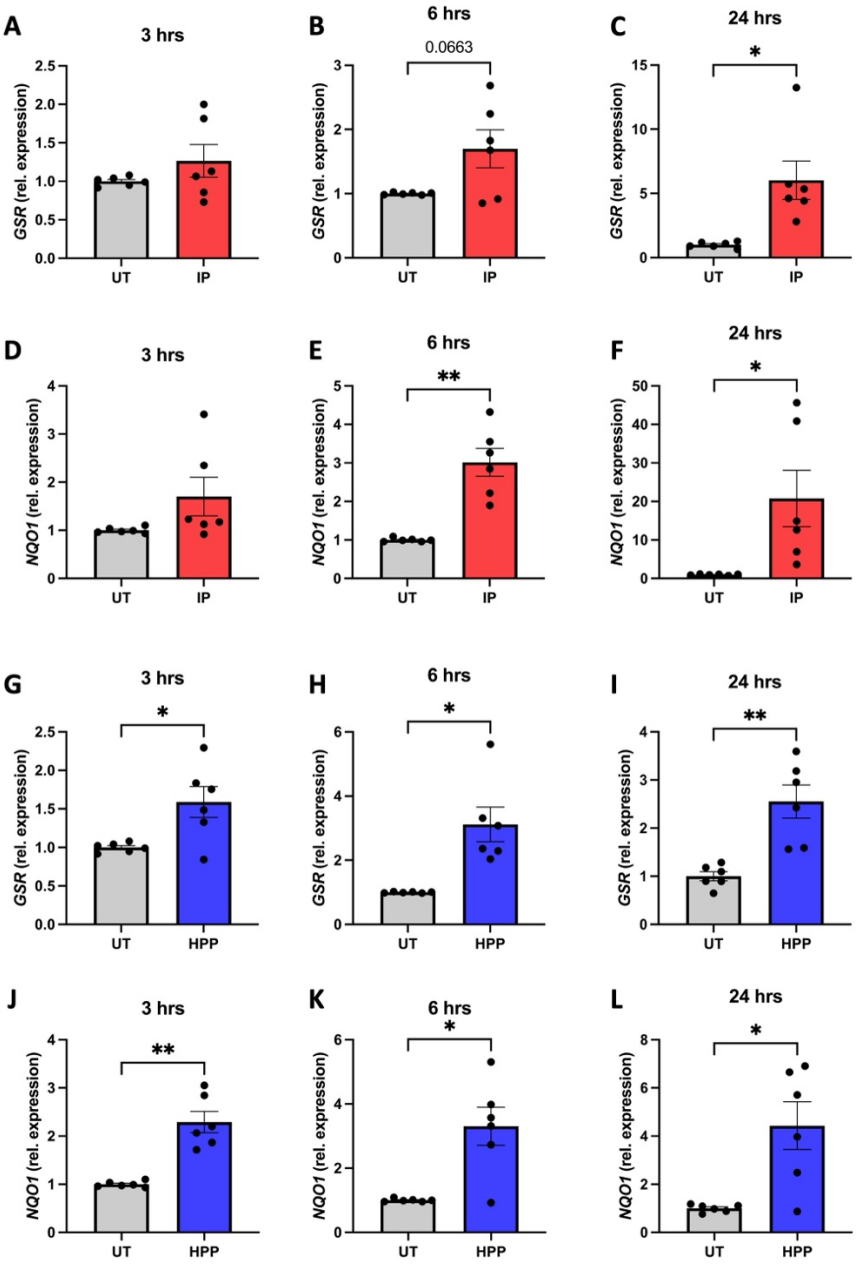

Figure 4.4 IP and HPP upregulate mRNA expression of *GSR* and *NQO1* over time in primary human macrophages.

Primary human macrophages (1 x 10^6 cells) were left untreated (UT) or incubated with **(A-F)** IP or **(G-L)** HPP (both 1000 μM) for 3, 6, or 24 hours. mRNA expression of *NQO1* and *GSR* was analysed by RT-qPCR. Pooled data (N=6) are represented as mean ± SEM. Data were analysed using Student's t-test (*P≤0.05, **P≤0.01).

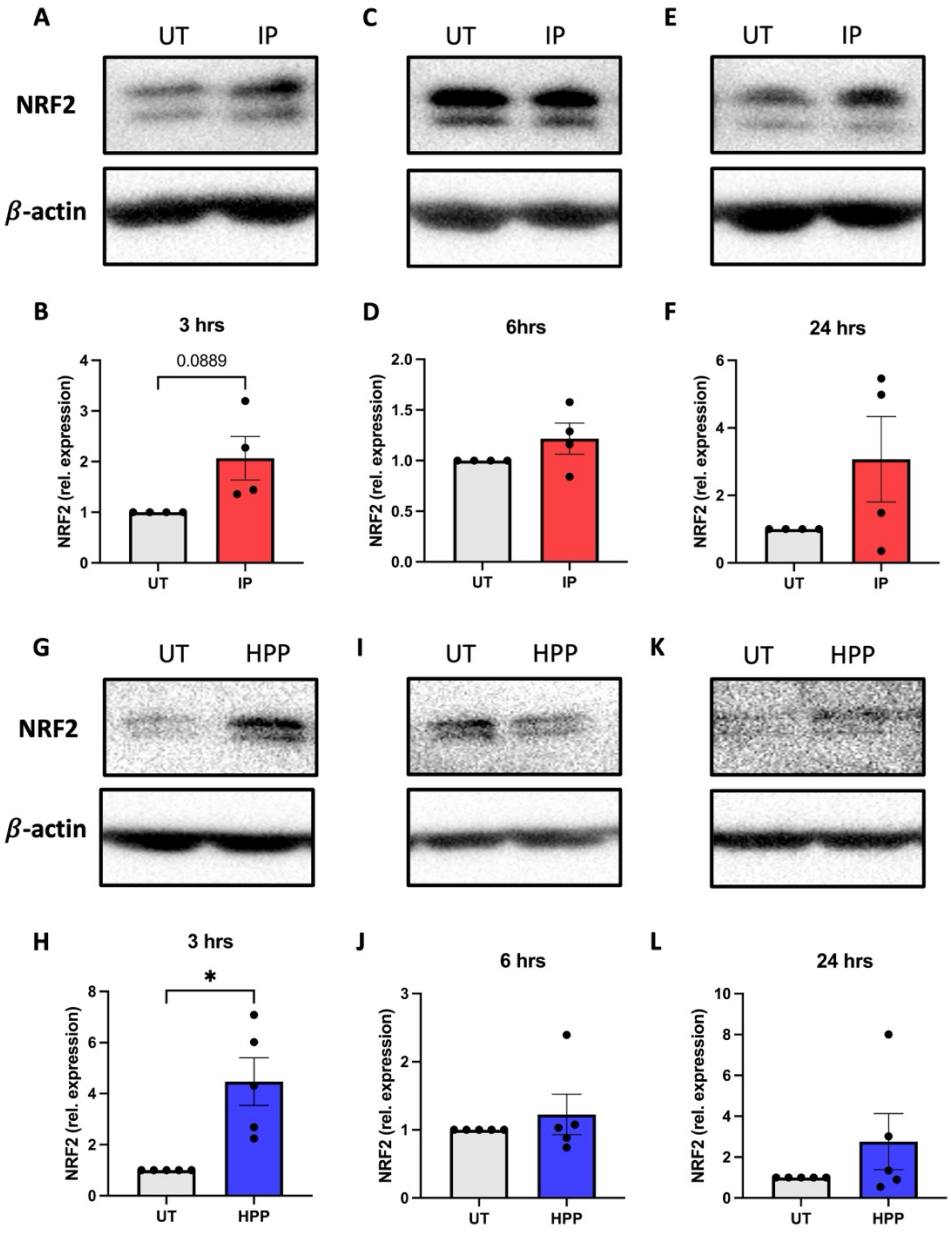

Figure 4.5 IP and HPP activate Nrf2 at 3 hours in primary human macrophages.

Primary human macrophages (1 x 10^6 cells) were left untreated (UT) or incubated with **(A-F)** IP or **(G-L)** HPP (both 1000 µM) for 3, 6, or 24 hours. Nrf2 expression was detected by western blot. **(A,C,E,G,I,K)** Representative blots of Nrf2 and corresponding β-actin protein. **(B,D,F,H,J,L)** Pooled data (N=4-5) depicting densitometric analysis of immunoblots using BioRad Software. Bar graphs illustrate mean ± SEM increase in protein expression relative to untreated control and normalised to β-actin housekeeping protein. Data were analysed using Student's t-test (*P≤0.05).

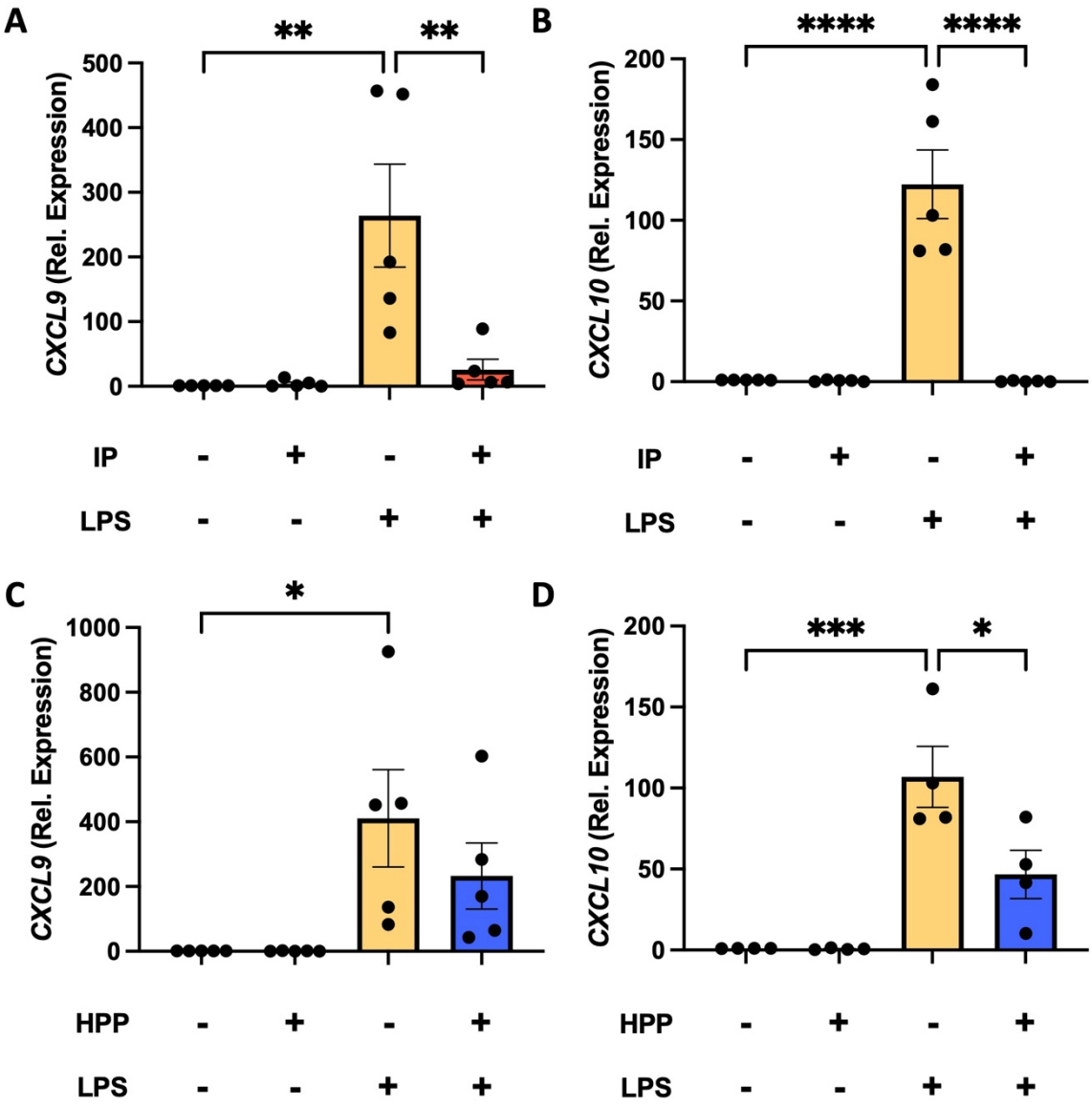

Figure 4.6 IP and HPP attenuate LPS-induced mRNA expression of *CXCL9* and *CXCL10* in primary human macrophages.

Primary human macrophages (1 x 10^6 cells) were treated with **(A-B)** IP or **(C-D)** HPP (both 1000 µM) for 6 hours prior to LPS stimulation (100 ng/ml) for 24 hours. mRNA expression of **(A, C)** *CXCL9* and **(B, D)** *CXCL10* was analysed by RT-qPCR. Pooled data (N=4-5) are represented as mean ± SEM. Data were analysed using one-way ANOVA with Tukey's post-test (*P≤0.05, **P≤0.01, ***P≤0.001, ****P≤0.0001).

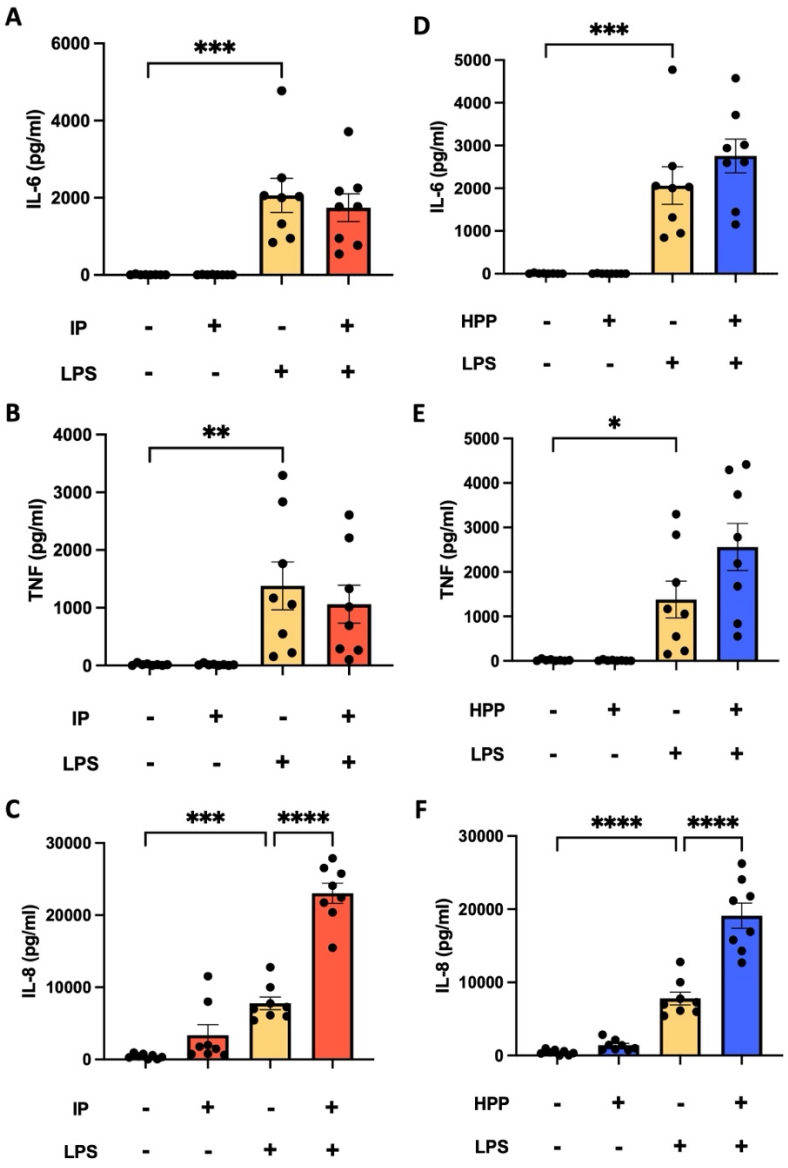

Figure 4.7 IP and HPP have no significant effect on the production of pro-inflammatory cytokines TNF and IL-6, but increase production of IL-8, in LPS-stimulated primary human macrophages.

Primary human macrophages (1 x 10^6 cells) were treated with **(A,B,C)** IP or **(D,E,F)** HPP (both 1000 µM) for 6 hours prior to LPS stimulation (100 ng/ml) for 24 hours. Supernatants were assessed using ELISA for **(A, D)** IL-6, **(B, E)** TNF and **(C, F)** IL-8 production in the presence or absence of ketoacid, LPS, or both. Data are represented as mean ± SEM and were analysed using one-way ANOVA with Tukey's post-test (*P≤0.05, **P≤0.01, ***P≤0.001, ****P≤0.0001).

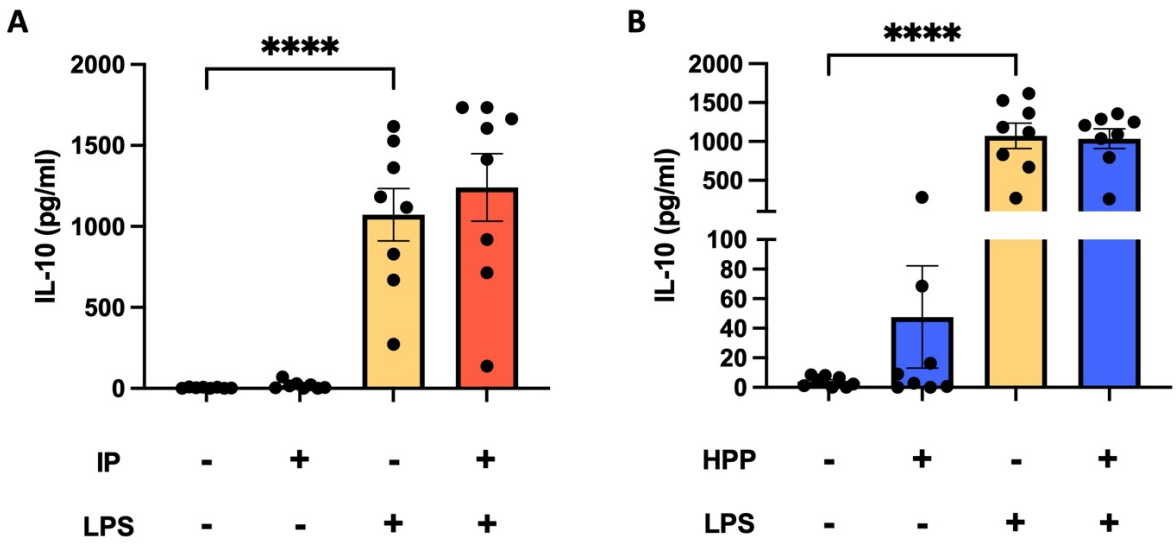

Figure 4.8 IP and HPP have no significant effect on the production of anti-inflammatory cytokine IL-10 in primary human macrophages.

Primary human macrophages (1 x 10^6 cells/ml) were treated with **(A)** IP or **(B)** HPP (both 1000 μM) for 6 hours prior to LPS stimulation (100 ng/ml) for 24 hours. Supernatants were assessed by ELISA for IL-10 production in the presence or absence of ketoacid, LPS, or both. Data are represented as mean ± SEM and were analysed using one-way ANOVA with Tukey's post-test (****P≤0.0001).

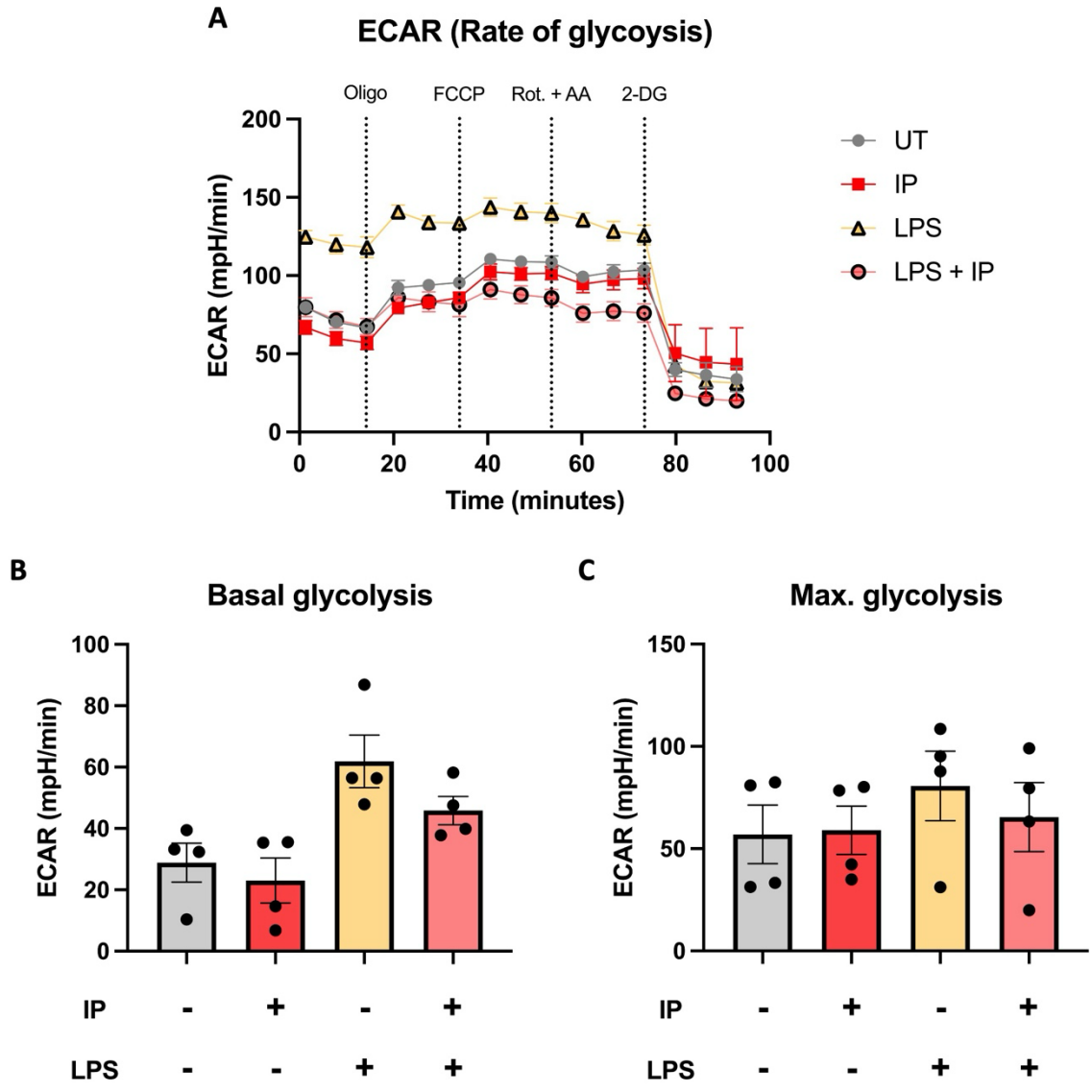

Figure 4.9 IP attenuates glycolysis in LPS-stimulated macrophages.

Primary human macrophages ($2x10^5$ cells) were treated with IP (1000 µM) for 6 hours followed by LPS stimulation (100 ng/ml) for 3 hours prior to placement in a Seahorse XF96 analyser. The extracellular acidification rate (ECAR) was measured before and after injections of oligomycin (1 µM), FCCP (1 µM), antimycin A (500 nM)/Rotenone (500 nM), and 2-DG (25 mM). **(A)** Representative ECAR measurements depicting rate of glycolysis. **(B-C)** Pooled data (N=4) depicting the calculated mean basal and maximum rates of glycolysis. Data are represented as mean ± SEM and were analysed using Kruskal-Wallis with Dunn's post-test.

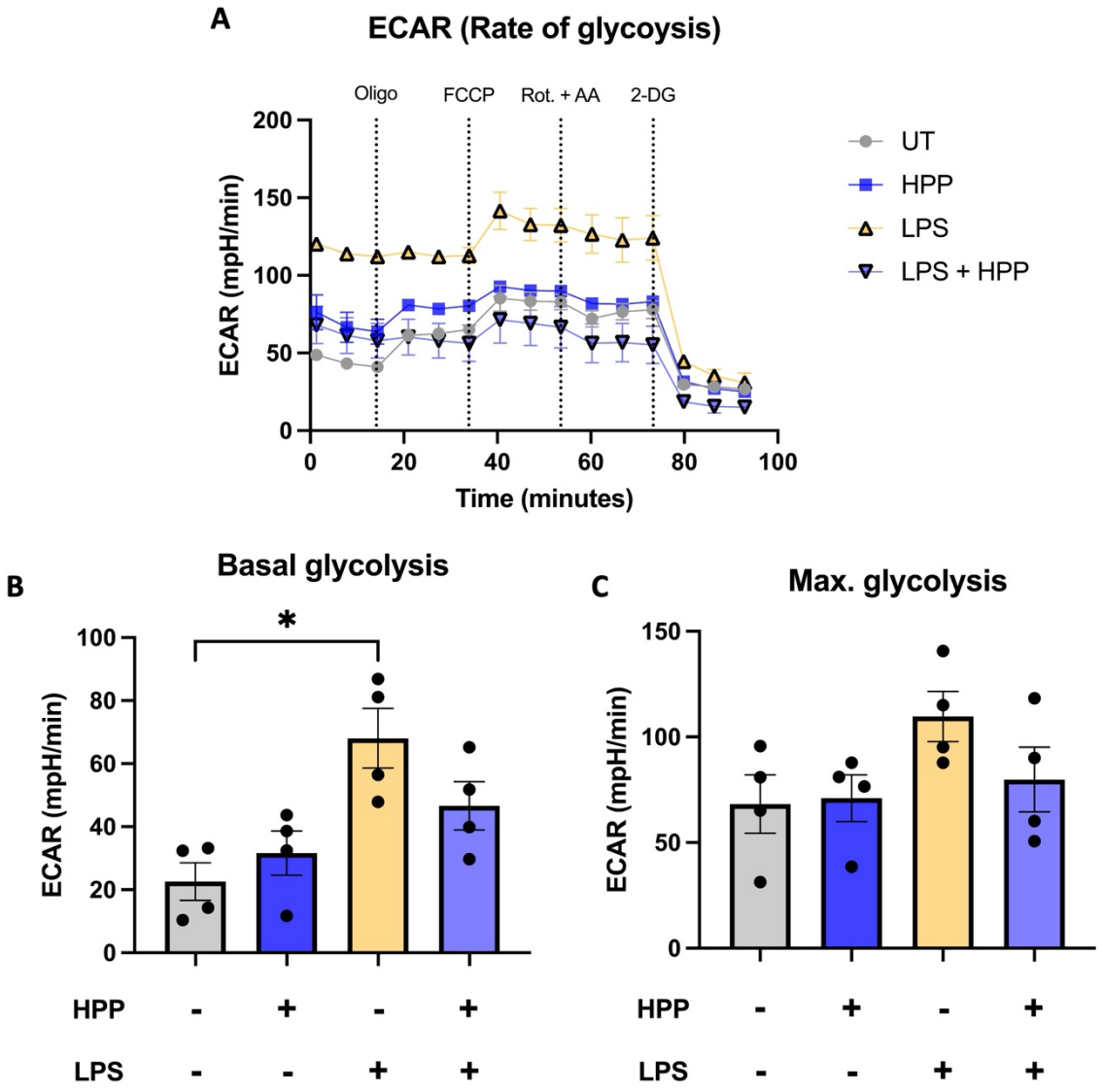

Figure 4.10 HPP attenuates glycolysis in LPS-stimulated macrophages.

Primary human macrophages ($2x10^5$ cells) were treated with HPP (1000 µM) for 6 hours followed by LPS stimulation (100 ng/ml) for 3 hours prior to placement in a Seahorse XF96 analyser. The extracellular acidification rate (ECAR) was measured before and after injections of oligomycin (1 µM), FCCP (1 µM), antimycin A (500 nM)/Rotenone (500 nM), and 2-DG (25 mM). **(A)** Representative ECAR measurements depicting rate of glycolysis. **(B-C)** Pooled data (N=4) depicting the calculated mean basal and maximum rates of glycolysis. Data are represented as mean ± SEM and were analysed using Kruskal-Wallis with Dunn's post-test (*P≤0.05).

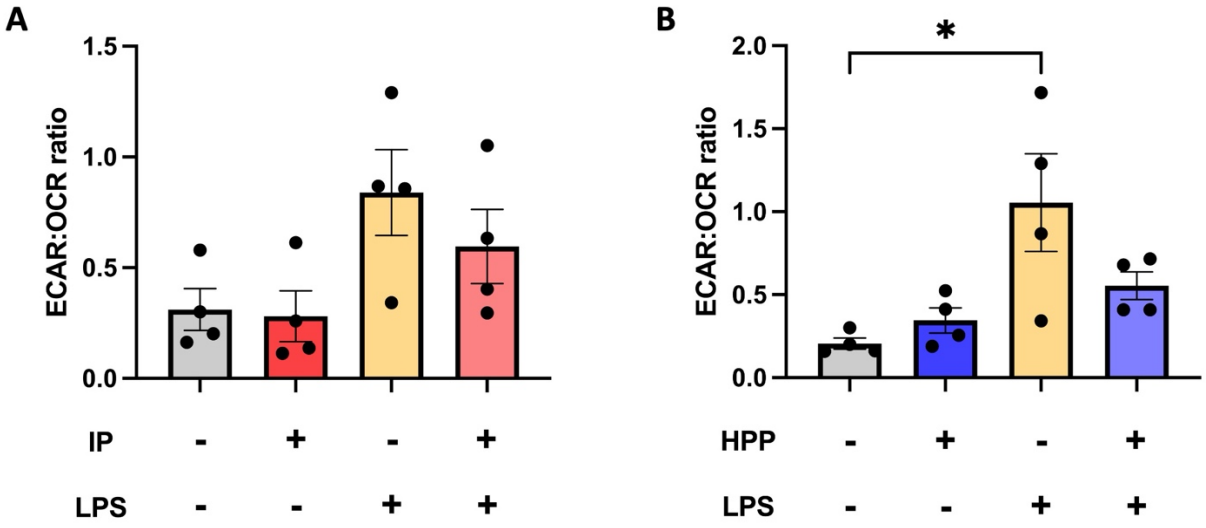

Figure 4.11 IP and HPP attenuate the glycolytic shift that occurs in LPS-stimulated macrophages.

Primary human macrophages ($2x10^5$ cells) were treated with IP or HPP (1000 µM) for 6 hours followed by LPS stimulation (100 ng/ml) for 3 hours prior to placement in a Seahorse XF96 analyser. The extracellular acidification rate (ECAR) was measured before and after injections of oligomycin (1 µM), FCCP (1 µM), antimycin A (500 nM)/Rotenone (500 nM), and 2-DG (25 mM). **(A-B)** Pooled data (N=4) depicting the calculated ECAR:OCR ratio. Data are represented as mean ± SEM and were analysed using Kruskal-Wallis with Dunn's post-test (*P≤0.05).

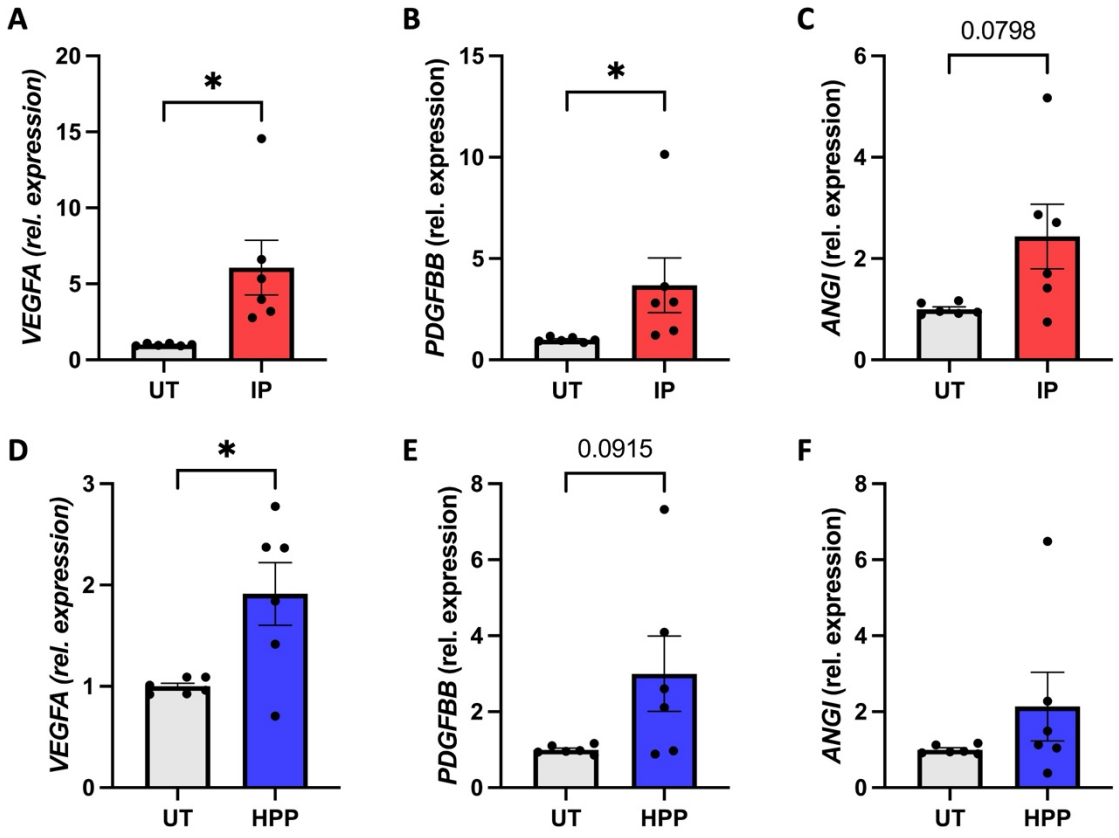

Figure 4.12 IP and HPP upregulate vascularisation-associated genes in primary human macrophages.

Primary human macrophages (1 x 10^6 cells) were left untreated (UT) or incubated with **(A-C)** IP or **(D-F)** HPP (both 1000 µM) for 24 hours. mRNA expression of **(A, D)** *VEGF-A* and **(B, E)** *PDGF-BB*, and **(C, F)** *ANG1* was analysed by real-time PCR. Pooled data (N=6) are represented as mean ± SEM. Data were analysed using Student's t-test (*P≤0.05).

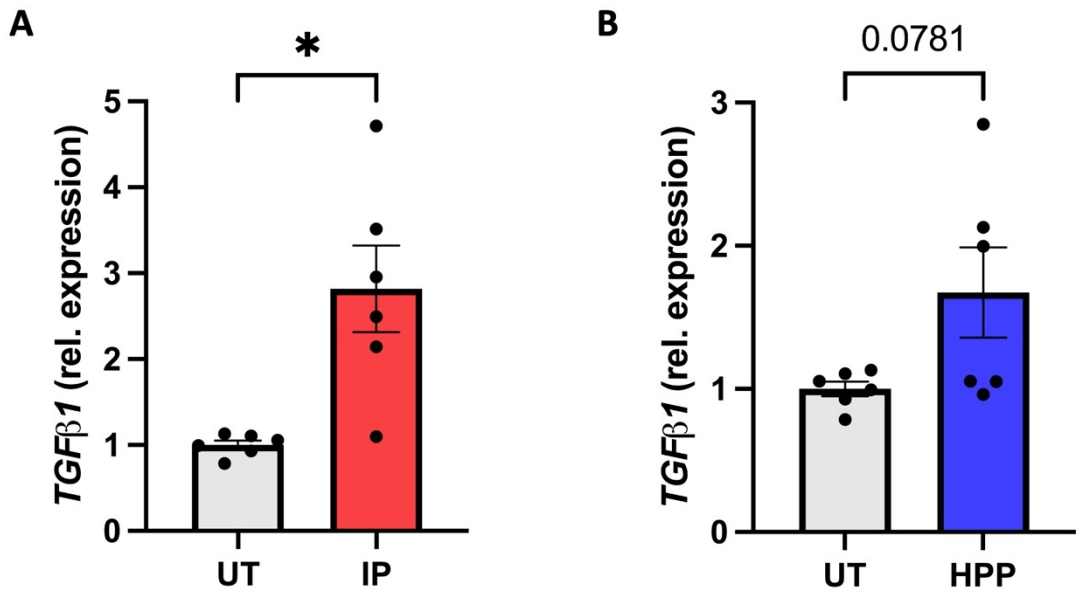

Figure 4.13 IP and HPP upregulate mRNA expression of growth factor *TGFβ1* in primary human macrophages.

Primary human macrophages (1 x 10^6 cells) were left untreated (UT) or incubated with **(A)** IP or **(B)** HPP (both 1000 μM) for 24 hours. mRNA expression of **(A, B)** *TGFβ1* was analysed by real-time PCR. Pooled data (N=6) is represented as mean ± SEM. Data were analysed using Student's t-test (*P≤0.05).

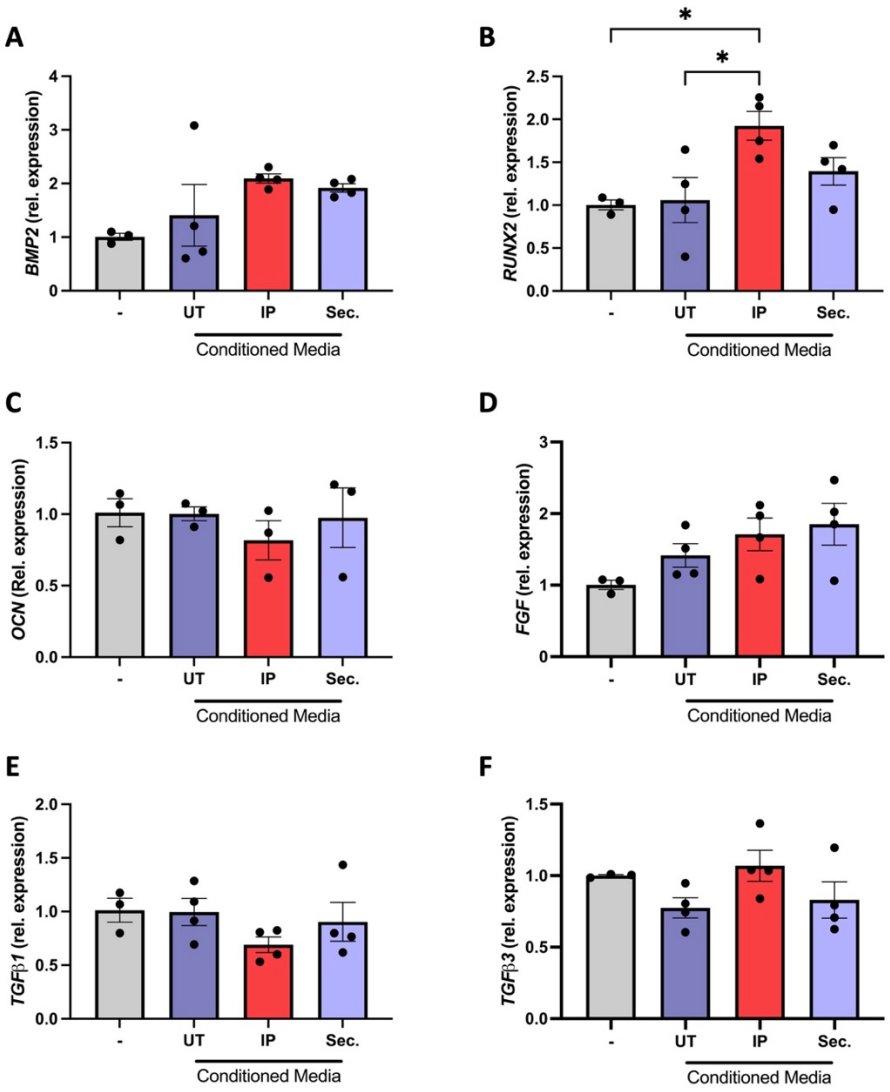

Figure 4.14 The effect of IP-conditioned macrophage media on osteogenic gene expression and growth factor gene expression in human mesenchymal stem cells.

Primary human macrophages (1 x 10^6 cells) were left untreated (UT) or stimulated with IP (1000 µM) for 24 hours. UT macrophage media (CM) and IP-conditioned media (IP-CM) was harvested, and RPMI was replenished on those that had received IP. Replenished media was collected after 24 hours (SEC-CM). Human mesenchymal stem cells (1 x 10^5 cells/ml) were treated with media control (1:1 RPMI to DMEM) or 1:1 DMEM to conditioned media for 48 hours. mRNA expression of **(A)** *BMP2,* **(B)** *RUNX2,* **(C)** *OCN,* **(D)** *FGF*, **(E)** *TGFβ1,* and **(F)** *TGFβ3* was analysed by RT-qPCR. Pooled data (N=3-4) are represented as mean ± SEM. Data were analysed using one-way ANOVA with Tukey's post hoc test (*P≤0.05).

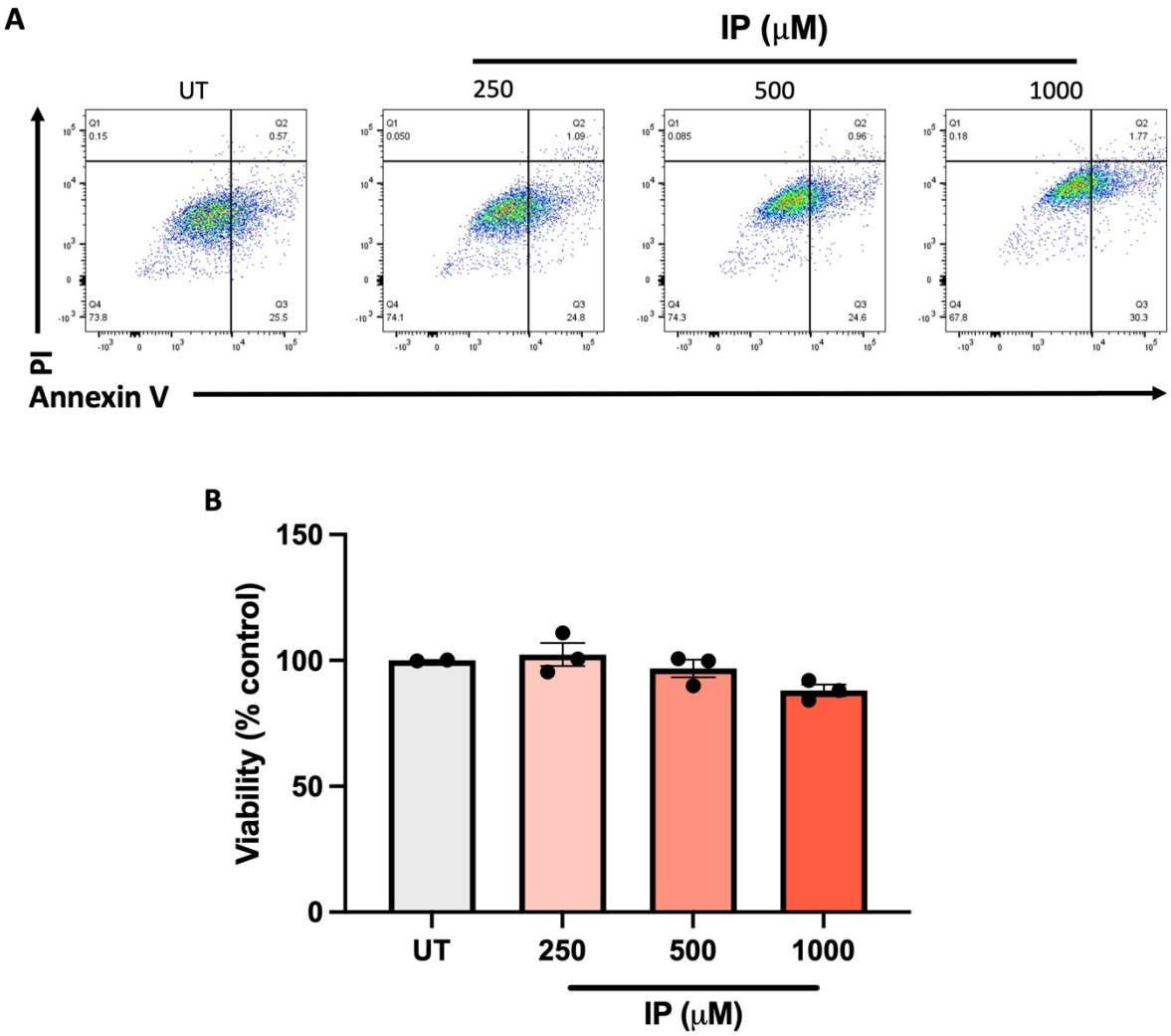

Figure 4.15 IP is non-toxic to human mesenchymal stem cells.

Human mesenchymal stem cells were left untreated (UT) or incubated with IP (250-1000 μM) for 24 hours. Cells were stained for Annexin V and PI uptake as indicators of apoptosis and necrosis, and analysed by flow cytometry. Viable cells were defined as Annexin V^- PI^- (non-apoptotic/necrotic cells). **(A)** Dot plots depicting Annexin V and PI expression from one representative experiment. **(B)** Pooled data showing the mean (± SEM) of Annexin V^- PI^- cells as a percentage of untreated (n=3). Data were analysed using one-way ANOVA with Dunnett's post hoc test.

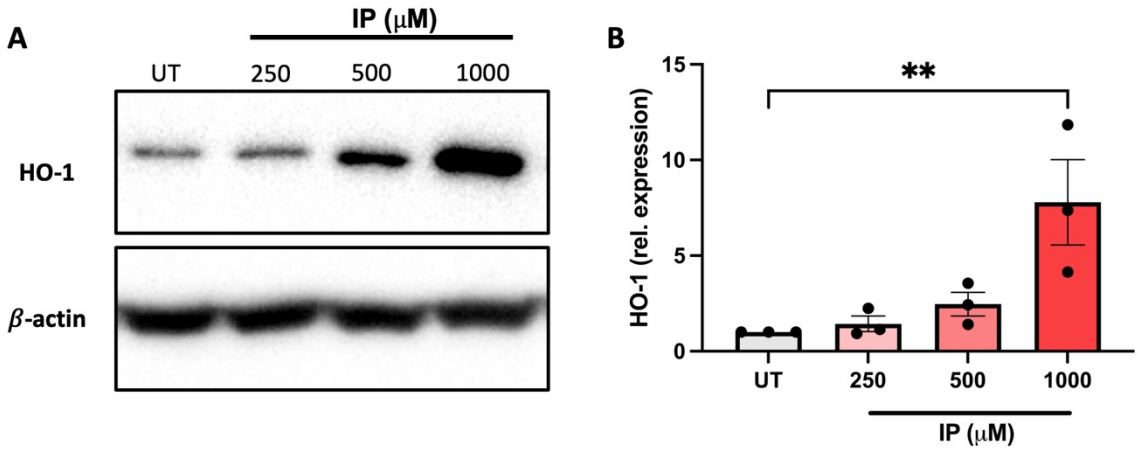

Figure 4.16 IP induces HO-1 in a dose-dependent manner in human mesenchymal stem cells.

Human mesenchymal stem cells were left untreated (UT) or incubated with IP (250-1000 μM) for 24 hours. HO-1 expression was detected by western blot. **(A)** Representative blot of HO-1 and β-actin protein. **(B)** Pooled data (n=3) depicting densitometric analysis of immunoblots using BioRad Software. Bar graphs illustrate mean ± SEM increase in protein expression relative to untreated control and normalised to β-actin housekeeping protein. Data were analysed using one-way ANOVA with Dunnett's post hoc test (**P≤0.01).

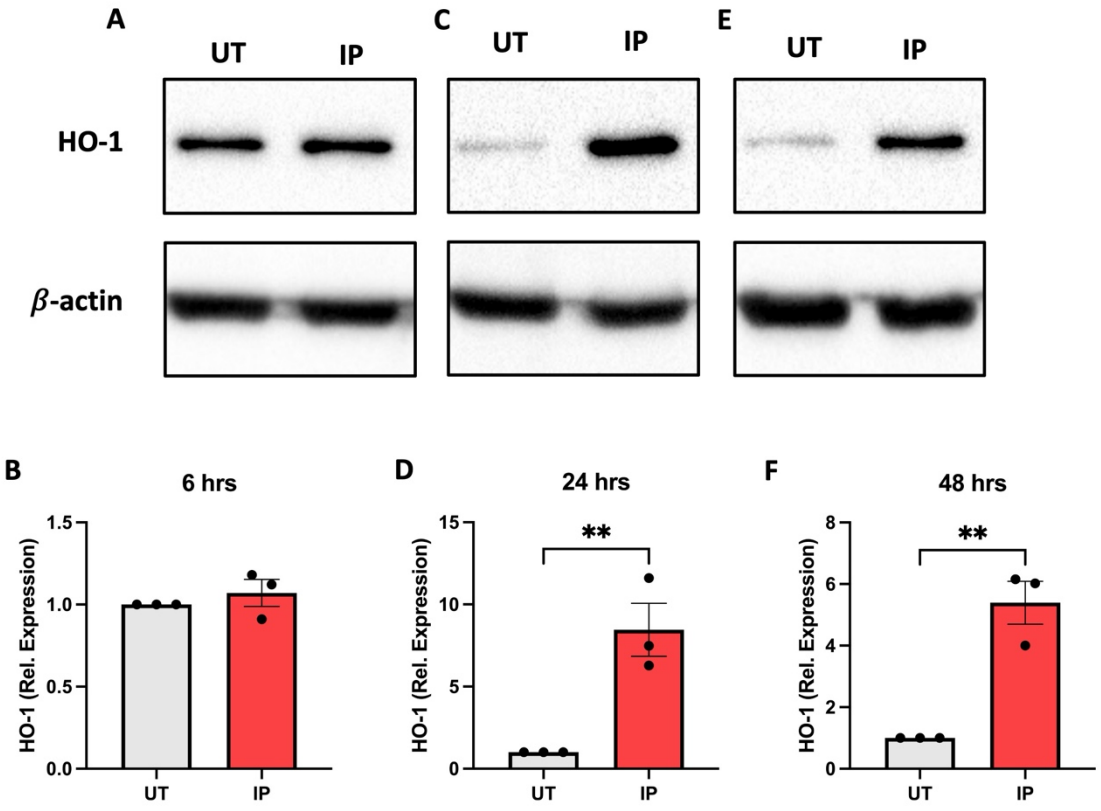

Figure 4.17 IP induces HO-1 in a temporal manner in human mesenchymal stem cells.

Human mesenchymal stem cells were left untreated (UT) or incubated with IP (1000 µM) for 6, 24, and 48 hours. HO-1 expression was detected by western blot. **(A, C, E)** Representative blots of HO-1 and β-actin protein. **(B, D, F)** Pooled data (n=3) depicting densitometric analysis of immunoblots using BioRad Software. Bar graphs illustrate mean ± SEM increase in protein expression relative to untreated control and normalised to β-actin housekeeping protein. Data were analysed using Student's t-test (**P≤0.01).

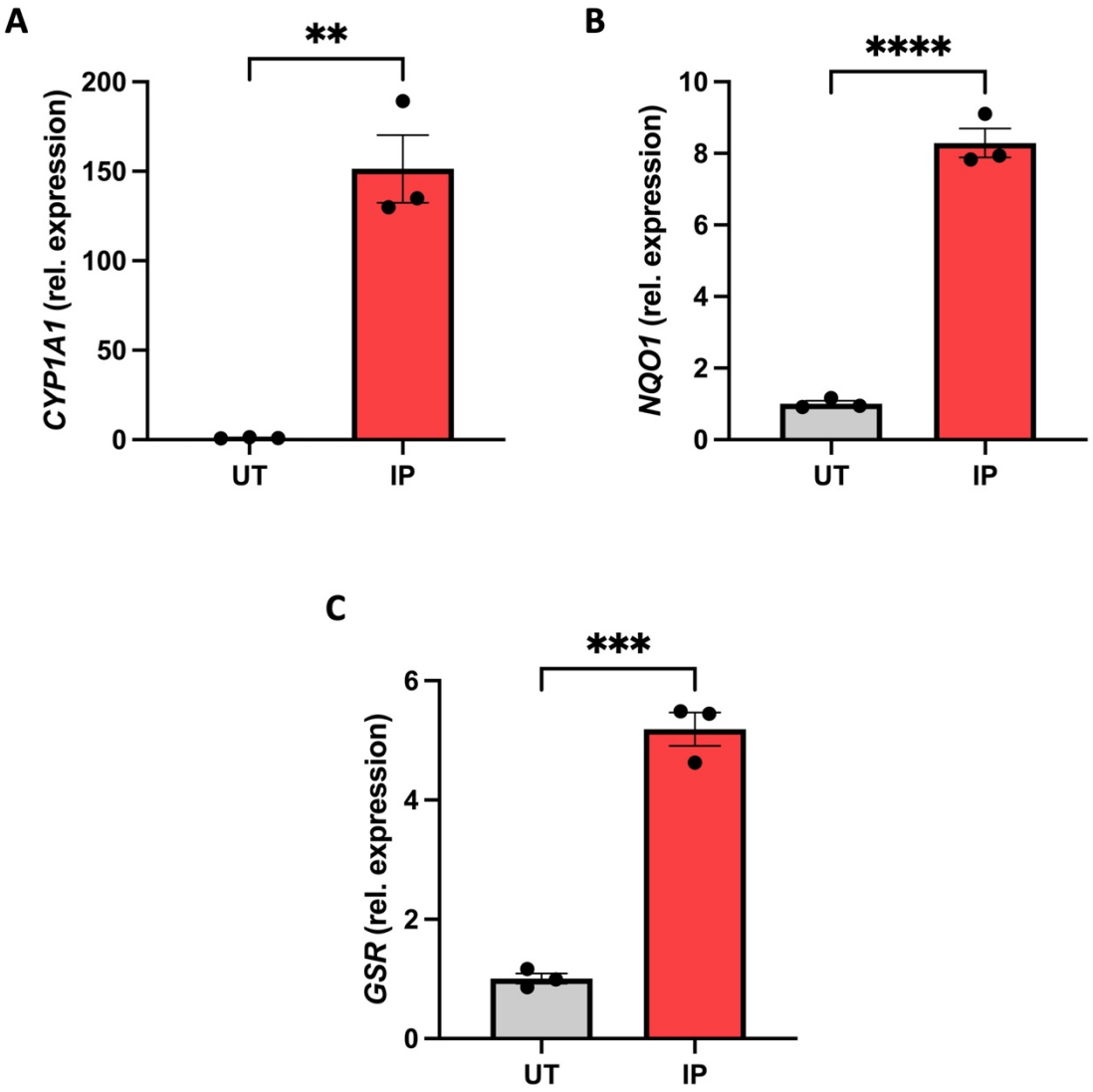

Figure 4.18 IP induces AhR and Nrf2-associated genes *CYP1A1* and *NQO1*, and Nrf2-associated gene *GSR* in human mesenchymal stem cells.

Human mesenchymal stem cells were left untreated (UT) or incubated with IP (1000 µM) for 24 hours. mRNA expression of **(A)** *CYP1A1,* **(B)** *NQO1*, and **(C)** *GSR* was analysed by RT-qPCR. Pooled data (n=3) is represented as mean ± SEM. Data were analysed using Student's t-test (**P≤0.01, ***P≤0.001, ****P≤0.0001).

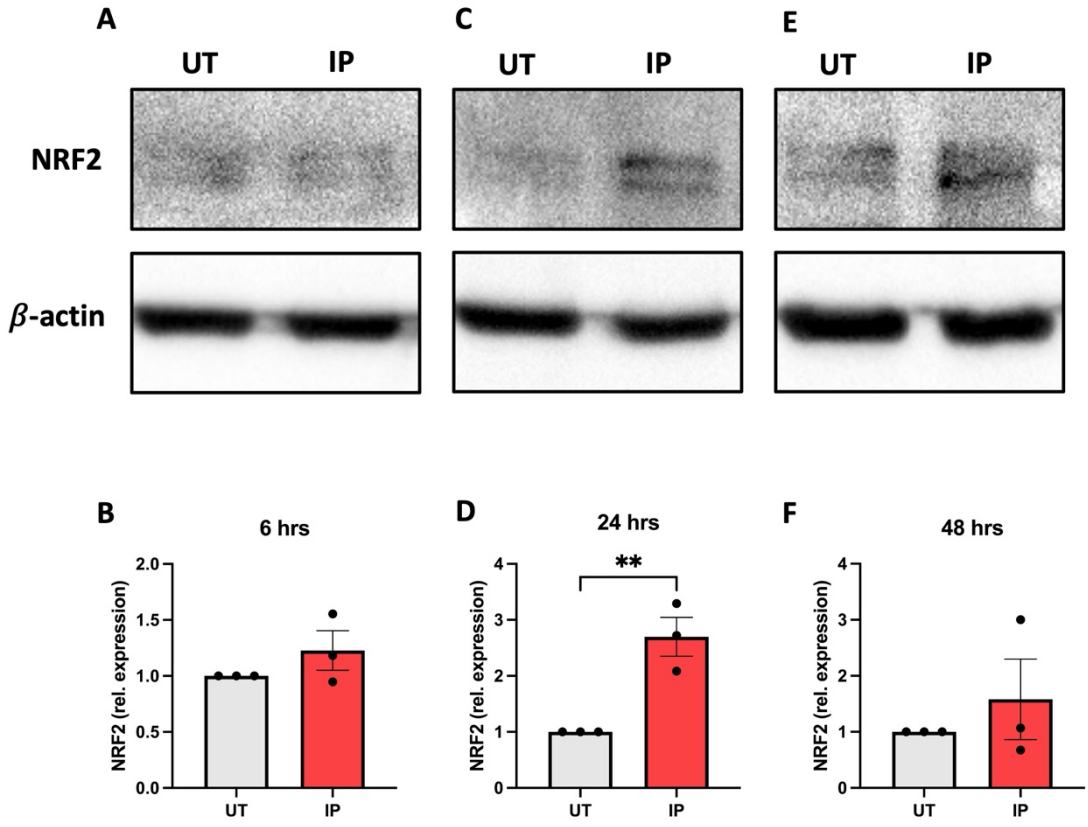

Figure 4.19 IP activates Nrf2 in human mesenchymal stem cells at 24 hours.

Human mesenchymal stem cells were left untreated (UT) or incubated with IP (1000 µM) for 6, 24, and 48 hours. Nrf2 expression was detected by western blot. **(A, C, E)** Representative blots of Nrf2 and β-actin protein. **(B, D, F)** Pooled data (n=3) depicting densitometric analysis of immunoblots using BioRad Software. Bar graphs illustrate mean ± SEM increase in protein expression relative to untreated control and normalised to β-actin housekeeping protein. Data were analysed using Student's t-test (**P≤0.01).

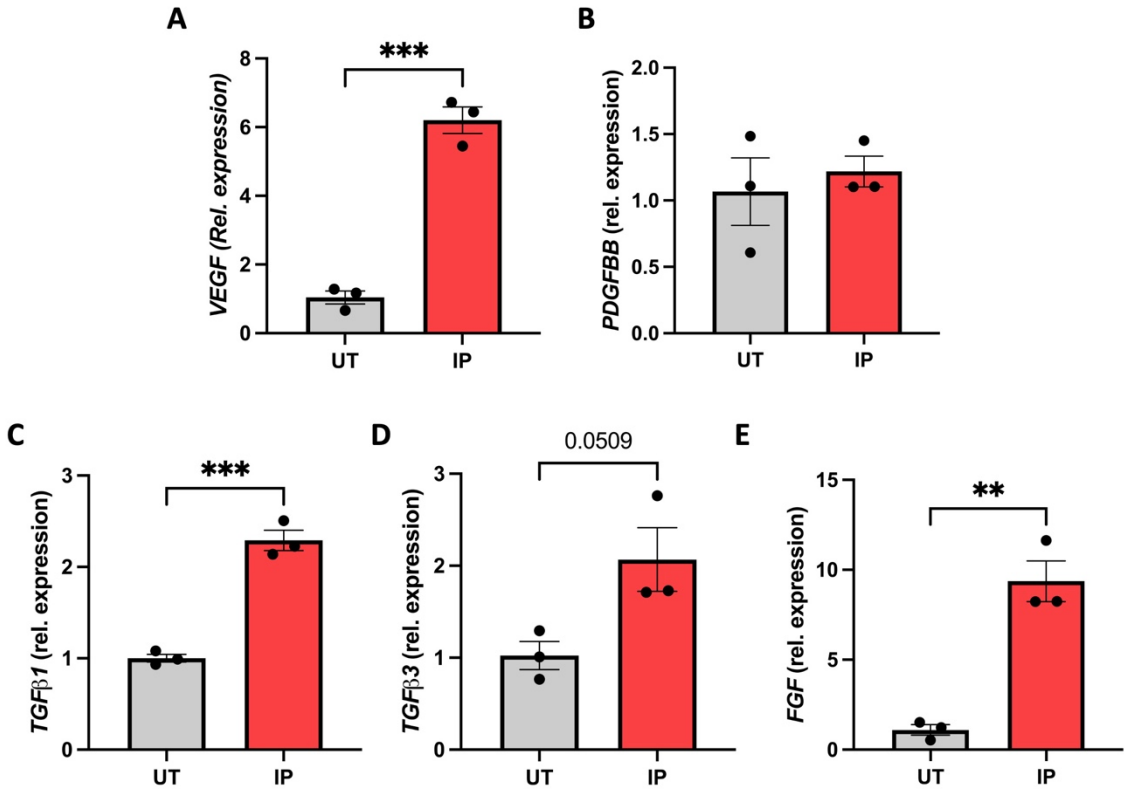

Figure 4.20 IP upregulates vascularisation-associated and growth factor genes in human mesenchymal stem cells.

Human mesenchymal stem cells were left untreated (UT) or incubated with IP (1000 µM) for 48 hours. mRNA expression of **(A)** *VEGF-A,* **(B)** *PDGF-BB*, **(C)** *TGFβ1*, **(D)** *TGFβ3,* and **(E)** *FGF* was analysed by RT-qPCR. Pooled data (n=3) is represented as mean ± SEM. Data were analysed using Student's t-test (**P≤0.01, ***P≤0.001).

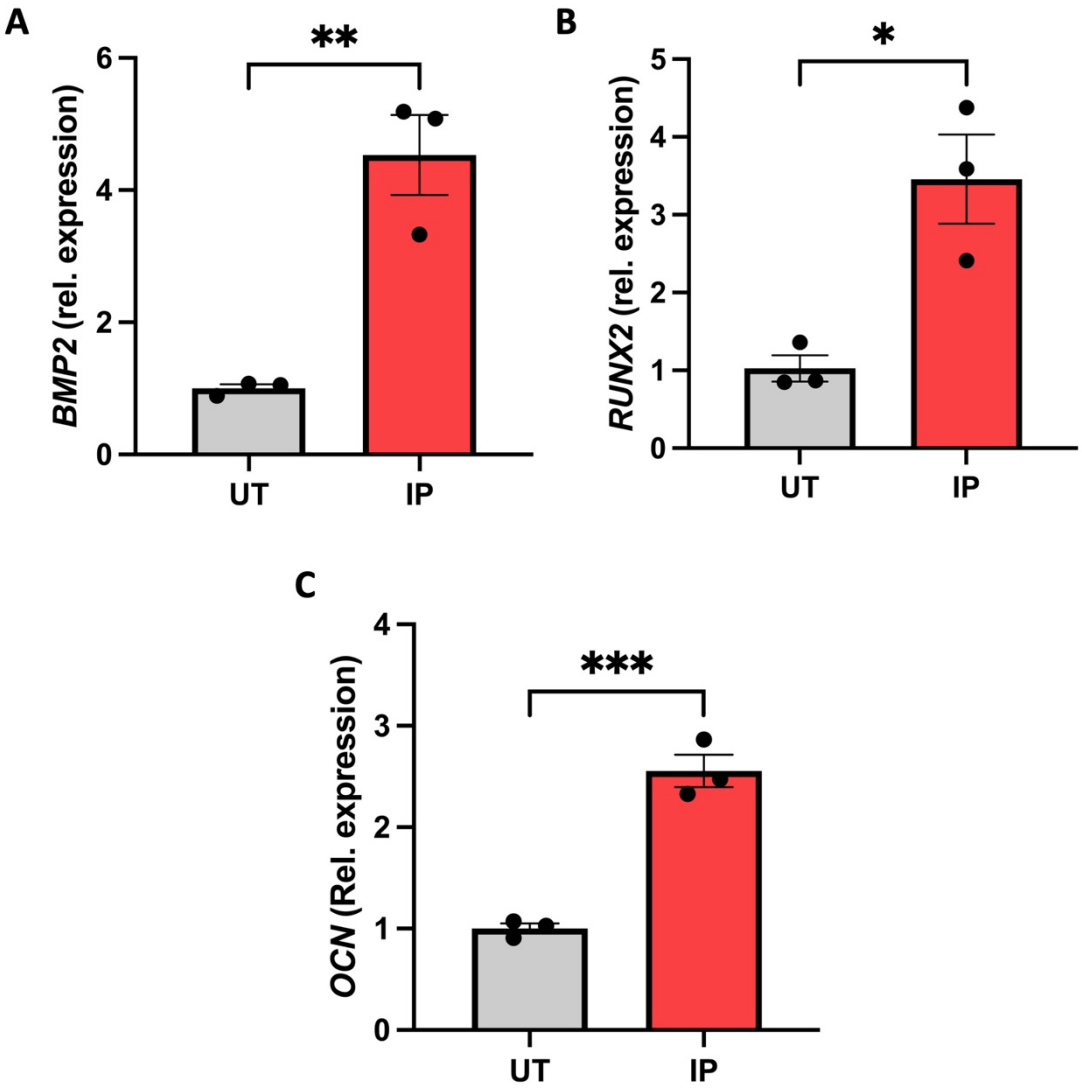

Figure 4.21 IP upregulates osteogenic genes in human mesenchymal stem cells.

Human mesenchymal stem cells were left untreated (UT) or incubated with IP (1000 µM) for 48 hours. mRNA expression of **(A)** *BMP2,* **(B)** *RUNX2*, and **(C)** *OCN* was analysed by RT-qPCR. Pooled data (n=3) is represented as mean ± SEM. Data were analysed using Student's t-test (*P≤0.05, **P≤0.01, ***P≤0.001).

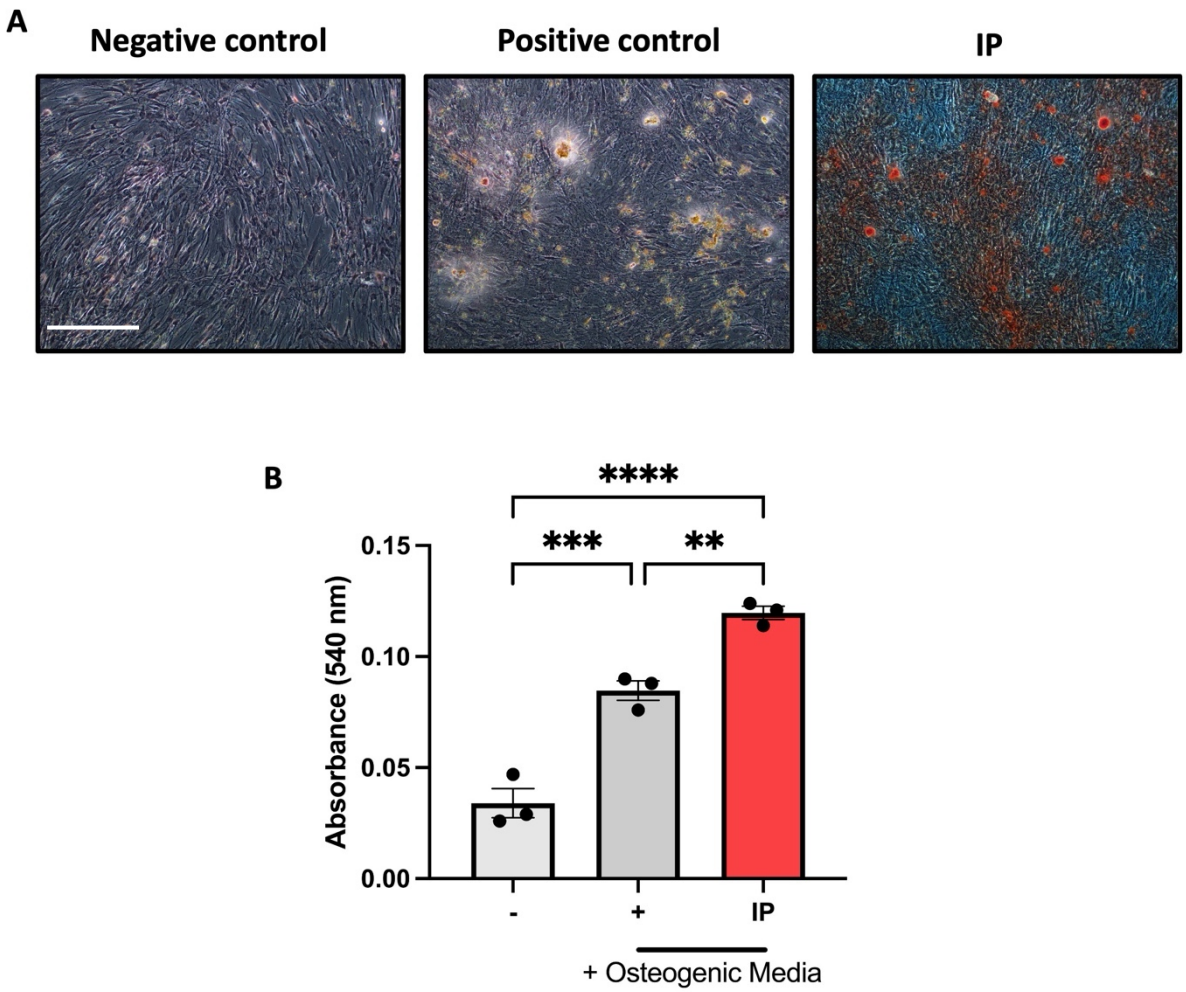

Figure 4.22 IP exposure enhances mineralisation of human mesenchymal stem cells at 14 days.

Human mesenchymal stem cells were left untreated (UT) or incubated with IP (1000 µM) for 48 hours before culture for a further 14 days in in osteogenic media, or expansion media only as a negative control. On day 14, cells were stained with Alizarin Red (AR) and imaged. **(A)** Representative images of negative control, positive control, and IP-conditioned MSC at day 14. Images 4X, scale bar=250 µm. **(B)** Pooled data (n=3) of cells destained with cetylpyrinidium chloride and AR dye quantification by measuring absorbance at 540 nm. Data were analysed using one-way ANOVA with Tukey's post hoc test. (**P≤0.01, ***P≤0.001, ****P≤0.0001).

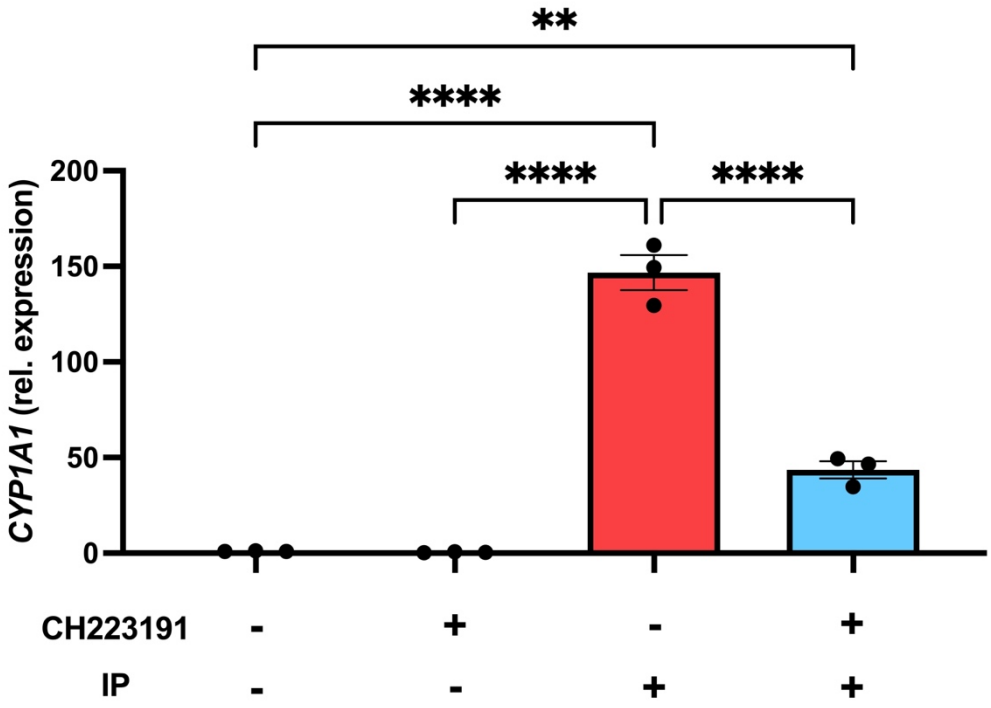

Figure 4.23 AhR antagonist CH223191 reduces IP-induced upregulation of *CYP1A1* gene expression in human mesenchymal stem cells.

Human mesenchymal stem cells were left untreated (UT), treated with CH223191 (10 µM), incubated with IP (1000 µM), or pre-treated with CH223191 for 1 hour prior to incubation with IP for a further 24 hours. Expression of *CYP1A1* was assessed by RT-qPCR. Pooled data (n=3) are represented as mean ± SEM. Data were analysed using one-way ANOVA with Tukey post hoc test (**P≤0.01, ****P≤0.0001).

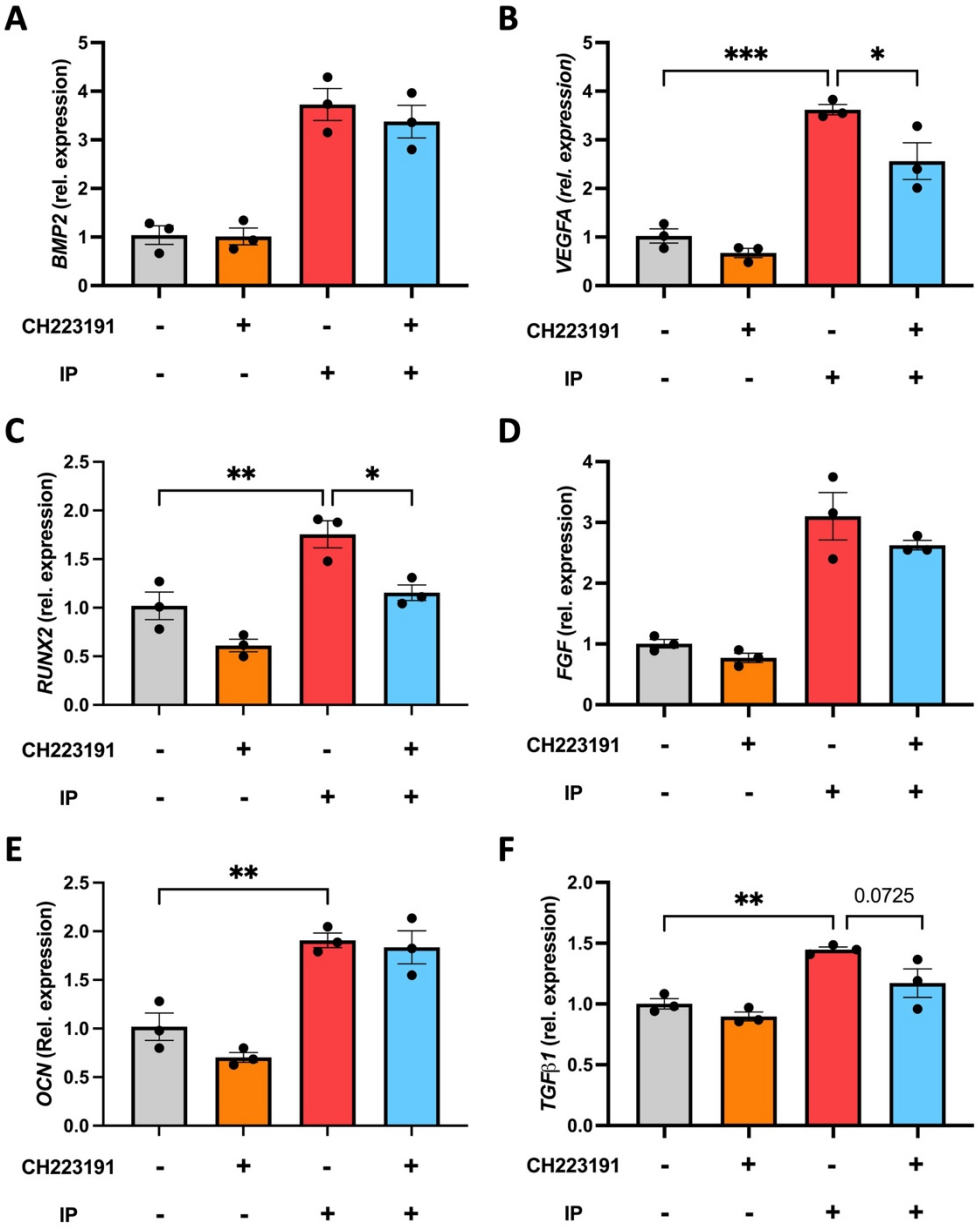

Figure 4.24 AhR antagonist CH223191 attenuates IP-induced mRNA expression of *VEGF-A* and *RUNX2* in human mesenchymal stem cells.

Human mesenchymal stem cells were left untreated (UT), treated with CH223191 (10 µM), incubated with IP (1000 µM), or pre-treated with CH223191 for 1 hour prior to incubation with IP for a further 24 hours. mRNA expression of **(A)** *BMP2,* **(B)** *VEGF-A,* **(C)** *RUNX2,* **(D)** *FGF,* **(E)** *OCN,* and **(F)** *TGFβ1* were analysed by RT-qPCR. Pooled data (n=3) are represented as mean ± SEM. Data were analysed using one-way ANOVA with Tukey post hoc test (*P≤0.05, **P≤0.01, ***P≤0.001).

4.5 Discussion

A growing understanding as to how our immune system influences and directs tissue repair and regeneration has led to a wealth of research into leveraging our immune response for desirable clinical outcomes. Generally, in the case of tissue damage or destruction, there is a need for an initial pro-inflammatory response that can initiate and propagate reparative processes, which must then transition to a primarily anti-inflammatory immune environment in order to allow continued healing and tissue regeneration [242, 243]. In the event that this pro- to anti-inflammatory transition does not occur or is halted, chronic inflammation at the defect site propagates further destructive processes [253, 254]. Therefore, there is a growing need to identify novel anti-inflammatory therapeutics that can modulate the immune response in the context of promoting tissue repair. Moreover, there is expanding interest into co-opting anti-inflammatory therapeutics for dual anti-inflammatory and pro-regenerative effects in order to mitigate immune-led destructive processes. Work in the previous chapter established immunometabolism as a potential therapeutic target in the context of host-biomaterial interactions, in which it is important to modulate inflammation and promote regeneration, and as such this chapter has further interrogated the potential of immunomodulatory metabolites to influence not only human immune cells, but also human mesenchymal stem cells for potential pro-regenerative ability in the context of bone tissue regeneration.

The *T.brucei*-secreted aromatic ketoacids IP and HPP have been studied in the context of their immunomodulatory capacity, as it is thought that the parasite secretes these ketoacids as a means of dampening the host immune response and promoting parasitic survival [78]. Indeed, these ketoacids have shown immense promise in their ability to dampen inflammatory responses of murine glia and BMDM, as well as human DC [78, 108]. These studies attribute the anti-inflammatory properties of these ketoacids to their induction of the stress-inducible enzyme HO-1, which is emerging as a potential therapeutic strategy in the context of autoimmune and inflammatory diseases [63]. Both IP and HPP are shown here to upregulate HO-1 to different extents in primary human

macrophages, with HPP appearing to act as a more potent HO-1 inducer compared to IP. This differs from murine cells and could potentially indicate a difference in the mechanism of action of IP and HPP in human macrophages. In addition, Nrf2 activation was observed as a result of both IP and HPP treatment, again aligning with what has been shown in other immune cell types such as BMDM and human DC [78, 108]. This implies a potential for immunomodulatory activity and can be likened to other metabolites that have been shown to signal through Nrf2 such as Urolithin A (UroA), a polyphenolic metabolite which has proven efficacious in pre-clinical models of colitis by exerting anti-inflammatory activity mediated *via* Nrf2-AhR pathway activation [255]. Additionally, the anti-inflammatory metabolite, itaconate, has also been shown to exert its effects via Nrf2 by alkylation of cysteine residues of KEAP1 [256]. Therefore, it is possible that a similar mechanism of action could take place in primary human macrophages under ketoacid treatment conditions, with further investigation needed.

In addition to HO-1 induction, IP and HPP can act via signalling through the AhR. Targeting the AhR is implicated in a number of autoimmune and inflammatory diseases, and has been shown to modulate immune cell functionality in cells of both the innate and adaptive immune system [257]. In murine macrophages, studies involving AhR-deficient cells have demonstrated that AhR activation is required to negatively regulate production of LPS-driven IL-6 via suppression of histamine, which functions as part of an alternative pathway to IL-6 production in macrophages versus MyD88-driven NFkB activation [258]. AhR KO macrophages were shown to increase production of IL-6, TNF, and IL-12 in response to LPS stimulation, and this was further confirmed in an *in vivo* LPS-challenge model, with the anti-inflammatory effects of the AhR found to be mediated via formation of an AhR-STAT1 complex that then binds to NFkB to regulate its transcriptional activity [259]. Indeed, it is plausible that the ability of IP and HPP observed here to downregulate LPS-induced M1-associated genes *CXCL9* and *CXCL10* is linked with their ability to activate the AhR, given that it has been shown in human carcinoma cell lines that CXCL9 and CXCL10 production is dependent on constitutive NFkB activation [260]. It was also observed in this chapter that IP is capable of upregulating expression of the AhR-associated gene, *CYP1A1,* to a greater extent than HPP, which could be linked to the comparatively more potent effects of IP versus HPP observed in reduction of LPS-induced IL-6 and TNF production, albeit not

to a significant extent. Additionally, LPS-induced production of IL-10 has been demonstrated to be hampered in AhR KO murine macrophages, and adoptive transfer of AhR-overexpressing macrophages was effective in protecting mice against LPS-induced peritonitis via production of IL-10 [261]. This ties in with the observed effects in this chapter on LPS-driven IL-10 production in macrophages with IP pre-treatment, in which LPS-stimulated macrophages pre-treated with IP were seen to moderately increase IL-10 production compared to LPS-stimulation alone, and so could potentially be linked with the more potent promotion of AhR activity by IP compared to HPP.

It is interesting to further consider how the mechanistic differences in the interaction of IP and HPP in primary human macrophages could potentially be linked to the functional differences observed in this cell type. As noted, it is observed that HPP upregulates HO-1 and Nrf2 protein expression to a greater extent than IP, whilst IP upregulates *CYP1A1* gene expression to a greater extent than HPP. Interestingly, IP is capable of suppressing the mRNA expression of LPS-induced M1-associated chemokines CXCL9 and CXCL10 to a greater extent than HPP and, although not to a significant degree, attenuating LPS-induced cytokines IL-6 and TNF. AhR ligands are documented to interact with and activate the AhR, which exert functional effects via binding of the AhR-Arnt complex to the XRE, and subsequent upregulation of genes that are under control of the XRE. Linked with, but also acting separately from, AhR activation, is the activation of Nrf2, which can subsequently bind to and upregulate anti-oxidant genes that are under the control of the ARE. It is notable that the effects mediated by IP at the functional level appear to be more potent than those of HPP in a number of cell types studied, and is therefore plausible that genes under the control of the XRE are contributing to stronger functional outcomes in terms of combatting inflammation and, as shown in this thesis, upregulating regeneration-associated genes. The evidence in the literature, and that generated in this thesis, implicate both mechanisms as potentially important to the anti-inflammatory activity of these ketoacids, and further exploration into the possible synergy between IP and HPP may yield interesting results. Indeed, early work demonstrated that the *in vivo* induction of quinone reductase, linked to the anti-cancer properties of crambene, was postulated to result from the co-activation of the ARE and XRE [262].

Building on this, different cell types are impacted to different extents by these ketoacids, as is observed in the case of murine glia and BMDM in which IP and HPP do not exert anti-inflammatory effects in BMDM to the same extent as in glia [78]. In this chapter, primary human macrophages pre-treated with IP and HPP were seen to exhibit minimal to no change in IL-6 and TNF production under LPS stimulation compared to those subject to LPS stimulation alone, which is in line with what has been documented to occur in BMDM [78, 105], and contrasts the reduction in pro-inflammatory mediators seen in murine glia and human DC [78, 108]. This could indicate a potential cell/tissue-specific effect of *T.brucei*-secreted immunomodulators that not only could provide further insight into parasitic survival mechanisms, but also indicates that any potential immunomodulatory therapeutic is worth investigation in a range of immune cell types in order to identify potential roadblocks to developing treatment, or potential for off-target effects. Alternatively, this may be advantageous from a therapeutic point of view for autoimmune diseases such as IBD where DC play a more dominant role than macrophages [263, 264]. This would negate the issues associated with potent immunotherapies which can lead to secondary infection, as seen for example in patients receiving anti-TNF therapy who require monitoring for infectious diseases such as TB and other respiratory illnesses [265-267]. It was also shown that IP and HPP could impact on the glycolytic metabolic shift driven by inflammatory stimuli such as LPS in primary human macrophages. This aligns with what has been shown in the literature regarding the ability of IP to inhibit LPS-induced glycolysis in BMDM, which was demonstrated to be mediated via targeting of HIF1α [105], and in human DC treated with IP and HPP [108].

The mild-to-moderate effects observed as a result of IP and HPP treatment in primary human macrophages may also be beneficial from the perspective of tissue regeneration. While it is appreciated that an anti-inflammatory immune environment is ultimately beneficial in the ensuing of tissue reparative responses, it is also understood that an initial inflammatory reaction is necessary to initiate the repair process and recruit other immune and progenitor cells to the defect area. In this, the effect of IP and HPP on increased IL-8 production in macrophages could be viewed as a positive aspect for tissue regeneration, given that IL-8 functions as an important chemokine in cellular recruitment and coordinating and guiding bone tissue regeneration [268]. Early IL-8 delivery from a

mesoporous bioactive glass (MBG) scaffold was shown to enhance osteogenesis *in vivo* in a murine subcutaneous and a rabbit segmental defect model, and increase BMP-2 receptors in rat bone marrow stromal cells (rBMSC) *in vitro*, resulting in a synergistic effect of IL-8 and BMP-2 on enhancement of early osteogenesis [269]. Therefore, it is plausible that ketoacid driven IL-8 production could have positive early effects on osteogenesis, as well as in recruitment of immune cells for initiation of the early immune response to tissue damage, and warrants further investigation in a bone regenerative context.

In order to further interrogate the potential for ketoacid treatment to impact on the regenerative potential of macrophages, gene expression of the angiogenic markers, *VEGF-A*, *PDGF-BB*, and *ANG1* was assessed, as well as *TGFβ1,* which are secreted by macrophages and contribute to a pro-regenerative environment in the wake of tissue injury or destruction [240]. IP and HPP were found to upregulate all markers tested, with IP again having the more pronounced effect when compared to HPP. This further indicates that possible pro-regenerative effects mediated by IP may not be entirely dependent on HO-1 induction given relatively low levels of HO-1 induction compared to HPP, but rather a result of multiple processes upon ketoacid exposure that is worthy of further investigation. The upregulation of pro-angiogenic genes in response to the ketoacids aligns with what is known in the case of certain parasitic infections such as those caused by the helminth *Heligmosomoides polygyrus (H.polygyrus)*. *H.polygyrus* infection, which has been employed as a therapy for autoimmune diseases, was accompanied by upregulation of VEGF-A and PDGF-BB in the brains of EAE mice, demonstrating the effect on angiogenic growth factors as a result of nematode infection [270], and indeed it is documented that helminths generally exhibit pro-angiogenic effects to create a niche for parasitic survival [271]. Interestingly, another type of Trypanosome, *T.Cruzi*, has been linked to exacerbated angiogenesis of the cardiac tissue in an *in vivo* model of infection, displaying increased levels of VEGF [272]. Another indole derivative produced from tryptophan, indole-3-aldehyde, was shown to have direct pro-angiogenic effects in human umbilical vein endothelial cells (HUVECs) [273]. Together, these results are in agreement with what is seen in macrophages with IP and HPP in terms of pro-angiogenic gene upregulation, and could be linked with a pro-survival mechanism employed by *T.brucei* in the case of host infection. Further experiments into assessment of soluble mediators of vascularisation,

such as by ELISA, or angiogenesis assays using direct administration of ketoacid or macrophage ketoacid-conditioned media on HUVECs will be necessary to fully elucidate the angiogenic potential of IP and HPP.

In a similar vein, TGFβ has been documented to be upregulated in response to soluble proteins secreted from the parasite, *Schistosoma mansoni* (*S.mansoni*) [274], and helminths are well-documented to leverage the TGFβ pathway as a means of immunosuppression to promote parasitic survival [275]. For example, they release TGFβ mimics that activate TGFβ signalling pathways in multiple cell types, which has been demonstrated to induce the expansion of regulatory T cells [276]. Therefore it is plausible that the upregulation seen at the mRNA level in TGFβ1 as a result of IP and HPP treatment is linked with pro-survival and immunomodulatory mechanisms used by *T.brucei*, with further investigation at the protein level required for confirmation. The possibility for these ketoacids to hold regenerative potential is further bolstered by recent work in which it was shown that ketoacids including PP and HPP are reduced in the serum of patients with multiple sclerosis (MS) compared to healthy controls. Furthermore, in this study it was demonstrated that *in vivo* administration of a combination of IP, HPP, as well as PP led to resolution of inflammation and increased remyelination in a murine EAE model [277].

Work in this chapter also sought to investigate the potential of IP to impact on the osteogenic differentiation of MSC. It was demonstrated here, for the first time, that IP is capable of inducing HO-1 and activating Nrf2 in MSC at different doses. Indeed, HO-1 induction in MSC has been linked to immunomodulatory and immunosuppressive effects, with Nrf2 activation and HO-1 induction in MSC shown to protect against inflammatory damage in the case of acute liver failure [278], and ameliorate hepatic fibrosis in a rodent model [279]. Although this investigation further focused on the regenerative potential of IP-induced HO-1 induction in MSC, it is therefore also plausible that IP could exert anti-inflammatory and immunomodulatory effects on the immune environment via interaction with MSC. It will be of interest in future studies to assess the immunomodulatory potential of IP-conditioned MSC, for example by assessment of cytokine production, conditioned media experiments, or direct/indirect co-culture involving a range of immune cell types, in order to elucidate the full potential of IP on MSC.

With respect to osteogenesis and general regenerative potential in the context of bone tissue, HO-1 induction has shown promise in promoting the osteoblastic differentiation of MSC [61, 62], while Nrf2 activation plays a more contentious role [280, 281]. With this in mind, it was of interest to interrogate whether IP could impact on the osteogenic ability of MSC by assessment of osteogenesis-associated marker expression and downstream mineralisation, as well as other pro-regenerative markers that contribute to bone formation. It was first confirmed that IP was indeed able to act as a HO-1 inducer in this cell type, and had no effect on MSC viability. It was also confirmed that Nrf2 expression was increased in MSC treated with IP, indicating that HO-1 induction could be mediated via Nrf2 activation. This aligns with known HO-1 inducers in the literature such as curcumin, in which it has been shown that curcumin can induce HO-1 and Nrf2 in MSC, in addition to mitigation of damage-causing ROS production and promotion of osteoblastic differentiation [282, 283]. This was encouraging in the exploration of IP for osteogenic benefit, and further promoted interrogation of osteogenic markers at the gene expression level. It was found that IP induced the mRNA upregulation of osteoblast-associated growth factor *BMP2*, BMP2-induced transcription factor *RUNX2*, and interestingly, *OCN*, which contributes to mineralisation as well as regulation of differentiation [284]. Additionally, this was verified at the mineralisation level by Alizarin red staining, implying that IP not only upregulates early markers of osteoblastic differentiation, but aids in maturation of differentiated osteoblasts. Given evidence in the literature that HO-1 contributes to osteoblastic differentiation, it is plausible that the observed upregulation of osteogenic genes and downstream mineralisation are at least partially driven by IP-induced HO-1 expression. However, further investigation is required to confirm the putative osteogenic effects of IP in a long-term bone regeneration model, as well as further *in vitro* and *in vivo* testing to elucidate the mechanism of action, for example by the use of HO-1 inhibitors. Traditional inhibitors such as metalloporphyrins zinc protoporphyrin (ZnPP) and tin protoporphyrin (SnPP) prove challenging when used in conjunction with potent HO-1 inducers such as IP, with these metalloporphyrins documented to reduce HO-1 activity but upregulate HO-1 mRNA and protein expression in 293T cells [285]. Additionally, previous attempts to surmount this issue in our lab by increasing the dose of HO-1 inhibitors resulted in cell death when used in combination with ketoacid treatment [78]. An

alternative approach would be to employ HO-1 knockout models, with greater efficacy seen using shRNA and CRISPR/Cas9 to knock-down or knock-out HO-1 in 293T cells when compared to the use of traditional metalloporphyrin inhibitors [285].

It is also known that MSC express the AhR, and given the strong upregulation of *CYP1A1* as a result of IP treatment observed, it was decided to investigate whether IP could exert its observed effects via AhR activation. To this end, established AhR antagonist CH223191 was used prior to IP treatment and assessment of gene expression. Interestingly, it was seen that CH223191 pre-treatment downregulated certain markers, with more pronounced effects seen in genes such as *VEGF-A* and *RUNX2* than in others such as *BMP2* and *FGF*. Given this, it would be of interest in future work to elucidate which genes are under the control of which pathway, as it appears as though certain genes may be more heavily under the control of the AhR, while IP may also be signalling through different pathways. It is interesting to note that there is contention on the role of AhR signalling in osteoblasts in the literature, with some studies implicating AhR agonists such as 2,3,7,8-tetrachlorodibenzo-p-dioxin (TCDD) and benzo[*a*]pyrene (BaP) as impairing osteoblastic differentiation via AhR activation in MSC [286-290], and with constitutive AhR activation linked to inhibition of bone formation in mice [291]. Conversely, other work reports the ability of TCDD to increase bone mass in a murine model [292], and further links AhR activation in MSC to a decrease in adipogenesis [293], which is known to be favourable for osteoblastic differentiation [294]. Quite interestingly, a recent work investigated the effects of two AhR ligands, BaP and 6-formylindolo[3,2-b]carbazole (FICZ), which are an environmental toxin and a natural compound derived from tryptophan metabolism respectively, in a murine model of TMJ osteoarthritis and osteoblastic MC3T3 E1 cells. It was found that while BaP exposure resulted in bone resorption and osteoclastogenesis mediated through AhR activation, FICZ, which transiently activates the AhR compared to the sustained AhR activation seen with TCDD and BaP, inhibited bone-resorbing osteoclasts and enhanced bone volume *in vivo*. Furthermore, it increased expression of the osteoblastic markers, *ALPL*, *OCN*, and *COL1A1 in vitro* [295]. This could potentially explain some of the effects observed with IP in this study that contrast with studies implicating AhR activation as a negative regulator of osteoblastogenesis in MSC, and further implies that it may not be solely AhR activation, but rather the extent to which the

AhR is activated (whether this is transient or sustained) that determines the osteogenic potential of MSC. IP, therefore, could act more akin to FICZ in that the AhR is transiently activated, and signalling *via* this pathway could impact on the upregulation of certain genes as a result of IP treatment. This also implies that the nature of the AhR ligand used also plays a role in differentiation capacity, with TCDD and BaP being known environmental toxins compared to the naturally occurring FICZ and IP. Consensus on the role of the AhR in osteoblastic differentiation has therefore yet to be reached, and this study further advocates for a nuanced approach in study of the AhR in osteogenesis.

Overall, this chapter has provided further characterisation of the impact of the ketoacids, IP and HPP, on primary human macrophage phenotype and function, an area previously under-explored. In demonstration that IP and HPP do not significantly impact on the LPS-induced human macrophage inflammatory profile when compared to murine macrophages, as well as human DC, this study further emphasises the need for study of immunomodulatory therapeutics across a range of immune cell types, with particular focus on human immune cells if the goal is clinical translatability. Furthermore, this study has identified IP and HPP as potential regulators of cell recruitment and tissue regeneration, further compounded by promising effects observed in MSC. Although there does not appear to be a macrophage-mediated component in promotion of MSC differentiation, this study has shown IP itself to be a potential promoter of osteoblastic differentiation, with additional upregulation of certain pro-regenerative factors. In summary, this investigation has further implicated naturally-derived metabolites as potential therapeutics worthy of exploration not only in the context of putative anti-inflammatory effects, but also in the context of tissue regeneration for a dual-effect therapeutic.

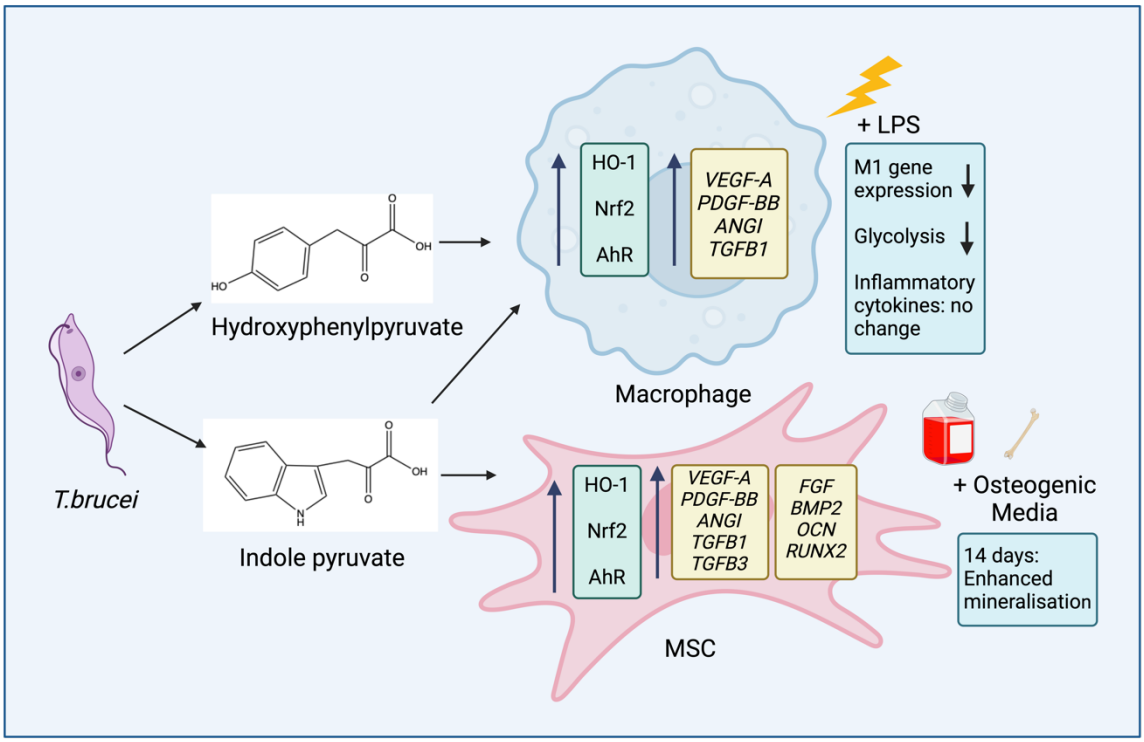

Figure 4.25 Summary schematic of research findings.

Indole pyruvate (IP) and hydroxyphenylpyruvate (HPP) upregulate HO-1 and activate Nrf2 and the AhR in primary human macrophages, as well as promote vascularisation and regeneration-associated gene expression. IP and HPP treatment attenuates LPS-induced M1-like macrophage gene expression and potentially attenuates LPS-induced glycolytic reprogramming in primary human macrophages. IP and HPP have no significant effect on LPS-induced cytokine secretion. IP upregulates HO-1 and activates Nrf2 and the AhR in human mesenchymal stem cells (MSC). IP upregulates vascularisation, regeneration, and osteogenesis-associated gene expression in MSC, and enhances mineralisation of MSC after 14 days *in vitro*.

Chapter Five

A hyaluronic acid hydrogel delivery system for immunomodulators in the context of bone regeneration

5.1 Introduction

The site of biomaterial implantation is often a hotspot for aberrant inflammatory activity that can hamper reparative and regenerative processes and can ultimately lead to the need for replacement surgeries [254]. There is much study underway into engineering a pro- to anti-inflammatory immune environment in the wake of implanted materials to facilitate repair and promote tissue growth. However, while impressive progress has been made in the field of regenerative medicine with the incorporation of bioengineering approaches, regenerative strategies for bone tissue are yet to see significant advancements that translate to the clinical level. Critical-sized defects in particular pose immense challenges to bone tissue regeneration given the need for a sufficiently stable osteoinductive biomaterials with inherent or imbued immunomodulatory properties capable of engineering a pro-regenerative environment [296].

Hydrogels are three-dimensional polymer networks formed from hydrophilic homopolymers, copolymers, or macromers that are crosslinked to form polymer matrices [297]. They exhibit many advantages in tissue engineering: their composition and structure bears similarity to natural ECM, and they can be delivered by injection and crosslinked *in situ*, allowing for a minimally invasive implantation strategy [298]. Hydrogels are derived from both naturally occurring and synthetic materials, with photo-crosslinking, pH-dependent crosslinking, ionic-crosslinking, and thermo-crosslinking all means by which gelation of hydrogels can be induced [299]. Despite displaying weaker mechanical properties, natural hydrogels offer an advantage over synthetic hydrogels in that they display excellent biocompatibility and bioactivity [300], and can be combined with other bioactive factors to enhance integration and promote regeneration at the site of implantation.

Hyaluronic acid is one such natural biopolymer that has garnered attention in recent years as a highly biocompatible material for hydrogel synthesis, and offers potential for use in bone tissue engineering given its biocompatible, biodegradable, and osteoinductive properties [299, 301, 302]. Hyaluronic acid is a non-sulphated glycosaminoglycan (GAG)

present in the ECM that aids in maintenance of form and hydration and can interact with cells expressing the surface receptors CD44 and the receptor for hyaluronan-mediated motility (RHAMM). Hyaluronic acid and hyaluronic acid derivates have begun to be used in the design of cell-seeded scaffolds or acting as delivery systems to modulate the post-implantation environment, with notable success in the fields of cardiovascular and cartilage tissue engineering [302]. Hyaluronic acid has been shown to possess inherent immunomodulatory potential at varying molecular weights: low molecular weight hyaluronic acid has been shown to promote a more pro-inflammatory environment and polarise macrophages towards an M1-like state, while in its high molecular weight form, hyaluronic acid has been shown to promote a more M2-like macrophage population and an anti-inflammatory environment [138].

In the context of bone tissue engineering, an early study demonstrated that high molecular weight (1900 kDa) hyaluronic acid enhanced bone formation through stimulating the differentiation of MSC into osteoblasts in a rat femoral bone marrow ablation model [303], with more recent work examining the effect of hyaluronic acid on induction of osteoblastic differentiation *via* enhancement of BMP2-linked Smad-signalling [304]. Indeed, as well as the pro-osteogenic effects of hyaluronic acid, the ease of tunability of hyaluronic acid hydrogel parameters posits these materials as potential modulators of the immune response. Hydrogel stiffness is one such parameter that has been implicated as a modulator of macrophage response [116, 130, 305, 306], with stiffer surfaces appearing to enhance the inflammatory profile of macrophages versus their softer counterparts. Given that many immune cells possess mechanosensing properties and this has been linked with their overall functionality, including not only macrophages but also, for example, B cells [307], DCs [308], and T cells [309], tuning hydrogel stiffness offers a possible avenue for manipulation of the overall immune microenvironment post-hydrogel implantation.

In addition to stiffness, the easily modifiable nature of hyaluronic acid hydrogels allows for the incorporation of bioactive factors such as growth factors that can further enhance integration and bone formation. Hyaluronic acid has shown success *in vivo* when used as a carrier for osteoinductive growth factors such as BMP2 [310, 311], or combined with

nanohydroxyapatite particles to prolong release and promote sustained osteogenic activity [312]. Hyaluronic acid hydrogels have also shown promise as a carrier for anti-inflammatory agents, with direct dissolution of the anti-inflammatory drug infliximab into hyaluronic acid hydrogels dampening inflammation and promoting bone repair within a critical sized defect in a rabbit model of RA [313].

The hyaluronic acid hydrogel (HyA-gel) under investigation in this chapter was studied in collaboration with the Duffy lab, NUIG. It has previously been studied in the Duffy lab by Gallagher *et al.* in MSC in the context of cardiac repair [314], and a similar hyaluronic acid hydrogel has been developed as a 3D microenvironment for monocyte cultivation [315]; however, it has not yet been thoroughly investigated in an immunomodulatory context, or utilised for the purpose of bone tissue engineering. This HyA-gel is tyramine-conjugated to allow for covalent crosslinking by an oxidative coupling reaction using HRP and H_20_2, with this method also allowing for a level of control over the mechanical strength and rate of gelation of the HyA-gel [316]. This chapter aims to assess HyA-gel biocompatibility with respect to primary human macrophages and interrogate whether macrophage phenotype is altered in response to HyA-gels of varying stiffnesses achieved by modification of crosslinker concentration. Using a rat femoral defect model, the *in vivo* effect of HyA-gel stiffness on the immune microenvironment in a bone regenerative context is then examined. Finally, the use of HyA-gel as a delivery system for the immunomodulatory metabolite indole-3-pyruvate (IP) studied in the previous chapter is interrogated in a rat femoral defect model, examining the ability of the HyA-gel to locally deliver IP as a potential immunomodulatory, pro-regenerative strategy for immune-assisted bone repair.

5.2 Hypothesis

A hyaluronic acid hydrogel can impact on the post-implantation immune microenvironment and deliver immunomodulatory therapeutics for bone tissue regeneration.

5.3 Specific Aims

- To characterise the macrophage response to a novel hyaluronic acid hydrogel.
- To determine whether hyaluronic acid hydrogel stiffness can impact on macrophage phenotype and function.
- To investigate the ability of hyaluronic acid hydrogels of different stiffnesses to impact on the *in vivo* immune environment in a rat femoral defect model.
- To investigate whether a hyaluronic acid hydrogel can be used as a delivery system for an immunomodulatory ketoacid, indole-3-pyruvate, in a rat femoral defect model.

5.4 Results

5.4.1 Hyaluronic acid hydrogels do not impact on the viability or differentiation ability of primary human macrophages and monocytes.

To first examine the biocompatibility of the HyA-gels, it was necessary to test whether HyA-gels impacted on the viability of primary human macrophages. Macrophages were seeded into tissue culture plastic (TCP) or HyA-gel surfaces for 24 hours prior to lifting and staining with Fixable eFluor 506 viability dye. Cell viability was assessed using flow cytometry. It was found that HyA-gels do not impact on macrophage viability, and HyA-gels were deemed suitable for further experimentation (Figure 5.1 A-B). It was next of interest to ascertain whether HyA-gels could impact on the M-CSF-driven differentiation of $CD14^+$ monocytes into macrophages over 6 days in culture. To this end, primary human monocytes were seeded onto either TCP or HyA-gel surfaces and differentiated with M-CSF over 6 days as described in Chapter 2 (section 2.2.1.1-2.2.1.3). On day 6, cells were lifted and stained for CD14 and CD11b, with macrophages defined as the $CD14^+/CD11b^+$ cell population. It was found that monocytes are capable of differentiation on HyA-gel surfaces at a level comparable to that of the TCP control (Figure 5.2 A-B) and therefore HyA-gels do not impede monocyte differentiation.

5.4.2 Macrophages can polarise in response to stimuli when seeded on hyaluronic acid hydrogel surfaces of different stiffnesses, and stiffness does not impact on macrophage polarisation.

Once it was confirmed that HyA-gels are non-toxic and do not hinder monocyte differentiation into macrophages, it was next of interest to investigate whether hydrogels themselves, as well as modulation of hydrogel stiffness, can impact on the phenotype of primary human macrophages. Tuning of stiffness of the HyA-gel was achieved *via* varying the amount of crosslinker. Soft gels were made using 0.06 U/ml HRP + 0.25 µM H_2O_2; medium gels were made with 0.12 U/ml HRP + 0.5 µM H_2O_2, and stiff gels with 0.48 U/ml HRP + 2 µM H_2O_2. 2% HyA-gels differing in crosslinker concentration were mechanically

stimulated and found to range between averages of 1 kPa – 10 kPa (Figure 5.3). As such, the 1 kPa gel was chosen as the "soft" gel and the 10 kPa gel chosen as the comparatively "stiff" gel with which to conduct subsequent investigation. HyA-gels of 200 µl volume ranging from 1 kPa – 10 kPa were made as described in Chapter 2 (section 2.2.10) in order to provide surfaces of varying stiffness. Given confirmation that HyA-gels do not impact on the viability of macrophages, nor on the differentiation capacity of primary human monocytes to macrophages in response to M-CSF, the impact of HyA-gel and HyA-gel stiffness on macrophage polarisation was then interrogated. To this end, macrophages were seeded on TCP, HyA-gels of 1 kPa, or HyA-gels of 10 kPa, and either left untreated, or treated with either LPS (100 ng/ml) and IFNγ (100 ng/ml) to promote M1-like polarisation, or IL-4 (20 ng/ml) to promote M2-like polarisation. M1-associated activation markers CD40, CD80, and CD86, and the M2-associated marker, CD206, were assessed by flow cytometry. It was found that neither HyA-gels of 1 kPa (Figure 5.4 E-G) or 10 kPa (Figure 5.4 I-K) hinder the ability of macrophages to upregulate CD40, CD80, and CD86 in response to LPS and IFNγ when compared to their ability to polarise on TCP (Figure 5.4 A-D), and while CD206 was not significantly upregulated on either 1 kPa (Figure 5.3 H) or 10 kPa (Figure 5.4 L) HyA-gels, there was a non-significant trend towards upregulation in response to IL-4 stimulation.

Having confirmed that macrophages were capable of polarisation in response to stimuli when seeded atop HyA-gel surfaces, and to further probe whether HyA-gel stiffness can impact on macrophage phenotype, the levels of activation markers of unpolarised (M0) macrophages seeded on 1 kPa HyA-gels, 10 kPa HyA-gels, or TCP surfaces as control for 24 hours as assessed by flow cytometry were compared, with the average of untreated TCP controls used for normalisation. It was found that stiffness does not significantly impact on the ability of macrophages to upregulate maturation markers CD40, CD80, and CD206 in response to stimuli (Figure 5.5 A-B, D), with a moderate trend towards a decrease in expression of CD86 in macrophages seeded atop HyA-gels of 10 kPa when compared to 1 kPa HyA-gels or TCP control (Figure 5.5 C). As studies examining the effect of stiffness on macrophage phenotype have shown that stiffness can act to 'prime' macrophage ability to respond to stimuli [116], it was also of interest to assess whether stimulation of macrophages seeded atop HyA-gel surfaces revealed stiffness-driven alterations in

resultant phenotype. To this end, activation markers CD40, CD80, CD86, or CD206 in macrophages seeded atop 1 kPa or 10 kPa HyA-gels, or TCP controls, prior to stimulation with LPS (100 ng/ml) and IFNγ (100 ng/ml), or IL-4 (20 ng/ml) for 24 hours were compared to examine whether stiffness had a 'priming' effect on macrophage marker expression. Marker expression was normalised to macrophages polarised atop TCP controls and expressed as mean fluorescence intensity (MFI) as percentage of control. It was found that stiffness does not significantly impact on macrophage expression of these markers in response to stimuli (Figure 5.8 A-D). To further investigate the impact of HyA-gel stiffness on macrophage polarisation at the protein level, expression of pro-inflammatory cytokines IL-6, IL-8, and TNF was compared in collected supernatants of macrophages post-stimulation with LPS and IFNγ on TCP, 1 kPa, or 10 kPa HyA-gel surfaces. No significant difference in IL-6 or IL-8 production between macrophages seeded atop 1 kPa and 10 kPa HyA-gel surfaces and polarised to an M1-like state was observed, both when compared against each other and against TCP control (Figure 5.9 A-B). However, a significant decrease in TNF production was observed for macrophages polarised atop both 1 kPa and 10 kPa HyA-gels when compared to TCP control (Figure 5.9 C). Together, this indicates that HyA-gels themselves may impede stimuli-induced expression of TNF when compared to TCP but that, overall, HyA-gel stiffness in the range investigated does not appear to significantly impact on the overall phenotype of primary human macrophages *in vitro*.

5.4.3 The impact of hyaluronic acid hydrogel stiffness on the immune cell environment in a rat femoral defect model.

While results in the *in vitro* investigation suggested that primary human macrophages are not impacted on by altering the stiffness of HyA-gels in the range achieved in this study (1-10 kPa), it is well known that, often, the *in vivo* environment can dictate responses differing to those observed *in vitro* given a complex interplay between a plethora of cell types. It was therefore of interest to investigate whether HyA-gel stiffness could influence the immune microenvironment *in vivo*. Given the potential application of hyaluronic acid hydrogels in bone tissue engineering, a rat femoral defect model was employed to provide the physiologically relevant context of the immune environment surrounding a critical bone defect. 1 kPa or 10 kPa HyA-gels were fit into a 5 mm femoral defect, or the defect

site remained empty as a control. Tissue surrounding the HyA-gel, including the HyA-gel itself, was harvested 7 days post-implantation, and the tissue was digested and analysed for characterisation of the immune microenvironment surrounding each gel type. Flow cytometric analysis revealed no significant differences in any of the immune cell subtypes assessed (Figure 5.8 A-N). However, it was observed that a potential increase in $CD68^{+}/CD11b^{+}$ macrophages as a proportion of $CD45^{+}$/Live cells surrounded the 1 kPa HyA-gels (Figure 5.8 H) when compared to empty or 10 kPa HyA-gels. Overall, a slight decrease in the absolute number of $CD45^{+}$/Live cells at the site of the 1 kPa and 10 kPa HyA-gels was observed versus empty controls (Figure 5.8 A). This was mirrored in a slightly lower absolute number of $CD3^{-}/CD161a^{-}/CD45R^{-}/CD43^{+}$ monocytes (Figure 5.8 C), $CD3^{-}/CD161a^{-}/CD45R^{-}/CD43^{+}$ neutrophils (Figure 5.8 E), $CD3^{-}/His48^{-}/CD161a^{+}$ NK Cells (Figure 5.8 I), $CD3^{+}/CD11b^{-}$ T cells (Figure 5.8 K), and $CD45R^{+}/CD161a^{-}$ B cells (Figure 5.8 M). However, when $CD45^{+}$/Live immune cells were plotted as proportion of total cells collected, and immune cell subsets as proportion of $CD45^{+}$/Live immune cells, these decreases were not observed to as great an extent (Figure 5.8 B, D, F, H, J, L, N). From this, it can be seen that HyA-gels of 1 kPa and 10 kPa do not appear to impact on the overall immune microenvironment in a rat femoral defect when compared to empty control. In order to provide further characterisation of the immune microenvironment in response to HyA-gels of varying stiffness, the phenotype of monocytes, macrophages, and T cells was further investigated. It was observed that both HyA-gels of 1 kPa and 10 kPa resulted in fewer inflammatory monocytes as determined by $CD43^{lo}$ $HIS48^{hi}$ marker expression (Figure 5.9 A) compared to empty control, with a significant decrease seen in the case of 1 kPa HyA-gels with respect to proportion of total monocytes that are $CD43^{lo}$ $HIS48^{hi}$ (Figure 5.9 B). No significant difference in the absolute number of regenerative monocytes ($CD43^{hi}$ $HIS48^{lo}$) was observed (Figure 5.9 C), but both 1 kPa and 10 kPa HyA-gels promoted an increased proportion of total monocytes that are $CD43^{hi}$ $HIS48^{lo}$ as compared to empty control, with significance achieved in the case of 1 kPa HyA-gels (Figure 5.9 D). Macrophage phenotype was assessed using CD86 as an M1-like marker, and CD163 as M2-like. It was observed that there was no difference in absolute cell numbers of $CD86^{+}$ macrophages between either gel or empty control (Figure 5.10 A), and a slight decrease in $CD163^{+}$ macrophages in 1 kPa and 10 kPa HyA-gel groups compared to empty control (Figure 5.10 B). When this was interrogated as proportion of total macrophage population

that was CD86 or CD163 positive, however, no significant differences were observed between all three groups (Figure 5.10 C-D). The MFI of both of these markers was also assessed across all three groups. It was observed that CD86 MFI was moderately, albeit not significantly, increased in macrophages surrounding 1 kPa HyA-gels (Figure 5.10 E), with no difference observed in CD163 MFI across all groups (Figure 5.10 F). $CD3^+$ T cells were further gated on for CD4 or CD8 expression, distinguishing potential 'T-helper' and 'cytotoxic' T cell subsets respectively. There was no difference in $CD4^+$ T cells as proportion of total T cell population across all three groups (Figure 5.11 A-B), but an increase in $CD8^+$ T cells as proportion of total T cell population in 10 kPa HyA-gels was observed when compared to 1 kPa HyA-gels (Figure 5.11 D). Taken together, the above data indicate that HyA-gel stiffness potentially has minor effects on immune cell phenotype in a rat femoral defect model.

5.4.4 The impact of hyaluronic acid hydrogel stiffness on gene expression in a rat femoral defect model.

In order to validate and further explore findings observed at the flow cytometric level and expand on profiling the immune response, and also to further extrapolate the potential impact of HyA-gel stiffness to a bone regenerative context, digested tissue was assessed for gene expression of inflammatory, regenerative, and osteogenic genes by RT-qPCR. It was observed that HyA-gels of 1 kPa and 10 kPa resulted in a non-significant decrease in pro-inflammatory associated *TNF* and *VEGF-A* mRNA compared to empty control (Figure 5.12 A, E). Expression of anti-inflammatory-associated *IL1Rα* was decreased in 1 kPa HyA-gels compared to empty controls, with 10 kPa HyA-gel levels comparable to those of the empty controls (Figure 5.12 D). An increase in *TGFβ3* compared to empty controls was seen with 1 kPa HyA-gels but no significance was achieved with 10 kPa HyA-gels (Figure 5.12 H). No difference was observed in mRNA expression of inflammation-associated *IFNγ* and *TIMP1* (Figure 5.12 B-C), or Treg-associated *FOXP3* expression (Figure 5.12 F) across all groups. There was no significant difference in *TGFβ1* mRNA expression across all three groups, with a mild increase seen in the case of the 10 kPa HyA-gel group (Figure 5.12 G). mRNA expression of macrophage activation markers *CD80*, *CD86*, and *CD163* was also assessed. No significant difference was seen across all groups in *CD80* and *CD163* (Figure

5.13 A, C), and although *CD86* mRNA expression was also not significantly altered, a slight upregulation in tissue surrounding the HyA-gel implanted groups compared to empty control was observed (Figure 5.13 B). Analysis of the expression of osteogenic genes *BMP2* and *RUNX2* demonstrated that there was no significant alteration in mRNA expression of *BMP2* across all three groups (Figure 5.14 A), although HyA-gels of 10 kPa significantly promoted *RUNX2* mRNA expression when compared to HyA-gels of 1 kPa (Figure 5.14 B). Overall, HyA-gels do not significantly impact on the immune microenvironment following induction of a critical sized femoral defect, but minor differences are observed in certain immune cell subsets and mRNA expression that implicate hyaluronic acid hydrogel stiffness as a potential modulator of immune cell phenotype and regenerative outcomes.

5.4.5 IP-loaded hyaluronic acid hydrogels behave similarly to stiff (10 kPa) hyaluronic acid hydrogels.

Given that stiffness was found not to significantly modulate immune cell phenotype *in vitro* and *in vivo*, it was decided to investigate whether HyA-gel can be used as a delivery system for local drug delivery into a defect site. As it was observed in the previous chapter that IP can potentially impact on macrophage phenotype, as well as the *in vitro* effects observed as a result of IP treatment on MSC osteogenesis that are worthy of exploration in an *in vivo* system, IP was chosen as the candidate immunomodulatory ketoacid for delivery into a critical sized bone defect. To this end, IP was dissolved directly in HyA-gel at a concentration of 2 mM and IP-loaded HyA-gel (IP-gel) was assessed for degradative activity when compared against 1 kPa and 10 kPa gels. For gel handleability, as well as yielding a lesser impact on the surrounding immune environment observed in comparison of 10 kPa HyA-gels with 1 kPa HyA-gels, it was decided to incorporate IP into the 10 kPa HyA-gel. To confirm that the degradation rate of IP-gel remained similar to that of the 10 kPa gel, 1 kPa HyA-gel, 10 kPa HyA-gel, and IP-gel were incubated over time in a 0.5 mg/ml or 1 mg/ml hyaluronidase solution and weighed hourly. It was found that IP-gel degrades at a similar rate to 10 kPa HyA-gel compared to the 1 kPa HyA-gel (Figure 5.15 A-B), and thus 10 kPa HyA-gel without IP was confirmed as the appropriate gel-only control implant.

5.4.6 IP-loaded hydrogels are capable of temporally upregulating aryl hydrocarbon receptor associated gene *CYP1A1* in human mesenchymal stem cells.

To investigate whether the IP-loaded HyA-gel was capable of releasing IP post-dissolution of IP (2 mM) within the gel and subsequent gelation, IP-gel, HyA-gel only, or IP only was incubated in media over 7 days with media being collected and replenished on each day. MSC were then incubated in conditioned media or aged media control for 24 hours prior to assessment of *CYP1A1* gene expression to indicate activity of the AhR. MSC were treated with conditioned media collected on day 1, day 2, day 3, and day 7, with conditioned media from days 4-6 being pooled due to limited MSC numbers, in order to assess for any residual effect of IP between these timepoints. It was found that IP-gel conditioned media was capable of upregulating *CYP1A1* on day 1, day 2, day 3, and between days 4-6 (Figure 5.16 A-D), with expression significantly decreasing by day 7 (Figure 5.16 E). Interestingly, *CYP1A1* expression was higher in IP-gel conditioned MSC than IP-conditioned MSC alone on day 2, 3, and between days 4-6, indicating a possible synergistic effect of IP and HyA-gel over time (Figure 5.16 B-D). This demonstrated that dissolved IP can be released from IP-gel as early as day 1, and this release is sustained until between days 4-6, while by day 7 IP is no longer being released from the HyA-gel.

5.4.7 The early effect of IP-loaded hyaluronic acid hydrogels on inflammatory, regenerative, and osteogenic gene expression in human mesenchymal stem cells.

As it was observed that IP release from IP-gel occurs at an early timepoint, it was of interest to investigate the impact of early release of IP from IP-gel on established IP-induced gene expression in MSC in order to determine whether IP release from HyA-gel can drive similar osteoinductive effects as previously observed with direct IP treatment. IP-gel and HyA-gel only conditioned media was collected on day 1 and MSC were treated with IP-gel conditioned media, HyA-gel only conditioned media, IP alone, and aged media control for 48 hours prior to assessment of mRNA expression of *BMP2*, *RUNX2*, *OCN*, and *VEGF-A* by RT-qPCR. It was found that IP alone upregulated expression of all genes assessed (Figure 5.17 A-D). *RUNX2*, *OCN,* and *VEGF-A* were not upregulated in MSCs exposed to IP-gel conditioned media when compared to aged media or HyA-gel only control (Figure 5.17 A-

C). Interestingly, *BMP2* mRNA was upregulated by both IP alone and HyA-gel conditioned media, with IP-gel conditioned media significantly upregulating *BMP2* compared to media, IP only, and HyA-gel conditioned media (Figure 5.17 A). This indicates a potential synergistic effect of HyA-gel and IP in *BMP2* induction, as observed with *CYP1A1* expression, as described above.

5.4.8 IP-loaded hydrogels do not impact on immune cell environment in a rat femoral defect model.

In order to examine whether release of IP from HyA-gel can influence the early immune microenvironment post-implantation, HyA-gel or IP-gel were fit into a 5 mm rat femoral defect, or the defect site remained empty as a control. Tissue surrounding the HyA-gel, including the HyA-gel itself, was harvested at 7 days post-implantation, and the tissue analysed for characterisation of the immune microenvironment in the wake of gel implantation. Flow cytometric analysis revealed no significant differences in absolute cell numbers or as a proportion of $CD45^+$/Live cells in any of the immune cell subtypes assessed (Figure 5.18 A-N). On further assessment of immune cell phenotype, it was found that there were no significant differences in the number of inflammatory monocytes at the implant site (Figure 5.19 A-B), and while there was no significant change in absolute cell number of regenerative monocytes (Figure 5.19 C), a potential increase in regenerative monocytes as proportion of total monocyte population was observed in the HyA-gel only group, and to a lesser extent in the IP-gel group, both compared to empty control (Figure 5.19 D). No significant differences were seen in absolute cell number, or in proportion of total macrophages, of $CD86^+$ or $CD163^+$ macrophage subsets (Figure 5.20 A-D), further reflected in no differences seen in the MFI of either marker across all three groups (Figure 5.20 E-F). In analysis of T cell subsets, it appeared that, while there was a slightly increased number of absolute $CD4^+/CD8^-$ T cells in the IP-gel group compared to empty or HyA-gel alone (Figure 5.21 A), there was no significant difference in proportion of total $CD3^+$ T cells that were $CD4^+/CD8^-$ across all three groups (Figure 5.21 B). This was similarly observed for $CD8^+/CD4^-$ T cells (Figure 5.21 C-D). Overall, IP-loaded hydrogels do not appear to impact on the immune response compared to hydrogels alone or empty controls.

5.4.9 IP-loaded hydrogels upregulate pro-osteogenic *BMP2* and *RUNX2* gene expression, and pro-regenerative *TGFβ1* gene expression, in a rat femoral defect model.

Given the results observed *in vitro* in macrophages and MSC treated with IP, it was decided to further probe specific inflammatory and regenerative markers at the gene expression level by RT-qPCR. Gene expression analysis revealed no significant changes in *TNF*, *IFNγ*, *TIMP1*, *IL1Ra*, *VEGF-A*, *FOXP3* or *TGFβ3* across all three groups (Figure 5.22 A-F, H), although a slight increase in *TNF*, *TIMP1*, *IL1Ra*, and *TGFβ3* was observed in the IP-gel group compared to empty control or HyA-gel alone (Figure 5.22 A, C, D, H). *TGFβ1* was significantly upregulated in the IP-gel group compared to empty control (Figure 5.22 G). Gene expression of activation markers *CD80*, *CD86*, and *CD163* were also assessed. It was observed that HyA-gel alone promoted an increase in *CD80* gene expression compared to empty controls, and while an increase was also seen in IP-gel versus empty control, this was not significant (Figure 5.23 A). *CD86* expression was upregulated in both HyA-gel and IP-gel groups compared to empty controls (Figure 5.23 B). There was no significant difference in mRNA of *CD163* across all three groups (Figure 5.23 C). Finally, and given the promising *in vitro* effects observed in the previous chapter, gene expression of osteogenic genes *BMP2* and *RUNX2* were assessed by RT-qPCR in order to test whether the pro-osteogenic effects of IP on MSCs *in vitro* could be translated into an *in vivo* context. An increase approaching significance (P=0.061) in *BMP2* expression was observed in the IP-gel group compared to empty controls, with a non-significant increase also observed in the HyA-gel alone group (Figure 5.24 A). Encouragingly, *RUNX2* expression was upregulated in the IP-gel group compared to empty controls and HyA-gel alone (Figure 5.24 B). Taken with the data above, it would appear that IP is not only being released from HyA-gel and activating the AhR of MSC *in vitro*, but may also be capable of promoting early osteogenesis in an *in vivo* bone defect model.

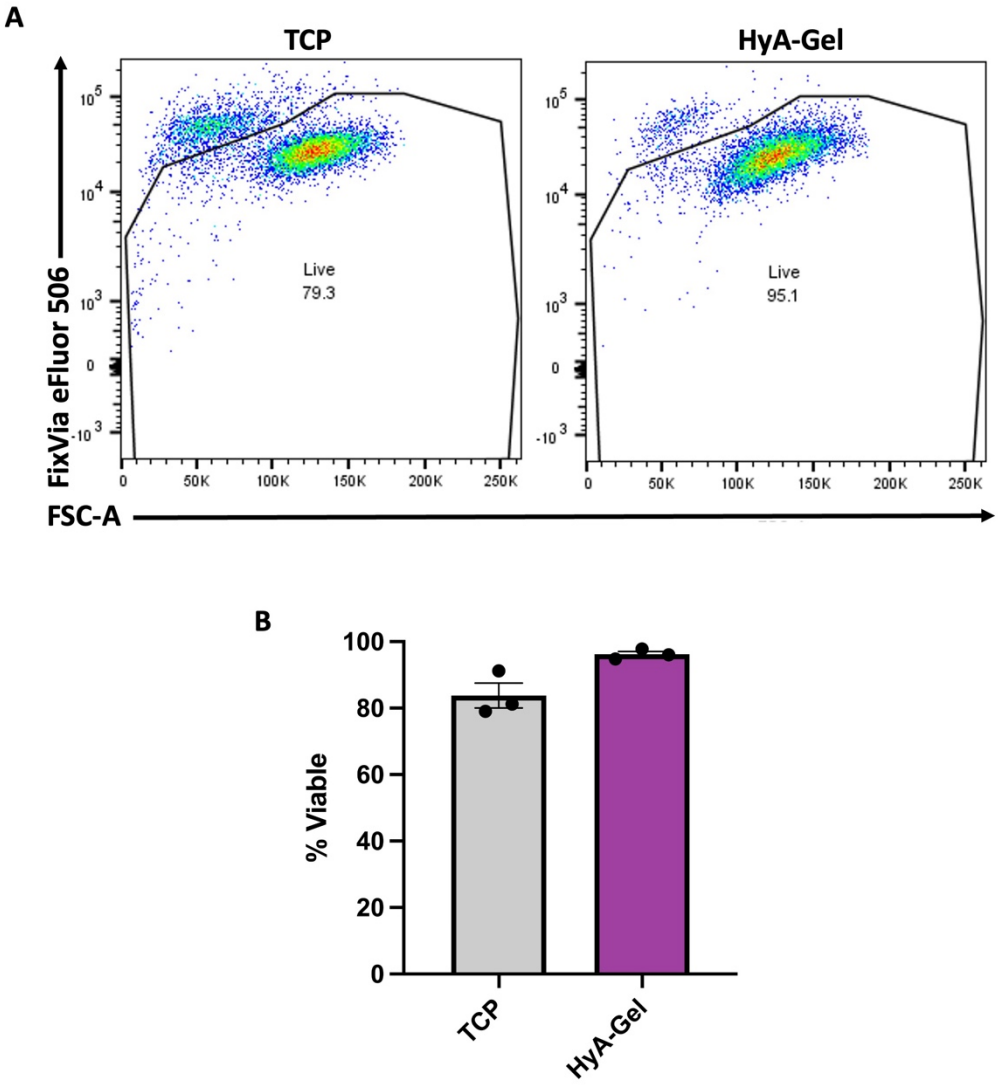

Figure 5.1 Hyaluronic acid hydrogels do not impact on primary human macrophage viability.

Primary human macrophages were seeded atop HyA-gel surfaces or TCP controls for 24 hours. Cells were stained with FixVia eFluor 506 viability dye and analysed by flow cytometry. **(A)** Dot plots depicting one representative experiment. **(B)** Pooled data showing the mean (± SEM) of viable cells as compared to respective untreated control (N=3). Data were analysed using Student's t-test.

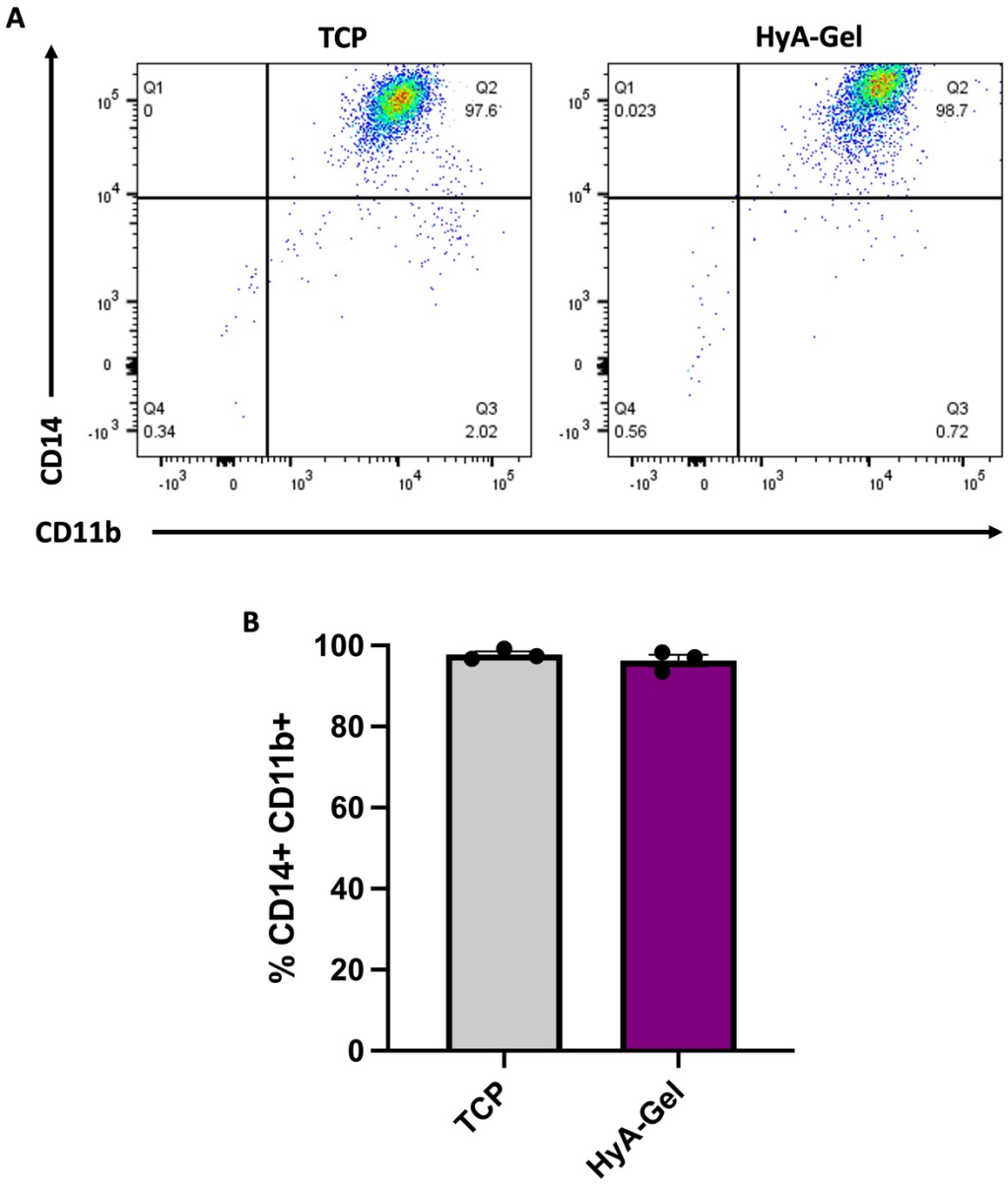

Figure 5.2 Hyaluronic acid hydrogels do not impact on the ability of monocytes to differentiate into macrophages.

Primary human monocytes (2 x 10^5) were seeded atop HyA-gel surfaces or TCP controls and cultured in RPMI supplemented with M-CSF (50 ng/ml) for 6 days. Cells were stained for CD14 and CD11b expression and analysed by flow cytometry. Macrophages were defined as cells that were $CD14^+/CD11b^+$. **(A)** Dot plots depicting one representative experiment. **(B)** Pooled data showing the mean (± SEM) of viable cells as compared to respective untreated control (N = 3). Data were analysed using Student's t-test.

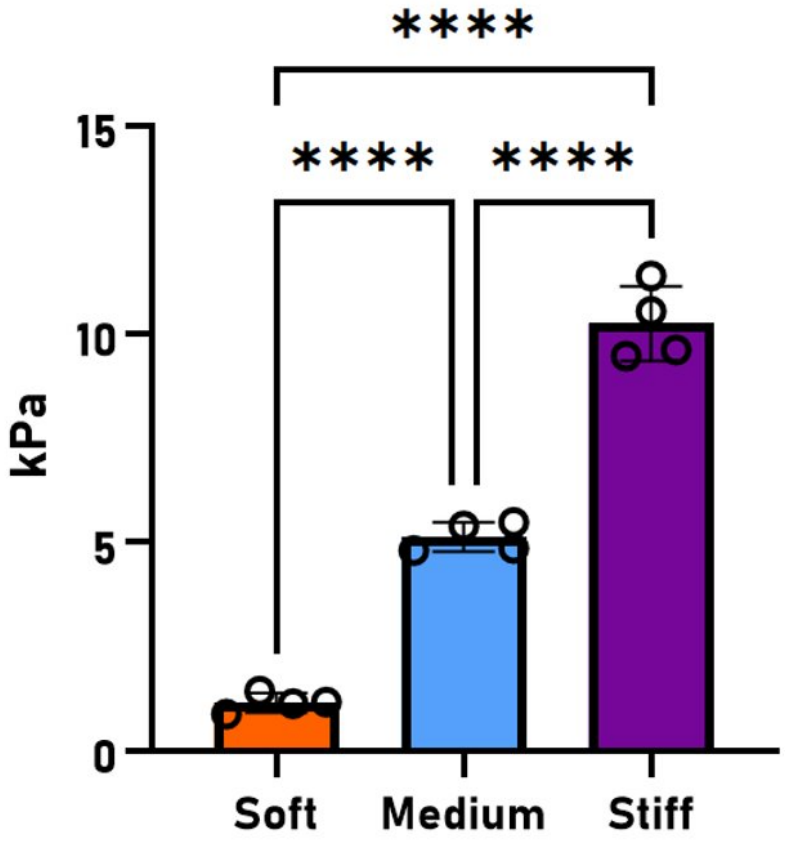

Figure 5.3 Alteration of crosslinker concentration produces 2% hyaluronic acid hydrogels ranging in stiffness between 1 kPa and 10 kPa.

Youngs modulus in compression of HyA-gels with varying concentrations of crosslinker (soft: 0.06 U/ml HRP + 0.25 µM H_2O_2; medium: 0.12 U/ml HRP + 0.5 µM H_2O_2; stiff 0.48 U/ml HRP + 2 µM H_2O_2). Pooled data (n=4) are represented as mean ± SEM (****P≤0.0001).

This experiment was performed and figure generated by Dr. David C. Browe.

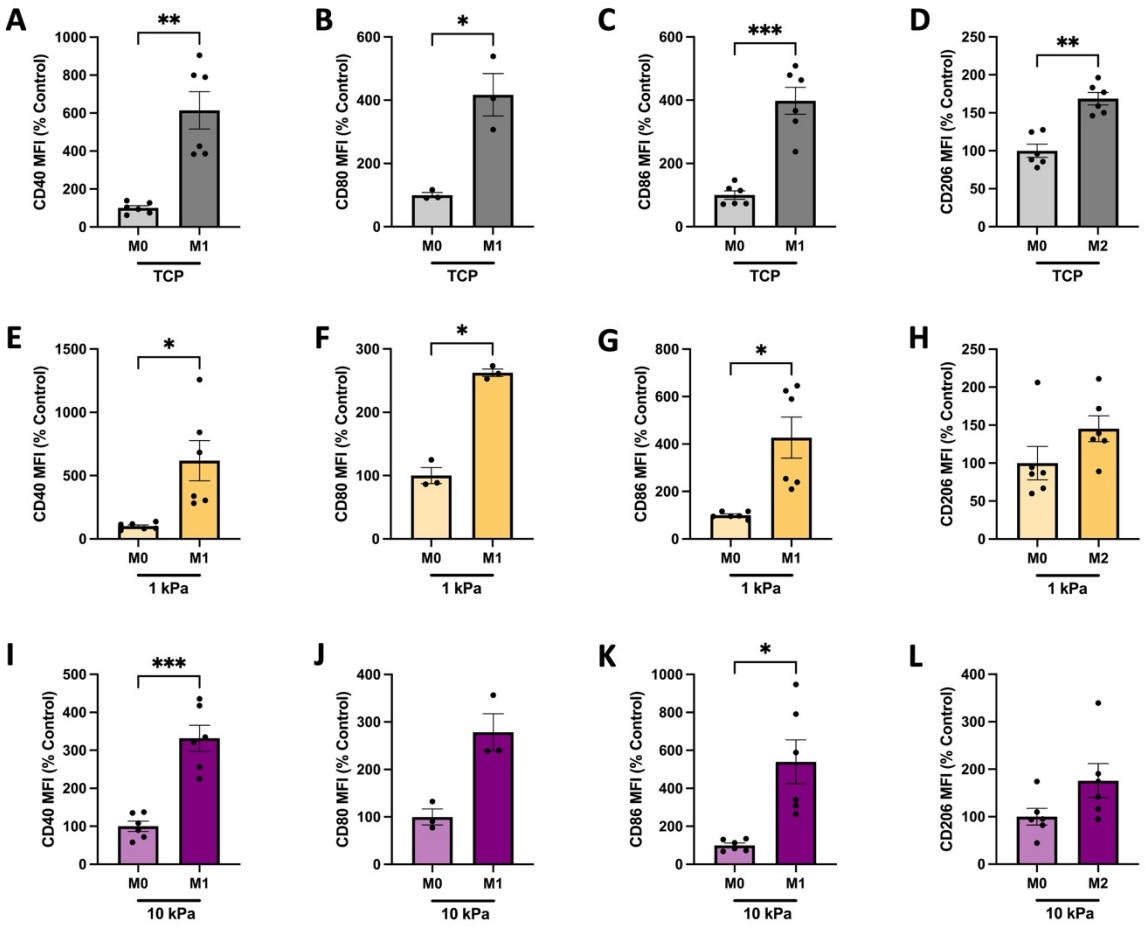

Figure 5.4 Macrophages can polarise in response to stimuli when seeded atop hyaluronic acid hydrogel surfaces of 1 kPa and 10 kPa.

Primary human macrophages (2 x 10^5) were seeded atop TCP, 1 kPa HyA-gels, or 10 kPa HyA-gels and stimulated with M1-polarising stimuli LPS (100 ng/ml) and IFNγ (100 ng/ml), or M2-polarising cytokine IL-4 (20 ng/ml) for 24 hours prior to assessment by flow cytometry. CD40, CD80, CD86, and CD206 expression was assessed in macrophages polarised atop **(A-D)** TCP, **(E-H)** 1 kPa HyA-gel, and **(I-L)** 10 kPa HyA-gel surfaces. Pooled data (N=3-6) are represented as mean ± SEM. Data were analysed using Student's t-test (*P≤0.05, **P≤0.01, ***P≤0.001).

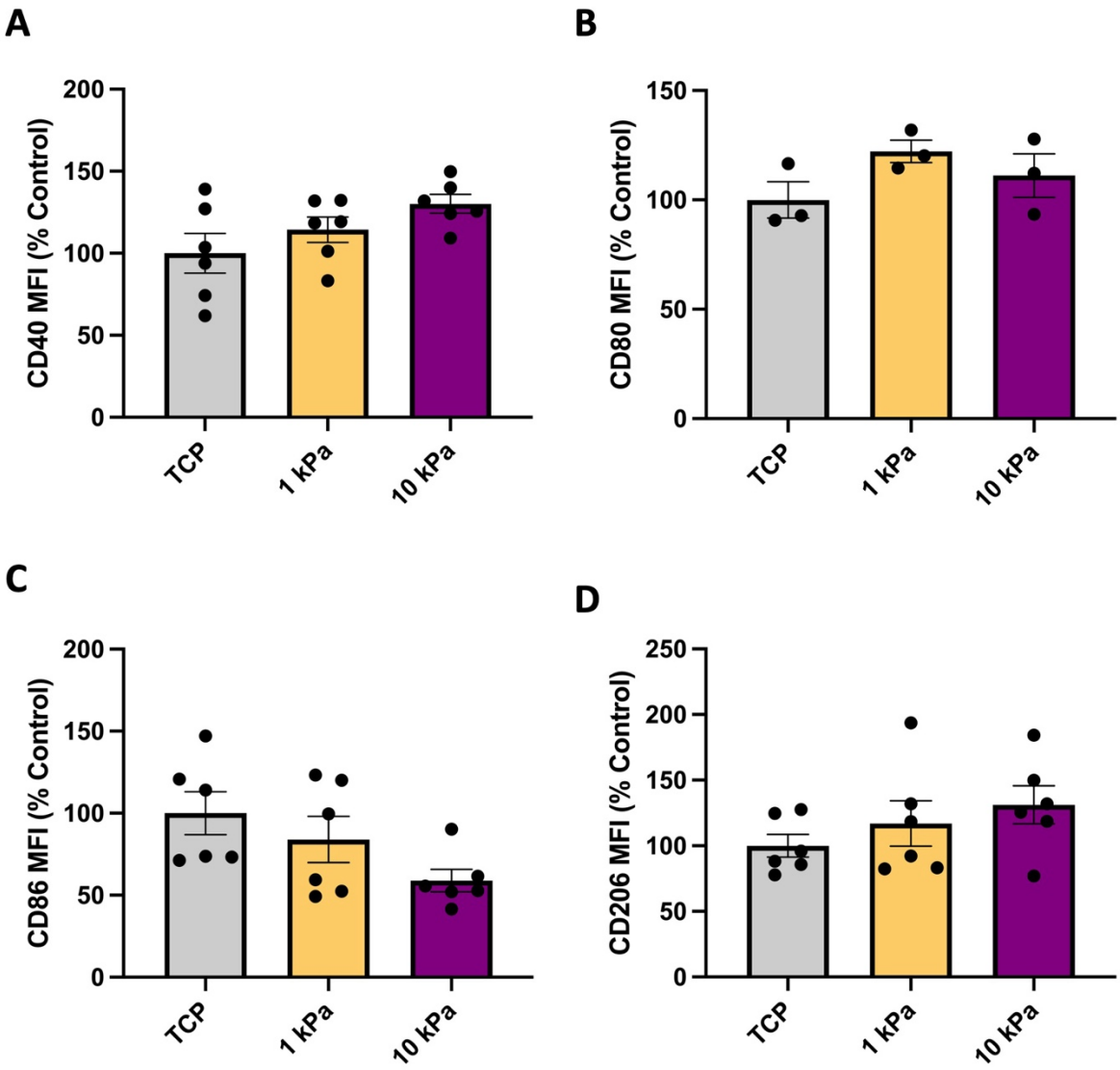

Figure 5.5 Hyaluronic acid hydrogel surfaces and stiffness do not significantly impact on macrophage polarisation marker expression.

Primary human macrophages (2 x 10^5) were seeded atop TCP, 1 kPa HyA-gels, or 10 kPa HyA-gel for 24 hours prior to assessment of maturation markers **(A)** CD40, **(B)** CD80, **(C)** CD86 and **(D)** CD206 by flow cytometry, and normalised to the average of untreated TCP control. Pooled data (N=3-6) is represented as mean ± SEM. Data were analysed using one-way ANOVA with Tukey's post-test.

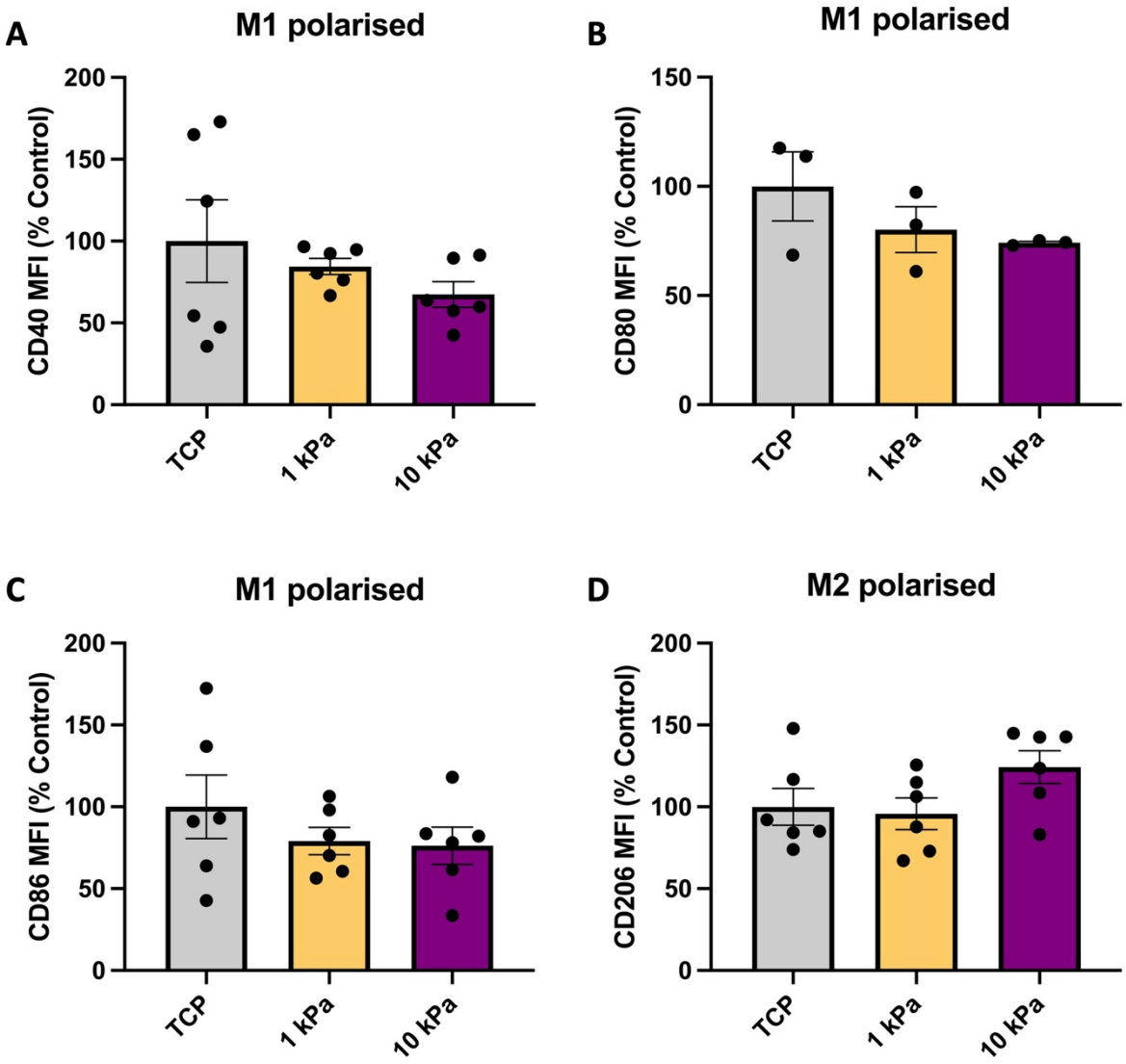

Figure 5.6 Hyaluronic acid hydrogel stiffness does not significantly impact on macrophage polarisation marker expression in response to stimuli.

Primary human macrophages were seeded atop TCP, 1 kPa HyA-gels, or 10 kPa HyA-gels and stimulated with M1-polarising stimuli LPS (100 ng/ml) and IFNγ (100 ng/ml), or M2-polarising cytokine IL-4 (20 ng/ml) for 24 hours prior to assessment by flow cytometry. Macrophage activation markers **(A)** CD40, **(B)** CD80, **(C)** CD86 or **(D)** CD206 were assessed by flow cytometry, and normalised to the average of M1 polarised TCP control. Pooled data (N=3-6) are represented as mean ± SEM. Data were analysed using one-way ANOVA with Tukey's post-test.

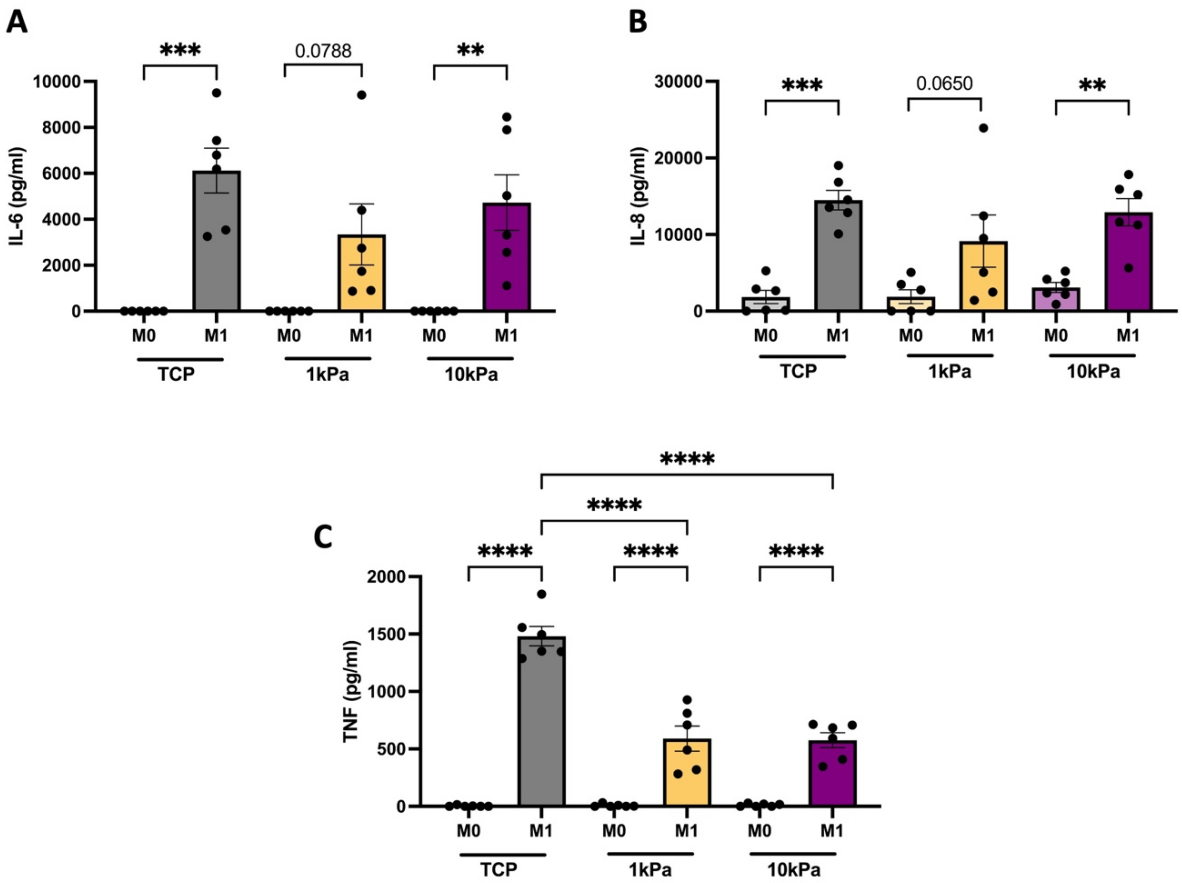

Figure 5.7 Hyaluronic acid hydrogel surfaces, but not hydrogel stiffness, impact on macrophage secretion of TNF, but not IL-6 or IL-8.

Primary human macrophages were seeded atop TCP, 1 kPa HyA-gels, or 10 kPa HyA-gels and stimulated with M1-polarising stimuli LPS (100 ng/ml) and IFNγ (100 ng/ml) for 24 hours. Supernatants were collected and assessed by ELISA for expression levels of M1-associated cytokines **(A)** IL-6, **(B)** IL-8, and **(C)** TNF. Pooled data (N=6) are represented as mean ± SEM. Data were analysed using one-way ANOVA with Tukey's post-test (**P≤0.01, ***P≤0.001, ****P≤0.0001).

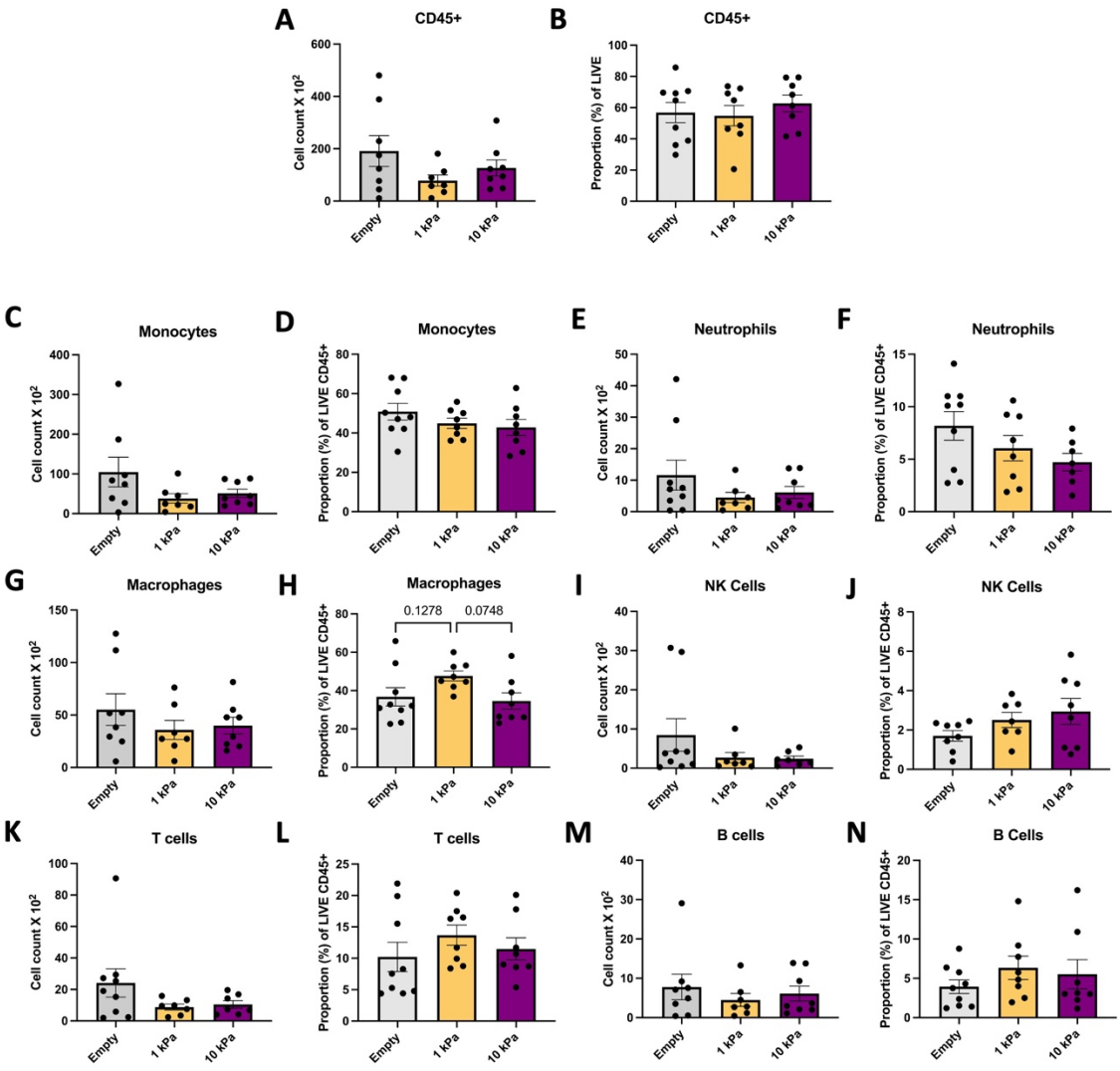

Figure 5.8 Hyaluronic acid hydrogel stiffness does not impact on immune microenvironment in a rat femoral defect model.

1 kPa HyA-gels or 10 kPa HyA-gels were implanted into a 5 mm rat femoral defect, or the defect site was left empty as a control. Tissue and hydrogel was harvested 7 days post-implantation and digested for staining and analysis by flow cytometry. Immune cells were gated on as **(A-B)** $CD45^+$/Live cells, and immune cell subsets **(C-D)** $CD3^-/CD161a^-/CD45R^-/CD43^+$ monocytes, **(E-F)** $CD3^-/CD161a^-/CD45R^-/CD43^+$ neutrophils (both based on marker expression and SSC-A), **(G-H)** $CD68^+/CD11b^+$ macrophages, **(I-J)** $CD3^-/His48^-/CD161a^+$ NK Cells, **(K-L)** $CD3^+/CD11b^-$ T cells, and **(M-N)** $CD45R^+/CD161a^-$ B cells were analysed by flow cytometry. Pooled data (n=9 rats) are represented as mean ± SEM. Outliers were excluded using Grubb's outlier test. Data were analysed using Kruskal-Wallis with Dunn's post-test.

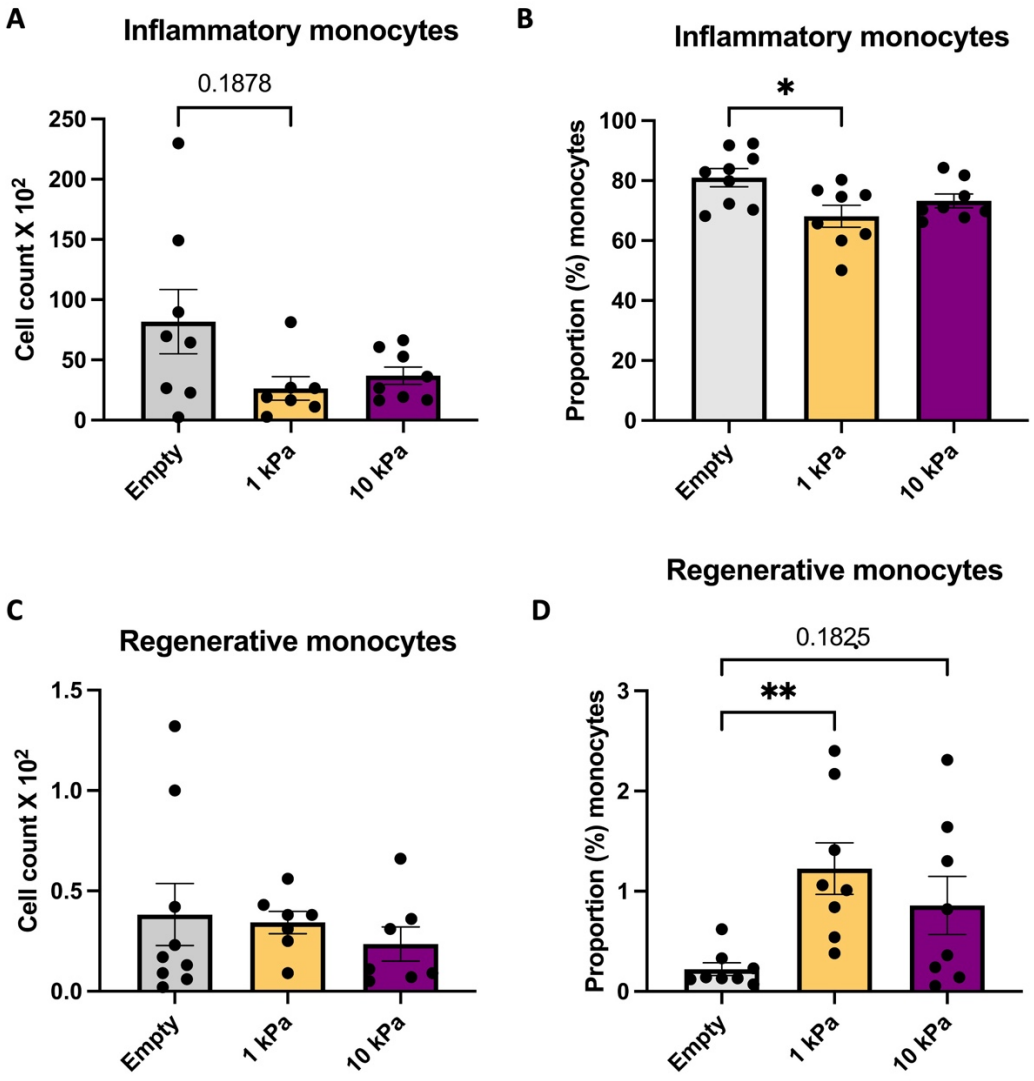

Figure 5.9 1 kPa hyaluronic acid hydrogels decrease inflammatory and promote regenerative monocytes compared to empty defect.

1 kPa HyA-gels or 10 kPa HyA-gels were implanted into a 5 mm rat femoral defect, or the defect site was left empty as a control. Tissue and hydrogel was harvested 7 days post-implantation and digested for staining and analysis by flow cytometry. Immune cells were gated on as (**A-B)** $CD45^+$/Live cells, and monocytes determined as $CD3^-$/$CD161a^-$/$CD45R^-$/$CD43^+$. **(A-B)** Inflammation-associated monocytes were gated on as $CD43^{lo}$ $HIS48^{hi}$ and **(C-D)** regeneration-associated monocytes as $CD43^{hi}$ $HIS48^{lo}$. Pooled data (n=9 rats) are represented as mean ± SEM. Outliers were excluded using Grubb's outlier test. Data were analysed using Kruskal-Wallis with Dunn's post-test (*P≤0.05, **P≤0.01).

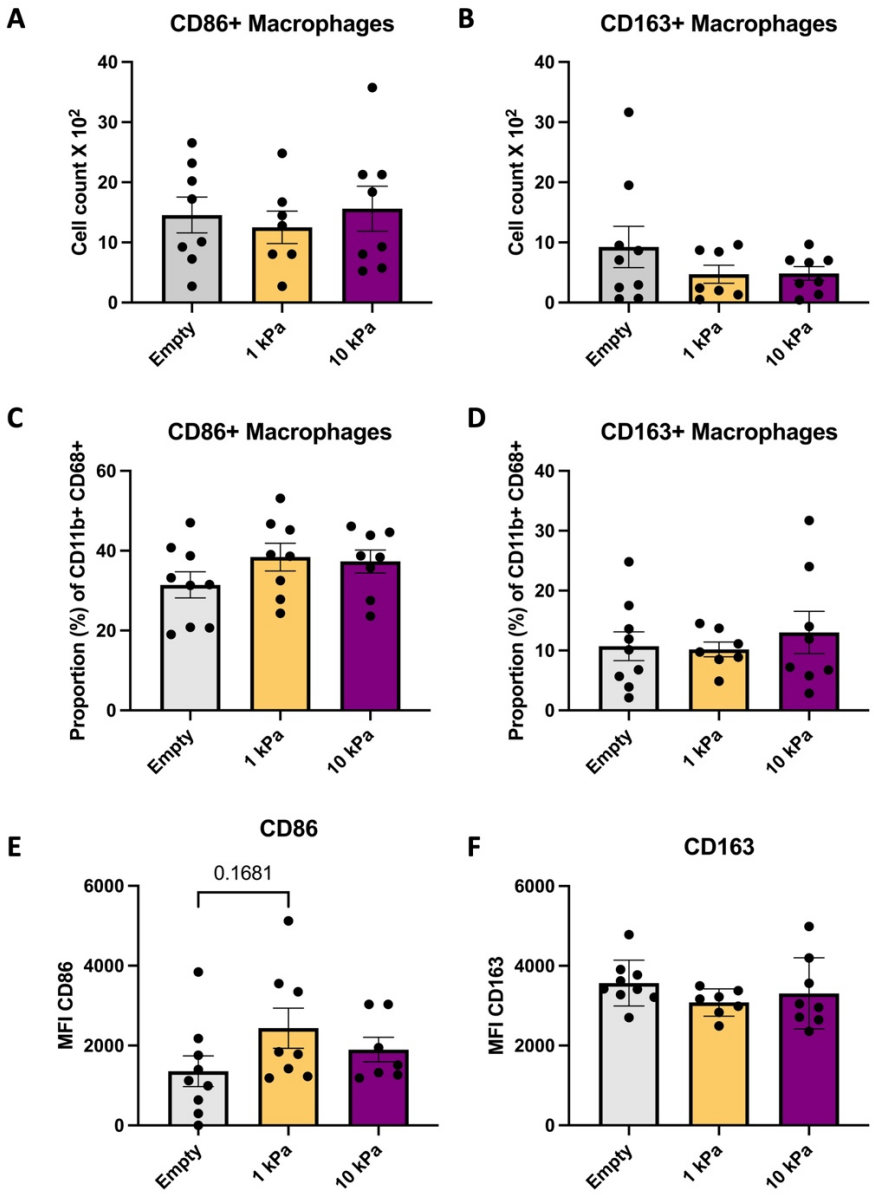

Figure 5.10 1 kPa and 10 kPa hyaluronic acid hydrogels do not significantly impact on macrophage phenotype in a rat femoral defect model.

1 kPa HyA-gels or 10 kPa HyA-gels were implanted into a 5 mm rat femoral defect, or the defect site was left empty as a control. Tissue and hydrogel was harvested 7 days post-implantation and digested for staining and analysis by flow cytometry. Immune cells were gated on as **(A-B)** $CD45^+$/Live cells, and macrophages determined as $CD68^+/CD11b^+$ and assessed for **(A, C, E)** M1-associated CD86 and **(B, D, F)** M2-associated CD163 expression. Pooled data (n=9 rats) are represented as mean ± SEM. Outliers were excluded using Grubb's outlier test. Data were analysed using Kruskal-Wallis with Dunn's post-test.

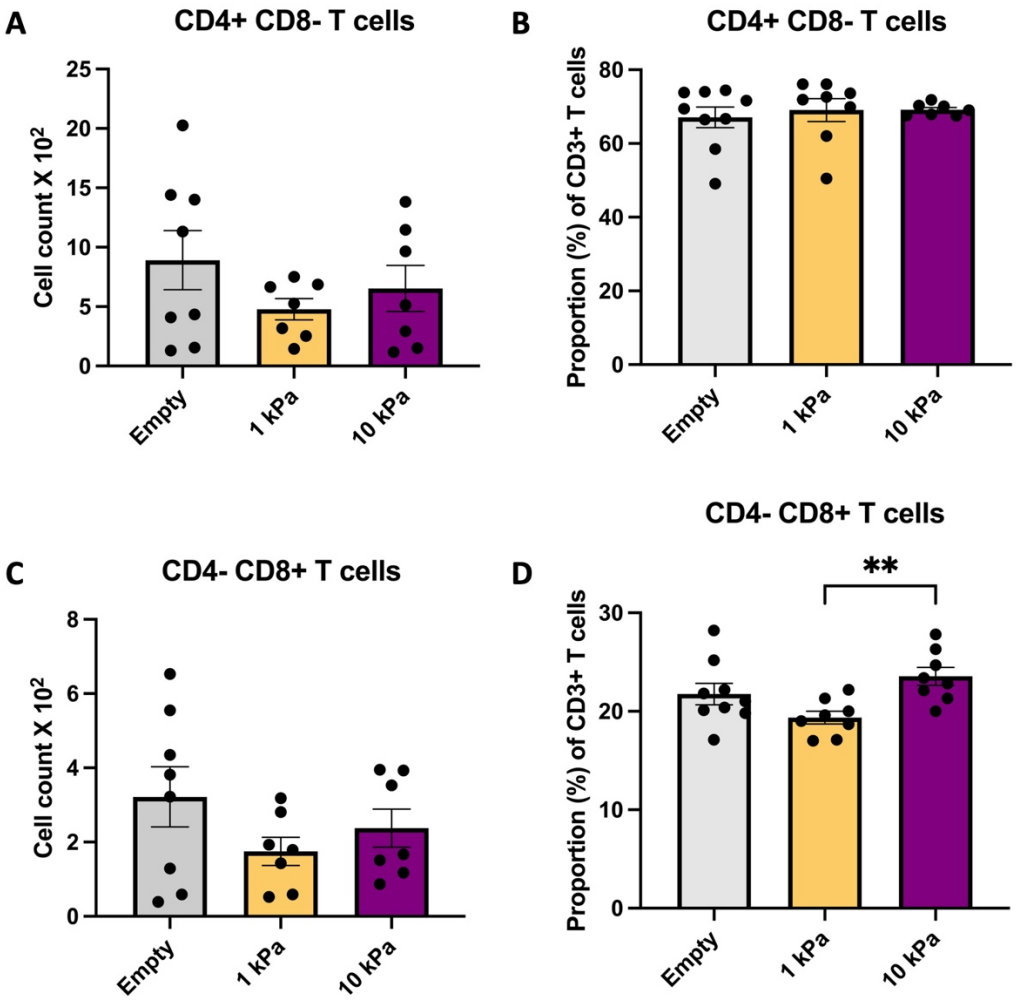

Figure 5.11 10 kPa hyaluronic acid hydrogels promote an increase in $CD4^-/CD8^+$ T cells compared to 1 kPa hydrogels a rat femoral defect model.

1 kPa HyA-gels or 10 kPa HyA-gels were implanted into a 5 mm rat femoral defect, or the defect site was left empty as a control. Tissue and hydrogel was harvested 7 days post-implantation and digested for staining and analysis by flow cytometry. Immune cells were gated on as **(A-B)** $CD45^+$/Live cells, and T cells determined as $CD3^+$. T cell subsets **(A-D)** $CD4^+/CD8^-$ and **(C-D)** $CD4^-/CD8^+$ were assessed by flow cytometry. Pooled data (n=9 rats) are represented as mean ± SEM. Outliers were excluded using Grubb's outlier test. Data were analysed using Kruskal-Wallis with Dunn's post-test (**P≤0.01).

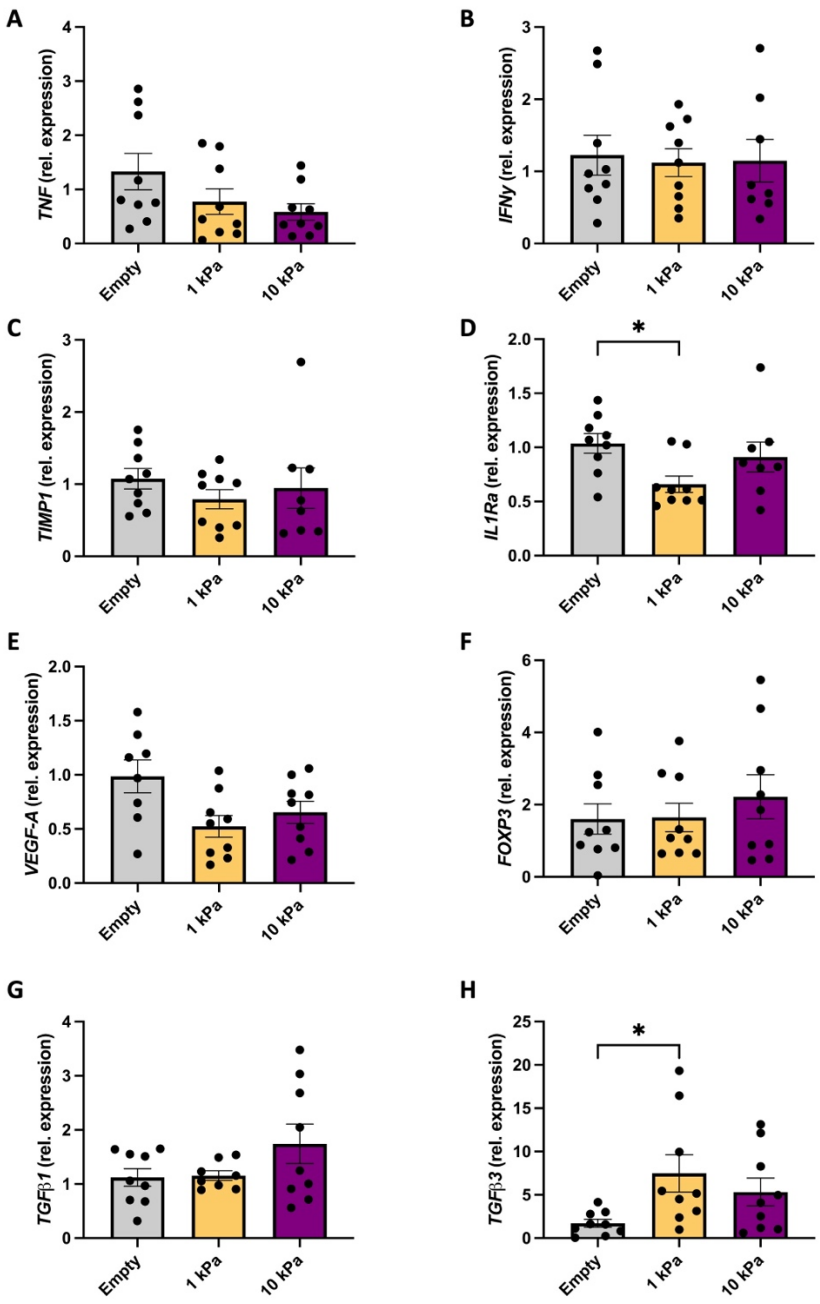

Figure 5.12 1 kPa hyaluronic acid hydrogels decrease *IL1Ra* and increase *TGFβ3* mRNA expression in a rat femoral defect model.

1 kPa HyA-gels or 10 kPa HyA-gels were implanted into a 5 mm rat femoral defect, or the defect site was left empty as a control. Tissue and hydrogel was harvested 7 days post-implantation and analysed by RT-qPCR for mRNA expression of **(A)** *TNF*, **(B)** *IFNγ*, **(C)** *TIMP1*, **(D)** *IL1Ra*, **(E)** *VEGF-A*, **(F)** *FOXP3*, **(G)** *TGFβ1*, and **(H)** *TGFβ3*. Pooled data (n=9 rats) are represented as mean ± SEM. Outliers were excluded using Grubb's outlier test. Data were analysed using Kruskal-Wallis with Dunn's post-test (*P≤0.05).

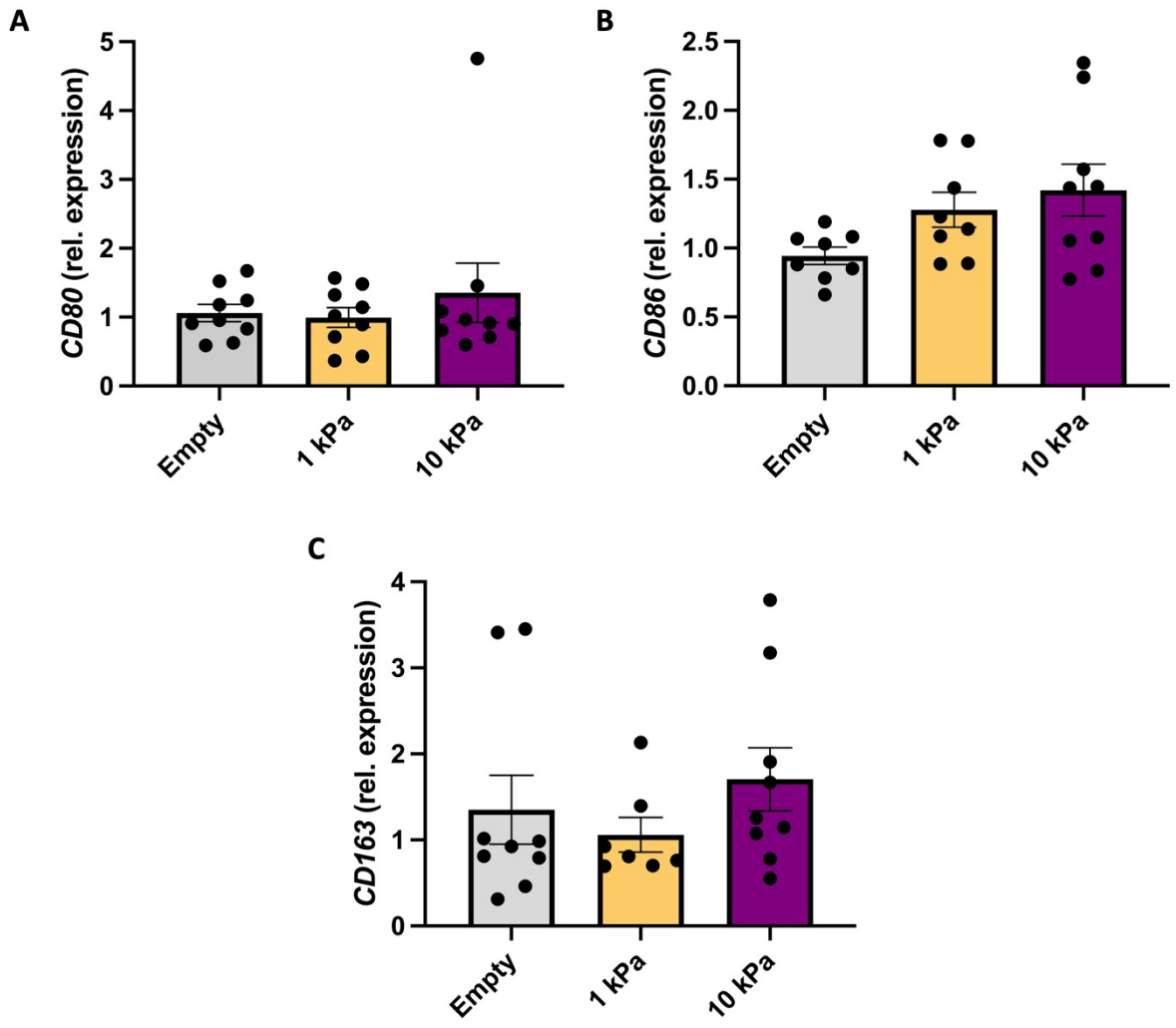

Figure 5.13 mRNA expression of macrophage activation markers *CD80*, *CD86*, and *CD163* are not affected by hyaluronic acid hydrogel stiffness in a rat femoral defect model.

1 kPa HyA-gels or 10 kPa HyA-gels were implanted into a 5 mm rat femoral defect, or the defect site was left empty as a control. Tissue and hydrogel was harvested 7 days post-implantation and analysed by RT-qPCR for mRNA expression of **(A)** *CD80*, **(B)** *CD86*, and **(C)** *CD163*. Pooled data (n=9 rats) are represented as mean ± SEM. Outliers were excluded using Grubb's outlier test. Data were analysed using Kruskal-Wallis with Dunn's post-test.

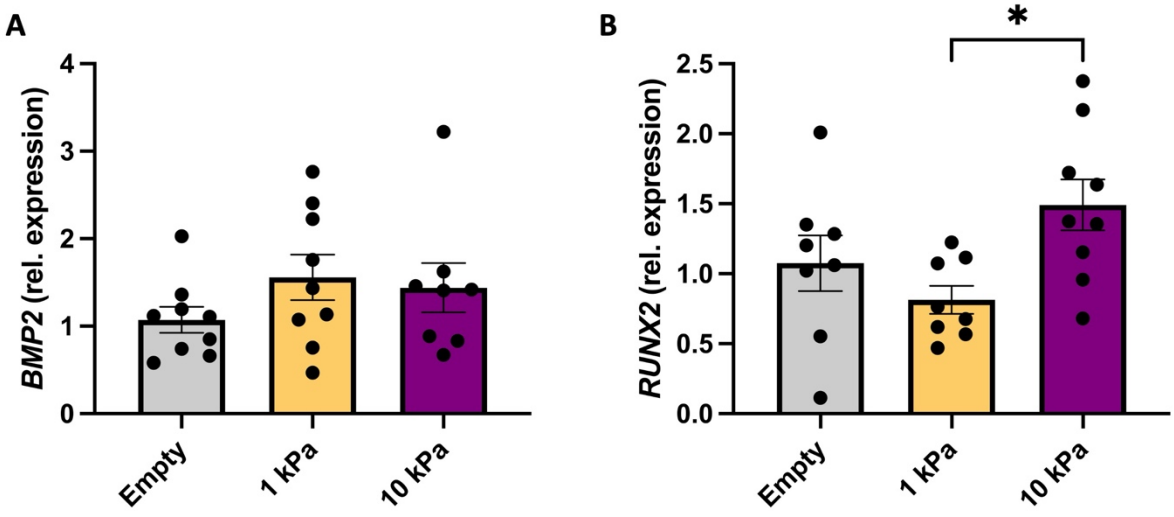

Figure 5.14 mRNA expression of osteogenic genes *BMP2* and *RUNX2* following implantation of 1 kPa or 10 kPa hydrogels into a rat femoral defect model.

1 kPa HyA-gels or 10 kPa HyA-gels were implanted into a 5 mm rat femoral defect, or the defect site was left empty as a control. Tissue and hydrogel was harvested 7 days post-implantation and analysed by RT-qPCR for mRNA expression of **(A)** *BMP2* and **(B)** *RUNX2*. Pooled data (n=9 rats) are represented as mean ± SEM. Outliers were excluded using Grubb's outlier test. Data were analysed using Kruskal-Wallis with Dunn's post-test (*P≤0.05).

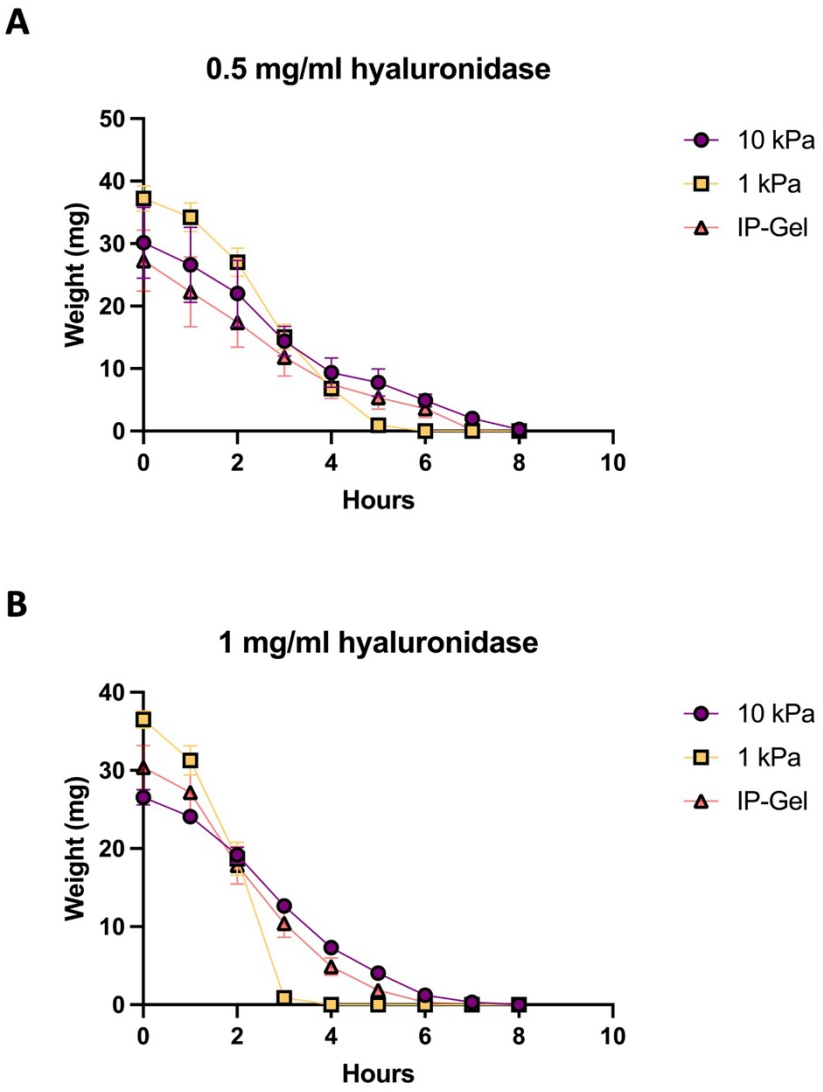

Figure 5.15 IP-gel behaves similarly to 10 kPa HyA-gel in the presence of hyaluronidase.

1 kPa HyA-gels, 10 kPa HyA-gels, or IP-loaded HyA gels were incubated in 0.5 mg/ml or 1 mg/ml hyaluronidase solution over time and weighed hourly, starting at 0 hrs. Weight is given in milligrams (mg).

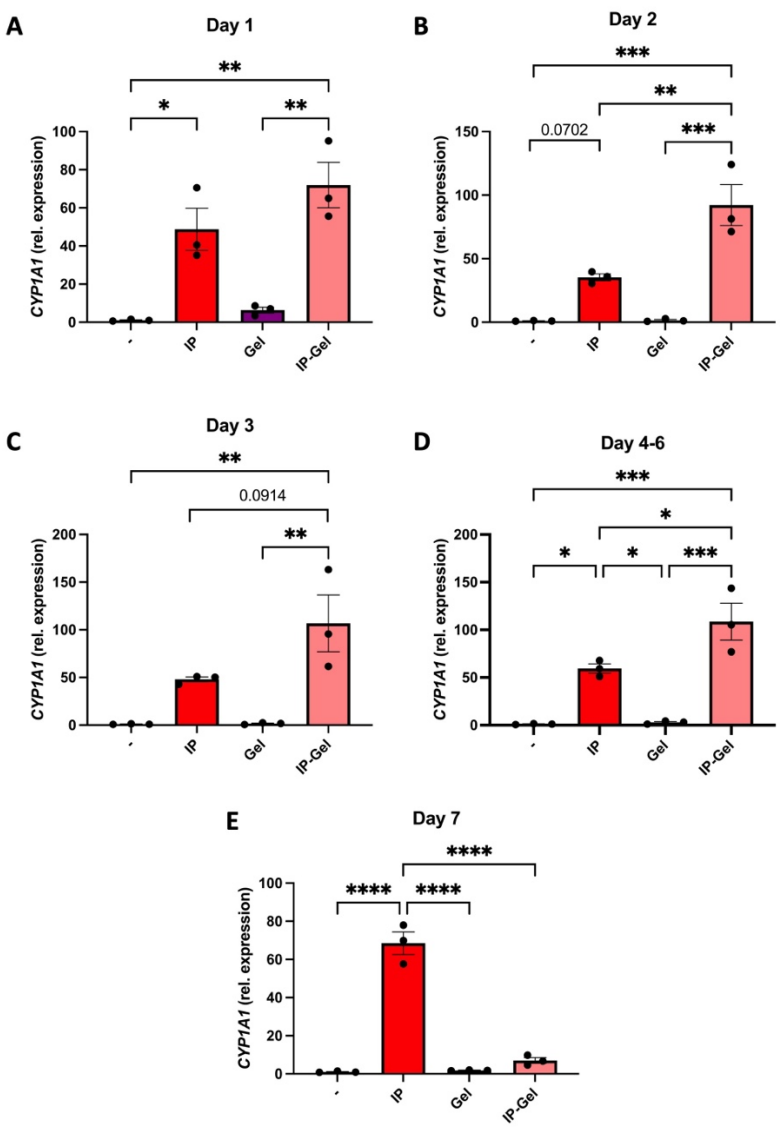

Figure 5.16 *CYP1A1* mRNA expression is upregulated at days 1, 2, 3, and between days 4-6, in human mesenchymal stem cells treated with IP-gel conditioned media.

HyA-gel with and without IP were incubated in DMEM over 7 days, with media collected and replenished on each day. MSCs (1 x 10^5 cells/ml) were then treated with the collected HyA-gel conditioned media, IP-gel conditioned media, IP alone, or aged media alone. mRNA expression of *CYP1A1* with **(A)** day 1 media, **(B)** day 2 media, **(C)** day 3 media, **(D)** days 4-6 media, and **(E)** day 7 media was then assessed using RT-qPCR. Pooled data (n=3) are represented as mean ± SEM. Data were analysed using one-way ANOVA with Tukey's post-test (*P≤0.05, **P≤0.01, ***P≤0.001, ****P≤0.0001).

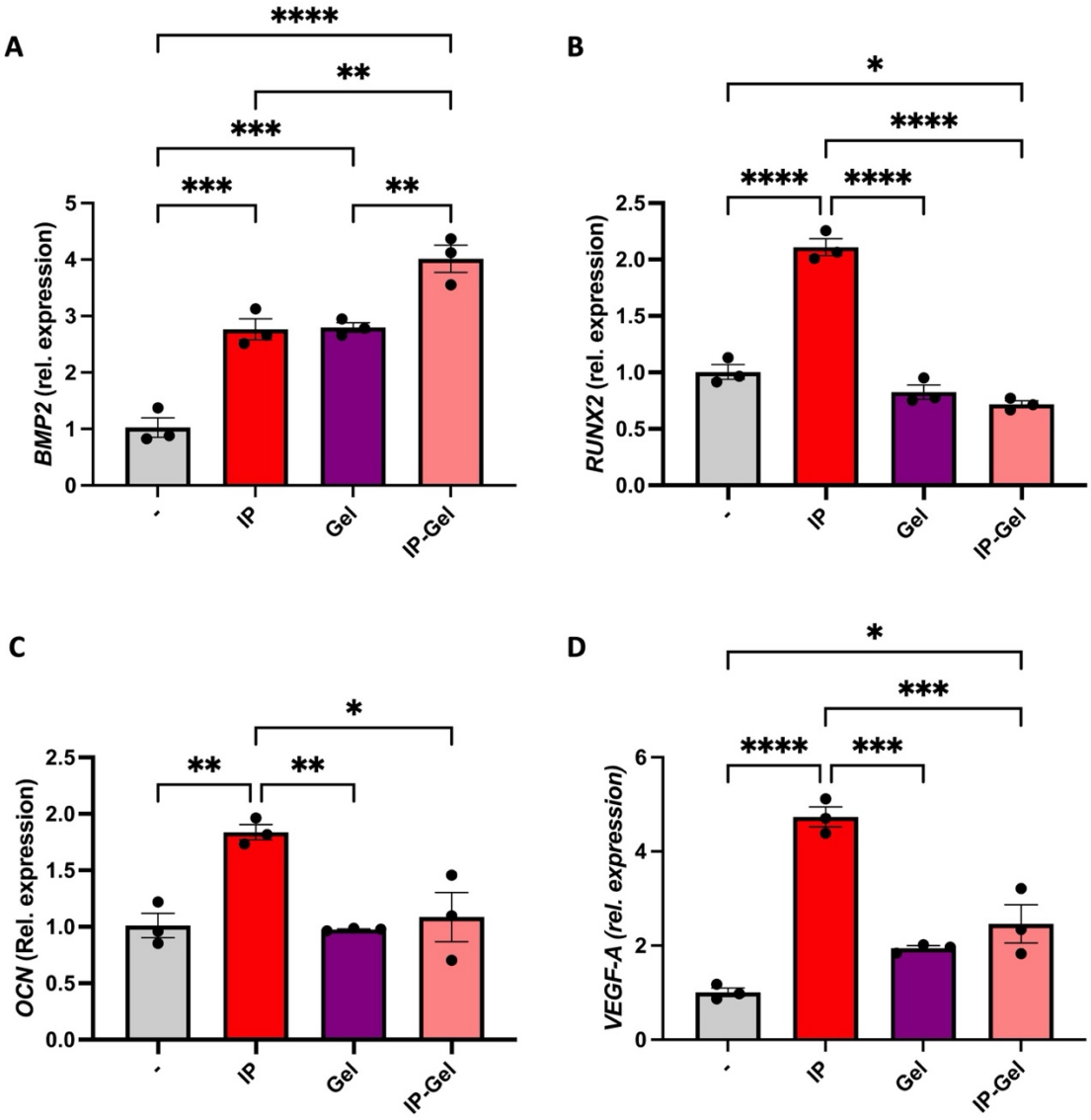

Figure 5.17 *BMP2* mRNA expression, but not *RUNX2*, *OCN*, or *VEGF-A*, is upregulated in human mesenchymal stem cells treated with IP, HyA-gel conditioned media, and IP-gel conditioned media at day 1.

HyA-gel with and without IP were incubated in DMEM for 24 hours. Media was then collected and MSC (1 x 10^5 cells/ml) were treated with collected HyA-gel conditioned media, IP-gel conditioned media, IP alone, or aged media alone. Gene expression of **(A)** *BMP2*, **(B)** *RUNX2*, **(C)** *OCN*, and **(D)** *VEGF-A* was assessed. Pooled data (n=3) are represented as mean ± SEM. Data were analysed using one-way ANOVA with Tukey's post-test (*P≤0.05, **P≤0.01, ***P≤0.001, ****P≤0.0001).

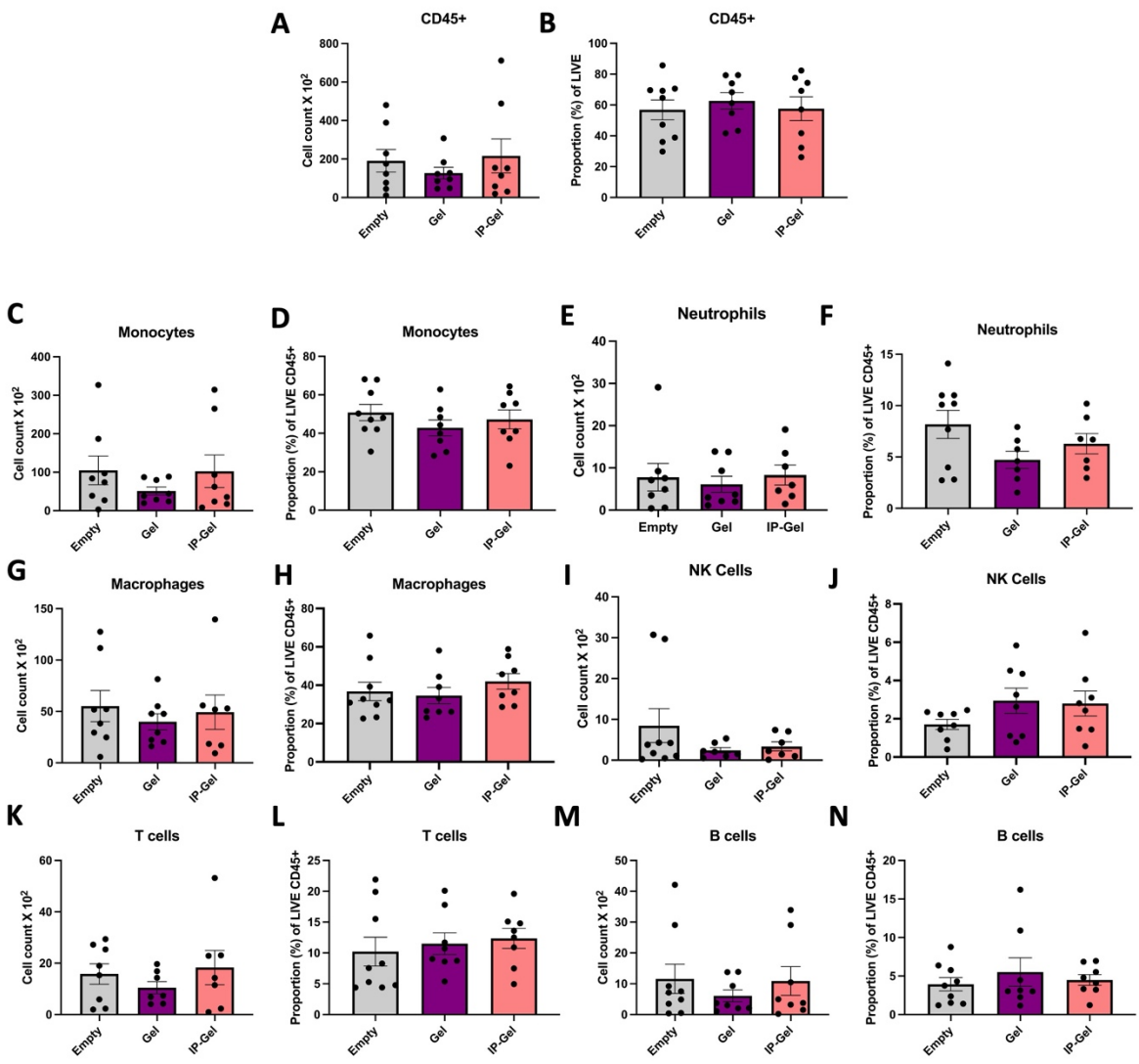

Figure 5.18 IP-loaded hyaluronic acid hydrogel does not impact on immune microenvironment in a rat femoral defect model.

HyA-gel with and without IP were implanted into a 5 mm rat femoral defect, or the defect site was left empty as a control. Tissue and hydrogel was harvested 7 days post-implantation and digested for staining and analysis by flow cytometry. Immune cells were gated on as **(A-B)** $CD45^+$/Live cells, and immune cell subsets **(C-D)** $CD3^-/CD161a^-/CD45R^-/CD43^+$ monocytes, **(E-F)** $CD3^-/CD161a^-/CD45R^-/CD43^+$ neutrophils (both based on marker expression and SSC-A), **(G-H)** $CD68^+/CD11b^+$ macrophages, **(I-J)** $CD3^-/His48^-/CD161a^+$ NK Cells, **(K-L)** $CD3^+/CD11b^-$ T cells, and **(M-N)** $CD45R^+/CD161a^-$ B cells were analysed by flow cytometry. Pooled data (n=9 rats) are represented as mean ± SEM. Outliers were excluded using Grubb's outlier test. Data were analysed using Kruskal-Wallis with Dunn's post-test.

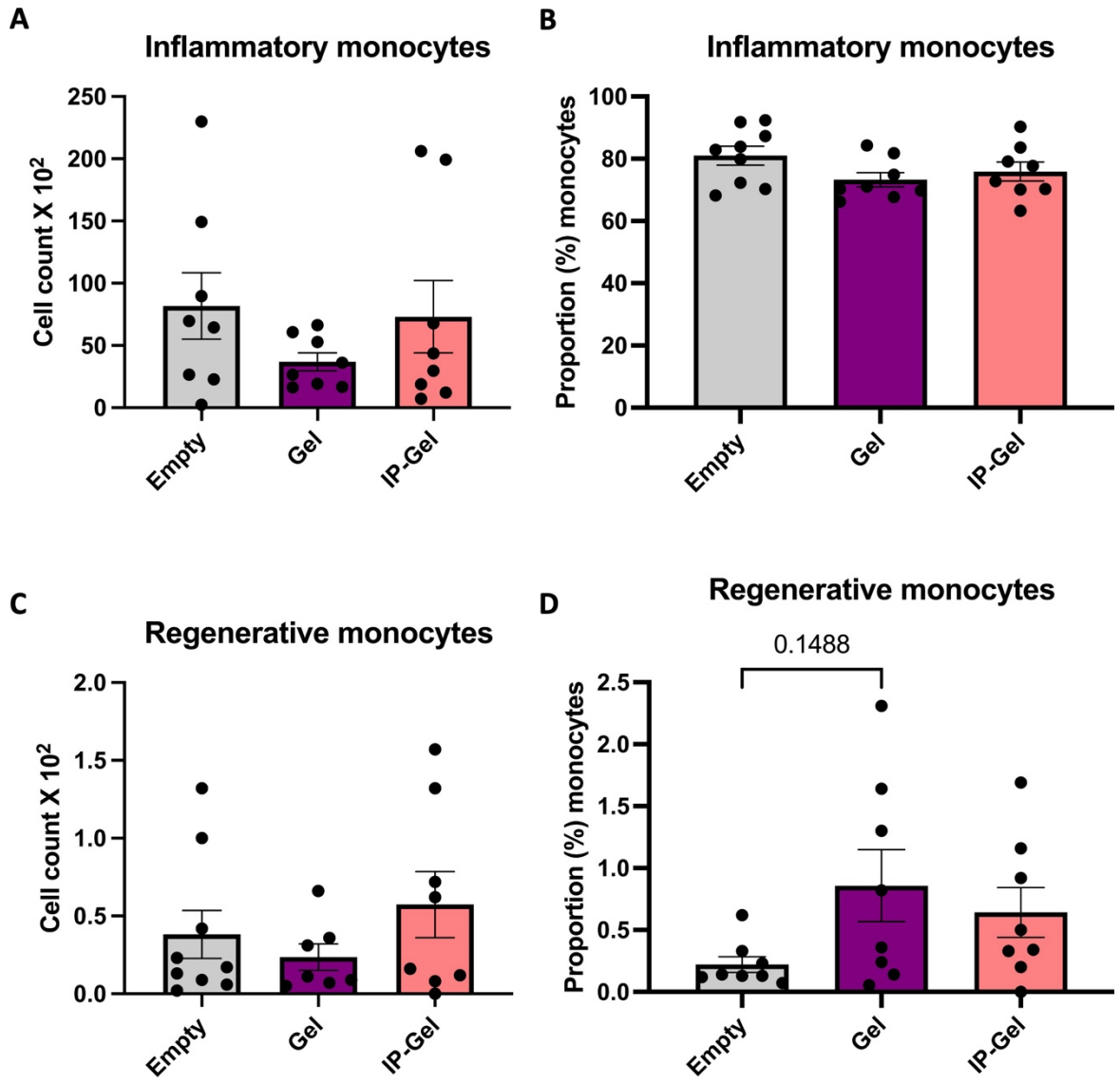

Figure 5.19 Monocyte subsets are not significantly impacted on following implantation of hyaluronic acid hydrogels with and without IP into a rat femoral defect model.

HyA-gel with and without IP were implanted into a 5 mm rat femoral defect, or the defect site was left empty as a control. Tissue and hydrogel was harvested 7 days post-implantation and digested for staining and analysis by flow cytometry. Immune cells were gated on as $CD45^+$/Live cells, and monocytes determined as $CD3^-/CD161a^-/CD45R^-/CD43^+$. **(A-B)** Inflammation-associated monocytes were gated on as $CD43^{lo}$ $HIS48^{hi}$ and **(C-D)** regeneration-associated monocytes as $CD43^{hi}$ $HIS48^{lo}$. Pooled data (n=9 rats) are represented as mean ± SEM. Outliers were excluded using Grubb's outlier test. Data were analysed using Kruskal-Wallis with Dunn's post-test.

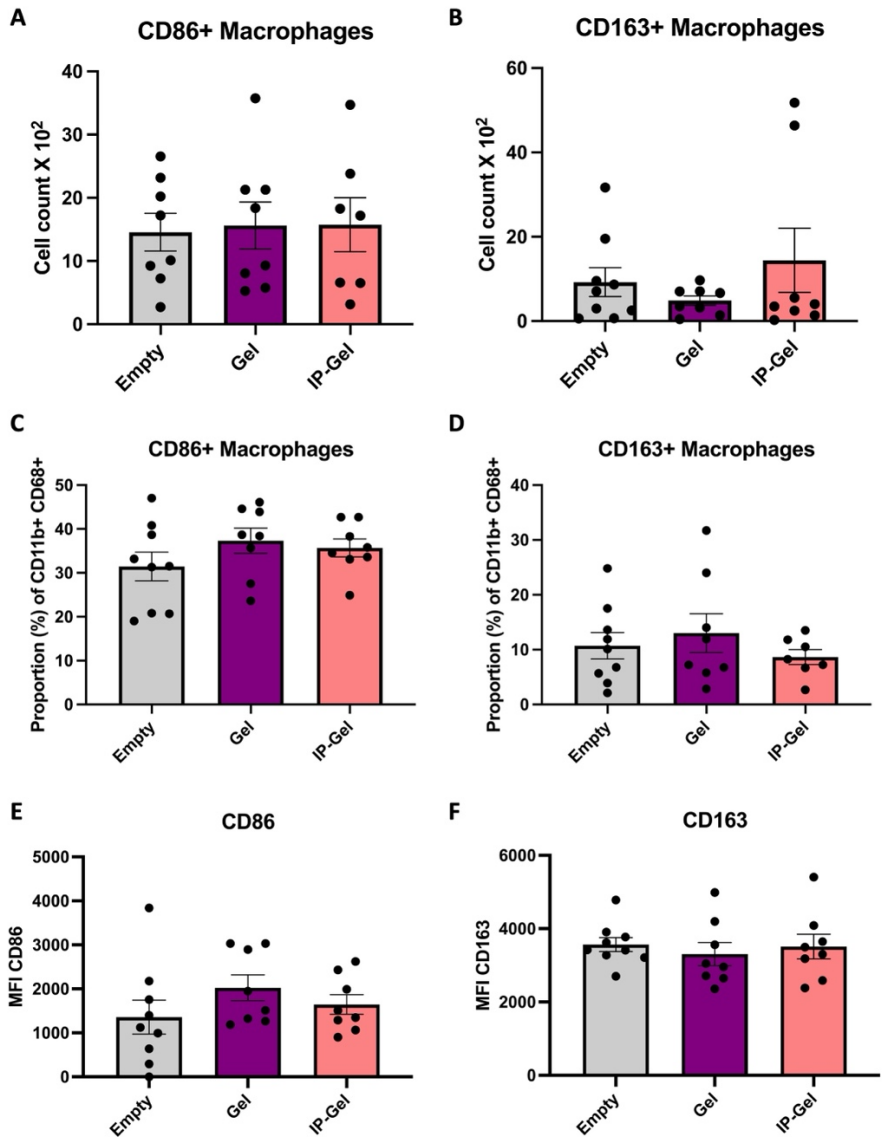

Figure 5.20 Macrophage subsets are not significantly impacted on following implantation of hyaluronic acid hydrogels with and without IP into a rat femoral defect model.

HyA-gel with and without IP were implanted into a 5 mm rat femoral defect, or the defect site was left empty as a control. Tissue and hydrogel was harvested 7 days post-implantation and digested for staining and analysis by flow cytometry. Immune cells were gated on as $CD45^+$/Live cells, and macrophages determined as $CD68^+/CD11b^+$ and assessed for **(A, C, E)** M1-associated CD86 and **(B, D, F)** M2-associated CD163 expression. Pooled data (n=9 rats) are represented as mean ± SEM. Outliers were excluded using Grubb's outlier test. Data were analysed using Kruskal-Wallis with Dunn's post-test.

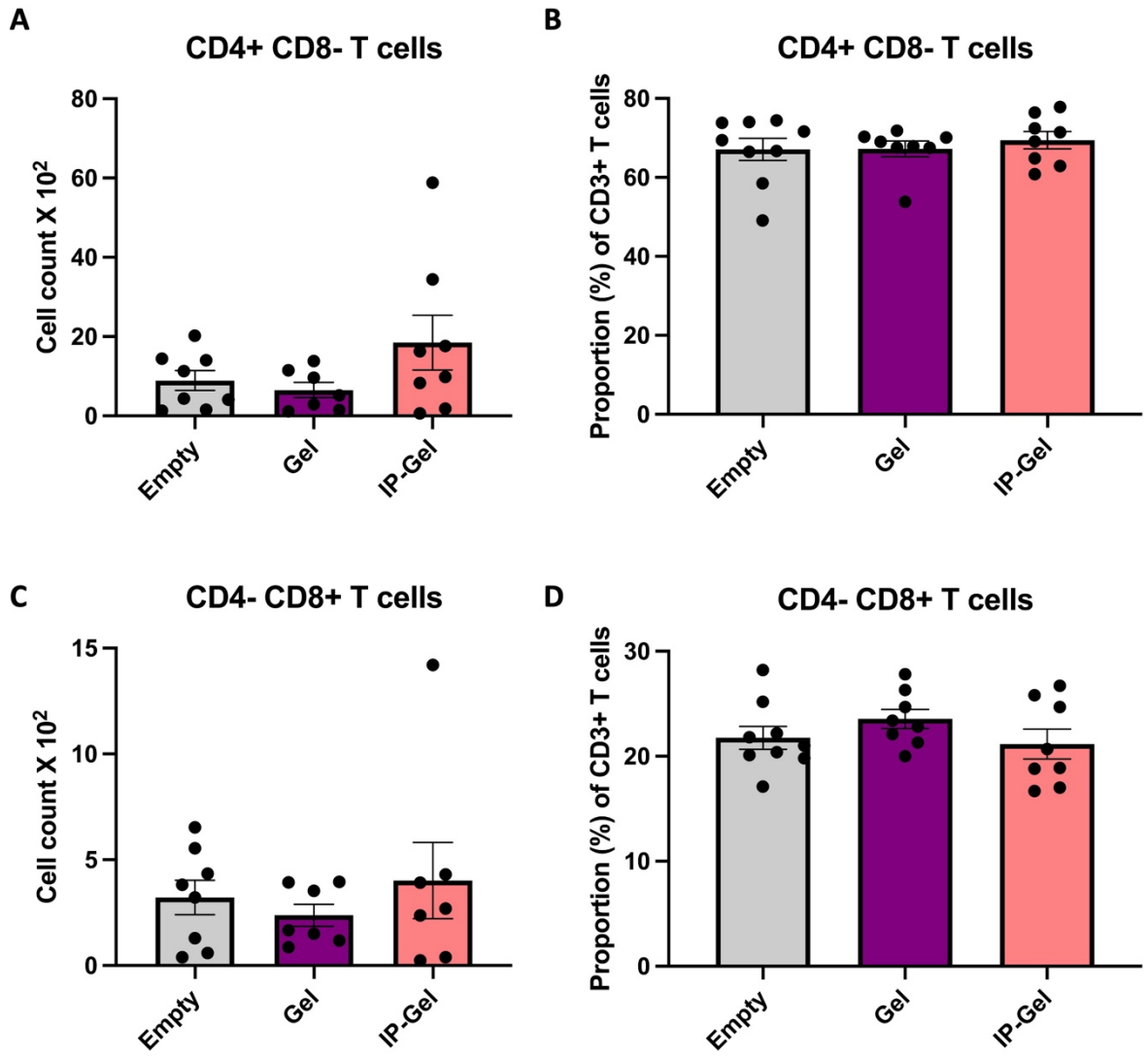

Figure 5.21 T cell subsets are not significantly impacted on following implantation of hyaluronic acid hydrogels with and without IP into a rat femoral defect model.

HyA-gels with and without IP were implanted into a 5 mm rat femoral defect, or the defect site was left empty as a control. Tissue and hydrogel was harvested 7 days post-implantation and digested for staining and analysis by flow cytometry. Immune cells were gated on as $CD45^+$/Live cells, and T cells determined as $CD3^+$. T cell subsets **(A-D)** $CD4^+/CD8^-$ and **(C-D)** $CD4^-/CD8^+$ were assessed by flow cytometry. Pooled data (n=9 rats) are represented as mean ± SEM. Outliers were excluded using Grubb's outlier test. Data were analysed using Kruskal-Wallis with Dunn's post-test.

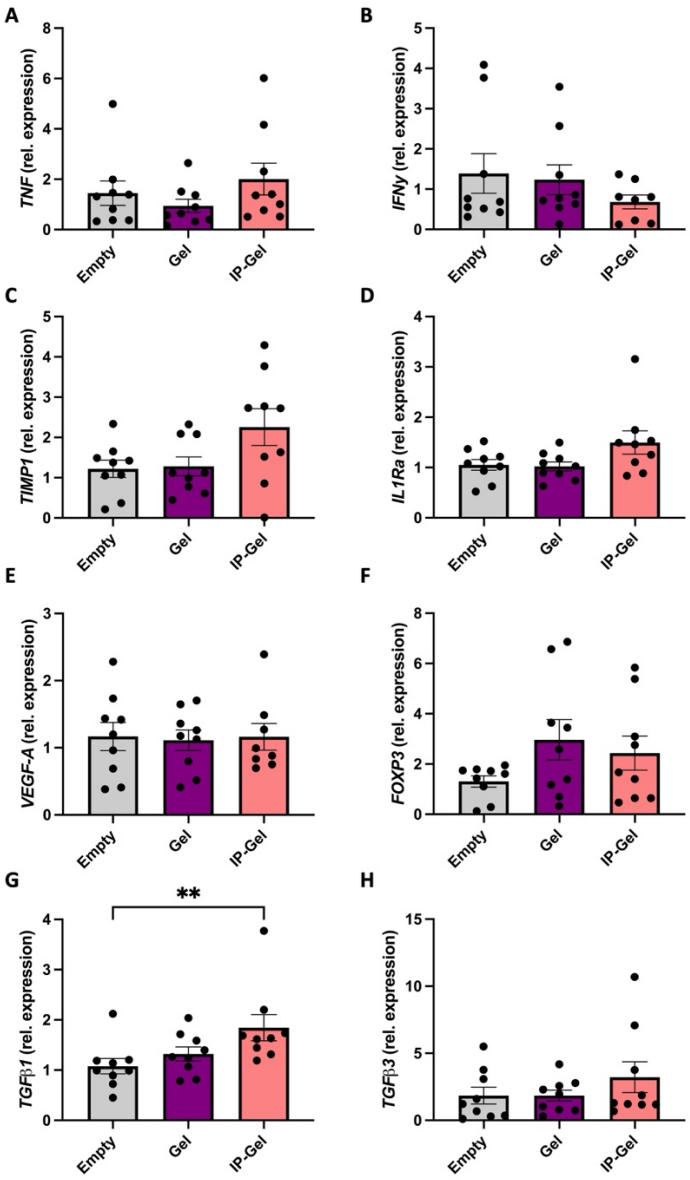

Figure 5.22 mRNA expression of inflammatory and regenerative-associated genes following implantation of hyaluronic acid hydrogels with and without IP into a rat femoral defect model.

HyA-gel with and without IP were implanted into a 5 mm rat femoral defect, or the defect site was left empty as a control. Tissue and hydrogel was harvested 7 days post-implantation and analysed by RT-qPCR for mRNA expression of **(A)** *TNF*, **(B)** *IFNγ,* **(C)** *TIMP1*, **(D)** *IL1Ra*, **(E)** *VEGF-A*, **(F)** *FOXP3*, **(G)** *TGFβ1*, and **(H)** *TGFβ3*. Pooled data (n=9 rats) are represented as mean ± SEM. Outliers were excluded using Grubb's outlier test. Data were analysed using Kruskal-Wallis with Dunn's post-test (**P≤0.01).

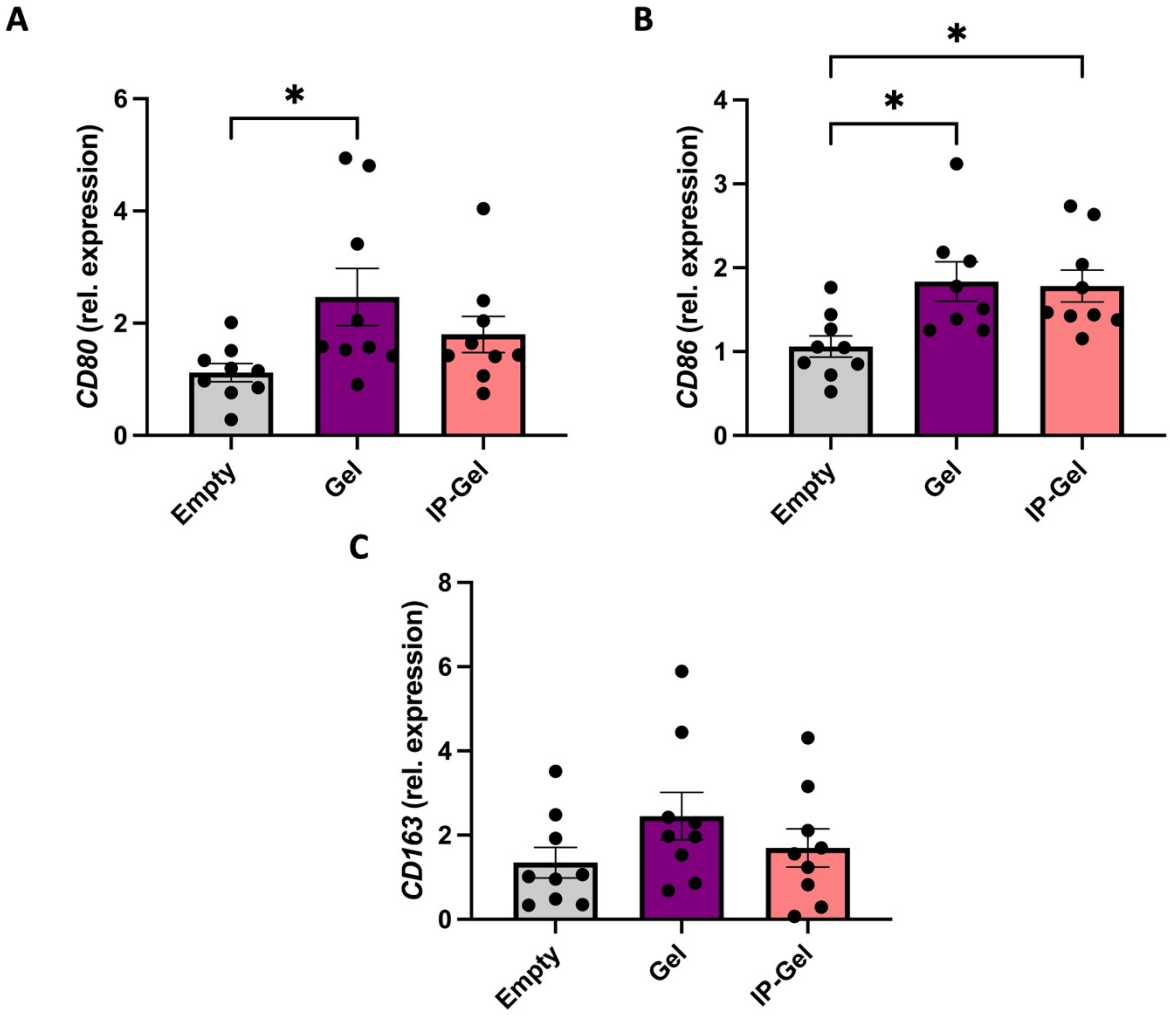

Figure 5.23 mRNA expression of macrophage activation markers *CD80* and *CD86*, but not *CD163*, are upregulated following implantation of hyaluronic acid hydrogels with and without IP into a rat femoral defect model.

HyA-gel with and without IP were implanted into a 5 mm rat femoral defect, or the defect site was left empty as a control. Tissue and hydrogel was harvested 7 days post-implantation and analysed by RT-qPCR for mRNA expression of **(A)** *CD80*, **(B)** *CD86*, and **(C)** *CD163*. Pooled data (n=9 rats) is represented as mean ± SEM. Outliers were excluded using Grubb's outlier test. Data were analysed using Kruskal-Wallis with Dunn's post-test (*P≤0.05).

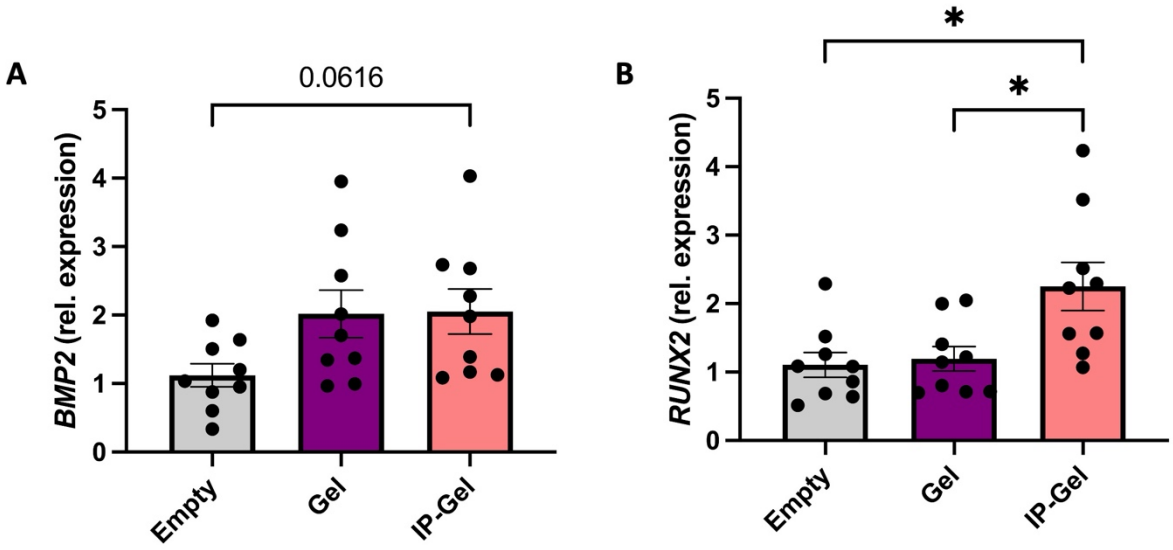

Figure 5.24 mRNA expression of osteogenic genes *BMP2* and *RUNX2* are upregulated following implantation of IP-loaded hyaluronic acid hydrogels into a rat femoral defect model.

HyA-gel with and without IP were implanted into a 5 mm rat femoral defect, or the defect site was left empty as a control. Tissue and hydrogel was harvested 7 days post-implantation and analysed by RT-qPCR for mRNA expression of **(A)** *BMP2* and **(B)** *RUNX2*. Pooled data (n=9 rats) are represented as mean ± SEM. Outliers were excluded using Grubb's outlier test. Data were analysed using Kruskal-Wallis with Dunn's post-test (*P≤0.05).

5.5 Discussion

There is a growing need for new and improved biomaterials to meet the rising demand for clinically translatable implant materials, notably in the case of orthopaedic implants which are prone to loosening and often require replacement surgeries [317]. As such, biomaterial design is based around a wide and varied range of natural and synthetic base materials, with a wider and ever-expanding range of potential modifications to enhance host-biomaterial integration and long-term success. Given the critical immune component of the host response to biomaterials and tissue regeneration [3], interest is growing into examining the effect of biomaterials and biomaterial modification on immune cell responses. Hyaluronic acid is garnering interest as a potential biomaterial for bone tissue engineering given its highly biocompatible, biodegradable, and osteoinductive properties [299, 301, 302]. Hyaluronic acid, while documented as a non-immunogenic material, is known to induce a pro-inflammatory immune response at low molecular weights, and an anti-inflammatory response at high molecular weights [138], and holds great potential as a carrier for immunomodulatory factors [318]. The hyaluronic acid hydrogel (HyA-gel) under investigation in this chapter has not been subject to study in the context of the immune response thus far, and therefore it was necessary to conduct *in vitro* testing using primary human macrophages to ascertain the biocompatibility of this HyA-gel, as determined by viability and differentiation capacity.

It was found that macrophages seeded onto HyA-gel exhibit cell viability comparable to, or greater than, those seeded on tissue culture polystyrene (TCP). Cell death that appears to result from culture on TCP compared to HyA-gel can be postulated to be due to the pre-staining processing; as macrophages are highly adherent on TCP, more force is needed to cause them to lift which can in turn result in cell death [319], compared to the gentle scraping that is needed to detach the loosely adherent macrophages from the HyA-gel surface. This also indicates that the HyA-gel's ability to bind via CD44 and RHAMM, receptors which are expressed on macrophages, results in a much looser adhesion than that of macrophages on TCP, thus potentially precluding integrin-mediated macrophage signalling and associated effector functions [320]. Further investigation into the binding of primary human macrophages to HyA-gel surfaces by receptor assessment would be

required to fully elucidate the mechanism behind their responsivity when cultured on these surfaces. Once the HyA-gel was confirmed not to induce cell death, the differentiation potential of monocytes was assessed. It was shown that the HyA-gel did not impact monocyte-to-macrophage differentiation, with $CD14^+$ $CD11b^+$ subpopulations comparable to that of the TCP control. This is similar to what has been seen in other hydrogels in the literature [321], and posits the HyA-gel as an attractive material for facilitating normal progression of the host immune response that allows for the transition from homing monocytes to mature macrophages necessary for facilitating the tissue repair process.

To complement the findings above, it was then necessary to ascertain that HyA-gel did not impact on the ability of macrophages to respond to polarisation stimuli, and assess whether contact with the HyA-gel itself impacted on macrophage polarisation state. Hyaluronic acid is documented to polarise macrophages towards an M1-like phenotype at low molecular weights and an M2-like phenotype at higher molecular weights [138]. The hyaluronic acid used to manufacture this HyA-gel has a molecular weight of ~340kDa, placing it at an intermediate level in the range used to investigate immunomodulatory potential of hyaluronic acid. Mature macrophage markers were assessed by flow cytometry in order to investigate the polarisation state of monocyte-derived macrophages seeded atop the HyA-gels. It was interesting to note that there were no significant differences between M1-like and M2-like macrophage markers between the HyA-gel and TCP control, suggesting that the HyA-gel does not have an inherently immunomodulatory effect on macrophage polarisation. This is in line with what could be expected given that low molecular weight hyaluronic acid required to upregulate pro-inflammatory responses tends to fall far below that used to manufacture the HyA-gel, whilst high molecular weight hyaluronic acid generally is reported as being 800kDa+ [138].

As stiffness has been shown to modulate macrophage phenotype, it was next of interest to investigate whether tuning of HyA-gel stiffness can influence macrophage polarisation state and thus render the material inherently immunomodulatory. Hydrogel manufacture was optimised to yield 1kPa and 10kPa hydrogels, which falls on the lower end of the stiffnesses reported for granulation tissue post-fracture and therefore recapitulates

stiffnesses found in the beginning states of the bone healing process [322, 323]. Overall, it was found that there was no significant change in macrophage polarisation markers upon culture on the HyA-gels of varying stiffness. The lack of significant change in polarisation marker expression could be due to the relatively narrow stiffness range achievable with modification of crosslinker concentration, with published *in vitro* studies investigating macrophage response to gel stiffness interrogating a wider range of gel stiffnesses. For example, one study showing that softer hydrogel surfaces promote anti-inflammatory macrophage gene expression while stiffer surfaces favour pro-inflammatory gene expression used hydrogels of 11, 88, and 323 kPa, with 11 and 88 kPa gels shown to promote anti-inflammatory gene expression [116]. Another investigation revealed increases in TNF secretion across gels of 1, 20, and 280 kPa, and this was further shown to be mediated *via* Yes-associated protein (YAP) translocation into the cell nucleus, which increases macrophage ability to respond to inflammatory stimuli [305]. It would therefore be of potential benefit to examine a wider range of hydrogel stiffnesses in future works. It would also be interesting to examine cellular YAP expression and translocation in response to the HyA-gels used in this chapter in order to interrogate this putative link between stiffness and inflammatory response.

It is also interesting to note that, while several studies have indicated softer substrates as skewing immune cells towards an anti-inflammatory phenotype compared to their stiffer counterparts, a recent study has shown that murine-derived BMDM cultured on soft ECM-derived gel surfaces are more pro-inflammatory than those cultured on stiffer surfaces, suggesting that the effect of tuning stiffness could be biomaterial-specific and not to be taken as a sole influencer of macrophage phenotype and function [133]. In addition, an earlier study by Friedemann *et al* demonstrated that macrophages cultured on a 0.1 kPa collagen surface were more M2-like than those seeded on a 0.03 kPa pure collagen control, again advocating for consideration of the effects of an interplay of factors on macrophage phenotype [132]. It was particularly notable that varying the stiffness of the HyA-gels did not appear to influence macrophage polarisation when compared to TCP controls, which provide a much stiffer surface (in the GPa range) than hydrogels. This could be due to the importance of material composition and multiple physiochemical properties in dictating immune cell response, with differences in the relative hydrophilicity and

binding ability of TCP compared to HyA-gels, and indicates that stiffness alone is not to be taken as sole determinant of immune cell response.

Given the lack of notable effect on macrophage polarisation markers, and in order to provide a more functional readout in the interests of biomaterial design, preliminary investigation into cytokine production as a result of culture on soft and stiff gels was conducted. The pro-inflammatory cytokines, IL-6, IL-8, and TNF were chosen as macrophages secrete high levels of all three in response to inflammatory stimuli, with IL-6 and IL-8 promoting recruitment of immune cells and propagation of immune cell activation, whilst TNF is particularly implicated in tissue destruction and destruction-associated inflammation. It was observed that macrophages cultured on HyA-gel surfaces trend towards secretion of lower levels of both IL-8 and IL-6 compared to TCP, and significantly lower levels of TNF compared to TCP controls, suggesting that HyA-gels can dampen the pro-inflammatory response of macrophages exposed to inflammatory stimuli. The lack of sufficient binding to the HyA-hydrogel could potentially be implicated as a reason for a muted pro-inflammatory response to M1-like polarising stimuli, with no binding sites present for integrin-mediated signalling. This weak cellular adherence is in line with results observed by Gallagher *et al* when investigating this particular HyA-gel in the context of MSC spreading [314], with subsequent modification by arginylglycylaspartic acid (RGD) peptide necessary to enhance cellular adhesion and subsequent effects. Therefore, modification of HyA-gel with binding motifs for cellular adhesion, or incorporation of other ECM components that bind macrophages such as fibronectin, offers a potential strategy for promotion of an immune-active, as opposed to a relatively immune-inert, HyA-gel in future works.

It is also important to note the wealth of emerging evidence for ‘hybrid’ macrophages exhibiting functions associated with either end of the macrophage polarisation spectrum and their role in bone tissue repair [239, 240]. This ties in with a growing appreciation for the plasticity of macrophages along a vast spectrum of polarisation states, and the inability to adequately characterise the response of macrophages by adhering to the overly simplistic ‘M1 vs M2’ paradigm. With this in mind, future studies could aim to incorporate more extensive means of interrogation of macrophage phenotype, such as by RNA-seq or

mass spectrometry, in order to gain a robust picture of macrophage response to not only HyA-gels used here, but any biomaterial under investigation. Taken together, this investigation has shown that this novel HyA-gel is not cytotoxic to primary human macrophages, does not have a significant effect on macrophage polarisation, and provides a surface on which monocytes can differentiate to macrophages at comparable levels to TCP control. In addition, it has been demonstrated that the stiffness range achievable with manufacture of this hydrogel does not appear to influence macrophage polarisation state to a significant degree. This indicates that, in its present form, our HyA-gel is biocompatible and neither hinders nor promotes the immune response to a significant degree, with further investigation into the extent with which this gel can bind macrophages necessary to fully elucidate how macrophages interact with this material.

It is well known that effects observed *in vitro* can often differ to those *in vivo* due to a complex microenvironment that cannot be adequately recapitulated outside of a model system. To this end, further investigation into the effect of hydrogel stiffness in an *in vivo* setting was conducted using a rat femoral defect model to recapitulate the *in vivo* immune environment surrounding a bone defect. As known rat immune cell markers are different to those typically displayed by human and murine immune cells, and consequently are less well characterised, an immune cell panel for flow cytometry was designed using two recent papers classifying rat immune cell subsets in LPS-induced inflammation and volumetric muscle loss (VML) rat models as a guide [324, 325]. It was seen across all major immune cell subsets that neither implantation of HyA-gel, nor tuning of HyA-gel stiffness influenced their absolute number or their relative proportion of $CD45^{+}$/Live cells to a significant degree, which is in line with the lack of significant effects observed in earlier *in vitro* work. The lack of impact on the immune environment also complements what has been documented in the literature, with the non-immunogenicity of hyaluronic acid hydrogels often cited as a reason for their use *in vivo*, and indicates that this biomaterial is not only biocompatible *in vitro*, but also does not promote a strong immune response in a host system. The relative lack of stiffness-mediated effects could be due to the relatively small range of stiffnesses achieved in this study, with published work showing differences in the *in vivo* immune response using a wider range of hydrogel stiffnesses in their investigation. In one example, hydrogel stiffness was shown to influence macrophage

migration and FBR in a subcutaneous implantation model, with these hydrogels ranging from 130 to 840 kPa as compared to the 1-10 kPa HyA-gels used in this study [130]. Another murine subcutaneous implantation model used poly (ethylene glycol) diacrylate (PEGDA) hydrogels of 1 kPa and 140 kPa to demonstrate the preferential *in vivo* recruitment of macrophages to stiffer as opposed to softer substrates [305]. It was seen in this chapter that 1 kPa HyA-gel surfaces appear to recruit a significantly lesser proportion of inflammatory monocytes than empty controls, and a trend towards a lesser proportion than 10 kPa HyA-gels, while the proportion of regenerative monocytes was increased around 1 kPa HyA-gel implants versus empty controls, and non-significantly increased around 10 kPa HyA-gels. This aligns with the literature demonstrating the anti-inflammatory potential of softer materials on the innate immune system, and indicates that softer HyA-gel implants may have a more pronounced effect in the context of the *in vivo* environment than that which was observed in the *in vitro* investigation. Hydrogel stiffness has also been shown to have an effect on the adaptive immune system, with *in vitro* work evidencing an increase in activation and secretion of IL-2 in $CD4^+$ T cells over a 10 – 200 kPa range [326], and B cells displaying increased activation when encountering antigens tethered to stiffer (22.1 kPa) substrates versus softer materials (2.6 kPa) [327]. As with the *in vitro* work, future work should aim to examine HyA-gels across a wider range of stiffnesses found in progression of bone fracture healing *in vivo*, to fully elucidate whether the parameter of stiffness can be tuned to produce an immunomodulatory effect with respect to this biomaterial. It is interesting to note that one study interrogated the effect of hydrogel stiffness in a rat VML model using a range of stiffnesses more comparable to those used in this chapter. This study demonstrated that defect sites in which higher stiffness hydrogels (10 kPa) had been implanted displayed higher levels of M1-like macrophages (as defined by $CD68^+/CD163^-$) at 24 weeks post-VML as compared to those which had received soft and medium gels (1 and 3 kPa respectively) [328]. It is worth noting that this study looked at macrophage phenotype at a later timepoint than that which was investigated in this chapter, and therefore examined the persistent immune response as opposed to the early immune timepoint investigated here. It is also worth considering that hydrogel degradative products are exerting more potent effects on the immune response over time compared to effects observed at an early timepoint. In line with the possible effect of hydrogel degradation on immune cell activation, it was also

observed that an upregulation of mRNA expression of activation marker *CD86* in HyA-gels versus empty control was observed, which may imply that although macrophage phenotype is not being significantly altered by these biomaterials, their degradation products may be capable of promoting macrophage activation. It will therefore be of interest in future work to quantify and examine the effect of the degradative products of this hydrogel on macrophage phenotype to gain a more robust picture of immune cell-hydrogel interaction.

Given the excellent biocompatibility displayed by the HyA-gel with respect to macrophage viability, differentiation, and polarisation ability, as well as the potential for HyA-gel to reduce LPS-induced TNF production, and as it did not appear that tuning the parameter of HyA-gel stiffness impacted on the polarisation state of macrophages, it was next decided to test the potential for our HyA-gel in drug delivery. Hyaluronic acid hydrogels have shown promise in delivery of anti-inflammatory therapeutics such as epigallocatechine-3-gallate (EGCG) in enhancement of osteoarthritic cartilage repair [329] and diclofenac potassium (DK) in a rat model of osteoarthritis, as well as displaying demonstrable efficacy in bone tissue regeneration by delivery of osteogenic agents such as BMP2 [311, 330, 331] and simvastatin [332]. To this end, it was decided to incorporate the immunomodulatory ketoacid, IP, into the HyA-gel in order to assess the effect of local IP delivery from this biomaterial on the immune microenvironment in a rat femoral defect model. IP was incorporated directly into the gel by dissolution. This method of physical entrapment, while being straightforward regarding experimental procedure, is also known to produce release kinetics that are difficult to control [333]. Upon assessment of IP-induced AhR activation in MSCs by *CYP1A1* mRNA expression, IP appeared to be released from the HyA-gel on day 1, and this release was not sustained by day 7. It is possible that IP is being released in a burst upon contact of the IP-gel with surrounding media, with further investigation using shorter timepoints in the minutes-to-hours range required to fully elucidate the release profile of IP from HyA-gel. Given the structure of IP and that of the HyA-gel, there may not be binding sites within the HyA-gel to which IP could attach, and hence this method of burst release is likely. IP also presents an issue with respect to quantification in that it has been found in our lab to auto fluoresce as it breaks down in solution over time, and preliminary experiments into quantification using fluorometric readouts proved inconclusive. It was therefore difficult to uncouple IP release from IP

breakdown within the parameters of the experimental protocol used. Further experiments are needed to elucidate the extent of IP release from the HyA-gel, such as by investigation of bioactivity of IP-gel as compared to IP or HyA-gel alone. This approach is confounded by the apparent ability of HyA-gel and IP to exert synergistic effects on MSC *CYP1A1* and *BMP2* mRNA expression and will require further interrogation of bioactive readouts specific to IP without apparent synergistic involvement of hyaluronic acid. The apparent synergy of IP and HyA is similar to what has been seen in the literature with respect to hyaluronic acid and other bioactive agents, with one study demonstrating the synergistic effect of hyaluronic acid chemically conjugated to the known antioxidant carnosine which, when used in combination, resulted in antioxidant effects to a greater extent than hyaluronic acid or carnosine alone as assessed by Trolox equivalents and RNS-derived nitric oxide production [334]. From an osteogenic perspective, it has been observed that a combination of hyaluronic acid and dexamethasone resulted in increased osteogenic differentiation of human MSC, with increased calcium and ECM-remodelling TIMP3 production as a result of hyaluronic acid and dexamethasone combination treatment as opposed to either single treatment alone [335]. This is similar to the upregulation in *BMP2* mRNA expression observed here as a result of HyA-gel and IP treatment in MSC. It is known that hyaluronic acid can activate the WNT/β-catenin pathway [336], which has been shown to in turn promote BMP2 production in osteoblasts [337]. It is possible that HyA-gel degradative products could be promoting WNT signalling in MSC, which is in turn driving the upregulation in BMP2 seen here. Further interrogation of the effect of both HyA-gel and IP exposure on components of the WNT/β-catenin signalling pathway are necessary to fully elucidate the means by which HyA-gel and IP can promote BMP2 production in MSC. The lack of upregulation seen with mRNA of *RUNX2*, *OCN*, and *VEGF-A* in MSC as a result of treatment with day 1 IP-gel conditioned media versus IP alone can be postulated to be due to the low concentration of IP in the conditioned media at day 1, and indicates that although some IP does appear to be released in a burst, as seen by the upregulation of *CYP1A1* and *BMP2* at the day 1 timepoint, IP may still be retained within the HyA-gel to a degree, with more extensive investigation using alternative timepoints for media collection required to gain a more robust picture of IP release from HyA-gel. Alternatively, encapsulation within the HyA-gel could be impacting on the breakdown of IP, and as it is highly possible that the effects of IP are mediated *via* its breakdown products, which have

yet to be characterised, the effect of HyA-gel on IP breakdown could be attenuating its effects on upregulation of gene expression. Further work employing techniques such as high-performance liquid chromatography (HPLC) could prove beneficial in characterising IP breakdown products for direct interrogation of their effects, and their interactions with materials such as hyaluronic acid.

In examination of overall immune cell subsets, IP-gel was not found to significantly impact on the immune environment in terms of immune cell recruitment, nor on monocyte, macrophage, and T cell phenotypic state. Additionally, only minor effects were observed in mRNA expression of inflammation and regeneration-associated markers, with the upregulation of certain markers such as *VEGF-A* and *TGFβ3* seen *in vitro* unable to be recapitulated *in vivo*. One explanation for this could be the discrepancies between human and rodent cellular responses to stimuli. Although little work has compared rat to human immune responses, there is literature documenting discrepancies seen in response to murine and human immune cell subsets in response to LPS, for example [338], and similar discrepancies could be seen between rat and human. It is, therefore, a worthy avenue of investigation to examine the effect of IP on rat immune and progenitor cells *in vitro* in order to more accurately recapitulate what is observed here *in vivo*. It is also worth noting that the actual amount of IP encapsulated within in the HyA-gel is low in relation to the doses documented to exert anti-inflammatory effects in the literature, with studies on the efficacy of IP in a rat collagen-induced arthritis model reporting a dosage of 10 - 20 mg/kg, as well as repeated administration as opposed to the single-delivery used in this chapter [109]. By comparison, the maximum concentration of IP dissolvable within the HyA-gel to allow for gelation and retention of structure was at a concentration of 2 mM, which equates to a total amount of 16.65 µg IP (based on HyA-gels of 40 µL volume), corresponding to a dosage of ~0.05 mg/kg total (based on an average of 350 g/rat). Hence there may not be a high enough dose of IP available to exert discernible effects on the immune environment, and future works could examine alternative means of IP encapsulation for sustained and increased delivery, for example by encapsulation within nanoparticles or PLGA-microparticles. It is also worth noting that the rat femoral defect model used here was employed as a means of interrogating the immune environment surrounding a critical sized bone defect for an ultimate goal of immunomodulation for

bone regeneration. If effects were to be studied specifically on IP release from HyA-gel in the context of inflammation, models of inflammatory disease such as RA could instead be used, with IP-gel being administered locally to examine its effects in an established inflammatory environment.

Despite the low dose of IP from the HyA-gel, upregulation in *TGFβ1* at the mRNA level was observed, which is in line with *in vitro* observations. Additionally, and most promisingly, upregulation of *BMP2* and *RUNX2* mRNA was also seen as a result of IP-gel treatment. It is interesting to note that HyA-gel alone does not promote increased *RUNX2* despite an increase seen in *BMP2* in MSC at 48 hours and a trend towards an increase in *BMP2 in vivo* at 7 days, as it is known that BMP2 can act to upregulate *RUNX2* activity. This further suggests IP as an advantageous pro-osteogenic therapeutic for delivery from HyA-gel. A limitation of this study is that was not extended to a timepoint that would allow for assessment of bone tissue regeneration. It would therefore be of interest in future studies to examine the potential for IP delivery to impact on bone regeneration *in vivo* beyond the preliminary indications provided in this chapter.

Overall, this chapter has provided evidence that a novel hyaluronic acid hydrogel exhibits high biocompatibility, as assessed by viability, differentiation, and polarisation ability, with respect to primary human macrophages. It has also shown that modulation of hydrogel stiffness within the range of 1 – 10 kPa does not exert potent effects on macrophage phenotype, but that culture on these hydrogels may dampen production of certain pro-inflammatory cytokines in response to LPS-stimulation. *In vivo*, modulation of hydrogel stiffness in the 1 – 10 kPa range achieved minimal effects on the resulting immune environment but demonstrated that softer hydrogels potentially reduce the number of inflammatory monocytes and increase pro-regenerative monocytes present at the defect site compared to empty defect. This chapter also demonstrated that HyA-gel may provide a suitable delivery platform for immunomodulators such as IP. IP-gel was not found to significantly affect overall immune cell environment in terms of absolute numbers and proportion of subsets surrounding the implant, but was found to increase *TGFβ1* mRNA expression *in vivo*. Additionally, incorporation of IP into HyA-gel was found to increase *BMP2* and *RUNX2* mRNA expression *in vivo*, which aligns with what was seen in

preliminary *in vitro* investigation and posits IP as a potential strategy in promotion of osteoblastic differentiation when delivered locally into a bone defect site. In summary, this chapter established a novel hyaluronic acid hydrogel as a biocompatible, non-immunogenic delivery platform for novel immunomodulatory therapeutics with potential pro-osteogenic effects.

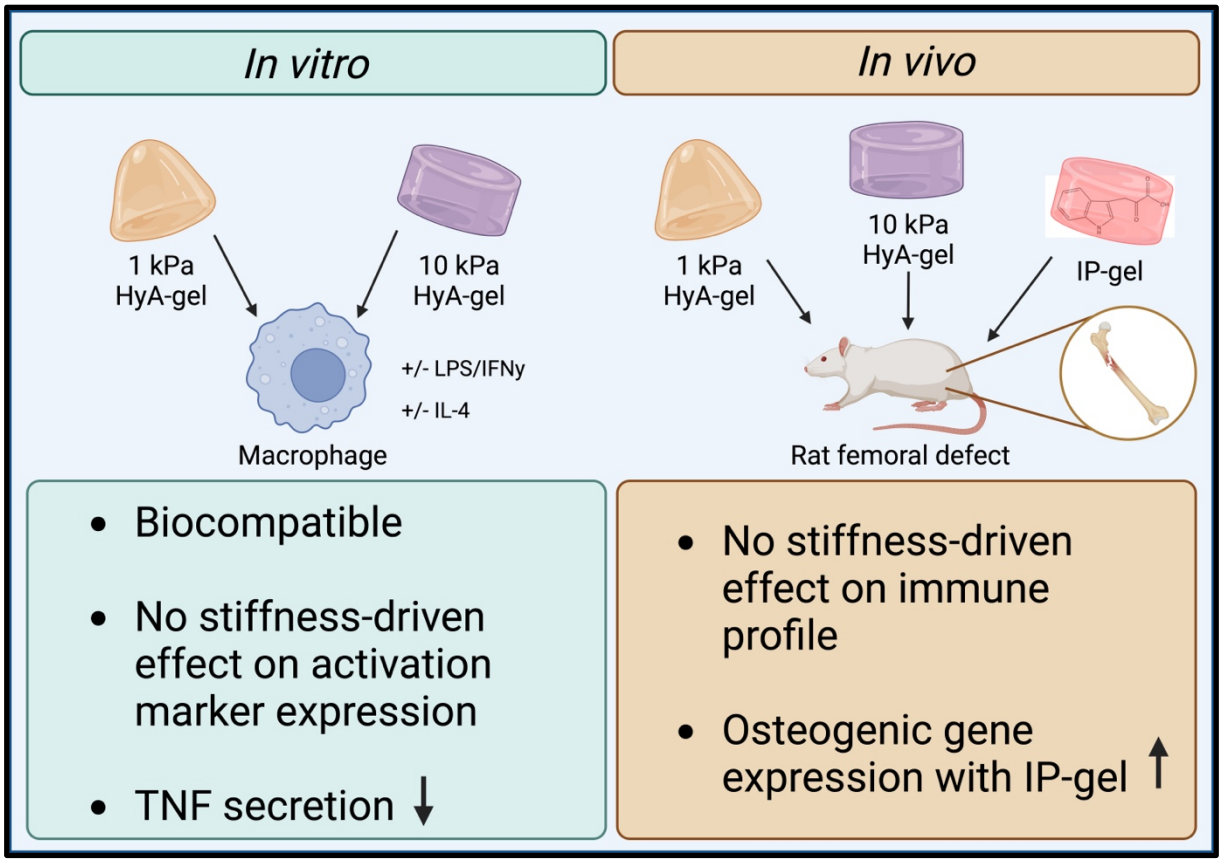

Figure 5.25 Summary schematic of findings.

Hyaluronic acid hydrogels are well tolerated by human macrophages *in vitro*. Primary human macrophages seeded on 1 kPa and 10 kPa hydrogels do not exhibit differential gene expression/marker expression/cytokine secretion in the presence or absence of M1 and M2-like polarising stimuli. The *in vivo* immune profile surrounding a rat femoral defect is not affected by hyaluronic acid hydrogel stiffness. Delivery of indole-3-pyruvate from a hyaluronic acid hydrogel in a rat femoral defect model does not impact on the surrounding immune cell profile, but does increase osteogenic gene expression.

Chapter Six

General Discussion

6.1 General Discussion

It is evident that the immune system functions as a crucial component of tissue reparative and regenerative processes, with immune cell-mediated activities acting as key drivers of processes that can either hamper or facilitate tissue healing and regeneration. Biomaterial intervention is often employed as a strategy in the treatment of damaged tissue with limited intrinsic regenerative capacity, with the optimal biomaterial traditionally considered to be one that is immunologically 'inert'. However, as our understanding of the interaction of the immune system with various clinically employed biomaterials grows, so too does our appreciation that no biomaterial is truly inert, and so our efforts to characterise and modulate the immune response to biomaterials serves to enhance our ability to design biomaterials with superior integrative and regenerative properties. Bone tissue in particular stands to benefit from incorporation of immunological insights into bone tissue engineering approaches.

As our understanding of the biomaterial-immune system interaction evolves, there is mounting evidence of a need for novel approaches to modulate this interaction for therapeutic benefit. The study of immunometabolism has led to vast advances in the field of immunology [161], but to date has not been extensively studied in the context of bioengineering. Indeed, recent works have only just begun to explore the potential application of immunometabolic insights in bioengineering [172, 339]. The majority have focused on metabolic changes in murine immune cells such as RAW 264.7 cells and primary BMDM [172, 238]. Human macrophages, however, have been documented to display different metabolic responses to those of murine origin in response to stimuli such as LPS [338, 340]. The work in this thesis provides one of the first examples of direct interrogation of the metabolic changes that occur in human immune cells in response to biomaterial particulates, furthering our efforts to bring immune-informed biomaterial design closer to clinical translatability. The results of chapter 3 provided evidence of metabolic reprogramming favouring glycolysis in primary human macrophages by micron, but not nano-sized hydroxyapatite particles. Encouragingly, since the completion of this project, studies have been published in the biomaterials space that corroborate the

findings presented here. Maduka *et al* has recently produced several works demonstrating the ability of clinically employed biomaterials, such as polylactide, to impact on immune cell metabolism [341]. Particularly, regarding biomaterial particulates, it has been shown that polyethylene (PE) wear particles enhance glycolysis in BMDM, with pro-inflammatory cytokine secretion that is driven by particle exposure attenuated with the use of glycolytic inhibitors, 3PO and 2-DG. These results complement those which were observed in this thesis regarding the effect of hydroxyapatite particles on primary human macrophages in the presence or absence of glycolytic inhibitors [224]. Maduka furthered this study to demonstrate that oxidative phosphorylation was elevated in BMDM exposed to PE particles, an effect which again aligns with moderate effects seen on human macrophage maximum respiration with the micronHA particles used here [225]. More encouragingly still, this work has since been translated into an *in vivo* model of particle-induced inflammation, in which small molecule inhibitors of glycolysis (aminooxyacetic acid and 2-DG) incorporated into a composite material of polylactide and HA and subcutaneously implanted into a mouse model were able to reduce pro-inflammatory immune cell proportions and increase anti-inflammatory immune cell populations, concomitant with an increase in arginase 1 (Arg1) which drives osteogenesis and tissue regeneration [342]. From the perspective of bone repair and regeneration, glycolytic inhibition may also prove beneficial in that MSC, which rely basally on glycolysis and utilise this pathway during chondrogenic differentiation [343], have been shown to upregulate oxidative phosphorylation and glutaminolysis when undergoing osteogenic differentiation [344, 345]. Therefore, pushing MSC metabolism from favouring glycolysis towards oxidative phosphorylation, for example through use of glycolytic inhibitors, could assist in the promotion of bone tissue regeneration *in vivo*. However, it must be noted that caution is to be used when interrogating metabolic inhibitors for therapeutic benefit, with many immune cells and progenitor cells relying on different metabolic pathways in a spatiotemporal manner to ensure optimal repair and regeneration *in situ*. It is also becoming appreciated that, while useful in terms of characterisation and establishing potential targets, it is overly simplistic to assign a particular metabolic pathway to one established functional phenotype given that an interplay of different metabolic pathways are required for different immune cell functions. For example, it is coming to be appreciated that M2-like macrophages also rely on induction of glycolysis to fuel their

activation [173, 174], whilst M1-like macrophages also employ FAO, a pathway traditionally associated with M2-like activation [346], and therefore careful and considered interrogation of metabolism is required when seeking to target metabolic pathways and metabolites for therapeutic benefit. Given that the work performed in this thesis demonstrates the impact of HA particles on human immune cell metabolism, chapter 3 contributes important new insights into the human immune response to biomaterial particulates, and highlights targeting of immunometabolism as an exciting clinical avenue to mitigate tissue destructive processes and promote tissue repair and regeneration. This may have implications not only for design of orthopaedic implant materials, furthering the rationale for the increasingly popular use of nano as opposed to micron-sized hydroxyapatite, but also offers new insight into the inflammatory processes that contribute to implant wear and, ultimately, failure [347].

As briefly mentioned in chapter 3, endotoxin contamination poses a major challenge in the field of biomaterial implantation [209, 210]. As such, a number of experimental strategies can be employed to mitigate the effects observed as a result of endotoxin contamination, such as the testing of micronHA and nanoHA with the HEK-blue TLR4 cell line described in this thesis, as well as other techniques, such as the use of polymyxin B, that act to neutralise endotoxin. That being said, it cannot be ignored that endotoxin contamination may in fact result in responses that are more clinically relevant in the context of biomaterial implantation, given that infections due to bacterial contamination commonly occur at the implantation site and pose a major clinical concern. As such, responses observed as a result of synergistic interaction between contaminants and biomaterials may also provide useful insight into clinical outcomes of biomaterial implantation and, whilst it is important to examine the direct impact of the biomaterial itself in the absence of endotoxin as a preliminary step, provide useful additional information as to how an implant will behave in the clinical setting.

The need for identification of novel immunomodulators in order to tackle and surmount challenges that currently exist at the clinical level is pressing, with one class of immunomodulators under investigation in our lab being that of novel HO-1 inducers/Nrf2 activators. HO-1 inducers show immense promise in the promotion of anti-inflammatory

activity in inflammatory and autoimmune diseases such as RA, multiple sclerosis, and IBD. The immunomodulatory ketoacids, IP and HPP, have recently begun to be investigated in our group for their ability to exert anti-inflammatory activity in certain immune cell subsets such as DC [108], and murine macrophages and glia [78], and IP in particular is garnering attention as a putative anti-inflammatory therapeutic in disease models of colitis and arthritis [107, 109]. However, prior to investigation conducted in chapter 4 of this thesis, very little work examined the effect of IP and HPP in primary human macrophages. At the time of study, one known work documented the ability of IP to reduce prostaglandin production in primary human macrophages [106]. Work presented in this thesis therefore expands our understanding of the effect of both ketoacids in human macrophages, and provides interesting insight into the differences in how immunomodulators can impact on various immune cell subsets. It was observed in this thesis that HPP was a more potent inducer of HO-1 than IP in human macrophages but that, interestingly, IP exerted more potent effects in the attenuation of LPS-driven M1-like macrophage marker gene expression and slight reduction in pro-inflammatory cytokine secretion, with the relative potency of IP documented in other immune cell types and evidenced by greater interrogation of therapeutic potential in the literature [107-109]. The results presented here highlight not only the variability that exists between immune cells in their response to various stimuli, but further advocate for study of multiple immune cell types in interrogation of putative immunomodulators for greater recapitulation of *in vivo* effects. They also highlight that, despite the anti-inflammatory benefit conferred by the induction of HO-1 and the documented link between HO-1 induction, Nrf2 activation, and the anti-inflammatory properties of IP, this ketoacid may be exerting immunomodulatory effects through alternative mechanisms that are worth investigation for thorough characterisation and therapeutic exploitation. There is also a possibility for synergy between HPP and IP in combination to confer greater therapeutic benefit than either ketoacid in isolation.

The work in chapter 4 of this thesis builds on the existing literature documenting the anti-inflammatory properties of the ketoacids IP and HPP, and furthers the investigation to interrogate their potential in tissue regeneration. This work provides the first example of these ketoacids impacting on the expression of pro-regenerative genes in primary human

macrophages. This chapter further builds on the potential pro-regenerative effects of IP in human MSC and it is demonstrated for the first time that this ketoacid can induce HO-1 and activate Nrf2 in these cells. While much work remains to be done, HO-1 inducers may represent a new class of potential drug to promote stem cell differentiation. This is supported by the recently established link between HO-1 and osteoblastic differentiation of MSC [60-62, 282]. It is further shown in chapter 4 that IP is capable of upregulating mRNA expression of angiogenesis-associated genes and growth factors in MSC, with exposure of MSC to IP additionally promoting MSC mineralisation, suggesting that IP does not only influence the differentiation, but also the maturation of osteoblasts *in vitro*. It is also notable that some of the growth factors interrogated at the mRNA level are important for chondrogenesis as well as osteogenesis, such as *TGFB1*, which further holds implications for potential in repair of osteochondral defects. Additionally, given that the process of endochondral ossification initially involves chondrogenic differentiation of MSC and cartilage deposition, which is then replaced by bone, IP could be an interesting candidate to interrogate for chondrogenic as well as osteogenic potential. Overall, the results shown here provide interesting preliminary results not only in establishing a novel means of promoting MSC differentiation, but also in identification of a compound with dual anti-inflammatory/pro-osteogenic effects. This work therefore also advocates for the interrogation of traditional anti-inflammatories for their regenerative effects, not only for bone tissue applications, but across a range of tissue types depending on intended therapeutic application. Additionally, MSC have come to be regarded as immunomodulatory cells themselves, functioning to suppress immune cell responses and promote the differentiation of anti-inflammatory macrophages [348-350]. It is therefore of interest to further interrogate the immunomodulatory effects of IP and HPP, as well as emerging immunomodulators, on MSC functionality with respect to immunomodulatory cytokine production and direct effects on other immune cell types, in order to gain a more robust understanding of the immunomodulatory and regenerative potential of these novel ketoacids.

Studies into hyaluronic acid hydrogels for bone tissue regeneration have indicated hyaluronic acid to be a highly biocompatible biomaterial for clinical application [333], and indeed hyaluronic acid itself is widely used as a therapy for rheumatoid arthritis as an

intra-articular injection intended to alleviate inflammation and improve joint lubrication [351], as well as in osteochondral defects as an adjunct therapy to microfracture [352]. In knee osteoarthritis the application of hyaluronic acid has been shown to be effective in follow-up studies in tempering of inflammation and pain management [353, 354]. This study therefore further profiles the human macrophage response to hyaluronic acid in the form of a novel hyaluronic acid hydrogel, with demonstration that it does not affect cell viability and allows for monocyte differentiation into macrophages as well as polarisation of macrophages to M1- or M2-like phenotypes. This study further verifies the relative safety of hyaluronic acid for clinical use in that no adverse effects such as cytotoxicity or significant impact on cell function were observed. Indeed, in the tempering of LPS-induced pro-inflammatory cytokines, the documented anti-inflammatory properties of hyaluronic acid were supported by chapter 5 in which TNF secretion was shown to be lessened on HyA-gel surfaces when compared to tissue culture plastic (TCP), further supporting the clinical use of hyaluronic acid.

Modulating biomaterial stiffness has produced conflicting results in the literature, with the majority of studies supporting the findings that stiffer materials promote a more pro-inflammatory immune cell profile [116, 130, 305, 306], while other studies argue for the opposite effect [132, 133]. In this thesis, it was observed that modulating hydrogel stiffness produced no discernible effects on primary human macrophages *in vitro*, and very slight effects in the context of the immune microenvironment *in vivo*. As well as indicating that modulation of this parameter within the range investigated here does not produce immunomodulatory effects, somewhat encouragingly, the lack of immune response supports the relative non-immunogenicity of this material, and this implicates hyaluronic acid hydrogels as a potential suitable drug delivery platform for experimental interrogation of deliverable therapeutics. Indeed, further work in this thesis assessed hyaluronic acid hydrogels for this purpose, and were used to deliver the novel immunomodulator, IP. It was shown here that, when physically encapsulated within the HyA-gel, IP is released to a degree at which it can activate the AhR in MSC and, with hyaluronic acid, synergistically promote *BMP2* mRNA expression. The results in this thesis also provide evidence that AhR activation is worthy of further investigation in MSC. Much of the literature reports that AhR activation in MSC is associated with negative outcomes in osteoblastic differentiation

and bone regeneration [287, 290], but fails to account for discrepancies seen in the type of AhR agonist used, and the extent to which the AhR is activated by these agonists. It is common for studies into AhR activation in MSC to use environmental toxins such as TCDD and BaP as AhR agonists, but fewer studies employ naturally-derived AhR agonists such as FICZ, or the ketoacids used in this thesis. This study therefore provides an example of an AhR agonist that is capable of promoting pro-osteoblastic effects in MSC, which may be attributable to not only AhR activation, but the extent to which the AhR is activated in these cells. This notion is supported by the increase in bone volume seen when administering FICZ *in vivo* [295] and the ability of FICZ to rescue alveolar bone loss in a murine model [355], and advocates for use of transient AhR activators as a potential pro-osteogenic strategy.

Given the established link between an anti-inflammatory immune response and bone formation, a number of studies have examined the therapeutic benefit of delivering both anti-inflammatory and osteogenic agents in combination [356, 357]. The work provided in chapter 4 explored the potential of a single drug to exert dual effects in an *in vivo* bone defect model. It was encouraging to find that results seen *in vitro* with MSC cultures translated to the *in vivo* level, with osteogenic genes *BMP2* and *RUNX2* upregulated after seven days of IP-gel exposure within a rat femoral defect. Additionally, this work furthers evidence in the literature for the beneficial effects of antioxidant-driven dampening of inflammation in promotion of osteogenesis and implant success [358, 359]. Given the lack of control achievable using a method of physical entrapment, future work should look to refine means of drug delivery from this hydrogel, also potentially allowing for delivery of an increased IP dose given the low dose used in this thesis compared to what is administered *in vivo* in the literature [107, 109].

It is additionally notable that work in chapters 3 and 4 considered the impact of biomaterials and immunomodulators on macrophage polarisation, and links the attenuation of chemokines CXCL9 and CXCL10, as well as CXCL11 and CXCL19, with the attenuation of the LPS-induced pro-inflammatory profile of these cells. In a wider context, it must also be noted that downregulation of these chemokines may additionally impact on the recruitment of other immune cells, including those of the adaptive immune system,

to an injury site. This therefore holds implications for downstream reparative and regenerative processes. This may not only contribute to the attenuation of inflammation and facilitation of repair processes, but may also hamper the recruitment of cells that may play beneficial roles in tissue repair and regeneration, such as Tregs, and further highlights the necessity of interrogating biomaterial implantation in the context of an interplay of immune and progenitor cells.

6.2 Limitations and Future Work:

- As indicated throughout, assessment of macrophage phenotype was limited to interrogation of a small number of selected markers for M1-like and M2-like polarisation. Additionally, assessment of macrophage metabolic profile in response to hydroxyapatite particles examined only two major metabolic pathways: glycolysis and oxidative phosphorylation. It would therefore be of interest in future work to interrogate a wider range of macrophage markers and functional outputs in response to these particles by using, for example, RNA-seq and metabolomics approaches, which could also implicate other metabolic pathways in the macrophage response to biomaterials. This robust approach is particularly relevant in light of emerging evidence for the role of 'hybrid' macrophages in contributing to tissue reparative and regenerative processes, in which macrophages displaying both markers and functions traditionally associated with either 'M1-like' or 'M2-like' classifications are proving vital in driving regenerative outcomes.
- Work interrogating the effect of the ketoacid IP on MSC was limited to one human MSC donor. While common in bioengineering approaches in the assessment of MSC response to materials, donor variability is a known limitation of human work, and evidence with variability found among primary human immune cells strongly advocates for interrogation of multiple human donors, if available. Future work should aim to replicate results in at least two more human MSC donors in order to ensure effects are reproducible and reliable across humans. Additionally, *in vitro* readouts herein provided preliminary indication of effects in that mRNA expression of angiogenesis-related genes and growth factors were assessed. Next steps could be to assess production of soluble mediators of regeneration at the protein level by ELISA and western blot, as well as the use of co-culture models using macrophages, MSC, and other immune cell types.
- The hyaluronic acid hydrogel under investigation was limited in supply, with production being halted shortly after the beginning of this project due to the repurposing of factory equipment. As a result, hyaluronic acid hydrogels of 2% w/v

were constructed, with the resulting range of achievable stiffnesses as a consequence of crosslinker modification ranging between ~1 – 10 kPa. Given that this range of stiffness falls far below that which is commonly studied in the literature in interrogation of immune response to stiffness, it would be of interest in future work to construct hydrogels of higher hyaluronic acid percentages in order to achieve a wider stiffness range, which may be more likely to produce effects on immune cells investigated. Additionally, it is known that increasing hyaluronic acid concentration can improve the mechanical strength of hydrogels, albeit resulting in reduced swelling capacity [360], and so this method may be beneficial in improving the suitability of our HyA-gel for bone tissue engineering applications in which higher mechanical strength is required.

- The immunomodulatory ketoacid, IP, has been shown in our lab to auto fluoresce over time in solution, rendering some common techniques such as flow cytometry and confocal microscopy difficult to perform. This limited the approach that could be taken in assessment of, for example, macrophage marker expression, and so mRNA and cytokine expression were taken as a more reliable initial indication of IP-mediated effects. Future work should focus primarily on the functional effects as a result of IP exposure in immune cells and MSC, such as the effect of the IP-induced secretome on other immune cell subsets. Additionally, the tendency of IP to auto fluoresce as it breaks down over time also proved a barrier to assessment of drug release, as it was difficult to uncouple fluorescence from IP breakdown, particularly as it is possible that IP interacts with hyaluronic acid to break down at a different rate or into different products than when free in solution. Therefore, future work involving characterisation of the breakdown products of IP, as well as different means of quantification in solution, is needed to provide a means of profiling drug release. Alternatively, the use of bioactivity, such as activation of AhR and Nrf2, as a proxy readout for IP release could be employed. However, it is worth noting that the results in this work were hampered by an apparent synergistic effect of hyaluronic acid and IP. Therefore, further interrogation of cellular responses that are specific to IP are therefore needed in order to utilise bioactivity as a readout for drug release.

- The direct physical entrapment route of encapsulating IP within the hyaluronic hydrogel was chosen due to time constraints regarding duration of animal ethics, with dissolution prior to gelation being the most straightforward route of encapsulation. However, as stated in chapter 4, a maximum amount of 16.65 µg IP was able to be encapsulated within the hydrogel that would fit in the defect site in accordance with procedures outlined in the HPRA-approved project authorisation, with higher amounts resulting in incomplete dissolution or loss of hydrogel structure. This low dose administered could go towards explaining the lack of pronounced effects seen *in vivo*, as IP has proven efficacious in inflammatory disease models at doses of 10 – 20 mg/kg, as well as published studies using repeated administration compared to the single-dose used here. Future work would benefit from alternative routes of drug encapsulation, perhaps by the use of PLGA nanoparticles or microspheres, which would allow for not only increased dosage of drug, but also provide means of controlled, sustained release over time which may provide more tangible *in vivo* benefit.

6.3 Conclusion

Overall, the work in this thesis has provided further characterisation of the innate immune response to biomaterials currently employed in the clinic for bone-based applications. It has highlighted immunometabolism as an exciting emerging area worthy of exploration for bioengineering applications, not only to further our understanding of the immune response to biomaterials, but also to potentially identify novel therapeutic targets that can elevate current therapies for tissue repair and regeneration. This work has also identified the potential for a novel immunomodulatory ketoacid to exert anti-inflammatory and pro-regenerative effects in human macrophages and MSC, and has highlighted interrogation of known and emerging immunomodulators for regenerative capacity in order to develop superior therapeutics in enhancement of tissue reparative and regenerative processes. Finally, a hyaluronic acid hydrogel has been identified as a potential drug delivery platform to deliver immunomodulators *in vivo* for experimental interrogation and possible eventual clinical application.

References

[1] T.A. Wynn, T.R. Ramalingam, Mechanisms of fibrosis: therapeutic translation for fibrotic disease, Nat Med 18(7) (2012) 1028-40.
[2] A.B. Aurora, E.N. Olson, Immune modulation of stem cells and regeneration, Cell Stem Cell 15(1) (2014) 14-25.
[3] Z. Julier, A.J. Park, P.S. Briquez, M.M. Martino, Promoting tissue regeneration by modulating the immune system, Acta Biomater 53 (2017) 13-28.
[4] J. Larouche, S. Sheoran, K. Maruyama, M.M. Martino, Immune Regulation of Skin Wound Healing: Mechanisms and Novel Therapeutic Targets, Adv Wound Care (New Rochelle) 7(7) (2018) 209-231.
[5] M. Rodrigues, N. Kosaric, C.A. Bonham, G.C. Gurtner, Wound Healing: A Cellular Perspective, Physiol Rev 99(1) (2019) 665-706.
[6] J.W. Godwin, A.R. Pinto, N.A. Rosenthal, Macrophages are required for adult salamander limb regeneration, Proc Natl Acad Sci U S A 110(23) (2013) 9415-20.
[7] J.W. Godwin, A.R. Pinto, N.A. Rosenthal, Chasing the recipe for a pro-regenerative immune system, Semin Cell Dev Biol 61 (2017) 71-79.
[8] A. Sindrilaru, K. Scharffetter-Kochanek, Disclosure of the Culprits: Macrophages-Versatile Regulators of Wound Healing, Adv Wound Care (New Rochelle) 2(7) (2013) 357-368.
[9] E. Kolaczkowska, P. Kubes, Neutrophil recruitment and function in health and inflammation, Nat Rev Immunol 13(3) (2013) 159-75.
[10] G.Y. Chen, G. Nuñez, Sterile inflammation: sensing and reacting to damage, Nat Rev Immunol 10(12) (2010) 826-37.
[11] D. Bausch, T. Pausch, T. Krauss, U.T. Hopt, C. Fernandez-del-Castillo, A.L. Warshaw, S.P. Thayer, T. Keck, Neutrophil granulocyte derived MMP-9 is a VEGF independent functional component of the angiogenic switch in pancreatic ductal adenocarcinoma, Angiogenesis 14(3) (2011) 235-43.
[12] D.P. Stirling, S. Liu, P. Kubes, V.W. Yong, Depletion of Ly6G/Gr-1 leukocytes after spinal cord injury in mice alters wound healing and worsens neurological outcome, J Neurosci 29(3) (2009) 753-64.
[13] E.O. Long, H.S. Kim, D. Liu, M.E. Peterson, S. Rajagopalan, Controlling natural killer cell responses: integration of signals for activation and inhibition, Annu Rev Immunol 31 (2013) 227-58.
[14] J. Rosenberg, J. Huang, CD8, Curr Opin Chem Eng 19 (2018) 9-20.
[15] R. Nikzad, L.S. Angelo, K. Aviles-Padilla, D.T. Le, V.K. Singh, L. Bimler, M. Vukmanovic-Stejic, E. Vendrame, T. Ranganath, L. Simpson, N.L. Haigwood, C.A. Blish, A.N. Akbar, S. Paust, Human natural killer cells mediate adaptive immunity to viral antigens, Sci Immunol 4(35) (2019).
[16] T. Barkhausen, C. Frerker, C. Pütz, H.C. Pape, C. Krettek, M. van Griensven, Depletion of NK cells in a murine polytrauma model is associated with improved outcome and a modulation of the inflammatory response, Shock 30(4) (2008) 401-10.
[17] D. Toben, I. Schroeder, T. El Khassawna, M. Mehta, J.E. Hoffmann, J.T. Frisch, H. Schell, J. Lienau, A. Serra, A. Radbruch, G.N. Duda, Fracture healing is accelerated in the absence of the adaptive immune system, J Bone Miner Res 26(1) (2011) 113-24.
[18] A. Tosello-Trampont, F.A. Surette, S.E. Ewald, Y.S. Hahn, Immunoregulatory Role of NK Cells in Tissue Inflammation and Regeneration, Front Immunol 8 (2017) 301.

[19] S.K. Panda, M. Colonna, Innate Lymphoid Cells in Mucosal Immunity, Front Immunol 10 (2019) 861.
[20] J. Yang, L. Zhao, M. Xu, N. Xiong, Establishment and function of tissue-resident innate lymphoid cells in the skin, Protein Cell 8(7) (2017) 489-500.
[21] J. Kim, S. Ryu, H.Y. Kim, Innate Lymphoid Cells in Tissue Homeostasis and Disease Pathogenesis, Mol Cells 44(5) (2021) 301-309.
[22] V.K. Raker, M.P. Domogalla, K. Steinbrink, Tolerogenic Dendritic Cells for Regulatory T Cell Induction in Man, Front Immunol 6 (2015) 569.
[23] M.P. Domogalla, P.V. Rostan, V.K. Raker, K. Steinbrink, Tolerance through Education: How Tolerogenic Dendritic Cells Shape Immunity, Front Immunol 8 (2017) 1764.
[24] M. Vinish, W. Cui, E. Stafford, L. Bae, H. Hawkins, R. Cox, T. Toliver-Kinsky, Dendritic cells modulate burn wound healing by enhancing early proliferation, Wound Repair Regen 24(1) (2016) 6-13.
[25] B. Chazaud, Macrophages: supportive cells for tissue repair and regeneration, Immunobiology 219(3) (2014) 172-8.
[26] J.G. Tidball, M. Wehling-Henricks, Macrophages promote muscle membrane repair and muscle fibre growth and regeneration during modified muscle loading in mice in vivo, J Physiol 578(Pt 1) (2007) 327-36.
[27] R. Londono, S. Tighe, B. Milnes, C. DeMoya, L.M. Quijano, M.L. Hudnall, J. Nguyen, E. Tran, S. Badylak, T.P. Lozito, Single Cell Sequencing Analysis of Lizard Phagocytic Cell Populations and Their Role in Tail Regeneration, J Immunol Regen Med 8 (2020).
[28] M.F. Gutknecht, A.H. Bouton, Functional significance of mononuclear phagocyte populations generated through adult hematopoiesis, J Leukoc Biol 96(6) (2014) 969-80.
[29] K.J. Lavine, S. Epelman, K. Uchida, K.J. Weber, C.G. Nichols, J.D. Schilling, D.M. Ornitz, G.J. Randolph, D.L. Mann, Distinct macrophage lineages contribute to disparate patterns of cardiac recovery and remodeling in the neonatal and adult heart, Proc Natl Acad Sci U S A 111(45) (2014) 16029-34.
[30] V.E. Miron, A. Boyd, J.W. Zhao, T.J. Yuen, J.M. Ruckh, J.L. Shadrach, P. van Wijngaarden, A.J. Wagers, A. Williams, R.J.M. Franklin, C. Ffrench-Constant, M2 microglia and macrophages drive oligodendrocyte differentiation during CNS remyelination, Nat Neurosci 16(9) (2013) 1211-1218.
[31] D. Dal-Secco, J. Wang, Z. Zeng, E. Kolaczkowska, C.H. Wong, B. Petri, R.M. Ransohoff, I.F. Charo, C.N. Jenne, P. Kubes, A dynamic spectrum of monocytes arising from the in situ reprogramming of CCR2+ monocytes at a site of sterile injury, J Exp Med 212(4) (2015) 447-56.
[32] C.D. Mills, K. Kincaid, J.M. Alt, M.J. Heilman, A.M. Hill, M-1/M-2 macrophages and the Th1/Th2 paradigm, J Immunol 164(12) (2000) 6166-73.
[33] N.X. Landén, D. Li, M. Ståhle, Transition from inflammation to proliferation: a critical step during wound healing, Cell Mol Life Sci 73(20) (2016) 3861-85.
[34] M. Pakyari, A. Farrokhi, M.K. Maharlooei, A. Ghahary, Critical Role of Transforming Growth Factor Beta in Different Phases of Wound Healing, Adv Wound Care (New Rochelle) 2(5) (2013) 215-224.
[35] Y. Liu, Y. Li, N. Li, W. Teng, M. Wang, Y. Zhang, Z. Xiao, TGF-β1 promotes scar fibroblasts proliferation and transdifferentiation via up-regulating MicroRNA-21, Sci Rep 6 (2016) 32231.
[36] G.J. Kotwal, S. Chien, Macrophage Differentiation in Normal and Accelerated Wound Healing, Results Probl Cell Differ 62 (2017) 353-364.

[37] S. McArthur, G. Juban, T. Gobbetti, T. Desgeorges, M. Theret, J. Gondin, J.E. Toller-Kawahisa, C.P. Reutelingsperger, B. Chazaud, M. Perretti, R. Mounier, Annexin A1 drives macrophage skewing to accelerate muscle regeneration through AMPK activation, J Clin Invest 130(3) (2020) 1156-1167.
[38] B.N. Brown, B.D. Ratner, S.B. Goodman, S. Amar, S.F. Badylak, Macrophage polarization: an opportunity for improved outcomes in biomaterials and regenerative medicine, Biomaterials 33(15) (2012) 3792-802.
[39] L. Bai, L. Fu, L. Li, F. Ren, Q. Zheng, S. Liu, Y. Han, S. Zheng, Y. Chen, Z. Duan, Cellular Mechanisms of Hepatoprotection Mediated by M2-Like Macrophages, Med Sci Monit 24 (2018) 2675-2682.
[40] A. Mauro, V. Russo, L. Di Marcantonio, P. Berardinelli, A. Martelli, A. Muttini, M. Mattioli, B. Barboni, M1 and M2 macrophage recruitment during tendon regeneration induced by amniotic epithelial cell allotransplantation in ovine, Res Vet Sci 105 (2016) 92-102.
[41] P. Starkey Lewis, L. Campana, N. Aleksieva, J.A. Cartwright, A. Mackinnon, E. O'Duibhir, T. Kendall, M. Vermeren, A. Thomson, V. Gadd, B. Dwyer, R. Aird, T.Y. Man, A.G. Rossi, L. Forrester, B.K. Park, S.J. Forbes, Alternatively activated macrophages promote resolution of necrosis following acute liver injury, J Hepatol (2020).
[42] F.C. Simões, T.J. Cahill, A. Kenyon, D. Gavriouchkina, J.M. Vieira, X. Sun, D. Pezzolla, C. Ravaud, E. Masmanian, M. Weinberger, S. Mayes, M.E. Lemieux, D.N. Barnette, M. Gunadasa-Rohling, R.M. Williams, D.R. Greaves, L.A. Trinh, S.E. Fraser, S.L. Dallas, R.P. Choudhury, T. Sauka-Spengler, P.R. Riley, Macrophages directly contribute collagen to scar formation during zebrafish heart regeneration and mouse heart repair, Nat Commun 11(1) (2020) 600.
[43] Y. Iwata, A. Yoshizaki, K. Komura, K. Shimizu, F. Ogawa, T. Hara, E. Muroi, S. Bae, M. Takenaka, T. Yukami, M. Hasegawa, M. Fujimoto, Y. Tomita, T.F. Tedder, S. Sato, CD19, a response regulator of B lymphocytes, regulates wound healing through hyaluronan-induced TLR4 signaling, Am J Pathol 175(2) (2009) 649-60.
[44] R.F. Sîrbulescu, C.K. Boehm, E. Soon, M.Q. Wilks, I. Ilieş, H. Yuan, B. Maxner, N. Chronos, C. Kaittanis, M.D. Normandin, G. El Fakhri, D.P. Orgill, A.E. Sluder, M.C. Poznansky, Mature B cells accelerate wound healing after acute and chronic diabetic skin lesions, Wound Repair Regen 25(5) (2017) 774-791.
[45] S. Reinke, S. Geissler, W.R. Taylor, K. Schmidt-Bleek, K. Juelke, V. Schwachmeyer, M. Dahne, T. Hartwig, L. Akyüz, C. Meisel, N. Unterwalder, N.B. Singh, P. Reinke, N.P. Haas, H.D. Volk, G.N. Duda, Terminally differentiated $CD8^+$ T cells negatively affect bone regeneration in humans, Sci Transl Med 5(177) (2013) 177ra36.
[46] P.A. Davis, D.J. Corless, R. Aspinall, C. Wastell, Effect of CD4(+) and CD8(+) cell depletion on wound healing, Br J Surg 88(2) (2001) 298-304.
[47] K. Sadtler, K. Estrellas, B.W. Allen, M.T. Wolf, H. Fan, A.J. Tam, C.H. Patel, B.S. Luber, H. Wang, K.R. Wagner, J.D. Powell, F. Housseau, D.M. Pardoll, J.H. Elisseeff, Developing a pro-regenerative biomaterial scaffold microenvironment requires T helper 2 cells, Science 352(6283) (2016) 366-70.
[48] J. Li, J. Tan, M.M. Martino, K.O. Lui, Regulatory T-Cells: Potential Regulator of Tissue Repair and Regeneration, Front Immunol 9 (2018) 585.
[49] H. Lei, K. Schmidt-Bleek, A. Dienelt, P. Reinke, H.D. Volk, Regulatory T cell-mediated anti-inflammatory effects promote successful tissue repair in both indirect and direct manners, Front Pharmacol 6 (2015) 184.

[50] M.M. Tiemessen, A.L. Jagger, H.G. Evans, M.J. van Herwijnen, S. John, L.S. Taams, CD4+CD25+Foxp3+ regulatory T cells induce alternative activation of human monocytes/macrophages, Proc Natl Acad Sci U S A 104(49) (2007) 19446-51.
[51] M.D. Rosenblum, I.K. Gratz, J.S. Paw, K. Lee, A. Marshak-Rothstein, A.K. Abbas, Response to self antigen imprints regulatory memory in tissues, Nature 480(7378) (2011) 538-42.
[52] N.K. Campbell, H.K. Fitzgerald, A. Malara, R. Hambly, C.M. Sweeney, B. Kirby, J.M. Fletcher, A. Dunne, Naturally derived Heme-Oxygenase 1 inducers attenuate inflammatory responses in human dendritic cells and T cells: relevance for psoriasis treatment, Sci Rep 8(1) (2018) 10287.
[53] K. Nurmi, I. Kareinen, J. Virkanen, K. Rajamäki, V.P. Kouri, K. Vaali, A.L. Levonen, N. Fyhrquist, S. Matikainen, P.T. Kovanen, K.K. Eklund, Hemin and Cobalt Protoporphyrin Inhibit NLRP3 Inflammasome Activation by Enhancing Autophagy: A Novel Mechanism of Inflammasome Regulation, J Innate Immun 9(1) (2017) 65-82.
[54] N.K. Campbell, H.K. Fitzgerald, J.M. Fletcher, A. Dunne, Plant-Derived Polyphenols Modulate Human Dendritic Cell Metabolism and Immune Function via AMPK-Dependent Induction of Heme Oxygenase-1, Front Immunol 10 (2019) 345.
[55] Y. Yang, X. Zhang, M. Xu, X. Wu, F. Zhao, C. Zhao, Quercetin attenuates collagen-induced arthritis by restoration of Th17/Treg balance and activation of Heme Oxygenase 1-mediated anti-inflammatory effect, Int Immunopharmacol 54 (2018) 153-162.
[56] C.F.S. Guazelli, L. Staurengo-Ferrari, A.C. Zarpelon, F.A. Pinho-Ribeiro, K.W. Ruiz-Miyazawa, F.T.M.C. Vicentini, J.A. Vignoli, D. Camilios-Neto, S.R. Georgetti, M.M. Baracat, R. Casagrande, W.A. Verri, Quercetin attenuates zymosan-induced arthritis in mice, Biomed Pharmacother 102 (2018) 175-184.
[57] A. Grochot-Przeczek, R. Lach, J. Mis, K. Skrzypek, M. Gozdecka, P. Sroczynska, M. Dubiel, A. Rutkowski, M. Kozakowska, A. Zagorska, J. Walczynski, H. Was, J. Kotlinowski, J. Drukala, K. Kurowski, C. Kieda, Y. Herault, J. Dulak, A. Jozkowicz, Heme oxygenase-1 accelerates cutaneous wound healing in mice, PLoS One 4(6) (2009) e5803.
[58] D. Kumar, G.R. Jena, M. Ram, M.C. Lingaraju, V. Singh, R. Prasad, S. Kumawat, V. Kant, P. Gupta, S.K. Tandan, Hemin attenuated oxidative stress and inflammation to improve wound healing in diabetic rats, Naunyn Schmiedebergs Arch Pharmacol 392(11) (2019) 1435-1445.
[59] Q.Y. Chen, G.G. Wang, W. Li, Y.X. Jiang, X.H. Lu, P.P. Zhou, Heme Oxygenase-1 Promotes Delayed Wound Healing in Diabetic Rats, J Diabetes Res 2016 (2016) 9726503.
[60] L.F. Zhang, J. Qi, G. Zuo, P. Jia, X. Shen, J. Shao, H. Kang, H. Yang, L. Deng, Osteoblast-secreted factors promote proliferation and osteogenic differentiation of bone marrow stromal cells via VEGF/heme-oxygenase-1 pathway, PLoS One 9(6) (2014) e99946.
[61] L. Vanella, D.H. Kim, D. Asprinio, S.J. Peterson, I. Barbagallo, A. Vanella, D. Goldstein, S. Ikehara, A. Kappas, N.G. Abraham, HO-1 expression increases mesenchymal stem cell-derived osteoblasts but decreases adipocyte lineage, Bone 46(1) (2010) 236-43.
[62] I. Barbagallo, A. Vanella, S.J. Peterson, D.H. Kim, D. Tibullo, C. Giallongo, L. Vanella, N. Parrinello, G.A. Palumbo, F. Di Raimondo, N.G. Abraham, D. Asprinio, Overexpression of heme oxygenase-1 increases human osteoblast stem cell differentiation, J Bone Miner Metab 28(3) (2010) 276-88.
[63] N.K. Campbell, H.K. Fitzgerald, A. Dunne, Regulation of inflammation by the antioxidant haem oxygenase 1, Nat Rev Immunol 21(7) (2021) 411-425.

[64] J. Alam, D. Stewart, C. Touchard, S. Boinapally, A.M. Choi, J.L. Cook, Nrf2, a Cap'n'Collar transcription factor, regulates induction of the heme oxygenase-1 gene, J Biol Chem 274(37) (1999) 26071-8.
[65] K. Itoh, N. Wakabayashi, Y. Katoh, T. Ishii, K. Igarashi, J.D. Engel, M. Yamamoto, Keap1 represses nuclear activation of antioxidant responsive elements by Nrf2 through binding to the amino-terminal Neh2 domain, Genes Dev 13(1) (1999) 76-86.
[66] T. Ishii, K. Itoh, S. Takahashi, H. Sato, T. Yanagawa, Y. Katoh, S. Bannai, M. Yamamoto, Transcription factor Nrf2 coordinately regulates a group of oxidative stress-inducible genes in macrophages, J Biol Chem 275(21) (2000) 16023-9.
[67] L. Baird, M. Yamamoto, The Molecular Mechanisms Regulating the KEAP1-NRF2 Pathway, Mol Cell Biol 40(13) (2020).
[68] E. Kansanen, S.M. Kuosmanen, H. Leinonen, A.L. Levonen, The Keap1-Nrf2 pathway: Mechanisms of activation and dysregulation in cancer, Redox Biol 1(1) (2013) 45-9.
[69] J.F. Reichard, G.T. Motz, A. Puga, Heme oxygenase-1 induction by NRF2 requires inactivation of the transcriptional repressor BACH1, Nucleic Acids Res 35(21) (2007) 7074-86.
[70] J. Sun, H. Hoshino, K. Takaku, O. Nakajima, A. Muto, H. Suzuki, S. Tashiro, S. Takahashi, S. Shibahara, J. Alam, M.M. Taketo, M. Yamamoto, K. Igarashi, Hemoprotein Bach1 regulates enhancer availability of heme oxygenase-1 gene, EMBO J 21(19) (2002) 5216-24.
[71] Y. Zenke-Kawasaki, Y. Dohi, Y. Katoh, T. Ikura, M. Ikura, T. Asahara, F. Tokunaga, K. Iwai, K. Igarashi, Heme induces ubiquitination and degradation of the transcription factor Bach1, Mol Cell Biol 27(19) (2007) 6962-71.
[72] P.J. Lee, B.H. Jiang, B.Y. Chin, N.V. Iyer, J. Alam, G.L. Semenza, A.M. Choi, Hypoxia-inducible factor-1 mediates transcriptional activation of the heme oxygenase-1 gene in response to hypoxia, J Biol Chem 272(9) (1997) 5375-81.
[73] Y. Lavrovsky, M.L. Schwartzman, R.D. Levere, A. Kappas, N.G. Abraham, Identification of binding sites for transcription factors NF-kappa B and AP-2 in the promoter region of the human heme oxygenase 1 gene, Proc Natl Acad Sci U S A 91(13) (1994) 5987-91.
[74] J. Alam, J.L. Cook, How many transcription factors does it take to turn on the heme oxygenase-1 gene?, Am J Respir Cell Mol Biol 36(2) (2007) 166-74.
[75] R.L. Cho, W.N. Lin, C.Y. Wang, C.C. Yang, L.D. Hsiao, C.C. Lin, C.M. Yang, Heme oxygenase-1 induction by rosiglitazone via PKCα/AMPKα/p38 MAPKα/SIRT1/PPARγ pathway suppresses lipopolysaccharide-mediated pulmonary inflammation, Biochem Pharmacol 148 (2018) 222-237.
[76] G.A. Ricchetti, L.M. Williams, B.M. Foxwell, Heme oxygenase 1 expression induced by IL-10 requires STAT-3 and phosphoinositol-3 kinase and is inhibited by lipopolysaccharide, J Leukoc Biol 76(3) (2004) 719-26.
[77] T.S. Lee, L.Y. Chau, Heme oxygenase-1 mediates the anti-inflammatory effect of interleukin-10 in mice, Nat Med 8(3) (2002) 240-6.
[78] N.K. Campbell, D.G. Williams, H.K. Fitzgerald, P.J. Barry, C.C. Cunningham, D.P. Nolan, A. Dunne, Secreted Aromatic Ketoacids Activate the Nrf2/HO-1 Pathway and Suppress Pro-inflammatory Responses in Primary Murine Glia and Macrophages, Front Immunol 10 (2019) 2137.
[79] S.W. Ryter, Heme Oxygenase-1: An Anti-Inflammatory Effector in Cardiovascular, Lung, and Related Metabolic Disorders, Antioxidants (Basel) 11(3) (2022).

[80] N. Radhakrishnan, S.P. Yadav, A. Sachdeva, P.K. Pruthi, S. Sawhney, T. Piplani, T. Wada, A. Yachie, Human heme oxygenase-1 deficiency presenting with hemolysis, nephritis, and asplenia, J Pediatr Hematol Oncol 33(1) (2011) 74-8.
[81] M.H. Kapturczak, C. Wasserfall, T. Brusko, M. Campbell-Thompson, T.M. Ellis, M.A. Atkinson, A. Agarwal, Heme oxygenase-1 modulates early inflammatory responses: evidence from the heme oxygenase-1-deficient mouse, Am J Pathol 165(3) (2004) 1045-53.
[82] A. Yachie, Heme Oxygenase-1 Deficiency and Oxidative Stress: A Review of 9 Independent Human Cases and Animal Models, Int J Mol Sci 22(4) (2021).
[83] S. Tzima, P. Victoratos, K. Kranidioti, M. Alexiou, G. Kollias, Myeloid heme oxygenase-1 regulates innate immunity and autoimmunity by modulating IFN-beta production, J Exp Med 206(5) (2009) 1167-79.
[84] Y. Kishimoto, K. Kondo, Y. Momiyama, The Protective Role of Heme Oxygenase-1 in Atherosclerotic Diseases, Int J Mol Sci 20(15) (2019).
[85] B.Z. Li, B. Guo, H.Y. Zhang, J. Liu, S.S. Tao, H.F. Pan, D.Q. Ye, Therapeutic potential of HO-1 in autoimmune diseases, Inflammation 37(5) (2014) 1779-88.
[86] A. Yachie, Y. Niida, T. Wada, N. Igarashi, H. Kaneda, T. Toma, K. Ohta, Y. Kasahara, S. Koizumi, Oxidative stress causes enhanced endothelial cell injury in human heme oxygenase-1 deficiency, J Clin Invest 103(1) (1999) 129-35.
[87] K.D. Poss, S. Tonegawa, Heme oxygenase 1 is required for mammalian iron reutilization, Proc Natl Acad Sci U S A 94(20) (1997) 10919-24.
[88] Y. Wei, J. Jia, X. Jin, W. Tong, H. Tian, Resveratrol ameliorates inflammatory damage and protects against osteoarthritis in a rat model of osteoarthritis, Mol Med Rep 17(1) (2018) 1493-1498.
[89] P. Fagone, K. Mangano, M. Coco, V. Perciavalle, G. Garotta, C.C. Romao, F. Nicoletti, Therapeutic potential of carbon monoxide in multiple sclerosis, Clin Exp Immunol 167(2) (2012) 179-87.
[90] H. Zhou, H. Qian, J. Liu, D. Zhu, W. Ding, P. Pan, D. Jin, J. Wang, W. Li, Protection against lung graft injury from brain-dead donors with carbon monoxide, biliverdin, or both, J Heart Lung Transplant 30(4) (2011) 460-6.
[91] D. Corona, B. Ekser, R. Gioco, M. Caruso, C. Schipa, P. Veroux, A. Giaquinta, A. Granata, M. Veroux, Heme-Oxygenase and Kidney Transplantation: A Potential for Target Therapy?, Biomolecules 10(6) (2020).
[92] K. Kotsch, M. Francuski, A. Pascher, R. Klemz, M. Seifert, J. Mittler, G. Schumacher, R. Buelow, H.D. Volk, S.G. Tullius, P. Neuhaus, J. Pratschke, Improved long-term graft survival after HO-1 induction in brain-dead donors, Am J Transplant 6(3) (2006) 477-86.
[93] A. Toro, M.S. Ruiz, S. Lage-Vickers, P. Sanchis, A. Sabater, G. Pascual, R. Seniuk, F. Cascardo, S. Ledesma-Bazan, F. Vilicich, E. Vazquez, G. Gueron, A Journey into the Clinical Relevance of Heme Oxygenase 1 for Human Inflammatory Disease and Viral Clearance: Why Does It Matter on the COVID-19 Scene?, Antioxidants (Basel) 11(2) (2022).
[94] M. Rossi, M. Piagnerelli, A. Van Meerhaeghe, K. Zouaoui Boudjeltia, Heme oxygenase-1 (HO-1) cytoprotective pathway: A potential treatment strategy against coronavirus disease 2019 (COVID-19)-induced cytokine storm syndrome, Med Hypotheses 144 (2020) 110242.
[95] L.L. Ma, P. Zhang, H.Q. Wang, Y.F. Li, J. Hu, J.D. Jiang, Y.H. Li, heme oxygenase-1 agonist CoPP suppresses influenza virus replication through IRF3-mediated generation of IFN-α/β, Virology 528 (2019) 80-88.

[96] G. Williamson, M.N. Clifford, Role of the small intestine, colon and microbiota in determining the metabolic fate of polyphenols, Biochem Pharmacol 139 (2017) 24-39.
[97] D. Del Rio, A. Rodriguez-Mateos, J.P. Spencer, M. Tognolini, G. Borges, A. Crozier, Dietary (poly)phenolics in human health: structures, bioavailability, and evidence of protective effects against chronic diseases, Antioxid Redox Signal 18(14) (2013) 1818-92.
[98] C.F. Wang, Z.Y. Wang, J.Y. Li, Dual protective role of HO-1 in transplanted liver grafts: a review of experimental and clinical studies, World J Gastroenterol 17(26) (2011) 3101-8.
[99] B. Stijlemans, G. Caljon, J. Van Den Abbeele, J.A. Van Ginderachter, S. Magez, C. De Trez, Immune Evasion Strategies of Trypanosoma brucei within the Mammalian Host: Progression to Pathogenicity, Front Immunol 7 (2016) 233.
[100] D.M. Paulnock, B.E. Freeman, J.M. Mansfield, Modulation of innate immunity by African trypanosomes, Parasitology 137(14) (2010) 2051-63.
[101] J.E. Hall, J.R. Seed, Increased urinary excretion of aromatic amino acid catabolites by Microtus montanus chronically infected with Trypanosoma brucei gambiense, Comp Biochem Physiol B 77(4) (1984) 755-60.
[102] G.R. Newport, C.R. Page, P.U. Ashman, H.H. Stibbs, J.R. Seed, Alteration of free serum amino acids in voles infected with Trypanosoma brucei gambiense, J Parasitol 63(1) (1977) 15-24.
[103] A. El Sawalhy, J.R. Seed, J.E. Hall, H. El Attar, Increased excretion of aromatic amino acid catabolites in animals infected with Trypanosoma brucei evansi, J Parasitol 84(3) (1998) 469-73.
[104] J.E. Hall, J.R. Seed, J.B. Sechelski, Multiple alpha-keto aciduria in Microtus montanus chronically infected with Trypanosoma brucei gambiense, Comp Biochem Physiol B 82(1) (1985) 73-8.
[105] A.F. McGettrick, S.E. Corcoran, P.J. Barry, J. McFarland, C. Crès, A.M. Curtis, E. Franklin, S.C. Corr, K.H. Mok, E.P. Cummins, C.T. Taylor, L.A. O'Neill, D.P. Nolan, Trypanosoma brucei metabolite indolepyruvate decreases HIF-1α and glycolysis in macrophages as a mechanism of innate immune evasion, Proc Natl Acad Sci U S A 113(48) (2016) E7778-E7787.
[106] C. Diskin, S.E. Corcoran, V.J. Tyrrell, A.F. McGettrick, Z. Zaslona, V.B. O'Donnell, D.P. Nolan, L.A.J. O'Neill, The Trypanosome-Derived Metabolite Indole-3-Pyruvate Inhibits Prostaglandin Production in Macrophages by Targeting COX2, J Immunol 207(10) (2021) 2551-2560.
[107] R. Aoki, A. Aoki-Yoshida, C. Suzuki, Y. Takayama, Indole-3-Pyruvic Acid, an Aryl Hydrocarbon Receptor Activator, Suppresses Experimental Colitis in Mice, J Immunol 201(12) (2018) 3683-3693.
[108] H.K. Fitzgerald, S.A. O'Rourke, E. Desmond, N.G.B. Neto, M.G. Monaghan, M. Tosetto, J. Doherty, E.J. Ryan, G.A. Doherty, D.P. Nolan, J.M. Fletcher, A. Dunne, The *Trypanosoma brucei* -Derived Ketoacids, Indole Pyruvate and Hydroxyphenylpyruvate, Induce HO-1 Expression and Suppress Inflammatory Responses in Human Dendritic Cells, Antioxidants (Basel) 11(1) (2022).
[109] T. Huang, L. Cheng, Y. Jiang, L. Zhang, L. Qian, Indole-3-pyruvic acid alleviates rheumatoid arthritis via the aryl hydrocarbon receptor pathway, Ann Transl Med 11(5) (2023) 213.

[110] V. Rothhammer, F.J. Quintana, The aryl hydrocarbon receptor: an environmental sensor integrating immune responses in health and disease, Nat Rev Immunol 19(3) (2019) 184-197.
[111] N.T. Nguyen, H. Hanieh, T. Nakahama, T. Kishimoto, The roles of aryl hydrocarbon receptor in immune responses, Int Immunol 25(6) (2013) 335-43.
[112] J.J. Green, Immunoengineering has arrived, J Biomed Mater Res A 109(4) (2021) 397-403.
[113] J. Zandstra, C. Hiemstra, A.H. Petersen, J. Zuidema, M.M. van Beuge, S. Rodriguez, A.A. Lathuile, G.J. Veldhuis, R. Steendam, R.A. Bank, E.R. Popa, Microsphere size influences the foreign body reaction, Eur Cell Mater 28 (2014) 335-47.
[114] F. Lebre, R. Sridharan, M.J. Sawkins, D.J. Kelly, F.J. O'Brien, E.C. Lavelle, The shape and size of hydroxyapatite particles dictate inflammatory responses following implantation, Sci Rep 7(1) (2017) 2922.
[115] K.A. Beningo, Y.L. Wang, Fc-receptor-mediated phagocytosis is regulated by mechanical properties of the target, J Cell Sci 115(Pt 4) (2002) 849-56.
[116] R. Sridharan, B. Cavanagh, A.R. Cameron, D.J. Kelly, F.J. O'Brien, Material stiffness influences the polarization state, function and migration mode of macrophages, Acta Biomater 89 (2019) 47-59.
[117] N.E. Paul, C. Skazik, M. Harwardt, M. Bartneck, B. Denecke, D. Klee, J. Salber, G. Zwadlo-Klarwasser, Topographical control of human macrophages by a regularly microstructured polyvinylidene fluoride surface, Biomaterials 29(30) (2008) 4056-64.
[118] P.C. Bota, A.M. Collie, P. Puolakkainen, R.B. Vernon, E.H. Sage, B.D. Ratner, P.S. Stayton, Biomaterial topography alters healing in vivo and monocyte/macrophage activation in vitro, J Biomed Mater Res A 95(2) (2010) 649-57.
[119] S. Chen, J.A. Jones, Y. Xu, H.Y. Low, J.M. Anderson, K.W. Leong, Characterization of topographical effects on macrophage behavior in a foreign body response model, Biomaterials 31(13) (2010) 3479-91.
[120] H.C. Bygd, K.D. Forsmark, K.M. Bratlie, Altering in vivo macrophage responses with modified polymer properties, Biomaterials 56 (2015) 187-97.
[121] J.A. Jones, D.T. Chang, H. Meyerson, E. Colton, I.K. Kwon, T. Matsuda, J.M. Anderson, Proteomic analysis and quantification of cytokines and chemokines from biomaterial surface-adherent macrophages and foreign body giant cells, J Biomed Mater Res A 83(3) (2007) 585-96.
[122] K.M. Hotchkiss, N.M. Clark, R. Olivares-Navarrete, Macrophage response to hydrophilic biomaterials regulates MSC recruitment and T-helper cell populations, Biomaterials 182 (2018) 202-215.
[123] J. Vlacic-Zischke, S.M. Hamlet, T. Friis, M.S. Tonetti, S. Ivanovski, The influence of surface microroughness and hydrophilicity of titanium on the up-regulation of TGFβ/BMP signalling in osteoblasts, Biomaterials 32(3) (2011) 665-71.
[124] E.M. Sussman, M.C. Halpin, J. Muster, R.T. Moon, B.D. Ratner, Porous implants modulate healing and induce shifts in local macrophage polarization in the foreign body reaction, Ann Biomed Eng 42(7) (2014) 1508-16.
[125] T. Tylek, C. Blum, A. Hrynevich, K. Schlegelmilch, T. Schilling, P.D. Dalton, J. Groll, Precisely defined fiber scaffolds with 40 µm porosity induce elongation driven M2-like polarization of human macrophages, Biofabrication 12(2) (2020) 025007.
[126] O.R. Mahon, D.C. Browe, T. Gonzalez-Fernandez, P. Pitacco, I.T. Whelan, S. Von Euw, C. Hobbs, V. Nicolosi, K.T. Cunningham, K.H.G. Mills, D.J. Kelly, A. Dunne, Nano-particle

mediated M2 macrophage polarization enhances bone formation and MSC osteogenesis in an IL-10 dependent manner, Biomaterials 239 (2020) 119833.
[127] T. Padmore, C. Stark, L.A. Turkevich, J.A. Champion, Quantitative analysis of the role of fiber length on phagocytosis and inflammatory response by alveolar macrophages, Biochim Biophys Acta Gen Subj 1861(2) (2017) 58-67.
[128] K. Niikura, T. Matsunaga, T. Suzuki, S. Kobayashi, H. Yamaguchi, Y. Orba, A. Kawaguchi, H. Hasegawa, K. Kajino, T. Ninomiya, K. Ijiro, H. Sawa, Gold nanoparticles as a vaccine platform: influence of size and shape on immunological responses in vitro and in vivo, ACS Nano 7(5) (2013) 3926-38.
[129] Z. Sheikh, P.J. Brooks, O. Barzilay, N. Fine, M. Glogauer, Macrophages, Foreign Body Giant Cells and Their Response to Implantable Biomaterials, Materials (Basel) 8(9) (2015) 5671-5701.
[130] A.K. Blakney, M.D. Swartzlander, S.J. Bryant, The effects of substrate stiffness on the in vitro activation of macrophages and in vivo host response to poly(ethylene glycol)-based hydrogels, J Biomed Mater Res A 100(6) (2012) 1375-86.
[131] T. Okamoto, Y. Takagi, E. Kawamoto, E.J. Park, H. Usuda, K. Wada, M. Shimaoka, Reduced substrate stiffness promotes M2-like macrophage activation and enhances peroxisome proliferator-activated receptor γ expression, Exp Cell Res 367(2) (2018) 264-273.
[132] M. Friedemann, L. Kalbitzer, S. Franz, S. Moeller, M. Schnabelrauch, J.C. Simon, T. Pompe, K. Franke, Instructing Human Macrophage Polarization by Stiffness and Glycosaminoglycan Functionalization in 3D Collagen Networks, Adv Healthc Mater 6(7) (2017).
[133] M. Chen, Y. Zhang, P. Zhou, X. Liu, H. Zhao, X. Zhou, Q. Gu, B. Li, X. Zhu, Q. Shi, Substrate stiffness modulates bone marrow-derived macrophage polarization through NF-κB signaling pathway, Bioact Mater 5(4) (2020) 880-890.
[134] D.P. Vasconcelos, A.P. Águas, M.A. Barbosa, P. Pelegrín, J.N. Barbosa, The inflammasome in host response to biomaterials: Bridging inflammation and tissue regeneration, Acta Biomater 83 (2019) 1-12.
[135] E. Mariani, G. Lisignoli, R.M. Borzì, L. Pulsatelli, Biomaterials: Foreign Bodies or Tuners for the Immune Response?, Int J Mol Sci 20(3) (2019).
[136] Q. Wang, H. Li, Y. Xiao, S. Li, B. Li, X. Zhao, L. Ye, B. Guo, X. Chen, Y. Ding, C. Bao, Locally controlled delivery of TNFα antibody from a novel glucose-sensitive scaffold enhances alveolar bone healing in diabetic conditions, J Control Release 206 (2015) 232-42.
[137] I. Somasuntharam, K. Yehl, S.L. Carroll, J.T. Maxwell, M.D. Martinez, P.L. Che, M.E. Brown, K. Salaita, M.E. Davis, Knockdown of TNF-α by DNAzyme gold nanoparticles as an anti-inflammatory therapy for myocardial infarction, Biomaterials 83 (2016) 12-22.
[138] J.E. Rayahin, J.S. Buhrman, Y. Zhang, T.J. Koh, R.A. Gemeinhart, High and low molecular weight hyaluronic acid differentially influence macrophage activation, ACS Biomater Sci Eng 1(7) (2015) 481-493.
[139] E.E. Friedrich, L.T. Sun, S. Natesan, D.O. Zamora, R.J. Christy, N.R. Washburn, Effects of hyaluronic acid conjugation on anti-TNF-α inhibition of inflammation in burns, J Biomed Mater Res A 102(5) (2014) 1527-36.
[140] M.M. Martino, K. Maruyama, G.A. Kuhn, T. Satoh, O. Takeuchi, R. Müller, S. Akira, Inhibition of IL-1R1/MyD88 signalling promotes mesenchymal stem cell-driven tissue regeneration, Nat Commun 7 (2016) 11051.

[141] Z. Julier, R. Karami, B. Nayer, Y.Z. Lu, A.J. Park, K. Maruyama, G.A. Kuhn, R. Müller, S. Akira, M.M. Martino, Enhancing the regenerative effectiveness of growth factors by local inhibition of interleukin-1 receptor signaling, Sci Adv 6(24) (2020) eaba7602.
[142] R. Haenold, F. Weih, K.H. Herrmann, K.F. Schmidt, K. Krempler, C. Engelmann, K.A. Nave, J.R. Reichenbach, S. Löwel, O.W. Witte, A. Kretz, NF-κB controls axonal regeneration and degeneration through cell-specific balance of RelA and p50 in the adult CNS, J Cell Sci 127(Pt 14) (2014) 3052-65.
[143] L. Lu, S. Qi, Y. Chen, H. Luo, S. Huang, X. Yu, Q. Luo, Z. Zhang, Targeted immunomodulation of inflammatory monocytes across the blood-brain barrier by curcumin-loaded nanoparticles delays the progression of experimental autoimmune encephalomyelitis, Biomaterials 245 (2020) 119987.
[144] J. Chang, F. Liu, M. Lee, B. Wu, K. Ting, J.N. Zara, C. Soo, K. Al Hezaimi, W. Zou, X. Chen, D.J. Mooney, C.Y. Wang, NF-κB inhibits osteogenic differentiation of mesenchymal stem cells by promoting β-catenin degradation, Proc Natl Acad Sci U S A 110(23) (2013) 9469-74.
[145] Q. Wang, H. Jiang, Y. Li, W. Chen, H. Li, K. Peng, Z. Zhang, X. Sun, Targeting NF-kB signaling with polymeric hybrid micelles that co-deliver siRNA and dexamethasone for arthritis therapy, Biomaterials 122 (2017) 10-22.
[146] J. Oyama, C. Blais, X. Liu, M. Pu, L. Kobzik, R.A. Kelly, T. Bourcier, Reduced myocardial ischemia-reperfusion injury in toll-like receptor 4-deficient mice, Circulation 109(6) (2004) 784-9.
[147] H. Wu, G. Chen, K.R. Wyburn, J. Yin, P. Bertolino, J.M. Eris, S.I. Alexander, A.F. Sharland, S.J. Chadban, TLR4 activation mediates kidney ischemia/reperfusion injury, J Clin Invest 117(10) (2007) 2847-59.
[148] S. Munir, A. Basu, P. Maity, L. Krug, P. Haas, D. Jiang, G. Strauss, M. Wlaschek, H. Geiger, K. Singh, K. Scharffetter-Kochanek, TLR4-dependent shaping of the wound site by MSCs accelerates wound healing, EMBO Rep (2020) e48777.
[149] H. Suga, M. Sugaya, H. Fujita, Y. Asano, Y. Tada, T. Kadono, S. Sato, TLR4, rather than TLR2, regulates wound healing through TGF-β and CCL5 expression, J Dermatol Sci 73(2) (2014) 117-24.
[150] D. Kwon, B.G. Cha, Y. Cho, J. Min, E.B. Park, S.J. Kang, J. Kim, Extra-Large Pore Mesoporous Silica Nanoparticles for Directing in Vivo M2 Macrophage Polarization by Delivering IL-4, Nano Lett 17(5) (2017) 2747-2756.
[151] M. Li, F. Wei, X. Yin, L. Xiao, L. Yang, J. Su, J. Weng, B. Feng, Y. Xiao, Y. Zhou, Synergistic regulation of osteoimmune microenvironment by IL-4 and RGD to accelerate osteogenesis, Mater Sci Eng C Mater Biol Appl 109 (2020) 110508.
[152] M.H. Abdelaziz, S.F. Abdelwahab, J. Wan, W. Cai, W. Huixuan, C. Jianjun, K.D. Kumar, A. Vasudevan, A. Sadek, Z. Su, S. Wang, H. Xu, Alternatively activated macrophages; a double-edged sword in allergic asthma, J Transl Med 18(1) (2020) 58.
[153] T.M. Raimondo, D.J. Mooney, Functional muscle recovery with nanoparticle-directed M2 macrophage polarization in mice, Proc Natl Acad Sci U S A 115(42) (2018) 10648-10653.
[154] N. Bloise, I. Rountree, C. Polucha, G. Montagna, L. Visai, K.L.K. Coulombe, F. Munarin, Engineering Immunomodulatory Biomaterials for Regenerating the Infarcted Myocardium, Front Bioeng Biotechnol 8 (2020) 292.
[155] K.L. Spiller, S. Nassiri, C.E. Witherel, R.R. Anfang, J. Ng, K.R. Nakazawa, T. Yu, G. Vunjak-Novakovic, Sequential delivery of immunomodulatory cytokines to facilitate the

M1-to-M2 transition of macrophages and enhance vascularization of bone scaffolds, Biomaterials 37 (2015) 194-207.
[156] S. Jain, T.H. Tran, M. Amiji, Macrophage repolarization with targeted alginate nanoparticles containing IL-10 plasmid DNA for the treatment of experimental arthritis, Biomaterials 61 (2015) 162-77.
[157] M.C.P. Sok, N. Baker, C. McClain, H.S. Lim, T. Turner, L. Hymel, M. Ogle, C. Olingy, J.I. Palacios, J.R. Garcia, K. Srithar, A.J. García, P. Qiu, E.A. Botchwey, Dual delivery of IL-10 and AT-RvD1 from PEG hydrogels polarize immune cells towards pro-regenerative phenotypes, Biomaterials 268 (2020) 120475.
[158] R.W.D. Gilbert, M.K. Vickaryous, A.M. Viloria-Petit, Signalling by Transforming Growth Factor Beta Isoforms in Wound Healing and Tissue Regeneration, J Dev Biol 4(2) (2016).
[159] K. Delaney, P. Kasprzycka, M.A. Ciemerych, M. Zimowska, The role of TGF-β1 during skeletal muscle regeneration, Cell Biol Int 41(7) (2017) 706-715.
[160] P.S. Hume, J. He, K. Haskins, K.S. Anseth, Strategies to reduce dendritic cell activation through functional biomaterial design, Biomaterials 33(14) (2012) 3615-25.
[161] L.A. O'Neill, R.J. Kishton, J. Rathmell, A guide to immunometabolism for immunologists, Nat Rev Immunol 16(9) (2016) 553-65.
[162] U. Fearon, M.M. Hanlon, S.M. Wade, J.M. Fletcher, Altered metabolic pathways regulate synovial inflammation in rheumatoid arthritis, Clin Exp Immunol 197(2) (2019) 170-180.
[163] M. Biniecka, M. Canavan, T. McGarry, W. Gao, J. McCormick, S. Cregan, L. Gallagher, T. Smith, J.J. Phelan, J. Ryan, J. O'Sullivan, C.T. Ng, D.J. Veale, U. Fearon, Dysregulated bioenergetics: a key regulator of joint inflammation, Ann Rheum Dis 75(12) (2016) 2192-2200.
[164] F.J. Blanco, M.J. López-Armada, E. Maneiro, Mitochondrial dysfunction in osteoarthritis, Mitochondrion 4(5-6) (2004) 715-28.
[165] V. Pucino, M. Certo, G. Varricchi, G. Marone, F. Ursini, F.W. Rossi, A. De Paulis, C. Mauro, K. Raza, C.D. Buckley, Metabolic Checkpoints in Rheumatoid Arthritis, Front Physiol 11 (2020) 347.
[166] Y. Ohashi, N. Takahashi, K. Terabe, S. Tsuchiya, T. Kojima, C.B. Knudson, W. Knudson, S. Imagama, Metabolic reprogramming in chondrocytes to promote mitochondrial respiration reduces downstream features of osteoarthritis, Sci Rep 11(1) (2021) 15131.
[167] X.S. Chen, L.Y. Li, Y.D. Guan, J.M. Yang, Y. Cheng, Anticancer strategies based on the metabolic profile of tumor cells: therapeutic targeting of the Warburg effect, Acta Pharmacol Sin 37(8) (2016) 1013-9.
[168] R.L. Aft, F.W. Zhang, D. Gius, Evaluation of 2-deoxy-D-glucose as a chemotherapeutic agent: mechanism of cell death, Br J Cancer 87(7) (2002) 805-12.
[169] J. Zhu, Y. Zheng, H. Zhang, H. Sun, Targeting cancer cell metabolism: The combination of metformin and 2-Deoxyglucose regulates apoptosis in ovarian cancer cells via p38 MAPK/JNK signaling pathway, Am J Transl Res 8(11) (2016) 4812-4821.
[170] E.M. Pålsson-McDermott, L.A.J. O'Neill, Targeting immunometabolism as an anti-inflammatory strategy, Cell Res (2020).
[171] L.D. Huyer, S. Mandla, Y. Wang, S. Campbell, B. Yee, C. Euler, B.F. Lai, D. Bannerman, D.S.Y. Lin, M. Montgomery, K. Nemr, T. Bender, S. Epelman, R. Mahadevan, M. Radisic, Macrophage immunomodulation through new polymers that recapitulate functional effects of itaconate as a power house of innate immunity, Adv Funct Mater 31(6) (2021).

[172] X.T. He, X. Li, M. Zhang, B.M. Tian, L.J. Sun, C.S. Bi, D.K. Deng, H. Zhou, H.L. Qu, C. Wu, F.M. Chen, Role of molybdenum in material immunomodulation and periodontal wound healing: Targeting immunometabolism and mitochondrial function for macrophage modulation, Biomaterials 283 (2022) 121439.
[173] A. Viola, F. Munari, R. Sánchez-Rodríguez, T. Scolaro, A. Castegna, The Metabolic Signature of Macrophage Responses, Front Immunol 10 (2019) 1462.
[174] J. Van den Bossche, L.A. O'Neill, D. Menon, Macrophage Immunometabolism: Where Are We (Going)?, Trends Immunol 38(6) (2017) 395-406.
[175] L.A. O'Neill, E.J. Pearce, Immunometabolism governs dendritic cell and macrophage function, J Exp Med 213(1) (2016) 15-23.
[176] X. Wei, H. Song, L. Yin, M.G. Rizzo, R. Sidhu, D.F. Covey, D.S. Ory, C.F. Semenkovich, Fatty acid synthesis configures the plasma membrane for inflammation in diabetes, Nature 539(7628) (2016) 294-298.
[177] J.S. Moon, S. Lee, M.A. Park, I.I. Siempos, M. Haslip, P.J. Lee, M. Yun, C.K. Kim, J. Howrylak, S.W. Ryter, K. Nakahira, A.M. Choi, UCP2-induced fatty acid synthase promotes NLRP3 inflammasome activation during sepsis, J Clin Invest 125(2) (2015) 665-80.
[178] J. Van den Bossche, J. Baardman, N.A. Otto, S. van der Velden, A.E. Neele, S.M. van den Berg, R. Luque-Martin, H.J. Chen, M.C. Boshuizen, M. Ahmed, M.A. Hoeksema, A.F. de Vos, M.P. de Winther, Mitochondrial Dysfunction Prevents Repolarization of Inflammatory Macrophages, Cell Rep 17(3) (2016) 684-696.
[179] S.C. Huang, A.M. Smith, B. Everts, M. Colonna, E.L. Pearce, J.D. Schilling, E.J. Pearce, Metabolic Reprogramming Mediated by the mTORC2-IRF4 Signaling Axis Is Essential for Macrophage Alternative Activation, Immunity 45(4) (2016) 817-830.
[180] S.C. Huang, B. Everts, Y. Ivanova, D. O'Sullivan, M. Nascimento, A.M. Smith, W. Beatty, L. Love-Gregory, W.Y. Lam, C.M. O'Neill, C. Yan, H. Du, N.A. Abumrad, J.F. Urban, M.N. Artyomov, E.L. Pearce, E.J. Pearce, Cell-intrinsic lysosomal lipolysis is essential for alternative activation of macrophages, Nat Immunol 15(9) (2014) 846-55.
[181] W. Wang, K.W.K. Yeung, Bone grafts and biomaterials substitutes for bone defect repair: A review, Bioact Mater 2(4) (2017) 224-247.
[182] Y. Xie, C. Hu, Y. Feng, D. Li, T. Ai, Y. Huang, X. Chen, L. Huang, J. Tan, Osteoimmunomodulatory effects of biomaterial modification strategies on macrophage polarization and bone regeneration, Regen Biomater 7(3) (2020) 233-245.
[183] O.B. F.J., Biomaterials & scaffolds for tissue engineering, Materials Today 14(3) (2011) 88-95.
[184] J. Jeong, J.H. Kim, J.H. Shim, N.S. Hwang, C.Y. Heo, Bioactive calcium phosphate materials and applications in bone regeneration, Biomater Res 23 (2019) 4.
[185] H. Yamasaki, H. Sakai, Osteogenic response to porous hydroxyapatite ceramics under the skin of dogs, Biomaterials 13(5) (1992) 308-12.
[186] S.W. Ha, H.L. Jang, K.T. Nam, G.R. Beck, Nano-hydroxyapatite modulates osteoblast lineage commitment by stimulation of DNA methylation and regulation of gene expression, Biomaterials 65 (2015) 32-42.
[187] J.I. Andorko, C.M. Jewell, Designing biomaterials with immunomodulatory properties for tissue engineering and regenerative medicine, Bioeng Transl Med 2(2) (2017) 139-155.
[188] J. Liu, L. Yang, K. Liu, F. Gao, Hydrogel scaffolds in bone regeneration: Their promising roles in angiogenesis, Front Pharmacol 14 (2023) 1050954.

[189] S. Abdulghani, G.R. Mitchell, Biomaterials for In Situ Tissue Regeneration: A Review, Biomolecules 9(11) (2019).
[190] L. Bai, G. Tao, M. Feng, Y. Xie, S. Cai, S. Peng, J. Xiao, Hydrogel Drug Delivery Systems for Bone Regeneration, Pharmaceutics 15(5) (2023).
[191] S. Nadine, C.R. Correia, J.F. Mano, Engineering immunomodulatory hydrogels and cell-laden systems towards bone regeneration, Biomater Adv 140 (2022) 213058.
[192] G.M. Cunniffe, F.J. O'Brien, S. Partap, T.J. Levingstone, K.T. Stanton, G.R. Dickson, The synthesis and characterization of nanophase hydroxyapatite using a novel dispersant-aided precipitation method, J Biomed Mater Res A 95(4) (2010) 1142-9.
[193] A.C. Daly, P. Pitacco, J. Nulty, G.M. Cunniffe, D.J. Kelly, 3D printed microchannel networks to direct vascularisation during endochondral bone repair, Biomaterials 162 (2018) 34-46.
[194] C.H. Chang, J. Qiu, D. O'Sullivan, M.D. Buck, T. Noguchi, J.D. Curtis, Q. Chen, M. Gindin, M.M. Gubin, G.J. van der Windt, E. Tonc, R.D. Schreiber, E.J. Pearce, E.L. Pearce, Metabolic Competition in the Tumor Microenvironment Is a Driver of Cancer Progression, Cell 162(6) (2015) 1229-41.
[195] C. La Rocca, F. Carbone, V. De Rosa, A. Colamatteo, M. Galgani, F. Perna, R. Lanzillo, V. Brescia Morra, G. Orefice, I. Cerillo, C. Florio, G.T. Maniscalco, M. Salvetti, D. Centonze, A. Uccelli, S. Longobardi, A. Visconti, G. Matarese, Immunometabolic profiling of T cells from patients with relapsing-remitting multiple sclerosis reveals an impairment in glycolysis and mitochondrial respiration, Metabolism 77 (2017) 39-46.
[196] L. Morel, Immunometabolism in systemic lupus erythematosus, Nat Rev Rheumatol 13(5) (2017) 280-290.
[197] S.A. O'Rourke, N.G.B. Neto, E. Devilly, L.C. Shanley, H.K. Fitzgerald, M.G. Monaghan, A. Dunne, Cholesterol crystals drive metabolic reprogramming and M1 macrophage polarisation in primary human macrophages, Atherosclerosis 352 (2022) 35-45.
[198] F. Renaudin, L. Orliaguet, F. Castelli, F. Fenaille, A. Prignon, F. Alzaid, C. Combes, A. Delvaux, Y. Adimy, M. Cohen-Solal, P. Richette, T. Bardin, J.P. Riveline, N. Venteclef, F. Lioté, L. Campillo-Gimenez, H.K. Ea, Gout and pseudo-gout-related crystals promote GLUT1-mediated glycolysis that governs NLRP3 and interleukin-1β activation on macrophages, Ann Rheum Dis 79(11) (2020) 1506-1514.
[199] O.R. Mahon, D.J. Kelly, G.M. McCarthy, A. Dunne, Osteoarthritis-associated basic calcium phosphate crystals alter immune cell metabolism and promote M1 macrophage polarization, Osteoarthritis Cartilage 28(5) (2020) 603-612.
[200] M.P. Bernardo, B.C.R. da Silva, A.E.I. Hamouda, M.A.S. de Toledo, C. Schalla, S. Rütten, R. Goetzke, L.H.C. Mattoso, M. Zenke, A. Sechi, PLA/Hydroxyapatite scaffolds exhibit in vitro immunological inertness and promote robust osteogenic differentiation of human mesenchymal stem cells without osteogenic stimuli, Sci Rep 12(1) (2022) 2333.
[201] N.A. Abdul Halim, M.Z. Hussein, M.K. Kandar, Nanomaterials-Upconverted Hydroxyapatite for Bone Tissue Engineering and a Platform for Drug Delivery, Int J Nanomedicine 16 (2021) 6477-6496.
[202] H. Samadian, H. Mobasheri, M. Azami, R. Faridi-Majidi, Osteoconductive and electroactive carbon nanofibers/hydroxyapatite nanocomposite tailored for bone tissue engineering: in vitro and in vivo studies, Sci Rep 10(1) (2020) 14853.
[203] D. Arcos, M. Vallet-Regí, Substituted hydroxyapatite coatings of bone implants, J Mater Chem B 8(9) (2020) 1781-1800.

[204] J. Fang, P. Li, X. Lu, L. Fang, X. Lü, F. Ren, A strong, tough, and osteoconductive hydroxyapatite mineralized polyacrylamide/dextran hydrogel for bone tissue regeneration, Acta Biomater 88 (2019) 503-513.
[205] P. Laquerriere, A. Grandjean-Laquerriere, E. Jallot, G. Balossier, P. Frayssinet, M. Guenounou, Importance of hydroxyapatite particles characteristics on cytokines production by human monocytes in vitro, Biomaterials 24(16) (2003) 2739-47.
[206] R.J. Christiansen, H.J. Münch, C.M. Bonefeld, J.P. Thyssen, J.J. Sloth, C. Geisler, K. Søballe, M.S. Jellesen, S.S. Jakobsen, Cytokine Profile in Patients with Aseptic Loosening of Total Hip Replacements and Its Relation to Metal Release and Metal Allergy, J Clin Med 8(8) (2019).
[207] R. Wang, H. Hu, J. Guo, Q. Wang, J. Cao, H. Wang, G. Li, J. Mao, X. Zou, D. Chen, W. Tian, Nano-Hydroxyapatite Modulates Osteoblast Differentiation Through Autophagy Induction via mTOR Signaling Pathway, J Biomed Nanotechnol 15(2) (2019) 405-415.
[208] F. Guo, C. Yuan, H. Huang, X. Deng, Z. Bian, D. Wang, K. Dou, L. Mei, Q. Zhou, Regulation of T Cell Responses by Nano-Hydroxyapatite to Mediate the Osteogenesis, Front Bioeng Biotechnol 10 (2022) 884291.
[209] M.B. Gorbet, M.V. Sefton, Endotoxin: the uninvited guest, Biomaterials 26(34) (2005) 6811-7.
[210] R. Lieder, P.H. Petersen, Ó. Sigurjónsson, Endotoxins-the invisible companion in biomaterials research, Tissue Eng Part B Rev 19(5) (2013) 391-402.
[211] A.F. McGettrick, L.A.J. O'Neill, The Role of HIF in Immunity and Inflammation, Cell Metab 32(4) (2020) 524-536.
[212] G.M. Tannahill, A.M. Curtis, J. Adamik, E.M. Palsson-McDermott, A.F. McGettrick, G. Goel, C. Frezza, N.J. Bernard, B. Kelly, N.H. Foley, L. Zheng, A. Gardet, Z. Tong, S.S. Jany, S.C. Corr, M. Haneklaus, B.E. Caffrey, K. Pierce, S. Walmsley, F.C. Beasley, E. Cummins, V. Nizet, M. Whyte, C.T. Taylor, H. Lin, S.L. Masters, E. Gottlieb, V.P. Kelly, C. Clish, P.E. Auron, R.J. Xavier, L.A. O'Neill, Succinate is an inflammatory signal that induces IL-1β through HIF-1α, Nature 496(7444) (2013) 238-42.
[213] M. Canton, R. Sánchez-Rodríguez, I. Spera, F.C. Venegas, M. Favia, A. Viola, A. Castegna, Reactive Oxygen Species in Macrophages: Sources and Targets, Front Immunol 12 (2021) 734229.
[214] S.Y. Kim, J.M. Jeong, S.J. Kim, W. Seo, M.H. Kim, W.M. Choi, W. Yoo, J.H. Lee, Y.R. Shim, H.S. Yi, Y.S. Lee, H.S. Eun, B.S. Lee, K. Chun, S.J. Kang, S.C. Kim, B. Gao, G. Kunos, H.M. Kim, W.I. Jeong, Pro-inflammatory hepatic macrophages generate ROS through NADPH oxidase 2 via endocytosis of monomeric TLR4-MD2 complex, Nat Commun 8(1) (2017) 2247.
[215] B. Brüne, N. Dehne, N. Grossmann, M. Jung, D. Namgaladze, T. Schmid, A. von Knethen, A. Weigert, Redox control of inflammation in macrophages, Antioxid Redox Signal 19(6) (2013) 595-637.
[216] Q. Yu, Y. Wang, L. Dong, Y. He, R. Liu, Q. Yang, Y. Cao, A. Jia, Y. Bi, G. Liu, Regulations of Glycolytic Activities on Macrophages Functions in Tumor and Infectious Inflammation, Front Cell Infect Microbiol 10 (2020) 287.
[217] W. Yu, X. Wang, J. Zhao, R. Liu, J. Liu, Z. Wang, J. Peng, H. Wu, X. Zhang, Z. Long, D. Kong, W. Li, C. Hai, Stat2-Drp1 mediated mitochondrial mass increase is necessary for pro-inflammatory differentiation of macrophages, Redox Biol 37 (2020) 101761.
[218] Y. Wang, N. Li, X. Zhang, T. Horng, Mitochondrial metabolism regulates macrophage biology, J Biol Chem 297(1) (2021) 100904.

[219] R. Kapetanovic, S.F. Afroz, D. Ramnath, G.M. Lawrence, T. Okada, J.E. Curson, J. de Bruin, D.P. Fairlie, K. Schroder, J.C. St John, A. Blumenthal, M.J. Sweet, Lipopolysaccharide promotes Drp1-dependent mitochondrial fission and associated inflammatory responses in macrophages, Immunol Cell Biol 98(7) (2020) 528-539.
[220] C. Jin, P. Frayssinet, R. Pelker, D. Cwirka, B. Hu, A. Vignery, S.C. Eisenbarth, R.A. Flavell, NLRP3 inflammasome plays a critical role in the pathogenesis of hydroxyapatite-associated arthropathy, Proc Natl Acad Sci U S A 108(36) (2011) 14867-72.
[221] O.R. Mahon, S. O'Hanlon, C.C. Cunningham, G.M. McCarthy, C. Hobbs, V. Nicolosi, D.J. Kelly, A. Dunne, Orthopaedic implant materials drive M1 macrophage polarization in a spleen tyrosine kinase- and mitogen-activated protein kinase-dependent manner, Acta Biomater 65 (2018) 426-435.
[222] F.M. Davis, A. denDekker, A. Kimball, A.D. Joshi, M. El Azzouny, S.J. Wolf, A.T. Obi, J. Lipinski, J.E. Gudjonsson, X. Xing, O. Plazyo, C. Audu, W.J. Melvin, K. Singer, P.K. Henke, B.B. Moore, C. Burant, S.L. Kunkel, K.A. Gallagher, Epigenetic Regulation of TLR4 in Diabetic Macrophages Modulates Immunometabolism and Wound Repair, J Immunol (2020).
[223] Z. Yan, X. Tian, J. Zhu, Z. Lu, L. Yu, D. Zhang, Y. Liu, C. Yang, Q. Zhu, X. Cao, Metformin suppresses UHMWPE particle-induced osteolysis in the mouse calvaria by promoting polarization of macrophages to an anti-inflammatory phenotype, Mol Med 24(1) (2018) 20.
[224] C.V. Maduka, O.M. Habeeb, M.M. Kuhnert, M. Hakun, S.B. Goodman, C.H. Contag, Glycolytic reprogramming underlies immune cell activation by polyethylene wear particles, Biomater Adv 152 (2023) 213495.
[225] C.V. Maduka, M.M. Kuhnert, O.M. Habeeb, A. Tundo, A.V. Makela, S.B. Goodman, C.H. Contag, Elevated oxidative phosphorylation is critical for immune cell activation by polyethylene wear particles, Journal of Immunology and Regenerative Medicine 19 (2023).
[226] L.C. Shanley, O.R. Mahon, S.A. O'Rourke, N.G.B. Neto, M.G. Monaghan, D.J. Kelly, A. Dunne, Macrophage metabolic profile is altered by hydroxyapatite particle size, Acta Biomater 160 (2023) 311-321.
[227] S. Ye, P. Yang, K. Cheng, T. Zhou, Y. Wang, Z. Hou, Y. Jiang, L. Ren, Drp1-Dependent Mitochondrial Fission Mediates Toxicity of Positively Charged Graphene in Microglia, ACS Biomater Sci Eng 2(5) (2016) 722-733.
[228] J. Herman, B. Le Goff, J. De Lima, R. Brion, C. Chevalier, F. Blanchard, C. Darrieutort-Laffite, Pro-inflammatory effects of human apatite crystals extracted from patients suffering from calcific tendinopathy, Arthritis Res Ther 23(1) (2021) 131.
[229] I. Nadra, A.R. Boccaccini, P. Philippidis, L.C. Whelan, G.M. McCarthy, D.O. Haskard, R.C. Landis, Effect of particle size on hydroxyapatite crystal-induced tumor necrosis factor alpha secretion by macrophages, Atherosclerosis 196(1) (2008) 98-105.
[230] A. Grandjean-Laquerriere, O. Tabary, J. Jacquot, D. Richard, P. Frayssinet, M. Guenounou, D. Laurent-Maquin, P. Laquerriere, S. Gangloff, Involvement of toll-like receptor 4 in the inflammatory reaction induced by hydroxyapatite particles, Biomaterials 28(3) (2007) 400-4.
[231] I. Cobo, A. Cheng, J. Murillo-Saich, R. Coras, A. Torres, Y. Abe, A.J. Lana, J. Schlachetzki, R. Liu-Bryan, R. Terkeltaub, E. Sanchez-Lopez, C.K. Glass, M. Guma, Monosodium urate crystals regulate a unique JNK-dependent macrophage metabolic and inflammatory response, Cell Rep 38(10) (2022) 110489.

[232] P. Doddapattar, R. Dev, M. Ghatge, R.B. Patel, M. Jain, N. Dhanesha, S.R. Lentz, A.K. Chauhan, Myeloid Cell PKM2 Deletion Enhances Efferocytosis and Reduces Atherosclerosis, Circ Res 130(9) (2022) 1289-1305.
[233] X. Zhang, Y. Yang, L. Jing, W. Zhai, H. Zhang, Q. Ma, C. Li, F. Yan, D. Cheng, J. Zhang, Z. Ning, H. Shi, C. Wang, M. Zhao, J. Dai, Z. Li, J. Ming, M. Yu, H. Wang, H. Cheng, H. Xiong, G. Dong, Pyruvate Kinase M2 Contributes to TLR-Mediated Inflammation and Autoimmunity by Promoting Pyk2 Activation, Front Immunol 12 (2021) 680068.
[234] S.Y. Lee, S.H. Lee, E.J. Yang, E.K. Kim, J.K. Kim, D.Y. Shin, M.L. Cho, Metformin Ameliorates Inflammatory Bowel Disease by Suppression of the STAT3 Signaling Pathway and Regulation of the between Th17/Treg Balance, PLoS One 10(9) (2015) e0135858.
[235] H.J. Son, J. Lee, S.Y. Lee, E.K. Kim, M.J. Park, K.W. Kim, S.H. Park, M.L. Cho, Metformin attenuates experimental autoimmune arthritis through reciprocal regulation of Th17/Treg balance and osteoclastogenesis, Mediators Inflamm 2014 (2014) 973986.
[236] Y.H. Youm, K.Y. Nguyen, R.W. Grant, E.L. Goldberg, M. Bodogai, D. Kim, D. D'Agostino, N. Planavsky, C. Lupfer, T.D. Kanneganti, S. Kang, T.L. Horvath, T.M. Fahmy, P.A. Crawford, A. Biragyn, E. Alnemri, V.D. Dixit, The ketone metabolite β-hydroxybutyrate blocks NLRP3 inflammasome-mediated inflammatory disease, Nat Med 21(3) (2015) 263-9.
[237] M. Cicuéndez, M. Fernandes, M. Ayán-Varela, H. Oliveira, M.J. Feito, R. Diez-Orejas, J.I. Paredes, S. Villar-Rodil, M. Vila, M.T. Portolés, I.F. Duarte, Macrophage inflammatory and metabolic responses to graphene-based nanomaterials differing in size and functionalization, Colloids Surf B Biointerfaces 186 (2020) 110709.
[238] R. Saborano, T. Wongpinyochit, J.D. Totten, B.F. Johnston, F.P. Seib, I.F. Duarte, Metabolic Reprogramming of Macrophages Exposed to Silk, Poly(lactic-co-glycolic acid), and Silica Nanoparticles, Adv Healthc Mater 6(14) (2017).
[239] O.R. Mahon, D.C. Browe, P.J. Diaz-Payno, P. Pitacco, K.T. Cunningham, K.H.G. Mills, A. Dunne, D.J. Kelly, Extracellular matrix scaffolds derived from different musculoskeletal tissues drive distinct macrophage phenotypes and direct tissue-specific cellular differentiation, Journal of Immunology and Regenerative Medicine 12 (2021).
[240] C.E. Witherel, K. Sao, B.K. Brisson, B. Han, S.W. Volk, R.J. Petrie, L. Han, K.L. Spiller, Regulation of extracellular matrix assembly and structure by hybrid M1/M2 macrophages, Biomaterials 269 (2021) 120667.
[241] M. Karin, H. Clevers, Reparative inflammation takes charge of tissue regeneration, Nature 529(7586) (2016) 307-15.
[242] A.M. Soliman, D.R. Barreda, Acute Inflammation in Tissue Healing, Int J Mol Sci 24(1) (2022).
[243] L.C. Shanley, O.R. Mahon, D.J. Kelly, A. Dunne, Harnessing the innate and adaptive immune system for tissue repair and regeneration: Considering more than macrophages, Acta Biomater 133 (2021) 208-221.
[244] F.A. Dauchy, C. Contin-Bordes, R. Nzoumbou-Boko, M. Bonhivers, N. Landrein, D.R. Robinson, J. Rambert, P. Courtois, S. Daulouède, P. Vincendeau, Trypanosoma brucei gambiense excreted/secreted factors impair lipopolysaccharide-induced maturation and activation of human monocyte-derived dendritic cells, Parasite Immunol 41(8) (2019) e12632.
[245] R. Aoki, A. Aoki-Yoshida, C. Suzuki, Y. Takayama, Protective effect of indole-3-pyruvate against ultraviolet b-induced damage to cultured HaCaT keratinocytes and the skin of hairless mice, PLoS One 9(5) (2014) e96804.

[246] G. Paul, F. Bataille, F. Obermeier, J. Bock, F. Klebl, U. Strauch, D. Lochbaum, P. Rümmele, S. Farkas, J. Schölmerich, M. Fleck, G. Rogler, H. Herfarth, Analysis of intestinal haem-oxygenase-1 (HO-1) in clinical and experimental colitis, Clin Exp Immunol 140(3) (2005) 547-55.
[247] S.C. Funes, M. Rios, A. Fernández-Fierro, C. Covián, S.M. Bueno, C.A. Riedel, J.P. Mackern-Oberti, A.M. Kalergis, Naturally Derived Heme-Oxygenase 1 Inducers and Their Therapeutic Application to Immune-Mediated Diseases, Front Immunol 11 (2020) 1467.
[248] Y. Yin, K.A. Corry, J.P. Loughran, J. Li, Moderate Nrf2 Activation by Genetic Disruption of Keap1 Has Sex-Specific Effects on Bone Mass in Mice, Sci Rep 10(1) (2020) 348.
[249] C. Sánchez-de-Diego, L. Pedrazza, C. Pimenta-Lopes, A. Martinez-Martinez, N. Dahdah, J.A. Valer, P. Garcia-Roves, J.L. Rosa, F. Ventura, NRF2 function in osteocytes is required for bone homeostasis and drives osteocytic gene expression, Redox Biol 40 (2021) 101845.
[250] A.J. Freemerman, A.R. Johnson, G.N. Sacks, J.J. Milner, E.L. Kirk, M.A. Troester, A.N. Macintyre, P. Goraksha-Hicks, J.C. Rathmell, L. Makowski, Metabolic reprogramming of macrophages: glucose transporter 1 (GLUT1)-mediated glucose metabolism drives a proinflammatory phenotype, J Biol Chem 289(11) (2014) 7884-96.
[251] B. Kelly, L.A. O'Neill, Metabolic reprogramming in macrophages and dendritic cells in innate immunity, Cell Res 25(7) (2015) 771-84.
[252] K. Khezri, S. Maleki Dizaj, Y. Rahbar Saadat, S. Sharifi, S. Shahi, E. Ahmadian, A. Eftekhari, E. Dalir Abdolahinia, F. Lotfipour, Osteogenic Differentiation of Mesenchymal Stem Cells via Curcumin-Containing Nanoscaffolds, Stem Cells Int 2021 (2021) 1520052.
[253] Z. Tu, Y. Zhong, H. Hu, D. Shao, R. Haag, M. Schirner, J. Lee, B. Sullenger, K.W. Leong, Design of therapeutic biomaterials to control inflammation, Nat Rev Mater 7(7) (2022) 557-574.
[254] T.H. Lin, Y. Tamaki, J. Pajarinen, H.A. Waters, D.K. Woo, Z. Yao, S.B. Goodman, Chronic inflammation in biomaterial-induced periprosthetic osteolysis: NF-κB as a therapeutic target, Acta Biomater 10(1) (2014) 1-10.
[255] R. Singh, S. Chandrashekharappa, S.R. Bodduluri, B.V. Baby, B. Hegde, N.G. Kotla, A.A. Hiwale, T. Saiyed, P. Patel, M. Vijay-Kumar, M.G.I. Langille, G.M. Douglas, X. Cheng, E.C. Rouchka, S.J. Waigel, G.W. Dryden, H. Alatassi, H.G. Zhang, B. Haribabu, P.K. Vemula, V.R. Jala, Enhancement of the gut barrier integrity by a microbial metabolite through the Nrf2 pathway, Nat Commun 10(1) (2019) 89.
[256] C. Diskin, E.A. Day, Ó. Henry, J.E. Toller-Kawahisa, L.A.J. O'Neill, 4-Octyl Itaconate and Dimethyl Fumarate Induce Secretion of the Anti-Inflammatory Protein Annexin A1 via NRF2, J Immunol 211(6) (2023) 1032-1041.
[257] C. Gutiérrez-Vázquez, F.J. Quintana, Regulation of the Immune Response by the Aryl Hydrocarbon Receptor, Immunity 48(1) (2018) 19-33.
[258] K. Masuda, A. Kimura, H. Hanieh, N.T. Nguyen, T. Nakahama, I. Chinen, Y. Otoyo, T. Murotani, A. Yamatodani, T. Kishimoto, Aryl hydrocarbon receptor negatively regulates LPS-induced IL-6 production through suppression of histamine production in macrophages, Int Immunol 23(10) (2011) 637-45.
[259] A. Kimura, T. Naka, T. Nakahama, I. Chinen, K. Masuda, K. Nohara, Y. Fujii-Kuriyama, T. Kishimoto, Aryl hydrocarbon receptor in combination with Stat1 regulates LPS-induced inflammatory responses, J Exp Med 206(9) (2009) 2027-35.

[260] M. Hiroi, Y. Ohmori, Constitutive nuclear factor kappaB activity is required to elicit interferon-gamma-induced expression of chemokine CXC ligand 9 (CXCL9) and CXCL10 in human tumour cell lines, Biochem J 376(Pt 2) (2003) 393-402.
[261] J. Zhu, L. Luo, L. Tian, S. Yin, X. Ma, S. Cheng, W. Tang, J. Yu, W. Ma, X. Zhou, X. Fan, X. Yang, J. Yan, X. Xu, C. Lv, H. Liang, Aryl Hydrocarbon Receptor Promotes IL-10 Expression in Inflammatory Macrophages Through Src-STAT3 Signaling Pathway, Front Immunol 9 (2018) 2033.
[262] C.W. Nho, E. Jeffery, Crambene, a bioactive nitrile derived from glucosinolate hydrolysis, acts via the antioxidant response element to upregulate quinone reductase alone or synergistically with indole-3-carbinol, Toxicol Appl Pharmacol 198(1) (2004) 40-8.
[263] S. Rutella, F. Locatelli, Intestinal dendritic cells in the pathogenesis of inflammatory bowel disease, World J Gastroenterol 17(33) (2011) 3761-75.
[264] J. Bates, L. Diehl, Dendritic cells in IBD pathogenesis: an area of therapeutic opportunity?, J Pathol 232(2) (2014) 112-20.
[265] G. Murdaca, S. Negrini, M. Pellecchio, M. Greco, C. Schiavi, F. Giusti, F. Puppo, Update upon the infection risk in patients receiving TNF alpha inhibitors, Expert Opin Drug Saf 18(3) (2019) 219-229.
[266] Y.M. Chiu, D.Y. Chen, Infection risk in patients undergoing treatment for inflammatory arthritis: non-biologics versus biologics, Expert Rev Clin Immunol 16(2) (2020) 207-228.
[267] R. Ha, Y. Keynan, Z.V. Rueda, Increased susceptibility to pneumonia due to tumour necrosis factor inhibition and prospective immune system rescue, Front Cell Infect Microbiol 12 (2022) 980868.
[268] A. Yang, Y. Lu, J. Xing, Z. Li, X. Yin, C. Dou, S. Dong, F. Luo, Z. Xie, T. Hou, J. Xu, IL-8 Enhances Therapeutic Effects of BMSCs on Bone Regeneration via CXCR2-Mediated PI3k/Akt Signaling Pathway, Cell Physiol Biochem 48(1) (2018) 361-370.
[269] D. Lin, Y. Chai, Y. Ma, B. Duan, Y. Yuan, C. Liu, Rapid initiation of guided bone regeneration driven by spatiotemporal delivery of IL-8 and BMP-2 from hierarchical MBG-based scaffold, Biomaterials 196 (2019) 122-137.
[270] M. Maruszewska-Cheruiyot, K. Krawczak-Wójcik, M. Michniowska, M.J. Stear, M. Machcińska, M. Doligalska, K. Donskow-Łysoniewska, Nematode-Induced Growth Factors Related to Angiogenesis in Autoimmune Disease Attenuation, Life (Basel) 13(2) (2023).
[271] R.D. Dennis, U. Schubert, C. Bauer, Angiogenesis and parasitic helminth-associated neovascularization, Parasitology 138(4) (2011) 426-39.
[272] L.M. Nisimura, R.R. Ferreira, L.L. Coelho, E.M. Souza, B.M. Gonzaga, P.M. Ferrão, M.C. Waghabi, L.B. Mesquita, M.C.S. Pereira, O.D.C. Moreira, J. Lannes-Vieira, L.R. Garzoni, Increased angiogenesis parallels cardiac tissue remodelling in experimental acute Trypanosoma cruzi infection, Mem Inst Oswaldo Cruz 117 (2022) e220005.
[273] D. Langan, D.J. Perkins, S.N. Vogel, K.D. Moudgil, Microbiota-Derived Metabolites, Indole-3-aldehyde and Indole-3-acetic Acid, Differentially Modulate Innate Cytokines and Stromal Remodeling Processes Associated with Autoimmune Arthritis, Int J Mol Sci 22(4) (2021).
[274] N.E. Ruyssers, B.Y. De Winter, J.G. De Man, A. Loukas, M.S. Pearson, J.V. Weinstock, R.M. Van den Bossche, W. Martinet, P.A. Pelckmans, T.G. Moreels, Therapeutic potential of helminth soluble proteins in TNBS-induced colitis in mice, Inflamm Bowel Dis 15(4) (2009) 491-500.

[275] T.C. Freitas, E.J. Pearce, Growth factors and chemotactic factors from parasitic helminths: molecular evidence for roles in host-parasite interactions versus parasite development, Int J Parasitol 40(7) (2010) 761-73.
[276] C.J.C. Johnston, D.J. Smyth, R.B. Kodali, M.P.J. White, Y. Harcus, K.J. Filbey, J.P. Hewitson, C.S. Hinck, A. Ivens, A.M. Kemter, A.O. Kildemoes, T. Le Bihan, D.C. Soares, S.M. Anderton, T. Brenn, S.J. Wigmore, H.V. Woodcock, R.C. Chambers, A.P. Hinck, H.J. McSorley, R.M. Maizels, A structurally distinct TGF-β mimic from an intestinal helminth parasite potently induces regulatory T cells, Nat Commun 8(1) (2017) 1741.
[277] J. Hu, G.S. Melchor, D. Ladakis, J. Reger, H.W. Kim, K.A. Chamberlain, N.V. Shults, H.C. Oft, V.N. Smith, L.M. Rosko, E. Li, M. Baydyuk, M.M. Fu, P. Bhargava, J.K. Huang, Myeloid cell-associated aromatic amino acid metabolism facilitates CNS myelin regeneration, NPJ Regen Med 9(1) (2024) 1.
[278] Z.H. Zhang, W. Zhu, H.Z. Ren, X. Zhao, S. Wang, H.C. Ma, X.L. Shi, Mesenchymal stem cells increase expression of heme oxygenase-1 leading to anti-inflammatory activity in treatment of acute liver failure, Stem Cell Res Ther 8(1) (2017) 70.
[279] S.M. Khadrawy, H.M. Mohamed, A.M. Mahmoud, Mesenchymal stem cells ameliorate oxidative stress, inflammation, and hepatic fibrosis via Nrf2/HO-1 signaling pathway in rats, Environ Sci Pollut Res Int 28(2) (2021) 2019-2030.
[280] J. Han, K. Yang, J. An, N. Jiang, S. Fu, X. Tang, The Role of NRF2 in Bone Metabolism - Friend or Foe?, Front Endocrinol (Lausanne) 13 (2022) 813057.
[281] J. Che, X. Yang, Z. Jin, C. Xu, Nrf2: A promising therapeutic target in bone-related diseases, Biomed Pharmacother 168 (2023) 115748.
[282] Y. Li, Z.Z. Zhang, Sustained curcumin release from PLGA microspheres improves bone formation under diabetic conditions by inhibiting the reactive oxygen species production, Drug Des Devel Ther 12 (2018) 1453-1466.
[283] N. Wang, F. Wang, Y. Gao, P. Yin, C. Pan, W. Liu, Z. Zhou, J. Wang, Curcumin protects human adipose-derived mesenchymal stem cells against oxidative stress-induced inhibition of osteogenesis, J Pharmacol Sci 132(3) (2016) 192-200.
[284] Y.T. Tsao, Y.J. Huang, H.H. Wu, Y.A. Liu, Y.S. Liu, O.K. Lee, Osteocalcin Mediates Biomineralization during Osteogenic Maturation in Human Mesenchymal Stromal Cells, Int J Mol Sci 18(1) (2017).
[285] O. Mucha, P. Podkalicka, M. Czarnek, A. Biela, M. Mieczkowski, N. Kachamakova-Trojanowska, J. Stepniewski, A. Jozkowicz, J. Dulak, A. Loboda, Pharmacological versus genetic inhibition of heme oxygenase-1 - the comparison of metalloporphyrins, shRNA and CRISPR/Cas9 system, Acta Biochim Pol 65(2) (2018) 277-286.
[286] A.T.D. Watson, R.C. Nordberg, E.G. Loboa, S.W. Kullman, Evidence for Aryl hydrocarbon Receptor-Mediated Inhibition of Osteoblast Differentiation in Human Mesenchymal Stem Cells, Toxicol Sci 167(1) (2019) 145-156.
[287] X. Liu, X. Li, Y. Tao, N. Li, M. Ji, X. Zhang, Y. Chen, Z. He, K. Yu, Z. Yu, TCDD inhibited the osteogenic differentiation of human fetal palatal mesenchymal cells through AhR and BMP-2/TGF-β/Smad signaling, Toxicology 431 (2020) 152353.
[288] M. Korkalainen, E. Kallio, A. Olkku, K. Nelo, J. Ilvesaro, J. Tuukkanen, A. Mahonen, M. Viluksela, Dioxins interfere with differentiation of osteoblasts and osteoclasts, Bone 44(6) (2009) 1134-42.
[289] Y. Zhou, R. Jiang, L. An, H. Wang, S. Cheng, S. Qiong, Y. Weng, Benzo[a]pyrene impedes self-renewal and differentiation of mesenchymal stem cells and influences fracture healing, Sci Total Environ 587-588 (2017) 305-315.

[290] Y. Tong, M. Niu, Y. Du, W. Mei, W. Cao, Y. Dou, H. Yu, X. Du, H. Yuan, W. Zhao, Aryl hydrocarbon receptor suppresses the osteogenesis of mesenchymal stem cells in collagen-induced arthritic mice through the inhibition of β-catenin, Exp Cell Res 350(2) (2017) 349-357.
[291] C. Wejheden, S. Brunnberg, S. Larsson, P.M. Lind, G. Andersson, A. Hanberg, Transgenic mice with a constitutively active aryl hydrocarbon receptor display a gender-specific bone phenotype, Toxicol Sci 114(1) (2010) 48-58.
[292] K.A. Fader, R. Nault, S. Raehtz, L.R. McCabe, T.R. Zacharewski, 2,3,7,8-Tetrachlorodibenzo-p-dioxin dose-dependently increases bone mass and decreases marrow adiposity in juvenile mice, Toxicol Appl Pharmacol 348 (2018) 85-98.
[293] N. Podechard, O. Fardel, M. Corolleur, M. Bernard, V. Lecureur, Inhibition of human mesenchymal stem cell-derived adipogenesis by the environmental contaminant benzo(a)pyrene, Toxicol In Vitro 23(6) (2009) 1139-44.
[294] Q. Chen, P. Shou, C. Zheng, M. Jiang, G. Cao, Q. Yang, J. Cao, N. Xie, T. Velletri, X. Zhang, C. Xu, L. Zhang, H. Yang, J. Hou, Y. Wang, Y. Shi, Fate decision of mesenchymal stem cells: adipocytes or osteoblasts?, Cell Death Differ 23(7) (2016) 1128-39.
[295] Y. Yoshikawa, T. Izawa, Y. Hamada, H. Takenaga, Z. Wang, N. Ishimaru, H. Kamioka, Roles for B[a]P and FICZ in subchondral bone metabolism and experimental temporomandibular joint osteoarthritis via the AhR/Cyp1a1 signaling axis, Sci Rep 11(1) (2021) 14927.
[296] E. Roddy, M.R. DeBaun, A. Daoud-Gray, Y.P. Yang, M.J. Gardner, Treatment of critical-sized bone defects: clinical and tissue engineering perspectives, Eur J Orthop Surg Traumatol 28(3) (2018) 351-362.
[297] B.V. Slaughter, S.S. Khurshid, O.Z. Fisher, A. Khademhosseini, N.A. Peppas, Hydrogels in regenerative medicine, Adv Mater 21(32-33) (2009) 3307-29.
[298] I.M. El-Sherbiny, M.H. Yacoub, Hydrogel scaffolds for tissue engineering: Progress and challenges, Glob Cardiol Sci Pract 2013(3) (2013) 316-42.
[299] X. Bai, M. Gao, S. Syed, J. Zhuang, X. Xu, X.Q. Zhang, Bioactive hydrogels for bone regeneration, Bioact Mater 3(4) (2018) 401-417.
[300] M.C. Catoira, L. Fusaro, D. Di Francesco, M. Ramella, F. Boccafoschi, Overview of natural hydrogels for regenerative medicine applications, J Mater Sci Mater Med 30(10) (2019) 115.
[301] K.T. Dicker, L.A. Gurski, S. Pradhan-Bhatt, R.L. Witt, M.C. Farach-Carson, X. Jia, Hyaluronan: a simple polysaccharide with diverse biological functions, Acta Biomater 10(4) (2014) 1558-70.
[302] M. Hemshekhar, R.M. Thushara, S. Chandranayaka, L.S. Sherman, K. Kemparaju, K.S. Girish, Emerging roles of hyaluronic acid bioscaffolds in tissue engineering and regenerative medicine, Int J Biol Macromol 86 (2016) 917-28.
[303] T. Sasaki, C. Watanabe, Stimulation of osteoinduction in bone wound healing by high-molecular hyaluronic acid, Bone 16(1) (1995) 9-15.
[304] M. Kawano, W. Ariyoshi, K. Iwanaga, T. Okinaga, M. Habu, I. Yoshioka, K. Tominaga, T. Nishihara, Mechanism involved in enhancement of osteoblast differentiation by hyaluronic acid, Biochem Biophys Res Commun 405(4) (2011) 575-80.
[305] V.S. Meli, H. Atcha, P.K. Veerasubramanian, R.R. Nagalla, T.U. Luu, E.Y. Chen, C.F. Guerrero-Juarez, K. Yamaga, W. Pandori, J.Y. Hsieh, T.L. Downing, D.A. Fruman, M.B. Lodoen, M.V. Plikus, W. Wang, W.F. Liu, YAP-mediated mechanotransduction tunes the macrophage inflammatory response, Sci Adv 6(49) (2020).

[306] R.A. Scott, K.L. Kiick, R.E. Akins, Substrate stiffness directs the phenotype and polarization state of cord blood derived macrophages, Acta Biomater 122 (2021) 220-235.
[307] F.N.U. Apoorva, Y.F. Tian, T.M. Pierpont, D.M. Bassen, L. Cerchietti, J.T. Butcher, R.S. Weiss, A. Singh, Award Winner in the Young Investigator Category, 2017 Society for Biomaterials Annual Meeting and Exposition, Minneapolis, MN, April 05-08, 2017: Lymph node stiffness-mimicking hydrogels regulate human B-cell lymphoma growth and cell surface receptor expression in a molecular subtype-specific manner, J Biomed Mater Res A 105(7) (2017) 1833-1844.
[308] S.F.B. Mennens, M. Bolomini-Vittori, J. Weiden, B. Joosten, A. Cambi, K. van den Dries, Substrate stiffness influences phenotype and function of human antigen-presenting dendritic cells, Sci Rep 7(1) (2017) 17511.
[309] D.J. Yuan, L. Shi, L.C. Kam, Biphasic response of T cell activation to substrate stiffness, Biomaterials 273 (2021) 120797.
[310] M. Kisiel, M.M. Martino, M. Ventura, J.A. Hubbell, J. Hilborn, D.A. Ossipov, Improving the osteogenic potential of BMP-2 with hyaluronic acid hydrogel modified with integrin-specific fibronectin fragment, Biomaterials 34(3) (2013) 704-12.
[311] G. Bhakta, B. Rai, Z.X. Lim, J.H. Hui, G.S. Stein, A.J. van Wijnen, V. Nurcombe, G.D. Prestwich, S.M. Cool, Hyaluronic acid-based hydrogels functionalized with heparin that support controlled release of bioactive BMP-2, Biomaterials 33(26) (2012) 6113-22.
[312] M.R. Todeschi, R.M. El Backly, O.P. Varghese, J. Hilborn, R. Cancedda, M. Mastrogiacomo, Host cell recruitment patterns by bone morphogenetic protein-2 releasing hyaluronic acid hydrogels in a mouse subcutaneous environment, Regen Med 12(5) (2017) 525-539.
[313] Y. Zhao, C. Gao, H. Liu, Y. Feng, Z. Li, J. Wang, B. Yang, Q. Lin, Infliximab-based self-healing hydrogel composite scaffold enhances stem cell survival, engraftment, and function in rheumatoid arthritis treatment, Acta Biomater 121 (2021) 653-664.
[314] L.B. Gallagher, E.B. Dolan, J. O'Sullivan, R. Levey, B.L. Cavanagh, L. Kovarova, M. Pravda, V. Velebny, T. Farrell, F.J. O'Brien, G.P. Duffy, Pre-culture of mesenchymal stem cells within RGD-modified hyaluronic acid hydrogel improves their resilience to ischaemic conditions, Acta Biomater 107 (2020) 78-90.
[315] J. Bystronova, I. Scigalkova, L. Wolfova, M. Pravda, N.E. Vrana, V. Velebny, Creating a 3D microenvironment for monocyte cultivation: ECM-mimicking hydrogels based on gelatine and hyaluronic acid derivatives, RSC Advances 8(14) (2018) 7606-7614.
[316] F. Lee, J.E. Chung, M. Kurisawa, An injectable enzymatically crosslinked hyaluronic acid- hydrogel system with independent tuning of mechanical strength and gelation rate, Soft Matter 4(4) (2008) 880-887.
[317] Y. Abu-Amer, I. Darwech, J.C. Clohisy, Aseptic loosening of total joint replacements: mechanisms underlying osteolysis and potential therapies, Arthritis Res Ther 9 Suppl 1 (2007) S6.
[318] S. Trombino, C. Servidio, F. Curcio, R. Cassano, Strategies for Hyaluronic Acid-Based Hydrogel Design in Drug Delivery, Pharmaceutics 11(8) (2019).
[319] G.E. Yan, T. Efferth, Cell Harvesting Methods Affect Cellular Integrity of Adherent Cells During Apoptosis Detection, Anticancer Res 38(12) (2018) 6669-6672.
[320] T.D. Zaveri, J.S. Lewis, N.V. Dolgova, M.J. Clare-Salzler, B.G. Keselowsky, Integrin-directed modulation of macrophage responses to biomaterials, Biomaterials 35(11) (2014) 3504-15.

[321] N. Mehrban, C. Pineda Molina, L.M. Quijano, J. Bowen, S.A. Johnson, J. Bartolacci, J.T. Chang, D.A. Scott, D.N. Woolfson, M.A. Birchall, S.F. Badylak, Host macrophage response to injectable hydrogels derived from ECM and α-helical peptides, Acta Biomater 111 (2020) 141-152.
[322] D. Lacroix, P.J. Prendergast, A mechano-regulation model for tissue differentiation during fracture healing: analysis of gap size and loading, J Biomech 35(9) (2002) 1163-71.
[323] M.S. Ghiasi, J.E. Chen, E.K. Rodriguez, A. Vaziri, A. Nazarian, Computational modeling of human bone fracture healing affected by different conditions of initial healing stage, BMC Musculoskelet Disord 20(1) (2019) 562.
[324] A. Barnett-Vanes, A. Sharrock, M.A. Birrell, S. Rankin, A Single 9-Colour Flow Cytometric Method to Characterise Major Leukocyte Populations in the Rat: Validation in a Model of LPS-Induced Pulmonary Inflammation, PLoS One 11(1) (2016) e0142520.
[325] K.M. Adusei, T.B. Ngo, A.L. Alfonso, R. Lokwani, S. DeStefano, M. Karkanitsa, J. Spathies, S.M. Goldman, C.L. Dearth, K.N. Sadtler, Development of a High-Color Flow Cytometry Panel for Immunologic Analysis of Tissue Injury and Reconstruction in a Rat Model, Cells Tissues Organs 212(1) (2023) 84-95.
[326] E. Judokusumo, E. Tabdanov, S. Kumari, M.L. Dustin, L.C. Kam, Mechanosensing in T lymphocyte activation, Biophys J 102(2) (2012) L5-7.
[327] Z. Wan, S. Zhang, Y. Fan, K. Liu, F. Du, A.M. Davey, H. Zhang, W. Han, C. Xiong, W. Liu, B cell activation is regulated by the stiffness properties of the substrate presenting the antigens, J Immunol 190(9) (2013) 4661-75.
[328] I.M. Basurto, J.A. Passipieri, G.M. Gardner, K.K. Smith, A.R. Amacher, A.I. Hansrisuk, G.J. Christ, S.R. Caliari, Photoreactive Hydrogel Stiffness Influences Volumetric Muscle Loss Repair, Tissue Eng Part A 28(7-8) (2022) 312-329.
[329] Y. Jin, R.H. Koh, S.H. Kim, K.M. Kim, G.K. Park, N.S. Hwang, Injectable anti-inflammatory hyaluronic acid hydrogel for osteoarthritic cartilage repair, Mater Sci Eng C Mater Biol Appl 115 (2020) 111096.
[330] J. Kim, I.S. Kim, T.H. Cho, K.B. Lee, S.J. Hwang, G. Tae, I. Noh, S.H. Lee, Y. Park, K. Sun, Bone regeneration using hyaluronic acid-based hydrogel with bone morphogenic protein-2 and human mesenchymal stem cells, Biomaterials 28(10) (2007) 1830-7.
[331] E. Martínez-Sanz, D.A. Ossipov, J. Hilborn, S. Larsson, K.B. Jonsson, O.P. Varghese, Bone reservoir: Injectable hyaluronic acid hydrogel for minimal invasive bone augmentation, J Control Release 152(2) (2011) 232-40.
[332] M.S. Bae, D.H. Yang, J.B. Lee, D.N. Heo, Y.D. Kwon, I.C. Youn, K. Choi, J.H. Hong, G.T. Kim, Y.S. Choi, E.H. Hwang, I.K. Kwon, Photo-cured hyaluronic acid-based hydrogels containing simvastatin as a bone tissue regeneration scaffold, Biomaterials 32(32) (2011) 8161-71.
[333] H.S. Hwang, C.S. Lee, Recent Progress in Hyaluronic-Acid-Based Hydrogels for Bone Tissue Engineering, Gels 9(7) (2023).
[334] V. Lanza, V. Greco, E. Bocchieri, S. Sciuto, R. Inturri, L. Messina, S. Vaccaro, F. Bellia, E. Rizzarelli, Synergistic Effect of L-Carnosine and Hyaluronic Acid in Their Covalent Conjugates on the Antioxidant Abilities and the Mutual Defense against Enzymatic Degradation, Antioxidants (Basel) 11(4) (2022).
[335] J.R. Schmidt, S. Vogel, S. Moeller, S. Kalkhof, K. Schubert, M. von Bergen, U. Hempel, Sulfated hyaluronic acid and dexamethasone possess a synergistic potential in the differentiation of osteoblasts from human bone marrow stromal cells, J Cell Biochem 120(5) (2019) 8706-8722.

[336] R.M. Liu, R.G. Sun, L.T. Zhang, Q.F. Zhang, D.X. Chen, J.J. Zhong, J.H. Xiao, Hyaluronic acid enhances proliferation of human amniotic mesenchymal stem cells through activation of Wnt/β-catenin signaling pathway, Exp Cell Res 345(2) (2016) 218-29.
[337] R. Zhang, B.O. Oyajobi, S.E. Harris, D. Chen, C. Tsao, H.W. Deng, M. Zhao, Wnt/β-catenin signaling activates bone morphogenetic protein 2 expression in osteoblasts, Bone 52(1) (2013) 145-56.
[338] V. Vijayan, P. Pradhan, L. Braud, H.R. Fuchs, F. Gueler, R. Motterlini, R. Foresti, S. Immenschuh, Human and murine macrophages exhibit differential metabolic responses to lipopolysaccharide - A divergent role for glycolysis, Redox Biol 22 (2019) 101147.
[339] S.L. Macias, B.G. Keselowsky, Perspectives on immunometabolism at the biomaterials interface, Mol Aspects Med 83 (2022) 100992.
[340] A.M. Sabogal-Guáqueta, A. Marmolejo-Garza, M. Trombetta-Lima, A. Oun, J. Hunneman, T. Chen, J. Koistinaho, S. Lehtonen, A. Kortholt, J.C. Wolters, B.M. Bakker, B.J.L. Eggen, E. Boddeke, A. Dolga, Species-specific metabolic reprogramming in human and mouse microglia during inflammatory pathway induction, Nat Commun 14(1) (2023) 6454.
[341] C.V. Maduka, M. Alhaj, E. Ural, O.M. Habeeb, M.M. Kuhnert, K. Smith, A.V. Makela, H. Pope, S. Chen, J.M. Hix, C.L. Mallett, S.J. Chung, M. Hakun, A. Tundo, K.R. Zinn, K.D. Hankenson, S.B. Goodman, R. Narayan, C.H. Contag, Polylactide Degradation Activates Immune Cells by Metabolic Reprogramming, Adv Sci (Weinh) 10(31) (2023) e2304632.
[342] C.V. Maduka, A.V. Makela, E. Ural, K.B. Stivers, M.M. Kuhnert, A. Tundo, M. Alhaj, E.H. Apu, K.D. Ashammakhi, R. Narayan, J.H. Elisseeff, C.H. Contag, Regulating the proinflammatory response to implanted composite biomaterials comprising polylactide and hydroxyapatite by targeting immunometabolism, bioRxiv (2023).
[343] N.M. Khan, M.E. Diaz-Hernandez, S. Chihab, P. Priyadarshani, P. Bhattaram, L.J. Mortensen, R.M. Guzzo, H. Drissi, Differential chondrogenic differentiation between iPSC derived from healthy and OA cartilage is associated with changes in epigenetic regulation and metabolic transcriptomic signatures, Elife 12 (2023).
[344] W. Yan, S. Diao, Z. Fan, The role and mechanism of mitochondrial functions and energy metabolism in the function regulation of the mesenchymal stem cells, Stem Cell Res Ther 12(1) (2021) 140.
[345] N.G.B. Neto, M. Suku, D.A. Hoey, M.G. Monaghan, 2P-FLIM unveils time-dependent metabolic shifts during osteogenic differentiation with a key role of lactate to fuel osteogenesis via glutaminolysis identified, Stem Cell Res Ther 14(1) (2023) 364.
[346] A. Batista-Gonzalez, R. Vidal, A. Criollo, L.J. Carreño, New Insights on the Role of Lipid Metabolism in the Metabolic Reprogramming of Macrophages, Front Immunol 10 (2019) 2993.
[347] X. Feng, J. Gu, Y. Zhou, Primary total hip arthroplasty failure: aseptic loosening remains the most common cause of revision, Am J Transl Res 14(10) (2022) 7080-7089.
[348] N. Song, M. Scholtemeijer, K. Shah, Mesenchymal Stem Cell Immunomodulation: Mechanisms and Therapeutic Potential, Trends Pharmacol Sci 41(9) (2020) 653-664.
[349] K. Hyvärinen, M. Holopainen, V. Skirdenko, H. Ruhanen, P. Lehenkari, M. Korhonen, R. Käkelä, S. Laitinen, E. Kerkelä, Mesenchymal Stromal Cells and Their Extracellular Vesicles Enhance the Anti-Inflammatory Phenotype of Regulatory Macrophages by Downregulating the Production of Interleukin (IL)-23 and IL-22, Front Immunol 9 (2018) 771.

[350] C. Lo Sicco, D. Reverberi, C. Balbi, V. Ulivi, E. Principi, L. Pascucci, P. Becherini, M.C. Bosco, L. Varesio, C. Franzin, M. Pozzobon, R. Cancedda, R. Tasso, Mesenchymal Stem Cell-Derived Extracellular Vesicles as Mediators of Anti-Inflammatory Effects: Endorsement of Macrophage Polarization, Stem Cells Transl Med 6(3) (2017) 1018-1028.
[351] H. Sprott, C. Fleck, Hyaluronic Acid in Rheumatology, Pharmaceutics 15(9) (2023).
[352] J.E. Dilley, J.S. Everhart, R.G. Klitzman, Hyaluronic acid as an adjunct to microfracture in the treatment of osteochondral lesions of the talus: a systematic review of randomized controlled trials, BMC Musculoskelet Disord 23(1) (2022) 313.
[353] J. Hermans, S.M.A. Bierma-Zeinstra, P.K. Bos, D.D. Niesten, J.A.N. Verhaar, M. Reijman, The effectiveness of high molecular weight hyaluronic acid for knee osteoarthritis in patients in the working age: a randomised controlled trial, BMC Musculoskelet Disord 20(1) (2019) 196.
[354] H. Zhang, K. Zhang, X. Zhang, Z. Zhu, S. Yan, T. Sun, A. Guo, J. Jones, R.G. Steen, B. Shan, J. Zhang, J. Lin, Comparison of two hyaluronic acid formulations for safety and efficacy (CHASE) study in knee osteoarthritis: a multicenter, randomized, double-blind, 26-week non-inferiority trial comparing Durolane to Artz, Arthritis Res Ther 17(1) (2015) 51.
[355] J. Huang, X. Cai, Y. Ou, L. Fan, Y. Zhou, Y. Wang, Protective roles of FICZ and aryl hydrocarbon receptor axis on alveolar bone loss and inflammation in experimental periodontitis, J Clin Periodontol 46(9) (2019) 882-893.
[356] I. Fasolino, A. Soriente, L. Ambrosio, M.G. Raucci, Osteogenic and Anti-Inflammatory Behavior of Injectable Calcium Phosphate Loaded with Therapeutic Drugs, Nanomaterials (Basel) 10(9) (2020).
[357] C. Giordani, G. Matacchione, A. Giuliani, D. Valli, E.S. Scarpa, A. Antonelli, J. Sabbatinelli, G. Giacchetti, S. Sabatelli, F. Olivieri, M.R. Rippo, Pro-Osteogenic and Anti-Inflammatory Synergistic Effect of Orthosilicic Acid, Vitamin K2, Curcumin, Polydatin and Quercetin Combination in Young and Senescent Bone Marrow-Derived Mesenchymal Stromal Cells, Int J Mol Sci 24(10) (2023).
[358] X. Li, K. Xu, Y. He, B. Tao, K. Li, C. Lin, J. Hu, J. Wu, Y. Wu, S. Liu, P. Liu, H. Wang, K. Cai, ROS-responsive hydrogel coating modified titanium promotes vascularization and osteointegration of bone defects by orchestrating immunomodulation, Biomaterials 287 (2022) 121683.
[359] J. Zhang, D. Tong, H. Song, R. Ruan, Y. Sun, Y. Lin, J. Wang, L. Hou, J. Dai, J. Ding, H. Yang, Osteoimmunity-Regulating Biomimetically Hierarchical Scaffold for Augmented Bone Regeneration, Adv Mater 34(36) (2022) e2202044.
[360] S. Ibrahim, Q.K. Kang, A. Ramamurthi, The impact of hyaluronic acid oligomer content on physical, mechanical, and biologic properties of divinyl sulfone-crosslinked hyaluronic acid hydrogels, J Biomed Mater Res A 94(2) (2010) 355-70.

Acta Biomaterialia 160 (2023) 311–321

Contents lists available at ScienceDirect

Acta Biomaterialia

journal homepage: www.elsevier.com/locate/actbio

Full length article

Macrophage metabolic profile is altered by hydroxyapatite particle size

Lianne C. Shanley[a,b], Olwyn R. Mahon[a,b,e], Sinead A. O'Rourke[a,c], Nuno G.B. Neto[c], Michael G. Monaghan[b,c], Daniel J. Kelly[b,c], Aisling Dunne[a,b,d,*]

[a] School of Biochemistry & Immunology, Trinity College, The University of Dublin, Dublin 2, Ireland
[b] Centre for Advanced Materials and Bioengineering Research Amber
[c] Department of Mechanical, Manufacturing and Biomedical Engineering, School of Engineering, Trinity College Dublin, Dublin, Ireland
[d] School of Medicine, Trinity College, The University of Dublin, Dublin 2, Ireland
[e] Health Research Institute and the Bernal Institute, University of Limerick, Limerick, V94 T9PX, Ireland

article info

Article history:
Received 30 September 2022
Revised 9 January 2023
Accepted 30 January 2023
Available online 7 February 2023

Keywords:
Immunometabolism
Macrophages
Hydroxyapatite
Particle size
Immunomodulation

abstract

Since the recent observation that immune cells undergo metabolic reprogramming upon activation, there has been immense research in this area to not only understand the basis of such changes, but also to exploit metabolic rewiring for therapeutic benefit. In a resting state, macrophages preferentially utilise oxidative phosphorylation to generate energy; however, in the presence of immune cell activators, glycolytic genes are upregulated, and energy is generated through glycolysis. This facilitates the rapid production of biosynthetic intermediates and a pro-inflammatory macrophage phenotype. While this is essential to mount responses to infectious agents, more evidence is accumulating linking dysregulated metabolism to inappropriate immune responses. Given that certain biomaterials are known to promote an inflammatory macrophage phenotype, this prompted us to investigate if biomaterial particulates can impact on macrophage metabolism. Using micron and nano sized hydroxyapatite (HA), we demonstrate for the first time that these biomaterials can indeed drive changes in metabolism, and that this occurs in a size-dependent manner. We show that micronHA, but not nanoHA, particles upregulate surrogate markets of glycolysis including the glucose transporter (GLUT1), hexokinase 2 (HK2), GAPDH, and PKM2. Furthermore, we demonstrate that micronHA alters mitochondrial morphology and promotes a bioenergetic shift to favour glycolysis. Finally, we demonstrate that glycolytic gene expression is dependent on par- ticle uptake and that targeting glycolysis attenuates the pro-inflammatory profile of micronHA-treated macrophages. These results not only further our understanding of biomaterial-based macrophage activation, but also implicate immunometabolism as a new area for consideration in intelligent biomaterial design and therapeutic targeting.

Statement of significance

Several recent studies have reported that immune cell activation occurs concurrently with metabolic reprogramming. Furthermore, metabolic reprogramming of innate immune cells plays a prominent role in determining cellular phenotype and function. In this study we demonstrate that hydroxyapatite particle size alters macrophage metabolism, in turn driving their functional phenotype. Specifically, the pro-inflammatory phenotype promoted by micron-sized HA-particles is accompanied by changes in mitochondrial dynamics and a bioenergetic shift favouring glycolysis. This effect is not seen with nano-HA particles and can be attenuated upon inhibition of glycolysis. This study therefore not only identifies immunometabolism as a useful tool for characterising the immune response to biomaterials, but also highlights immunometabolism as a targetable aspect of the host response for therapeutic benefit.

© 2023 The Author(s). Published by Elsevier Ltd on behalf of Acta Materialia Inc.
This is an open access article under the CC BY license (http://creativecommons.org/licenses/by/4.0/)

Introduction

Immunometabolism is a rapidly expanding field that focuses on the intimate link between the metabolic phenotype of immune cells and their functionality. Innate immune cells such

* Correspondence author.
E-mail address: aidunne@tcd.ie (A. Dunne).

https://doi.org/10.1016/j.actbio.2023.01.058
1742-7061/© 2023 The Author(s). Published by Elsevier Ltd on behalf of Acta Materialia Inc. This is an open access article under the CC BY license (http://creativecommons.org/licenses/by/4.0/)

as macrophages generally rely on oxidative phosphorylation as their basal means of energy production, but exhibit a switch to favour glycolysis on exposure to cellular stressors and under conditions in which oxygen is limiting. This in turn allows for the rapid generation of metabolic and biosynthetic intermediates that contribute to the production of inflammatory mediators and reactive oxygen species (ROS) [1]. Such metabolic reprogramming is generally associated with polarisation towards a pro-inflammatory phenotype and, not surprisingly, dysregulated immunometabolism has now been recognised as a feature of many immune mediated diseases and cancers [2–5]. While it is well accepted that pathogen-associated molecules such as lipopolysaccharide (LPS) can promote a glycolytic environment in macrophages, focus is now turning to other drivers of altered macrophage metabolism. For example, it has recently been shown that exposure to damage or disease-associated molecular patterns (DAMPs) such as gout-associated monosodium urate (MSU) crystals, osteoarthritis-associated calcium-containing crystals, or cholesterol crystals that are deposited in atherosclerotic plaques, drive a glycolytic metabolic profile, concomitant with the polarisation of primary human macrophages to an M1-like phenotype [6–8].

While MSU and cholesterol crystals represent endogenous disease-associated particulates, bone-mimetic hydroxyapatite (HA) is commonly employed in the development of scaffolds for bone tissue engineering and as a coating for orthopaedic implant materials given its known osteoconductive properties [9–13]. Indeed, HA has been well studied in the context of macrophage responses, and it has been found that accumulation and recognition of HA particulates can have potent effects on subsequent immune cell-driven inflammatory responses. For example, it has been shown that the shape and size of HA particles can differentially modulate immune cell effector function, with needle-shaped [14,15] and micron-sized [8] particles preferentially driving an inflammatory monocyte and macrophage phenotype, characterised by production of pro-inflammatory cytokines such as TNFα, IL-6, and IL-1β. These cytokines are well documented contributors to the foreign body response (FBR) at the orthopaedic implant site and have also been shown to contribute to osteoclast differentiation and activation, leading to bone resorption, periprosthetic osteolysis and eventual aseptic implant loosening [16]. As a result, orthopaedic biomaterial design is relying on insights gained from immunological studies to mitigate these destructive processes and facilitate superior implant integration and tissue regeneration.

Nano-sized hydroxyapatite (nanoHA) has become an attractive alternative to traditionally used micronHA given its ability to promote an anti-inflammatory macrophage phenotype and exert pro-osteogenic effects on mesenchymal stem cells (MSCs) [17]. NanoHA has been shown to promote differentiation of osteoblasts [18], with recent work further exploring the interaction of nanoHA with the adaptive immune cell component to regulate osteoblastic differentiation [19]. However, there remains a pressing need for more thorough mechanistic studies into the means by which particulate biomaterials in general drive immune cell responses preclusive to repair, and those that facilitate tissue regeneration. In this study, we use HA particles in the micron and nanometre range to investigate whether particle size alters the metabolism of primary human macrophages. We link macrophage metabolic phenotype to alterations in mitochondrial dynamics and further examine the role that micron particle-induced metabolic changes play in HA-driven pro-inflammatory macrophage polarisation. Given the range of particulate biomaterials known to promote macrophage activation, we postulate that incorporation of immunometabolism into biomaterial research holds immense potential to further our understanding of the host-biomaterial response and may even facilitate the identification of novel therapeutic targets.

Materials and methods

Human blood monocyte-derived macrophage isolation

This study was approved by the research ethics committee of the School of Biochemistry and Immunology, Trinity College Dublin and was conducted in accordance with the Declaration of Helsinki. Leucocyte-enriched buffy coats from anonymous healthy donors (N ranging from 3-11 depending on experimental technique) were obtained with permission from the Irish Blood Transfusion Service (IBTS), St. James's Hospital, Dublin. Donors provided informed written consent to the IBTS for their blood to be used for research purposes. PBMCs were isolated and differentiated into macrophages as described previously [20]. The purity of $CD14^+CD11b^+$ macrophages was assessed by flow cytometry and was routinely >95% (Fig. S1).

Synthesis of nanohydroxyapatite particles (nHA)

Nano-sized hydroxyapatite particles were prepared following a previously described protocol [21]. Briefly, a solution of 20 mM calcium chloride was added to a solution of 12 mM sodium phosphate, containing 0.017% DARVAN 821 A (RT Vanderbilt) as the dispersant, and nanohydroxyapatite particles were precipitated. This solution was centrifuged, reconstituted in endotoxin-free water, and filtered through a 0.2 μm filter to remove aggregated particles and stored at 4°C for up to one month. Cell viability in the presence of nHA was assessed using a neutral red based cytotoxicity assay (TOX4, Sigma) (Fig. S2). Particles were characterised as previously published and shown to be 50-100 nm in length and 15-25 nm in width [17].

Preparation of micron hydroxyapatite particle (micronHA) suspension

Commercial micronHA particles ($Ca_5(OH)(PO_4)_{3\ 18\text{-}20}$ were purchased from Sigma Aldrich (Cat# 04238), weighed out and resuspended at a concentration of 5 mg/ml in endotoxin-free water, sonicated for 10 min, and stored at 4°C. Cell viability in the presence of micronHA was assessed using a neutral red based cytotoxicity assay (TOX4, Sigma) (Fig. S2). Particles were characterised as previously published and shown to be 1-2 μM in size [17].

Cytokine measurements

Primary human macrophages (1×10^6 cells/ml) were pre-treated with 2-deoxyglucose (2-DG) (25 mM), 3-(3-Pyridinyl)-1-(4-pyridinyl)-2-propen-1-one (3PO) (10 μM), or cytochalasin B (5 μm) prior to stimulation with particles for 24 hours, or particles alone, in order to assess the impact of glycolytic inhibition and phagocytic inhibition on the ability of micronHA to promote a pro-inflammatory macrophage phenotype. Supernatants were harvested and cytokine concentrations of TNFα, IL-6 and IL-8 were quantified by ELISA (eBioscience, San Diego, CA) according to manufacturer's protocol. Cell viability in the presence of all inhibitors was assessed by flow cytometry (Fig. S3).

Real-time PCR

Primary human macrophages (1×10^6 cells/ml) were treated with micronHA or nanoHA alone, or in the presence of indicated inhibitors (2-DG (25 mM), 3PO (10 μM), Cytochalasin B (5 μM)). RNA was extracted using High-Pure RNA Isolation Kits (Roche), and assessed for concentration and purity using the NanoDrop 2000c UV–Vis spectrophotometer. RNA was normalised and reverse transcribed using the Applied Biosystems High-Capacity cDNA reverse transcription kit. Real-time PCR was carried out on triplicate cDNA

samples using the CFX96 Touch Real-Time PCR Detection System (Bio-Rad Laboratories, California). Reactions included iTaq Univer- sal SYBR Green Supermix (Bio-rad Laboratories), cDNA, TaqMan fast universal PCR Master Mix and pre-designed TaqMan gene expres- sion probes (Applied Biosystems) for *CXCL9, CXCL10, CXCL11, CCL19*, and the housekeeping gene, 18S ribosomal RNA. The $2-.6.6$CT method was used to analyse relative gene expression. Oligonu- cleotide primer sequences for SYBR primers for *HK2, Glut1, HIF1α, PKM2, PFKFB3, GAPDH,* and *β-actin* are provided in Supplementary Table 1.

Immunoblotting

Primary human macrophages (1×10^6 cells/ml) were stimu- lated with micron or nano hydroxyapatite particles (250 μg/ml) for 3, 6, or 24 hours for the detection HK2 or GLUT1 protein. Cells were lysed by addition of RIPA buffer (Tris 50 mM; NaCl 150 mM; SDS 0.1%; sodium deoxycholate 0.5%; Triton X 100). Lysates were electrophoresed on SDS-PAGE gels (12% gel for GLUT1, 10% gel for HK2) and transferred to PVDF membranes (Millipore, Massachusetts) prior to detection with anti-HK2 (CST, 2867S) or anti-GLUT1 (abcam, 32551) antibodies (Supplementary Table 2). Densitometric analysis was performed using Bio-Rad software.

Seahorse analyser

Primary human macrophages were cultured at 1×10^6 cells/ml for 6 days prior to re-seeding at 2×10^5 cells/well in a Seahorse 96-well microplate and allowed to rest for 5 hours prior to micronHA or nanoHA (250 μg/ml) stimulation. The Seahorse cartridge plate was hydrated with XF calibrant fluid and incubated in a non-CO_2 incubator at 37°C for a minimum of 8 hours prior to use. To determine the effect of micronHA or nanoHA, macrophages were incubated with previously published doses of micronHA or nanoHA (250 μg/ml) for 3, 6, and 24 hours prior to analysis using a Seahorse XFe24 analyser. 30 min prior to placement into the XF/XFe analyser, cell culture medium was replaced with complete XF assay medium (Seahorse Biosciences; supplemented with 10 mM glucose, 1 mM sodium pyruvate, 2 mM L-glutamine, and pH adjusted to 7.4) and incubated in a non-CO_2 incubator at 37°C. Blank wells (XF assay medium only) were prepared without cells for subtracting the background oxygen consumption rate (OCR) and extracellular acidification rate (ECAR) during analysis. Oligomycin (1 μM; Cayman Chemicals), carbonyl cyanide-p-trifluoromethoxyphenylhydrazone (FCCP) (1 μM; Santa Cruz biotechnology), rotenone (500 nM), and antimycin A (500 nM) and 2-deoxy-D-glucose (2-DG) (25 mM; all Sigma–Aldrich) were prepared in XF assay medium and loaded into the appropriate injection ports on the cartridge plate and incu- bated for 10 min in a non-CO_2 incubator at 37°C. OCR and ECAR were measured over time with sequential injections of oligomycin, FCCP, rotenone and antimycin A, and 2-DG. Analysis of results was performed using Wave software (Agilent Technologies). The rates of basal glycolysis, max glycolysis, glycolytic reserve etc. were calculated as detailed in the manufacturer's protocol and supplied in Supplementary Table 3.

FLIM imaging and analysis

Primary human macrophages (1×10^6 cells/ml) were treated with micronHA or nanoHA (250 μg/ml) for 24 hours in phenol free RPMI. Two-photon excited NAD(P)H-FLIM imaging was used to measure levels of free and protein-bound NADH using a custom upright (Olympus BX61WI) laser multiphoton microscopy system equipped with Titanium:sapphire laser (Chameleon Ultra, Coherent, USA) and water-immersion 25 x objective (Olympus 1.05NA) with a temperature controlled stage. Two photon excitation of NAD(P)H was performed at an excitation wavelength of 760 nm and a 455/90 nm bandpass filter was used for NAD(P)H fluores- cence emission. 512×512 pixel images were acquired with a pixel dwell time of 3.81 μs and 30 s collection time. A Picoharp 300 TCSPC system operating in the time-tagged mode coupled with a photomultiplier detector assembly (PMA) hybrid detector (PicoQuanT GmbH, Germany) was used for fluorescence decay measurements yielding 256-time bins per pixel.

Fluorescence lifetime images with their associated decay curves for NAD(P)H were obtained and fitted using a double exponential decay curve for NAD(P)H, as previously described [25].

For NAD(P)H, a two-component fitting was also used to differentiate between the free (τ_1) and protein-bound (τ_2) NAD(P)H: the average lifetime (τ_{avg}) of NAD(P)H for each pixel was calculated by a weighted average of both free and bound lifetime contributions (Eq. (1)), with fraction α_1 relating to free NAD(P)H, and fraction α_2 corresponds to protein-bound NAD(P)H. Eq. 1:

$$\tau_{avg} = \frac{\tau_1 \times \alpha_1 + \tau_2 \times \alpha_2}{\alpha_1 + \alpha_2} \quad (1)$$

Confocal imaging of mitochondria

Primary human macrophages (1×10^6 cells/ml) were treated with micronHA or nanoHA (250 μg/ml) for 24 hours. Macrophages were incubated with MitoTracker Red CMXRos (Life technologies) (50 nM) and Hoescht (Thermofisher) (5 μg/ml), and maintained for 30 min at 37°C in a 5% CO_2 atmosphere. Images were taken using a Leica SP8 scanning confocal microscope at 63x magnification and imaged using Leica LASX Software. Micrographs were assessed for mitochondrial morphology with eccentricity and aspect ratios used as defining parameters in the analysis. This was performed using an automated script generated in CellProfiler.

Flow cytometry

Cells were stained with CD14 as cell marker and MitoSox Red™ or Mitotracker Red™ before being acquired using a FACSCantoTM II (BD Biosciences). The model antigen DQ-Ova, which fluoresces upon processing by proteases inside the cell, was used to assess phagocytic capacity of the cells. Macrophages were pre-treated with 2DG (25 mM), 3PO (10 μM), or cytochalasin B (5 μm) for 45 mins prior to being cultured with complete RPMI containing DQ- Ovalbumin (500 ng/ml; Invitrogen) for 20 min at 37°C, followed by incubation for 10 min at 4°C. Cells were then washed in PBS and immediately acquired. Cells were acquired on a FACSCanto TM II (BD Biosciences) and analysis was performed with FlowJo v.10 soft- ware (Tree Star Inc.). DQ-Ova gating shown in Supplemental Fig. S9.

Statistical analysis

Each experiment was performed in at least three healthy donors (defined by N). Paired one-way ANOVA or Kruskal–Wallis tests were used for the comparison of more than two groups for analysis, with the Tukey or Dunn's post-test (where applicable). All statistical analysis was performed on GraphPad Prism 9.00 (Graph- Pad Software). P value < 0.05 were deemed significant.

Results

MicronHA particles, but not nanoHA particles, upregulate surrogate markers of glycolysis in primary human macrophages

We have previously demonstrated that micronHA treatment results in the polarisation of primary human macrophages towards

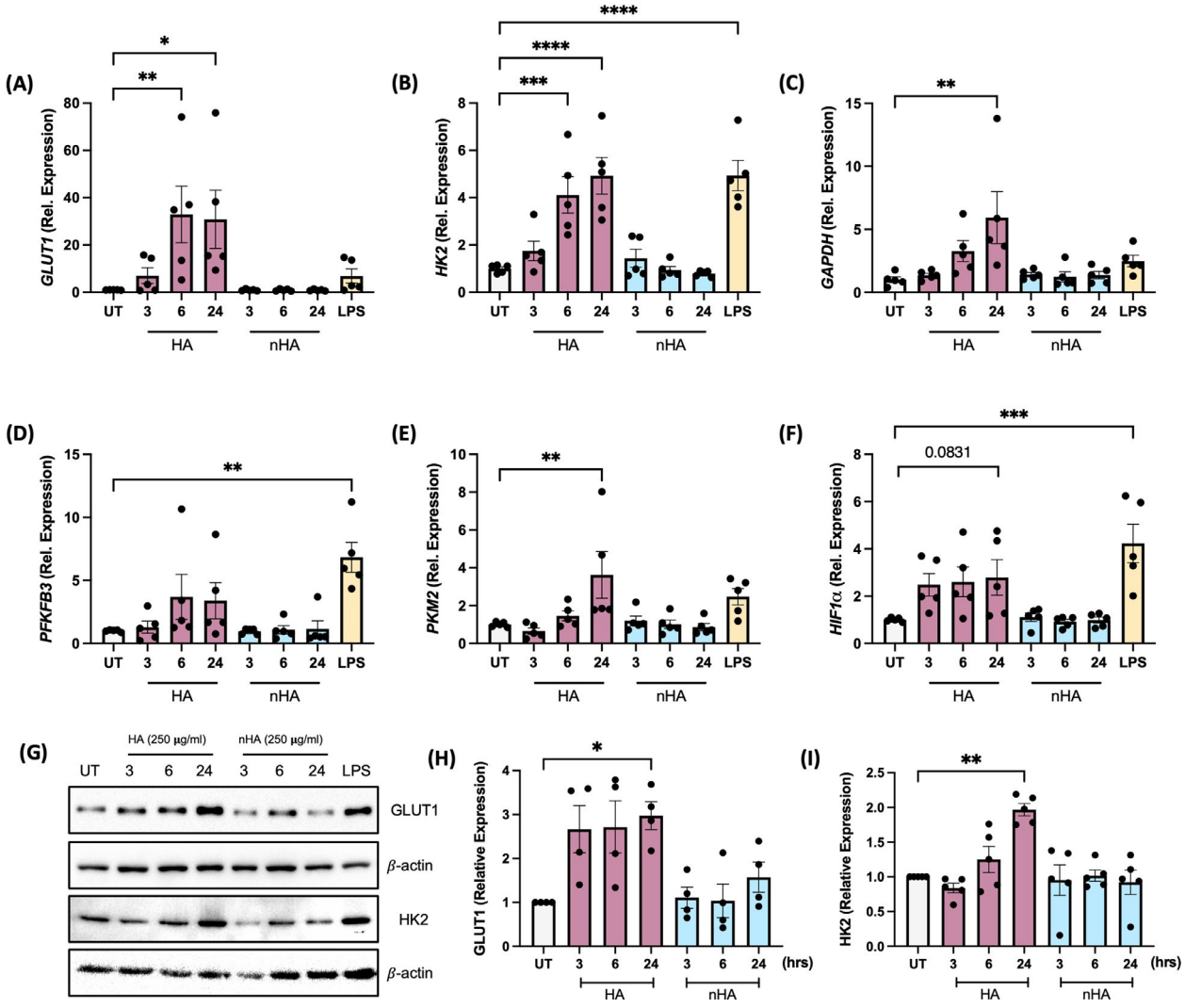

Fig. 1. MicronHA stimulation upregulates surrogate markers of glycolysis in primary human macrophages.
Primary human macrophages (1 × 10^6 cells/ml) were stimulated with particles (250 µg/ml) for 3, 6 or 24 hours. mRNA expression of glycolytic markers **(A)** *GLUT1*, **(B)** *HK2*, **(C)** *PFKFB3*, **(D)** *GAPDH*, **(E)** *HIF1α*, **(F)** *PKM2* were analysed by real-time PCR. Pooled data ($N = 5$) is represented as mean ± SEM. **(G)** Representative western blots demonstrating expression of GLUT1 and HK2 in whole cell lysates in response to micron or nanoHA particles post 3, 6 or 24 hour stimulation. **(H,I)** Pooled data (N = 4-5) depicting densitometric analysis of immunoblots using BioRad software. Bar graphs depict the mean ± SEM increase in protein expression relative to untreated control and normalised to β-actin housekeeping protein. Data was analysed using one-way ANOVA with Tukey post-test (*$P \leq 0.05$, ** $P \leq 0.01$, *** $P \leq 0.001$, **** $P \leq 0.0001$).

a pro-inflammatory phenotype, while nanoHA treatment preferentially results in anti-inflammatory macrophage polarisation [8,17]. As pro-inflammatory immune cell function is strongly associated with a metabolic shift to favour glycolysis [1], we first investi- gated the expression of genes encoding for key glycolytic markers upon micron and nanoHA treatment. Primary human macrophages were treated with micron or nanoHA particles over 3, 6, and 24 hours, or the positive control, LPS (100 ng/ml), for 24 hours, be- fore established markers of glycolysis were assessed using RT- qPCR. It was observed that *GLUT1*, which encodes for the glu- cose transporter, and *HK2*, the rate-limiting enzyme in glycolysis, were significantly upregulated at 6 and 24 hours post-stimulation with micronHA particles (Fig. 1A and B). The mRNA encoding glyceraldehyde-3-phosphate dehydrogenase (*GAPDH*) and pyruvate kinase M2 (*PKM2*), key enzymes involved in regulation of glycolysis, were also found to be significantly upregulated at 24 hours post micronHA stimulation (Fig. 1C and E). An increase in phosphofructokinase (*PFKFB3*) was observed at 6 and 24 hours in micronHA particle-treated macrophages, albeit this was not signifi- cant (Fig. 1D). This was also the case for the transcription factor, *HIF1α*, which is known to be upregulated in macrophages undergoing a metabolic shift towards glycolysis, where it translo- cates to the nucleus to upregulate expression of pro-inflammatory cytokines [22,23] (P=0.08 @ 24 hours) (Fig. 1F). In contrast, nanoHA did not appear to impact on expression of any of the glycolytic genes assessed (Fig. 1A-F). This suggests that exposure of macrophages to micronHA particles, but not nanoHA, induces enhanced transcription of key genes involved in glycolysis. Inter- estingly, we also observed an increase in glycolytic genes *GLUT1, HK2, GAPDH,* and *HIF1α* upon exposure to micronHA particles in macrophages pre-polarised to an M2-like phenotype with IL-4, al- though not to as great an extent as that achieved upon micronHA stimulation of untreated macrophages alone (Fig. S7). This suggests that the micron HA particles are still capable of promoting a gly- colytic phenotype even in the presence of M2 polarising stimuli, which are known to induce a greater reliance on oxidative phosphorylation.

Having observed an upregulation of key glycolytic markers upon stimulation with micron-sized HA, it was next of interest to validate this at the protein level. GLUT1 and HK2 were cho-

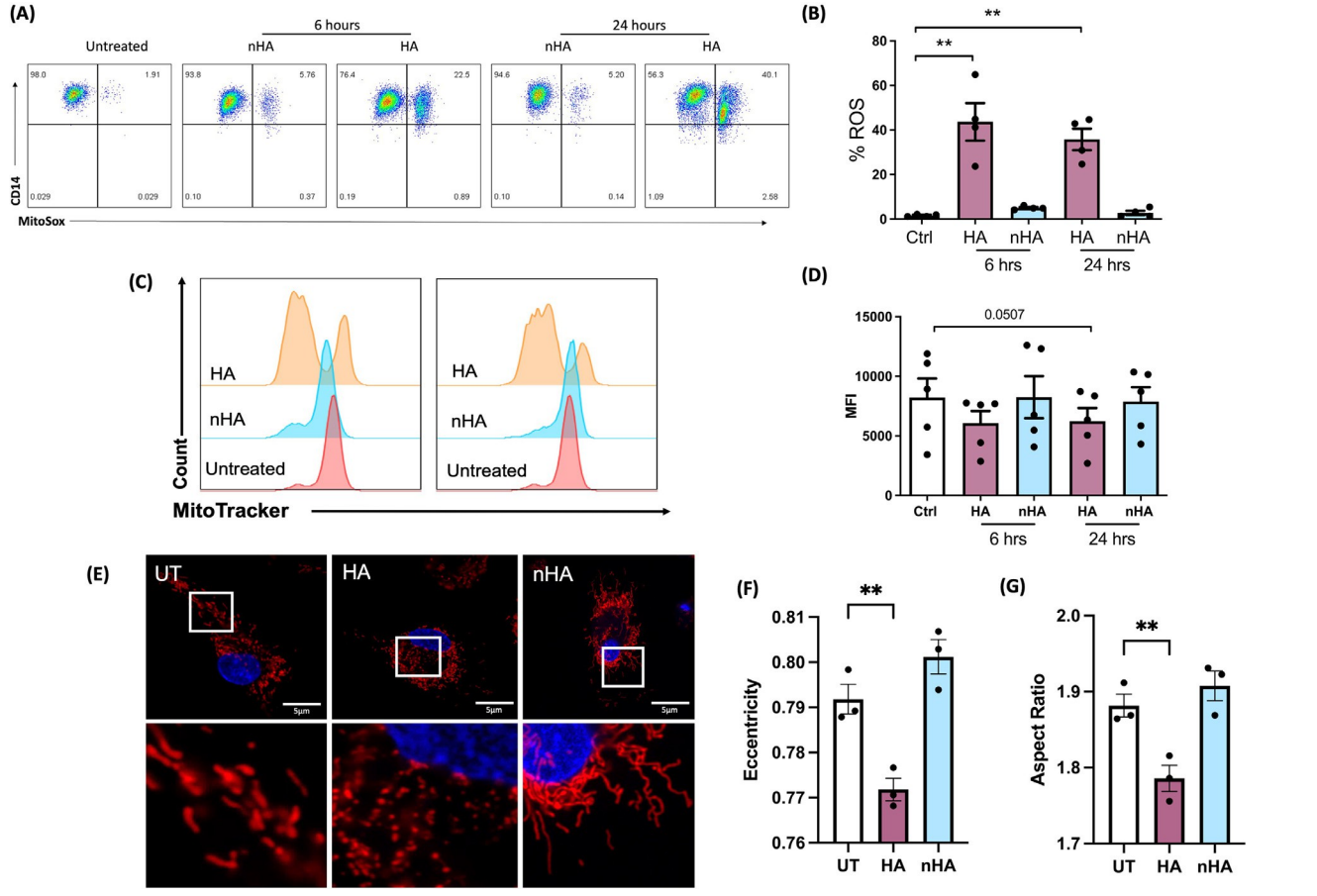

Fig. 2. MicronHA stimulation alters mitochondrial dynamics and drives mitochondrial ROS production in primary human macrophages.
(A) Representative dot plots depicting MitoSox Red staining in control, micronHA, and nanoHA stimulated macrophages from one representative experiment. **(B)** Pooled data ($N = 4$) depicting MitoSox Red staining in control, micronHA and nanoHA-treated macrophages. Results shown are mean percentages ± SEM of MitoSox™ positive cells. Mitochondrial biomass was measured by flow cytometry. **(C)** Histogram depicting Mitotracker Red staining in control, micronHA and nanoHA stimulated macrophages from one representative experiment. **(D)** Pooled data ($N = 5$) depicting Mitotracker Red staining in control, micronHA and nanoHA stimulated macrophages Results shown are mean ± SEM of the measured Mean Fluorescence Intensities (MFI). Primary human macrophages (1×10^6 cells) were stimulated with particles (250 μg/ml) for 24 hours. Cells were stained with MitoTracker Red™ (50 nM) for visualisation of the mitochondrial network and Hoechst 33342 (5 μg/μl) for visualisation of the nucleus. **(E)** Representative images of untreated, micronHA, and nanoHA stimulated primary human macrophages. **(F)** Eccentricity and **(G)** aspect ratio (measures of deviation from circularity) were calculated using CellProfiler ($N = 3$). Data was analysed using Kruskal Wallis with Dunn's post-test ($^{**}P < 0.01$).

sen, being the glucose transporter and first rate-limiting enzyme in glycolysis respectively, and therefore would provide reliable indication that the upregulation observed at the mRNA level was being translated to the protein level. Macrophages were treated with micron and nanoHA over 3, 6, and 24 hours, before assessment by immunoblotting. Both GLUT1 and HK2 were found to be upregulated over time, with peak induction occurring at 24 hours post micronHA stimulation (Fig. 1G). Densitometric analysis revealed a significant increase in GLUT1 and HK2 at 24 hours post micronHA stimulation (Fig. 1H,I). In contrast, nanoHA stimulated macrophages did not drive expression of GLUT1 or HK2, with levels found to be comparable to that of untreated control cells (Fig. 1G- I).

MicronHA particles alter mitochondrial dynamics in primary human macrophages

Alterations in mitochondrial dynamics are closely linked with the metabolic state of immune cells. Mitochondrial ROS (mROS) production occurs as a result of, and promotes, pro-inflammatory macrophage polarisation [24–26], and macrophages undergoing a shift to favour glycolysis exhibit a reduction in mitochon- drial biogenesis and hence mitochondrial mass [27,28]. It is also documented that mitochondrial fission, in which mitochondrial networks are broken apart into punctate structures, occurs in macrophages following LPS treatment and is associated with an upregulation in glycolysis [29,30]. Given the observed upregula- tion of surrogate glycolytic markers upon micronHA treatment, it was of interest to investigate whether mitochondrial dynamics are altered as a result of stimulation with micron and nanoHA par- ticles. Macrophages were treated with micron or nanoHA for 6 and 24 hours, then stained with CD14 and MitoSox Red™, which allows for detection of mROS production. It was found that mi- cronHA treatment significantly induced mROS production at 6 and 24 hours post-stimulation when compared to untreated control, an effect not observed for nanoHA treated macrophages (Fig. 2A and B).

Mitochondrial biogenesis was assessed using Mitotracker Red™ staining which links to thiol groups within the mitochondria and thus accumulates as mitochondrial mass increases. Macrophages were stained with Mitotracker Red™ for 6 or 24 hours and as- sessed using flow cytometry. It was found that micronHA treat- ment resulted in a loss of Mitotracker straining at 6 hours, and a non-significant decrease at 24 hours post micronHA stimulation. In contrast, there was no observable change between nanoHA stimu- lated macrophages and untreated control cells (Fig. 2C and D). This suggested that micronHA treatment resulted in a loss of mitochon- drial mass whilst nanoHA induced no change.

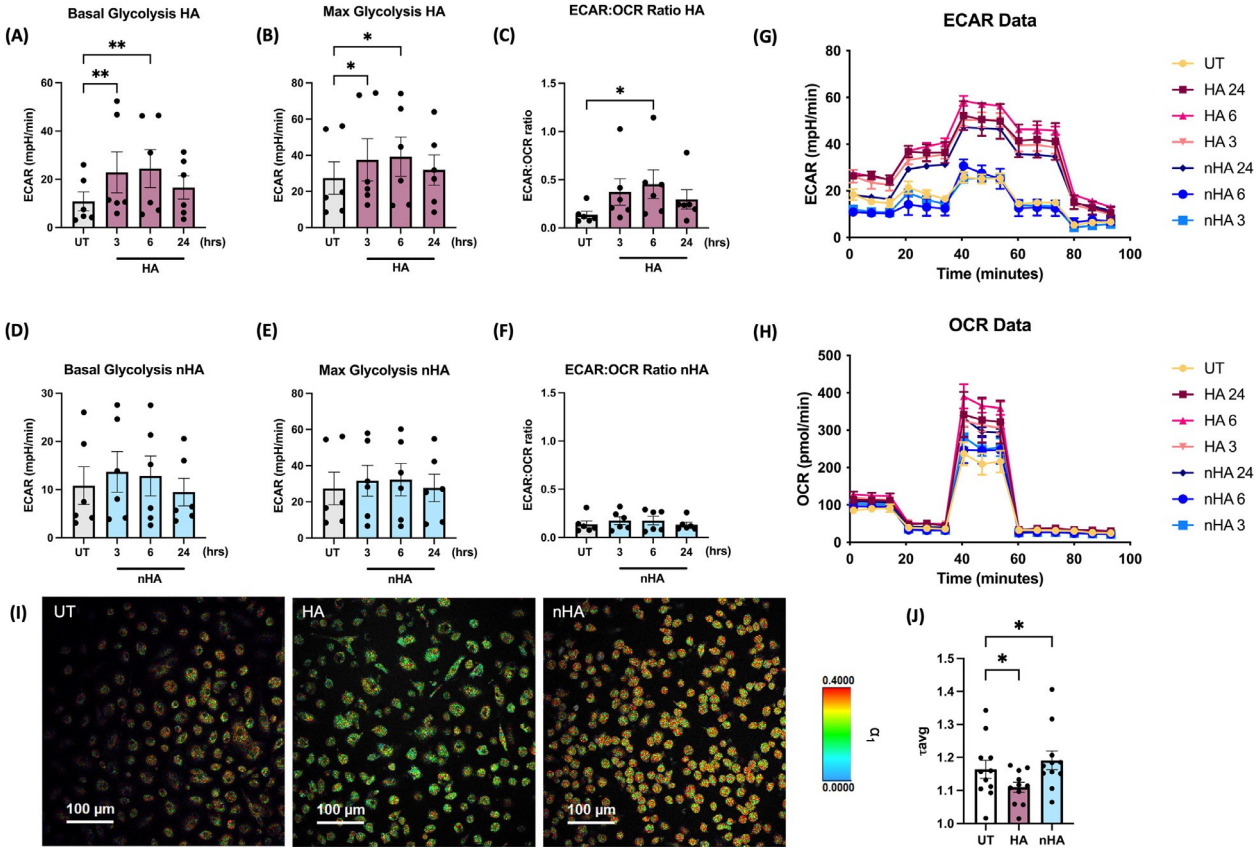

Fig. 3. Primary human macrophages stimulated with micronHA exhibit a bioenergetic shift to favour glycolysis.
Primary human macrophages (2×10^5 cells) were stimulated with particles (250 µg/ml) for 3, 6, or 24 hours. Seahorse data ($N = 6$) with bar graphs depicting **(A)** basal glycolysis, **(B)** max glycolysis, and **(C)** ECAR:OCR ratio of primary human macrophages in response to micronHA stimulation. Bar graphs depicting **(D)** basal glycolysis, **(E)** max glycolysis, and **(F)** ECAR:OCR ratio of primary human macrophages in response to nanoHA stimulation. **(G)** Representative glycolysis (ECAR) and **(H)** oxidative phosphorylation (OCR) Seahorse bioenergetic profiles before and after injections of oligomycin (1μM), FCCP (1μM), antimycin A (500 nM)/Rotenone (500 nM), and 2-DG (25 mM) post stimulation with micron and nanoHA (250 μg/ml). Cells were imaged using fluorescence lifetime imaging microscopy (FLIM) to assess the endogenously fluorescent metabolic molecule NADH. **(I)** Representative FLIM images from control, micronHA or nanoHA treated macrophages. **(J)** Bar graphs depicting the ratio of bound:free NADH (τ avg). Pooled data ($N = 11$) is represented as mean ± SEM. Data was analysed using Kruskal Wallis with Dunn's post-test for all Seahorse calculations and is represented as mean ± SEM (*$P \leq 0.05$, ** $P \leq 0.01$).

To further interrogate mitochondrial dynamics upon parti- cle stimulation, macrophages were stained with MitoTracker Red™ following stimulation with micron or nanoHA for 24 hours (Fig. 2E). The mitochondrial networks of micronHA treated macrophages showed significantly more punctate structures and had a lower aspect ratio and eccentricity (measures of deviation from circularity), indicating significantly more mitochondrial fis- sion in micronHA stimulated macrophages compared to untreated and nanoHA-treated counterparts (Fig. 2F and G). By contrast, and while not significant, there was a trend towards an increase in mitochondrial aspect ratio and eccentricity upon nanoHA particle stimulation, with mitochondrial structures appearing as fused net- works within the macrophages, indicating that nanoHA potentially promotes mitochondrial fusion (Fig. 2F and G). While further anal- ysis is required, this data suggests that micronHA particle stimula- tion promotes mitochondrial fission and hence a reduced reliance on oxidative phosphorylation, whilst nanoHA stimulation appears to favour mitochondrial fusion and suggests a greater reliance on oxidative phosphorylation.

MicronHA, but not nanoHA, favours a bioenergetic shift towards glycolysis in primary human macrophages

Having observed an upregulation of surrogate markers of gly- colysis as a result of micronHA treatment, as well as changes in mitochondrial dynamics in response to micron and nano-sized HA particles, it was next of interest to investigate the effect of HA particle size on the bioenergetic profile of macrophages. To this end, macrophage bioenergetics were assessed using the Seahorse XF analyser. Macrophages were seeded into a Seahorse microplate and stimulated with micron and nanoHA particles for 3, 6, or 24 hours. They were then placed in a Seahorse XF96 analyser in which the extracellular acidification rate (ECAR) and oxygen consump- tion rate (OCR) before and after injections of metabolic inhibitors oligomycin, FCCP, rotenone and antimycin A, and 2-deoxyglucose (2-DG) were measured. The basal and maximum rates of glycol- ysis were increased at all time-points with micronHA stimulation, with significance achieved at 3 and 6 hours post particle treatment (Fig. 3A and B). NanoHA stimulation, by contrast, did not upregu- late basal or max glycolysis in macrophages (Fig. 3D and E). Most notably, the ECAR:OCR ratio of micronHA treated macrophages was increased at all timepoints, with a significant increase occurring at 6 hours post micronHA stimulation (Fig. 3C). NanoHA treatment resulted in no observable increase in ECAR:OCR when compared to untreated control cells (Fig. 3F). Basal and max respiration, and res- piratory reserve, were modestly increased upon micronHA stimula- tion, with no significance achieved. This is reflected in the expres- sion of ox.phos-associated genes *ATP5b, MFN1,* and *MFN2* following treatment with micronHA, where increased *ATP5b* expression was observed at 24 hours post-micronHA stimulation, with no increase

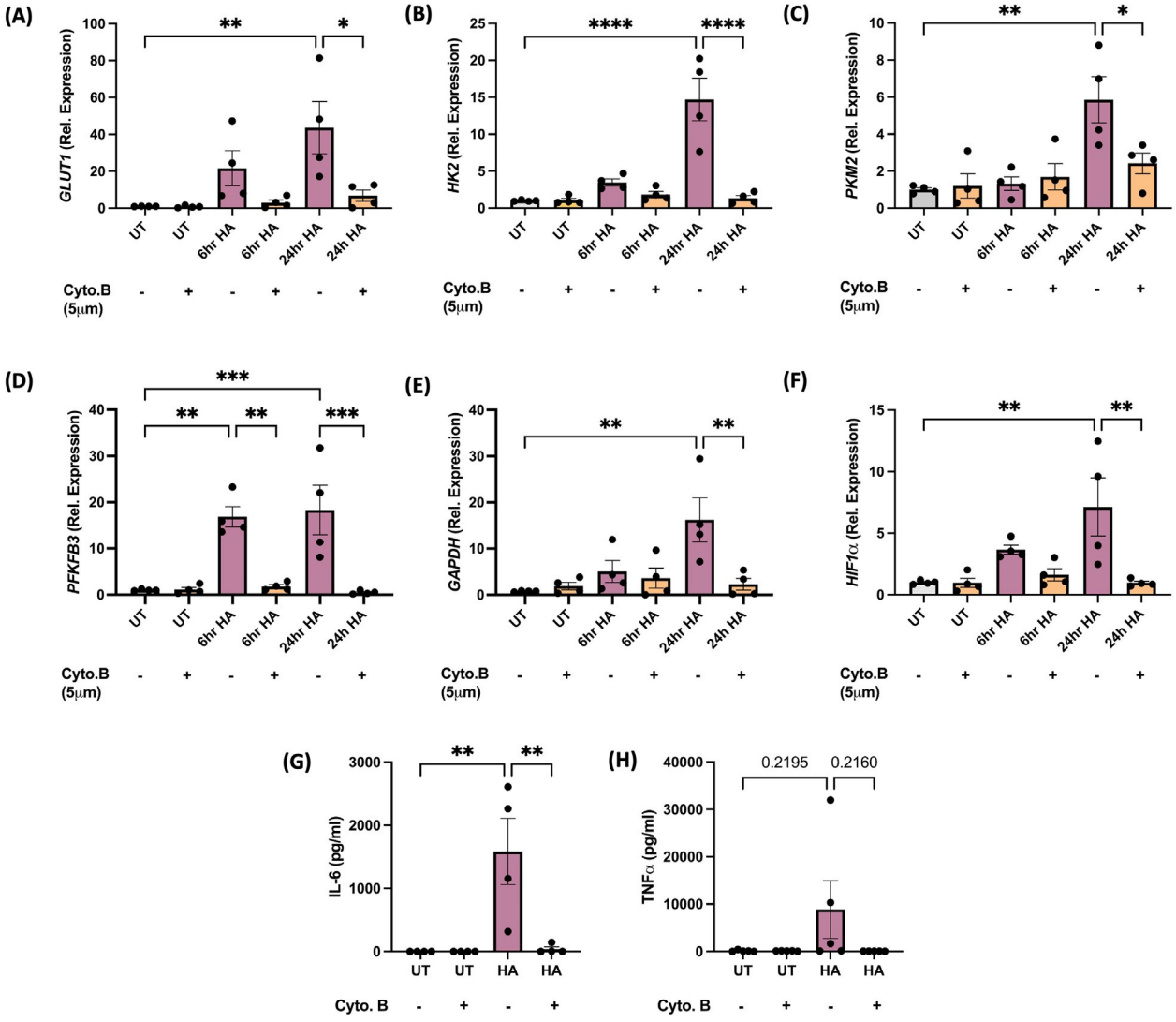

Fig. 4. Inhibition of phagocytosis attenuates micronHA-induced upregulation of surrogate markers of glycolysis and pro-inflammatory cytokine secretion in primary human macrophages.

Primary human macrophages (1×10^6 cells/ml) were stimulated with micronHA particles (250 μg/ml) for 6 or 24 hours in the presence or absence of phagocytic inhibitor cytochalasin B. mRNA expression of glycolytic markers **(A)** *GLUT1*, **(B)** *HK2*, **(C)** *PKM2* **(D)** *PFKFB3*, **(E)** *GAPDH*, **(F)** *HIF1α*, were assessed by RT-qPCR ($N = 4$). **(G,H)** Supernatants were assessed for IL-6 and TNFα production in the presence and absence of inhibitor, micronHA, or both inhibitor and micronHA ($N = 4$-5). Data was analysed using one-way ANOVA with Tukey post-test (*$P \leq 0.05$, ** $P \leq 0.01$, *** $P \leq 0.001$, **** $P \leq 0.0001$).

seen at 3 and 6 hours, and no differences in *MFN1* and *MFN2* expression seen at all timepoints (Fig. S8). NanoHA, by contrast, did not appear to alter macrophage respiration (Fig. S4).

In order to validate and complement the findings of our Seahorse analysis, an emerging non-invasive imaging technique termed fluorescence lifetime imaging microscopy (FLIM) was em- ployed, allowing for assessment of overall metabolic profile post- particle stimulation. FLIM provides a quantitative live readout of particle-stimulated macrophage metabolism based on the excited state lifetime of endogenously fluorescent NADH. Free NADH has a short emission lifetime and is associated with glycolysis, whereas protein bound NADH has a longer emission lifetime and is as- sociated with oxidative phosphorylation, thus providing a means to identify both forms of respiration. The calculated ratio of bound:free NADH is then used to indicate the metabolic state of the cell, with a lower τ_{avg} corresponding to a glycolytic metabolic profile and vice versa. Primary human macrophages were treated with micron or nanoHA for 24 hours to assess sustained metabolic profile and imaged using FLIM. MicronHA stimulated macrophages were found to have a significantly lower τ_{avg} than untreated and nanoHA stimulated macrophages, suggesting a heightened reliance on glycolysis as their primary metabolic pathway. NanoHA treated macrophages, by contrast, exhibited a significantly higher τ_{avg} than the untreated or micronHA treated macrophages, suggesting a preference for oxidative phosphorylation and a downregulation of glycolysis (Fig. 3I and J). FLIM also showed an increase in glycolysis upon micronHA exposure at 6 hours post-stimulation, whilst nanoHA-induced reliance on oxidative phosphorylation appeared modestly, although not significantly, increased (Fig. S5).

Inhibition of phagocytosis attenuates micronHA-induced upregulation of surrogate markers of glycolysis and pro-inflammatory cytokine secretion in primary human macrophages

In order to further investigate the mechanism by which metabolic alteration is induced in primary human macrophages in response to micronHA stimulation, and thus link metabolic pheno- type with pro-inflammatory polarisation, we investigated whether

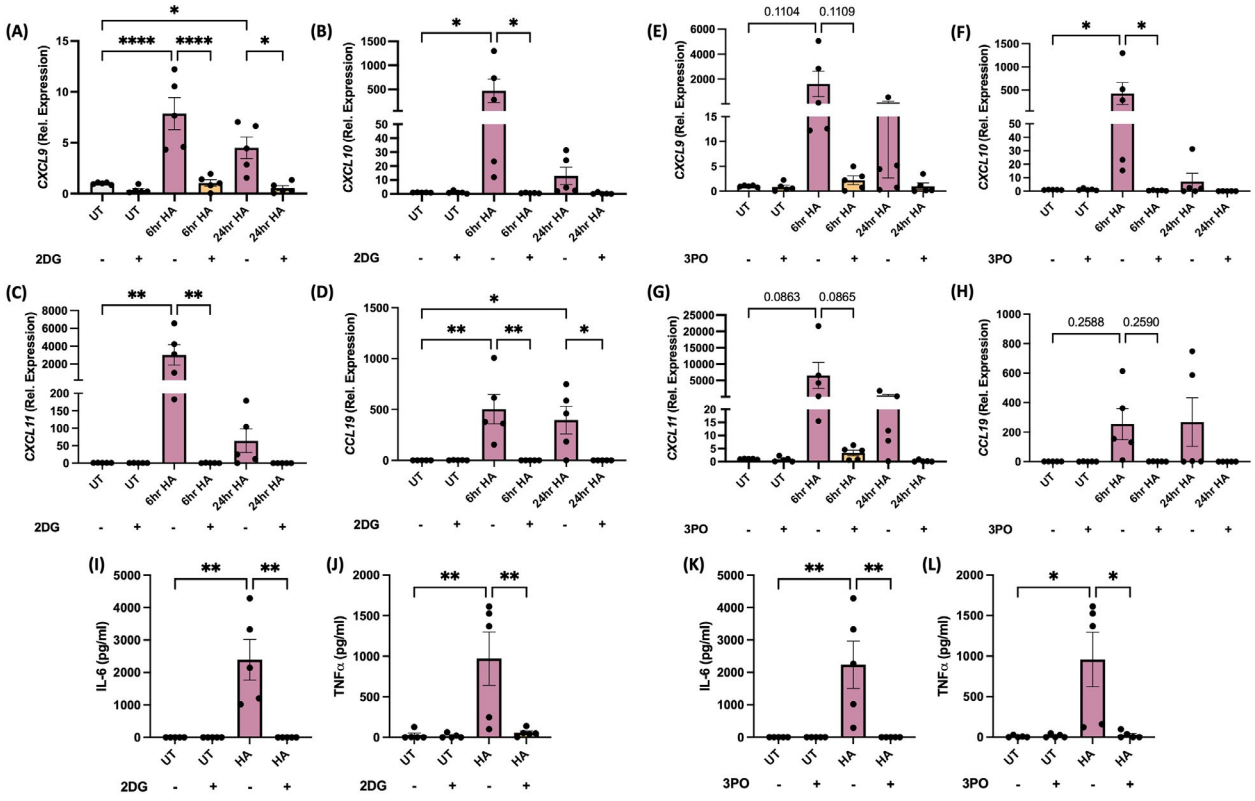

Fig. 5. Inhibition of glycolysis attenuates M1 macrophage marker expression in micronHA treated macrophages.
Primary human macrophages (1 × 10^6 cells/ml) were stimulated with micronHA particles (250 μg/ml) for 6 or 24 hours in the presence or absence of glycolytic inhibitors 2DG (25 mM) or 3PO (10 μm). mRNA expression of glycolytic markers **(A,E)** *CXCL9*, **(B,F)** *CXCL10*, **(C,G)** *CXCL11*, **(D,H)** *CCL19* were analysed by real-time PCR. Pooled data (N = 5) is represented as mean ± SEM. Supernatants were assessed for **(I,K)** IL-6 and **(J,L)** TNFα production in the presence and absence of inhibitor, micronHA, or both inhibitor and micronHA (N = 5). Data was analysed using one-way ANOVA with Tukey post-test (*$P \leq 0.05$, ** $P \leq 0.01$, **** $P \leq 0.0001$).

particle uptake is required for the observed effects on macrophage metabolism and effector function. To test this, macrophages were treated with the inhibitor of actin polymerization, cytochalasin B (5μm), for 45 minutes prior to stimulation with micronHA par- ticles, and then assessed for expression of surrogate markers of glycolysis *GLUT1, HK2, PKM2, PFKFB3, GAPDH*, and *HIF1α*. It was found that inhibition of phagocytosis significantly attenuated the upregulation of all surrogate markers assessed at 24 hours post- stimulation (Fig. 4A-F), with additional attenuation of *PFKFB3* at 6 hours post micronHA-stimulation (Fig. 4D). This was coupled to decreased secretion of micronHA-induced IL-6 (Fig. 4G) and a trend towards reduced expression of TNFα (Fig. 4H), suggesting that micronHA-induced metabolic rewiring to favour glycolysis and pro-inflammatory macrophage polarisation is dependent on par- ticle uptake. MicronHA-driven IL-8 was also found to be moder- ately decreased as a result of pre-treatment with cytochalasin B (Fig. S6).

Inhibition of glycolysis attenuates M1 macrophage marker expression in micronHA treated macrophages

Given the established link between macrophage metabolism and polarisation state, it was of interest to investigate whether metabolic alteration as a result of particle stimulation could be linked with the known effect of HA particle size on macrophage phenotype. RT-qPCR was used to investigate mRNA expression of M1-like macrophage markers *CXCL9, CXCL10, CXCL11,* and *CCL19* in macrophages treated with micronHA in the presence or absence of glycolytic inhibitors 2-DG (25 mM) or 3PO (10 μM). Results demonstrate that 2-DG potently inhibited micronHA-induced ex- pression of *CXCL9* and *CCL19* at 6 and 24 hours post stimulation (Fig. 5A and D). *CXCL10* and *CXCL11* were more highly expressed at 6 hours and both genes were inhibited by 2-DG at this time- point (Fig. 5B and C). 3PO, an inhibitor of PFKFB3, significantly re- duced mRNA expression of *CXCL10* at 6 hours post micronHA stim- ulation (Fig. 5F), while there was a trend towards decreased ex- pression of *CXCL9* and *CXCL11* (Fig. 5E and G). Although not signif- icant, a decrease in *CCL19* expression at 6 and 24 hours post mi- cronHA stimulation was also observed (Fig. 5H). To validate these findings at the protein level, secretion of the pro-inflammatory cy- tokines, IL-6 and TNFα, was assessed by ELISA. Pre-treatment of macrophages with 2-DG or 3PO was found to significantly decrease micronHA-induced production of both cytokines, confirming the observed attenuation of pro-inflammatory markers at the mRNA level (Fig. 5I-L). Production of pro-inflammatory cytokine IL-8 was assessed given its contributory role in recruitment of inflammatory cells and propagation of tissue destructive processes, with a signif- icant decrease in micronHA-driven induction observed upon 2-DG pretreatment, and a trend towards a reduction in micronHA-driven IL-8 secretion upon 3PO treatment (Fig. S6).

Discussion

Wear debris generated at the host-biomaterial interface of orthopaedic implants is known to mediate detrimental effects through interactions with innate immune cells. For example, in- soluble particulates such as hydroxyapatite crystals have been im- plicated as directly contributing to destructive arthropathy [31], and are well documented to resist digestion by macrophages [32]. This results in a host of clinical challenges, including peripros- thetic osteolysis at the implant site, and the eventual need for revi- sion/replacement surgeries. As a result, measures are currently un-

derway to mitigate these destructive processes, and investigations into nanoscale materials such as nanoHA have yielded promising results, with nano-scale particles reported to preferentially polarise macrophages to an anti-inflammatory, pro-regenerative phenotype [17]. It is also becoming increasingly evident that immune cell phenotype is intricately linked to metabolic status, and that dysregulated metabolic reprogramming contributes to inflamma- tory processes in a number of diseases including OA, RA, and di- abetes [2,33,34]. In this paper, we demonstrate for the first time that micron, but not nano-sized HA particles, drive a metabolic shift to favour glycolysis, as evidenced by increased expression of surrogate markets of glycolysis, changes in cellular bioener- getics, and altered mitochondrial dynamics. Uptake of the parti- cles is required for these metabolic changes to occur, while in- hibition of micronHA-driven metabolic reprogramming attenuates pro-inflammatory macrophage responses. We thus provide a novel mechanistic link between particle size, glycolytic profile, and pro-inflammatory macrophage polarisation.

It is now well established that pro-inflammatory macrophage polarisation correlates with metabolic rewiring to favour glycol- ysis over oxidative phosphorylation. Termed 'the Warburg effect', this phenomenon occurs even when oxygen is plentiful and facil- itates the production of biosynthetic intermediates needed for a rapid inflammatory response [1,35]. Key indicators of this shift in- clude upregulation of enzymes and proteins required to drive gly- colytic pathways. In line with this, treatment of macrophages with micronHA resulted in upregulation of *GLUT1*, *HK2, GAPDH, PFKFB3,* and *HIF1α*, in addition to *PKM2*, which is a key regulator of glycolytic pathways. It is worth noting that, while *GAPDH* is often used as a housekeeping gene for data normalisation, it functions as a key enzyme in the glycolytic pathway and, as we demonstrate with our micronHA particles, is altered by modulators of cellular metabolism. We would argue for the use of alternative housekeeping genes for studies in which glycolysis, and indeed metabolism in general, is under investigation.

While the extracellular acidification rate of the cells was increased upon micronHA stimulation compared to nanoHA treatment (demonstrating a significantly higher rate of glycolysis), we also observed an increase in basal and max respiration, indicating that micronHA treated macrophages are more metabolically active overall. It will therefore be of interest to examine a wider range of metabolic pathways such as fatty acid oxidation and the pentose phosphate pathway to further characterise the metabolic pheno- type induced by HA particle size.

In terms of mitochondrial morphology and function, it has been shown that macrophage mitochondrial networks undergo fission in response to pro-glycolytic stimuli such as LPS [30], and we now report that this phenomenon occurs upon stimulation with micron, but not nanoHA. This is accompanied by decreased mitochondrial mass and increased ROS production. Mitochondrial mass increases as immune cells shift to favour oxidative phosphorylation in re- sponse to M2-promoting stimuli such as IL-4 [27], while mitochon- drial mass decreases in mononuclear cells in inflammatory settings and conditions such as type II diabetes, in which mitochondria are known to undergo fission and exhibit membrane hyperpolar- isation [36]. It should be noted that, although not significant, we did observe a modest increase in mitochondrial fusion in nanoHA treated macrophages, suggesting that nanoHA treatment may be playing a role in the promotion of cellular respiration linked with their known activation state. More detailed studies of particle size and surface topography are required to determine if these proper- ties can be altered to promote favourable changes in mitochondrial bioenergetics. Of note, the micronHA particles used in this study have a mean size of 1.3 μm and we, and others, have demonstrated that particle size of >1 m can be conducive to pro-inflammatory macrophage polarisation [32,37-39]. Other studies have demonstrated that needle versus spherical shaped particles induce higher levels of pro-inflammatory cytokine secretion, hence it is possible that shape is also a determining factor in altering mitochondrial dynamics. Regarding ROS production, this has been implicated in the induction of bone resorption via the promotion of osteoclast differentiation [40]; therefore the increase in ROS observed in response to micronHA treatment may have further implications for the destructive processes that occur in periprosthetic inflamma- tion. Mitochondrial dysfunction is also known to prevent repolari- sation of M1-like macrophages to an M2-like state [41]; therefore, these combined effects on mitochondrial morphology and func- tion may preclude the pro-inflammatory to pro-reparative transi- tion necessary for normal healing processes to occur.

In summary, there is a growing body of research implicating particulate-mediated metabolic reprogramming as key driver of inflammation [6,8]. The list to date consists of endogenous disease-associated particulates such as gout-associated MSU crystals, osteoarthritis-associated calcium containing crystals and atherosclerosis-associated cholesterol crystals [6,7,42]. We can now add hydroxyapatite particles to this growing list of metabolic modulators. Other biomaterials such as PMMA particles likely have a similar effect, given their propensity to drive pro-inflammatory macrophage polarisation [32]. Indeed, and as mentioned above, further study will determine how particle size/shape can differentially affect metabolic pathways, and whether this can be artificially manipulated. Further research in this area may also lead to the identification of novel therapeutic targets. For example, inhibitors of PKM2 are currently being explored in the context of atherosclerosis [43] and SLE [44], while the metabolism altering drug, metformin, which is traditionally used to treat type II diabetes, is now showing potential as a treatment for autoimmune and inflammatory diseases, including RA and colitis [45,46]. Of note, it was recently demonstrated that a 3D-printed glass ceramic scaffold coated with the trace element, molybdenum, promotes M2 macrophage polarisation and a shift from glycolysis to oxidative phosphorylation in LPS-stimulated murine macrophages, as well as promoting periodontal tissue regeneration in canines [47]. Furthermore, metabolomics studies have identified anti-inflammatory metabolites such as itaconate and ß-hydroxybutyrate (BHB) that could potentially be incorporated into biomaterial scaffolds [48,49]. Of note, ^{1}H NMR metabolomics has emerged as a valuable technique for interrogating cellular metabolism on a deep level, allowing for a thorough characterisation of the intracellular metabolome of immune cells. Graphene-based nanoparticles were shown to induce different metabolic profiles in murine RAW 264.7 macrophages depending on their size and functionalisation, with flavin mononucleotide-stabilised pristine graphene (PF-FMN) particles from 200 – 400 nm, and 100 – 200 nm, capable of increasing nitric oxide production and altering metabolites such as phosphocreatine and creatine in a manner similar to that seen upon LPS treatment [50]. It has also been shown that murine RAW 264.7 macrophages alter their metabolism and inflammatory response upon exposure to silk, silica, and PLGA nanoparticles ranging from 100 – 125 nm [51]. This study posits ^{1}H NMR metabolomics as a useful means of identifying not only immunometabolic reprogramming induced by particulate materials, but allows for identification of metabolites and other metabolic pathways at play. These works also highlight the ability of other nanoparticles, in addition to the potential of our nanoHA, to modulate cellular metabolism and macrophage phenotype in a manner similar to that seen in this manuscript, with silica, silk, and PLGA particles inducing production of TNFα at concentrations of 500 μg/ml and induction of M1-like macrophage markers. This also emphasises that not only size, but also particle composition plays a role in dictating macrophage metabolic and functional responses, given that our nanoHA parti-

cles of 50 - 150 nm induce an anti-inflammatory macrophage by contrast.

Indeed, in our hands, treatment of human macrophages with glycolytic inhibitors prevented micron HA-driven pro-inflammatory macrophage polarisation and inflammatory cytokine production, suggesting that targeting this aspect of particulate induced inflammation warrants further *in vivo* investigation. This undoubtedly requires careful consideration given the potential for 'off-target' effects and the differential use of metabolic pathways by chondrocytes versus macrophages, for example. Furthermore, it is impor- tant to note that we use a limited number of macrophage sur- face markers to perform phenotypic analysis in this study. It is now widely accepted that the traditional "M1/M2" paradigm of macrophage classification is overly simplistic and it is far more likely that macrophages exhibit a much more complex response in displaying 'hybrid' phenotypic and functional characteristics of both pro and anti-inflammatory macrophages in response to ex- ternal stimuli [52,53]. Our findings nonetheless provide further in- sight into cellular changes that occur at the periprosthetic implant site and implicate metabolic targeting and/or manipulation as a potentially effective strategy for tempering adverse inflammatory processes associated with biomaterial implantation.

Conclusions

In this study, we demonstrate for the first time that macrophages alter their metabolic profile in response to hydroxyapatite exposure. Furthermore, we show that particle size is a determining factor in driving these changes. This not only broadens the range of immune cell parameters we can assess/manipulate when designing immune-informed biomaterials, but also highlights immunometabolism as a novel therapeutic avenue to explore in order to mitigate adverse post-implantation reactions.

Declaration of Competing Interest

The authors declare that they have no known competing financial interests or personal relationships that could have appeared to influence the work reported in this paper.

CRediT authorship contribution statement

Lianne C. Shanley: Conceptualization, Methodology, Data curation, Formal analysis, Writing – original draft, Investigation, Writing – review & editing. **Olwyn R. Mahon:** Conceptualization, Methodology, Data curation, Formal analysis, Investigation, Writing – review & editing. **Sinead A. O'Rourke:** Investigation. **Nuno G.B. Neto:** Investigation, Software. **Michael G. Monaghan:** Resources, Supervision, Funding acquisition. **Daniel J. Kelly:** Resources, Supervision, Funding acquisition. **Aisling Dunne:** Conceptualization, Methodology, Data curation, Formal analysis, Writing – original draft, Resources, Supervision, Funding acquisition.

Acknowledgements

This work was supported by Science Foundation Ireland (SFI), Ireland, through the Advanced Materials and Bioengineering Re- search (AMBER) Centre (SFI/12/RC/2278_P2, partly supported by the European Regional Development Fund).

Supplementary materials

Supplementary material associated with this article can be found, in the online version, at doi:10.1016/j.actbio.2023.01.058.

References

[1] L.A. O'Neill, R.J. Kishton, J. Rathmell, A guide to immunometabolism for immunologists, Nat. Rev. Immunol. 16 (9) (2016) 553–565.
[2] M. Biniecka, M. Canavan, T. McGarry, W. Gao, J. McCormick, S. Cregan, L. Gallagher, T. Smith, J.J. Phelan, J. Ryan, J. O'Sullivan, C.T. Ng, D.J. Veale, U. Fearon, Dysregulated bioenergetics: a key regulator of joint inflammation, Ann. Rheum. Dis. 75 (12) (2016) 2192–2200.
[3] C.H. Chang, J. Qiu, D. O'Sullivan, M.D. Buck, T. Noguchi, J.D. Curtis, Q. Chen, M. Gindin, M.M. Gubin, G.J. van der Windt, E. Tonc, R.D. Schreiber, E.J. Pearce, E.L. Pearce, Metabolic competition in the tumor microenvironment is a driver of cancer progression, Cell 162 (6) (2015) 1229–1241.
[4] C. La Rocca, F. Carbone, V. De Rosa, A. Colamatteo, M. Galgani, F. Perna, R. Lanzillo, V. Brescia Morra, G. Orefice, I. Cerillo, C. Florio, G.T. Maniscalco, M. Salvetti, D. Centonze, A. Uccelli, S. Longobardi, A. Visconti, G. Matarese, Immunometabolic profiling of T cells from patients with relapsing-remitting multiple sclerosis reveals an impairment in glycolysis and mitochondrial respiration, Metabolism 77 (2017) 39–46.
[5] L. Morel, Immunometabolism in systemic lupus erythematosus, Nat. Rev. Rheumatol. 13 (5) (2017) 280–290.
[6] S.A. O'Rourke, N.G.B. Neto, E. Devilly, L.C. Shanley, H.K. Fitzgerald, M.G. Monaghan, A. Dunne, Cholesterol crystals drive metabolic reprogramming and M1 macrophage polarisation in primary human macrophages, Atherosclerosis 352 (2022) 35–45.
[7] F. Renaudin, L. Orliaguet, F. Castelli, F. Fenaille, A. Prignon, F. Alzaid, C. Combes, A. Delvaux, Y. Adimy, M. Cohen-Solal, P. Richette, T. Bardin, J.P. Riveline, N. Venteclef, F. Lioté, L. Campillo-Gimenez, H.K. Ea, Gout and pseudo-gout-related crystals promote GLUT1-mediated glycolysis that governs NLRP3 and interleukin-1β activation on macrophages, Ann. Rheum. Dis. 79 (11) (2020) 1506–1514.
[8] O.R. Mahon, D.J. Kelly, G.M. McCarthy, A. Dunne, Osteoarthritis-associated basic calcium phosphate crystals alter immune cell metabolism and promote M1 macrophage polarization, Osteoarthr. Cartil. 28 (5) (2020) 603–612.
[9] M.P. Bernardo, B.C.R. da Silva, A.E.I. Hamouda, M.A.S. de Toledo, C. Schalla, S. Rütten, R. Goetzke, L.H.C. Mattoso, M. Zenke, A. Sechi, PLA/Hydroxyapatite scaffolds exhibit in vitro immunological inertness and promote robust osteogenic differentiation of human mesenchymal stem cells without osteogenic stimuli, Sci. Rep. 12 (1) (2022) 2333.
[10] N.A. Abdul Halim, M.Z. Hussein, M.K. Kandar, Nanomaterials-upconverted hydroxyapatite for bone tissue engineering and a platform for drug delivery, Int. J. Nanomed. 16 (2021) 6477–6496.
[11] H. Samadian, H. Mobasheri, M. Azami, R. Faridi-Majidi, Osteoconductive and electroactive carbon nanofibers/hydroxyapatite nanocomposite tailored for bone tissue engineering: in vitro and in vivo studies, Sci. Rep. 10 (1) (2020) 14853.
[12] D. Arcos, M. Vallet-Regí, Substituted hydroxyapatite coatings of bone implants, J. Mater. Chem. B 8 (9) (2020) 1781–1800.
[13] J. Fang, P. Li, X. Lu, L. Fang, X. Lü, F. Ren, A strong, tough, and osteoconductive hydroxyapatite mineralized polyacrylamide/dextran hydrogel for bone tissue regeneration, Acta Biomater. 88 (2019) 503–513.
[14] F. Lebre, R. Sridharan, M.J. Sawkins, D.J. Kelly, F.J. O'Brien, E.C. Lavelle, The shape and size of hydroxyapatite particles dictate inflammatory responses following implantation, Sci. Rep. 7 (1) (2017) 2922.
[15] P. Laquerriere, A. Grandjean-Laquerriere, E. Jallot, G. Balossier, P. Frayssinet, M. Guenounou, Importance of hydroxyapatite particles characteristics on cytokines production by human monocytes in vitro, Biomaterials 24 (16) (2003) 2739–2747.
[16] R.J. Christiansen, H.J. Münch, C.M. Bonefeld, J.P. Thyssen, J.J. Sloth, C. Geisler, K. Søballe, M.S. Jellesen, S.S. Jakobsen, Cytokine profile in patients with aseptic loosening of total hip replacements and its relation to metal release and metal allergy, J. Clin. Med. 8 (8) (2019).
[17] O.R. Mahon, D.C. Browe, T. Gonzalez-Fernandez, P. Pitacco, I.T. Whelan, S. Von Euw, C. Hobbs, V. Nicolosi, K.T. Cunningham, K.H.G. Mills, D.J. Kelly, A. Dunne, Nano-particle mediated M2 macrophage polarization enhances bone formation and MSC osteogenesis in an IL-10 dependent manner, Biomaterials 239 (2020) 119833.
[18] R. Wang, H. Hu, J. Guo, Q. Wang, J. Cao, H. Wang, G. Li, J. Mao, X. Zou, D. Chen, W. Tian, Nano-hydroxyapatite modulates osteoblast differentiation through autophagy induction via mTOR signaling pathway, J. Biomed. Nanotechnol. 15 (2) (2019) 405–415.
[19] F. Guo, C. Yuan, H. Huang, X. Deng, Z. Bian, D. Wang, K. Dou, L. Mei, Q. Zhou, Regulation of T cell responses by nano-hydroxyapatite to mediate the osteogenesis, Front. Bioeng. Biotechnol. 10 (2022) 884291.
[20] E.M. Corr, C.C. Cunningham, L. Helbert, G.M. McCarthy, A. Dunne, Osteoarthritis-associated basic calcium phosphate crystals activate membrane proximal kinases in human innate immune cells, Arthritis Res. Ther. 19 (1) (2017) 23.
[21] G.M. Cunniffe, F.J. O'Brien, S. Partap, T.J. Levingstone, K.T. Stanton, G.R. Dickson, The synthesis and characterization of nanophase hydroxyapatite using a novel dispersant-aided precipitation method, J. Biomed. Mater. Res. A 95 (4) (2010) 1142–1149.
[22] A.F. McGettrick, L.A.J. O'Neill, The role of HIF in immunity and inflammation, Cell Metab. 32 (4) (2020) 524–536.
[23] G.M. Tannahill, A.M. Curtis, J. Adamik, E.M. Palsson-McDermott, A.F. McGettrick, G. Goel, C. Frezza, N.J. Bernard, B. Kelly, N.H. Foley, L. Zheng, A. Gardet, Z. Tong, S.S. Jany, S.C. Corr, M. Haneklaus, B.E. Caffrey, K. Pierce, S. Walmsley, F.C. Beasley, E. Cummins, V. Nizet, M. Whyte, C.T. Taylor, H. Lin, S.L. Masters,

E. Gottlieb, V.P. Kelly, C. Clish, P.E. Auron, R.J. Xavier, L.A. O'Neill, Succinate is an inflammatory signal that induces IL-1β through HIF-1α, Nature 496 (7444) (2013) 238–242.

[24] M. Canton, R. Sánchez-Rodríguez, I. Spera, F.C. Venegas, M. Favia, A. Viola, A. Castegna, Reactive oxygen species in macrophages: sources and targets, Front. Immunol. 12 (2021) 734229.

[25] S.Y. Kim, J.M. Jeong, S.J. Kim, W. Seo, M.H. Kim, W.M. Choi, W. Yoo, J.H. Lee, Y.R. Shim, H.S. Yi, Y.S. Lee, H.S. Eun, B.S. Lee, K. Chun, S.J. Kang, S.C. Kim, B. Gao, G. Kunos, H.M. Kim, W.I. Jeong, Pro-inflammatory hepatic macrophages generate ROS through NADPH oxidase 2 via endocytosis of monomeric TLR4-MD2 complex, Nat. Commun. 8 (1) (2017) 2247.

[26] B. Brüne, N. Dehne, N. Grossmann, M. Jung, D. Namgaladze, T. Schmid, A. von Knethen, A. Weigert, Redox control of inflammation in macrophages, Antioxid. Redox. Signal. 19 (6) (2013) 595–637.

[27] Q. Yu, Y. Wang, L. Dong, Y. He, R. Liu, Q. Yang, Y. Cao, A. Jia, Y. Bi, G. Liu, Regulations of glycolytic activities on macrophages functions in tumor and infectious inflammation, Front. Cell Infect. Microbiol. 10 (2020) 287.

[28] W. Yu, X. Wang, J. Zhao, R. Liu, J. Liu, Z. Wang, J. Peng, H. Wu, X. Zhang, Z. Long, D. Kong, W. Li, C. Hai, Stat2-Drp1 mediated mitochondrial mass increase is necessary for pro-inflammatory differentiation of macrophages, Redox. Biol. 37 (2020) 101761.

[29] Y. Wang, N. Li, X. Zhang, T. Horng, Mitochondrial metabolism regulates macrophage biology, J. Biol. Chem. 297 (1) (2021) 100904.

[30] R. Kapetanovic, S.F. Afroz, D. Ramnath, G.M. Lawrence, T. Okada, J.E. Curson, J. de Bruin, D.P. Fairlie, K. Schroder, J.C. St John, A. Blumenthal, M.J. Sweet, Lipopolysaccharide promotes Drp1-dependent mitochondrial fission and associated inflammatory responses in macrophages, Immunol. Cell Biol. 98 (7) (2020) 528–539.

[31] C. Jin, P. Frayssinet, R. Pelker, D. Cwirka, B. Hu, A. Vignery, S.C. Eisenbarth, R.A. Flavell, NLRP3 inflammasome plays a critical role in the pathogenesis of hydroxyapatite-associated arthropathy, Proc. Natl. Acad. Sci. U. S. A. 108 (36) (2011) 14867–14872.

[32] O.R. Mahon, S. O'Hanlon, C.C. Cunningham, G.M. McCarthy, C. Hobbs, V. Nicolosi, D.J. Kelly, A. Dunne, Orthopaedic implant materials drive M1 macrophage polarization in a spleen tyrosine kinase- and mitogen-activated protein kinase-dependent manner, Acta Biomater. 65 (2018) 426–435.

[33] U. Fearon, M.M. Hanlon, S.M. Wade, J.M. Fletcher, Altered metabolic pathways regulate synovial inflammation in rheumatoid arthritis, Clin. Exp. Immunol. 197 (2) (2019) 170–180.

[34] F.M. Davis, A. denDekker, A. Kimball, A.D. Joshi, M. El Azzouny, S.J. Wolf, A.T. Obi, J. Lipinski, J.E. Gudjonsson, X. Xing, O. Plazyo, C. Audu, W.J. Melvin, K. Singer, P.K. Henke, B.B. Moore, C. Burant, S.L. Kunkel, K.A. Gallagher, Epigenetic regulation of TLR4 in diabetic macrophages modulates immunometabolism and wound repair, J. Immunol. (2020).

[35] E.M. Pålsson-McDermott, L.A.J. O'Neill, Targeting immunometabolism as an anti-inflammatory strategy, Cell Res. 30 (4) (2020) 300–314.

[36] M.E. Widlansky, J. Wang, S.M. Shenouda, T.M. Hagen, A.R. Smith, T.J. Kizhakekuttu, M.A. Kluge, D. Weihrauch, D.D. Gutterman, J.A. Vita, Altered mitochondrial membrane potential, mass, and morphology in the mononuclear cells of humans with type 2 diabetes, Transl. Res. 156 (1) (2010) 15–25.

[37] J. Herman, B. Le Goff, J. De Lima, R. Brion, C. Chevalier, F. Blanchard, C. Darrieutort-Laffite, Pro-inflammatory effects of human apatite crystals extracted from patients suffering from calcific tendinopathy, Arthritis Res. Ther. 23 (1) (2021) 131.

[38] I. Nadra, A.R. Boccaccini, P. Philippidis, L.C. Whelan, G.M. McCarthy, D.O. Haskard, R.C. Landis, Effect of particle size on hydroxyapatite crystal-induced tumor necrosis factor alpha secretion by macrophages, Atherosclerosis 196 (1) (2008) 98–105.

[39] A. Grandjean-Laquerriere, O. Tabary, J. Jacquot, D. Richard, P. Frayssinet, M. Guenounou, D. Laurent-Maquin, P. Laquerriere, S. Gangloff, Involvement of toll-like receptor 4 in the inflammatory reaction induced by hydroxyapatite particles, Biomaterials 28 (3) (2007) 400–404.

[40] T.S. Agidigbi, C. Kim, Reactive oxygen species in osteoclast differentiation and possible pharmaceutical targets of ROS-mediated osteoclast diseases, Int. J. Mol. Sci. 20 (14) (2019).

[41] J. Van den Bossche, J. Baardman, N.A. Otto, S. van der Velden, A.E. Neele, S.M. van den Berg, R. Luque-Martin, H.J. Chen, M.C. Boshuizen, M. Ahmed, M.A. Hoeksema, A.F. de Vos, M.P. de Winther, Mitochondrial dysfunction prevents repolarization of inflammatory macrophages, Cell Rep. 17 (3) (2016) 684–696.

[42] I. Cobo, A. Cheng, J. Murillo-Saich, R. Coras, A. Torres, Y. Abe, A.J. Lana, J. Schlachetzki, R. Liu-Bryan, R. Terkeltaub, E. Sanchez-Lopez, C.K. Glass, M. Guma, Monosodium urate crystals regulate a unique JNK-dependent macrophage metabolic and inflammatory response, Cell Rep. 38 (10) (2022) 110489.

[43] P. Doddapattar, R. Dev, M. Ghatge, R.B. Patel, M. Jain, N. Dhanesha, S.R. Lentz, A.K. Chauhan, Myeloid cell PKM2 deletion enhances efferocytosis and reduces atherosclerosis, Circ. Res. 130(9) (2022) 1289-1305.

[44] X. Zhang, Y. Yang, L. Jing, W. Zhai, H. Zhang, Q. Ma, C. Li, F. Yan, D. Cheng, J. Zhang, Z. Ning, H. Shi, C. Wang, M. Zhao, J. Dai, Z. Li, J. Ming, M. Yu, H. Wang, H. Cheng, H. Xiong, G. Dong, Pyruvate kinase M2 contributes to TLR-mediated inflammation and autoimmunity by promoting Pyk2 activation, Front. Immunol. 12 (2021) 680068.

[45] S.Y. Lee, S.H. Lee, E.J. Yang, E.K. Kim, J.K. Kim, D.Y. Shin, M.L. Cho, Metformin ameliorates inflammatory bowel disease by suppression of the stat3 signaling pathway and regulation of the between Th17/Treg balance, PLoS One 10 (9) (2015) e0135858.

[46] H.J. Son, J. Lee, S.Y. Lee, E.K. Kim, M.J. Park, K.W. Kim, S.H. Park, M.L. Cho, Metformin attenuates experimental autoimmune arthritis through reciprocal regulation of Th17/Treg balance and osteoclastogenesis, Mediators Inflamm. 2014 (2014) 973986.

[47] X.T. He, X. Li, M. Zhang, B.M. Tian, L.J. Sun, C.S. Bi, D.K. Deng, H. Zhou, H.L. Qu, C. Wu, F.M. Chen, Role of molybdenum in material immunomodulation and periodontal wound healing: Targeting immunometabolism and mitochondrial function for macrophage modulation, Biomaterials 283 (2022) 121439.

[48] Y.H. Youm, K.Y. Nguyen, R.W. Grant, E.L. Goldberg, M. Bodogai, D. Kim, D. D'Agostino, N. Planavsky, C. Lupfer, T.D. Kanneganti, S. Kang, T.L. Horvath, T.M. Fahmy, P.A. Crawford, A. Biragyn, E. Alnemri, V.D. Dixit, The ketone metabolite β-hydroxybutyrate blocks NLRP3 inflammasome-mediated inflammatory disease, Nat. Med. 21 (3) (2015) 263–269.

[49] L.D. Huyer, S. Mandla, Y. Wang, S. Campbell, B. Yee, C. Euler, B.F. Lai, D. Bannerman, D.S.Y. Lin, M. Montgomery, K. Nemr, T. Bender, S. Epelman, R. Mahadevan, M. Radisic, Macrophage immunomodulation through new polymers that recapitulate functional effects of itaconate as a power house of innate immunity, Adv. Funct. Mater. 31 (6) (2021).

[50] M. Cicuéndez, M. Fernandes, M. Ayán-Varela, H. Oliveira, M.J. Feito, R. Diez-Orejas, J.I. Paredes, S. Villar-Rodil, M. Vila, M.T. Portolés, I.F. Duarte, Macrophage inflammatory and metabolic responses to graphene-based nanomaterials differing in size and functionalization, Colloids Surf. B 186 (2020) 110709.

[51] R. Saborano, T. Wongpinyochit, J.D. Totten, B.F. Johnston, F.P. Seib, I.F. Duarte, Metabolic reprogramming of macrophages exposed to silk, poly(lactic-co-glycolic acid), and silica nanoparticles, Adv. Healthc. Mater. 6 (14) (2017).

[52] O.R. Mahon, D.C. Browe, P.J. Diaz-Payno, P. Pitacco, K.T. Cunningham, K.H.G. Mills, A. Dunne, D.J. Kelly, Extracellular matrix scaffolds derived from different musculoskeletal tissues drive distinct macrophage phenotypes and direct tissue-specific cellular differentiation, J. Immunol. Regenerat. Med. 12 (2021).

[53] C.E. Witherel, K. Sao, B.K. Brisson, B. Han, S.W. Volk, R.J. Petrie, L. Han, K.L. Spiller, Regulation of extracellular matrix assembly and structure by hybrid M1/M2 macrophages, Biomaterials 269 (2021) 120667.

Minireview

Endogenous drivers of altered immune cell metabolism

Lianne C Shanley[1,2], Hannah K Fitzgerald[1], Sinead A O'Rourke[1,3] and Aisling Dunne[1,2,4]

[1]School of Biochemistry & Immunology, Trinity College, University of Dublin, Dublin 2, Ireland; [2]Centre for Advanced Materials and Bioengineering Research (AMBER), Trinity College Dublin, Dublin 2, Ireland; [3]School of Engineering, Trinity College, University of Dublin, Dublin 2, Ireland; [4]School of Medicine, Trinity College, University of Dublin, Dublin 2, Ireland
Corresponding author: Aisling Dunne. Email: aidunne@tcd.ie

Impact Statement

Metabolic reprogramming of immune cells has emerged as a central mechanism governing the control of cell fate and function. Furthermore, the finding that dysregulated immunometabolism is a feature of many inflammatory and autoimmune disorders has opened up new therapeutic possibilities. Our knowledge of this area is continuing to grow, and in this review, we focus on damage or disease–associated molecular patterns (DAMPs), which are now coming to the fore as drivers of altered immune cell metabolism. This adds to a growing body of evidence highlighting the dynamic cross-talk between metabolic process and immune effector mechanisms. Furthermore, it underscores a new facet of DAMPs and expands our knowledge of how they contribute to sterile inflammatory disease.

Abstract

Dysregulated metabolism has long been recognized as a feature of many metabolic disorders. However, recent studies demonstrating that metabolic reprogramming occurs in immune cells have led to a growing interest in the relationship between metabolic rewiring and immune-mediated disease pathogeneses. It is clear now that immune cell subsets engage in different metabolic pathways depending on their activation and/or maturation state. As a result, it may be possible to modulate metabolic reprogramming for clinical benefit. In this review, we provide an overview of immune cell metabolism with focus on endogenous drivers of metabolic reprogramming given their link to a number of immune-mediated disorders.

Keywords: Immunometabolism, cellular respiration, metabolic reprogramming, damage or disease-associated molecular patterns

Experimental Biology and Medicine **2022; 247: 2192–2200. DOI: 10.1177/15353702221134093**

Introduction

Cellular respiration and fatty acid metabolism

Cellular respiration is a multistep, catabolic process, typically utilizing glucose as an energy source to drive the generation of adenosine triphosphate (ATP). Glucose first passes through glycolysis, which takes place in the cytosol of the cell. The first step in this pathway is catalyzed by the rate-limiting enzyme hexokinase 2 (HK2), which irreversibly phosphorylates glucose, resulting in the generation of glucose-6-phosphate. Glucose-6-phosphate is isomerized to fructose-6-phosphate, which is then converted to fruc- tose-1,6-bisphosphate by the enzyme phosphofructokinase, another key regulatory enzyme catalyzing an irreversible step in this pathway. Fructose-1,6-biphosphate is unstable, and is split into two sugars: glyceraldehyde-3-phosphate, which continues through the remaining steps in the glycolytic pathway, and dihydroxyacetone phosphate, which cannot continue through glycolysis unless it is first converted to glyceraldehyde-3-phosphate. The remaining steps in glycolysis are reversible, until the final step, which is catalyzed by pyruvate kinase. Under normoxic conditions, pyruvate is generated which passes further through the respiratory chain. However, glycolysis can also occur in the absence of oxygen (anaerobic glycolysis), resulting in the generation of lactate. Although glycolysis is a relatively fast process, it is relatively inefficient in terms of energy production, resulting in the generation of only two ATP molecules. Despite this low energy yield, it is the primary pathway for the generation of many intermediates that are utilized to produce nucleotides, fatty acids, and amino acids.

In order to yield additional energy, pyruvate is oxidized to acetyl-CoA, which then enters the tricarboxylic acid (TCA) cycle inside the mitochondria. The TCA cycle (also

Copyright © 2022 by the Society for Experimental Biology and Medicine

known as the Krebs cycle) is more efficient in terms of ATP production compared to glycolysis, and occurs in conjunction with oxidative phosphorylation in cells that are in a quiescent or non-proliferative state. Acetyl-CoA is first oxidized to CO_2, leading to the production of the intermediate metabolites, citrate and isocitrate. As isocitrate converts to α-ketoglutarate, CO_2 is produced and nicotinamide adenine dinucleotide (NAD^+) is reduced to NADH. α-ketoglutarate is converted to succinyl CoA by α-ketoglutarate dehydrogenase, and ATP is generated upon conversion of succinyl-CoA to succinate, which is then further converted to fumarate via the action of succinate dehydrogenase. Flavin adenine dinucleotide (FAD) is reduced to $FADH_2$ during this reaction, and fumarate is subsequently converted to malate. Finally, malate is converted to oxaloacetate (which is again accompanied by the reduction of NAD^+ to $NADH_2$), with oxaloacetate condensing with acetyl-CoA to form citrate, hence the term TCA "cycle." When intact, this fuels the process of oxidative phosphorylation (OXPHOS), whereby NADH and FADH function as sources of electrons that contribute to energy generation via a proton gradient set up by the electron transport chain that, in turn, powers ATP synthase. The electron transport chain is located at the inner mitochondrial membrane and consists of a series of complexes (I–V) and two electron carriers (coenzyme Q and cytochrome c). NADH donates electrons to complex I while $FADH_2$ donates electrons to complex II. This process powers the pumping of protons from the matrix into the intermembrane space and an electrochemical gradient is established, termed the "proton motive force." This then powers the final complex, ATP synthase, which operates by combining adenosine di-phosphate (ADP) and inorganic phosphate (Pi), resulting in the generation of ATP. This process is generally slower than glycolysis; however, the yield of ATP (32 molecules) is much higher.

Fatty acid metabolism consists of two pathways: fatty acid synthesis (FAS) and fatty acid oxidation (FAO). FAS, an anabolic process, generates fatty acids which act as precursors for other compounds. FAS takes place in the cytosol of the cell, and begins when acetyl-CoA exits the TCA cycle in the mitochondria and enters the cytosol, where it is carboxylated by acetyl-CoA carboxylase (ACC) to form malonyl-CoA. This is the first committed step in this pathway. Malonyl-CoA then continues through the remaining steps in FAS, which are catalyzed by enzymes known as fatty acid synthases (FASN). This results in the production of a 16-carbon palmitic acid, which can act as a building block for other compounds including phospholipids and hormones. However, in the catabolic process of FAO, or beta-oxidation as it is also known, fatty acids are broken down to generate energy. Fatty acids enter the cell and are first converted to acyl-CoA in order to be able to enter the mitochondria. Acyl-CoA enters the mitochondria through the carnitine shuttle, the first step of which is catalyzed by carnitine palmitoyltransferase 1 (CPT1), where acyl-CoA is temporarily transferred to carnitine. This acyl-carnitine is shuttled into the mitochondria while carnitine is shuttled out, before being converted back to acyl-CoA once inside. The acyl-CoA then continues through the four steps of FAO, resulting in the generation of acetyl-CoA, which can then enter the TCA cycle.

Regulation of cellular respiration

Engagement of cellular respiration is controlled in a number of ways, including regulation through feedback mechanisms by the enzymes and products involved in this process. Mammalian target of rapamycin (mTOR), which forms part of the mTORC1 complex, functions as a cellular energy and nutrient sensor and controls protein synthesis and other cellular processes including anabolic pathways, such as glycolysis. Activation of mTORC1 results in the induction of a number of glycolytic genes, including the glucose transporter, GLUT1, which transports glucose into the cell, and HK2, the enzyme crucial for the phosphorylation of glucose in the first step of glycolysis.[1] These glycolytic genes are upregulated by the mTORC1 pathway upon activation of the transcription factor hypoxia-inducible factor 1 (HIF1α).[1] mTOR also promotes FAS through activation of sterol regulatory element binding protein (SREBP), which activates the enzyme ACC. This results in the carboxylation of acetyl-CoA to malonyl-CoA. When malonyl-CoA becomes committed to FAS, FAO is subsequently inhibited, occurring as a result of ACC-mediated inhibition of the FAO-associated enzyme, CPT. The block on FAO can be lifted following inhibition of FAS by 5′ adenosine monophosphate–activated protein kinase (AMPK). This enzyme inhibits FAS in two ways: first by directly inhibiting mTOR activation, and second by phosphorylating and inactivating the FAS-associated enzyme, ACC (Figure 1).[2]

Immune cell metabolism

In 1956, Otto Warburg first observed that some cancer cells increase glucose uptake and glycolysis, despite the presence of oxygen.[3] Referred to as the "Warburg effect," this phenomenon has now been observed in other cell types, including activated immune cells where energy demands are increased. For example, despite the TCA cycle and oxidative phosphorylation generally remaining functional in activated dendritic cells (DCs) and macrophages, glycolytic rate is increased concomitant with a decrease in mitochondrial energy generation.[4,5] Many effector T cell subsets – including $CD8^+$ T cells, Th1, Th2, and Th17 cells – alter their metabolism in a similar manner to the innate immune cells specified above.[6] In the case of pro-inflammatory classically activated (M1) macrophages and activated DC, the TCA cycle has been shown to be broken in two places, once after isocitrate dehydrogenase which can be inhibited by a build-up of NADH, while a second break occurs upon inhibition of succinate dehydrogenase following accumulation of intermediate metabolites such as succinate and itaconate. Notably, the accumulation of these metabolites can also lead to stabilization of HIF1α, which can drive the production of pro-inflammatory cytokines, including interleukin (IL)-1β.[7–9] An impaired TCA cycle also results in the accumulation of citrate, which can feed into the process of FAS. Increased FAS is crucial for the activation of M1 macrophages and DC, and is elevated upon stimulation of pattern recognition receptors (PRRs) in both cell types.[9,10] However, FAO is more prominent in anti-inflammatory, alternatively activated (M2) macrophages, and contrib- utes to reduced production of inflammatory cytokines by inflammatory macrophages. (It should be noted that a spectrum of intermediary macrophage subtypes exist

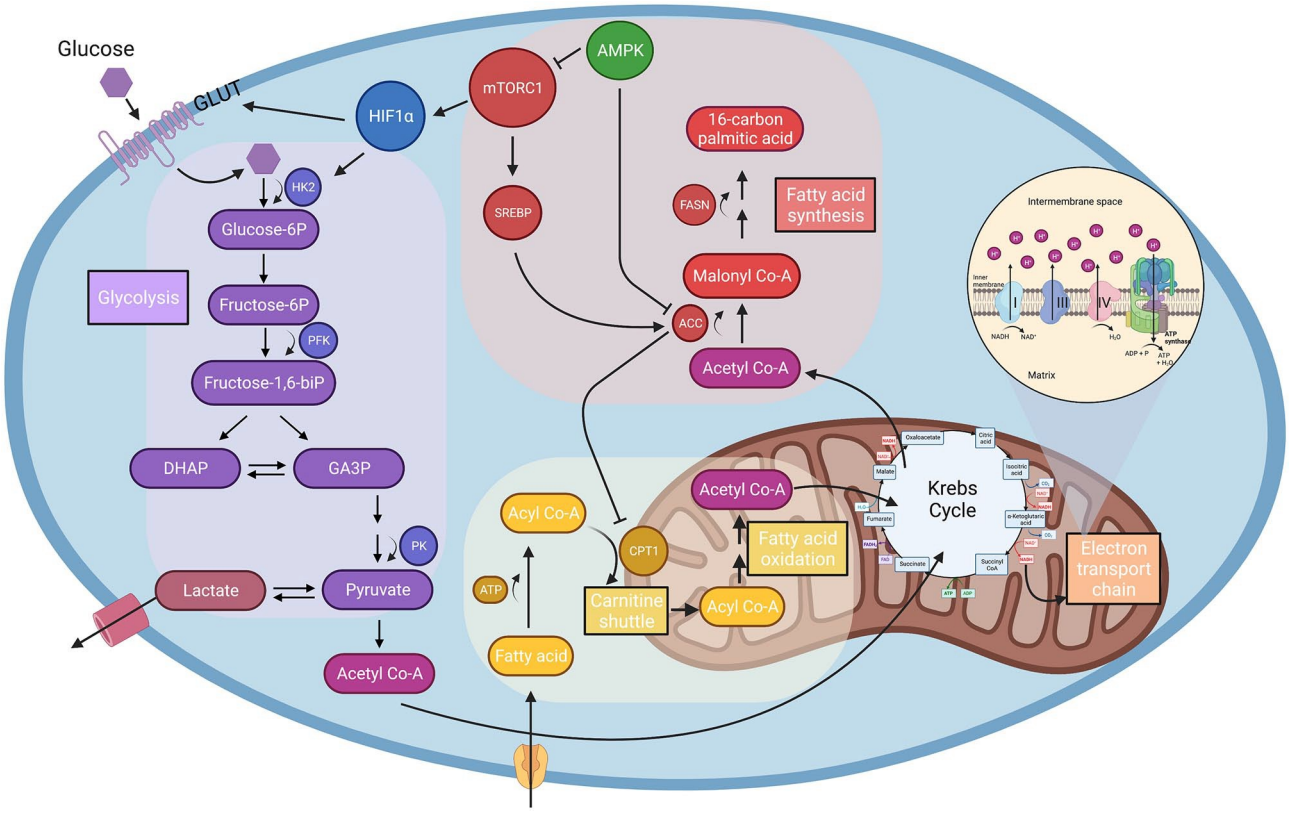

Figure 1. Cellular respiration and fatty acid metabolism. Cells engage a range of metabolic pathways depending on their needs. During glycolysis, glucose is first phosphorylated by hexokinase 2 (HK2) to generate glucose-6-phosphate (glucose-6P). Glucose-6P is isomerized to fructose-6-phosphate (fructose-6P), which is converted to fructose-1,6-biphosphate (fructose-1,6-biP) by phosphofructokinase (PFK). This is split into two: dihydroxyacetone phosphate (DHAP) and glyceraldehyde-3-phosphate (GA3P). GA3P continues through the remaining steps of glycolysis and is finally converted to pyruvate by pyruvate kinase (PK). Pyruvate can be exported from the cell as lactate under anaerobic conditions. In the presence of oxygen, pyruvate is converted to acetyl-CoA which enters the TCA cycle. NADH from the TCA cycle passes into the electron transport chain, completing oxidative phosphorylation and generating energy through a proton gradient. Acetyl-CoA can then enter the fatty acid synthesis pathway, where it is carboxylated by acetyl-CoA carboxylase (ACC) to form malonyl-CoA. Malonyl-CoA then passes through the remaining steps of this pathway, which are catalyzed by fatty acid synthases (FASN) resulting in 16-carbon palmitic acid. The fatty acid synthesis pathway is activated by mTORC1. mTORC1 is also responsible for the activation of HIF1α, which in turn can activate glycolysis by upregulating GLUT1 and HK2. Inhibition of fatty acid synthesis by AMPK results in activation of the fatty acid oxidation pathway, by lifting the inhibition placed on the enzyme carnitine palmitoyltransferase 1 (CPT1). Fatty acids first enter the cell and are converted to acyl-CoA, which then enters the carnitine shuttle to translocate into the mitochondria. Acyl-CoA then continues through the fatty acid oxidation pathway, generating acetyl-CoA, which can then enter the TCA cycle. (A color version of this figure is available in the online journal.)

in vivo and extensive metabolic profiling of these individual subtypes has not yet been carried out.).[11,12] The balance of fatty acid metabolism is also of particular importance for T cell responses and their effector function. Tregs exhibit increased levels of FAO and increased expression of the genes involved in this process, including CPT1A, while effector T cells downregulate FAO during activation.[13,14] Furthermore, effector T cells, and in particular Th17 cells, exhibit increased FAS (Figure 2).[15] This difference in T cell metabolism could be of particular importance for diseases in which the Th17/Treg balance is skewed.

While less well established, *in vitro* studies have revealed that B cells also undergo changes in their metabolic state upon activation. For example, B-cell receptor (BCR)–activated B cells upregulate GLUT1, increase glycolysis, and activate mTOR in a protein kinase Cβ (PKCβ)–dependent manner.[16] When B cells are fully activated upon engagement of co-stimulatory molecules such as CD40, glucose and glutamine uptake is further enhanced to support proliferation.[17] A link has also been established between antibody production by plasma cells (PCs) and energy metabolism, whereby long-lived PCs have been shown to exhibit enhanced glucose uptake compared to their shorter-lived counterparts. This is primarily utilized to glycosylate antibodies, although this can be diverted to glycolysis if energy demands are low.[18] Less is known regarding energy metabolism in memory B cells, but a recent study has demonstrated that, compared to naïve B cells, human memory B cells of the IgD isotype exhibit enhanced glycolysis and mTORC activation upon stimulation with interferon alpha (IFN-α) and Toll-like receptor (TLR) ligands.[19] They also differentiate into PCs to a greater extent, and it has been suggested that longevity and antibody secretion are regulated by metabolic pathways. In light of these findings, altered B cell metabolism should also be considered in the context of immune-mediated disease pathogenesis, as is currently the case for dysregulated T cell, DC, and macrophage metabolism.

Endogenous drivers of metabolic reprogramming

Cytokines

Cytokines can differentially alter immune cell metabolism.[20] For example, macrophages exhibit an increase in glycolysis in response to recombinant IL-1 treatment.[21] Tumor necrosis

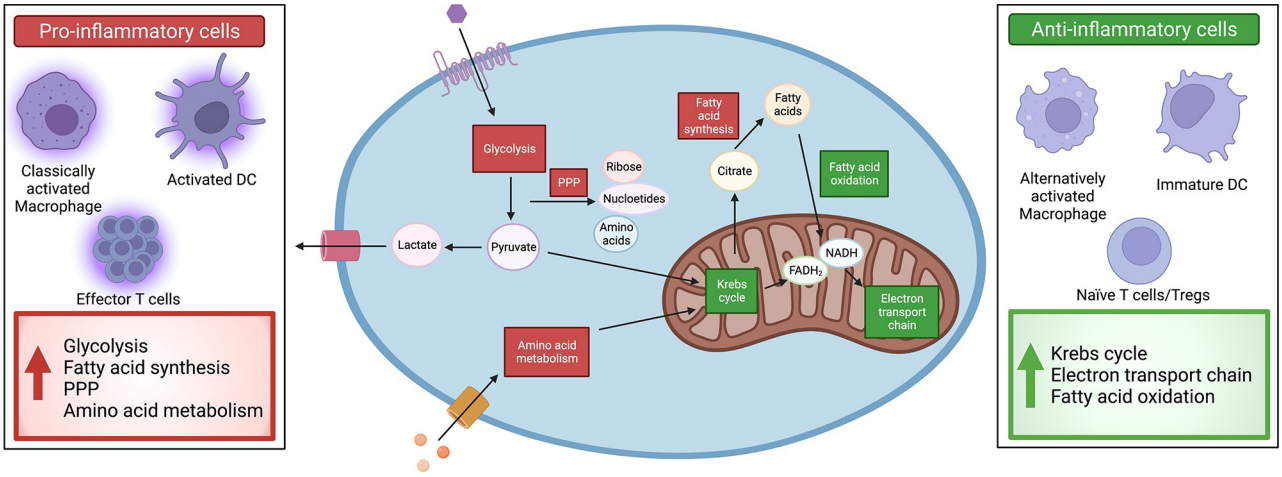

Figure 2. Major metabolic pathways engaged in immune cells. The metabolic pathways engaged by an immune cell depend on its activation state, maturation state, or specific effector subset. The pathways shown in red: glycolysis, fatty acid synthesis, amino acid metabolism, and the pentose phosphate pathway (PPP) are generally associated with activated and effector immune cells. Some examples of these cells include pro-inflammatory macrophages, activated DC, and specific effector T cell subsets. The pathways shown in green: TCA cycle and the electron transport chain (together comprising oxidative phosphorylation) and fatty acid oxidation are generally associated with naive, immature, or regulatory immune cells. Some examples of these cells include alternatively activated macrophages, immature DC, and naïve or regulatory T cells (Tregs). (A color version of this figure is available in the online journal.)

factor (TNF) has also has been linked to metabolic reprogramming via upregulation of the mitochondrial citrate carrier (CIC), leading to accumulation of citrate in the cytosol of inflammatory M1 macrophages, and is capable of upregulating ATP-citrate lyase (ACLY) which catalyses the conversion of glucose-derived citrate to acetyl-CoA.[22,23] TNF has also been shown to promote a potential glycolytic shift in human $CD4^+$ T cells, as well as human fibroblast–like synoviocytes.[24,25] In the case of the latter, this was accompanied by increased expression of inflammatory rheumatoid arthritis (RA) biomarkers, while in a clinical setting, treatment with anti-TNF significantly reduces glycolytic activity in the RA synovium.[26] This is coupled with a downregulation of the glucose transporter, GLUT1, and the glycolytic enzyme, glyceraldehyde 3-phosphate dehydrogenase (GAPDH),[26] further bolstering the evidence for TNF-α as driver of metabolic reprogramming in disease pathogenesis.

Blockade of IL-6 signaling appears to have a similar effect in RA, particularly in leukocytes, where inhibition of the IL-6 receptor results in reduced oxidative stress and inflammation.[27] A further example of IL-6-mediated metabolic reprogramming has been observed in $CD8^+$ T cells, which undergo IL-6-dependent metabolic rewiring to allow for pro-inflammatory cytokine production and proliferation in response to lipopolysaccharide (LPS).[28] The downstream modulation of metabolism by pro-inflammatory cytokines may be attributed to activation of the nuclear factor-κB (NF-κB) pathway, which is now understood to hold a criti- cal role in shaping the inflammatory response via metabolic rewiring.[29] In the presence of varying stimuli, including TNF or IL-1, the IkappaB kinase (IKK) complex becomes activated, resulting in the release of NF-κB, which subsequently translocates to the nucleus and promotes transcription of HIF1α. As mentioned above, HIF1α promotes glycolysis via upregulation of glycolytic genes such and HK2 and GLUT1. NF-κB is also capable of activating mTOR, which further stabilizes HIF1α, sustaining its transcriptional activity.

However, IL-10, which is considered an anti-inflammatory cytokine, limits glucose uptake and glycolysis in LPS-treated macrophages.[30] Furthermore, IL-10 has been shown to protect mitochondrial function and eliminate dysfunctional mitochondria through the upregulation of mitophagy in the cell. This response appears to be regulated through inhibition of mTOR activity, as mice lacking the IL-10 receptor demonstrate sustained mTOR activation, and consequential impaired mitochondrial activity. IL-4 signaling has also been linked to mTOR activity, via its interactions with the mTOR complexes, mTORC1 and mTORC2, which in turn modulate glycolytic activity and FAO in IL-4-treated macrophages.[31]

Nitric oxide

Nitric oxide (NO) plays a role in a plethora of biological functions, and is most notably generated by activated myeloid cells in response to inflammatory stimuli. NO synthases (NOSs) convert l-arginine and oxygen (O_2) to NO and l-citrulline, and NO is well documented as being produced at nanomolar concentrations under normal physiological conditions.[32] In the context of the immune response, however, NO functions at higher concentrations over time to kill infectious agents and plays a role in immunoregulation. There is a growing body of evidence to show that NO can do this through modulation of cellular metabolism, and furthermore, it is known that NO and NO-derivatives can act to reprogram macrophage cell function.[33]

NO has been shown to exert effects through interaction with metal ions found in proteins, notably associating with heme centers such as those found in cytochrome c oxidase, that is, complex IV of the mitochondrial electron transport chain. NO works in concert with inversely correlated O_2 levels to exert an inhibitory effect on complex IV, and therefore inhibit oxidative phosphorylation. Indeed, it has been shown that inhibition or ablation of inducible NO synthase (iNOS) in myeloid cells can rescue ATP-linked mitochondrial

respiration.[34,35] Early evidence also demonstrated that when NO levels are high, O_2 cannot be sufficiently utilized by the cell in a state termed "metabolic hypoxia." In the case of pro-inflammatory macrophage polarization, macrophages increase their utilization of the pentose phosphate pathway and consequent generation of reactive oxygen species (ROS) and reactive nitrogen species (RNS). Generation of the latter is, in part, mediated through iNOS to exert antimicrobial effects.[36,37] One notable study investigated the effect of NO on inflammatory macrophage metabolic reprogramming using NO-deficient macrophages, and demonstrated that NO modulates expression of the subunits forming complex I of the mitochondrial electron transport chain. Furthermore, it was shown that NO-deficient macrophages differentially modulate levels of important TCA cycle intermediates including succinate, citrate, and itaconate.[34] Interestingly, NO depletion resulted in enhanced IL-1β levels which may be attributed to the fact that NO can act to inhibit formation of the NLR family pyrin domain containing 3 (NLRP3) inflammasome through nitrosation.[38] It is worth noting that these studies were carried out in murine cells which dif- fer from human cells, given that human macrophages do not exhibit such a potent NO response; hence, it will be of interest to further explore how NO-induced metabolic reprogramming impacts on human disease.

DAMPs as drivers of altered immune cell metabolism

There is no doubt that pathogen-associated molecules (PAMPs) can alter immune cell metabolism, and this has been reviewed in detail elsewhere.[33,39] As outlined above, cytokines themselves and the hypoxic environment associated with diseased tissues can lead to metabolic reprogramming of immune cells; however, there is emerging evidence that disease or damage–associated molecular patterns (DAMPs) – also referred to as alarmins – can also contribute to alterations in immune cell metabolism. This is perhaps not so surprising, given that many DAMPs bind to the same receptors as PAMPs and stimulate immune effector responses akin to those generated during microbial infection. For example, many particulates including beta amyloid (Aβ) fibrils and cholesterol crystals activate the NLRP3 inflammasome, leading to the production of mature IL-1β, while other DAMPs such as HMGB1, S100 proteins, and oxLDL have been shown to activate members of the TLR family to drive inflammatory cytokine and chemokine production.[40–43] Hence, DAMPs themselves, and the pathways they activate, have become attractive therapeutic targets. Research into DAMP-induced metabolic changes is very much in its infancy; however, there have been recent studies highlighting the impact of certain DAMPs on macrophage and microglia metabolic phenotype as outlined below.

Aβ alters microglia metabolism

Although the brain primarily utilizes glucose to meet its energy demands, in disease states, it has been shown to shift toward consumption of other substances. In the aging brain, there is evidence of impaired glucose metabolism that is exacerbated under conditions of neuroinflammatory or neurodegenerative disease.[44,45] In the case of Alzheimer's disease (AD), primary focus has been on neurons and astrocytes as contributors to disease progression; however, metabolic reprogramming of microglia is receiving considerable attention, given the chronic inflammation and altered glucose metabolism that serve as hallmarks of this disease.[46] In a non-activated state, microglia rely primarily on OXPHOS and switch to favor glycolysis upon activation.[47] In early AD, this shift in metabolism toward aerobic glycolysis may facilitate Aβ clearance.[48] However, chronically activated or dysfunctional microglia can contribute to disease progression, with direct links shown between activated microglia and synapse loss.[49] Indeed, recent work has implicated Aβ itself as a driver of microglial metabolic reprogramming, and there is evidence of meta- bolic rewiring from OXPHOS to aerobic glycolysis follow- ing Aβ stimulation of primary microglia.[48] Furthermore, it has been demonstrated that inhibition of glycolysis using the glucose analogue, 2-deoxy-D-glucose (2-DG), leads to decreased oxidative stress and a reduction in Aβ oligomers in the brains of transgenic AD mice.[50] On a functional level, metabolic reprogramming of microglia has been directly linked to Aβ-induced-phosphorylation of mTOR and consequential activation of the mTOR-HIF1α-pathway, which facilitates the switch from OXPHOS to glycolysis.[48] In support of this, inhibition of the mTOR pathway was shown to reduce Aβ-induced microglial inflammation in primary microglia, as demonstrated by reduced expression of pro-inflammatory cytokines IL-1β and TNF-α.[48] A reduction in activation markers has also been observed in LPS-activated microglia following treatment with 2-DG.[51]

It is worth noting also that Aβ can activate the NLRP3 inflammasome, and recent studies have highlighted a link between glycolysis and inflammasome activation, with inhibition of glycolysis using aminooxyacetic acid (an inhibitor of aspartate aminotransferase) or 2-DG result- ing in attenuation of NLRP3 inflammasome activation in activated murine macrophages, and in a murine model of acute lung injury, respectively.[52,53] Furthermore, HK activity was shown to be essential for NLRP3 inflammasome activation in macrophages, as demonstrated by short hairpin RNA (shRNA) knockdown of HK1 in murine peritoneal macrophages, which resulted in decreased inflammasome-dependent IL-1β and IL-18 secretion.[54] HK2 has been shown to be upregulated in microglia favoring glycolysis under inflammatory conditions;[55] it will therefore be of interest to determine if Aβ-induced inflammasome activation is also dependent on HK activity in this cell type. The ketone body metabolite, β-hydroxybutyrate (BHB), was also shown to reduce macrophage activation and inhibit NLRP3 inflammasome activation in murine models of NLRP3-mediated disease.[56] Moreover, BHB reduced Aβ-induced mitochondrial dysfunction and ROS formation in primary cortical neurons, and further restored mitochondrial complex I activity when administered peripherally in a murine AD model. This effect was accompanied by a reduction in Aβ levels.[57] It might therefore be worth considering modulation of ketogenic metabolism, in addition to glucose metabolism, as a potential therapeutic avenue to attenuate Aβ- and other inflammasome-associated diseases.

Crystalline particulates alter immune cell metabolism

Dysregulated metabolism has been observed in several forms of joint disease including RA, osteoarthritis (OA), and gout.[26,58,59] The hypoxic environment of the RA joint promotes such alternations, where metabolites such as lactate and citrate can act on synovial fibroblasts and macrophages to enhance glycolysis, FAS, and inflammatory mediator production.[60] In OA and gout, crystalline particulates have been shown to directly impact on monocyte/macrophage metabolism. For example, in the case of gouty arthritis, insoluble monosodium urate (MSU) crystals were shown to enhance glucose uptake by driving increased GLUT1 expression in human macrophages and neutrophils, while treatment with either a GLUT1 inhibitor or 2-DG suppressed crystal-induced NLRP3 activation and IL-1β production in an *in vivo* model of MSU-induced inflammation. Peripheral blood mononuclear cell (PBMC) and monocytes stimulated with MSU crystals also exhibited enhanced mTOR activity, while mTOR pathway gene expression was found to be elevated in monocytes from gout patients versus healthy controls.[61] Furthermore, MSU crystals were recently shown to induce a metabolic-inflammatory transcriptional profile that is distinct from that promoted by the well-studied PAMP, LPS, and is dependent on activation of the mitogen-activated protein (MAP) kinase, c-Jun N-terminal kinase (JNK). Interestingly, despite MSU crystals being considered potent activators of the NLRP3 inflammasome, this study found no evidence that the inflammasome is required for the upregulation of metabolic genes by these particulates.[62] The ketone body, BHB, was, however, found to inhibit MSU-induced NLRP3 inflammasome formation, as has been shown for Aβ-dependent inflammasome activation.[63]

OA-associated basic calcium phosphate (BCP) crystals were also recently shown to directly promote M1 polarization and metabolic reprogramming in primary human macrophages, providing further evidence that targeting altered metabolism may serve to limit the inflammation associated with certain crystal arthropathies.[64] In this case, the BCP-mediated polarization of macrophages toward an inflammatory phenotype was prevented upon inhibition of glycolysis, as was the production of the key OA-associated DAMP, S100A8.[64] Indeed, it is worth noting that such findings extend beyond the joint, and we recently demonstrated that atherosclerosis-associated cholesterol crystals can alter macrophage bioenergetics by increasing the glycolytic profile of the cell.[65] This *in vitro* effect was dependent on the glycolytic enzyme, pyruvate kinase isoenzyme type M2 (PKM2), and supports a recent *in vivo* study demonstrating that inhibition of PKM2 nuclear translocation reduces glycolytic rate while also suppressing atherosclerosis and inflammation in $Ldlr^{-/-}$ mice.[66] Taken together, these studies reveal potential new targets to limit inflammation and macrophage polarization by modulating the metabolic state of pathogenic immune cells.

Immunometabolism as a therapeutic target

Given that the metabolism of immune cells plays an important role in their activation status and/or effector function, manipulation of metabolic pathways hold great potential as a therapeutic approach to treat many diseases characterized by dysregulated inflammation. Indeed, some autoimmune diseases show specific alterations to the metabolism of the immune cells involved. For example, in systemic lupus erythematosus (SLE), T cells exhibit persistent mitochondrial hyperpolarization (an early step in T cell activation), as well as ATP depletion,[67] while in RA, $CD4^+$ T cell metabolism is characterized by a reduced utilization of glycolysis and an increase in the amount of glucose passing through the pentose phosphate pathway.[68] Similarly, T cells from patients with MS exhibit dampened glycolysis and mitochondrial respiration, which is restored to levels comparable to healthy subjects upon treatment with IFN-β, a first-line treatment for MS.[69]

Comparable effects were also observed in T cells from patients with relapsing-remitting multiple sclerosis (RRMS) upon treatment with dimethyl fumarate (DMF), an oral, first-line RRMS treatment.[70] DMF is a citric acid cycle intermediate and is known to exhibit immunomod- ulatory effects through activation of the redox-sensitive transcription factor, nuclear factor erythroid 2–related factor 2 (NRF2), and further anti-inflammatory effects via inhibition of NF-κB.[70] The mechanism of action of DMF is complex; however, a recent study involving peripheral cells from RRMS patients demonstrated that the DMF increases monocyte ROS generation and epigenetic methylation changes in monocytes prior to exerting epigenetic changes in $CD4^+$ T cells.[71] While ROS production is generally associated with oxidative damage, there is evidence to show that myeloid-derived ROS can limit T cell activity *in vitro*.[71] Further study is required to uncover the complexity of DMF's mechanism of action, and effects are likely to be dependent on multiple factors including disease stage and immune cell phenotype.

In terms of targeting specific metabolites, effector T cells convert pyruvate to lactate, while Tregs utilize the enzyme pyruvate dehydrogenase (PDH) to convert pyruvate to acetyl-CoA to continue further through the TCA cycle. This is controlled by the enzyme pyruvate dehydrogenase kinase (PDHK), which inhibits PDH in effector T cells, thereby preventing them from converting pyruvate to acetyl-CoA. Inhibition of PDHK overcomes this effect and could therefore be used as a potential therapy to skew the metabolic pathways engaged in T cells by enhancing processes associated with regulatory T cells. This has shown promise in a number of animal models of disease, including experimental autoimmune encephalomyelitis (EAE).[14] Similarly, blockade of mTOR activity in the EAE model results in increased Tregs and an amelioration of disease progression.[72] Inhibition of ACC, a key enzyme involved in FAS downstream of mTOR, also increased Treg numbers while decreasing IL-17 and IFN-γ producing T cells in the EAE model. This was accompanied by reduced disease pathology.[15] Inhibition of mTORC1 with rapamycin also inhibits Th17 cells and promotes Tregs in patients with SLE.[73] Furthermore, metformin, a drug traditionally used to treat type II diabetes, is now showing potential as a treatment for autoimmune diseases by altering the metabolic state of immune cells. One of the established mechanisms of action for metformin is through

activation of AMPK, which in turn inhibits mTOR.[74,75] This likely accounts for some of the metabolism-altering functions it carries out, although multiple mechanisms cannot be ruled out. In the EAE model, metformin treatment was shown to decrease pro-inflammatory cytokines, increase Treg numbers, and slow disease progression.[76] Th17-mediated inflammation was also reduced by metformin treatment in animal models of RA and colitis, and again, effects were dependent on AMPK and mTOR signaling.[77,78] These studies provide further evidence that modulating metabolic pathways engaged by immune cells may have therapeutic potential for the treatment of autoimmune/inflammatory conditions. Further detailed evaluation of immunometabolism-based therapies can be found elsewhere.[79,80]

Conclusions

There a now wide ranging studies confirming that when immune cells are activated, they ramp up glycolysis as a requirement for many of their effector functions, includ- ing upregulation of co-stimulatory markers and cytokine production.[4,81,82] When glycolysis is blocked, these processes are impaired, leading to an inability to activate adaptive immune cells.[4,81,82] Further exploration of the metabolic switches, proteins, and metabolites that govern these changes will undoubtedly provide further insight into disease mechanisms, and how these pathways can be manipulated to halt the destructive processes associated with deleterious immune cell activation. Already, there is encouraging evidence from *in vivo* studies to support metabolic targeting in immune-mediated disease such as RA, SLE, and MS. However, direct inhibition of immune cell activation or promotion of regulatory immune cell activity via metabolic manipulation requires careful consideration, given the potential for "off target" effects. Nonetheless, dissecting the links between immune cell activation and metabolic status could have major implications for health and disease, where current strategies have thus far failed to make an impact.

AutHORS' CONtRIbutIONS

All authors participated in the conceptualization and writing of this manuscript.

DECLARAtION OF CONFLICtINg INtERESt S

The author(s) declared no potential conflicts of interest with respect to the research, authorship, and/or publication of this article.

FuNDINg

The author(s) disclosed receipt of the following financial support for the research, authorship, and/or publication of this article: LCS and AD are supported by the Science Foundation Ireland (SFI), Ireland, through the Advanced Materials and Bioengineering Research (AMBER) Centre (SFI/12/RC/2278_P2, partly supported by the European Regional Development Fund). HKF and AD are also supported by Enterprise Ireland (CF-2020-1340). SAO is funded by an IntraFaculty PhD Fellowship and the Schools of Engineering and Biochemistry and Immunology at Trinity College Dublin.

ORCID ID

Aisling Dunne https://orcid.org/0000-0002-2342-9518

REFERENCES

1. Düvel K, Yecies JL, Menon S, Raman P, Lipovsky AI, Souza AL, Triantafellow E, Ma Q, Gorski R, Cleaver S, Vander Heiden MG, MacKeigan JP, Finan PM, Clish CB, Murphy LO, Manning BD. Activation of a metabolic gene regulatory network downstream of mTOR complex 1. *Mol Cell* 2010;**39**:171–83
2. Ma EH, Poffenberger MC, Wong AH, Jones RG. The role of AMPK in T cell metabolism and function. *Curr Opin Immunol* 2017;**46**:45–52
3. Warburg O. On the origin of cancer cells. *Science* 1956;**123**:309–14
4. O'Neill LA, Pearce EJ. Immunometabolism governs dendritic cell and macrophage function. *J Exp Med* 2016;**213**:15–23
5. Pearce EJ, Everts B. Dendritic cell metabolism. *Nat Rev Immunol* 2015; **15**:18–29
6. Almeida L, Lochner M, Berod L, Sparwasser T. Metabolic pathways in T cell activation and lineage differentiation. *Semin Immunol* 2016;**28**: 514–24
7. Jha AK, Huang SC, Sergushichev A, Lampropoulou V, Ivanova Y, Loginicheva E, Chmielewski K, Stewart KM, Ashall J, Everts B, Pearce EJ, Driggers EM, Artyomov MN. Network integration of parallel metabolic and transcriptional data reveals metabolic modules that regulate macrophage polarization. *Immunity* 2015;**42**:419–30
8. Tannahill GM, Curtis AM, Adamik J, Palsson-McDermott EM, McGettrick AF, Goel G, Frezza C, Bernard NJ, Kelly B, Foley NH, Zheng L, Gardet A, Tong Z, Jany SS, Corr SC, Haneklaus M, Caffrey BE, Pierce K, Walmsley S, Beasley FC, Cummins E, Nizet V, Whyte M, Taylor CT, Lin H, Masters SL, Gottlieb E, Kelly VP, Clish C, Auron PE, Xavier RJ, O'Neill LA. Succinate is an inflammatory signal that induces IL-1β through HIF-1α. *Nature* 2013;**496**:238–42
9. Everts B, Amiel E, Huang SC, Smith AM, Chang CH, Lam WY, Redmann V, Freitas TC, Blagih J, van der Windt GJ, Artyomov MN, Jones RG, Pearce EL, Pearce EJ. TLR-driven early glycolytic reprogramming via the kinases TBK1-IKKε supports the anabolic demands of dendritic cell activation. *Nat Immunol* 2014;**15**:323–32
10. Ecker J, Liebisch G, Englmaier M, Grandl M, Robenek H, Schmitz G. Induction of fatty acid synthesis is a key requirement for phagocytic differentiation of human monocytes. *Proc Natl Acad Sci USA* 2010; **107**:7817–22
11. Vats D, Mukundan L, Odegaard JI, Zhang L, Smith KL, Morel CR, Wagner RA, Greaves DR, Murray PJ, Chawla A. Oxidative metabolism and PGC-1beta attenuate macrophage-mediated inflammation. *Cell Metab* 2006;**4**:13–24
12. Malandrino MI, Fucho R, Weber M, Calderon-Dominguez M, Mir JF, Valcarcel L, Escoté X, Gómez-Serrano M, Peral B, Salvadó L, Fernández-Veledo S, Casals N, Vázquez-Carrera M, Villarroya F, Vendrell JJ, Serra D, Herrero L. Enhanced fatty acid oxidation in adipocytes and macrophages reduces lipid-induced triglyceride accumulation and inflammation. *Am J Physiol Endocrinol Metab* 2015;**308**:E756–169
13. Wang R, Dillon CP, Shi LZ, Milasta S, Carter R, Finkelstein D, McCormick LL, Fitzgerald P, Chi H, Munger J, Green DR. The transcription factor Myc controls metabolic reprogramming upon T lymphocyte activation. *Immunity* 2011;**35**:871–82
14. Gerriets VA, Kishton RJ, Nichols AG, Macintyre AN, Inoue M, Ilkayeva O, Winter PS, Liu X, Priyadharshini B, Slawinska ME, Haeberli L, Huck C, Turka LA, Wood KC, Hale LP, Smith PA, Schneider MA, MacIver NJ, Locasale JW, Newgard CB, Shinohara ML, Rathmell JC. Metabolic programming and PDHK1 control CD4+ T cell subsets and inflammation. *J Clin Invest* 2015;**125**:194–207
15. Berod L, Friedrich C, Nandan A, Freitag J, Hagemann S, Harmrolfs K, Sandouk A, Hesse C, Castro CN, Bähre H, Tschirner SK, Gorinski N, Gohmert M, Mayer CT, Huehn J, Ponimaskin E, Abraham WR, Müller R, Lochner M, Sparwasser T. De novo fatty acid synthesis controls the fate between regulatory T and T helper 17 cells. *Nat Med* 2014;**20**:1327–33
16. Blair D, Dufort FJ, Chiles TC. Protein kinase Cβ is critical for the metabolic switch to glycolysis following B-cell antigen receptor engagement. *Biochem J* 2012;**448**:165–9

17. Egawa T, Bhattacharya D. Regulation of metabolic supply and demand during B cell activation and subsequent differentiation. *Curr Opin Immunol* 2019;**57**:8–14
18. Lam WY, Becker AM, Kennerly KM, Wong R, Curtis JD, Llufrio EM, McCommis KS, Fahrmann J, Pizzato HA, Nunley RM, Lee J, Wolfgang MJ, Patti GJ, Finck BN, Pearce EL, Bhattacharya D. Mitochondrial pyruvate import promotes long-term survival of antibody-secreting plasma cells. *Immunity* 2016;**45**:60–73
19. Torigoe M, Iwata S, Nakayamada S, Sakata K, Zhang M, Hajime M, Miyazaki Y, Narisawa M, Ishii K, Shibata H, Tanaka Y. Metabolic reprogramming commits differentiation of human CD27. *J Immunol* 2017;**199**:425–34
20. Zhang S, Carriere J, Lin X, Xie N, Feng P. Interplay between cellular metabolism and cytokine responses during viral infection. *Viruses* 2018;**10**:521
21. Finucane OM, Sugrue J, Rubio-Araiz A, Guillot-Sestier MV, Lynch MA. The NLRP3 inflammasome modulates glycolysis by increasing PFKFB3 in an IL-1β-dependent manner in macrophages. *Sci Rep* 2019; **9**:4034
22. Infantino V, Iacobazzi V, Palmieri F, Menga A. ATP-citrate lyase is essential for macrophage inflammatory response. *Biochem Biophys Res Commun* 2013;**440**:105–11
23. Infantino V, Iacobazzi V, Menga A, Avantaggiati ML, Palmieri F. A key role of the mitochondrial citrate carrier (SLC25A1) in TNFα- and IFNγ-triggered inflammation. *Biochim Biophys Acta* 2014;**1839**:1217–25
24. Chimenti MS, Tucci P, Candi E, Perricone R, Melino G, Willis AE. Metabolic profiling of human CD4+ cells following treatment with methotrexate and anti-TNF-α infliximab. *Cell Cycle* 2013;**12**:3025–36
25. Koedderitzsch K, Zezina E, Li L, Herrmann M, Biesemann N. TNF induces glycolytic shift in fibroblast like synoviocytes via GLUT1 and HIF1A. *Sci Rep* 2021;**11**:19385
26. Biniecka M, Canavan M, McGarry T, Gao W, McCormick J, Cregan S, Gallagher L, Smith T, Phelan JJ, Ryan J, O'Sullivan J, Ng CT, Veale DJ, Fearon U. Dysregulated bioenergetics: a key regulator of joint inflammation. *Ann Rheum Dis* 2016;**75**:2192–200
27. Ruiz-Limón P, Ortega R, Arias de la Rosa I, Abalos-Aguilera MDC, Perez-Sanchez C, Jimenez-Gomez Y, Peralbo-Santaella E, Font P, Ruiz-Vilches D, Ferrin G, Collantes-Estevez E, Escudero-Contreras A, López-Pedrera C, Barbarroja N. Tocilizumab improves the proatherothrombotic profile of rheumatoid arthritis patients modulating endothelial dysfunction, NETosis, and inflammation. *Transl Res* 2017; **183**:87–103
28. Dudek M, Lohr K, Donakonda S, Baumann T, Lüdemann M, Hegenbarth S, Dübbel L, Eberhagen C, Michailidou S, Yassin A, Prinz M, Popper B, Rose-John S, Zischka H, Knolle PA. IL-6-induced FOXO1 activity determines the dynamics of metabolism in CD8 T cells cross-primed by liver sinusoidal endothelial cells. *Cell Rep* 2022;**38**:110389
29. Kracht M, Müller-Ladner U, Schmitz ML. Mutual regulation of metabolic processes and proinflammatory NF-κB signaling. *J Allergy Clin Immunol* 2020;**146**:694–705
30. Ip WKE, Hoshi N, Shouval DS, Snapper S, Medzhitov R. Anti-inflammatory effect of IL-10 mediated by metabolic reprogramming of macrophages. *Science* 2017;**356**:513–9
31. Huang SC, Smith AM, Everts B, Colonna M, Pearce EL, Schilling JD, Pearce EJ. Metabolic reprogramming mediated by the mTORC2-IRF4 signaling axis is essential for macrophage alternative activation. *Immunity* 2016;**45**:817–30
32. Markiewicz R, Litowczenko J, Gapiński J, Woźniak A, Jurga S, Patkowski A. Nanomolar nitric oxide concentrations in living cells measured by means of fluorescence correlation spectroscopy. *Molecules* 2022;**27**:1010
33. Kelly B, O'Neill LA. Metabolic reprogramming in macrophages and dendritic cells in innate immunity. *Cell Res* 2015;**25**:771–84
34. Bailey JD, Diotallevi M, Nicol T, McNeill E, Shaw A, Chuaiphichai S, Hale A, Starr A, Nandi M, Stylianou E, McShane H, Davis S, Fischer R, Kessler BM, McCullagh J, Channon KM, Crabtree MJ. Nitric oxide modulates metabolic remodeling in inflammatory macrophages through TCA cycle regulation and itaconate accumulation. *Cell Rep* 2019;**28**:218–307
35. Everts B, Amiel E, van der Windt GJ, Freitas TC, Chott R, Yarasheski KE, Pearce EL, Pearce EJ. Commitment to glycolysis sustains survival of NO-producing inflammatory dendritic cells. *Blood* 2012;**120**:1422–31
36. MacMicking J, Xie QW, Nathan C. Nitric oxide and macrophage function. *Annu Rev Immunol* 1997;**15**:323–50
37. Palmieri EM, McGinity C, Wink DA, McVicar DW. Nitric oxide in macrophage immunometabolism: hiding in plain sight. *Metabolites* 2020;**10**:429
38. Mao K, Chen S, Chen M, Ma Y, Wang Y, Huang B, He Z, Zeng Y, Hu Y, Sun S, Li J, Wu X, Wang X, Strober W, Chen C, Meng G, Sun B. Nitric oxide suppresses NLRP3 inflammasome activation and protects against LPS-induced septic shock. *Cell Res* 2013;**23**:201–12
39. Ganeshan K, Chawla A. Metabolic regulation of immune responses. *Annu Rev Immunol* 2014;**32**:609–34
40. Piccinini AM, Midwood KS. DAMPening inflammation by modulating TLR signalling. *Mediators Inflamm* 2010;**2010**:672395
41. Foell D, Wittkowski H, Vogl T, Roth J. S100 proteins expressed in phagocytes: a novel group of damage-associated molecular pattern molecules. *J Leukoc Biol* 2007;**81**:28–37
42. Sims GP, Rowe DC, Rietdijk ST, Herbst R, Coyle AJ. HMGB1 and RAGE in inflammation and cancer. *Annu Rev Immunol* 2010;**28**:367–88
43. Rocha DM, Caldas AP, Oliveira LL, Bressan J, Hermsdorff HH. Saturated fatty acids trigger TLR4-mediated inflammatory response. *Atherosclerosis* 2016;**244**:211–5
44. Weise CM, Chen K, Chen Y, Kuang X, Savage CR, Reiman EM, Alzheimer's Disease Neuroimaging Initiative. Left lateralized cerebral glucose metabolism declines in amyloid-β positive persons with mild cognitive impairment. *Neuroimage Clin* 2018;**20**:286–96
45. Johnson KA, Fox NC, Sperling RA, Klunk WE. Brain imaging in Alzheimer disease. *Cold Spring Harb Perspect Med* 2012;**2**:a006213
46. Lu Y, Ren J, Cui S, Chen J, Huang Y, Tang C, Shan B, Nie B, Xinsheng L. Cerebral glucose metabolism assessment in rat models of Alzheimer's disease: an 18F-FDG-PET study. *Am J Alzheimers Dis Other Demen* 2016; **31**:333–40
47. Shippy DC, Ulland TK. Microglial immunometabolism in Alzheimer's disease. *Front Cell Neurosci* 2020;**14**:563446
48. Baik SH, Kang S, Lee W, Choi H, Chung S, Kim JI, Mook-Jung I. A breakdown in metabolic reprogramming causes microglia dysfunction in Alzheimer's disease. *Cell Metab* 2019;**30**:493.e–507.e6
49. Spangenberg EE, Green KN. Inflammation in Alzheimer's disease: lessons learned from microglia-depletion models. *Brain Behav Immun* 2017;**61**:1–11
50. Yao J, Chen S, Mao Z, Cadenas E, Brinton RD. 2-Deoxy-D-glucose treatment induces ketogenesis, sustains mitochondrial function, and reduces pathology in female mouse model of Alzheimer's disease. *PLoS ONE* 2011;**6**:e21788
51. Ghosh S, Castillo E, Frias ES, Swanson RA. Bioenergetic regulation of microglia. *Glia* 2018;**66**:1200–12
52. Zhao P, Zhou W, Zhang Y, Li J, Zhao Y, Pan L, Shen Z, Chen W, Hui J. Aminooxyacetic acid attenuates post-infarct cardiac dysfunction by balancing macrophage polarization through modulating macrophage metabolism in mice. *J Cell Mol Med* 2020;**24**:2593–609
53. Zhong WJ, Yang HH, Guan XX, Xiong JB, Sun CC, Zhang CY, Luo XQ, Zhang YF, Zhang J, Duan JX, Zhou Y, Guan CX. Inhibition of glycolysis alleviates lipopolysaccharide-induced acute lung injury in a mouse model. *J Cell Physiol* 2019;**234**:4641–54
54. Moon JS, Hisata S, Park MA, DeNicola GM, Ryter SW, Nakahira K, Choi AMK. mTORC1-induced HK1-dependent glycolysis regulates NLRP3 inflammasome activation. *Cell Rep* 2015;**12**:102–15
55. Lauro C, Limatola C. Metabolic reprograming of microglia in the regulation of the innate inflammatory response. *Front Immunol* 2020; **11**:493
56. Youm YH, Nguyen KY, Grant RW, Goldberg EL, Bodogai M, Kim D, D'Agostino D, Planavsky N, Lupfer C, Kanneganti TD, Kang S, Horvath TL, Fahmy TM, Crawford PA, Biragyn A, Alnemri E, Dixit VD. The ketone metabolite β-hydroxybutyrate blocks NLRP3 inflammasome-mediated inflammatory disease. *Nat Med* 2015;**21**:263–9
57. Yin JX, Maalouf M, Han P, Zhao M, Gao M, Dharshaun T, Ryan C, Whitelegge J, Wu J, Eisenberg D, Reiman EM, Schweizer FE, Shi J.

Ketones block amyloid entry and improve cognition in an Alzheimer's model. *Neurobiol Aging* 2016;**39**:25–37
58. Mobasheri A, Rayman MP, Gualillo O, Sellam J, van der Kraan P, Fearon U. The role of metabolism in the pathogenesis of osteoarthritis. *Nat Rev Rheumatol* 2017;**13**:302–11
59. Fearon U, Hanlon MM, Wade SM, Fletcher JM. Altered metabolic pathways regulate synovial inflammation in rheumatoid arthritis. *Clin Exp Immunol* 2019;**197**:170–80
60. Hanlon MM, Canavan M, Barker BE, Fearon U. Metabolites as drivers and targets in rheumatoid arthritis. *Clin Exp Immunol* 2022;**208**:167–80
61. Renaudin F, Orliaguet L, Castelli F, Fenaille F, Prignon A, Alzaid F, Combes C, Delvaux A, Adimy Y, Cohen-Solal M, Richette P, Bardin T, Riveline JP, Venteclef N, Lioté F, Campillo-Gimenez L, Ea HK. Gout and pseudo-gout-related crystals promote GLUT1-mediated glycolysis that governs NLRP3 and interleukin-1β activation on macrophages. *Ann Rheum Dis* 2020;**79**:1506–14
62. Cobo I, Cheng A, Murillo-Saich J, Coras R, Torres A, Abe Y, Lana AJ, Schlachetzki J, Liu-Bryan R, Terkeltaub R, Sanchez-Lopez E, Glass CK, Guma M. Monosodium urate crystals regulate a unique JNK-dependent macrophage metabolic and inflammatory response. *Cell Rep* 2022;**38**:110489
63. Goldberg EL, Asher JL, Molony RD, Shaw AC, Zeiss CJ, Wang C, Morozova-Roche LA, Herzog RI, Iwasaki A, Dixit VD. β-hydroxybutyrate deactivates neutrophil NLRP3 inflammasome to relieve gout flares. *Cell Rep* 2017;**18**:2077–87
64. Mahon OR, Kelly DJ, McCarthy GM, Dunne A. Osteoarthritis-associated basic calcium phosphate crystals alter immune cell metabolism and promote M1 macrophage polarization. *Osteoarth Cart* 2020;**28**:603–12
65. O'Rourke SA, Neto NGB, Devilly E, Shanley LC, Fitzgerald HK, Monaghan MG, Dunne A. Cholesterol crystals drive metabolic reprogramming and M1 macrophage polarisation in primary human macrophages. *Atherosclerosis* 2022;**352**:35–45
66. Doddapattar P, Dev R, Ghatge M, Patel RB, Jain M, Dhanesha N, Lentz SR, Chauhan AK. Myeloid cell PKM2 deletion enhances efferocytosis and reduces atherosclerosis. *Circ Res* 2022;**130**:1289–305
67. Gergely P Jr, Grossman C, Niland B, Puskas F, Neupane H, Allam F, Banki K, Phillips PE, Perl A. Mitochondrial hyperpolarization and ATP depletion in patients with systemic lupus erythematosus. *Arthritis Rheum* 2002;**46**:175–90
68. Weyand CM, Goronzy JJ. Immunometabolism in early and late stages of rheumatoid arthritis. *Nat Rev Rheumatol* 2017;**13**:291–301
69. La Rocca C, Carbone F, De Rosa V, Colamatteo A, Galgani M, Perna F, Lanzillo R, Brescia Morra V, Orefice G, Cerillo I, Florio C, Manis- calco GT, Salvetti M, Centonze D, Uccelli A, Longobardi S, Visconti A, Matarese G. Immunometabolic profiling of T cells from patients with relapsing-remitting multiple sclerosis reveals an impairment in glycolysis and mitochondrial respiration. *Metabolism* 2017;**77**:39–46
70. Montes Diaz G, Hupperts R, Fraussen J, Somers V. Dimethyl fumarate treatment in multiple sclerosis: recent advances in clinical and immunological studies. *Autoimmun Rev* 2018;**17**:1240–50
71. Carlström KE, Ewing E, Granqvist M, Gyllenberg A, Aeinehband S, Enoksson SL, Checa A, Badam TVS, Huang J, Gomez-Cabrero D, Gustafsson M, Al Nimer F, Wheelock CE, Kockum I, Olsson T, Jagodic M, Piehl F. Therapeutic efficacy of dimethyl fumarate in relapsing-remitting multiple sclerosis associates with ROS pathway in monocytes. *Nat Commun* 2019;**10**:3081
72. Procaccini C, De Rosa V, Galgani M, Abanni L, Calì G, Porcellini A, Carbone F, Fontana S, Horvath TL, La Cava A, Matarese G. An oscillatory switch in mTOR kinase activity sets regulatory T cell responsiveness. *Immunity* 2010;**33**:929–41
73. Lai ZW, Borsuk R, Shadakshari A, Yu J, Dawood M, Garcia R, Francis L, Tily H, Bartos A, Faraone SV, Phillips P, Perl A. Mechanistic target of rapamycin activation triggers IL-4 production and necrotic death of double-negative T cells in patients with systemic lupus erythematosus. *J Immunol* 2013;**191**:2236–46
74. Rena G, Hardie DG, Pearson ER. The mechanisms of action of metformin. *Diabetologia* 2017;**60**:1577–85
75. Dowling RJ, Zakikhani M, Fantus IG, Pollak M, Sonenberg N. Metformin inhibits mammalian target of rapamycin-dependent translation initiation in breast cancer cells. *Cancer Res* 2007;**67**:10804–12
76. Nath N, Khan M, Paintlia MK, Singh I, Hoda MN, Giri S. Metformin attenuated the autoimmune disease of the central nervous system in animal models of multiple sclerosis. *J Immunol* 2009;**182**:8005–14
77. Lee SY, Lee SH, Yang EJ, Kim EK, Kim JK, Shin DY, Cho ML. Metformin ameliorates inflammatory bowel disease by suppression of the STAT3 signaling pathway and regulation of the between Th17/Treg balance. *PLoS ONE* 2015;**10**:e0135858
78. Son HJ, Lee J, Lee SY, Kim EK, Park MJ, Kim KW, Park SH, Cho ML. Metformin attenuates experimental autoimmune arthritis through reciprocal regulation of Th17/Treg balance and osteoclastogenesis. *Mediators Inflamm* 2014;**2014**:973986
79. Pålsson-McDermott EM, O'Neill LAJ. Targeting immunometabolism as an anti-inflammatory strategy. *Cell Res* 2020;**30**:300–14
80. Piranavan P, Bhamra M, Perl A. Metabolic targets for treatment of autoimmune diseases. *Immunometabolism* 2020;**2**:e200012
81. Wculek SK, Khouili SC, Priego E, Heras-Murillo I, Sancho D. Metabolic control of dendritic cell functions: digesting information. *Front Immunol* 2019;**10**:775
82. O'Neill LA, Kishton RJ, Rathmell J. A guide to immunometabolism for immunologists. *Nat Rev Immunol* 2016;**16**:553–65

Acta Biomaterialia 133 (2021) 208–221

Contents lists available at ScienceDirect

Acta Biomaterialia

journal homepage: www.elsevier.com/locate/actbio

Review article

Harnessing the innate and adaptive immune system for tissue repair and regeneration: Considering more than macrophages ☆

Lianne C. Shanley[a,c,e], Olwyn R. Mahon[a,c,e], Daniel J. Kelly[c,d,e], Aisling Dunne[a,b,e,*]

[a] School of Biochemistry and Immunology, Trinity College Dublin, Dublin, Ireland
[b] School of Medicine, Trinity College Dublin, Dublin, Ireland
[c] Trinity Centre for Bioengineering, Trinity Biomedical Sciences Institute, Trinity College Dublin, Dublin, Ireland
[d] Department of Mechanical and Manufacturing Engineering, School of Engineering, Trinity College Dublin, Dublin, Ireland
[e] Advanced Materials and Bioengineering Research (AMBER) Centre, Trinity College Dublin, Ireland

article info

Article history:
Received 9 October 2020
Revised 5 February 2021
Accepted 15 February 2021
Available online 28 February 2021

Keywords:
Innate immunity
Adaptive immunity
Immune modulation
Macrophage polarization
Tissue engineering
Tissue healing
Tissue regeneration

abstract

Tissue healing and regeneration is a complex, choreographed, spatiotemporal process involving a plethora of cell types, the activity of which is stringently regulated in order for effective tissue repair to ensue post injury. A number of globally prevalent conditions such as heart disease, organ failure, and severe musculoskeletal disorders require new therapeutic strategies to repair damaged or diseased tissue, particularly given an ageing population in which obesity, diabetes, and consequent tissue defects have reached epidemic proportions. This is further compounded by the lack of intrinsic healing and poor regenerative capacity of certain adult tissues. While vast progress has been made in the last decade regarding tissue regenerative strategies to direct self-healing, for example, through implantation of tissue engineered scaffolds, several challenges have hampered the clinical application of these technologies. Control of the immune response is growing as an attractive approach in regenerative medicine and it is becoming increasingly apparent that an in depth understanding of the interplay between cells of the immune system and tissue specific progenitor cells is of paramount importance. Furthermore, the integration of immunology and bioengineering promises to elevate the efficacy of biomaterial-based tissue repair and regeneration. In this review, we highlight the role played by individual immune cell subsets in tissue repair processes and describe new approaches that are being taken to direct appropriate healing outcomes via biomaterial mediated targeting of immune cell activity.

Statement of significance

It is becoming increasingly apparent that controlling the immune response is as an attractive approach in regenerative medicine. Here, we propose that an in-depth understanding of immune system and tissue specific progenitor cell interactions may reveal mechanisms by which tissue healing and regeneration takes place, in addition to identifying novel therapeutic targets that could be used to enhance the tissue repair process. To date, most reviews have focused solely on macrophage subsets. This manuscript details the role of other innate and adaptive immune cells such as innate lymphoid cells (ILCs), natural killer (NK) cells and $\gamma\delta$T cells (in addition to macrophages) in tissue healing. We also describe new approaches that are being taken to direct appropriate healing outcomes via biomaterial mediated cytokine and drug delivery.

© 2021 Acta Materialia Inc. Published by Elsevier Ltd. All rights reserved.

Contents

1. Introduction 209
2. Immune cell mediators of tissue healing and repair 209

☆ Part of the Special Issue on Immunomodulatory Biomaterials, guest-edited by Professor Georg Duda and Doctor Taimoor Qazi.

* Corresponding author.
E-mail address: aidunne@tcd.ie (A. Dunne).

https://doi.org/10.1016/j.actbio.2021.02.023
1742-7061/© 2021 Acta Materialia Inc. Published by Elsevier Ltd. All rights reserved.

2.1. Macrophages in tissue healing and repair 209
2.2. Neutrophils in tissue healing and repair 211
2.3. Natural killer cells in tissue healing and repair 211
2.4. Innate lymphoid cells in tissue healing and repair 212
2.5. Dendritic cells in tissue healing and repair 212
2.6. B cells in tissue healing and repair 213
2.7. T cells in tissue healing and repair 213
3. Immunomodulation for tissue repair and regeneration 214
3.1. Immunomodulation through targeting pro-inflammatory factors 214
3.2. Immunomodulation through targeting anti-inflammatory factors 215
4. Concluding remarks and future directions 216
Declaration of Competing Interest 218
References 218

1. Introduction

The limited capacity of many tissues and organs to regenerate is at the heart of numerous healthcare challenges. When controlled, the tissue healing response allows for resolution of inflammation and restoration of tissue architecture and homeostasis. A dysfunctional response, on the other hand, often leads to fibrosis and scarring at the injury site which can impair healing and result in organ failure [1]. A number of globally prevalent conditions such as heart disease, severe musculoskeletal defects, and organ failure comprise those most urgently demanding improved therapeutic strategies that enhance the tissue repair process. A thorough understanding of the cellular processes underlying tissue healing and repair is therefore crucial in the development of appropriate and effective therapies that engineer regenerative mechanisms to combat debilitating disease processes.

As the number of tissue repair models used in research has grown and evolved over the last few decades, our understanding of tissue repair and the ability to integrate this knowledge with the pathogenesis of relevant diseases has also expanded. A prevailing concept derived from study findings across a number of species indicates that the tissue regenerative capacity inherent to organ- isms lesser in complexity, such as fish and amphibians, diminishes as the immune competency of more complex organisms, namely mammals, increases [2,3]. It is now well accepted that the im- mune system plays a pivotal role in tissue healing, with immune cells directly affecting the host response at the injury site and influencing the activity of related tissue-specific cell populations and both recruited and tissue-resident stem cells. Indeed, the immune system has been shown to both positively and negatively regulate the tissue repair process, resulting in either effective tissue regeneration or fibrosis and scarring, respectively [2,4].

In this review, we highlight the contribution of a number of immune cell subsets across the innate and adaptive arms of the immune system, and the underlying cellular mechanisms that impact on tissue healing processes. We focus not just on macrophage populations which have been at the center of immunology-based tis- sue engineering strategies and hence the majority of such reviews to date, but also consider the contribution of neutrophils, natural killer (NK) cells and the more recently characterized innate lym- phoid cell (ILC) subsets as members of the innate immune system at play in tissue regeneration. Furthermore, we highlight the role played by cells of the adaptive immune system and move to sum- marize current efforts to integrate immunology and biomaterial- mediated therapeutic development in order to elicit a favorable immune response to facilitate tissue repair and regeneration.

2. Immune cell mediators of tissue healing and repair

In mammals, the normal tissue healing process progresses in four overlapping phases: hemostasis, inflammation, repair (also termed proliferation or granulation), and remodeling (also termed maturation [5] (Fig. 1). To ensure optimal healing, these phases must progress in a tightly controlled manner, with aberration resulting in impairment that can lead to fibrosis and heightened potential for organ failure. The progression of these phases is heavily reliant on the contribution of immune cells, particularly during the inflammatory phase which dictates the efficacy of subsequent tissue repair and remodeling [6,7].

Inflammation begins with neutrophil influx, followed by monocyte infiltration and their subsequent differentiation into macrophages, in a process that is dependent on location and stimuli received [8]. Signals from these innate cells recruit lymphocytes to the site of injury, which engage in crosstalk and influence further innate immune responses. This phase resolves naturally in the case of acute wounds and is marked primarily by the transition of inflammatory macrophages at the injury site to a pro-reparative population. The subsequent repair phase is characterized by the onset of angiogenesis along with collagen synthesis and the deposition of ECM, with the final phase of regeneration involving the maturation of the newly formed vessels and remodeling of tissue. Immune cells exert critical influence over the processes of remodeling and regeneration in their clearance of cellular debris, along with their effects on the proliferation and differentiation of tissue specific stem/progenitor cell populations. This is exemplified in the case of bone regeneration, in which the crosstalk between immune cells and osteoprogenitor cells is integral to the initiation and propagation of osteogenesis and associated activities. The concerted activity of macrophages and bone marrow derived stem/stromal cells (BMSCs) is particularly well-studied in this regard, exemplified by demonstration of the initial M1-like macrophage population's ability to enhance bone mineralization by BMSCs *in vitro*, pointing to the importance of the M1-like macrophage in the initiation of osteogenesis [9].

An ever-growing wealth of evidence supports our understanding that aberrant cellular activity in the inflammatory phase often results in impaired tissue healing and defective host responses, with over-fibrosis and scarring a major outcome of such. Given the complex role immune cells of both the innate and adaptive immune system play in the tissue repair process, a thorough understanding of their individual contributions to healing and their interaction with other cells that are involved in tissue repair and regeneration, particularly the aforementioned tissue specific stem/progenitor cells, is required.

2.1. Macrophages in tissue healing and repair

Whilst tissue healing and tissue repair requires the presence and concerted actions of a plethora of cell types, the involvement of macrophages across all stages of tissue repair and their ex- tensive interaction with stem and progenitor cells has indicated that targeting macrophage-mediated responses holds wide-ranging

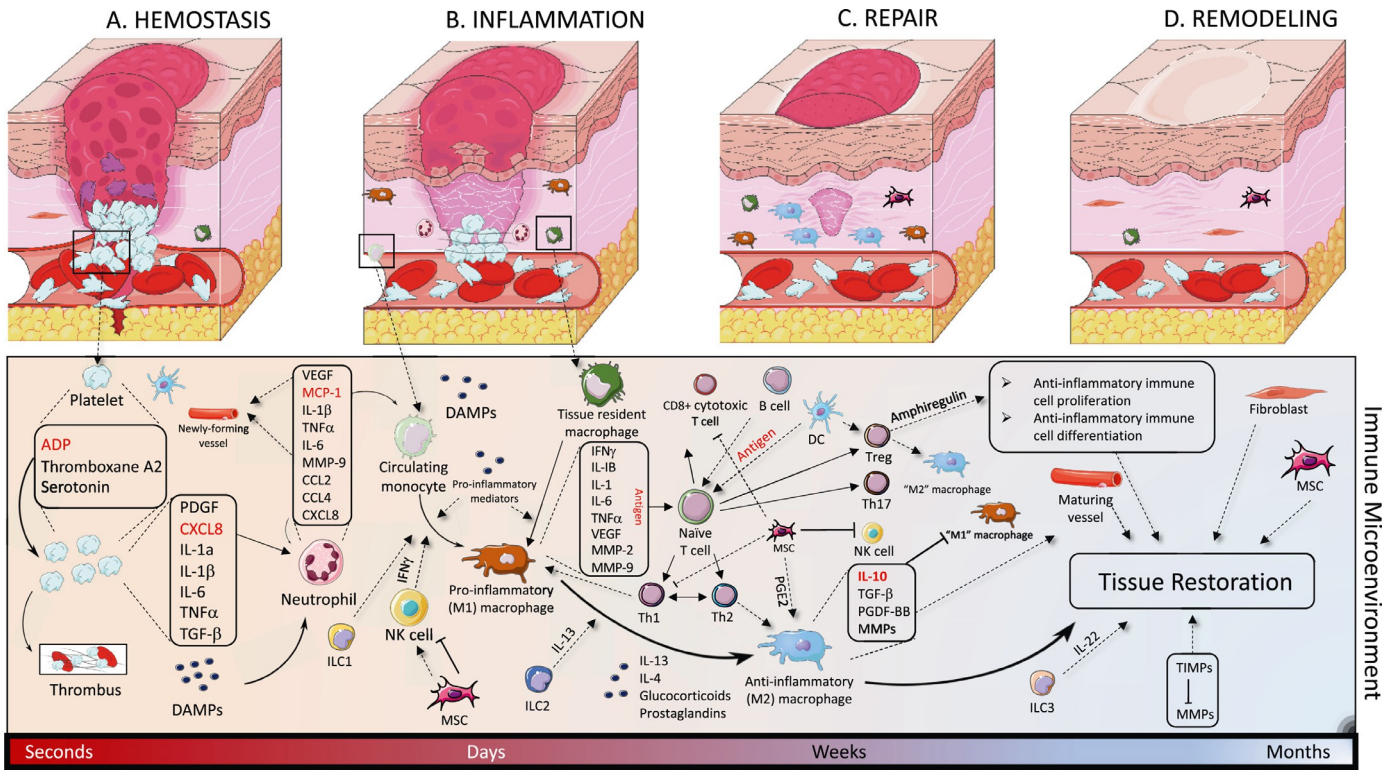

Fig. 1. The Immune Microenvironment in Tissue Healing.
a) Immediately post-injury, platelets are recruited and secrete chemoattractant factors such as ADP, thromboxane A2, and serotoninto further recruit platelets to the injury site. Thrombocytes and leukocytes migrate towards a fibrin-rich provisional matrix where platelets then degranulate and activate the complement cascade, with resultant DAMPs facilitating inflammatory immune cell activation. **b)** Neutrophils first migrate to the site of injury, particularly facilitated by CXCL8 family chemokines. Here they secrete antimicrobial factors including ROS, and sequester and phagocytose pathogens assisted by the process of NETosis. They secrete a variety of growth factors and cytokines, stimulate recruitment of inflammatory cells, and facilitate angiogenesis and proliferation of cells such as fibroblasts and epithelial cells. MCP-1, also secreted by these neutrophils, stimulates circulating monocytes to migrate from the surrounding blood vessels and differentiate into macrophages upon encountering further pro-inflammatory stimuli in the injury microenvironment. At this point, ILC1s and NK cells contribute to the inflammatory microenvironment in their secretion of pro-inflammatory cytokine IFNγ . A population of tissue resident macrophages are also stimulated to proliferate and differentiate by pro-inflammatory mediators at the injury site. The predominant macrophage subpopulation during this inflammatory phase of tissue healing are pro-inflammatory/M1-like. The pro-inflammatory secretome of M1-like macrophages per- petuates inflammatory immune cell recruitment. **c)** As the phases progress from inflammation to repair, the macrophage subpopulation shifts from being predominately M1-like to M2-like (this can be driven by ILC2 derived IL-13) and secrete anti-inflammatory and pro-resolutory cytokines such as TGF-β1, while also depositing ECM. M2- like macrophages exert potent anti-inflammatory effects, including suppression of the M1-like phenotype by their secretion of IL-10 and maturation of newly-formed vessels via secretion of PDGF-BB. T cells are recruited by macrophage secreted cytokines and the two most crucial T cell subsets in tissue repair and remodeling are the Th2 and Treg subsets, both of which secrete factors contributing to matrix formation such as TGF-β1, IL-4, -5, -13, and -21. Treg-derived amphiregulin stimulates immune cells to differentiate and proliferate and exert anti-inflammatory functions in the latter stages of healing.

therapeutic potential [10]. Their crucial role in the repair process across multiple tissue types has been demonstrated by deplet- ing macrophage populations in several models of tissue injury. Seminal works in salamander and murine models exemplified the detrimental effect of macrophage depletion on limb regeneration and muscle repair [6,11]. Bolstering this, a recent comparative study in which single-cell RNA-seq was used to compare immune cell populations between salamander and murine models of tis- sue regeneration showed an earlier recruitment of macrophages exhibiting heightened expression of matrix metalloproteinases (MMPs) in the salamander as compared to the more immuno- competent murine model [12].

Macrophages originate from myeloid precursor cells in the bone marrow compartment and persist in the host system either within the circulation where they differentiate from monocytes through extravasation through the endothelium or residing in tissues in which they rapidly proliferate in response to injury [13]. There is evidence to support the belief that these subsets can play opposing but important roles in healing in a tissue-dependent manner, with studies involving inhibition or depletion of mono- cytes and macrophages showing a more pro-inflammatory role for macrophages derived from monocytes, in comparison to a more regenerative role for those macrophages that are tissue resident [14–16].

An early paradigm introduced in 2000 that has greatly evolved in recent years is that depicting macrophage plasticity and po- larization states. These states exist across a spectrum of diverse, plastic phenotypes, with one end of the spectrum correlating to an "M1-like" or pro-inflammatory macrophage phenotype and the other referring to an anti-inflammatory "M2-like" macrophage phenotype, which in turn determines their functionality [17].

Broadly speaking, M1-like macrophages are induced by pro-inflammatory stimuli (*in vitro*, the classic "M1-like" activators are lipopolysaccharide (LPS) and interferon-γ (IFN-γ)) and they act to orchestrate the initial acute inflammatory response to tissue assault. M1-like macrophages engage in phagocytosis of foreign particles and clearance of debris at the wound site, a process which propagates a pro-inflammatory secretome. The release of pro-inflammatory cytokines and growth factors acts to counter the hypoxic conditions at the site of tissue damage or injury, with molecules including platelet-derived growth factor (PDGF) and vascular endothelial growth factor (VEGF-A) prompting formation of new vessels and cellular proliferation.

M2-like macrophages are induced *in vitro* and in certain *in vivo* settings by anti-inflammatory cytokines such as interleukin (IL)-4 and IL-13, along with glucocorticoids, prostaglandins, and modu- lators of metabolism, and these macrophages play a key role in tissue healing and remodeling [18]. They secrete factors including

TGF-β1 and anti-inflammatory cytokine IL-10 that instruct cells at the injury site such as fibroblasts to move towards a reparative phenotype and deposit extracellular matrix (ECM) [19,20]. The latter phases of repair and remodeling require precedence of the M2-like macrophage population, facilitating dampening of inflammation and destructive processes and upregulation of healing-associated activities. Under normal healing conditions, the initial predominant population of M1-like macrophages shifts to- wards M2-like as the reparative phase begins [21]. This shift from M1-like to M2-like can be attributed to the effect of a number of stimulatory molecules, and was recently shown in a murine model of musculoskeletal injury to be particularly dependent on the protein annexin A1 (ANXA1), a major driver of resolution of inflammation signalling through the AMP-activated protein kinase (AMPK)-governed pathway [22].

Indeed, a large number of studies have shown that higher M2/M1 ratios correlate with heightened tissue repair and a reduc- tion in fibrosis and scarring in the wake of tissue injury, largely caused by a local reduction in inflammatory mediators [23–26]. A caveat to macrophage modulation lies in the critical temporal roles of various macrophage phenotypes and functions, with their del- icate balance and inextricable interplay with cells of the adaptive immune system rendering them both an attractive therapeutic tar- get and a potential hinderance to immunomodulation. Supporting this, a recent study uncovering the contribution of macrophages to deleterious collagen deposition during scar formation in both a zebrafish and a murine model of cardiac tissue repair impli- cates macrophages as an apparent 'double-edged sword' in tissue restorative processes [27], further pointing to the importance of macrophages in immunoengineering research and indicating that they should continue to be considered as either central or periph- eral components in the majority of immunomodulation strategies, depending on the intended target cell population or populations and tissue types. An in-depth account of macrophages in tissue healing can be found in the following recent reviews [28,29].

2.2. Neutrophils in tissue healing and repair

Like macrophages, neutrophils function on the frontline of the innate immune system and are the first immune cell to arrive at the site of injury. They are derived from common myeloid progenitors in the immune reservoirs of the body (the bone marrow and spleen) and function by secreting antimicrobial agents and proteases that control infection at the wound site [30]. They predominate during the beginning of the acute in- flammatory response and large numbers are recruited from the peripheral blood by chemoattractants released by cells in response to damage associated molecular patterns (DAMPs) following injury [30,31]. The activated neutrophils are known to secrete immuno-regulatory factors, namely CX chemokine ligand (CXCL) 8 (a target of neutrophils), C chemokine ligand (CCL) 2, and CCL4 (both chemoattractants and activators of monocytes, macrophages, immature dendritic cells (DCs), and lymphocytes) [32].

Generally regarded as being short-lived, it is now accepted that neutrophils can persist at the injury site in a cyclical relationship with inflammation for days beyond assault [33]. Here, they release granules or undergo the respiratory burst to facilitate degradation of necrotic tissue in addition to their phagocytic action. Regulation of neutrophils, primarily mediated by macrophages and dependent on prostaglandin E2 (PGE2), is a vital component of the healing process, with the shift towards the reparative macrophage subset leading to clearance of neutrophils that would otherwise result in matrix degradation and delayed deposition of collagen [34,35]. Upon increased monocyte infiltration to the injury site in response to neutrophil derived CCL2 and CCL4, neutrophil recruitment is suppressed and, without further signalling, neutrophils apoptose and are cleared from the site. Importantly, macrophages that clear apoptosed neutrophils by phagocytosis have been shown to polarize to an M2-like, pro-reparative phenotype, facilitating progression of the normal tissue repair process [36,37].

In addition to resolution of neutrophil activation by macrophages, neutrophils also employ the process of neutrophil extracellular trap (NET)-osis, which typically involves release of neutrophil extracellular traps (NETs) and functions at the site of injury to trap and sequester pathogens and can dampen inflam- mation. While this process has been shown to aid the healing re- sponse, it has also been shown to play a role in a sustained foreign body reaction (FBR), a severe result of aberrant healing in the case of encountering a non-native material, and resultant production of a dense fibrotic matrix that can preclude further repair [38–40].

Further supporting a role for neutrophils in tissue healing is evidence that neutrophils function as players in angiogenesis, a crucial requirement for the onset of repair and precursor to tissue remodeling. This occurs via the secretion of MMP-9 by neutrophils which has been demonstrated to be a VEGF-independent mechanism of initiating the switch to angiogenesis [41]. Moreover, they have been implicated in wound repair in a murine model of spinal cord injury, in which Ly6G leukocyte depletion correlated with impaired healing ability [42].

Similar to the M1/M2-like macrophage paradigm, recent in- terest has grown in the concept of an N1/N2-like neutrophil spectrum of polarization states. In the field of cardiovascular dis- ease and atherosclerosis, investigation is being conducted into the differential effects of neutrophil polarization on disease states and resolution. Neutrophils polarized to a pro-inflammatory state upon LPS stimulation, as characterized by the expression of inflamma- tory mediators such as CD11b, MMP-9, and Dectin-1, were shown to contribute to an exacerbated atherosclerotic state in a murine model. The converse was seen following transfer of neutrophils polarized to an anti-inflammatory state by the stimulation of LPS-stimulated neutrophils with 4-phenylbutarate (PBA) [43], con- comitant with a reduction in the expression of the inflammatory mediators expressed by the N1 phenotype. As with macrophages, polarized neutrophils as defined by Ly6G and CD206 expression have been shown to exert similar temporal effects post myocardial infarction (MI), with the authors defining $Ly6G^{+}CD206^{+}$ neutrophils as 'N1', shifting to 'N2' upon loss of CD206 expression [44]. This implicates the targeting of neutrophil polarization as a potential immunomodulatory strategy in a similar manner to the targeting of macrophage polarization that has dominated the field thus far, with additional considerations for therapeutic design and experimental investigation lying in the relatively short lifespan of primary neutrophils both in culture and *in vivo*. Given the 'first responder' role of neutrophils in the healing response and their ability to initiate angiogenesis, targeting of neutrophil phenotypes has the potential to influence subsequent immunological events to gear the immune response towards that of a pro-regenerative state by acting at an earlier stage to that of macrophage infiltration, introducing the possibility of an attractive new key player in the field of immunoengineering.

2.3. Natural killer cells in tissue healing and repair

Natural killer (NK) cells function as the sentinels of the innate immune system. Depending on their received stimuli, NK cells are instructed to either tolerate or attack an invading pathogen [45], and parallels are drawn between NK cells and cytotoxic CD8+ T cells of the adaptive immune system regarding their functionality [46]. They are well-defined in terms of their regulation of the adaptive immune system, with a growing body of evidence detail- ing their efficacy in mediating host immunity to viral pathogens [47]. In the case of tissue healing, NK cells have been shown to

function as regulators of the inflammatory phase, with evidence to date indicating a net negative effect of NK cells on the tissue repair process. Using a murine polytrauma model, NK depletion resulted in 50% mortality reduction and an overall decrease in inflammatory response as measured by IL-6 expression [48]. One study investigating femur fracture in Rag1-null mice, a murine model of adaptive immunodeficiency, implicated NK cells as a ma- jor contributor of IFN-γ during fracture healing, which indicates that that they have the ability to polarize macrophages towards a proinflammatory phenotype, particularly when highly activated as they are known to secrete large amounts of IFN-γ in this state [49,50]. IFN-γ production by NK cells has been shown to be enhanced by IL-33 (in combination with IL-12), a cytokine which is constitutively expressed in the bone and has been hypothesized to play opposing roles in bone homeostasis depending on the differentiation stage of the osteoclasts it acts to stimulate [51,52]. From a pro-healing perspective, one investigation used a model of corneal epithelial abrasion to demonstrate that NK depletion led to neutrophil influx to the wound site and was reported to hamper nerve regeneration and healing [53].

Studies so far largely indicate the ability of NK cells to in- fluence inflammation as being their major contribution to tissue healing. This is supported by investigation into NK cell interaction with bone marrow-derived mesenchymal stromal cells (BM-MSCs) in the context of bone fracture repair, with pro-inflammatory cytokine-activated NK cells inducing reactive oxygen species (ROS) generation within BM-MSCs and leading to decreased MSC viability [54]. It should be noted that MSCs have been shown to inhibit the cytotoxic capabilities of NK cells in turn, supporting a need for more thorough characterization of NK cell-MSC interac- tions [55–57], additionally advocating for further consideration of MSCs as potential complementary components of immunomod- ulatory strategies and therapeutic design, particularly in NK-cell focused immunotherapeutics such as those employed in cancer immunotherapies.

2.4. Innate lymphoid cells in tissue healing and repair

Innate lymphoid cells (ILCs), a recently classified family of innate immune cells, have emerged as cellular populations that share properties with cells of the adaptive immune system but do not display antigen-specific receptors. In this way, they are often described as the “innate counterparts of T cells” [58]. ILCs can be found in both lymphoid organs and non-lymphoid tis- sues. They are primarily tissue-resident and found in abundance in mucosal tissues, interacting with immune cells to promote immunity and mediate inflammation and tissue repair [59]. Of particular relevance to tissue healing, ILCs are enriched in barrier tissues such as the skin, intestine, and the lung, and have been documented to play a role in the maintenance of tissue integrity and promotion of chronic inflammatory disease [60]. They are grouped into three distinctive subsets: ILC1s, ILC2s, and ILC3s which are functionally considered to correspond to the adaptive immune cell subsets $CD4^+$ T helper (Th)1, Th2, and Th17 cells in their ability to respond to intracellular pathogens, response to extracellular pathogens and mediation of allergic responses, and response to microbial pathogens respectively [61].

ILC1s share features with NK cells in their expression of over- lapping markers such as NKp46 (humans and mice) and Tbet, similar effector functions, and production of IFN-γ . ILC1s are activated by cytokines such as IL-12, IL-15, and IL-18, and respond quickly to infections and certain bacteria [61]. They are distinguished from NK cells by their production of CD127 and IL-7R (a receptor for the pro-survival cytokine IL-7), and their lack of the eomesoder- min (Eomes) transcription factor. Whilst their active role in tis- sue regeneration and repair is less established than that of ILC2s and ILC3s, a recent study also indicated ILC1s as being drivers of intestinal epithelial matrix remodeling by their secretion of TGF- β1 and its consequent promotion of WNT/β-catenin pathway signalling via upregulation of CD44v6, a variant of the CD44 cell surface adhesion receptor [62]. ILC2s respond to cytokines IL-33, IL-25, and thymic stromal lymphopoietin (TSLP) and, like their functional Th2 counterparts, have been shown to be producers of IL-5 and the M2-like macrophage polarizing cytokine IL-13 in murine visceral adipose tissue (VAT) and a model of allergic asthma [63,64]. They are also producers of the M2-like macrophage po- larizing IL-4 and have been shown to contribute to the expansion of the anti-inflammatory regulatory T cell (Treg) subset, helping to establish disease resistance in a murine model of experimen- tal cerebral malaria [65]. This role as a type 2 cytokine producing cellular subset and demonstrated effects on M2-like macrophage polarization and Treg expansion advocate for ILC2s as a notable player in pro-healing responses. In addition, ILC2-secreted IL-13 has recently been shown to promote the renewal of stem cells via the β-catenin pathway in both human and murine intestinal stem cells [66]. A subset of ILC2s that are dependent on epithelial cell- derived IL-33 to drive their responses were also shown to improve wound healing in a cutaneous wound model [67]. ILC2s have been shown to drive Th2 cell polarization by inhibition of Th1 cells, sup- porting their role in tissue repair and regeneration given the pro- regenerative functions of the Th2 cell subset [68].

ILC3s exert a protective role by the secretion of IL-22, a cytokine that has been linked to reduced liver fibrosis and hepato- cyte cell death, in addition to having been shown to drive thymic tissue regeneration in mice [69–71]. During tissue healing, ILC3s exert an immunomodulatory influence as shown by their recruit- ment to the wound site, with depletion of this subset leading to hampered skin repair in a murine model [72]. Furthermore, a subset of ILC3s referred to as lymphoid tissue-inducing cells (LTis) has been shown to play a role in promoting the formation of secondary lymphoid organs during embryonic development and mediating tissue repair [73].

Taken together, delineation of the direct contribution of each ILC subset to tissue specific repair processes may prove a promis- ing avenue of exploration for identification of novel targets for enhanced tissue healing, with the potential for incorporation of each subset into both innate and adaptive immunomodulatory strategies as either direct influencers or peripheral contributors.

2.5. Dendritic cells in tissue healing and repair

Dendritic cells (DCs) are considered as “bridging” cells between the innate and adaptive arms of the immune system. DCs play a similar phagocytic role to macrophages in their recognition of invading pathogens and are heavily involved in the instruction of T and B cell responses post-trauma, primarily in their antigen-presenting capabilities. They can also activate the pro-reparative T cell subset, regulatory T cells (Tregs), an adaptive immune cell subset vital for regeneration [74].

DCs express pattern recognition receptors (PRRs) which recognize pathogenic and foreign materials and propagate signalling. Depending on the PRR stimulated, DCs exhibit an immunogenic or tolerogenic phenotype, the latter of which is responsible for the activation of various immunosuppressive pathways allowing for tolerance of self-antigen [75]. Tolerogenic DCs, in turn, polarize T cells towards a similarly tolerant state and can potentially reduce the extent of inflammation and thus attenuate aberrant host responses that can preclude tissue healing.

DCs play a putative immunoprotective role in the heart following MI in their regulation of anti-inflammatory monocytes and M2-like macrophage recruitment to the infarcted myocardium, with DC ablation resulting in sustained inflammation [76]. There is also

evidence that enrichment of DCs facilitates wound closure in a murine model of burn wound healing, with resultant increased TGFβ1 expression and enhancement of fibroblast proliferation confirmed not to adversely affect quality of wound healing by contributing to scar formation, supporting a beneficial role of DCs in the host healing response [77]. Furthermore, depletion of plasma- cytoid DC (pDCs), a specialized type of DC that produces large amounts of type I interferon (IFN-α/β), was found to delay reep- ithelialization of skin wounds in a murine model of skin injury, indicating a requirement for pro-inflammatory IFN-α/β and an acute inflammatory response in the initiation of epithelialization [78]. This can be likened to the requirement for an initial pro- inflammatory macrophage response in the tissue healing process and further implicates the inflammatory response as a major mod- ulator of tissue repair. While these studies highlight the important role of DCs in the tissue healing process across varied tissue types, it appears likely that they primarily play a regulatory role, particu- larly in their signaling to macrophages and T cells, rather than act- ing as a pronounced component of tissue repair and remodeling.

2.6. B cells in tissue healing and repair

The major role of B cells is in their presentation of antigen to T cells and resultant influence of the adaptive immune response. While studies regarding the role of B cells in tissue repair and wound healing are limited in number as compared to T cells, it has been shown that CD19-null mice (a murine model of B cell deficiency) in which cutaneous wound healing was examined, a lack of B cells resulted in inhibited healing accompanied by an increase in pro-inflammatory cellular infiltration and cytokine expression [79]. Mature B cells have been shown to accelerate wound healing when administered topically as a purified cell suspension in phosphate-buffered saline (PBS) to wounds sus- tained in a murine model of skin wound healing, with efficiency of wound healing scored by collagen deposition, angiogenesis, and nerve regeneration [80]. In this study, splenic mature naïve B cells were shown to significantly accelerate wound closure in both wild-type and diabetic murine wounds, showing their efficacy in the case of both acute and chronic wounds. Of note, a marked neutrophil influx was also observed at early time points in acute wounds treated with the mature B cell suspension, followed by neutrophil depletion at an accelerated rate when compared to the saline-only control cohort and further indicating accelerated tissue repair as a result of B cell administration. B cell depletion has been shown to result in delayed wound healing, with B cell reintroduction leading to the rescue of the healing phenotype in a splenectomized murine model [81].

B cells have been shown to predominate at the later stages of bone healing in a murine model of femoral fracture [82]. Under normal tissue homeostasis B cells secrete osteoprotegerin (OPG), an anti-osteoclastogenic factor. Under inflammatory conditions, however, B cells are known to secrete pro-osteoclastogenic factors such as receptor activator of nuclear factor kappa-B ligand (RANKL) [83,84]. While this is supportive of a temporal role for B cells in fracture healing, there is still much more extensive characterization required regarding the contribution for B cells and their specific secreted factors in tissue repair in various tissue types. Nonethe- less, targeting of B cells during healing may prove an important strategy for enhanced tissue repair, particularly in the case of bone and skin repair, when considered in the context of inflammation- modulating strategy design.

2.7. T cells in tissue healing and repair

There is now ample evidence supporting the crucial role of T cells in tissue repair and regeneration through modulation of inflammation during the healing process. Naïve T cells differentiate into either CD8+ cytotoxic T cells or CD4+ T helper (Th) cells which can exert positive or negative effects on tissue healing. Seminal work in the field has indicated that cytotoxic CD8+ T cell presence at the injury site is associated with poor tissue regen- erative outcomes, with a high number of CD8+ cytotoxic T cells at the bone fracture site having a negative impact on bone regener- ation in both mice and humans [85,86]. In contrast, a prevalence of CD4+ Th cells has been shown to contribute to effective tis- sue regeneration [87]. The main CD4+ T cell subset involved in tis- sue repair is the CD4+ Th subset, largely functioning in its ability to switch from a Th1 to Th2 phenotype analogous to the M1-like to M2-like macrophage transition and is marked by a pro to anti- inflammatory cytokine expression profile promoting the resolution of inflammation and resultant regeneration of tissue. Both Th1 and Th2 subtypes of CD4+ Th cells play a role in the chronic inflamma- tory phase of healing by the production of cytokines that modulate the inflammatory state of the injury site. An early study demon- strated CD4+ T cells to be the predominant T cell population per- sisting throughout the tissue repair process in a murine model of dermal wound healing. This study also demonstrated the impor- tance of both CD4+ and CD8+ T cell presence for tempering of in- flammation during the healing process, with severe-compromised immunodeficient (SCID) mice exhibiting exacerbated inflammation, heightened scarring, and decreased formation of new vessels post-dermal wound introduction, yet displayed accelerated wound closure time compared to their WT counterparts [88]. This addition- ally indicates that the speed at which wound closure processes oc- cur is not to be taken as definitive indicator of superior tissue re- pair, with a number of factors to be considered when addressing the question of tissue regeneration. It becomes necessary in ex- perimental investigation to further define the criteria that must be met to identify 'superior' healing and tissue regeneration, and rec- ognize the elements, such as faster wound closure, that appear to be beneficial but ultimately prove preclusive to adequate regener- ation of functional host tissue.

Notably as regards tissue repair, one study which involved re-populating Rag1-null mice with wild-type (WT) CD4+ T cells post-injury resulted in improved running capacity accompanied by up-regulated Th2-associated cytokine IL-4 at 3 weeks post repopulation, further supporting a role for Th2 cells in injury-related repair [87]. A recent investigation into bladder tissue regeneration using chymase-deficient mice, which do not undergo natural exfoliation of bladder tissue during infection to the same extent as their WT counterparts, found that bladder infection and requirement for tis- sue regeneration stimulated a Th2-biased response to promote ep- ithelial cell proliferation in the WT cohort at the expense of host ability to clear bacteria and control infection, indicating a dampen- ing of the Th1-mediated anti-bacterial response in favor of a Th2- biased pro-reparative immune response. This study exemplifies the tissue-specific action of certain immune cell subsets, and the po- tential compromises resulting from such, to be an additional con- sideration in therapeutic design [89]. It is worth considering in- vestigation into immune cell activity not only in the general con- text of tissue repair, but with added scrutiny of the tissue-specific microenvironment with which immune cells interact, given certain tissues may require particular immune responses to facilitate re- pair that would otherwise prove disadvantageous.

Regulatory T cells (Tregs) exert an influential role in tissue regeneration by engaging in crosstalk with neutrophils, directing macrophage polarization, and regulating helper T cells, and have been shown in a number of tissue repair models to be regulators of the healing response [90,91]. Tregs polarize macrophages towards an M2-like phenotype and are seen to persist as a T cell subpop- ulation at the injury site even as overall T cell numbers decrease [92,93]. Treg depletion has been shown to result in increased mus-

cle damage and inflammation in a murine model of muscular dystrophy, while mice treated with compounds promoting Treg differentiation and development displayed reduced muscle damage when compared to untreated control mice [94,95], highlighting the necessity of Tregs for tissue regeneration. Mechanistically, Tregs homing to an injury site are drawn by mast cell-secreted growth factor amphiregulin [96] (also secreted by the ILC2 subset and $\gamma\delta$T cells), and can then in turn secrete their own amphiregulin, which plays a role in tissue regeneration and is required for the differentiation and proliferation of surrounding immune cells [96–98]. The dependency on paracrine signalling by Tregs for cardiomyocyte proliferation, a critical factor in regeneration of the myocardium, has been demonstrated in a murine model of Treg depletion and re-supplementation with six Treg-secreted factors (Cst7, Tnfsf11, Il33, Fgl2, Matn2, and Igf2) as chosen by performance of an *in sil- ico* analysis followed by a test of ability to induce cardiomyocyte proliferation, resulting in rescue of the Treg-dependent therapeutic effect [99].

CD4+ Tregs are also known to mediate immunosuppression and the presence of these cells has been reported to have a pro-reparative role in the repair of skin, kidney, lung, and skeletal muscle [90,100,101]. Tregs have been shown to modulate monocyte and macrophage phenotypes to promote tissue healing post-MI and promote pro-resolving macrophage activity in the regression of atherosclerotic inflammation and tissue remodeling [97,102]. A recent review highlights the necessity for Tregs in repair of skin injury in governing interaction between lymphocytes and non-hematopoietic cells during the healing process [103]. On this ba- sis, it is reasonable to suggest that Treg-targeting strategies may be employed in immunomodulatory therapeutic design in which it is sought to influence a number of immune cell subsets. In par- ticular, strategies that facilitate the tissue repair process by inhibition of deleterious immune cell contributions, namely those of T cell subsets such as CD8+ cytotoxic T cells and Th1 cells, would stand to benefit from harnessing the immunosuppressive functions of Tregs.

Other T cell subsets have been shown to play a role in orchestrating the healing response. Th17 cells and the Th17 secreted pro-inflammatory cytokine IL-17 are emerging as players in the development of fibrosis. A recent body of work has shed light upon the previously unexplored dynamic between Th17 cells and senes- cent cells in the context of tissue regeneration. It was shown that Th17 cells and senescent fibroblasts engage in a positive feedback loop that fosters chronic inflammation and ultimately inhibits tis- sue repair processes, with *in vitro* application of Th17 cells induc- ing senescence in healthy fibroblasts, and senescent fibroblasts in turn skewing differentiation of naive T cells towards Th17. Using a murine model of osteoarthritis, it was then shown that clearance of senescent cells in turn reduced the prevalence of Th17 cells and thus resulted in decreased tissue damage, also highlighting the requirement for IL-4 post clearance to allow healing activity to ensue [104].

Furthermore, a recent study highlighted an IL-36γ-producing macrophage subset as the driver of IL-17 mediated fibrosis [105]. It was shown that application of urine-derived stem cells down-regulated Th17 (as well as Th1) immune responses, leading to decreased inflammation and improved healing in a murine colitis model [106]. Further subsets of T cells include the $\alpha\beta$T cell and $\gamma\delta$T cell subpopulations; to date, $\alpha\beta$T have been shown to exert both positive and negative effects on tissue regeneration, whilst $\gamma\delta$T cells have primarily been demonstrated to display pro- reparative functions. This T cell subpopulation is particularly en- riched in the dermis, and has been shown in murine models to be required for wound repair [107]. As seen with Tregs, $\gamma\delta$T cells are also contributors of pro-healing factor amphiregulin, with $\gamma\delta$T cell-secreted amphiregulin demonstrated to be crucial in the maintenance of barrier tissue homeostasis [108]. In the regenera- tion of bone tissue, an important pro-regenerative role for IL-17A-production by $\gamma\delta$T cells has been demonstrated in vivo, in which it was shown that this pro-inflammatory cytokine plays a role in promoting the osteoblastic differentiation of mesenchymal progenitor cells [109].

Thus, it is well established that various T cell subsets and T cell specific cytokines are critical modulators of inflammation driven tissue repair, however details of their interactions with stem cells and progenitor cells, the major contributors to ECM deposition, is relatively underexplored and therefore warrants further investigation.

3. Immunomodulation for tissue repair and regeneration

With an array of immune cell subtypes implicated as crucial players in tissue repair and regeneration it is unsurprising that a vast range of immunomodulatory strategies are employed in the design of regenerative therapeutics. Although these strategies have advanced the field of regenerative medicine to a consider- able degree, there still exist multiple limitations and challenges when attempting to target various components of such a com- plex and interdependent system during tissue regeneration. The field of immunomodulatory bioengineering, or immunoengineer- ing, a field which marries the benefits of immunomodulatory ther- apeutics with those of biomaterial intervention, either alone or in combination with stem cells and growth factors, has the capacity to address many of these challenges. Here, we provide an overview of means by which immune cell processes, namely those relating to inflammatory activities, have been targeted to enhance tissue repair and regeneration, touching upon the limitations of each and providing examples as to how the incorporation of biomaterials has led to the advancement of regenerative therapeutics.

3.1. Immunomodulation through targeting pro-inflammatory factors

Given the critical role of inflammation in tissue repair and the extent to which inflammation dictates the subsequent reparative or destructive processes, the targeting of inflammatory pathways has proven to be a potent immunomodulatory strategy. In this re- gard many investigations into modulation of the immune response have focused on targeting pro and anti-inflammatory mediators, and there exists in-depth review of biomaterial-mediated induc- tion of the inflammatory response *via* formation of the inflamma- some [110]. Therapeutic strategies targeting inflammation are of particular relevance to biomaterial-mediated tissue regeneration in that they also pose an avenue for modulation or tempering of the foreign body reaction (FBR) and potential fibrosis and scarring that can result from inflammation in the wake of biomaterial implanta- tion.

The pro-inflammatory cytokine TNFα has been implicated as a major contributor to detrimental outcomes post-injury. This has been demonstrated particularly in the context of macrophage- mediated responses, and reduction or inhibition of TNFα as an as- sociated effect of common painkillers such as aspirin and ibupro- fen has shown promise in the context of tissue repair and regen- eration [3,111]. Serving as an example of the beneficial effect of TNFα inhibition, bone tissue regeneration was shown to be pos- itively influenced by the biomaterial mediated delivery of anti- TNFα antibodies in a diabetic rat model [112]. Cardiac tissue, too, has been shown to benefit from inhibiting TNFα, with the use of gold nanoparticles to knockdown TNFα in RAW264.7 macrophages *in vitro* and subsequently in an *in vivo* rodent model of MI, result- ing in improved cardiac function [113].

Hyaluronic acid, shown to exert an anti-inflammatory effect in its high molecular weight form [114], has also proven effec-

tive in delivering anti-TNFα to modulate inflammation in a burn wound model, resulting in a decrease in nonviable tissue and lessened pro-inflammatory cytokine secretion at the wound site when compared to HA alone and saline controls [115]. The efficacy of TNFα targeting, therefore, provides not only an effective strategy to modulate inflammation, but also supports the targeting of ma- jor pro-inflammatory cytokines to achieve a more pro-regenerative immune cell landscape.

Similar to our earlier caveat regarding the modulation of macrophage phenotype in the development of immunomodulatory strategies, TNFα too has been implicated to play a beneficial role at particular points during bone tissue repair [3]. A recent study particularly highlighted the role of TNFα and its interaction with TNFR2, expressed on many cells of the immune system, in mediating anti-inflammatory and immunosuppressive responses in the context of MSC-mediated immunomodulation, indicating TNFα as not only useful in inhibitory strategies, but also a potential deliverable therapeutic in a finely-tuned system [116].

Targeting of the pro-inflammatory cytokine interleukin-1 (IL- 1) and its receptor (IL-1R1) is particularly notable in the context of biomaterial-mediated immunomodulation, with inhibition of IL- 1R1 signalling shown to enhance the tissue regenerative activity of MSCs [117]. A recent investigation building on this demonstrated the negative impact of IL-1R1 activation on the osteo-regenerative capabilities of MSCs [118]. In this study, the inhibition of IL-1 pro-inflammatory signalling through the co-delivery of IL-1 receptor agonist (IL-1Ra) and pro-osteogenic growth factors BMP-2 and PDGF-BB via a fibrin-based biomaterial scaffold resulted in en- hanced bone regeneration *in vivo* when compared to growth fac- tors alone.

Further exemplifying the immunomodulatory potential of targeting pro-inflammatory IL-1R1 signalling with biomaterial intervention, it was demonstrated that electrodes coated with polyethylene glycol (PEG) functionalized with IL-1Ra improved over- all neuronal survival *in vitro* due to the imbued, controlled anti-inflammatory capability of the biomaterial [119], suggesting that in circumstances in which cell death and resultant inflammation triggered by necrotic cells and their secretome prove preclusive to tissue repair, inhibition of IL-1R1 may offer a combative strategy to enhance cell survival.

Given the potency of targeting pro-inflammatory signalling towards a pro-regenerative outcome, therapeutic strategies that seek to target the nuclear factor kappa b (NFkB) signalling path- way, a central pathway in pro-inflammatory mediation across a range of diseases and regenerative processes [3,120], have also proven useful in aiding tissue repair and regeneration. For exam- ple, it has been shown that curcumin-loaded nanoparticles effec- tively inhibited the activation of NF-kB and downregulated inflam- matory markers alongside decreased infiltration of inflammatory monocytes in an *in vivo* model of experimental autoimmune en- cephalomyelitis (EAE), holding promise for the future combatting of degenerative or destructive diseases such as multiple sclerosis (MS) and graft vs. host (GVD) [121]. In the context of bone re- generation, pro-inflammatory cytokine-stimulated NFkB signalling has previously been shown to inhibit osteogenic differentiation of MSCs [122], making inhibition of NFkB signalling an attractive strategy in bone regeneration. Small interfering RNA (siRNA) based NFkB targeting has also risen as an effective means of blocking NFkB signalling, with use of hybrid micelles to co-deliver siRNA targeting p65 (RelA, a member of the NFkB signalling family) and dexamethasone, a glucocorticoid that inhibits transcription of NFkB and is commonly employed in treatment of rheumatoid arthri- tis, effectively reducing inflammation and inducing polarization of macrophages from a pro- to anti-inflammatory state in a murine model of collagen-induced arthritis [123].

NFkB targeting has been shown to be an effective modulator of inflammation across a range of tissue types, with biomaterial-mediated delivery aiding localization and elevating efficacy. This means of NFkB targeting can also be employed to enhance signalling through the NFkB pathway, with recent evidence implicating the NFkB/IL-1 signalling pathway as critical in mediating murine lung tissue repair post influenza infection as part of a specific inflammatory niche required for removal of damaged tissue and activation of the required stem and progenitor cell populations for regeneration [124].

Toll-like receptors (TLRs), a set of pattern-recognition recep- tors expressed on many immune cell subsets, have been shown to play a role in tissue regeneration which can be attributed in part to their activation of the pro-inflammatory NFkB signalling pathway, as well as the induction of TNFα among other pro-inflammatory cytokines. They therefore pose a potential upstream target of pro-inflammatory signalling and have thus been employed in biomaterial-mediated immunomodulation, with TLR4 targeting proving particularly effective in tissue regeneration. TLR4 activation in murine renal and cardiac ischemia-reperfusion mod- els has been shown to contribute to pro-inflammatory responses that mediate organ failure, with TLR4-/- mice shown to exhibit decreased inflammation, smaller infarct sizes, and protection against tubular damage and immune cell infiltration [125,126]. However, it is clear that inhibiting certain influencers of inflammatory signalling must be considered in the context of the complex cellular interplay at the defect site, a caveat supported by a recent *in vitro* study using LPS-primed MSCs in which TLR4 had been silenced that displayed diminished wound healing ability, in contrast with their LPS-primed only MSC controls which promoted neutrophil activation, NET formation, and increased healing [127]. TLR4 signalling, too, has been demonstrated to be a regulator of wound healing in vivo, with TLR4-/- mice exhibiting slower wound healing, which was postulated to be as a result of TLR4-induced TGF-β and CCL5 activation, an immune cell chemokine [128].

3.2. *Immunomodulation through targeting anti-inflammatory factors*

In contrast to the targeting of pro-inflammatory pathways, which generally aims to inhibit or dampen the activity of pro- inflammatory mediators, anti-inflammatory strategies usually seek to skew host responses towards a desired state typically *via* the delivery of cytokines known to have a direct anti-inflammatory function. The appropriate temporal dampening or modulation of inflammation is often desirable in the context of tissue regenera- tion, with biomaterial-mediated delivery of anti-inflammatory fac- tors representing a promising route towards immunomodulation for tissue repair.

Delivery of IL-4, an M2-like macrophage polarizing cytokine, via mesoporous silica nanoparticles (MSNs) has been shown to induce M2-like macrophage polarization *in vivo* and lower ROS production, demonstrating the potential of exogenous IL-4 delivery for improving tissue repair [129]. Similarly, functionalization of TiO_2 nanotubes with IL-4 and attachment of RGD peptide resulted in M2-like macrophage polarization and enhanced production of the pro-reparative cytokine IL-10, and also appears to improve MSC osteogenic differentiation [130]. IL-4-conjugated gold nanoparticles implanted into murine skeletal muscle were shown to lead to a twofold increase in the M2a-like macrophage population (one of the four distinct M2-like macrophage subsets and most strongly associated with anti-inflammatory and wound healing actions [131]) and a twofold decrease in M1-like macrophages [132]. Another recent study has found that alginate hydrogels loaded with anti-inflammatory molecules, either CSF-1 alone or in conjunction with IL-4, or IL-4, IL-6, and IL-13, have resulted in faster tissue repair *in vivo* using a rat model of ischemia-reperfusion. Subsequent injection of biomaterials loaded with CSF-1 and IL-4 were then shown to result in reduced fibrosis and increased cardiac function in a rat MI model, supporting use of biomaterial-

mediated cytokine delivery for the healing of damaged cardiac tissue [133].

It is worth noting that, given the complex and spatiotemporal role of macrophage phenotype in tissue repair, appreciation for the need of an M1-like phenotype early on in the repair process has come to light. Demonstrating this, a bone scaffold that sequentially delivered M1-like and M2-like polarizing cytokines *via* physically adsorbed IFN-γ and biotinylated IL-4 respectively has been investigated in a murine subcutaneous implantation model. Overall, this sequential cytokine delivery method resulted in improved vascularization *in vivo* in comparison to either an IFN-γ or IL-4 scaffold alone, exemplifying the necessity of controlled transition of M1- like to M2-like macrophages required for vascularization and angiogenesis [134], and highlighting the tissue-specific requirements for a spectrum of inflammation states at different stages of repair as a consideration in therapeutic delivery of immunomodulatory cytokines.

In addition to loading of IL-4 as an M2-polarizing cytokine, delivery of IL-10 has also been investigated as a means of inducing M2-like macrophage polarization and promoting tissue repair. In- deed, loading of alginate nanoparticles with IL-10 has displayed a potent polarization towards a reparative phenotype in a rat model of arthritis [135], while more recently it has been demonstrated that direct supplementation of recombinant IL-10 in culture me- dia resulted in induction of robust BMP2, ALP and osteopontin gene expression in human MSCs, demonstrating a role for IL-10 not only in macrophage polarization but also in promoting os- teogenesis [136]. Further supporting the therapeutic use of tar- geted IL-10 delivery, an investigation by Kim et al. has demon- strated that delivery of IL-10 *via* a biomaterial nanocarrier resulted in significant regression of atherosclerotic plaques in a murine model of atherosclerosis. This employment of nanocarriers as de- livery molecules also resulted in greater IL-10 accumulation in the atherosclerotic lesions, surmounting the issue of rapid clearance encountered with delivery of free cytokine [137].

Of particular note, a recent study by Sok et al. employed PEG-hydrogels to locally deliver IL-10 and the specialized pro-resolving mediator (SPM) aspirin-triggered resolving D1 (AT-RvD1) resulting in increased infiltration of pro-regenerative macrophages, dendritic cells, and T cells in a murine model of tissue injury, highlighting the efficacy of local bioactive molecule delivery in inducing the de- sired response of multiple immune cell subtypes [138].

The TGF-β isoforms 1-3 have been shown to play a key role in multiple stages of tissue healing and regeneration [139], with the TGF-β1 isoform particularly implicated in skeletal muscle repair [140] and scar formation [20]. TGF-β1, although known to hold pro-inflammatory capabilities, has also been shown to func- tion as a major anti-inflammatory modulator in tissue regenera- tion and therefore indicated as a therapeutic target. Early work demonstrated *tgfb*-null SCID mice exhibited inferior tissue healing in comparison to their SCID only counterparts, implicating TGB- β1 as a crucial factor in healing and tissue regeneration [141]. The implantation of TGF-β1 releasing PLG scaffolds into a murine model of diabetes was then shown to result in a 40% decrease in the expression of pro-inflammatory mediators TNFα, IL-12, and MCP-1, and a decrease in subsequent leukocyte infiltration postu- lated to be as a result of the earlier tempering of inflammation [142]. TGFβ1 and IL-10 are frequently used to influence dendritic cell activity *in vitro*, and it was demonstrated that immobilization of TGFβ1 and IL-10 on PEG hydrogel surfaces inhibited immature dendritic cell (iDC) maturation, advocating for the efficacy of de- signing an immunosuppressive biomaterial for therapeutic benefit [143].

TGFβ has been also characterized as a key regulator of the immunosuppressive and anti-inflammatory activities of Tregs [144], with knockout of FoxP3+ Treg-specific TGFβ receptor 1 (TGF-βR1) leading to a decreased ability to modulate inflammation in the colon in a murine model of colitis [145]. Taken together, studies thus far indicate that TGFβ1 poses a promising target to employ in biomaterial-mediated drug delivery for an immunomodulatory goal, with the potential to exert pro-regenerative effects on multi- ple immune cell types involved in tissue repair.

Given the potency of targeting inflammatory signalling in the context of the immune response and the wealth of evidence strongly suggesting that such responses can be modulated *via* bio- material intervention, it is reasonable to suggest that biomaterial- mediated targeting of inflammatory activities represents a partic- ularly promising means of generating pro-regenerative environ- ments *in vivo*.

4. Concluding remarks and future directions

Despite a wealth of advances that have furthered our understanding of different immune cell subsets and their extensive interplay with tissue repair processes, macrophages remain the most extensively characterized cell type when determining the role of (and targeting) the immune system in tissue regeneration. How- ever, there is now growing evidence to suggest that various other immune cell subsets can both positively and negatively influence tissue regeneration in a tissue specific manner. For example, Th2 cells, Tregs, and $\gamma\delta$ T cells have been shown to be supportive of a more pro-regenerative phenotype, and indeed direct polarization of these subsets through cytokine delivery or blockade may prove a plausible and worthy strategy to enhance tissue repair. While less well characterized, a new appreciation for the temporal role of B cells, NK cells and ILCs in tissue healing positions these cells as po- tential candidates to target, although greater efforts must be made to extensively characterize and establish their role in the regener- ation of multiple tissue types. Understanding the role of these im- mune cells in the context of specific tissue microenvironments will be central to the design of elegant, tissue-specific immunomodula- tory strategies.

The incorporation of biomaterials into immunomodulatory therapeutics has the potential to transform the field of tissue engineer- ing and regenerative medicine. Existing approaches to manipulate immune cell responses at sites of injury generally aim to target pro or anti-inflammatory activities at play in the tissue microenvironment, with a particular focus on dampening the inflamma- tory activities of immune cells with the goal of promoting superior healing and tissue regeneration (Fig. 2). Incorporating biomateri- als into the design of such therapies enables the localized deliv- ery and temporally controlled release of cytokines and molecules targeting inflammatory processes, in addition to providing a phys- ical structure to guide the tissue repair process. Perhaps equally important, the physiochemical properties of biomaterials themselves will have a significant impact on the host immune system [3,111,146], which can be leveraged to design scaffolds and biomaterials that will invoke programmable immune responses. Future immunomodulatory therapeutics will likely leverage such biomaterial properties as well as their capacity to control the delivery of cytokines, chemokines and other regulatory factors.

As immunotherapies in tissue engineering and regenerative medicine develop in this way, it will become necessary to consider the host reaction to diverse immunomodulatory inputs. For example, how will the host-biomaterial response, which is commonly pro-inflammatory and skewed towards the adverse outcomes of fibrosis and scar formation, be influenced by the local delivery of anti-inflammatory cytokines from the same biomaterial? Fur- thermore, much of our understanding of how the physiochemi- cal properties of biomaterials, for example how surface topography or substrate stiffness can be tuned to promote anti-inflammatory

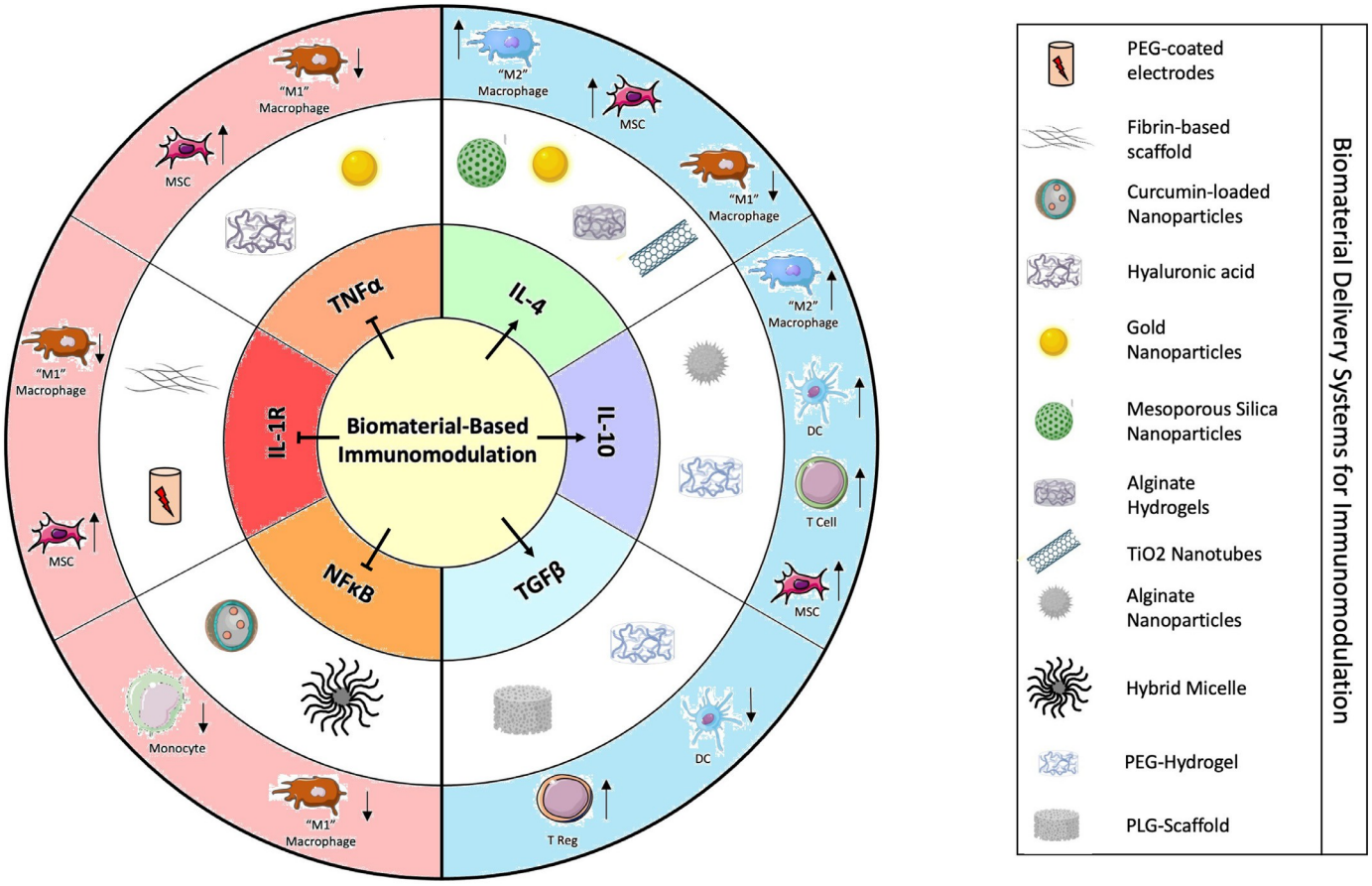

Fig. 2. Summary of Reviewed Biomaterial-Based Targeting of Pro and Anti-Inflammatory Factors for Immunomodulation.
A summary schematic of each of the biomaterials discussed in this review as examples of biomaterial-based immunomodulation by targeting pro and anti-inflammatory factors, plus a legend to identify key biomaterials discussed in this paper. From the center outwards this depicts the factor targeted whether by inhibition or delivery, the biomaterial used to implement this, and the cell type influenced.
From the upper right segment and going clockwise: Mesoporous silica nanoparticles, gold nanoparticles, alginate hydrogels, titanium dioxide (TiO_2) nanotubes delivering IL-4 enhances M2-like macrophage polarization and increases the M2:M1 macrophage ratio. Loading of alginate hydrogels with anti-inflammatory IL-10 increases the M2:M1 macrophage ratio and enhances osteogenesis. PEG-hydrogel delivery of IL-10 facilitates immunomodulation. Delivery of TGFβ *via* PEG-hydrogels and PLG scaffolds tempers inflammation and reduces iDC maturation, and can enhance immunosuppressive functions of Tregs. Inhibition of NFkB signaling through hybrid micelles delivering siRNA, or curcumin-loaded nanoparticles leads to an increase in anti-inflammatory macrophages and monocytes respectively. Coating of electrodes with IL-1R1-functionalized PEG leads to improved neuronal survival *in vitro*. Inhibition of IL-1R by delivering IL-1R agonist alongside pro-osteogenic growth factors on a fibrin-based matrix leads to enhanced bone regeneration in a murine host. Knockdown of TNFα with gold nanoparticles and delivery of anti-TNFα through hyaluronic acid (HA) based hydrogels results in lessened pro-inflammatory cytokine secretion and enhances the immunomodulatory capabilities of MSCs.

macrophage polarization *in vitro* [147–151] needs to be reevaluated in the context of the *in vivo* microenvironment where potentially pro- or anti-inflammatory factors are being released from the same device. Careful fine-tuning of biomolecule release will be central to the success of such therapeutics. Indeed, such advances hold the potential to inform further immunological studies and eluci- date the precise effects or modulate the action of immunomodu- latory factors to a greater extent than has been achieved without the backdrop of biomaterial design.

There also remains a substantial gap in our knowledge of cell- cell interactions between immune cells and tissue specific stem and progenitor cells, and further studies may reveal mechanisms by which tissue healing and regeneration takes place in addition to identifying novel therapeutic targets that could be used to en- hance the tissue repair process. As well as the interaction of im- mune cells with stem and progenitor cells, other cells types con- tinue to be identified as players in tissue regeneration and the im- mune response to biomaterials. A recent review briefly summarizes the role of pericytes, mural cells of blood microvessels that facili- tate immune cell extravasation, and their role in angiogenesis and potential to contribute to scar formation [3], highlighting not only pericytes as additional cellular players in tissue repair, but also the potential for targeting a range of cellular subsets closely linked to immune cell activity as another level to be considered in biomate- rial mediated immunotherapeutic design.

While current studies are scarce, therapeutic strategies involv- ing siRNA-mediated gene silencing or regulating the immune sys- tem through miRNAs and extracellular vesicles (EVs) are underway and offer alternative strategies to loading of exogenous cytokines and antibodies, proving beneficial to tissue healing. Another key remaining challenge lies in the development of biomaterials that can control specific immune system mediated responses for opti- mal healing and complete regain of tissue function *in situ*. As our understanding and characterization of the role of the immune sys- tem in tissue healing and regeneration continues to grow, com- pounded with ongoing investigation into the varied and potent ef- fects of biomaterial composition and properties on immune cell function, it is reasonable to assume that we will continue to see a vast expansion of our knowledge and resources in this area over the coming years.

Acronyms

NK	Natural Killer
ILC	Innate Lymphoid Cell
TGF	Transforming Growth Factor
VEGF	Vascular Endothelial Growth Factor
PDGF	Platelet-Derived Growth Factor
ECM	Extracellular Matrix
BMSC	Bone marrow-derived stem/stromal cells
MMP	Matrix Metalloproteinase
LPS	Lipopolysaccharide
IFN-γ	Interferon-γ
IL-	Interleukin-
ANXA1	Annexin A1
AMPK	AMP-activated protein kinase
DAMP	Danger Associated Molecular Pattern
CXCL-	CX Chemokine Ligand
CCL-	C Chemokine Ligand
DC	Dendritic Cell
PGE2	Prostaglandin E2
NET	Neutrophil Extracellular Trap
FBR	Foreign Body Reaction
PBA	4-phenylbutarate
MI	Myocardial Infarction
BM-MSC	Bone marrow-derived mesenchymal stromal cells
ROS	Reactive Oxygen Species
Th-	T helper
TSLP	Thymic Stromal Lymphopoietin
VAT	Visceral Adipose Tissue
Treg	Regulatory T Cells
LTi	Lymphoid Tissue-Inducing Cells
PRR	Pattern Recognition Receptor
pDC	Plasmacytoid Dendritic Cell
IFN-α/β	Type I Interferon
PBS	Phosphate Buffered Saline
OPG	Osteoprotegerin
RANKL	Receptor Activator of Nuclear Factor Kappa B Ligand
SCID	Severe Combined Immunodeficiency
WT	Wild Type
IL-1R1	Interleukin-1 Receptor
IL-1Ra	Interleukin-1 Receptor Agonist
PEG	Polyethylene Glycol
NFkB	Nuclear Factor Kappa B
EAE	Experimental Autoimmune Encephalomyelitis
MS	Multiple Sclerosis
GVD	Graft Vs. Host Disease
TLR	Toll-Like Receptor
MSN	Mesoporous Silica Nanoparticles
SPM	Specialized Pro-Resolving Mediator
AT-RvD1	Aspirin-Triggered Resolving D1
MCP	Monocyte Chemoattractant Protein
iDC	Immature Dendritic Cell
siRNA	Small Interfering RNA
miRNA	Micro RNA
EV	Extracellular vesicle

Declaration of Competing Interest

The authors declare that they have no known competing financial interests or personal relationships that could have appeared to influence the work reported in this paper.

References

[1] T.A. Wynn, T.R. Ramalingam, Mechanisms of fibrosis: therapeutic translation for fibrotic disease, Nat. Med. 18 (7) (2012) 1028–1040.
[2] A.B. Aurora, E.N. Olson, Immune modulation of stem cells and regeneration, Cell Stem Cell 15 (1) (2014) 14–25.
[3] Z. Julier, A.J. Park, P.S. Briquez, M.M. Martino, Promoting tissue regeneration by modulating the immune system, Acta Biomater 53 (2017) 13–28.
[4] J. Larouche, S. Sheoran, K. Maruyama, M.M. Martino, Immune regulation of skin wound healing: mechanisms and novel therapeutic targets, Adv. Wound Care (New Rochelle) 7 (7) (2018) 209–231.
[5] M. Rodrigues, N. Kosaric, C.A. Bonham, G.C. Gurtner, Wound healing: a cellular perspective, Physiol. Rev. 99 (1) (2019) 665–706.
[6] J.W. Godwin, A.R. Pinto, N.A. Rosenthal, Macrophages are required for adult salamander limb regeneration, Proc Natl Acad Sci USA 110 (23) (2013) 9415–9420.
[7] J.W. Godwin, A.R. Pinto, N.A. Rosenthal, Chasing the recipe for a pro-regenerative immune system, Semin. Cell Dev. Biol. 61 (2017) 71–79.
[8] A. Sindrilaru, K. Scharffetter-Kochanek, Disclosure of the culprits: macrophages-versatile regulators of wound healing, Adv. Wound Care (New Rochelle) 2 (7) (2013) 357–368.
[9] L.Y. Lu, F. Loi, K. Nathan, T.H. Lin, J. Pajarinen, E. Gibon, A. Nabeshima, L. Cordova, E. Jämsen, Z. Yao, S.B. Goodman, Pro-inflammatory M1 macrophages promote osteogenesis by mesenchymal stem cells via the COX-2-prostaglandin E2 pathway, J. Orthop. Res. 35 (11) (2017) 2378–2385.
[10] B. Chazaud, Macrophages: supportive cells for tissue repair and regeneration, Immunobiology 219 (3) (2014) 172–178.
[11] J.G. Tidball, M. Wehling-Henricks, Macrophages promote muscle membrane repair and muscle fibre growth and regeneration during modified muscle loading in mice in vivo, J. Physiol. 578 (Pt 1) (2007) 327–336.
[12] R. Londono, S. Tighe, B. Milnes, C. DeMoya, L.M. Quijano, M.L. Hudnall, J. Nguyen, E. Tran, S. Badylak, T.P. Lozito, Single cell sequencing analysis of lizard phagocytic cell populations and their role in tail regeneration, J. Im- munol. Regen. Med. 8 (2020).
[13] M.F. Gutknecht, A.H. Bouton, Functional significance of mononuclear phagocyte populations generated through adult hematopoiesis, J Leukoc Biol 96 (6) (2014) 969–980.
[14] K.J. Lavine, S. Epelman, K. Uchida, K.J. Weber, C.G. Nichols, J.D. Schilling, D.M. Ornitz, G.J. Randolph, D.L. Mann, Distinct macrophage lineages contribute to disparate patterns of cardiac recovery and remodeling in the neonatal and adult heart, Proc Natl Acad Sci USA 111 (45) (2014) 16029–16034.
[15] V.E. Miron, A. Boyd, J.W. Zhao, T.J. Yuen, J.M. Ruckh, J.L. Shadrach, P. van Wijngaarden, A.J. Wagers, A. Williams, R.J.M. Franklin, C. Ffrench-Constant, M2 microglia and macrophages drive oligodendrocyte differentiation during CNS remyelination, Nat. Neurosci. 16 (9) (2013) 1211–1218.
[16] D. Dal-Secco, J. Wang, Z. Zeng, E. Kolaczkowska, C.H. Wong, B. Petri, R.M. Ransohoff, I.F. Charo, C.N. Jenne, P. Kubes, A dynamic spectrum of monocytes aris- ing from the in situ reprogramming of CCR2+ monocytes at a site of sterile injury, J. Exp. Med. 212 (4) (2015) 447–456.
[17] C.D. Mills, K. Kincaid, J.M. Alt, M.J. Heilman, A.M. Hill, M-1/M-2 macrophages and the Th1/Th2 paradigm, J. Immunol. 164 (12) (2000) 6166–6173.
[18] N.X. Landén, D. Li, M. Ståhle, Transition from inflammation to proliferation: a critical step during wound healing, Cell Mol. Life Sci. 73 (20) (2016) 3861–3885.
[19] M. Pakyari, A. Farrokhi, M.K. Maharlooei, A. Ghahary, Critical role of transforming growth factor beta in different phases of wound healing, Adv. Wound Care (New Rochelle) 2 (5) (2013) 215–224.
[20] Y. Liu, Y. Li, N. Li, W. Teng, M. Wang, Y. Zhang, Z. Xiao, TGF-β1 promotes scar fibroblasts proliferation and transdifferentiation via up-regulating MicroRNA-21, Sci. Rep. 6 (2016) 32231.
[21] G.J. Kotwal, S. Chien, Macrophage differentiation in normal and accelerated wound healing, Results Probl. Cell Differ. 62 (2017) 353–364.
[22] S. McArthur, G. Juban, T. Gobbetti, T. Desgeorges, M. Theret, J. Gondin, J.E. Toller-Kawahisa, C.P. Reutelingsperger, B. Chazaud, M. Perretti, R. Mounier, Annexin A1 drives macrophage skewing to accelerate muscle regeneration through AMPK activation, J. Clin. Invest. 130 (3) (2020) 1156–1167.
[23] B.N. Brown, B.D. Ratner, S.B. Goodman, S. Amar, S.F. Badylak, Macrophage polarization: an opportunity for improved outcomes in biomaterials and regenerative medicine, Biomaterials 33 (15) (2012) 3792–3802.
[24] L. Bai, L. Fu, L. Li, F. Ren, Q. Zheng, S. Liu, Y. Han, S. Zheng, Y. Chen, Z. Duan, Cellular mechanisms of hepatoprotection mediated by M2-like macrophages, Med. Sci. Monit. 24 (2018) 2675–2682.
[25] A. Mauro, V. Russo, L. Di Marcantonio, P. Berardinelli, A. Martelli, A. Muttini, M. Mattioli, B. Barboni, M1 and M2 macrophage recruitment during tendon regeneration induced by amniotic epithelial cell allotransplantation in ovine, Res. Vet. Sci. 105 (2016) 92–102.
[26] P. Starkey Lewis, L. Campana, N. Aleksieva, J.A. Cartwright, A. Mackinnon, E. O'Duibhir, T. Kendall, M. Vermeren, A. Thomson, V. Gadd, B. Dwyer, R. Aird, T.Y. Man, A.G. Rossi, L. Forrester, B.K. Park, S.J. Forbes, Alternatively activated macrophages promote resolution of necrosis following acute liver injury, J. Hepatol. (2020).

[27] F.C. Simões, T.J. Cahill, A. Kenyon, D. Gavriouchkina, J.M. Vieira, X. Sun, D. Pezzolla, C. Ravaud, E. Masmanian, M. Weinberger, S. Mayes, M.E. Lemieux, D.N. Barnette, M. Gunadasa-Rohling, R.M. Williams, D.R. Greaves, L.A. Trinh, S.E. Fraser, S.L. Dallas, R.P. Choudhury, T. Sauka-Spengler, P.R. Riley, Macrophages directly contribute collagen to scar formation during zebrafish heart regeneration and mouse heart repair, Nat. Commun. 11 (1) (2020) 600.
[28] S.Y. Kim, M.G. Nair, Macrophages in wound healing: activation and plasticity, Immunol. Cell Biol. 97 (3) (2019) 258–267.
[29] Y. Oishi, I. Manabe, Macrophages in inflammation, repair and regeneration, Int. Immunol. 30 (11) (2018) 511–528.
[30] E. Kolaczkowska, P. Kubes, Neutrophil recruitment and function in health and inflammation, Nat. Rev. Immunol. 13 (3) (2013) 159–175.
[31] G.Y. Chen, G. Nuñez, Sterile inflammation: sensing and reacting to damage, Nat. Rev. Immunol. 10 (12) (2010) 826–837.
[32] V. Rungelrath, S.D. Kobayashi, F.R. DeLeo, Neutrophils in innate immunity and systems biology-level approaches, Wiley Interdiscip. Rev. Syst. Biol. Med. 12 (1) (2020) e1458.
[33] S. Jhunjhunwala, S. Aresta-DaSilva, K. Tang, D. Alvarez, M.J. Webber, B.C. Tang, D.M. Lavin, O. Veiseh, J.C. Doloff, S. Bose, A. Vegas, M. Ma, G. Sahay, A. Chiu, A. Bader, E. Langan, S. Siebert, J. Li, D.L. Greiner, P.E. Newburger, U.H. von An- drian, R. Langer, D.G. Anderson, Neutrophil responses to sterile implant ma- terials, PLoS One 10 (9) (2015) e0137550.
[34] O. Soehnlein, L. Lindbom, Phagocyte partnership during the onset and resolution of inflammation, Nat. Rev. Immunol. 10 (6) (2010) 427–439.
[35] C.A. Loynes, J.A. Lee, A.L. Robertson, M.J. Steel, F. Ellett, Y. Feng, B.D. Levy, M.K.B. Whyte, S.A. Renshaw, PGE, Sci. Adv. 4 (9) (2018) eaar8320.
[36] A. Mantovani, M.A. Cassatella, C. Costantini, S. Jaillon, Neutrophils in the activation and regulation of innate and adaptive immunity, Nat. Rev. Immunol. 11 (8) (2011) 519–531.
[37] M. Horckmans, L. Ring, J. Duchene, D. Santovito, M.J. Schloss, M. Drechsler, C. Weber, O. Soehnlein, S. Steffens, Neutrophils orchestrate post-myocardial infarction healing by polarizing macrophages towards a reparative phenotype, Eur. Heart J. 38 (3) (2017) 187–197.
[38] J. Hahn, C. Schauer, C. Czegley, L. Kling, L. Petru, B. Schmid, D. Weidner, C. Reinwald, M.H.C. Biermann, S. Blunder, J. Ernst, A. Lesner, T. Bäuerle, R. Palmisano, S. Christiansen, M. Herrmann, A. Bozec, R. Gruber, G. Schett, M.H. Hoffmann, Aggregated neutrophil extracellular traps resolve inflammation by proteolysis of cytokines and chemokines and protection from antiproteases, FASEB J. 33 (1) (2019) 1401–1414.
[39] C. Schauer, C. Janko, L.E. Munoz, Y. Zhao, D. Kienhöfer, B. Frey, M. Lell, B. Manger, J. Rech, E. Naschberger, R. Holmdahl, V. Krenn, T. Harrer, I. Jeremic, R. Bilyy, G. Schett, M. Hoffmann, M. Herrmann, Aggregated neutrophil extracellular traps limit inflammation by degrading cytokines and chemokines, Nat. Med. 20 (5) (2014) 511–517.
[40] S.L. Wong, M. Demers, K. Martinod, M. Gallant, Y. Wang, A.B. Goldfine, C.R. Kahn, D.D. Wagner, Diabetes primes neutrophils to undergo NETosis, which impairs wound healing, Nat. Med. 21 (7) (2015) 815–819.
[41] D. Bausch, T. Pausch, T. Krauss, U.T. Hopt, C. Fernandez-del-Castillo, A.L. Warshaw, S.P. Thayer, T. Keck, Neutrophil granulocyte derived MMP-9 is a VEGF independent functional component of the angiogenic switch in pancreatic ductal adenocarcinoma, Angiogenesis 14 (3) (2011) 235–243.
[42] D.P. Stirling, S. Liu, P. Kubes, V.W. Yong, Depletion of Ly6G/Gr-1 leukocytes af- ter spinal cord injury in mice alters wound healing and worsens neurological outcome, J. Neurosci. 29 (3) (2009) 753–764.
[43] S. Geng, Y. Zhang, C. Lee, L. Li, Novel reprogramming of neutrophils modulates inflammation resolution during atherosclerosis, Sci. Adv. 5 (2) (2019) eaav2309.
[44] Y. Ma, A. Yabluchanskiy, R.P. Iyer, P.L. Cannon, E.R. Flynn, M. Jung, J. Henry, C.A. Cates, K.Y. Deleon-Pennell, M.L. Lindsey, Temporal neutrophil polarization following myocardial infarction, Cardiovasc. Res. 110 (1) (2016) 51–61.
[45] E.O. Long, H.S. Kim, D. Liu, M.E. Peterson, S. Rajagopalan, Controlling natural killer cell responses: integration of signals for activation and inhibition, Annu. Rev. Immunol. 31 (2013) 227–258.
[46] J. Rosenberg, J. Huang, CD8, Curr. Opin. Chem. Eng. 19 (2018) 9–20.
[47] R. Nikzad, L.S. Angelo, K. Aviles-Padilla, D.T. Le, V.K. Singh, L. Bimler, M. Vukmanovic-Stejic, E. Vendrame, T. Ranganath, L. Simpson, N.L. Haigwood, C.A. Blish, A.N. Akbar, S. Paust, Human natural killer cells mediate adaptive immunity to viral antigens, Sci. Immunol. 4 (35) (2019).
[48] T. Barkhausen, C. Frerker, C. Pütz, H.C. Pape, C. Krettek, M. van Griensven, Depletion of NK cells in a murine polytrauma model is associated with improved outcome and a modulation of the inflammatory response, Shock 30 (4) (2008) 401–410.
[49] D. Toben, I. Schroeder, T. El Khassawna, M. Mehta, J.E. Hoffmann, J.T. Frisch, H. Schell, J. Lienau, A. Serra, A. Radbruch, G.N. Duda, Fracture healing is accelerated in the absence of the adaptive immune system, J. Bone Miner Res. 26 (1) (2011) 113–124.
[50] A. Tosello-Trampont, F.A. Surette, S.E. Ewald, Y.S. Hahn, Immunoregulatory role of NK cells in tissue inflammation and regeneration, Front. Immunol. 8 (2017) 301.
[51] F.A. da Luz, A.P. Oliveira, D. Borges, P.C. Brígido, M.J. Silva, The physiopathological role of IL-33: new highlights in bone biology and a proposed role in periodontal disease, Mediators Inflamm. (2014) 342410 2014.
[52] M.D. Smithgall, M.R. Comeau, B.R. Yoon, D. Kaufman, R. Armitage, D.E. Smith, IL-33 amplifies both Th1- and Th2-type responses through its activity on human basophils, allergen-reactive Th2 cells, iNKT and NK cells, Int. Immunol. 20 (8) (2008) 1019–1030.
[53] Q. Liu, C.W. Smith, W. Zhang, A.R. Burns, Z. Li, NK cells modulate the inflammatory response to corneal epithelial abrasion and thereby support wound healing, Am. J. Pathol. 181 (2) (2012) 452–462.
[54] M. Najar, M. Fayyad-Kazan, N. Meuleman, D. Bron, H. Fayyad-Kazan, L. Lagneaux, Mesenchymal stromal cells of the bone marrow and natural killer cells: cell interactions and cross modulation, J. Cell Commun. Signal 12 (4) (2018) 673–688.
[55] G.M. Spaggiari, A. Capobianco, H. Abdelrazik, F. Becchetti, M.C. Mingari, L. Moretta, Mesenchymal stem cells inhibit natural killer-cell proliferation, cytotoxicity, and cytokine production: role of indoleamine 2,3-dioxygenase and prostaglandin E2, Blood 111 (3) (2008) 1327–1333.
[56] P.A. Sotiropoulou, S.A. Perez, A.D. Gritzapis, C.N. Baxevanis, M. Papamichail, Interactions between human mesenchymal stem cells and natural killer cells, Stem Cells 24 (1) (2006) 74–85.
[57] M. Najar, M. Fayyad-Kazan, M. Merimi, A. Burny, D. Bron, H. Fayyad-Kazan, N. Meuleman, L. Lagneaux, Mesenchymal stromal cells and natural killer cells: a complex story of love and hate, Curr. Stem Cell Res. Ther. 14 (1) (2019) 14–21.
[58] S.K. Panda, M. Colonna, Innate lymphoid cells in mucosal immunity, Front. Immunol. 10 (2019) 861.
[59] J. Yang, L. Zhao, M. Xu, N. Xiong, Establishment and function of tissue-resident innate lymphoid cells in the skin, Protein Cell 8 (7) (2017) 489–500.
[60] A. Ignacio, C.N.S. Breda, N.O.S. Camara, Innate lymphoid cells in tissue homeostasis and diseases, World J. Hepatol. 9 (23) (2017) 979–989.
[61] E. Vivier, D. Artis, M. Colonna, A. Diefenbach, J.P. Di Santo, G. Eberl, S. Koyasu, R.M. Locksley, A.N.J. McKenzie, R.E. Mebius, F. Powrie, H. Spits, Innate lymphoid cells: 10 years on, Cell 174 (5) (2018) 1054–1066.
[62] G.M. Jowett, M.D.A. Norman, T.T.L. Yu, P. Rosell Arévalo, D. Hoogland, S.T. Lust, E. Read, E. Hamrud, N.J. Walters, U. Niazi, M.W.H. Chung, D. Marciano, O.S. Omer, T. Zabinski, D. Danovi, G.M. Lord, J. Hilborn, N.D. Evans, C.A. Dreiss, L. Bozec, O.P. Oommen, C.D. Lorenz, R.M.P. da Silva, J.F. Neves, E. Gentleman, ILC1 drive intestinal epithelial and matrix remodelling, Nat. Mater., 2020.
[63] A.B. Molofsky, J.C. Nussbaum, H.E. Liang, S.J. Van Dyken, L.E. Cheng, A. Mohapatra, A. Chawla, R.M. Locksley, Innate lymphoid type 2 cells sustain visceral adipose tissue eosinophils and alternatively activated macrophages, J. Exp. Med. 210 (3) (2013) 535–549.
[64] R.G. Klein Wolterink, A. Kleinjan, M. van Nimwegen, I. Bergen, M. de Bruijn, Y. Levani, R.W. Hendriks, Pulmonary innate lymphoid cells are major producers of IL-5 and IL-13 in murine models of allergic asthma, Eur. J. Immunol. 42 (5) (2012) 1106–1116.
[65] A.G. Besnard, R. Guabiraba, W. Niedbala, J. Palomo, F. Reverchon, T.N. Shaw, K.N. Couper, B. Ryffel, F.Y. Liew, IL-33-mediated protection against experimental cerebral malaria is linked to induction of type 2 innate lymphoid cells, M2 macrophages and regulatory T cells, PLoS Pathog. 11 (2) (2015) e1004607.
[66] P. Zhu, X. Zhu, J. Wu, L. He, T. Lu, Y. Wang, B. Liu, B. Ye, L. Sun, D. Fan, J. Wang, L. Yang, X. Qin, Y. Du, C. Li, W. Ren, X. Wu, Y. Tian, Z. Fan, IL-13 secreted by ILC2s promotes the self-renewal of intestinal stem cells through circular RNA circPan3, Nat. Immunol. 20 (2) (2019) 183–194.
[67] G.D. Rak, L.C. Osborne, M.C. Siracusa, B.S. Kim, K. Wang, A. Bayat, D. Artis, S.W. Volk, IL-33-dependent group 2 innate lymphoid cells promote cutaneous wound healing, J. Invest. Dermatol. 136 (2) (2016) 487–496.
[68] A.S. Mirchandani, A.G. Besnard, E. Yip, C. Scott, C.C. Bain, V. Cerovic, R.J. Salmond, F.Y. Liew, Type 2 innate lymphoid cells drive CD4+ Th2 cell responses, J. Immunol. 192 (5) (2014) 2442–2448.
[69] X. Kong, D. Feng, H. Wang, F. Hong, A. Bertola, F.S. Wang, B. Gao, Interleukin-22 induces hepatic stellate cell senescence and restricts liver fibrosis in mice, Hepatology 56 (3) (2012) 1150–1159.
[70] A. Matsumoto, T. Kanai, Y. Mikami, P.S. Chu, N. Nakamoto, H. Ebinuma, H. Saito, T. Sato, H. Yagita, T. Hibi, IL-22-producing RORγ t-dependent innate lymphoid cells play a novel protective role in murine acute hepatitis, PLoS One 8 (4) (2013) e62853.
[71] J.A. Dudakov, A.M. Hanash, R.R. Jenq, L.F. Young, A. Ghosh, N.V. Singer, M.L. West, O.M. Smith, A.M. Holland, J.J. Tsai, R.L. Boyd, M.R. van den Brink, Interleukin-22 drives endogenous thymic regeneration in mice, Science 336 (6077) (2012) 91–95.
[72] Z. Li, T. Hodgkinson, E.J. Gothard, S. Boroumand, R. Lamb, I. Cummins, P. Narang, A. Sawtell, J. Coles, G. Leonov, A. Reboldi, C.D. Buckley, T. Cupedo, C. Siebel, A. Bayat, M.C. Coles, C.A. Ambler, Epidermal Notch1 recruits RORγ (+) group 3 innate lymphoid cells to orchestrate normal skin repair, Nat. Commun. 7 (2016) 11394.
[73] D. Artis, H. Spits, The biology of innate lymphoid cells, Nature 517 (7534) (2015) 293–301.
[74] V.K. Raker, M.P. Domogalla, K. Steinbrink, Tolerogenic dendritic cells for regulatory T cell induction in man, Front. Immunol. 6 (2015) 569.
[75] M.P. Domogalla, P.V. Rostan, V.K. Raker, K. Steinbrink, Tolerance through Education: how tolerogenic dendritic cells shape immunity, Front. Immunol. 8 (2017) 1764.
[76] A. Anzai, T. Anzai, S. Nagai, Y. Maekawa, K. Naito, H. Kaneko, Y. Sugano, T. Takahashi, H. Abe, S. Mochizuki, M. Sano, T. Yoshikawa, Y. Okada, S. Koyasu, S. Ogawa, K. Fukuda, Regulatory role of dendritic cells in postinfarction healing and left ventricular remodeling, Circulation 125 (10) (2012) 1234–1245.
[77] M. Vinish, W. Cui, E. Stafford, L. Bae, H. Hawkins, R. Cox, T. Toliver-Kinsky, Dendritic cells modulate burn wound healing by enhancing early proliferation, Wound Repair Regen. 24 (1) (2016) 6–13.

[78] J. Gregorio, S. Meller, C. Conrad, A. Di Nardo, B. Homey, A. Lauerma, N. Arai, R.L. Gallo, J. Digiovanni, M. Gilliet, Plasmacytoid dendritic cells sense skin in- jury and promote wound healing through type I interferons, J. Exp. Med. 207 (13) (2010) 2921–2930.
[79] Y. Iwata, A. Yoshizaki, K. Komura, K. Shimizu, F. Ogawa, T. Hara, E. Muroi, S. Bae, M. Takenaka, T. Yukami, M. Hasegawa, M. Fujimoto, Y. Tomita, T.F. Tedder, S. Sato, CD19, a response regulator of B lymphocytes, regulates wound healing through hyaluronan-induced TLR4 signaling, Am. J. Pathol. 175 (2) (2009) 649–660.
[80] R.F. Sîrbulescu, C.K. Boehm, E. Soon, M.Q. Wilks, I. Ilies¸, H. Yuan, B. Maxner, N. Chronos, C. Kaittanis, M.D. Normandin, G. El Fakhri, D.P. Orgill, A.E. Sluder, M.C. Poznansky, Mature B cells accelerate wound healing after acute and chronic diabetic skin lesions, Wound Repair Regen. 25 (5) (2017) 774–791.
[81] N. Nishio, S. Ito, H. Suzuki, K. Isobe, Antibodies to wounded tissue enhance cutaneous wound healing, Immunology 128 (3) (2009) 369–380.
[82] I. Könnecke, A. Serra, T. El Khassawna, C. Schlundt, H. Schell, A. Hauser, A. Ellinghaus, H.D. Volk, A. Radbruch, G.N. Duda, K. Schmidt-Bleek, T and B cells participate in bone repair by infiltrating the fracture callus in a two-wave fashion, Bone 64 (2014) 155–165.
[83] Y. Han, Y. Jin, Y. Miao, T. Shi, X. Lin, Improved RANKL expression and osteoclastogenesis induction of CD27+CD38- memory B cells: a link between B cells and alveolar bone damage in periodontitis, J. Periodontal Res. 54 (1) (2019) 73–80.
[84] N. Meednu, H. Zhang, T. Owen, W. Sun, V. Wang, C. Cistrone, J. Rangel– Moreno, L. Xing, J.H. Anolik, Production of RANKL by memory B Cells: a link between B cells and bone erosion in rheumatoid arthritis, Arthritis Rheuma- tol. 68 (4) (2016) 805–816.
[85] S. Reinke, S. Geissler, W.R. Taylor, K. Schmidt-Bleek, K. Juelke, V. Schwachmeyer, M. Dahne, T. Hartwig, L. Akyüz, C. Meisel, N. Unterwalder, N.B. Singh, P. Reinke, N.P. Haas, H.D. Volk, G.N. Duda, Terminally differentiated CD8+ T cells negatively affect bone regeneration in humans, Sci. Transl. Med. 5 (177) (2013) 177ra36.
[86] P.A. Davis, D.J. Corless, R. Aspinall, C. Wastell, Effect of CD4(+) and CD8(+) cell depletion on wound healing, Br. J. Surg. 88 (2) (2001) 298–304.
[87] K. Sadtler, K. Estrellas, B.W. Allen, M.T. Wolf, H. Fan, A.J. Tam, C.H. Patel, B.S. Luber, H. Wang, K.R. Wagner, J.D. Powell, F. Housseau, D.M. Pardoll, J.H. Elisseeff, Developing a pro-regenerative biomaterial scaffold microenvironment requires T helper 2 cells, Science 352 (6283) (2016) 366–370.
[88] X. Wang, S. Balaji, E.H. Steen, H. Li, M.M. Rae, A.J. Blum, Q. Miao, M.J. Butte, P.L. Bollyky, S.G. Keswani, T Lymphocytes attenuate dermal scarring by regulating inflammation, neovascularization, and extracellular matrix remodeling, Adv. Wound Care (New Rochelle) 8 (11) (2019) 527–537.
[89] J. Wu, B.W. Hayes, C. Phoenix, G.S. Macias, Y. Miao, H.W. Choi, F.M. Hughes, J.Todd Purves, R.Lee Reinhardt, S.N. Abraham, A highly polarized TH2 bladder response to infection promotes epithelial repair at the expense of preventing new infections, Nat. Immunol. (2020).
[90] J. Li, J. Tan, M.M. Martino, K.O. Lui, Regulatory T-cells: potential regulator of tissue repair and regeneration, Front. Immunol. 9 (2018) 585.
[91] H. Lei, K. Schmidt-Bleek, A. Dienelt, P. Reinke, H.D. Volk, Regulatory T cell–mediated anti-inflammatory effects promote successful tissue repair in both indirect and direct manners, Front. Pharmacol. 6 (2015) 184.
[92] M.M. Tiemessen, A.L. Jagger, H.G. Evans, M.J. van Herwijnen, S. John, L.S. Taams, CD4+CD25+Foxp3+ regulatory T cells induce alternative activation of human monocytes/macrophages, Proc. Natl. Acad. Sci. USA 104 (49) (2007) 19446–19451.
[93] M.D. Rosenblum, I.K. Gratz, J.S. Paw, K. Lee, A. Marshak-Rothstein, A.K. Abbas, Response to self antigen imprints regulatory memory in tissues, Nature 480 (7378) (2011) 538–542.
[94] D. Burzyn, W. Kuswanto, D. Kolodin, J.L. Shadrach, M. Cerletti, Y. Jang, E. Sefik, T.G. Tan, A.J. Wagers, C. Benoist, D. Mathis, A special population of regulatory T cells potentiates muscle repair, Cell 155 (6) (2013) 1282–1295.
[95] S.A. Villalta, W. Rosenthal, L. Martinez, A. Kaur, T. Sparwasser, J.G. Tidball, M. Margeta, M.J. Spencer, J.A. Bluestone, Regulatory T cells suppress muscle inflammation and injury in muscular dystrophy, Sci. Transl. Med. 6 (258) (2014) 258ra142.
[96] D.M. Zaiss, J. van Loosdregt, A. Gorlani, C.P. Bekker, A. Gröne, M. Sibilia, P.M. van Bergen en Henegouwen, R.C. Roovers, P.J. Coffer, A.J. Sijts, Amphiregulin enhances regulatory T cell-suppressive function via the epidermal growth factor receptor, Immunity 38 (2) (2013) 275–284.
[97] J. Weirather, U.D. Hofmann, N. Beyersdorf, G.C. Ramos, B. Vogel, A. Frey, G. Ertl, T. Kerkau, S. Frantz, Foxp3+ CD4+ T cells improve healing after myocardial infarction by modulating monocyte/macrophage differentiation, Circ. Res. 115 (1) (2014) 55–67.
[98] L.A. Monticelli, L.C. Osborne, M. Noti, S.V. Tran, D.M. Zaiss, D. Artis, IL-33 promotes an innate immune pathway of intestinal tissue protection dependent on amphiregulin-EGFR interactions, Proc. Natl. Acad. Sci. USA 112 (34) (2015) 10762–10767.
[99] S. Zacchigna, V. Martinelli, S. Moimas, A. Colliva, M. Anzini, A. Nordio, A. Costa, M. Rehman, S. Vodret, C. Pierro, G. Colussi, L. Zentilin, M.I. Gutier- rez, E. Dirkx, C. Long, G. Sinagra, D. Klatzmann, M. Giacca, Paracrine effect of regulatory T cells promotes cardiomyocyte proliferation during pregnancy and after myocardial infarction, Nat. Commun. 9 (1) (2018) 2432.
[100] Y.Y. Wan, Regulatory T cells: immune suppression and beyond, Cell Mol. Immunol. 7 (3) (2010) 204–210.
[101] B.T. Garibaldi, F.R. D'Alessio, J.R. Mock, D.C. Files, E. Chau, Y. Eto, M.B. Drummond, N.R. Aggarwal, V. Sidhaye, L.S. King, Regulatory T cells reduce acute lung injury fibroproliferation by decreasing fibrocyte recruitment, Am. J. Respir. Cell Mol. Biol. 48 (1) (2013) 35–43.
[102] M. Sharma, M.P. Schlegel, M.S. Afonso, E.J. Brown, K. Rahman, A. Weinstock, B. Sansbury, E.M. Corr, C. van Solingen, G. Koelwyn, L.C. Shanley, L. Beckett, D. Peled, J.J. Lafaille, M. Spite, P. Loke, E.A. Fisher, K.J. Moore, Regulatory T cells license macrophage pro-resolving functions during atherosclerosis re- gression, Circ. Res., 2020.
[103] I.C. Boothby, J.N. Cohen, M.D. Rosenblum, Regulatory T cells in skin injury: at the crossroads of tolerance and tissue repair, Sci. Immunol. 5 (47) (2020).
[104] H.J. Faust, H. Zhang, J. Han, M.T. Wolf, O.H. Jeon, K. Sadtler, A.N. Peña, L. Chung, D.R. Maestas, A.J. Tam, D.M. Pardoll, J. Campisi, F. Housseau, D. Zhou, C.O. Bingham, J.H. Elisseeff, IL-17 and immunologically induced senescence regulate response to injury in osteoarthritis, J. Clin. Invest. (2020).
[105] S.D. Sommerfeld, C. Cherry, R.M. Schwab, L. Chung, D.R. Maestas, P. Laffont, J.E. Stein, A. Tam, S. Ganguly, F. Housseau, J.M. Taube, D.M. Pardoll, P. Cahan, J.H. Elisseeff, Interleukin-36γ -producing macrophages drive IL-17-mediated fibrosis, Sci. Immunol. 4 (40) (2019).
[106] C. Zhou, X.R. Wu, H.S. Liu, X.H. Liu, G.H. Liu, X.B. Zheng, T. Hu, Z.X. Liang, X.W. He, X.J. Wu, L.C. Smith, Y.Y. Zhang, P. Lan, Immunomodulatory effect of urine-derived stem cells on inflammatory bowel diseases via downregulating Th1/Th17 immune responses in a PGE2-dependent manner, J. Crohns Colitis (2019).
[107] J. Jameson, K. Ugarte, N. Chen, P. Yachi, E. Fuchs, R. Boismenu, W.L. Havran, A role for skin gammadelta T cells in wound repair, Science 296 (5568) (2002) 747–749.
[108] S. Krishnan, I.E. Prise, K. Wemyss, L.P. Schenck, H.M. Bridgeman, F.A. McClure, T. Zangerle-Murray, C. O'Boyle, T.A. Barbera, F. Mahmood, D.M.E. Bowdish, D.M.W. Zaiss, J.R. Grainger, J.E. Konkel, Amphiregulin-producing $\gamma\delta$ T cells are vital for safeguarding oral barrier immune homeostasis, Proc. Natl. Acad. Sci. USA 115 (42) (2018) 10738–10743.
[109] T. Ono, K. Okamoto, T. Nakashima, T. Nitta, S. Hori, Y. Iwakura, H. Takayanagi, IL-17-producing $\gamma\delta$ T cells enhance bone regeneration, Nat. Commun. 7 (2016) 10928.
[110] D.P. Vasconcelos, A.P. Águas, M.A. Barbosa, P. Pelegrín, J.N. Barbosa, The inflammasome in host response to biomaterials: bridging inflammation and tissue regeneration, Acta Biomater 83 (2019) 1–12.
[111] E. Mariani, G. Lisignoli, R.M. Borzì, L. Pulsatelli, Biomaterials: foreign bodies or tuners for the immune response? Int. J. Mol. Sci. 20 (3) (2019).
[112] Q. Wang, H. Li, Y. Xiao, S. Li, B. Li, X. Zhao, L. Ye, B. Guo, X. Chen, Y. Ding, C. Bao, Locally controlled delivery of TNFα antibody from a novel glucose-sensitive scaffold enhances alveolar bone healing in diabetic conditions, J. Control Release 206 (2015) 232–242.
[113] I. Somasuntharam, K. Yehl, S.L. Carroll, J.T. Maxwell, M.D. Martinez, P.L. Che, M.E. Brown, K. Salaita, M.E. Davis, Knockdown of TNF-α by DNAzyme gold nanoparticles as an anti-inflammatory therapy for myocardial infarction, Biomaterials 83 (2016) 12–22.
[114] J.E. Rayahin, J.S. Buhrman, Y. Zhang, T.J. Koh, R.A. Gemeinhart, High and low molecular weight hyaluronic acid differentially influence macrophage activation, ACS Biomater Sci. Eng. 1 (7) (2015) 481–493.
[115] E.E. Friedrich, L.T. Sun, S. Natesan, D.O. Zamora, R.J. Christy, N.R. Washburn, Effects of hyaluronic acid conjugation on anti-TNF-α inhibition of inflammation in burns, J. Biomed. Mater. Res. A 102 (5) (2014) 1527–1536.
[116] G. Beldi, M. Khosravi, M.E. Abdelgawad, B.L. Salomon, G. Uzan, H. Haouas, S. Naserian, TNFα/TNFR2 signaling pathway: an active immune checkpoint for mesenchymal stem cell immunoregulatory function, Stem Cell Res. Ther. 11 (1) (2020) 281.
[117] M.M. Martino, K. Maruyama, G.A. Kuhn, T. Satoh, O. Takeuchi, R. Müller, S. Akira, Inhibition of IL-1R1/MyD88 signalling promotes mesenchymal stem cell-driven tissue regeneration, Nat. Commun. 7 (2016) 11051.
[118] Z. Julier, R. Karami, B. Nayer, Y.Z. Lu, A.J. Park, K. Maruyama, G.A. Kuhn, R. Müller, S. Akira, M.M. Martino, Enhancing the regenerative effectiveness of growth factors by local inhibition of interleukin-1 receptor signaling, Sci. Adv. 6 (24) (2020) eaba7602.
[119] S.M. Gutowski, J.T. Shoemaker, K.L. Templeman, Y. Wei, R.A. Latour, R.V. Bellamkonda, M.C. LaPlaca, A.J. García, Protease-degradable PEG-maleimide coat- ing with on-demand release of IL-1Ra to improve tissue response to neural electrodes, Biomaterials 44 (2015) 55–70.
[120] R. Haenold, F. Weih, K.H. Herrmann, K.F. Schmidt, K. Krempler, C. Engelmann, K.A. Nave, J.R. Reichenbach, S. Löwel, O.W. Witte, A. Kretz, NF-κB controls axonal regeneration and degeneration through cell-specific balance of RelA and p50 in the adult CNS, J. Cell Sci. 127 (Pt 14) (2014) 3052–3065.
[121] L. Lu, S. Qi, Y. Chen, H. Luo, S. Huang, X. Yu, Q. Luo, Z. Zhang, Targeted immunomodulation of inflammatory monocytes across the blood-brain barrier by curcumin-loaded nanoparticles delays the progression of experimental autoimmune encephalomyelitis, Biomaterials 245 (2020) 119987.
[122] J. Chang, F. Liu, M. Lee, B. Wu, K. Ting, J.N. Zara, C. Soo, K. Al Hezaimi, W. Zou, X. Chen, D.J. Mooney, C.Y. Wang, NF-κB inhibits osteogenic differentiation of mesenchymal stem cells by promoting β-catenin degradation, Proc. Natl. Acad. Sci. USA 110 (23) (2013) 9469–9474.
[123] Q. Wang, H. Jiang, Y. Li, W. Chen, H. Li, K. Peng, Z. Zhang, X. Sun, Targeting NF-kB signaling with polymeric hybrid micelles that co-deliver siRNA and dexamethasone for arthritis therapy, Biomaterials 122 (2017) 10–22.

[124] H. Katsura, Y. Kobayashi, P.R. Tata, B.L.M. Hogan, IL-1 and TNFα contribute to the inflammatory niche to enhance alveolar regeneration, Stem Cell Rep. 12 (4) (2019) 657–666.
[125] J. Oyama, C. Blais, X. Liu, M. Pu, L. Kobzik, R.A. Kelly, T. Bourcier, Reduced myocardial ischemia-reperfusion injury in toll-like receptor 4-deficient mice, Circulation 109 (6) (2004) 784–789.
[126] H. Wu, G. Chen, K.R. Wyburn, J. Yin, P. Bertolino, J.M. Eris, S.I. Alexander, A.F. Sharland, S.J. Chadban, TLR4 activation mediates kidney ischemia/reperfusion injury, J. Clin. Invest. 117 (10) (2007) 2847–2859.
[127] S. Munir, A. Basu, P. Maity, L. Krug, P. Haas, D. Jiang, G. Strauss, M. Wlaschek, H. Geiger, K. Singh, K. Scharffetter-Kochanek, TLR4-dependent shaping of the wound site by MSCs accelerates wound healing, EMBO Rep. (2020) e48777.
[128] H. Suga, M. Sugaya, H. Fujita, Y. Asano, Y. Tada, T. Kadono, S. Sato, TLR4, rather than TLR2, regulates wound healing through TGF-β and CCL5 expression, J Dermatol. Sci. 73 (2) (2014) 117–124.
[129] D. Kwon, B.G. Cha, Y. Cho, J. Min, E.B. Park, S.J. Kang, J. Kim, Extra-large pore mesoporous silica nanoparticles for directing in vivo M2 macrophage polar- ization by delivering IL-4, Nano Lett. 17 (5) (2017) 2747–2756.
[130] M. Li, F. Wei, X. Yin, L. Xiao, L. Yang, J. Su, J. Weng, B. Feng, Y. Xiao, Y. Zhou, Synergistic regulation of osteoimmune microenvironment by IL-4 and RGD to accelerate osteogenesis, Mater. Sci. Eng. C Mater. Biol. Appl. 109 (2020) 110508.
[131] M.H. Abdelaziz, S.F. Abdelwahab, J. Wan, W. Cai, W. Huixuan, C. Jianjun, K.D. Kumar, A. Vasudevan, A. Sadek, Z. Su, S. Wang, H. Xu, Alternatively activated macrophages; a double-edged sword in allergic asthma, J. Transl. Med. 18 (1) (2020) 58.
[132] T.M. Raimondo, D.J. Mooney, Functional muscle recovery with nanoparti- cle-directed M2 macrophage polarization in mice, Proc. Natl. Acad. Sci. USA 115 (42) (2018) 10648–10653.
[133] N. Bloise, I. Rountree, C. Polucha, G. Montagna, L. Visai, K.L.K. Coulombe, F. Munarin, Engineering immunomodulatory biomaterials for regenerating the infarcted myocardium, Front. Bioeng. Biotechnol. 8 (2020) 292.
[134] K.L. Spiller, S. Nassiri, C.E. Witherel, R.R. Anfang, J. Ng, K.R. Nakazawa, T. Yu, G. Vunjak-Novakovic, Sequential delivery of immunomodulatory cytokines to facilitate the M1-to-M2 transition of macrophages and enhance vasculariza- tion of bone scaffolds, Biomaterials 37 (2015) 194–207.
[135] S. Jain, T.H. Tran, M. Amiji, Macrophage repolarization with targeted alginate nanoparticles containing IL-10 plasmid DNA for the treatment of experimental arthritis, Biomaterials 61 (2015) 162–177.
[136] O.R. Mahon, D.C. Browe, T. Gonzalez-Fernandez, P. Pitacco, I.T. Whelan, S. Von Euw, C. Hobbs, V. Nicolosi, K.T. Cunningham, K.H.G. Mills, D.J. Kelly, A. Dunne, Nano-particle mediated M2 macrophage polarization enhances bone forma- tion and MSC osteogenesis in an IL-10 dependent manner, Biomaterials 239 (2020) 119833.
[137] M. Kim, A. Sahu, Y. Hwang, G.B. Kim, G.H. Nam, I.S. Kim, I. Chan Kwon, G. Tae, Targeted delivery of anti-inflammatory cytokine by nanocarrier reduces atherosclerosis in Apo E, Biomaterials 226 (2020) 119550.
[138] M.C.P. Sok, N. Baker, C. McClain, H.S. Lim, T. Turner, L. Hymel, M. Ogle, C. Oli- ingy, J.I. Palacios, J.R. Garcia, K. Srithar, A.J. García, P. Qiu, E.A. Botchwey, Dual delivery of IL-10 and AT-RvD1 from PEG hydrogels polarize immune cells to- wards pro-regenerative phenotypes, Biomaterials 268 (2020) 120475.
[139] R.W.D. Gilbert, M.K. Vickaryous, A.M. Viloria-Petit, Signalling by transforming growth factor beta isoforms in wound healing and tissue regeneration, J. Dev. Biol. 4 (2) (2016).
[140] K. Delaney, P. Kasprzycka, M.A. Ciemerych, M. Zimowska, The role of TGF-β1 during skeletal muscle regeneration, Cell Biol. Int. 41 (7) (2017) 706–715.
[141] M.J. Crowe, T. Doetschman, D.G. Greenhalgh, Delayed wound healing in im- munodeficient TGF-beta 1 knockout mice, J. Invest. Dermatol. 115 (1) (2000) 3–11.
[142] J.M.H. Liu, J. Zhang, X. Zhang, K.A. Hlavaty, C.F. Ricci, J.N. Leonard, L.D. Shea, R.M. Gower, Transforming growth factor-beta 1 delivery from microporous scaffolds decreases inflammation post-implant and enhances function of transplanted islets, Biomaterials 80 (2016) 11–19.
[143] P.S. Hume, J. He, K. Haskins, K.S. Anseth, Strategies to reduce dendritic cell activation through functional biomaterial design, Biomaterials 33 (14) (2012) 3615–3625.
[144] Y.Y. Wan, R.A. Flavell, Yin-Yang' functions of transforming growth factor– beta and T regulatory cells in immune regulation, Immunol. Rev. 220 (2007) 199–213.
[145] J.E. Konkel, D. Zhang, P. Zanvit, C. Chia, T. Zangarle-Murray, W. Jin, S. Wang, W. Chen, Transforming growth factor-β signaling in regulatory T cells controls T helper-17 cells and tissue-specific immune responses, Immunity 46 (4) (2017) 660–674.
[146] J.I. Andorko, C.M. Jewell, Designing biomaterials with immunomodulatory properties for tissue engineering and regenerative medicine, Bioeng. Transl. Med. 2 (2) (2017) 139–155.
[147] M. Chen, Y. Zhang, P. Zhou, X. Liu, H. Zhao, X. Zhou, Q. Gu, B. Li, X. Zhu, Q. Shi, Substrate stiffness modulates bone marrow-derived macrophage polarization through NF-κB signaling pathway, Bioact. Mater. 5 (4) (2020) 880–890.
[148] R. Sridharan, B. Cavanagh, A.R. Cameron, D.J. Kelly, F.J. O'Brien, Material stiffness influences the polarization state, function and migration mode of macrophages, Acta Biomater 89 (2019) 47–59.
[149] A.K. Blakney, M.D. Swartzlander, S.J. Bryant, The effects of substrate stiff- ness on the in vitro activation of macrophages and in vivo host response to poly(ethylene glycol)-based hydrogels, J. Biomed. Mater. Res. A 100 (6) (2012) 1375–1386.
[150] P.C. Bota, A.M. Collie, P. Puolakkainen, R.B. Vernon, E.H. Sage, B.D. Rat- ner, P.S. Stayton, Biomaterial topography alters healing in vivo and mono- cyte/macrophage activation in vitro, J. Biomed. Mater. Res. A 95 (2) (2010) 649–657.
[151] M.J. Vassey, G.P. Figueredo, D.J. Scurr, A.S. Vasilevich, S. Vermeulen, A. Carlier, J. Luckett, N.R.M. Beijer, P. Williams, D.A. Winkler, J. de Boer, A.M. Ghaemmaghami, M.R. Alexander, Immune modulation by design: using topography to control human monocyte attachment and macrophage differentiation, Adv. Sci. (Weinh) 7 (11) (2020) 1903392.